U.S. Department
of Commerce

Volume 90
Number 2
April 1992

Fishery Bulletin

U.S. Department of Commerce
Barbara Hackman Franklin
Secretary

National Oceanic and Atmospheric Administration
John A. Knauss
Under Secretary for
Oceans and Atmosphere

National Marine Fisheries Service
William W. Fox Jr.
Assistant Administrator
for Fisheries

Fishery Bulletin

Scientific Editor
Dr. Linda L. Jones
National Marine Mammal Laboratory
National Marine Fisheries Service, NOAA
7600 Sand Point Way NE
Seattle, Washington 98115-0070

Editorial Committee
Dr. Andrew E. Dizon National Marine Fisheries Service
Dr. Charles W. Fowler National Marine Fisheries Service
Dr. Richard D. Methot National Marine Fisheries Service
Dr. Theodore W. Pietsch University of Washington
Dr. Joseph E. Powers National Marine Fisheries Service
Dr. Tim D. Smith National Marine Fisheries Service
Dr. Mia J. Tegner Scripps Institution of Oceanography

Managing Editor
Nancy Peacock
National Marine Fisheries Service
Scientific Publications Office
7600 Sand Point Way NE, BIN C15700
Seattle, Washington 98115-0070

The *Fishery Bulletin* (ISSN 0090-0656) is published quarterly by the Scientific Publications Office, National Marine Fisheries Service, NOAA, 7600 Sand Point Way NE, BIN C15700, Seattle, WA 98115-0070. Second class postage is paid in Seattle, Wash., and additional offices. POSTMASTER send address changes for subscriptions to Fishery Bulletin, Superintendent of Documents, Attn: Chief, Mail List Branch, Mail Stop SSOM, Washington, DC 20402-9373.

Although the contents have not been copyrighted and may be reprinted entirely, reference to source is appreciated.

The Secretary of Commerce has determined that the publication of this periodical is necessary in the transaction of the public business required by law of this Department. Use of funds for printing of this periodical has been approved by the Director of the Office of Management and Budget.

For sale by the Superintendent of Documents, U.S. Government Printing Office, Washington, DC 20402. Subscription price per year: $24.00 domestic and $30.00 foreign. Cost per single issue: $12.00 domestic and $15.00 foreign. **See back page for order form.**

The *Fishery Bulletin* carries original research reports and technical notes on investigations in fishery science, engineering, and economics. The Bulletin of the United States Fish Commission was begun in 1881; it became the Bulletin of the Bureau of Fisheries in 1904 and the Fishery Bulletin of the Fish and Wildlife Service in 1941. Separates were issued as documents through volume 46; the last document was No. 1103. Beginning with volume 47 in 1931 and continuing through volume 62 in 1963, each separate appeared as a numbered bulletin. A new system began in 1963 with volume 63 in which papers are bound together in a single issue of the bulletin. Beginning with volume 70, number 1, January 1972, the *Fishery Bulletin* became a periodical, issued quarterly. In this form, it is available by subscription from the Superintendent of Documents, U.S. Government Printing Office, Washington, DC 20402. It is also available free in limited numbers to libraries, research institutions, State and Federal agencies, and in exchange for other scientific publications.

U.S. Department
of Commerce
Seattle, Washington

Volume 90
Number 2
April 1992

Fishery Bulletin

Contents

iii **Publications Awards, 1989-90**

iv **List of recent NOAA Technical Reports**

217 **Armstrong, Michael P., John A. Musick, and James A. Colvocoresses**
Age, growth, and reproduction of the goosefish *Lophius americanus* (Pisces:Lophiiformes)

231 **Bowers, Michael J.**
Annual reproductive cycle of oocytes and embryos of yellowtail rockfish *Sebastes flavidus* (Family Scorpaenidae)

243 **Bullock, Lewis H., Michael D. Murphy, Mark F. Godcharles, and Michael E. Mitchell**
Age, growth, and reproduction of jewfish *Epinephelus itajara* in the eastern Gulf of Mexico

250 **Campton, Donald E., Carl J. Berg Jr., Lynn M. Robison, and Robert A. Glazer**
Genetic patchiness among populations of queen conch *Strombus gigas* in the Florida Keys and Bimini

260 **Dorn, Martin W.**
Detecting environmental covariates of Pacific whiting *Merluccius productus* growth using a growth-increment regression model

276 **Hyndes, Glenn A., Neil R. Loneragan, and Ian C. Potter**
Influence of sectioning otoliths on marginal increment trends and age and growth estimates for the flathead *Platycephalus speculator*

285 **Markle, Douglas F., Phillip M. Harris, and Christopher L. Toole**
Metamorphosis and an overview of early-life-history stages in Dover sole *Microstomus pacificus*

302 **Parrack, Michael L.**
Estimating stock abundance from size data

328 **Rajaguru, Arjuna**
Biology of two co-occurring tonguefishes, *Cynoglossus arel* and *C. lida* (Pleuronectiformes:Cynoglossidae), from Indian waters

368 **Somerton, David A., and Donald R. Kobayashi**
Inverse method for mortality and growth estimation: A new method for larval fishes

376 **Stone, Heath H., and Brian M. Jessop**
Seasonal distribution of river herring *Alosa pseudoharengus* and *A. aestivalis* off the Atlantic coast of Nova Scotia

Notes

390 **Bumguardner, Britt W., Robert L. Colura, and Gary C. Matlock**
Long-term coded wire tag retention in juvenile *Sciaenops ocellatus*

395 **Davis, Tim L.O., and Grant J. West**
Growth and mortality of *Lutjanus vittus* (Quoy and Gaimard) from the North West Shelf of Australia

405 **Hettler, William F.**
Correlation of winter temperature and landings of pink shrimp *Penaeus duorarum* in North Carolina

407 **Matlock, Gary C.**
Growth of five fishes in Texas Bays in the 1960s

412 **Restrepo, Victor R.**
A mortality model for a population in which harvested individuals do not necessarily die: The stone crab

417 **Salvadó, Carlos A.M., Pierre Kleiber, and Andrew E. Dizon**
Optimal course by dolphins for detection avoidance

421 **Toole, Christopher L., and Roger L. Nielsen**
Effects of microprobe precision on hypotheses related to otolith Sr:Ca ratios

U.S. Department of Commerce
Seattle, Washington

Publications Awards 1989-90

National Marine Fisheries Service, NOAA

The Publications Advisory Committee of the National Marine Fisheries Service is pleased to announce the awards for best publications authored by NMFS scientists and published in the *Fishery Bulletin* volume 88 and *Marine Fisheries Review* volume 51. Eligible papers are nominated by the Fisheries Science Centers and Regional Offices and are judged by the NMFS Editorial Board. Only articles which significantly contribute to the understanding and knowledge of NMFS-related studies are eligible. We offer congratulations to the following authors for their outstanding efforts.

Fishery Bulletin 1990

Joseph E. Hightower

Multispecies harvesting policies for Washington-Oregon-California rockfish trawl fisheries. *Fishery Bulletin* 88:645-656. Dr. Hightower is retired from his position with the Southwest Fisheries Science Center, and is now with the North Carolina Cooperative Fish and Wildlife Center, North Carolina State University, Raleigh.

Marine Fisheries Review 1989

Joseph M. Terry and Lewis E. Queirolo

U.S. fisheries management and foreign trade linkages: Policy implications for groundfish fisheries in the North Pacific EEZ. *Marine Fisheries Review* 51(1):23-43. Drs. Terry and Queirolo are with the Alaska Fisheries Science Center, Seattle.

U.S. Department of Commerce
Seattle, Washington

Recent publications in the NOAA Technical Reports NMFS Series

102 **Svrjcek, Ralph S. (editor)**
Marine ranching: Proceedings of the seventeenth U.S.-Japan meeting on aquaculture, Ise, Mie Prefecture, Japan, October 16, 17, and 18, 1988. May 1991, 180 p.

103 **Reid, Robert N., David J. Radosh, Ann B. Frame, Steven A. Fromm**
Benthic macrofauna of the New York Bight, 1979-89. December 1991, 50 p.

104 **Perez, Michael, and Thomas R. Loughlin**
Incidental catch of marine mammals by foreign and joint venture trawl vessels in the U.S. EEZ of the North Pacific, 1973-88. December 1991, 57 p.

105 **Wetherall, Jerry A. (editor)**
Biology, oceanography, and fisheries of the North Pacific Transition Zone and Subarctic Frontal Zone. December 1991, 111 p.

106 **Svrjcek, Ralph S. (editor)**
Marine ranching: Proceedings of the eighteenth U.S.-Japan meeting on aquaculture, Port Ludlow, Washington, 18-19 September 1989. February 1992, 136 p.

107 **Russell, Mike, Mark Grace, and Elmer J. Gutherz**
Field guide to the searobins (*Prionotus* and *Bellator*) in the western North Atlantic. March 1992, 26 p.

Some NOAA publications are available by purchase from the Superintendent of Documents, U.S. Government Printing Office, Washington, DC 20402.

Age, growth, and reproduction of the goosefish *Lophius americanus* (Pisces:Lophiiformes)*

Michael P. Armstrong

School of Marine Science, Virginia Institute of Marine Science
College of William and Mary, Gloucester Point, Virginia 23062
Present address: Department of Zoology, University of New Hampshire
Durham, New Hampshire 03824

John A. Musick
James A. Colvocoresses

School of Marine Science, Virginia Institute of Marine Science
College of William and Mary, Gloucester Point, Virginia 23062

Abstract. – Age, growth, and reproduction were studied in goosefish *Lophius americanus* collected from National Marine Fisheries Service groundfish surveys and commercial fishing cruises between Georges Bank and Cape Hatteras in the western North Atlantic. Age and growth of *L. americanus* were determined from vertebral annuli, which became visible at the edge of the vertebral centra in May. Maximum ages of males and females were 9 and 11 years, respectively. Males appeared to experience higher mortality than females in the older age-classes. Von Bertalanffy growth curves calculated for males and females had excellent agreement with back-calculated lengths. The growth rate of *L. americanus* was intermediate to its eastern Atlantic congeners, *L. piscatorius* and *L. budegassa*. Male *L. americanus* matured at 3+ years (~370 mm TL) and females at 4+ years (~485 mm TL). Spawning took place primarily in May and June. Fecundity in 17 individuals of 610–1048 mm TL ranged from 300,000 to 2,800,000 ova, and was linear with total length in that size range. Histological examination of the ovaries showed they are remarkably similar to ovaries of other lophiiform species. Females produced egg veils, which may function in dispersion, buoyancy, facilitating fertilization, and protection of the eggs and larvae.

Manuscript accepted 20 March 1992.
Fishery Bulletin, U.S. 90:217–230 (1992).

The goosefish *Lophius americanus* (Valenciennes in Cuvier and Valenciennes 1837) is a benthic fish which occurs in the Northwest Atlantic Ocean from the northern Gulf of Saint Lawrence, southward to Cape Hatteras, North Carolina (Bigelow and Schroeder 1953, Scott and Scott 1988) and less commonly to Florida (Caruso 1983). It has a eurybathic depth distribution, having been collected from the tideline (Bigelow and Schroeder 1953) to approximately 840 m (Markle and Musick 1974), although few large individuals occur deeper than 400 m (Wenner 1978). Goosefish have been taken in temperatures of 0–24°C (Grosslein and Azarovitz 1982), but seem to be most abundant in temperatures of about 9°C in the Mid-Atlantic Bight (Edwards 1965), 3–9°C in Canadian waters (Jean 1965), and 7–11°C on the continental slope off Virginia (Wenner 1978). The goosefish is sympatric with the black-finned goosefish *L. gastrophysus* in deep water (>100–150 m) from Cape Hatteras to the Florida coast, although strays of *L. gastrophysus* occur as far north as Washington Canyon, off Virginia (pers. observ., MPA).

Lophius americanus was confused with *L. piscatorius*, a European species, for many years. Thus all references to *L. piscatorius* in the western North Atlantic north of Cape Hatteras actually refer to *L. americanus* (Caruso 1977). There are several accounts of the species' life history (Gill 1905, Connolly 1920, Dahlgren 1928, Hildebrand and Schroeder 1928, Proctor et al. 1928, McKenzie 1936, Bigelow and Schroeder 1953, Grosslein and Azarovitz 1982, Scott and Scott 1988), but all are general in nature. Much of the information contained in these reports is anecdotal.

Goosefish are a bycatch of groundfishing and scalloping operations and are marketed under the name monkfish. They have traditionally been considered "trash" fish in the United States and discarded at sea or used in the production of fish meal, with a small amount being exported to Europe where *Lophius* has been highly esteemed as a food fish for centuries. Goosefish have become more popular with the American consumer due to dwindling catches and rising prices in recent years of the more traditional fishery products. Commercial landings have been increasing yearly since 1970 (Northeast Fisheries Science Center 1991). This

* Contribution 1735, Virginia Institute of Marine Science.

study describes age, growth, and reproduction of this increasingly exploited fish.

Methods

Goosefish were collected during the spring and autumn groundfish surveys (1982–85) conducted by the National Marine Fisheries Service (NMFS) in the Mid-Atlantic Bight and southern New England (for survey methodology see Grosslein and Azarovitz 1982). Additional samples were obtained during the NMFS 1983 summer scallop survey off southern New England and during cruises aboard commercial groundfish trawlers and scallopers operating out of Hampton, Virginia. Sampling effort was concentrated in the area from southern New England to Virginia.

Goosefish greater than ~180 mm were examined at sea. Smaller individuals were fixed in 10% formalin and saved for examination in the laboratory. Examination included measuring total and standard length and weight, excising a section of the vertebral column, removing both sagittal otoliths, recording stomach contents, macroscopic staging and weighing of the gonads, and preserving pieces of gonads for histological inspection and fecundity estimates.

Reproduction

Gonads were staged visually in the field and assigned to one of the following classes: immature, resting, developing, ripe, and spent. Both gonads were then removed from the body cavity and weighed to the nearest 0.1 g. A small representative piece was excised from the midsection of selected gonads and preserved in Davidson's fixative for histological study.

Late-developing and ripe ovaries were selected for fecundity analyses. The extremely large size of goosefish ovaries precluded saving the entire organ. A subsample of about 100 g was weighed to the nearest 0.1 g and placed in modified Gilson's solution (Simpson 1951). After several months of storage, most of the ovarian connective tissue had dissolved. Ova were removed from the Gilson's solution, separated from any remaining ovarian tissue, rinsed in water, blotted on absorbent paper, and weighed. Three subsamples, each containing about 1000 ova, were removed and weighed to the nearest 0.001 g. Ova in each sample were counted using a dissecting microscope. Fecundity was calculated as:

$$\text{Fecundity} = (W)(P)(N)$$

where W = total weight of both ovaries,

$$P = \frac{\text{weight of sample after Gilson's}}{\text{weight of sample before Gilson's}},$$

N = mean number of ova/g from 3 subsamples.

Gonad portions preserved in Davidson's fixative for histological preparations were dehydrated in a graded series of ethanol baths and Technicon reagents (S-29 dehydrant VC-670 solvent). They were then embedded in paraffin, sectioned at 7 μm and stained using Harris' hematoxylin and counterstained with eosin Y. Gonad sections were viewed at 40×, 100×, and 400× to determine stages of oogenesis and spermatogenesis to verify accuracy of macroscopic field staging and to examine the histology of the goosefish ovary.

A gonasomatic index (GSI) was calculated for each sex as:

$$\text{GSI} = \frac{\text{gonad weight}}{\text{total weight of fish}} \times 100.$$

Age and growth

Weights were taken to the nearest gram in fish <1200 g and to the nearest 25 g increment in fish >1200 g. Total length (TL) in millimeters was measured from the tip of the protruding lower jaw to the tip of the caudal fin rays. Because of the large size and loose suspension of the goosefish jaw apparatus, it was necessary to hold the head in a standard position while length was measured to reduce variation due to changes in head and jaw configuration. This position was achieved by applying light pressure to the top of the head, thereby causing a maximal amount of dorsal-ventral compression.

Vertebrae were chosen as the best method to age *L. americanus*, based on a preliminary examination which revealed that each vertebral centrum contained concentric rings which appeared to be annuli. Sagittal otoliths were also examined; however, otoliths from larger fish were opaque and had extremely irregular outer margins, which made it difficult or impossible to discern annuli.

A section of the vertebral column containing vertebrae numbers 3–11 was excised from each goosefish. These were stored in 50% isopropanol for 1–12 months. Vertebrae numbers 7–10 were similar in size and shape and also had the largest diameters. Vertebra number 8 was used in aging, but number 9 was used if number 8 was damaged in preparation.

Vertebra number 8 was disarticulated from the rest of the excised vertebral section. The neural and haemal arches and all excess fat, muscle, connective tissue and cartilage were removed by scalpel. The vertebra was then sliced along the midsagittal line producing two hourglass-shaped halves, similar to the method used by Lyczkowski (1971) and Lawler (1976) for preparing vertebrae from northern puffer *Sphaeroides maculatus*

and sandbar sharks *Carcharinus plumbeus*. These halves were then heated in an oven at 200°C for about 3 hours. Larger vertebra required one-half to 1 hour further heating. This heating made the alternating opaque and translucent bands of the vertebral centra more distinct.

Annuli were counted on the posterior face of the centrum. This was generally more concave than the anterior face, thus allowing greater separation of the rings. Each vertebra was read twice at an interval of at least one month to insure independence of readings. If they disagreed, a third reading was done. Agreement between any two readings was considered as the true count. If all three readings differed, the vertebra was considered unreadable and not used in the analysis. A random sample of fifty vertebrae was selected for verification by an independent reader.

Measurements of the vertebral rings and radius were made from the apex of the posterior and anterior faces of the centrum along an oblique line that followed the midline of the posterior centrum. All measurements and counts were made with a binocular dissecting microscope equipped with an ocular micrometer at 10× magnification using reflected light.

Regression analyses of vertebral radius on total length and weight on total length were calculated by the method of least squares. Length-at-age was back-calculated by the Lee method (Lagler 1956):

$$L' = C + S' (L - C)/S$$

where L' = total length of the fish at time of annulus formation,
L = total length of fish at time of capture,
S' = measurement to the annulus,
S = vertebral radius at time of capture,
C = correction factor; y-axis intercept of the regression of total length on vertebral radius.

Computation of the von Bertalanffy growth equations followed Ricker (1975).

Results

Reproduction

External sexual dimorphism was not apparent in *L. americanus*. Caruso (1975) noted sexual differences in nostril morphology, but this was not a useable field character. Sex was easily determined in mature individuals by examination of the gonads, which are markedly different in appearance. Gonads from small juveniles (<160–180 mm TL) were indistinguishable macroscopically. Both testes and ovaries from these juveniles were small, translucent, and string-like.

In females larger than ~180 mm TL the ovaries were long, wide, and ribbon-like. They were greatly coiled in the abdomen and supported by an extensive mesovarium. The two ovaries were fused at their posterior ends, forming a single, confluent organ. Dimensions of the ovary varied greatly depending on the stage of sexual development.

The testes were solid, sausage-like organs. A groove was present along the medial aspect of each testis. This groove contained blood vessels and served as the site of attachment for mesentary connective tissue.

A physical description of the gonads in the five developmental stages (immature, resting, developing, ripe, and spent) is presented in Table 1.

Table 1
Description of gonads at five maturity stages assigned to *Lophius americanus*, based on macroscopic examination.

Stage	Description
Ovaries	
Immature	Grayish-pink, relatively small, ribbon-like, appear almost empty, no vascularization.
Resting	Orangish-pink, contain material but no ova visible, larger than immature, little vascularization.
Developing	Pink, ova discernible by eye, abdominal cavity slightly bulging, highly vascular.
Ripe	Straw-colored to almost clear as ovary approaches spawning, distinct ova present, abdominal cavity greatly bulging, highly vascular.
Spent	Gray, extremely flaccid, appear almost empty, atretic ova appear as black or white dots, moderately vascular.
Testes	
Immature	White to tan, similar in shape as mature testes but very small, medial groove less distinct.
Resting	White to tan, much larger than immature, medial groove distinct, small amount of milt sometimes present when dissected.
Developing	Blotchy cream to tan, moderate to large amount of milt produced when dissected, very firm in texture.
Ripe	Blotchy cream to tan with areas of pink, extremely firm in texture, milt produced from genital pore when pressure is applied on abdomen, copious amounts present when dissected.
Spent	Grayish-tan, edges appear translucent, extremely flaccid, small amount of milt sometimes present when dissected.

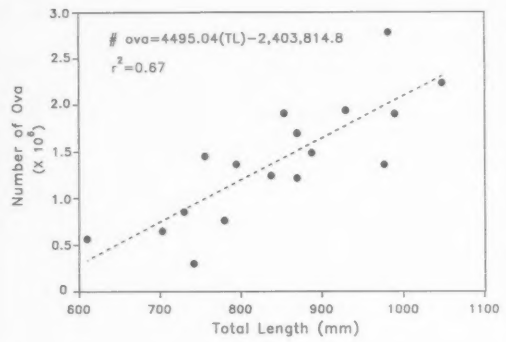

Figure 1

Relationship of fecundity with total length for *Lophius americanus*. Dashed line indicates least-squares regression. Regression equation and coefficient of determination are given. Each dot represents a single individual (n 17).

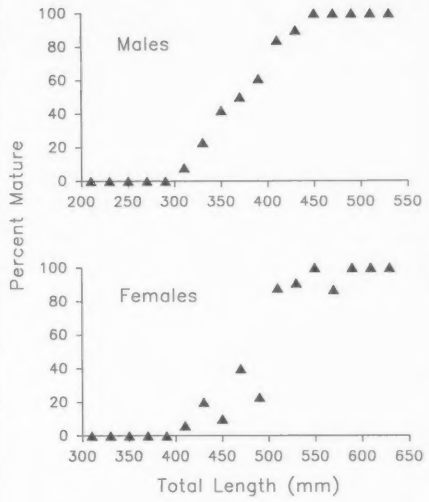

Figure 2

Percent of individuals sexually mature in relation to total length (mm) for *Lophius americanus*, based on macroscopic examination of the gonads. Lengths at 50% maturity are 368.9 mm for males and 485.3 mm for females.

Fecundity in 17 individuals of 610–1048 mm TL ranged from 301,150 to 2,780,632 ova. Fecundity increased linearly with TL in that size range (Fig. 1), the regression equation being

number of ova =

$$4495.04(TL) - 2{,}403{,}814.8 \quad (r^2\ 0.67).$$

Log transformations of one or both variables failed to provide a better fit.

Goosefish reached sexual maturity (by macroscopic staging) at 290–450 mm in males and 390–590 mm in females (Fig. 2). Linear regressions of proportion mature (arcsine-square root transformed) on TL for these size intervals were:

Proportion of males mature =

$$0.0089(TL) - 2.498 \quad (r^2\ 0.96)$$

Proportion of females mature =

$$0.0079(TL) - 3.056 \quad (r^2\ 0.86).$$

Values for length at 50% maturity were 368.9 mm in males and 485.3 mm in females.

Ovaries and testes followed similar patterns of development, with the exception that testes changed from a resting to developing state earlier in the year (Jan.–Feb.) (Fig. 3). No resting gonads were found for either sex in May or June. The percentage of spent gonads was highest in July–August, indicating that spawning had taken place in the previous time interval (May–June). Although the percentage of ripe gonads was highest in May–June, gonads in a near-spawning state were also found in March–April and July–August.

Gonasomatic values were calculated for 117 mature males and 98 mature females. The GSI peaked in May–June for females and March–April and May–June for males (Fig. 4). High index values in these months corresponded with the greatest incidence of ripe individuals (Fig. 3). Again, similar to observations based on gonad condition, males appeared to develop earlier in the season and remain ripe longer. No mature females were collected during the Jan.–Feb. interval.

GSI values for females were much greater than for males (Table 2). Females showed a large increase in GSI as the ovaries developed. The greatest value recorded was 50.9, from a ripe female. This value indicates that greater than half of the body weight was composed of ovarian mass. However, only a relatively small percentage of the ovarian weight from late-developing and ripe females was composed of ova. The actual percentage of the ovarian weight which was ova ranged from 12.9% to 33.5% for the seventeen females used for fecundity analysis. The remainder of the weight was ovarian tissue, and more importantly, the muco-gelatinous matrix surrounding the ova.

Slides were prepared from sections of 33 ovaries and 20 testes. Representatives from all the developmental

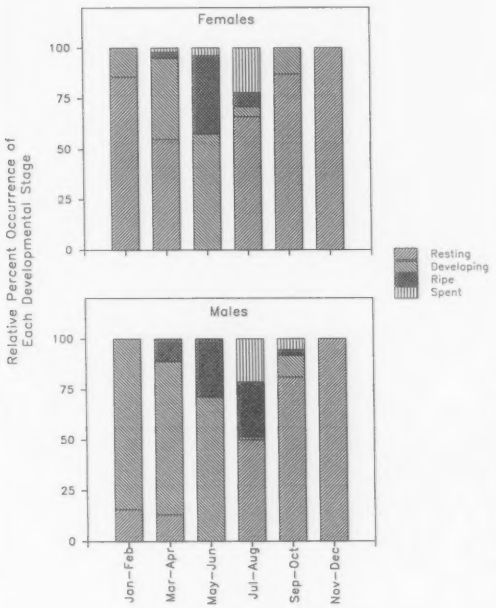

Figure 3
Seasonal progression of gonad condition in mature male and female *Lophius americanus*, based on macroscopic examination.

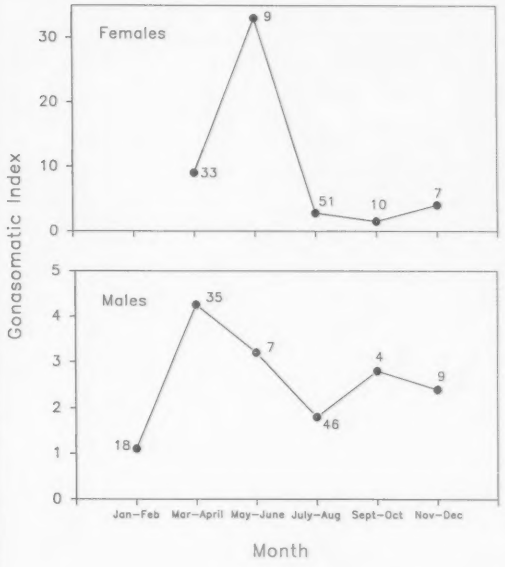

Figure 4
Seasonal progression of mean gonasomatic index values for male and female *Lophius americanus*. Numbers of mature individuals examined on each date are indicated.

classes (immature, resting, developing, ripe and spent) were included.

Oogenesis proceeds through six distinguishable morphological stages similar to other fishes, such as black sea bass *Centropristis striata* (Mercer 1978):

Oogonia (4.5–11 μm) Densely packed, granular, deeply basophilic cells.

Stage 1 Small (15–50 μm) oocytes with a large nucleus, single nucleolus, and small amount of basophilic cytoplasm.

Stage 2 (30–200 μm) Previtellogenic oocytes with strongly basophilic cytoplasm and multiple nucleoli around the nucleus margin.

Stage 3 (110–390 μm) Vitellogenesis begins with the deposition of yolk vesicles in the less darkly-staining cytoplasm. A thin zona radiata can be seen in late stage-3.

Stage 4 (270–970 μm) Cytoplasm filled with yolk vesicles and globules, lightly staining. Zona radiata well developed and strongly acidophilic.

Stage 5 (>600 μm) Mature or nearly mature oocytes, uniform in appearance due to the coalescence of yolk globules. Often fractured or irregular in outline due to fixation and sectioning.

Table 2
Gonasomatic index values at five gonad maturity stages for male and female *Lophius americanus*, based on macroscopic staging.

	Range	Mean(SE)	*n*
Females			
Immature	Trace–1.26	—	56
Resting	0.77–7.58	2.35(0.19)	53
Developing	3.82–22.12	12.26(1.18)	21
Ripe	18.23–50.90	33.96(2.73)	13
Spent	0.94–3.77	2.56(0.43)	12
Males			
Immature	Trace–0.83	—	37
Resting	0.31–3.42	1.46(0.17)	36
Developing	0.46–6.18	2.44(0.27)	43
Ripe	0.84–5.72	3.20(0.22)	23
Spent	0.18–4.19	1.16(0.20)	21

Based on the occurrence of these oocyte stages, the ovaries were placed in the following developmental classes:

Immature Stage 1 and 2 oocytes present, atretic bodies absent. The ovarian lamellae are pressed tightly together and lumen is small.

Resting Stage 1, 2, and 3 oocytes are present with stage 2 dominating.

Developing Oocyte stages 1, 2, 3, and small 4 are present with 3 dominating.

Ripe Oocyte stages 1, 2, 3, 4, and sometimes 5 are present with 4 dominating.

Spent Oocyte stages 1, 2, and 3 are present with 2 dominating. Atretic stage 4 and 5 oocytes and ruptured follicles are present.

Macroscopic and microscopic maturity classifications showed excellent agreement. Only two (6%) needed to be reclassified following histological examination. These included one reclassified from ripe to developing, and one from resting to immature.

Figures 5 and 6 show the histology of the ovary. The lumen is not centrally located but is at one side (Fig. 5). The ovigerous tissue extends into the lumen in the form of lamellae from one wall only. In late-developing and ripe ovaries, the mucogelatinous material that forms the egg veil can be seen surrounding the ovigerous lamellae and filling the lumen (Fig. 6). This material is produced by the epithelial cells (Fulton 1898), which can be seen lining the lumen and lamellae (Fig. 6).

Spermatogenesis proceeds through six distinct stages analogous to those described for *Tilapia* spp. (Hyder 1969) and *Caulolatilus microps* (Ross 1978). These stages are primary and secondary spermatogonia, primary and secondary spermatocytes, spermatids, and spermatozoa. Spermatogenesis in goosefish is not notably different from other teleosts, so the process is not described here.

The 20 testes examined histologically were placed in the following maturity classifications based on a modification of the system of Hyder (1969):

Immature Primary and/or secondary spermatogonia are present; primary and/or secondary spermatocytes may also be present.

Resting Primary and/or secondary spermatogonia and spermatocytes are present. Spermatids also

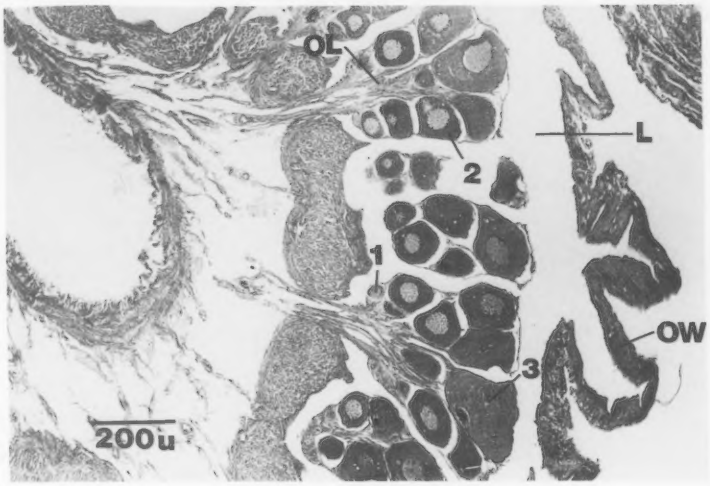

Figure 5

Photomicrograph of *Lophius americanus* ovary, classified as resting (40×): OL = ovigerous lamella; L = lumen of ovary; OW = nonovigerous ovarian wall; 1–3 = stages of oocyte development.

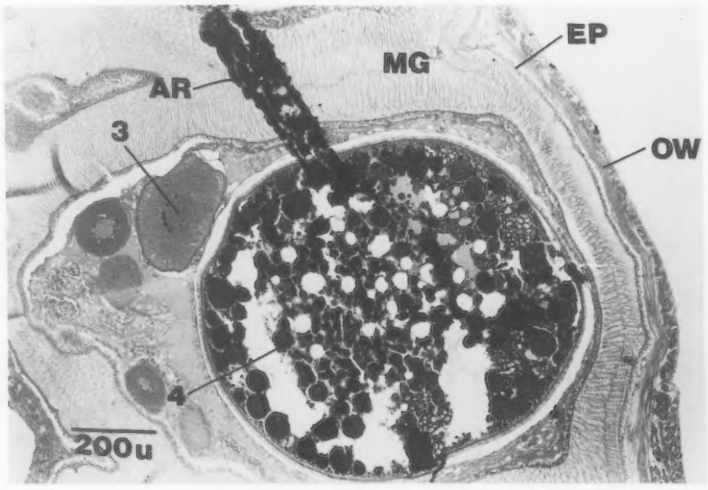

Figure 6

Photomicrograph of *Lophius americanus* ovary, classified as late developing (40×): MG = mucogelatinous matrix; EP = epithelial lining of lumen and lamellae; OW, = nonovigerous ovarian wall; AR = artifact; 3–4 = stages of oocyte development.

present. Small amount of spermatozoa may be present in lumen.

Developing Few primary and/or secondary spermatogonia visible; primary and/or secondary spermatocytes and spermatids present; spermatozoa present in lumen.

Ripe Few or no primary and/or secondary spermatogonia and spermatocytes visible; lumen densely packed with spermatozoa.

Spent No primary and/or secondary spermatogonia or spermatocytes visible; no spermatids present; few spermatozoa remaining in lumen.

In all cases, maturity classifications based on histological examination agreed with visual classifications applied in the field.

Age and growth

Growth marks on the vertebrae of *L. americanus* formed distinct steps on the centrum surface. Under magnification in reflected light, the surface texture of the step appeared coarser than the rest of the centrum. A narrow, dark, translucent band was on the outer side of each step. The step and the narrow band formed a continuous ring around the centrum and was considered to be the annulus. Broader, lighter opaque bands with relatively uniform surface texture were between the annuli. A broad, opaque band combined with a narrow, translucent band and step was interpreted as one year's growth. While these features were visible on fresh vertebrae, they became much more distinct when the vertebrae were heated. The step became deeper and the narrow, translucent band became opaque and dark relative to the rest of the centrum (Fig. 7).

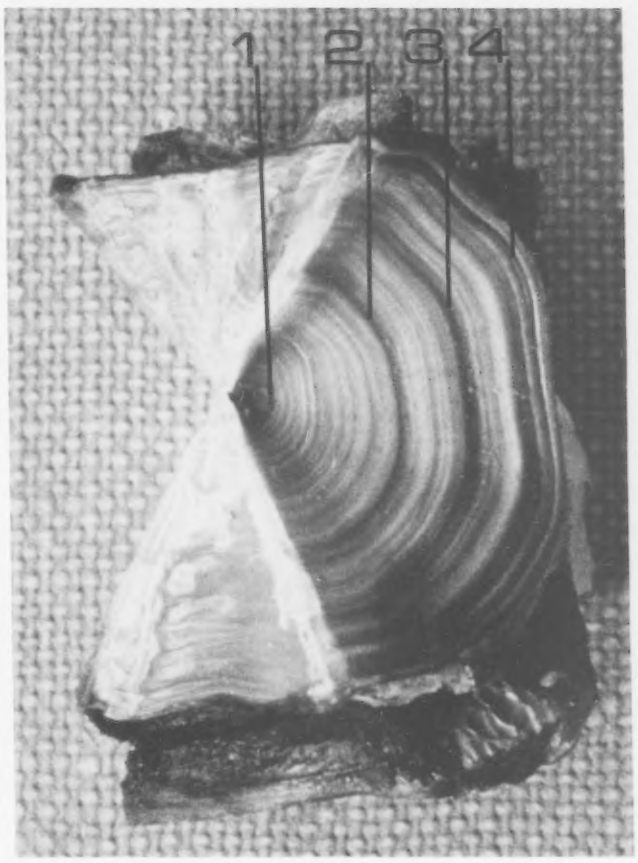

Figure 7
Vertebra from a 4-year-old *Lophius americanus*, after heating. Annuli are indicated.

Annuli were counted on vertebrae from 635 goosefish. In 200 (31.5%) cases, the first and second reading did not agree and a third reading was done. In most cases, the second reading differed by only one. In 25 (3.9%) cases, the third reading was different from both the first and second; these vertebrae were considered unreadable and discarded from the analysis.

Differences between readings were due to the presence of false annuli or because the true annuli were not distinct. False annuli appeared as dark bands but were not associated with a step. Another extraneous mark that sometimes occurred was a depression that formed a continuous ring on the centrum but was not a definitive step. This feature has also been found on black bullhead (Lewis 1949) and northern puffer (Lyczkowski 1971) vertebrae.

Annuli counts determined by the independent reader agreed with the original counts in 40 (80%) cases. In no case did the counts differ by more than one.

Van Oosten (1929) established the following criteria that must be met before checkmarks on scales or bones can be considered annuli: (1) Scales or bones must remain constant in number and identity throughout the life of the fish; (2) growth of the scale or bone must be proportional to the overall growth of the fish; (3) growth checkmarks must be formed at approximately the same time each year; and (4) back-calculated lengths should agree with empirical lengths. The first criterion is fulfilled by using vertebrae as the aging tool.

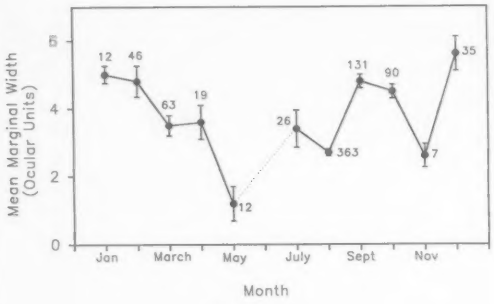

Figure 8

Monthly mean (±1 SE of mean) marginal width for *Lophius americanus* vertebrae. Number of vertebrae examined each month is indicated. No vertebrae were collected during June.

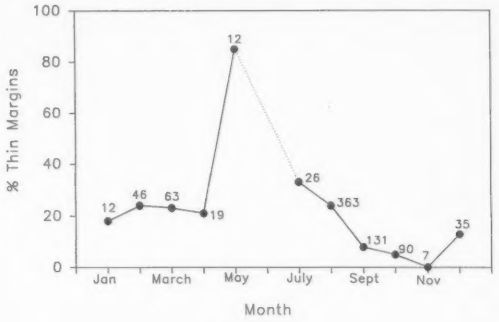

Figure 9

Percentage of *Lophius americanus* vertebrae having a marginal width less than one ocular unit by month. Number of vertebrae examined is indicated. No vertebrae were collected during June.

The regression of vertebral radius (VR) on TL revealed a strong linear relationship between the two variables. The regression equation based on 682 vertebrae from both sexes was as follows:

$$TL = 11.077(VR) + 40.018 \quad (r^2\ 0.97).$$

This indicates that growth of vertebrae is proportional to growth of the fish, thereby satisfying the second criterion.

Monthly mean marginal increments were plotted for all age groups combined (Fig. 8). Sample size was not large enough to plot the age-groups separately. However, inspection of the data indicated that the seasonal progression of marginal increment was similar for all age-groups. Percentage of vertebrae showing a very small marginal increment (less than 1 ocular unit), indicating that little or no growth had occurred since the annulus was deposited, was also plotted (Fig. 9). The annuli were found to be closest to the edge of the vertebrae in May. Marginal increments were highest in December–February, following a period of growth during July–December. The percent of vertebrae with thin margins showed less variation than marginal increments. The percent was highest in May and decreased as the season progressed. These plots indicate that May is the time of annulus formation, and only one checkmark is formed per year. This appears to fulfill the third criterion that states that growth checks must be formed at approximately the same time each year; however, because data were pooled from several years, this cannot be stated with certainty. Although there was a decrease in the marginal increment from February to March, there was no corresponding rise in the percentage of very small margins (i.e., the mean

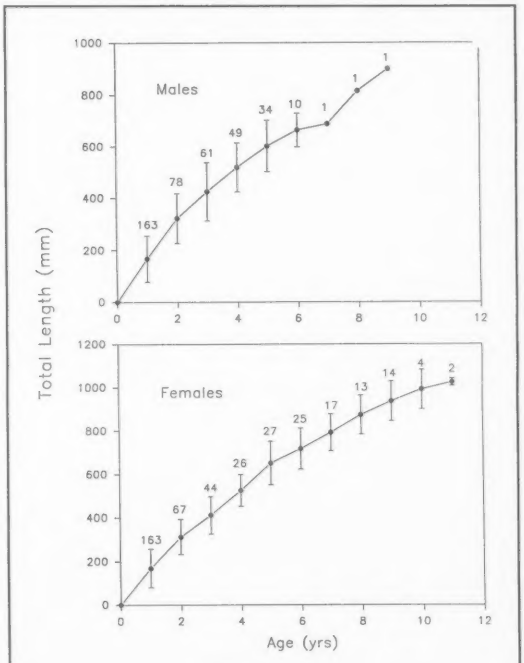

Figure 10

Mean observed lengths-at-age for *Lophius americanus*. Vertical bars indicate ranges of total length observed for each age. Sample sizes are indicated.

value of marginal width was not lowered by the presence of marginal widths <1). Although the relatively small sample sizes preclude making definitive conclusions, these data suggest that some process is causing

Table 3

Observed, von Bertalanffy, and back-calculated lengths-at-age (TL, mm) for male and female *Lophius americanus*, based on counts of vertebral annuli. The number examined for age 1 includes 142 unsexed individuals, which were used in the back-calculations for both sexes.

Age	Number examined	Mean observed length	von Bertalanffy length	Mean back-calculated lengths at successive annuli										
				I	II	III	IV	V	VI	VII	VIII	IX	X	XI
Males														
1	163	167	133	123										
2	78	322	256	127	267									
3	61	425	367	134	265	374								
4	49	519	469	127	263	377	472							
5	34	602	560	127	269	378	478	568						
6	10	664	644	109	241	352	465	549	634					
7	1	688	719	82	189	284	390	486	592	688				
8	1	815	788	109	255	367	473	602	675	731	793			
9	1	900	850	143	263	396	489	555	621	701	781	860		
			Mean	126	264	374	473	563	633	707	787	860		
		Annual growth increment		126	138	110	100	90	70	74	80	73		
Females														
1	163	169	121	124										
2	67	313	253	126	261									
3	44	412	373	124	257	361								
4	26	526	482	116	248	373	476							
5	27	652	581	130	278	405	507	600						
6	25	718	672	121	250	366	477	580	672					
7	17	792	754	124	265	386	485	573	662	757				
8	13	874	828	110	242	361	468	567	665	745	834			
9	14	937	896	119	250	373	475	567	652	740	821	901		
10	4	991	957	107	244	353	458	574	655	741	815	890	966	
11	2	1024	1014	117	254	380	488	591	677	757	826	894	962	1013
			Mean	123	258	374	483	581	664	748	826	898	965	1013
		Annual growth increment		123	135	116	109	98	83	84	78	72	67	48

the vertebrae to decrease slightly in diameter, possibly the resorbtion of the outer surfaces due to starvation in late winter.

Mean lengths were back-calculated for 256 males and 260 females. One hundred forty-two individuals, whose sex could not be determined because their gonads were undifferentiated (94–239 mm TL) but who were determined to have one annulus, were included in the back-calculations for each sex, bringing the total number used in the analysis to 398 males and 402 females.

The observed lengths were consistently higher than back-calculated or von Bertalanffy lengths for individual age-groups (Table 3). However, the differences are within the limits of seasonal growth, so the fourth criterion appears to have been fulfilled.

Males and females had very similar lengths-at-age until age 4. Above age 4, the mean lengths for females were slightly greater than males, with the difference becoming more pronounced with increasing age (Fig. 10).

The data suggest a difference in maximum age for the two sexes. The oldest male collected was 9 years old. Males older than 6 were exceptionally rare. Only one individual from each of the age groups 7, 8, and 9 was captured during the course of this study. The oldest female sampled was 11 years old. Fifty females greater than 6 years old were obtained. It appears that the number of older males is much fewer than females, indicating greater mortality of the males.

Mean back-calculated lengths-at-age were used to develop the vonBertalanffy growth equations. The resulting parameters and equation for females are:

$$K = 0.095$$
$$L_\infty = 1576 \text{ mm}$$
$$t_0 = 0.162$$
$$L_t = 1576.0\ (1 - e^{-0.095(t-0.162)}).$$

The growth equation for males was calculated using three slightly different data sets. It was first calculated using all the mean back-calculated lengths available. The equation was then formulated after eliminating the two fish in age-groups 8 and 9 from the data set and finally it was calculated without age-groups 7, 8, or 9.

Because there was only one individual in each of these three oldest age-groups, these were possibly not good estimates of length for these ages. The parameters and equations are as follows.

All males:

$K = 0.097$
$L_\infty = 1460.0$
$t_0 = 0.015$
$L_t = 1460.0\ (1 - e^{-0.097(t-0.015)})$

Age-groups 8 and 9 eliminated:

$K = 0.166$
$L_\infty = 1018.0$
$t_0 = 0.211$
$L_t = 1018.0\ (1 - e^{-0.166(t-0.211)})$

Age-groups 7, 8, and 9 eliminated:

$K = 0.157$
$L_\infty = 1059.0$
$t_0 = 0.196$
$L_t = 1059.0\ (1 - e^{-0.157(t-0.196)})$

The length-weight relationships (Fig. 11) for 305 males and 311 females were:

Males
$\log_{10} W = 2.833\ (\log_{10} TL) - 4.347 \quad (r^2\ 0.95)$

Females
$\log_{10} W = 3.001\ (\log_{10} TL) - 4.770 \quad (r^2\ 0.98)$

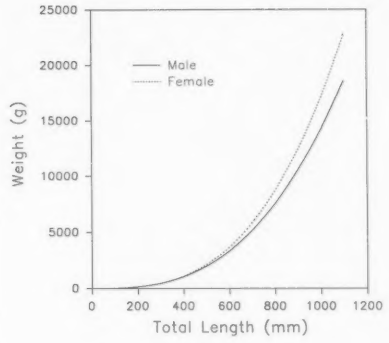

Figure 11
Length-weight relationship for male (n 305) and female (n 311) *Lophius americanus*.

Discussion

Reproduction

All female members of the Lophiiformes are thought to expel nonadhesive, mucoid egg rafts or veils with the possible exception of one species of antenariid angler fish (Pietsch and Grobecker 1980). These veils are buoyant and have a complex structure consisting of individual chambers, which each contain one to three eggs and an opening providing water circulation (Fulton 1898, Gill 1905, Rasquin 1958, Ray 1961). This method of egg production appears to be unique among the fishes.

The goosefishes, *Lophius* spp., have the most spectacular egg veils because of their large size. The egg veil of *L. americanus* can reach 6–12 m in length and 0.15–1.5 m in width (Martin and Drewry 1978). Several authors have provided detailed description of the egg veils of *L. americanus* (e.g., Agassiz and Whitman 1885, Connolly 1920, Dahlgren 1928) and *L. piscatorius* (Fulton 1898, Bowman 1919).

Estimates of fecundity presented by other authors are similar to those obtained in this study. Eaton et al. (1954) estimated 543,000 ova in the ovary of a 660 mm specimen. The regression of fecundity on TL presented here predicts 563,000 ova for a female of this size. Other estimates of fecundity range from 432,000 to 2,670,000 eggs, based on the examination of veils released from females of unknown size (Baird 1871, Nichols and Breder 1927, Berril 1929).

Female goosefish matured at a larger size and at a greater age (487 mm, age 4) than males (369 mm, age 3). This is a common trend among teleosts (Moyle and Cech 1982). In the case of goosefish, the female requires a larger body size to accommodate the large egg veil. Connolly (1920) was unable to determine size-at-maturity because of small sample size, but he stated that a goosefish 18 inches (457 mm) long (unstated sex) was immature, and all individuals over 31 inches (787 mm) were mature. McBride and Brown (1980), in a tabular summary of life-history parameters for several demersal fish species, present the age-at-maturity for *L. americanus* as 4 and 5 years for males and females, respectively. The source of their data is not stated. Martin and Drewry (1978) and several others also suggest that the age of maturity is 4 and 5 years for males and females. They state the source of this information as Connolly (1920). A review of Connolly's paper shows that he was quoting a publication by Fulton (1903), which deals with the growth of *L. piscatorius*, not *L. americanus*. At the time of Connolly's paper, the two species were considered synonymous. *L. piscatorius* is known to reach a larger maximum size and is larger at each age (based on data presented in the following age and growth discussion). The age-at-maturity cannot be considered the same

for the two species; in fact, it would be expected that the age- and length-at-maturity for *L. piscatorius* would probably be greater, as suggested here.

Data on gonad condition and the gonasomatic index indicate that spawning takes place in May–June in the area from Cape Hatteras to Southern New England. Because samples were collected and pooled from throughout this entire region, a seasonal progression of spawning from south to north as suggested in the literature cannot be demonstrated. Testes appear to develop earlier and remain ripe longer than ovaries. Fulton (1898) found the same to be true for *L. piscatorius*. This suggests that males may be multiple spawners. Multiple spawning in males would increase the chances of a ripe female encountering a ripe male, and thereby spawning successfully. It also serves to equalize the energetic investment of the sexes in reproduction. It appears that the investment of females is relatively high. The GSI was as high as 50%. Tsimenidis (1980) found values as high as 37% for the Mediterranean goosefish *L. budegassa*. A large part of the ovarian weight is composed of the mucogelatinous material that forms the veil. The caloric value of this material is unknown, but probably is rather low because of its low density and apparently high water content. However, the large amount of this material, combined with the great number of eggs produced, represents a sizeable energetic contribution by the female to reproduction.

Histological examination of the goosefish testes showed that spermatogenesis and the internal structure are not remarkably different from other teleosts. It also confirmed the validity of macroscopic staging of testes in the field. Examination of ovaries showed that oogenesis is similar to other teleosts but the structure of the ovary is somewhat different. The most significant differences were the presence of stalk-like lamellae containing the developing ova, and epithelium lining the lumen which is responsible for secreting the mucogelatinous matrix. Fulton (1898) was the first to suggest this mechanism of veil formation in the lophiids. His figures and descriptions of the histology of the ovaries of *L. piscatorius* indicate they are identical to those from *L. americanus* seen here. Rasquin (1958) provided detailed descriptions and photographs of the ovaries of two species of antennariid anglers (*Antennarius*, *Histrio*) and one species of ogcocephalid angler. These lophiiform species are known to produce egg veils. Although they are all only a fraction of the size of *L. americanus* and *L. piscatorius*, the histology of their ovaries was virtually identical to their larger relatives, including the presence of stalk-like ovigerous lamellae and secretory epithelium. It is reasonable to assume that all members of the order Lophiiformes known to produce egg veils have similar ovaries. This character may be useful in verifying veil production in some of the deepwater lophiiform families for which veil production has been assumed but not verified.

Pietsch and Grobecker (1980) suggest that the egg veil is an excellent device for broadcasting a large number of eggs over great geographical distances. In addition, the buoyancy of the veil causes the eggs to develop in relatively productive surface waters.

There seem to be additional selective advantages to the egg veil as well. It may function in facilitating fertilization of the eggs. When a veil is first extruded from the female, it absorbs a large quantity of water. As water is absorbed, sperm may be drawn into the egg chambers through the small circulation pores in the veil, thereby insuring fertilization. The veil likely functions by several methods in the protection of the eggs and embryos, since the embryos remain in the egg chamber for 2–3 days after hatching (Dahlgren 1928). Predators such as zooplankton are physically excluded from the egg chambers by the small size of the circulation pore. The veil may reduce or eliminate olfactory cues, thereby eliminating predators locating food items by this method. Wells (1977) suggests that the jelly coat of yellow perch *Perca flavescens* spawn may act in a similar manner. Finally, the mucogelatinous material of goosefish egg veils may be toxic or repugnant to potential predators. Newsome and Tompkins (1985) found that the egg mass of yellow perch contain some compound(s) that are not toxic but seem to deter predators. While such a protective device is rare among teleosts (Fuhrman et al. 1969, Orians and Janzen 1974), the presence of toxic or unpalatable compounds within the jelly coat of amphibian egg masses is well known (Licht 1969, Ward and Sexton 1981).

Age and growth

Females and males have about the same weight-at-length before maturity. After maturity the females are slightly heavier than males because of their large ovaries. As the ovaries ripen, weight differences between males and females become greater. The regression slopes for males and females approximate 3, implying isometric growth in the length-weight relationship. Tsimenidis and Ondrias (1980) calculated very similar length-weight regressions for *L. piscatorius* in the Mediterranean Sea.

Vertebrae appear to be valid aging tools for *L. americanus*. They satisfy all of Van Oosten's (1929) criteria. Vertebrae can readily be located and removed from goosefish and are relatively easy to prepare and read. The annuli are readily discernible since only 3% of the vertebrae were considered unreliable, and an inexperienced, independent reader agreed with the counts in 80% of the readings he performed.

These data indicate that the annuli become discernible in May. Because these rings are present on juveniles as well as adults, they appear to be related to seasonal patterns of growth rather than reproduction. The annuli are difficult to see when they are at the very edge of the vertebral centra. For this reason, they are probably not detected until some additional growth has occurred after they are laid down. Yasuda (1940) has shown that on vertebrae of *Scombrops* sp. annuli were formed 1.5 months later than on the otoliths. So it is likely that the annuli (composed of a step and a translucent band) found on goosefish vertebrae represent the end of fast growth (the step) in late-fall and a period of slow winter growth (the translucent band).

While several authors have studied growth in *L. piscatorius* and *L. budegassa* (Fulton 1903, Guillou and Njock 1978, Tsimenidis and Ondrias 1980), only Connolly (1920) has looked at growth in *L. americanus*. He based his growth estimates on vertebral annuli counts, but his sample size was only six individuals. His results were as follows: age 1, 114mm; age 4, 457mm; age 8, 737mm; age 9, 787mm; age 10, 940mm; age 12, 1016mm. These estimates are slightly lower than found in this study, but a slower growth rate would be expected in the colder Canadian waters in which Connolly conducted his study.

The growth rate of *L. americanus* is intermediate to *L. piscatorius* and *L. budegassa*. Figure 12 compares the mean back-calculated lengths for the two European species (from Tsimenidis and Ondrias 1980) with data presented here for *L. americanus*.

The differences in observed and back-calculated mean lengths between males and females past age 4 are small, but appear to be real. This is the most common form of sexual dimorphism among fishes (Moyle and Cech 1982). Tsimenidis and Ondrias (1980) found similar small differences between the sexes for *L. budegassa* and *L. piscatorius*.

More significant is the difference in mortality between the sexes implied by the data. The heavier mortality of males may be caused by increased predation due to their smaller size, but this does not seem likely. Perhaps the males exhibit behavioral or distributional differences which make them more susceptible to predation or fishing effort. A final possibility is that they simply reach senescence before females.

The von Bertalanffy growth equations fit the back-calculated lengths extremely well. The values for L_∞ for both sexes seem somewhat inflated. The maximum reported size for *L. americanus* is approximately 1220mm (Bigelow and Schroeder 1953). The largest female collected in this study was 1115mm and the calculated L_∞ was 1576mm. The largest male collected was 900mm compared with a calculated L of 1018–1460mm. The inflation of L_∞ is caused by a lack of representatives from the older age-classes. This is a common problem in age and growth studies. The asymptotic length is therefore not well defined for either sex in this study. The sampling effort was believed to be intense enough to sample these larger individuals if they were present in the population. It is concluded that these individuals are simply not present. This may be the result of commercial fishing pressure (groundfishing and scalloping), which tends to be selective towards larger individuals.

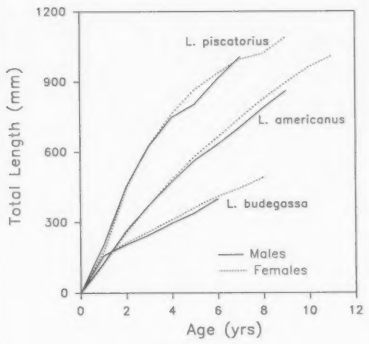

Figure 12
Back-calculated lengths-at-age for three species of *Lophius*. Data for *L. americanus* from present study; data for *L. piscatorius* and *L. budegassa* from Tsimenidis and Ondrias (1980).

Acknowledgments

We are indebted to all the graduate students and staff members at the Virginia Institute of Marine Science who assisted at various points in this study. D. Sved, M. Chittenden, and W. DuPaul provided helpful reviews of this manuscript. Ship time was provided by the Northeast Fisheries Science Center and the fishing vessels *Captain Wool*, *Virginia Queen*, *Virginia Cavalier*, and *Cara Lyn*. Funding was provided by Sea Grant, National Oceanic and Atmospheric Administration, U.S. Department of Commerce, under Grant NA86AA-D-SG042, through the Virginia Sea Grant Program, Project RC/F-10, J.A. Musick, Principal Investigator. This manuscript was based on a thesis submitted by the senior author in partial fulfillment of the M.A. degree, School of Marine Science, College of William and Mary.

Citations

Agassiz, A., and C.O. Whitman
1885 Studies from the Newport Marine Laboratory, XVI. The development of the osseus fishes. Part I. The pelagic stages of young fishes. Mem. Mus. Comp. Zool. 14(1):1–56.

Baird, S.F.
1871 Spawning of the goosefish *L. americanus*. Am. Nat. 5:785–786.

Berril, N.J.
1929 The validity of *L. americanus* as a species distinct from *L. piscatorius* with notes on rate of developement. Contrib. Can. Biol. Fish. 4(12):143–155.

Bigelow, H.B., and W.C. Schroeder
1953 Fishes of the Gulf of Maine. U.S. Fish. Wildl. Serv. Fish. Bull. 53(74), 577 p.

Bowman, A.
1919 The eggs and larvae of the angler (*Lophius piscatorius*) in Scottish waters. Rep. Fish. Board Scotl. Sci. Invest. for 1919, No. 1. 42 p.

Caruso, J.H.
1975 Sexual dimorphism of the olfactory organs of lophiids. Copeia 1975:380–381.
1977 The systematics of the fish family Lophiidae. Ph.D. diss., Tulane Univ., New Orleans, 220 p.
1983 The systematics and distribution of the lophiid angler fishes: II. Revision of the genera *Lophiomus* and *Lophius*. Copeia 1983:11–30.

Connolly, C.J.
1920 History of the new food fishes. III. The angler. Bull. Biol. Board Can. 3:1–17.

Cuvier, G., and A. Valenciennes
1837 Historie naturelle des poisons, vol. 12. F.G. Levrault, Paris, 507 p.

Dahlgren, U.
1928 The habits and life history of *Lophius*, the angler fish. Nat. Hist. 28(1):18–32.

Eaton, T.H. Jr., C.A. Edwards, M.A. McIntosh, and J.P. Rowland
1954 The structure and relationships of the anglerfish, *Lophius americanus*. J. Elisha Mitchell Sci. Soc. 70(2):205–218.

Edwards, R.L.
1965 Relation of temperature to fish abundance and distribution in the southern New England area. Int. Comm. Northwest Atl. Fish. Spec. Publ. 6:95–110.

Fuhrman, F.A., G.J. Fuhrman, D.L. Dull, and H.S. Moser
1969 Toxins from eggs of fishes and amphibia. J. Agric. Food Chem. 17:417–424.

Fulton, T.W.
1898 The ovaries and ovarian eggs of the angler or frog fish (*Lophius piscatorius*) and of the John Dory (*Zeus faber*). Sixteenth Annu. Rep. Fish. Board Scotl. 3:125–137.
1903 The distribution, growth, and food of the angler. Twenty-first Annu. Rep. Fish. Board Scotl. 3:186–199.

Gill, T.
1905 The life history of the angler. Smithson. Misc. Collect. 47(4):500–516.

Grosslein, M.D., and T.R. Azarovitz
1982 Goosefish, *Lophius americanus*. *In* Fish distribution. MESA N.Y. Bight Atlas Monogr. 15, New York Sea Grant Inst., Stony Brook.

Guillou, A., and J.C. Njock
1978 Analyse des structures de la peche dans les parts de la cote atlantique francaise de 1961 a 1975 et des incidences du chalutage sur les stocks des principales especes concernees par cette activite dans les mers adjacentes. Revue Trav. Inst. Peches Marit. 42(1,2):120–128 [in French].

Hildebrand, S.F., and W.C. Schroeder
1928 Fishes of Chesapeake Bay. Bull. U.S. Bur. Fish. 43, pt. 1, 388 p.

Hyder, M.
1969 Histological studies on the testes of *Tilapia leucesticta* and other species of the genus *Tilapia* (Pisces:Teleostei). Trans. Am. Microsc. Soc. 88(2):211–231.

Jean, Y.
1965 Seasonal distribution of monkfish along the Canadian Atlantic mainland. J. Fish. Res. Board Can. 22(2):621–624.

Lagler, K.F.
1956 Freshwater fishery biology, 2d ed. W.C. Brown, Dubuque, 248 p.

Lawler, E.F. Jr.
1976 The biology of the sandbar shark, *Carcharinus plumbeus*, in the lower Chesapeake Bay and adjacent waters. M.A. thesis, College of William and Mary, Williamsburg, 48 p.

Lewis, W.M.
1949 The use of vertebrae as indicators of the age of the northern black bullhead, *Ameriurus m. melas*. Iowa State Coll. J. Sci. 22(2):209–218.

Licht, L.E.
1969 Palatability of *Rana* and *Hyla* eggs. Am. Midl. Nat. 82:296–298.

Lyczkowski, J.M.
1971 Age and growth of the northern puffer, *Sphoeroides maculatus*. M.A. thesis, College of William and Mary, Williamsburg, 26 p.

Markle, D.F., and J.A. Musick
1974 Benthic-slope fishes found at 900 m depth along a transect in the western North Atlantic Ocean. Mar. Biol. (Berl.) 26: 225–233.

Martin, F.D., and G.E. Drewry
1978 Lophiidae. *In* Development of fishes of the mid-Atlantic Bight—An atlas of egg, larval and juvenile stages, vol. 6, Stromateidae through Ogocephalidae, p. 357–366. U.S. Fish Wildl. Serv. OBS 78/12, 416 p.

McBride, M.M., and B.E. Brown
1980 The status of the marine fishery resources of the northeastern United States. NOAA Tech. Memo. NMFS-F/NEC-5, Northeast Fish. Sci. Cent., Woods Hole, 13 p.

McKenzie, R.A.
1936 Some notes on the monkfish or angler (*Lophius piscatorius*). Can. Field Nat. 50:55–56.

Mercer, L.P.
1978 The reproductive biology and population dynamics of black sea bass, *Centropristis striata*. Ph.D. diss., College of William and Mary, Williamsburg, 196 p.

Moyle, P.B., and J.J. Cech Jr.
1982 Fishes, an introduction to ichthyology. Prentice-Hall, Englewood Cliffs, 593 p.

Newsome, G.E., and J. Tompkins
1985 Yellow perch egg masses deter predators. Can. J. Zool. 63:2882–2884.

Nichols, J.T., and C.M. Breder
1927 The marine fishes of New York and southern New England. Zoologica (NY) 9(1):1–192.

Northeast Fisheries Science Center
1991 Status of the fishery resources off the northeastern United States. NOAA Tech. Memo. NMFS-F/NEC-86, Northeast Fish. Sci. Cent., Woods Hole, 132 p.

Orians, G.H., and D.H. Janzen
1974 Why are embryos so tasty? Am. Nat. 108:581–592.

Pietsch, T.W., and D.B. Grobecker
1980 Parental care as an alternative reproductive mode in an antennariid angler fish. Copeia 1980:551–553.

Proctor, W., H.C. Tracy, E. Helwig, C.H. Blake, J.E. Morrison, and S. Cohen
1928 Fishes—A contribution to the life history of the angler (*Lophius piscatorius*). *In* Biological survey of the Mount Desert Region, Part 2, p. 1–29, Philadelphia.

Rasquin, P.
1958 Ovarian morphology and early embryology of the pediculate fishes *Antennarius* and *Histrio*. Bull. Am. Mus. Nat. Hist. 114(4):331–371.

Ray, C.
1961 Spawning behavior and egg raft morphology of the ocellated fringed frogfish, *Antennarius numifer* (Cuvier). Copeia 1961:230–231.

Ricker, W.E.
1975 Computation and interpretation of biological statistics of fish populations. Bull. Fish. Res. Board Can. 191, 382 p.

Ross, J.L.
1978 Life history aspects of the gray tilefish, *Caulolatilus microps* (Goode and Bean, 1878). M.A. thesis, College of William and Mary, Williamsburg, 120 p.

Scott, W.B., and M.G. Scott
1988 Atlantic fishes of Canada. Can. Bull. Fish. Aquat. Sci. 219, 731 p.

Simpson, A.C.
1951 The fecundity of the plaice. Fish. Invest. Ser. 2, Mar. Fish. G.B. Minist. Agric. Fish. Food 17(5), 27 p.

Tsimenidis, N.Ch.
1980 Contribution to the study of the angler-fishes *Lophius budegassa* Spinola, 1807 and *L. piscatorius* L., 1758 in Greek seas. Inst. Oceanogr. Fish. Res. (Athens) Spec. Publ. 4: 180–190.

Tsimenidis, N.Ch., and J.Ch. Ondrias
1980 Growth studies on the angler-fishes *L. piscatorius* and *L. budegassa* in Greek waters. Thalasographica 2(3):63–94.

Van Oosten, J.
1929 Life history of the lake herring (*Leucichthys artedi*, LeSeur) of Lake Huron as revealed by its scales, with a critique of the scale method. Bull. U.S. Bur. Fish. 44:265–428.

Ward, D., and O.J. Sexton
1981 Anti-predator role of salamander egg membranes. Copeia 1981:724–726.

Wells, L.
1977 Changes in yellow perch (*Perca flavescens*) populations of Lake Michigan, 1954–75. J. Fish. Res. Board Can. 34: 1821–1829.

Wenner, C.A.
1978 *Lophius americanus*. *In* Making a living on the continental slope and in the deep sea: Life history of some dominant fishes of the Norfolk Canyon area, p. 253–263, 267–268. Ph.D. diss., College of William and Mary, Williamsburg.

Yasuda, H.
1940 On the rings formed on scale, vertebral centrum, and otolith of the same individual fish. Jpn. Soc. Sci. Fish. Bull. 8:290–300.

Annual reproductive cycle of oocytes and embryos of yellowtail rockfish *Sebastes flavidus* (Family Scorpaenidae)

Michael J. Bowers

Tiburon Laboratory, Southwest Fisheries Science Center
National Marine Fisheries Service, NOAA
3150 Paradise Drive, Tiburon, California 94920

Abstract. – Female yellowtail rockfish *Sebastes flavidus*, a viviparous species employing intralumenal gestation following fertilization of ovulated eggs, were caught from Cordell Bank (seamount 20 miles west of Pt. Reyes, central California) on a monthly basis from May 1985 through April 1986 to determine their annual reproductive cycle. Since histological methods provide precise and detailed information, this method was employed to (1) examine oocytes and embryos to describe developmental stages, and (2) provide temporal assessment of the annual reproductive cycle. The description and staging scheme developed provide a basis to compare reproductive developmental patterns between cycles and populations.

Oogonia (Stage I) and early perinucleolus (Stage II) oocytes were present in samples from all months. Progressive growth of oocytes from early- to late perinucleolus (Stage III) was evident in spent and recovering ovaries, indicating the end of a reproductive year and the beginning of a new reproductive cycle. Initial yolk accumulation (Stage IV) occurred in July, and final yolk accumulation (Stage V) was predominant from September through January. In February, the majority of samples displayed fertilized ova in early-celled stages of embryonic development. Gestation continued for about 30 days with parturition occurring between January and March. Mature oocytes were also collected in March, suggesting the Cordell Bank yellowtail population has a prolonged reproductive season extending into April.

Manuscript accepted 9 March 1992.
Fishery Bulletin, U.S. 90:231–242 (1992).

Sixty species of rockfish (genus *Sebastes*) have been recorded in waters off the California coast; twenty species are utilized by commercial and recreational fisheries (Lenarz 1986). Rockfishes display a wide variety of life history patterns with respect to their habitat and seasonality of reproduction (Wyllie Echeverria 1987). The majority of investigations on rockfish reproduction have focused on the development, occurrence, and identification of larvae and juveniles. Evaluating annual reproductive success as a direct consequence of variations in oocyte viability has received less attention.

The *Sebastes* complex contributed approximately 37,806 mt to west coast fisheries in 1985 (PFMC 1990) and management of this resource is heavily dependent upon predictions of strong and weak year-classes. Since no single trait accurately represents reproductive capacities of fish populations (Eldridge et al. 1991), fisheries management is based on a variety of information. Year-class strength estimates may be enhanced by understanding factors influencing annual fluctuations in reproduction. Reproduction within this genus is characterized by intralumenal gestation, following fertilization of ovulated, mature eggs. This process is somewhat unique among teleosts occurring only in scorpaenids and zoarcids (Wourms et al. 1988). The investigation described here focuses on the development and temporal occurrence of oocytes and embryos within the ovary of yellowtail rockfish *Sebastes flavidus*. Characterization of oocyte growth and embryonic development provides a basis for assessing reproductive performance. This study is part of a larger effort to acquire information on the reproductive biology of yellowtail rockfish to ultimately determine factors that influence reproductive success.

Although characteristics of oocyte growth are generally similar among teleosts (Wallace and Selman 1981), numerous ovary maturity scales and oocyte classification schemes exist (Yamamoto 1956, Htun-Han 1978, Robb 1982, Howell 1983). These classification schemes are useful for determining reproductive strategies (synchronous, group-synchronous, or asynchronous) and evaluating aspects of reproductive trends. Each oocyte staging system is, however, less likely to be adapted for teleosts outside the genus of original study due to the variety of reproductive strategies. An oocyte classification scheme to assess the reproductive status of the marine, viviparous genus Sebastes in the Eastern Pacific has not been reported. Taking these factors under consideration, the objectives of the study reported here were two-fold: (1) to describe oocyte and embryonic development in *Sebastes flavidus* through one complete reproductive cycle, and (2) establish a staging

classification as a basis for the comparison of oocyte and embryonic development between populations, reproductive years, and other species of Sebastes. Such data may be used to monitor reproductive development during a particular year. In addition, descriptions of oocyte and embryonic development provide a basis to compare the impacts of environmental fluctuations and physiological responses with the production of viable offspring. An understanding of environmental and physiological interactions influencing reproductive success could provide valuable contributions to the understanding of recruitment dynamics and allow for more efficient resource management.

Materials and methods

Specimens were collected from Cordell Bank (38°00′N, 123°25′W), a seamount 20 miles west of Pt. Reyes, at monthly intervals. Adult female yellowtail rockfish were captured by hook-and-line at depths of 50–150 m, from May 1985 through April 1986. No samples were obtained in June 1985 due to inclement weather. Mean age and size of samples for each month are shown in Table 1.

Fish were held on ice and transported to the laboratory where pieces of ovaries (~4×4×6 mm) were dissected and fixed in 10% neutral buffered formalin. Routine paraffin embedding followed the guidelines of Humason (1967). Samples were sectioned at 6 μ thickness with a rotary microtome. Mounted sections were stained in hematoxylin and counterstained in eosin (H&E).

Cell measurements were made using a video coordinate digitizer (Model 582 AVCD, H.E. Inc., Las Vegas, NV) on cells sectioned through the nucleus. Oocytes were measured and staged randomly. Mean cell diameters were determined from a subsample of 10–20 cells for each stage. All cell diameters reported are from fixed tissues.

In each monthly sample, the first 200–400 cells encountered were counted and staged. Percent frequency distributions of the various oocyte stages were calculated by dividing the total number of a particular stage by the total number of oocytes observed, expressed as a percentage. Because the probability of an individual oocyte being sectioned is proportional to its size as well as its abundance, larger oocytes tend to be overestimated and smaller oocytes underestimated (Howell 1983). Nonetheless, frequency distributions do indicate seasonal changes within the ovary. Because of the wide range of cell diameters, overlapping sizes among oocyte stages, and shrinkage due to fixation, criteria for staging oocytes was based on histological appearances and cell structure.

Table 1

Monthly means and standard errors for age, standard length (SL), and weight (Wt) of *Sebastes flavidus* collected off central California, May 1985–April 1986, used for histological analysis.

Month	Age (yr)	SL (cm)	Wt (g)	*n*
May	14.7±2.0	37.4±1.0	1434±115	6
June	—	—	—	0
July	17.9±2.3	39.5±1.5	1600±146	9
Aug.	13.2±2.0	36.8±1.8	1387±181	4
Sept.	30.0±2.6	44.4±0.6	2349±111	6
Oct.	26.2±4.0	42.6±1.2	2017±157	7
Nov.	21.1±2.2	40.9±0.6	1780± 97	6
Dec.	18.7±2.1	39.3±1.1	1830±122	10
Jan.	15.4±1.8	36.1±1.1	1272±107	10
Feb.	14.6±1.8	36.1±1.1	1315± 83	10
Mar.	19.3±1.8	37.5±1.2	1489±102	10
Apr.	23.4±2.2	38.3±0.6	1387± 52	10

Although ovaries in varying stages of postfertilization development were observed, monthly collection of ovaries was inadequate for a detailed study of rapid embryonic development. Therefore, additional samples of embryonic stages were collected by catheterization from female yellowtail rockfish held in captivity. Ten adult female yellowtail rockfish captured after copulation were catheterized weekly for 6 weeks while being maintained in a flow-through, sand-filtered (to 10 μ) seawater system. Photoperiod was ambient. The mean temperature and salinity (10.4°C and 34.7‰) for the 2-month holding period (January and February) were well within the range of parameters at the sampling site.

Abbreviations used in figures

BC	blastodermal cap	MU	muscle
BR	brain	NC	notochord
C	capillary	NU	nucleoli
CH	chorion	N	nucleus
EB	embryonic body	OG	oil globule
EF	empty follicle	ON	oogonial nest
ER	erythrocyte	OP	optic vesicle
EY	eye	OV	oil vacuole
FOL	follicle	POF	postovulatory follicle
G	granulosa		
GR	germ ring	RE	retina
HG	hind gut	SO	somite
LC	lampbrush chromosome	T	theca
		VM	vitelline membrane
LN	lens		
LT	liver tissue	YG	yolk globule
MN	migratory nucleus	YM	yolk mass

Table 2

Classification and temporal occurrence of oocytes from *Sebastes flavidus* collected off central California, based on histological appearance. See text for additional histological descriptions.

Stage		Major histological characteristics	Temporal occurrence
I	Oogonia	Small cells (5–25 μ) found in clumps or "nests." Cytoplasm pale to clear. Basophilic nucleus occupying most of cell volume.	All year
II	Early perinucleolus	Wide range of cell diameters (20–100 μ). Intense basophilic cytoplasm. One or two large nucleoli in nucleus.	All year
III	Late perinucleolus	Diameters 50–140 μ. Small, clear vesicles present in cytoplasm. Cytoplasm pale-blue to light-gray. Several small nucleoli around inner margins of nuclear membrane.	Feb.–Oct.
IV	Initial yolk accumulation	Cell diameters 120–210 μ. Small spherical, eosinophilic yolk granules in a distinct cortical zone in cytoplasm. Cytoplasm vesicular and light-gray. Well-developed follicle surrounds a developing vitelline membrane. Several small nucleoli around the inner margins of nuclear membrane.	July–Oct.
V	Final yolk accumulation	Large cells (200–600 μ). Cell volume one-half to entirely full of yolk spheres. Lampbrush chromosomes visible in nucleoplasm. Lipid vacuoles appear larger as they coalesce.	Sept.–March
VI	Migratory nucleus	Cell diameters 600–750 μ. A single, large lipid vacuole present. Nuclear membrane indistinct or absent. Nuclear material irregularly shaped and no longer centrally located. Follicle may be distorted and irregularly shaped.	Dec.–March
VII	Ovulation & Fertilization	Mature oocyte free from follicle. The yolk mass is a single, large homogeneous mass, staining deep-purple. In fresh (unfixed) ovaries, ova appear clear or translucent.	Dec.–March

Results

Oocyte development

Major histological characteristics distinguishing stages for *S. flavidus* are listed in Table 2. All cells could be categorized into one of the seven stages. Terminology and nomenclature follow Moser (1967a) and Howell (1983).

Stage I: Oogonia These small cells were 5–25 μ in diameter and were found in clumps or "nests" along the lamellar branches (Figs. 1A, 4E). Larger oogonia in the 20 μ range possessed a deeply-stained chromatin network attached to a single, large basophilic nucleolus.

Stage II: Early perinucleolus These oocytes were 20–100 μ in cell diameter. While still closely associated with neighboring oogonia, there was noticeable movement away from oogonial nests. The most obvious feature of this cell was the intensely basophilic cytoplasm (Figs. 1B, 4E).

Stage III: Late perinucleolus Diameters were 50–140 μ. Clear vacuoles appeared in the cytoplasm of oocytes as small as 50 μ. Initially these vacuoles were distributed as a poorly organized ring surrounding the nucleus, but were seen randomly scattered throughout the cytoplasm of larger oocytes (Figs. 1B, 4E). As growth continued, they increased in size and number.

Stage IV: Initial yolk accumulation The earliest signs of yolk accumulation were seen in oocytes of 120–210 μ in diameter. Small, spherical globules of yolk were seen in a distinct cortical zone in the cytoplasm (Fig. 1C, D). The follicle enclosing the oocyte is more complex and composed of several identifiable structures (see below).

Stage V: Final yolk accumulation To simplify the staging of yolked oocytes, cells with approximately one-half their volume filled with yolk spheres, and cells whose volumes were entirely filled with yolk, were placed in Stage V. Yolk spheres increased in number and size. By the end of this stage, the cell diameter increased to about 650 μ. The cytoplasm was entirely filled with yolk spheres of various sizes (Fig. 2A). The vacuoles which were distributed throughout the cytoplasm began to coalesce, forming larger vacuoles.

An eosinophilic nucleoplasm with lampbrush chromosomes was visible (Fig. 2B). In the late Stage-V cell, the nucleus became irregularly shaped and the nuclear membrane was often indistinct (Fig. 2A).

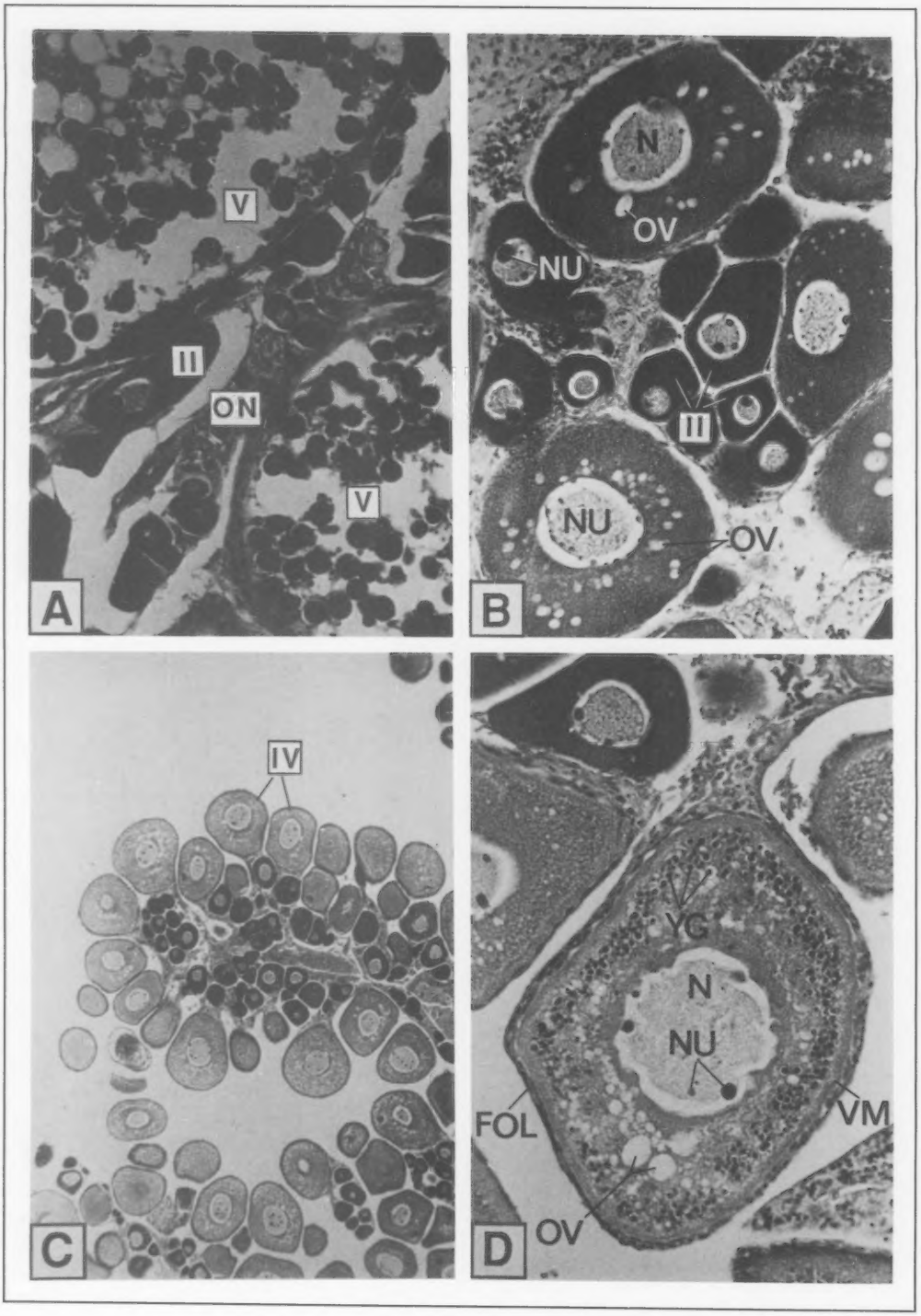
V
II
ON
V
A
N
OV
NU
II
NU
OV
B
IV
C
YG
N
NU
FOL
VM
OV
D

Figure 1 (left page)
(A) Oogonial nest (Stage-I oocyte) from *Sebastes flavidus*, containing several primary oocytes collected Dec. 1985, 400×. (B) Section of oocytes in ovary of *S. flavidus* collected May 1985, 250×. Basophilic properties of cytoplasm in Stage-II cells and their large nucleoli are shown. Distribution of vacuoles are seen in the larger Stage-III cells. (C) Cross-section of an ovary collected Aug. 1985 showing arrangement of Stage-IV oocytes in grape-like clusters on outer margins of a lamellar branch, 63×. (D) Typical Stage-IV (initial yolk accumulation) oocyte showing the first indications of yolk, 250×.

The cellular composition of the mature follicle was best observed in Stage-IV or Stage-V oocytes (Fig. 2D). A bilaminar vitelline membrane about 1 μ in thickness was next to the plasma membrane of the oocyte. Outside the vitelline membrane was a single inner epithelial layer, the granulosa. Encapsulating the granulosa was an intricate capillary network filled with erythrocytes. The theca, a single epithelial layer consisting of squamous cells with large nuclei, surrounded the profuse capillary system.

Stage VI: Migratory nucleus Cell diameters ranged from 600 to ~750 μ. Lipid material had coalesced to form a single, large vacuole, usually centrally located. Nuclear material was ameboid in appearance and no longer occupied a centralized position in the cell (Fig. 2C). Nucleoli were small, indistinct, or entirely absent.

Stage VII: Ovulation/Fertilization Histological evidence of ovulation was verified by observing the integrity of the surrounding follicle. Follicles appeared either as irregularly shaped and shrunken away from the oocyte or displayed a loss of continuity. Postovulatory follicles appeared throughout the sectioned ovary (Fig. 2C).

Because fertilization of the mature oocyte occurs rapidly after ovulation, distinction between ovulated oocytes and recently-fertilized oocytes was unnecessary. Therefore, fertilization was considered an event rather than a stage of histological distinction, and is included in Stage VII to maintain logical continuity of the developmental process. Following fertilization, however, the yolk material became a single homogeneous mass staining bright-purple in histological preparations, appearing clear or translucent in unfixed samples (Fig. 3A, B). This distinguishes fertilized from recently ovulated ova.

Embryonic development

A complete series of sequential embryonic developmental stages was not obtained from field collections due to the sampling interval and rapid development of embryos. Embryos from field collections were, however, satisfactorily placed into one of three broad categories: (1) early-celled, (2) embryonic body, or (3) eyed-larvae (where retinal pigmentation was visible).

Early-celled The early celled stage of embryonic development observed from field collections of yellowtail rockfish ovaries corresponded to stage 9 of Oppenheimer's classification for *Fundulus heteroclitus* (Oppenheimer 1937). The early-celled stage was seen as an undifferentiated mass of cells (blastodermal cap) on top of a large yolk mass (Fig. 3A). This stage was first collected in January, most frequently seen in February, and last occurred in March.

Embryos in a more advanced state (i.e., flattening or expansion of the blastula) occasionally occurred within an ovary primarily containing early-celled embryos. This suggests rapid cellular divisions and growth.

Embryonic body The appearance of an embryonic body was first seen in an ovary collected in February and last seen in March. This embryonic stage closely corresponds to Oppenheimer's stages 14 or 15 (Oppenheimer 1937). At the beginning of this stage, an undifferentiated mass of cells (taking on the appearance of tissue rather than individual cells) was located in a high ridge lying over the yolk mass. The oil globule was evident at the opposite pole (Fig. 3B). With further development, embryos displayed optic vesicles originating from lateral buds, distinguishing the cephalic region (Fig. 3C). By the end of this growth phase, somites along the trunk were visible along with lengthening of the tail. The head had further developed to include lens formation (Fig. 3D).

Figure 2 (overleaf, left page)
(A) Cross-section of ovary from *Sebastes flavidus* with clutch of oocytes in late Stage V, 63×. (B) Cross-section through nucleus of a Stage-V oocyte showing distribution of nucleoli and lampbrush chromosomes in the nucleoplasm, 400×. (C) Section through two nearly-mature oocytes in Stage VI (migratory nucleus), 63×. (D) Tangential section of Stage-V oocyte showing components of the follicle outside of vitelline membrane, 400×.

Figure 3 (overleaf, right page)
(A) Early-celled embryos from *Sebastes flavidus* ovary collected Feb. 1986, 63×. (B) First appearance of embryonic body, showing cellular differentiation. Whole embryo, formalin-fixed, 40×. (C) Section through developing embryo (embryonic body, late stage) showing optic vesicle formation originating from lateral expansions in cephalic region, 63×. (D) Embryonic body stage further developed than in Fig. 3C, with better definition of brain, retina, and lens formation, 63×.

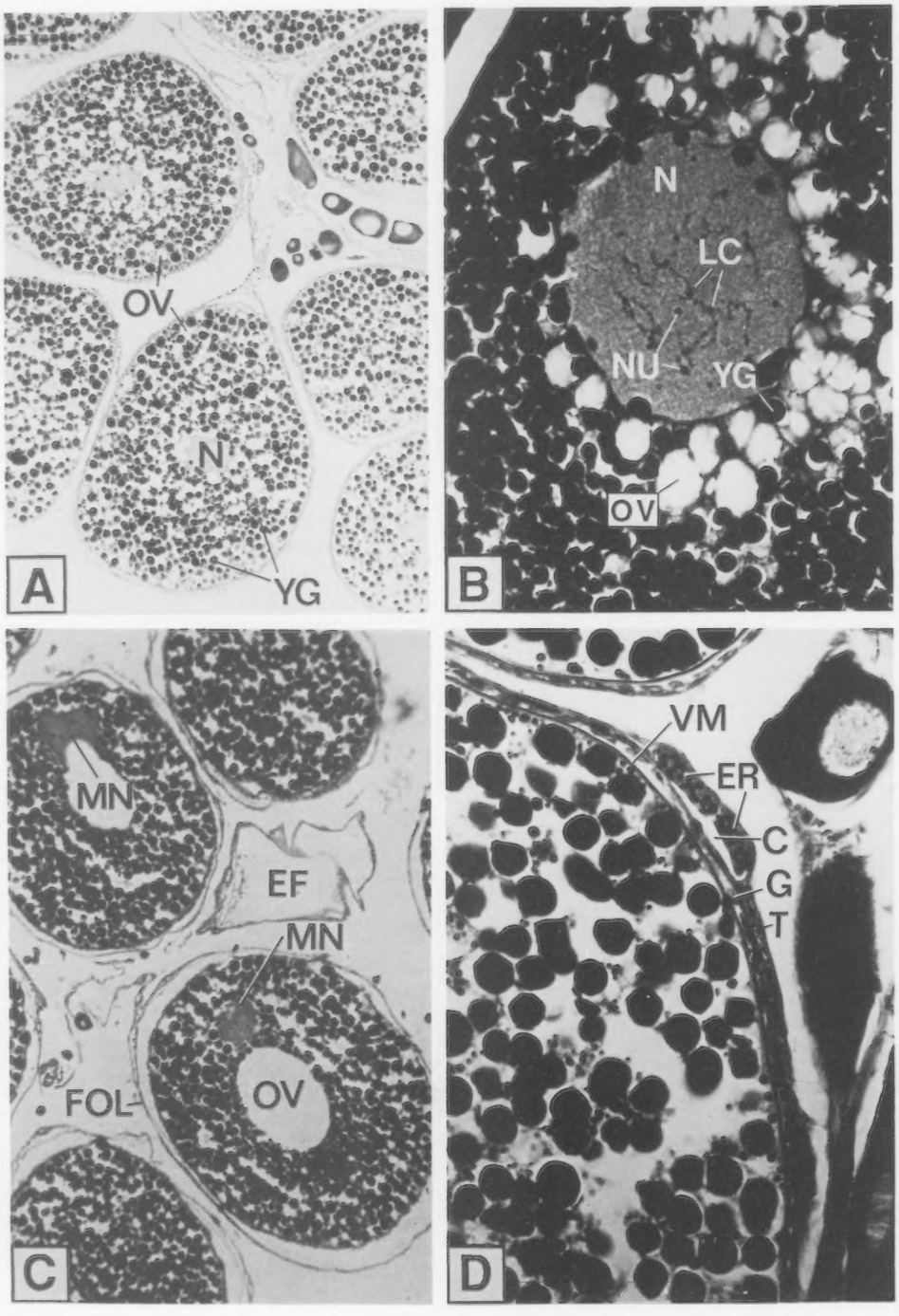

Figure 2

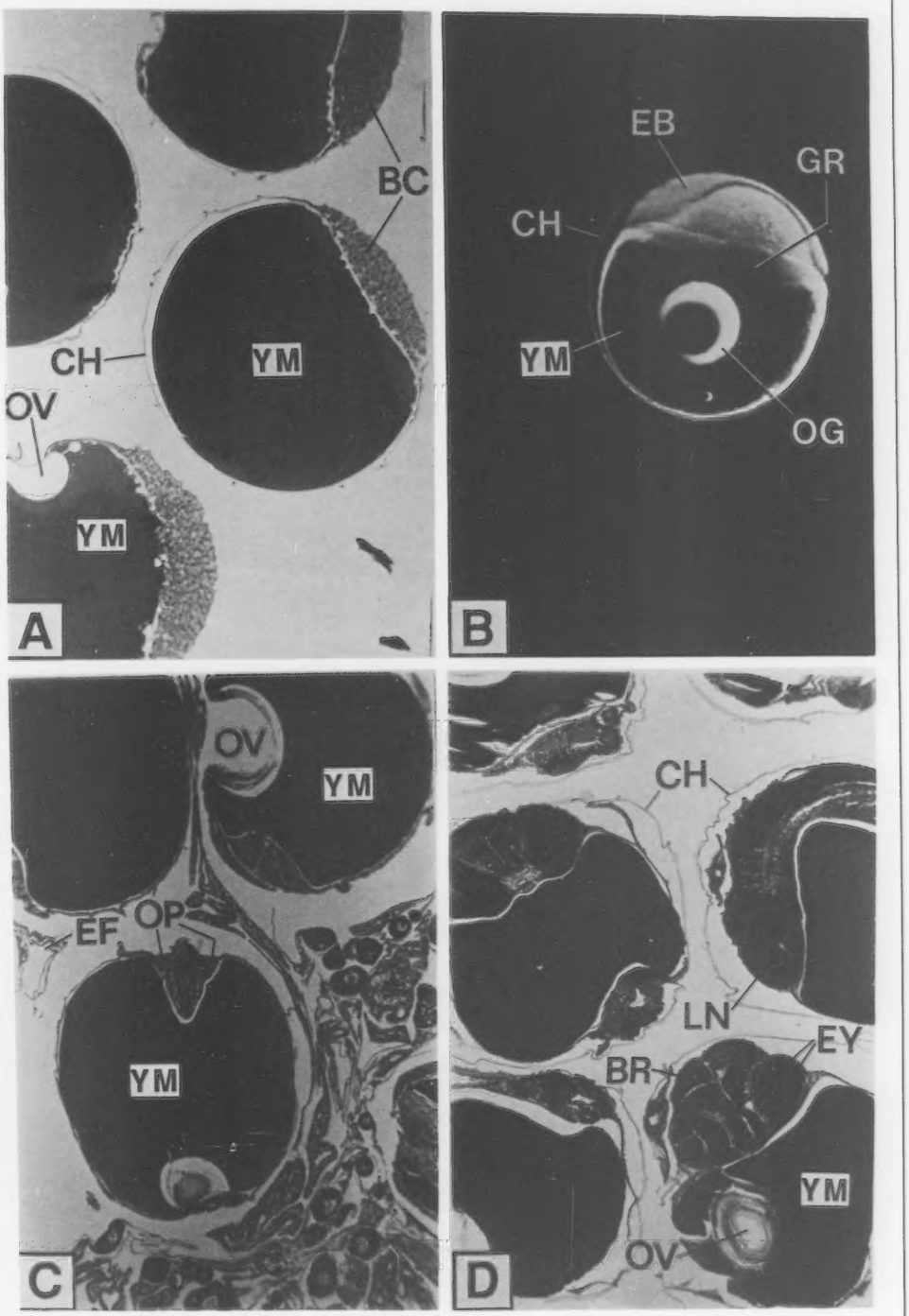

Figure 3

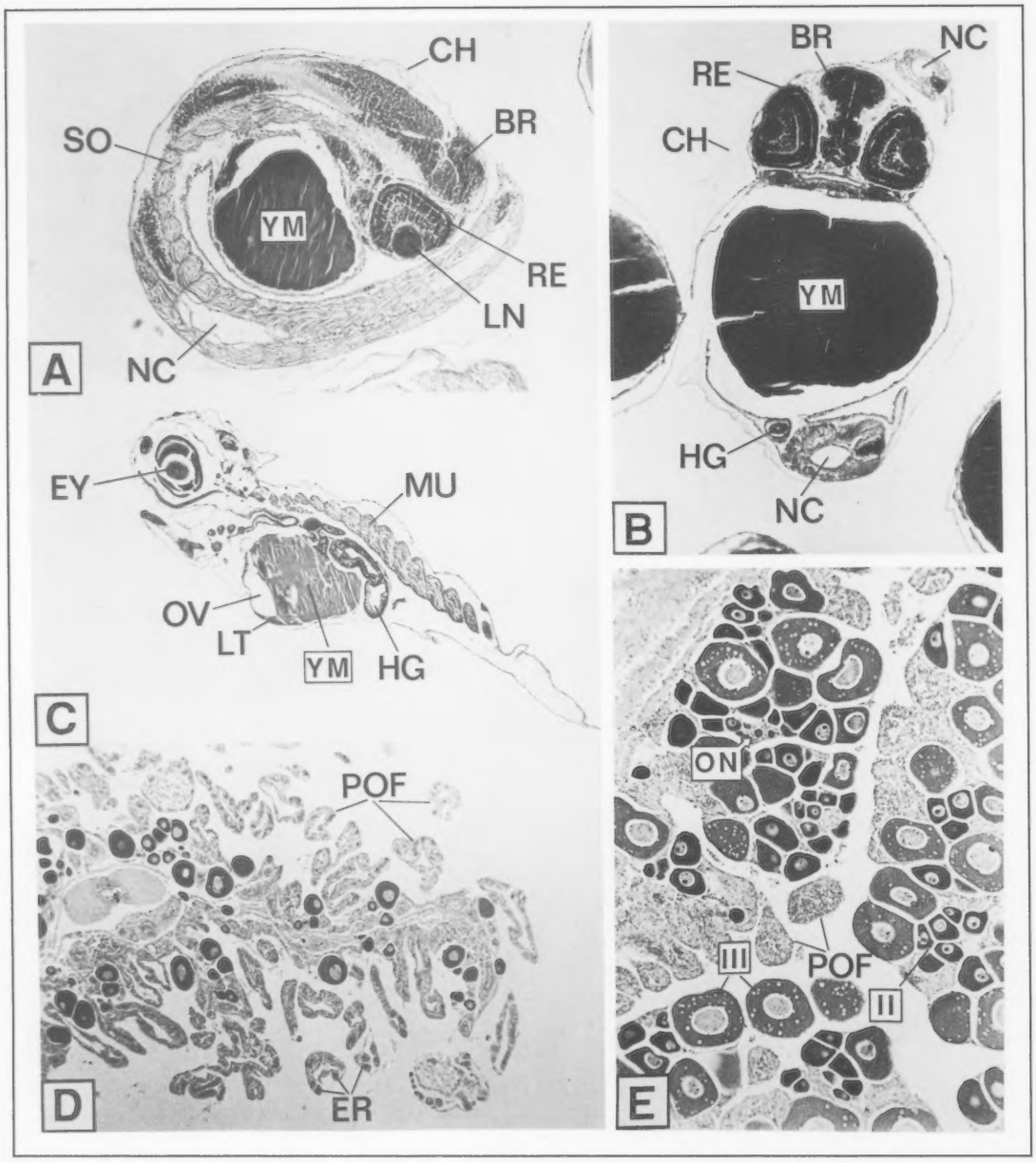

Figure 4 (above)

(A) Unhatched prolarvae of *Sebastes flavidus* collected Feb. 1986. Pigmentation of retina is apparent, as are well-formed somites, 63×. (B) Tangential section of unhatched prolarvae with completed pigmentation of the retina. Tail continues to lengthen and is seen to pass the head slightly, 63×. (C) Newly-hatched larva of *S. flavidus* showing close association of liver with oil vacuole, developing jaw and well-developed gut, 40×. (D) Cross-section of a recently-spent ovary of *S. flavidus* collected March 1986. Many empty and collapsed follicles are being resorbed, 40×. (E) Recovering and early developing ovary collected April 1986 showing reorganization of ovarian stroma as resorption nears completion, 63×.

Eyed-larvae Retinal pigmentation began as a black deposit outlining the periphery of the retina. Concurrently, somites were well formed in the thoracic and tail regions (Fig. 4A). Mature embryos (prehatching larvae) exhibited complete pigmentation of the eyes and a well-developed musculature system along the entire length of the tail (Fig. 4B). Embryos in this broad developmental category were in field samples collected in January and February. Had ovaries containing

hatched embryos (larvae) been collected in the field, they would have been included in this stage. Larvae were, however, taken from females held in the laboratory. These larvae were 4–6 mm in length and had open mouths with functional jaws. The yolk mass appeared to be reduced, and liver tissue was associated with a persistent oil globule (Fig. 4C).

Seasonal oocyte cycle Oogonial nests were observed in all samples, with about 25% frequency of occurrence throughout the entire reproductive cycle (Fig. 5). These Stage-I cells were most conspicuous early in the reproductive season and in ovaries of spent females.

Stage II or early-perinucleolus oocytes were also noted year-round and accounted for about one-third of all oocyte types observed (Fig. 5). The large nucleoli and dark cytoplasm were features that easily distinguish this stage. Mid- to late Stage-II cells were observed either singly or in groups around oocytes of later maturational stages (Stages III–VII) and were considered the 'resting' stage oocytes of other investigators (Bowers and Holliday 1961, Howell 1983).

In early spring, a broader range of Stage-II cell diameters was evident, indicating continued oocyte growth. Stage-III cells rapidly increased during March and April to a maximum frequency of 40% in April, and decreased in frequency by August as this clutch of oocytes developed (Fig. 5).

Copulation of yellowtail rockfish typically occurs over three months beginning in August and ending in October (Eldridge et al. 1991). The incidence and frequency of sperm in yellowtail rockfish ovaries were not evaluated in this study. However, small clumps or 'packages' of sperm were occasionally seen closely associated with the stroma or in spaces between developing (yolked) oocytes.

Initial yolk accumulation (Stage IV) was first documented in females collected in July, with all specimens collected in August showing this stage. In August, 34% of oocytes were Stage IV. Oocytes of Stage IV appeared as grape-like clusters on the outer margins of the lamellar branches, developing in a group-synchronous manner (Fig. 1C). The occurrence of Stage-IV oocytes sharply declined from August to November when no Stage-IV oocytes were observed (Fig. 5). As yolk accumulation continued, yolk spheres increased in size and number, filling the cytoplasm to about one-half its volume. At this point, oocytes were categorized as Stage V. Stage V was the most advanced oocyte observed from its first appearance in September until December when the frequency declined (Fig. 5). Oocytes in this developmental stage were most prevalent in November when they accounted for a mean of 48% of all oocytes. Stage-VI (Migratory nucleus) oocytes were first observed in December.

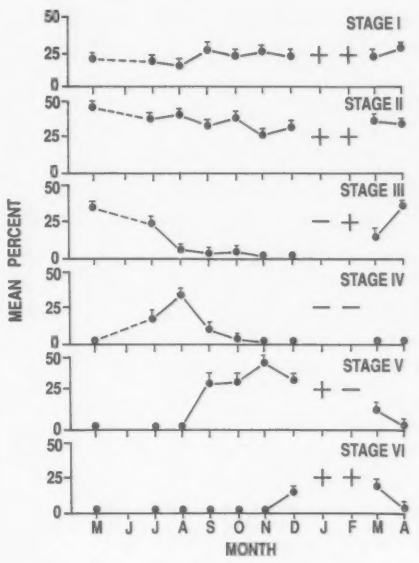

Figure 5
Mean monthly frequency distributions of oocyte Stages I–VI in ovaries of *Sebastes flavidus* during 1985–86. Error bars represent 1 SE. Plus signs = present, minus = not present. Monthly sample size same as in Table 1.

Ovaries with an advanced mode of Stage-VI oocytes continued to be collected over the next 3 months (January–March). This stage appeared to have a short duration, as ovaries containing Stage VII were also collected in some of the same months as Stage VI (December–February).

Ovary maturation was determined by using the most advanced oocyte or embryonic stage present in each monthly sample, and their frequency of occurrence was expressed as percent(s) (Fig. 6). Temporal ovarian development is illustrated and reflects a prolonged reproductive season.

While accurate frequency distributions on Stage-VII oocytes were not possible, the peak month of ovulation and fertilization appeared to be February. Sections of samples with Stage-VII oocytes showed eggs free from (e.g., outside) their follicular remnants. While continuity of follicular components (theca and granulosa) was disrupted, the integrity of the capillary network was maintained and there was a close association with the developing embryo.

Ovaries recently spawned (parturition) were seen as early as January and most frequently collected in March (Fig. 6). The ovary was greatly reduced in size,

reddish-blue in color, and very soft in texture. Histologically, the spent ovary displayed increased vascularization, a thickening of the tunica, and post-ovulatory follicles undergoing various stages of resorption (Fig. 4D). In addition, larvae remaining after parturition and yolked oocytes not reaching maturity are frequently seen in various stages of resorption.

Late-recovering and early-developing ovaries possessed reorganized lamellar branches containing Stages I, II, and early Stage-III oocytes as resorption nears completion (Fig. 4E). All samples collected in April were in this condition (Fig. 6), which marked the end of one reproductive season and the beginning of the next reproductive cycle.

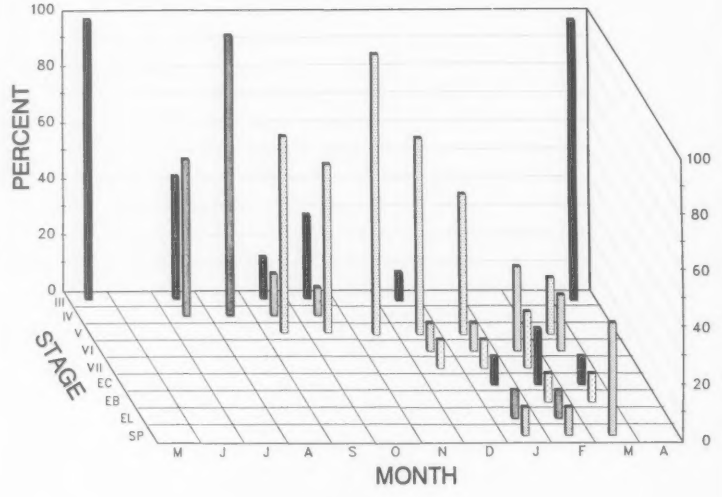

Figure 6

Percent distribution of ovarian maturation stages (derived from the most advanced oocyte or embryonic stage categorized histologically) from monthly collections of *Sebastes flavidus*; *n* is same as presented in Table 1. III = late perinucleolus, IV = early yolk, V = late yolk, VI = migratory nucleus, VII = ovulation/fertilization, EC = early-celled embryo, EB = embryonic body, EL = eyed-larvae, SP = spent.

Discussion

In the present study, I established an oocyte/embryonic classification that allows rapid determination of a rockfish population's status in the annual reproductive cycle. The use of this staging system allows one to establish oocyte frequency distributions and categorize ovaries as to their seasonal development, both temporally and spatially. This information, in turn, not only permits interannual and interpopulational comparisons, but may help reveal variations related to environmental factors.

Developmental events that occur in the oocytes of *Sebastes flavidus* are similar to those described for other teleosts with group-synchronous development (see review by Wallace and Selman 1981). Embryogenesis and the basic reproductive patterns follow observations reported for other members of the genus *Sebastes* (Moser 1967a, Wyllie Echeverria 1987). Temporal occurrence of reproductive events and seasonal variations of these events differ within the genus (Wyllie Echeverria 1987).

In the present work, oocyte development in *S. flavidus* has been categorized by separating oocyte growth into seven distinct stages. Oogonia and early-perinucleolus stages (Stages I and II, respectively) are found in the ovaries throughout the year. These stages appear to grow continuously, develop asynchronously, and, particularly in Stage-II cells, display a wide range of cell diameters. Development of unyolked oocytes in *S. flavidus* is similar to that described for *S. paucispinus* (Moser 1967a, b). However, seasonal occurrence of Stage-III oocytes differs between the two species. Stage-III oocytes in *S. flavidus* decline rapidly in number as yolk accumulation (Stage IV) is initiated. They are not observed again in the ovaries until after parturition and the beginning of the reorganization of the lamellar branches. While Moser (1967a) did not suggest a staging classification scheme, his descriptions for *S. paucispinus* included oocytes corresponding to Stage III (in the present study). In contrast to *S. flavidus*, these oocytes occurred in ovaries of *S. paucispinus* throughout the year (Moser 1967a). The temporal difference in occurrence of Stage-III oocytes between these two species is most likely a reflection of the number of broods produced annually. Viviparous species producing more than one brood annually require a reserve of Stage-III oocytes. In rockfish where two or more broods of young are produced in one reproductive season, a second clutch of yolked oocytes develops concurrently with the initial brood of gestating embryos. Moser (1967a) reported the second clutch of yolked oocytes to occur in *S. paucispinus* when the initial brood had reached eye-lens formation. A distinct seasonal absence of Stage-III oocytes, or a

clutch of yolked oocytes during embryonic gestation, distinguishes single from multiple spawners.

There were approximately 30–40 days between the appearance of fertilized ova and well-developed larvae or recently-spawned females. Therefore, gestation appears to be 30–40 days in *S. flavidus*. Moser (1967b) estimated 1–2 months gestation for the multiple-spawner *S. paucispinus*, and Boehlert and Yoklavich (1984) noted 37 days for *S. melanops*, a single-season spawner. Similarly, Mizue (1959) compared a multiple-spawner, *S. marmoratus* to a single-season spawner, *S. inermis*. His data suggest approximately 30–45 days for embryonic gestation in both species.

While the basic reproductive pattern among the various Sebastes species is similar, variations exist in reproductive strategy and life history (Boehlert and Yoklavich 1984). Temporal variations in reproductive seasonality of rockfishes are perhaps the most obvious and, therefore, well documented. Releasing larvae over an extended period of time increases the probability that a portion of the reproductive population would encounter favorable environmental conditions for the survival of the progeny. Wyllie Echeverria (1987) listed the peak parturition months for 34 species of *Sebastes* and reported that larval extrusion occurs for up to 9 months in some species. In her study, from samples collected over a 7-year period, the principal month of parturition for yellowtail rockfish was February. In the present study, and in more recent work (unpubl. data), March was the peak month of parturition; however, the samples were from a smaller geographical area. Phillips (1964), who sampled northern, central, and southern California rockfish populations, determined *S. flavidus* to be a "winter" spawner (November–March). Wyllie Echeverria (1987) reported parturition for yellowtail rockfish from north-central California to occur from January to July. In the present study, a shorter parturition time was observed for the Cordell Bank yellowtail population (January–March). This temporal variance may reflect a clinal reproductive variation in yellowtail rockfish populations. Care must be taken, however, when interpreting and comparing results where macroscopic characteristics are used. While field assessments by microscopic staging of whole oocytes or macroscopic examinations are less time-consuming, validation by histological methods is required for precise and detailed information (West 1990). Furthermore, studies on the impact of atresia and postovulatory follicles are relevant to understanding functional relationships between yellowtail rockfish reproduction and their environment. West (1990) suggests histology as the appropriate method of use for these types of studies.

A prolonged reproductive season is characteristic of the genus *Sebastes*, but the factors regulating such a mechanism are not clear. While temperature and photoperiod appear to effect later spawning in higher-latitude populations (Wooton 1984), inherent factors may also play a key role in the prolonged seasonality displayed by rockfishes. There is some evidence that age, at least in yellowtail rockfish, may account for some variation in parturition time within a season (M.J. Bowers, unpubl. data; Eldridge et al. 1991). In addition, Boehlert and Yoklavich (1984) estimated 5 days between hatching and birth in *S. melanops*, while parturition has been reported to occur immediately after hatching in the ovary in the subgenus *Sebasticus* (Tsukahara 1962). In this study, it could not be determined if hatched larvae remained in the ovaries of yellowtail rockfish. Further investigations are necessary to determine the occurrence, significance, and regulatory mechansims of larval retention.

Rockfish are an important economic resource to the Washington, Oregon, and California fisheries. Estimates of total commercial rockfish landings in 1985 were 37,806 mt (PFMC 1990). In the same year, recreational anglers landed approximately 4000 mt of rockfish in California alone. Yellowtail, blue, and black rockfishes represented 30% of the recreational landings (Lenarz 1986). Fluctuations in year-class strength cause the fishery to be somewhat unpredictable (Lenarz 1986), leaving it difficult for optimal management strategies to protect stock depletion and establish harvest guidelines. The earlier one can predict recruitment success, the more precise management decisions are likely to be. Leaman (1988) discussed the value of directing management models toward biological principles. Responses of yellowtail rockfish ovaries to environmental fluctuations are early indicators of reproductive performance. This study documents the process of oocyte development in yellowtail rockfish and provides a basis for interannual comparisons.

Acknowledgments

To Richard Powers, owner and operator of the *New Sea Angler*, my sincerest appreciation for his skill and assistance collecting samples. My greatest debt in connection with this work is to Dr. Bruce MacFarlane whose tireless enthusiasm, assistance, and patience are beyond mortal explanation.

Citations

Boehlert, G.W., and M. Yoklavich
1984 Reproduction, embryonic energetics, and the maternal-fetal relationships in the viviparous genus *Sebastes* (Pisces:Scorpaenidae). Biol. Bull. (Woods Hole) 167:354–370.

Bowers, A.B., and F. Holliday
1961 Histological changes in the gonad associated with the reproductive cycle of the herring (*Clupea harengus*). Dep. Agric. Fish. Scotl., Mar. Res. 5, p. 1–16.

Eldridge, M.B., J. Whipple, M. Bowers, B. Jarvis, and J. Gould
1991 Reproductive performances of yellowtail rockfish, *Sebastes flavidus*. Environ. Biol. Fishes 30:91–102.

Howell, W.H.
1983 Seasonal changes in the ovaries of adult yellowtail flounder, *Limanda ferruginea*. Fish. Bull., U.S. 81:341–355.

Htun-Han, M.
1978 The reproductive biology of the dab *Limanda limanda* (L.) in the North Sea: Seasonal changes in the ovary. J. Fish Biol. 13:351–359.

Humason, G.L.
1967 Animal tissue techniques, 3d ed. W.H. Freeman, San Francisco.

Leaman, B.M.
1988 Reproductive and population biology of Pacific ocean perch (*Sebastes alutus* (Gilbert)). Ph.D. thesis, Univ. Brit. Col., Vancouver, 200 p.

Lenarz, W.H.
1986 A history of California rockfish fisheries. *In* Proc., Int. Rockfish Symp., Oct. 1986, Anchorage, Alaska, p. 35–41. Alaska Sea Grant Rep. 87-2, Univ. Alaska, Fairbanks.

Mizue, K.
1959 Studies on a scorpaenous fish *Sebasticus marmoratus* Cuvier et Valenciennes. V. On the maturation and the seasonal cycle of the ovaries of the marine ovoviviparous teleost. Bull. Fac. Fish. Nagasaki Univ. 8:84-110 [in Jpn., Engl. summ.].

Moser, H.G.
1967a Seasonal histological changes in the gonads of *Sebastodes paucispinis* (Ayres), an ovoviviparous teleost (family Scorpaenidae). J. Morphol. 123:329–351.
1967b Reproduction and development of *Sebastodes paucispinis* and comparison with other rockfishes off southern California. Copeia 1967:773–797.

Oppenheimer, J.M.
1937 The normal stages of *Fundulus heteroclitus*. Anat. Rec. 68(1):1–15.

PFMC (Pacific Fishery Management Council)
1990 Status of the Pacific coast groundfish fishery through 1990 and recommended acceptable biological catches for 1991: Stock assessment and fishery evaluation. Document prepared for the Council and its advisory entities. Pac. Fish. Manage. Counc., Portland, OR 97201.

Phillips, J.B.
1964 Life history studies on ten species of rockfish (genus *Sebastodes*). Calif. Dep. Fish Game, Fish Bull. 126, 70 p.

Robb, A.P.
1982 Histological observations on the reproductive biology of the haddock, *Melanogrammus aeglefinus* (L.). J. Fish. Biol. 20:97–408.

Tsukahara, H.
1962 Studies on habits of coastal fishes in the Amakusa Islands. 2. Early life history of the rockfish, *Sebasticus marmoratus* (Cuvier et Valenciennes). Rec. Oceanogr. Works Jpn., Spec. 6:49–55.

Wallace, R.A., and K. Selman
1981 Cellular and dynamic aspects of oocyte growth in teleosts. Am. Zool. 21:325–343.

West, G.
1990 Methods of assessing ovarian development in fishes: A review. Aust. J. Mar. Freshwater Res. 41:199–222.

Wootton, R.J.
1984 Introduction: Strategies and tactics in fish reproduction. *In* Potts, G.W., and R.J. Wootton (eds.), Fish reproduction: Strategies and tactics, p. 1–12. Acad. Press, London.

Wourms, J.P., B.D. Grove, and J. Lombardi
1988 The maternal-embryonic relationship in viviparous fishes. *In* Hoar, W.S., and D.J. Randall (eds.), Fish physiology, Vol. XI, Part B, p. 1–34. Acad. Press, San Diego.

Wyllie Echeverria, T.
1987 Thirty-four species of California rockfishes: Maturity and seasonality of reproduction. Fish. Bull., U.S. 85:229–250.

Yamamoto, K.
1956 Studies on the formation of fish eggs. I. Annual cycle in the development of the ovarian eggs of the flounder, *Liopsetta obscura*. J. Fac. Sci. Hokkaido Univ., Ser. VI Zool. 12:362–373.

Age, growth, and reproduction of jewfish *Epinephelus itajara* in the eastern Gulf of Mexico

Lewis H. Bullock
Michael D. Murphy
Florida Marine Research Institute, Florida Department of Natural Resources
100 Eighth Avenue SE, St. Petersburg, Florida 33701-5095

Mark F. Godcharles
Southeast Region, National Marine Fisheries Service, NOAA
9450 Koger Boulevard, St. Petersburg, Florida 33702

Michael E. Mitchell
Florida Marine Research Institute, Florida Department of Natural Resources
1481-A Market Circle, Port Charlotte, Florida 33953

Abstract.–We sampled jewfish from recreational and commercial catches in the eastern Gulf of Mexico from November 1977 to January 1990 to obtain life history information. A single annual minimum in mean marginal increment ratios during May–August supported the hypothesis that jewfish up to at least age 10 can be aged by counting the opaque marks observed on otolith sections. Annual opaque mark formation was observed for a 3- and a 4-year-old jewfish using oxytetracycline (OTC) reference marks on otoliths (sagittae). Male jewfish (N 41) ranged 3–26 years old; females, 0–37 years (N 85). Growth was similar for males and females, averaging >100 mm/year through age 6, then slowing to about 30 mm/year by age 15, and finally declining to <10 mm/year after age 25. Observed total length and age data were described well by the following von Bertalanffy growth model: total length (mm) = $2006\ (1 - e^{(-0.126(\text{age(yrs)}+0.49))})$. Jewfish spawned from June through December, with peak activity from July through September. Male jewfish matured at about 1100–1150 mm when 4–6 years old; females matured at 1200–1350 mm when 6 or 7 years old. The extensive overlap of length and age distributions of males and females, and the slight differences between their sizes and ages at maturity, prevent us from designating jewfish as a protogynous hermaphrodite. No transitional individuals were found. Their relatively slow growth, longevity, and behavioral characteristics, such as the tendency to form spawning aggregations, make jewfish populations highly susceptible to overfishing.

Manuscript accepted 11 March 1992.
Fishery Bulletin, U.S. 90:243–249 (1992).

The jewfish *Epinephelus itajara*, largest of the western North Atlantic groupers (possibly reaching 455 kg; Robins et al. 1986), ranges from the east coast of Florida throughout the Gulf of Mexico, Caribbean Sea, and south to Brazil (Smith 1971), and also in the Pacific Ocean from Costa Rica to Peru. Jewfish occur at depths ranging from several meters (shallow estuarine areas) to about 50 m. Juveniles can be found in holes and below undercut ledges in swift tidal creeks draining mangrove swamps. Large adults occur both inshore around structures such as piers and bridges, and offshore around ledges and wrecks (Bullock and Smith 1991).

Jewfish have recently been granted protected status, eliminating harvest in both the U.S. Exclusive Economic Zone (NMFS 1990a, b) and Florida's territorial waters (Florida Marine Fisheries Commission 1990). Prior to this designation, jewfish were captured by hook-and-line, speargun, shark and grouper/snapper longlines, and as a bycatch of shrimp trawling. Historically, the majority of the U.S. commercial catch has been landed along the Florida Gulf coast, where landings reached a high of approximately 61,700 kg in 1988 (Fla. Dep. Nat. Resour. Annual Landings Summ., Fla. Mar. Res. Inst., St. Petersburg, unpubl. data).

A comprehensive study of jewfish life history does not exist. Smith (1971) discussed their systematics, distribution, and ecology. Randall (1967) described food habits from nine individuals. Other researchers have contributed incidental observations on diet (Beebe and Tee-Van 1928, Tabb and Manning 1961, Odum 1971), habitat (Smith 1976, Odum et al. 1982), spawning (Schroeder 1924, Colin 1990), and parasites/pseudoparasites (Breder and Nigrelli 1934, Pearse 1934 and 1952, Manter 1947, Olsen 1952). Bullock and Smith (1991) provided basic life-history information on jewfish in the eastern Gulf of Mexico, but did not discuss age and growth or size/age-at-maturity. In this paper, we describe age and growth, spawning seasonality, and approximate size- and age-at-maturity for jewfish in the eastern Gulf of Mexico. We also briefly discuss the implications of these life-history characteristics as they relate to the jewfish's susceptibility to overfishing.

Methods and materials

Jewfish were sampled aperiodically from recreational and commercial catches from the eastern Gulf of Mexico, November 1977 through January 1990. Fifty-six percent (269/481) of the sampled jewfish were captured using spearguns, 27% by hook-and-line, 8% by bottom longline (either grouper/snapper or shark fisheries), and the remaining 9% by shrimp trawl, trap, or unrecorded methods. We attempted to determine sex, whole (WW) and/or gutted (GW) weight (kg), and total length (mm TL) for each specimen, although we could not determine whole weight and sex when fish had been eviscerated (N 271). Although eviscerated, unsexed fish could not be included in our study of reproduction, they were used in the age and growth analyses. If sagittae could be located, they were removed from the otic capsule (N 384) and stored dry. A portion of the gonad, if available (N 173), was preserved in 10% formalin and later transferred to 70% ethanol.

Otolith sections were examined for evidence of age marks. Transverse sections, approximately 0.5 mm thick, were cut from each sagitta with a Buehler Isomet low-speed saw. Sections were mounted on microscope slides with Histomount mounting media and examined for age marks under a dissecting microscope using reflected light. Age marks were counted independently by two readers. Later, a joint reading was conducted in an attempt to resolve differences between counts.

Monthly mean marginal increment ratios were calculated for fish with 1–10 annuli to determine the periodicity of mark formation. Marginal increment was standardized for differences in growth among age-classes by dividing the marginal increment for each fish by the distance between its penultimate and outermost annuli. We called this calculated value the 'marginal increment ratio' (*sensu* percentage of marginal increment; Hood et al. Unpubl. manuscr.). Fish were assigned ages based on the number of annuli and a biologically realistic hatching date of 1 September (time of peak spawning; see Results). All fish were assigned an age equal to their annulus count, except for fish collected prior to 1 September and that had already deposited an annulus during the most recent period of mark deposition (April–August; see Results). The assigned age for these fish was one less than their number of annuli.

Observations to determine the validity of age marks were made from two jewfish (290 mm TL, 509 g; and 375 mm TL, 934 g) that were injected intramuscularly with 50 mg oxytetracycline (OTC) per kg body weight on 3 November 1990 and 21 October 1989, respectively. These fish were maintained at ambient light and temperature in flow-through 1038-gallon seawater tanks located at the Keys Marine Laboratory in the Florida Keys. The smaller specimen survived 11 months after OTC treatment; the larger fish was sacrificed after 22 months.

Nonlinear regression of all available age and length data (using FSAS; Saila et al. 1988) was used to estimate parameters of the von Bertalanffy growth equation,

$$l_t = L_\infty(1-e^{(-K(t-t_0))}),$$

where l_t is total length (mm), t is age (years), L_∞ is asymptotic length, K is the Brody growth coefficient, and t_0 is the age at zero length (von Bertalanffy 1957). Likelihood ratio tests were used to compare male and female von Bertalanffy parameter estimates (Kimura 1980, Cerrato 1990). Nonlinear regression was used to fit the exponential equation, WW or $GW = aTL^b$, to whole- or gutted-weight and total-length data.

Histological preparations of gonads were made to determine gonad developmental class, following the criteria presented by Moe (1969) for red grouper *Epinephelus morio*. Initially, gonad samples were embedded in paraffin, but beginning with fish sampled in 1988, gonads were embedded in plastic (glycol methacrylate) because of its superior tissue-infiltrating abilities. Gonad samples were sectioned to a thickness of 3.5 μm and stained with Weigert's hematoxylin and eosin Y for microscopic examination. Spawning was inferred from seasonal changes in the relative abundance of fish having ovaries containing vitellogenic oocytes or testes containing sperm in their efferent ducts. Sizes or ages at maturity were determined from changes in the proportion of mature fish over the entire age range or across 50 mm size-classes.

Results

Age and growth

Opaque bands can be recognized and counted on thin-sectioned jewfish sagittae. Initial counts of opaque bands by two independent readers agreed on 62% (237/384 fish) of sections analyzed, with 91% (348/384) of all counts either in agreement or differing by one. After a second, joint reading, agreement was reached on opaque-band counts for all but two sections, leaving 382 specimens for analysis of age and growth.

The annual pattern of monthly mean marginal increment ratios and observations from two OTC-marked jewfish support the hypothesis that annuli form once each year. Mean marginal increment ratios were greater than 70% during November–April and declined to a minimum of 20% in June. The mean marginal increment ratio remained less than 30% through August (Fig. 1). For a large number of specimens captured

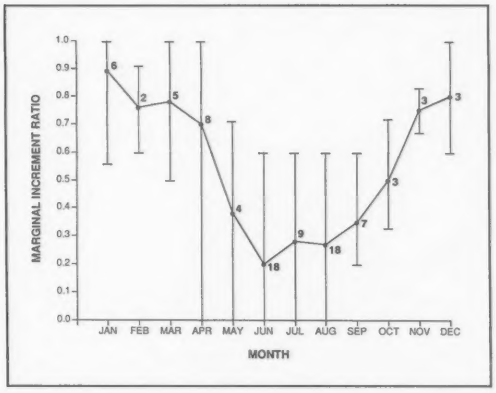

Figure 1

Monthly mean marginal increment ratios for jewfish with 1–10 opaque marks on otolith sections. Vertical lines indicate range of observations; sample size indicated by the number adjacent to the mean (*N* 86).

during April–August, we observed an opaque band at the outer edge of the otolith section and interpreted this as the deposition of a new annulus. After August, the mean marginal increment ratio increased until reaching a maximum during November–April. The observed annual minimum in monthly mean marginal increment ratios suggests that opaque bands form once each year in the otoliths of jewfish ≤ 10 years of age. The validity of age marks was confirmed for two OTC-marked jewfish. The OTC reference mark was clearly evident on otoliths of each of the two specimens. The otolith of the 3-year-old jewfish that had survived for 11 months in captivity contained a single annulus distal to the OTC mark. This fish, injected with OTC in November 1990, had apparently deposited an annulus prior to its death in October 1991. Its total length and weight were 505 mm TL and 2.7 kg. The 4-year-old specimen, injected with OTC in October 1989 and sacrificed in August 1991 after 22 months in captivity (total length and weight of ~735 mm TL and 9 kg), had deposited two annuli distal to the OTC reference mark.

Table 1

Number of aged jewfish *Epinephelus itajara* from the eastern Gulf of Mexico, and average observed and predicted total lengths for age groups 0–37 years old. Predicted lengths are based on the von Bertalanffy growth equation $\text{mm TL} = 2006\,(1 - e^{(-0.126(\text{age (yr)} + 0.49))})$.

	Average observed total length (mm)						Predicted total length (mm)		
Age	*N*	Male	*N*	Female	*N*	Unknown	Male	Female	Pooled*
0	0	—	1	338	4	170			—
1	0	—	3	517	0	—	434	382	344
2	0	—	5	717	1	711	605	563	541
3	2	863	4	708	4	751	759	725	714
4	1	1184	3	924	4	913	897	871	867
5	2	1080	1	1218	8	1067	1021	1002	1002
6	4	1078	0	—	5	1161	1132	1119	1121
7	5	1318	0	—	4	1423	1232	1225	1226
8	2	1476	2	1333	8	1437	1322	1319	1318
9	2	1400	2	1399	12	1368	1403	1404	1400
10	2	1398	6	1515	12	1516	1475	1481	1471
11	1	1660	6	1632	23	1544	1540	1549	1535
12	1	1690	7	1647	31	1612	1598	1611	1590
13	5	1620	10	1653	26	1644	1651	1666	1640
14	2	1849	7	1762	15	1723	1698	1715	1683
15	4	1828	4	1913	12	1737	1740	1760	1721
16	3	1909	4	1860	8	1735	1778	1800	1755
17	1	1770	2	1878	6	1879	1812	1836	1785
18	0	—	4	1820	8	1750	1843	1868	1811
19	0	—	0	—	6	1833	1870	1897	1834
20	0	—	2	1990	11	1842	1895	1923	1854
21	0	—	4	2023	8	1818	1917	1946	1872
22	0	—	2	2011	9	1820	1937	1967	1888
23	0	—	0	—	4	1938	1955	1986	1902
24	1	1905	1	1950	7	1936	1971	2003	1914
25	2	1955	0	—	4	1821	1985	2018	1925
26	1	1930	0	—	5	1891	1998	2032	1935
27	0	—	2	2065	3	1853	2010	2044	1943
28	0	—	1	1935	2	2006	2020	2055	1951
29	0	—	0	—	1	2090	2030	2065	1957
30	0	—	0	—	1	2040	2038	2073	1963
33	0	—	1	2015	2	1820	2058	2095	1977
34	0	—	0	—	1	2032	2064	2101	1980
36	0	—	0	—	1	1908	2073	2110	1986
37	0	—	1	1970	0	—	2077	2115	1988

* Including fish of unknown sex

A total of 481 jewfish were sampled for life-history data. Age data were determined for 382 individuals. Age range was 3–26 years for males (*N* 41), 0–37 for females (*N* 85), and 0–36 for fish of undetermined sex (*N* 256). Total lengths of jewfish sampled were 795–2057 mm for males (*N* 75), 338–2155 mm for females (*N* 131), and 75–2160 mm for fish of undetermined sex (*N* 275).

Jewfish grow slowly relative to their potential maximum size. Annual growth was most rapid (averaging >100 mm/year) through age 6, then declined to about 30 mm/year by age 15, and to less than 10 mm/year after age 25 (Table 1,

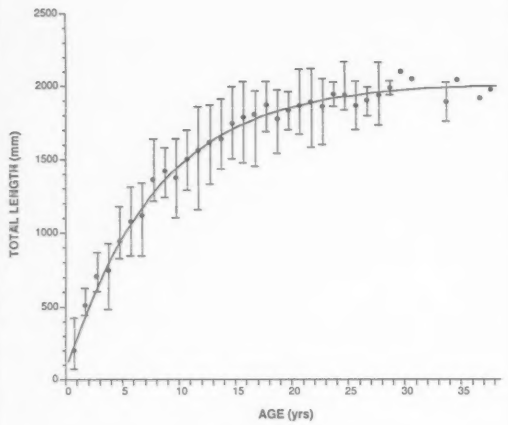

Figure 2

Observed ages (years) and total lengths (mm), and predicted growth modeled for jewfish collected from the eastern Gulf of Mexico. Parameters for the von Bertalanffy growth model are $L_\infty = 2006$ mm TL, K = 0.126/year, and $t_0 = -0.49$ year (N 382).

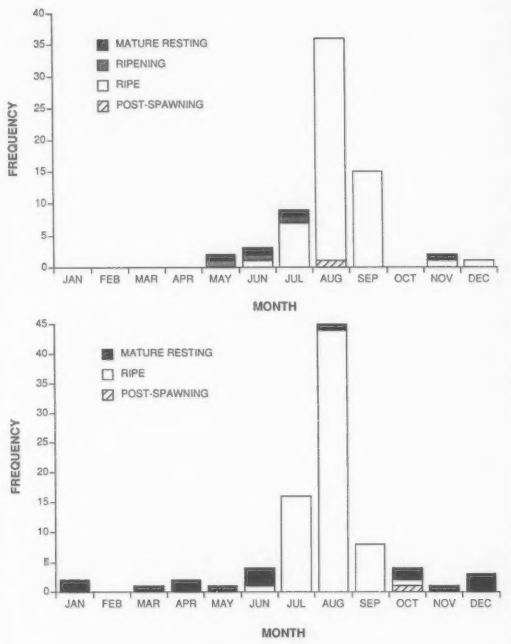

Figure 3

Monthly distribution of gonad classes for mature (upper) male (N 66) and (lower) female (N 86) jewfish collected from the eastern Gulf of Mexico. Histological criteria for gonad classes correspond to Moe's (1969) descriptions for red grouper.

Fig. 2). Average observed and predicted (von Bertalanffy equation) sizes-at-age were similar between sexes (Table 1). Results of likelihood ratio tests indicated no significant differences between sex-specific estimates of L_∞ (χ^2 0.136, df 1, $P>0.70$), K (χ^2 4.0×10^{-5}, df 1, $P>0.90$), or t_0 (χ^2 0.138, df 1, $P>0.70$). Estimates of the growth equation parameters (asymptotic standard error) for pooled length and age data were $L_\infty = 2006$ mm TL (23.3), K = 0.126/year (0.0057), and $t_0 = -0.49$ years (0.200).

The relationships of whole and gutted weight (kg) to total length (mm) were

$$WW = 1.31 \times 10^{-8} TL^{3.056} \quad (N\ 66,\ r^2\ 0.964)$$
$$GW = 2.94 \times 10^{-8} TL^{2.941} \quad (N\ 402,\ r^2\ 0.941).$$

Gutted and whole weights were linearly related (N 50, r^2 0.995) as follows:

$$WW = -0.717 + 1.1039\,GW$$
$$GW = 1.001 + 0.9018\,WW.$$

Reproduction

Jewfish spawn during June–December in the eastern Gulf of Mexico, with peak activity during July–September (Fig. 3). Ripe males and females first appeared in our collections during June. Nearly all gonads collected from mature fish in July, August, and September were classified as ripe. Most spawning appears to end by October, although a ripe male was collected in November and another in December. Spent fish were collected in August (one male) and October (one female). No transitional fish were found.

Male jewfish become sexually mature at a slightly smaller size and younger age than females. Male jewfish were first mature when about 1100–1150 mm TL at 4–6 years of age. All males <1150 mm TL (N 6, 795–1100 mm) were immature, whereas all larger males in our samples (N 55, 1155–2057 mm) were mature. Both 3-year-old males sampled were immature, whereas one large (1184 mm TL) 4-year-old male was mature. Fifty percent of males 5 or 6 years old (3 of 6 individuals) and all males age 7 or older (N 31) were mature. Female jewfish first mature when about 1200–1350 mm TL at age 6 or 7. All females <1225 mm (N 21, 338–1218 mm) and <6 years old (N 17, 0–5 yr) were immature. All larger (N 90, 1350–2155 mm) and older (N 68, 8–37 yr) females sampled were mature.

Discussion

Age and growth

The spring–summer period of annulus formation in jewfish seems somewhat protracted. However, there appears to be a considerable range for the duration of annulus deposition in grouper populations: 2 or 3 months for *Epinephelus morio*, *E. nigritis*, *E. drummondhayi*, and *E. niveatus* (Moe 1969, Matheson and Huntsman 1984, Moore and Labisky 1984, Manooch and Mason 1987) to 5–7 months for *Mycteroperca phenax* and *M. microlepis* (Matheson et al. 1986, Hood and Schlieder 1992). Moe (1969) discussed factors affecting annulus formation and concluded that spawning and its associated physiological processes probably caused annulus formation in red grouper. However, annulus formation does not always occur in phase with spawning in epinephelines. For example, Matheson et al. (1986) found *M. phenax* to spawn during April–August in the South Atlantic Bight, but annulus formation occurred during December–April.

The annual deposition of opaque bands, seen in 3- and 4-year old OTC-marked jewfish, needs to be validated for fish older than 10 years. Due to the difficulty in sampling large numbers of these older fish year-round, it is probably not feasible to utilize indirect validation techniques (i.e., marginal increment analysis). Validation will probably require direct observations of individuals that have been injected with OTC and recaptured after annulus deposition.

The growth rate of jewfish (i.e., K 0.13/year) falls within or near the range observed for some of its congeners in the South Atlantic Bight and Gulf of Mexico: speckled hind, 0.13/year (Matheson and Huntsman 1984) and red grouper, 0.11–0.18/year (Moe 1969, Muhlia-Melo 1975). However, jewfish growth is somewhat faster than that of the deepwater snowy grouper *E. niveatus* (K 0.07–0.09/year; Matheson and Huntsman 1984, Moore and Labisky 1984) and considerably greater than that of the second-largest grouper in the western North Atlantic Ocean, the warsaw grouper *E. nigritis* (K 0.05/year; Manooch and Mason 1987), which may reach weights >200 kg.

Reproduction

We found jewfish to be in peak spawning condition during July–September in the eastern Gulf of Mexico. This agrees with Schroeder's (1924) finding that jewfish spawned during July–August, when heavily exploited aggregations of jewfish appeared off the Florida Keys. Furthermore, Colin (1990) observed what he interpreted as courtship behavior in jewfish off southwest Florida during the full moons of August and September.

When compared with that of females, the slightly smaller size and younger age of males at first maturity is unexpected, given that jewfish are assumed to be protogynous hermaphrodites (Smith 1971). Furthermore, whereas the youngest fish in our sample was female, as would be expected for a protogynous fish, so was the oldest. However, Sadovy and Shapiro (1987) point out several factors that may obscure differences in length, age, and maturity between males and females of a protogynous fish: (1) Some females may never change sex for lack of genetic or environmental cues and therefore may attain sizes (ages) equal to or greater than males, (2) a fraction of the population may initiate female development but change to males prior to sexual maturation, and (3) size at sex-reversal may differ among subpopulations of the same species and thus may obscure differences in length or age distribution between the sexes. Conclusive evidence for protogynous hermaphroditism in jewfish (i.e., the presence of transitional individuals) was not found in this study. Transitional individuals in confirmed protogynous hermaphrodites, such as *E. morio* (Moe 1969) and *M. microlepis* (Collins et al. 1987, Hood and Schlieder 1992), never represent a large percentage of the population; therefore, more extensive collections than ours may be needed to detect the presence of these individuals.

Fisheries implications

The life-history characteristics that we describe imply that jewfish are highly vulnerable to overfishing. Their slow growth, longevity, and presumed low natural mortality specify a population composed of cohorts that reach their maximum biomass at relatively old ages (Alverson and Carney 1975). Thus the greatest yield from a cohort of jewfish would be attained at either low rates of fishing or when only large fish are harvested. If jewfish are indeed protogynous hermaphrodites, fishing may also disrupt their spawning and recruitment by limiting the number of older males available for spawning (Smith 1982, Bannerot et al. 1987, Huntsman and Waters 1987). In addition, behavioral traits exhibited by large jewfish, such as their general unwariness of spearfishermen and apparent site-specific spawning aggregations (Shroeder 1924, Colin 1990), make them readily available for capture. Fisheries managers of Florida territorial and U.S. Exclusive Economic Zone waters have recognized the jewfish's susceptibility to overfishing and have recently banned all harvest of jewfish from waters under their jurisdictions.

Acknowledgments

We would like to thank the following fishermen for providing juvenile specimens: D. Bellamy, I. Bellamy, J. Rhodes, and R. Woodring. This study would not have been possible without the fine cooperation from the following: T. Nachman, G. Brown, G. Migliano, M. Nahon, W. Tappan, F. Devens, D. Harger, E. McManus, R. Ruiz-Carus, J. Swanson, W. Gibbs, W. Bell, and Capt. T. Reynolds. Special thanks go to Capt. D. DeMaria, who not only permitted us to thoroughly sample his catches but was also the major impetus for bringing about protection for the jewfish in Florida.

This manuscript benefited from review by R. Taylor, R. Crabtree, and P. Hood of the Florida Marine Research Institute, Department of Natural Resources. This study was partially supported by funds provided to the State of Florida under PL 99-659 of the Department of Commerce.

Citations

Alverson, D.L., and M.J. Carney
1975 A graphic review of the growth and decay of population cohorts. J. Cons. Cons. Int. Explor. Mer 36:133–143.

Bannerot, S., W.W. Fox Jr., and J.E. Powers
1987 Reproductive strategies and the management of snappers and groupers in the Gulf of Mexico and Caribbean. *In* Polovina, J.J., and S. Ralston (eds.), Tropical snappers and groupers: Biology and fisheries management, p. 561–603. Westview Press, Boulder.

Beebe, W., and J. Tee-Van
1928 The fishes of Port-au-Prince Bay, Haiti, with a summary of the known species of marine fish of the Island of Haiti and Santo Domingo. Zoologica (NY) 10:1–279.

Breder, C.M. Jr., and R.F. Nigrelli
1934 The penetration of a grouper's digestive tract by a sharp-tailed eel. Copeia 1934(4):162–164.

Bullock, L.H., and G.B. Smith
1991 Seabasses (Pisces: Serranidae). Mem. Hourglass Cruises VIII (II), 243 p.

Cerrato, R.M.
1990 Interpretable statistical tests for growth comparisons using parameters in the von Bertalanffy equation. Can. J. Fish. Aquat. Sci. 47:1416–1426.

Colin, P.L.
1990 Preliminary investigations of reproductive activity of the jewfish, *Epinephelus itajara*. *In* Abstr. Gulf Caribb. Fish. Inst., 43rd Annu. Sess., Miami, 4–9 Nov. 1990, p. 9,10.

Collins, M.R., C.W. Waltz, W.A. Roumillat, and D.L. Stubbs
1987 Contribution to the life history and reproductive biology of gag, *Mycteroperca microlepis* (Serranidae), in the South Atlantic Bight. Fish. Bull., U.S. 85:648–653.

Florida Marine Fisheries Commission
1990 Jewfish: Designation as protected species; prohibition of harvest in state waters; possession, landing, and sale prohibited. Florida Administrative Code 46-14.008, Tallahassee.

Hood, P.B., and R.C. Schlieder
1992 Age, growth and reproduction of gag, *Mycteroperca microlepis*, in the eastern Gulf of Mexico. Bull. Mar. Sci. 51(3).

Hood, P.B., M.F. Godcharles, and R. Barco
Unpubl. Age, growth, reproduction, and the feeding ecology of black sea bass, *Centropristis striata* (Pisces: Serranidae). Fla. Mar. Res. Inst., Fla. Dep. Nat. Resour., St. Petersburg, 38 p.

Huntsman, G.R., and J.R. Waters
1987 Development of management plans for reef fishes—Gulf of Mexico and U.S. South Atlantic. *In* Polovina, J.J., and S. Ralston (eds.), Tropical snappers and groupers: Biology and fisheries management, p. 533–560. Westview Press, Boulder.

Kimura, D.K.
1980 Likelihood methods for the von Bertalanffy growth curve. Fish. Bull., U.S. 77:765–776.

Manooch, C.S. III, and D.L. Mason
1987 Age and growth of the warsaw grouper and black grouper from the southeast region of the United States. Northeast Gulf Sci. 9:65–75.

Manter, H.W.
1947 The digenetic trematodes of marine fishes of Tortugas, Florida. Am. Midl. Nat. 38:257–416.

Matheson, R.H. III, and G.R. Huntsman
1984 Growth, mortality, and yield-per-recruit models for speckled hind and snowy grouper from the United States South Atlantic Bight. Trans. Am. Fish. Soc. 113:607–616.

Matheson, R.H. III, G.R. Huntsman, and C.S. Manooch III
1986 Age, growth, mortality, food, and reproduction of the scamp, *Mycteroperca phenax*, collected off North Carolina and South Carolina. Bull. Mar. Sci. 38:300–312.

Moe, M.A. Jr.
1969 Biology of the red grouper *Epinephelus morio* (Valenciennes) from the eastern Gulf of Mexico. Fla. Dep. Nat. Resour. Mar. Res. Lab. Prof. Pap. Ser. 10, 95 p.

Moore, C.M., and R.F. Labisky
1984 Population parameters of a relatively unexploited stock of snowy grouper in the lower Florida Keys. Trans. Am. Fish. Soc. 113:322–329.

Muhlia-Melo, A.
1975 Aspectos biológicos pesqueros de *Epinephelus morio* (Val.). M.S. thesis, Univ. Nac. Autónoma México, Mexico City, D.F., 68 p.

NMFS (National Marine Fisheries Service)
1990a Fishery management plan for the reef fish of the Gulf of Mexico, Amendment 2. Gulf of Mexico Fish. Manage. Counc., Tampa, 20 p.
1990b Fishery management plan for the snapper-grouper fishery of the South Atlantic Region, Amendment 2. South Atl. Fish. Manage. Counc., Charleston, 28 p.

Odum, W.E.
1971 Pathways of energy flow in a south Florida estuary. Univ. Miami Sea Grant Prog. Sea Grant Tech. Bull. 7, 162 p.

Odum, W.E., C.C. McIvor, and T.J. Smith III
1982 The ecology of the mangroves of south Florida: A community profile. U.S. Fish Wildl. Serv. Biol. Serv. FWS-OBS-81/24, 144 p.

Olsen, L.S.
1952 Some nematodes parasitic in marine fishes. Publ. Inst. Mar. Sci. Univ. Tex. 2:173–215.

Pearse, A.S.
1934 Observations on the parasites and commensals found associated with crustaceans and fishes at Dry Tortugas, Florida. Carnegie Inst. Washington Publ. Pap. Tortugas Lab. 28(435):104–115.

1952 Parasitic crustacea from the Texas coast. Publ. Inst. Mar. Sci. Univ. Tex. 2(2):5–42.

Randall, J.E.

1967 Food habits of reef fishes of the West Indies. Stud. Trop. Oceanogr. Inst. Mar. Sci. Univ. Miami 5:665–847.

Robins, C.R., G.C. Ray, J. Douglass, and R. Freund

1986 A field guide to Atlantic coast fishes of North America. Peterson Field Guide Ser. 32, Houghton Mifflin, Boston, 354 p.

Sadovy, Y., and D.Y. Shapiro

1987 Criteria for the diagnosis of hermaphroditism in fishes. Copeia 1987:136–156.

Saila, S.B., C.W. Recksiek, and M.H. Prager

1988 Basic fishery science programs, a compendium of microcomputer programs and manual of operation. Elsevier Sci. Publ., NY, 230 p.

Schroeder, W.C.

1924 Fisheries of Key West and the clam industry of southern Florida. Appendix XII to the Report of the U.S. Commissioner of Fisheries for 1923. Bur. Fish. Doc. 962, 74 p.

Smith, C.L.

1971 A revision of the American groupers: *Epinephelus* and allied genera. Bull. Am. Mus. Nat. Hist. 146:67–242.

1982 Patterns of reproduction in coral reef fishes. *In* Huntsman, G.R., W.R. Nicholson, and W.W. Fox Jr. (eds.), The biological bases for reef fishery management, p. 49–66. NOAA Tech. Memo. NOAA-TM-NMFS-SEFC-80, Beaufort Lab., Southeast Fish. Sci. Cent., Beaufort, NC.

Smith, G.B.

1976 Ecology and distribution of eastern Gulf of Mexico reef fishes. Fla. Mar. Res. Publ. 19, 78 p.

Tabb, D.C., and R.B. Manning

1961 A checklist of the flora and fauna of northern Florida Bay and adjacent brackish waters of the Florida mainland collected during the period July 1957 through September 1960. Bull. Mar. Sci. Gulf Caribb. 11:552–649.

von Bertalanffy, L.

1957 Quantitative laws in metabolism and growth. Q. Rev. Biol. 32:217–231.

Genetic patchiness among populations of queen conch *Strombus gigas* in the Florida Keys and Bimini*

Donald E. Campton
Department of Fisheries and Aquaculture, University of Florida
7922 NW 71st Street, Gainesville, Florida 32606-0300

Carl J. Berg Jr.
Florida Marine Research Institute, Florida Department of Natural Resources
13365 Overseas Highway, Marathon, Florida 33050
Current address: P.O. Box 769, Kilauea, Hawaii 90754

Lynn M. Robison
Department of Fisheries and Aquaculture, University of Florida
7922 NW 71st Street, Gainesville, Florida 32606-0300
Current address: Department of Fisheries and Allied Aquacultures
Auburn University, Auburn, Alabama 36849

Robert A. Glazer
Florida Marine Research Institute, Florida Department of Natural Resources
13365 Overseas Highway, Marathon, Florida 33050

Abstract.– Allozymes were used to examine spatial and temporal components of genetic variation among populations of queen conch in the Florida Keys and Bimini over a 4-year period. Spatial and temporal genetic variation were both significant ($P<0.001$) despite high levels of genetic similarity among samples (mean Nei's I, 0.994). However, no consistent pattern of variation was observed. The gene diversity among localities (G_{LT} 0.50%) did not differ significantly ($P>0.05$) from the diversity among years or samples within localities (G_{SL} 0.60%). In addition, Florida Keys and Bimini populations were very similar genetically to those studied previously in the Caribbean Sea and Bermuda (mean Nei's I, 0.988). In general, populations of queen conch appear to be structured as a mosaic of spatial and temporal genetic patchiness within a continuum of high genetic similarity. This genetic similarity is presumably maintained by larval drift and gene flow. However, the observed patterns of genetic variation suggest a dynamic population structure. This structure may reflect presettlement stochastic events and processes in the marine environment.

The queen conch *Strombus gigas* is a large marine gastropod of significant economic importance to the Caribbean Sea area (reviewed by Berg and Olsen 1989). The native range of the species extends from south Florida to Venezuela and eastward from Central America to the Bahama and West Indies Islands. An isolated population also inhabits the coastal waters of Bermuda. The species has been heavily exploited in commercial, recreational, and subsistance fisheries throughout its geographic range. Many populations are considered depleted or overfished.

The life history of queen conch suggests the potential for extensive gene flow through larval dispersal (Scheltema 1971, 1986). Laboratory studies indicate that larvae maintain the planktonic stage for 12–35 days ($\bar{x}$ 21 days) before settling and metamorphosis (Ballantine and Appledoorn 1983, Davis and Hesse 1983). Larvae entrained in swift, Caribbean currents (1–3 km/h) could thus be transported significant distances (Kinder et al. 1985). However, dispersal and recruitment patterns of *S. gigas* during the planktonic stage are largely unknown. Effective management and rehabilitation of the species throughout its geographic range necessitate an understanding of population structure, patterns of gene flow, and genetic relationships.

In a recent allozyme study, Mitton et al. (1989) found a high level of genetic similarity among populations of queen conch from eight localities throughout the Caribbean Sea. However, significant spatial heterogeneity in allele frequencies indicated that the sampled populations were not totally panmictic. In addition, allele frequencies for the geographically disjunct population of Bermuda were distinctive at one locus.

Manuscript accepted 4 March 1992.
Fishery Bulletin, U.S. 90:250–259 (1992).

* Journal Series R-01534, Florida Agricultural Experiment Station.

In the study described here, allozymes were used to examine the genetic structure of queen conch populations in the Florida Keys and Bimini. We collected conch from the same localities in multiple years to compare spatial and temporal components of genetic variation. Testing the relative significance of those two components was a major objective of our study.

Materials and methods

Sampled populations

Queen conch were collected between 1987 and 1990 from four localities in the Florida Keys and from Bimini, a linear distance of approximately 350 km (Table 1, Fig. 1). Samples of conch were obtained in multiple years from Ballast Key, Coffins Patch, and Craig Key. Single samples were obtained from Key Biscayne and Bimini. All animals were collected by scuba diving or snorkeling.

The shell length, or major axis, of each conch was measured with calipers to the nearest mm. Based on size distributions, the Coffins Patch population (or aggregation) appeared to be a single year-class or cohort that we sampled in three consecutive years (Table 1). All other populations represented mixtures of year-classes with new recruits added each year.

Tissues

Conch collected in 1987 (three samples) were processed according to the methods of Mitton et al. (1989): Only the distal tip of the digestive gland, including gonad and associated connective tissue, was retained for enzyme extraction. We were not able to resolve some of the enzymes or presumptive loci reported by Mitton et al. (1989) but were able to resolve some enzymes and loci not examined previously. Consequently, from each of 12 conch collected from Ballast Key in February, 1988 (Table 1), we dissected six tissues for further screening of enzymes and loci: (1) foot muscle, (2) proboscis with radula, (3) eyes and eyestalks, (4) crystalline style, (5) mantle tissue, and (6) distal tip of the digestive gland (Little 1965). Thirty-eight enzymes

Table 1

Means ± standard errors (SE) and ranges of shell length for samples of queen conch *Strombus gigas* collected from four localities in the Florida Keys and Bimini, 1987–90.

			Length (mm)	
Locality	Year	*N*	Mean ± SE	Range
Ballast Key	1987	56	167 ± 6.2	96–241
	1988[a]	12	125 ± 5.6	91–157
	1988[b]	30	135 ± 4.2	69–167
Coffins Patch	1988	100	58 ± 0.4	46–71
	1989	102	98 ± 0.6	87–112
	1990	100	142 ± 0.9	117–170
Craig Key	1987	105	177 ± 2.5	127–267
	1989	71	225 ± 3.5	137–257
	1990	92	187 ± 3.5	125–252
Key Biscayne	1987	79	155 ± 3.5	99–216
Bimini	1989	96	194 ± 2.0	127–236

[a] February collection.
[b] April collection.

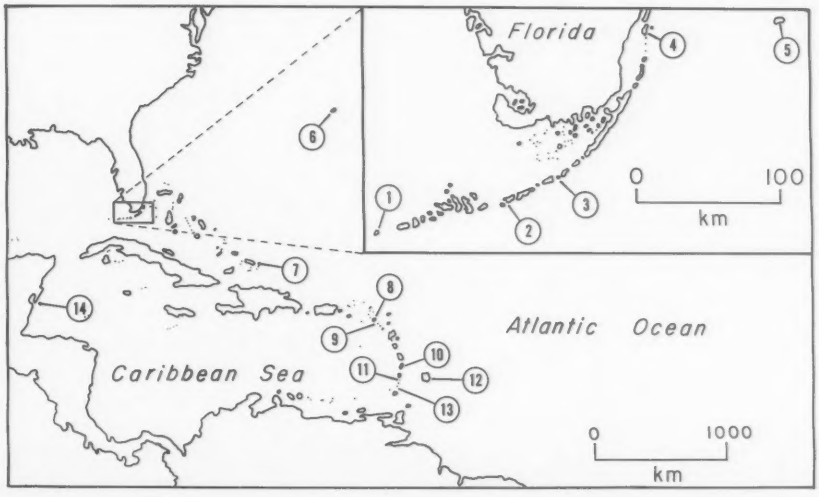

Figure 1

Localities from which queen conch *Strombus gigas* were collected. For the study described here, conch were collected from (1) Ballast Key, (2) Coffins Patch, (3) Craig Key, (4) Key Biscayne, and (5) Bimini. Localities 6–14 are from Mitton et al. (1989): (6) Bermuda, 1 site; (7) Turks and Caicos Islands, 4 sites; (8) St. Kitts, 2 sites; (9) Nevis, 1 site; (10) St. Lucia, 2 sites; (11) Bequia, 1 site; (12) Barbados, 1 site; (13) Grenadines, 3 sites; and (14) Belize, 2 samples, 1 each of the normal and melanic forms.

were assayed in each tissue using a variety of electrophoresis buffers.

On the basis of the aforementioned analyses, three tissues were retained from all conch collected subsequently in 1988–90: (1) foot muscle, (2) proboscis with radula, and (3) digestive gland with gonad. The three tissues were dissected from each individual, placed in separate cryotubes or plastic bags, and frozen in the field with liquid nitrogen or dry ice. All tissues were stored at −80°C until prepared for enzyme extraction.

Table 2
Enzymes and loci resolved in queen conch *Strombus gigas*. Tissues are digestive gland (D), foot muscle (F), and proboscis (P).

Enzyme	Enzyme number	Locus	Tissue	Optimum buffer[a]
Aspartate aminotransferase	2.6.1.1	*AAT-1**	D,P	TC
		*AAT-2**	F,P	TC
Argenine kinase	2.7.3.3	*ARGK**	F	TC
Dipeptidase[b] (substrates: Leu-Ala, Leu-Tyr)	3.4.13.11	[b]*DPEP-1**	D,F,P	TLBC-2,TC
		*DPEP-2**	D,F,P	TLBC-1
		*DPEP-3**	D,F,P	TLBC-1
Glucose-6-phosphate dehydrogenase	1.1.1.49	*G6PDH**	D	TLBC-2
Glucose-6-phosphate isomerase	5.3.1.9	*GPI**	D,F,P	TC
Isocitrate dehydrogenase ($NADP^+$)	1.1.1.42	*IDHP-1**	D,F,P	AC
		*IDHP-2**	D,F,P	AC
Malate dehydrogenase[b]	1.1.1.37	*MDH-1**	F,P	AC
		[b]*MDH-2**	D,P	AC
Octopine dehydrogenase	1.5.1.11	*ODH**	F,P	TLBC-1
Phosphoglucomutase[b]	5.4.2.2	[b]*PGM-1**	D,F,P	TC
		[b]*PGM-2**	D,F,P	TC
		*PGM-3**	F	TC
Phosphogluconate dehydrogenase[b]	1.1.1.44	[b]*PGDH**	F,P	AC
Tripeptide aminopeptidase (substrate: Leu-Gly-Gly)	3.4.11.4	*TPEP-1**	D,F,P	TLBC-1
		*TPEP-2**	D,F,P	TLBC-1

[a] AC: 0.04 M citric acid adjusted to pH 7.5 with N-(3-aminopropyl) morpholine (Clayton and Tretiak 1972); TBE: Tris-borate-EDTA, pH 8.6 (Boyer et al. 1963); TC: TC buffer of Siciliano and Shaw 1976; TLBC-1: LiOH buffer of Ridgway et al. (1970); TLBC-2: LiOH buffer of Selander et al. (1971).
[b] Enzymes and loci assayed also by Mitton et al. (1989).

Electrophoresis

Allozymes were detected by horizontal starch-gel electrophoresis following the procedures of Aebersold et al. (1987). Enzymes were extracted by homogenizing each tissue separately in 0.5–1.0 volumes of 0.05 M PIPES, 0.05% Triton X-100, and 0.2 mM pyridoxal-5′-phosphate (adjusted to pH 6.8 with 1.0 M NaOH). Gels were prepared with a 12.5% mixture (wt:vol) of Connaught starch (Fisher Sci. Co.) and one of five buffer solutions (Table 2). Histochemical staining of gels followed standard procedures (Morizot and Schmidt 1990). Gels were stained by agar overlay for all enzymes except AAT.

Presumptive loci and alleles were designated by the nomenclature system outlined by Shaklee et al. (1990), except peptidase loci were identified by their di- or tripeptide acronyms (DPEP, TPEP). Multiple loci of a particular enzyme were designated numerically (1, 2, etc.) from fastest to slowest anodic mobility. Alleles of a particular locus were designated by their relative, anodic mobilities (most frequent allele = **100*).

Statistics

Genotypic proportions at each locus were tested for goodness-of-fit to Hardy-Weinberg expectations using the likelihood-ratio test or G-statistic (Sokal and Rohlf 1981). Allele frequencies at each locus were tested for homogeneity among samples by contingency table (samples × alleles) G-tests (Sokal and Rohlf 1981). This total G-statistic, or likelihood ratio, was then partitioned into hierarchical components representing temporal and spatial components of genetic variation within and among localities, respectively (e.g., Smouse and Ward 1978). An approximate F-ratio was then constructed as (G among localities/df)/(G among years within localities/df) to test whether the genetic heterogeneity among localities was significantly greater than the heterogeneity among years within localities. The total gene diversity (Nei 1973) was similarly partitioned into within- and among-locality components following the algorithm of Chakraborty et al. (1982). In all tests of statistical significance, significance probabilities were adjusted for the number of tests (loci) evaluated simultaneously (Rice 1989).

Nei's (1972) index of gene identity was calculated between all population samples. The genetic similarities among all populations, including those sampled by Mitton et al. (1989), were represented graphically in a UPGMA dendrogram (Sneath and Sokal 1973). The 1987 sample from Ballast Key was excluded from these latter analyses because of small sample size (n 12).

Table 3

Allele frequencies for samples of queen conch *Strombus gigas* from the Florida Keys (4 sites) and Bimini. "ND" indicates no data for that locus.

		Ballast Key			Coffins Patch			Craig Key			Key Biscayne	Bimini
Locus	Alleles	1987	1988[a]	1988[b]	1988	1989	1990	1987	1989	1990	1987	1990
*AAT-1**	*100*	0.713	1.00	0.62	0.723	0.755	0.696	0.663	0.671	0.678	0.648	0.591
	120	0.287	—	0.38	0.277	0.245	0.304	0.338	0.329	0.322	0.352	0.403
	130	—	—	—	—	—	—	—	—	—	—	0.005
*AAT-2**	*100*	ND	1.00	1.00	0.975	0.980	0.955	ND	0.993	0.973	ND	0.973
	150		—	—	0.025	0.020	0.045		0.007	0.022		0.016
	31		—	—	—	—	—		—	—		0.011
	180		—	—	—	—	—		—	0.005		—
*DPEP-1**	*100*	0.472	0.42	0.57	0.536	0.536	0.460	0.567	0.521	0.522	0.513	0.565
	108	0.528	0.58	0.43	0.464	0.464	0.540	0.433	0.479	0.478	0.487	0.435
*GPI**	*100*	0.929	1.00	0.98	1.000	0.990	1.000	0.985	1.000	0.995	0.994	0.995
	117	0.071	—	0.02	—	—	—	0.015	—	0.005	0.006	0.005
	78	—	—	—	—	0.010	—	—	—	—	—	—
*IDH-2**	*100*	ND	1.00	1.00	1.000	0.975	0.976	1.000	0.979	0.956	1.000	0.978
	82		—	—	—	0.025	0.024	—	0.021	0.044	—	0.022
*MDH-1**	*100*	ND	1.00	1.00	1.000	0.951	0.960	ND	0.944	0.944	ND	0.982
	120		—	—	—	0.049	0.040		0.056	0.056		0.018
*MDH-2**	*100*	0.794	1.00	1.00	1.000	1.000	1.000	0.955	1.000	1.000	1.000	1.000
	138	0.206	—	—	—	—	—	0.005	—	—	—	—
*ODH**	*100*	ND	1.00	1.00	0.990	0.990	1.000	ND	0.993	0.995	ND	0.995
	68		—	—	0.005	0.010	—		0.007	0.005		0.005
	134		—	—	0.005	—	—		—	—		—
*PGM-1**	*100*	0.723	0.83	0.62	0.665	0.706	0.645	0.737	0.697	0.658	0.709	0.660
	111	0.250	0.17	0.38	0.335	0.279	0.350	0.263	0.275	0.342	0.291	0.340
	89	0.027	—	—	—	0.015	0.005	—	0.028	—	—	—
*PGDH**	*100*	ND	0.59	0.63	0.686	0.721	0.695	ND	0.641	0.696	ND	0.681
	150		0.41	0.37	0.314	0.279	0.305		0.359	0.293		0.319
	200		—	—	—	—	—		—	0.011		—

[a] Data for these conch (February collection) were excluded from the statistical analyses because of small sample size.
[b] April collection.

Results

Nineteen presumptive loci encoding 11 enzymes were resolved electrophoretically (Table 2). Ten loci were polymorphic and were used exclusively in the population analyses (Table 3).

Florida Keys and Bimini populations

Allele frequencies for samples of queen conch from the Florida Keys and Bimini were very similar (Table 3). The gene identity between samples, averaged over the ten polymorphic loci, ranged from 0.978 to 0.999 and averaged 0.994 for all pairwise comparisons. Most alleles were present in all samples, but some rare ($P<0.01$) alleles were detected as only one or two heterozygotes (e.g., *AAT-1*130*). An exception to this latter generalization was the presence of the *MDH-2*138* allele at a frequency of 0.206 (35 **100/100*, 11 **100/138*, and 5 **138/138*) among 51 scored individuals collected from Ballast Key in 1987. Only one heterozygote for this allele was observed elsewhere during the study.

Genotypes conformed ($P>0.05$) to Hardy-Weinberg proportions at all loci except *DPEP-1**. At this latter locus, significant ($P<0.01$) deficits of heterozygotes were detected in 7 of 10 samples. Overall, 285, 279, and 244 individuals had the **100/100*, **100/108*, and **108/108* genotypes, respectively, at *DPEP-1**. This overall deficit of heterozygotes occurred despite similar ($P>0.05$) allele frequencies among samples (Table 3).

Spatial and temporal variation in allele frequencies accounted for minor but approximately equal amounts of gene diversity. The total gene diversity (H_T) averaged 0.202 for the ten polymorphic loci. Of this total, 0.60% and 0.50% were due to temporal and spatial variation within and among localities, respectively

Table 4

Hierarchical likelihood-ratio tests (G-statistics) for homogeneity of allele frequencies among samples of queen conch *Strombus gigas* from the Florida Keys and Bimini. Degrees of freedom are in parentheses.

Source of variation	*AAT-1**	*AAT-2**	*DPEP-1**	*GPI**	*IDH-2**	*MDH-1**
Total	19.68(18)	20.03(18)	7.84(9)	43.22(18)**	21.09(8)*	24.51(6)**
Among localities	16.26(8)	15.21(9)	2.42(4)	32.66(8)*	9.48(4)	9.57(3)
Within localities	3.42(5)	4.82(4)	5.42(5)	10.57(5)	11.61(4)	14.95(3)*
Ballast Key	1.62(1)	—	1.38(1)	2.81(1)	—	—
Coffins Patch	1.71(2)	2.37(2)	3.04(2)	4.36(2)	4.41(2)	14.94(2)**
Craig Key	0.09(2)	2.45(2)	1.00(2)	3.40(2)	7.20(2)	0.01(1)
(Approx. F-ratio[a])	2.97(8,5)	1.40(9,4)	0.56(4,5)	1.93(8,5)	0.82(4,4)	0.64(3,3)

Source of variation	*MDH-2**	*ODH**	*PGM-1**	*PGDH**	Total
Total	116.83(9)***	7.03(12)	34.13(18)	10.97(12)	305.33(128)***
Among localities	95.42(4)***	2.02(6)	8.79(8)	6.65(6)	198.48(60)***
Within localities	21.41(3)***	5.00(5)	25.34(10)*	4.32(4)	106.86(48)***
Ballast Key	19.54(1)***	—	5.49(2)	—	30.84(6)***
Coffins Patch	—	4.97(4)	6.58(4)	0.61(2)	42.99(22)**
Craig Key	1.87(2)	0.03(1)	13.27(4)	3.71(2)	33.03(20)*
(Approx. F-ratio[a])	3.34(4,3)	0.37(6,5)	0.43(8,10)	1.03(6,4)	1.49(60,48)

[a] Approximate F-ratio = (G among localities/df)/(G within localities/df).
*$P<0.05$; **$P<0.01$; ***$P<0.001$; after adjustment for number of tests (Rice 1989).

(G_{SL} 0.0060, G_{LT} 0.0050). The remaining 98.9% (H_S/H_T) was due to within-sample heterozygosity.

Allele-frequency heterogeneity among samples was significant ($P<0.05$) at several loci and was due to both spatial and temporal components of variation (Table 4). Temporal variation at Ballast Key ($P<0.001$) and Coffins Patch ($P<0.01$) was due primarily to variation at *MDH-2** and *MDH-1**, respectively. On the other hand, the heterogeneity among years at Craig Key ($P<0.05$) was due primarily to the cumulative effects of variation at *IDH-2** and *PGM-1**. Significant allele-frequency variation also existed among localities, but this latter variation did not exceed the temporal variation within localities as measured by F-ratio comparisons ($P>0.05$) at each locus.

Comparisons with Caribbean Sea and Bermuda populations

Allele frequencies at *DPEP-1**, *MDH-2**, *PGM-1**, and *PGDH** for the Florida Keys and Bimini populations of *S. gigas* can be compared directly with those for populations sampled by Mitton et al. (1989). In that previous study, queen conch were collected from 16 sampling sites representing eight major localities throughout the Caribbean Sea area (Fig. 1). In addition, conch were collected from one site in Bermuda.

Patterns of genetic variation among populations in the Caribbean Sea and Bermuda were similar to those for populations in the Florida Keys and Bimini (Table 5). Total gene diversities (H_T) for the two groups of populations were essentially equal (0.355 and 0.354, respectively). However, the diversity within and among localities was somewhat greater for Caribbean Sea and Bermuda populations (G_{LT} 1.69%, G_{SL} 1.14%) than for populations from the Florida Keys and Bimini (G_{LT} 0.39%, G_{SL} 0.68%). This latter result might be expected considering the relative geographic scales over which populations were sampled in the two studies (Fig. 1). In this context, summing G_{LT} and G_{SL} for Florida Keys and Bimini populations yields a percentage of gene diversity (1.07%) that is approximately equal to G_{SL} (sites within localities) for the Caribbean Sea and Bermuda populations (1.14%).

A dendrogram based on Nei's index of gene identity clearly reflected the high genetic similarity among populations of *S. gigas* (Fig. 2). The average gene identity (based on the four aforementioned loci) among populations sampled by Mitton et al. (1989) was 0.984, among those sampled here was 0.993, and between populations (samples) of the two studies was 0.988. Twenty-three of these populations clustered together at the 0.99 level or above. The Bermuda population and the 1987 Ballast Key population (sample) formed a separate subcluster, due primarily to divergent allele frequencies at *MDH-2**. The Vieux Fort (St. Lucia) and Six Hill Cay (Turks and Caicos Islands) populations also clustered separately, due primarily to slightly divergent

Table 5

Percentages of total gene diversity (H_T) among localities (G_{LT}), among samples and sites within localities (G_{SL}), and within samples and sites (H_S/H_T) for populations of queen conch *Strombus gigas* from the Florida Keys and Bimini (this study) and from the Caribbean Sea and Bermuda (Mitton et al. 1989). Data represent the means for *DPEP-1**, *MDH-2**, *PGM-1**, *PGDH**.

		Gene diversity (%)		
Populations	H_T	G_{LT}	G_{SL}	H_S/H_T
Florida Keys and Bimini	0.354	0.39	0.68	98.94
Caribbean Sea and Bermuda	0.355	1.69	1.14	97.17
All populations	0.354	1.24	1.01	97.75

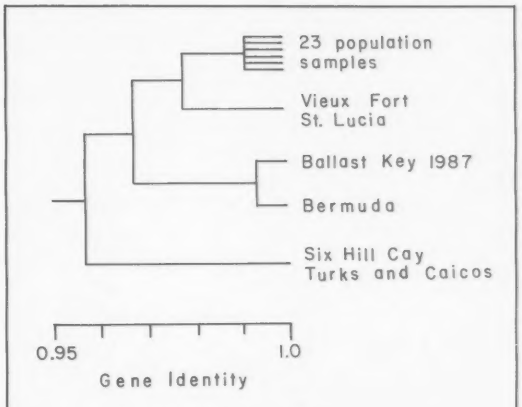

Figure 2

UPGMA dendrogram of genetic similarities among population samples of queen conch *Strombus gigas* based on allele frequencies at *DPEP-1**, *MDH-2**, *PGDH**, and *PGM-1**, and Nei's (1972) index of genetic identity.

allele frequencies at *PGDH** and *DPEP-1**, respectively (Mitton et al. 1989).

In summary, populations of *S. gigas* are very similar genetically and do not appear to be structured geographically. However, those populations cannot be considered totally panmictic.

Discussion

Population structure

Benthic marine invertebrates with planktonic larvae often exhibit spatial and temporal genetic variation similar to that described here for *S. gigas*. For example, Watts et al. (1990) found significant allele-frequency variation among three populations of sea urchin *Echinometra mathaei* separated by only 4km. Moreover, that heterogeneity over a 4km distance was approximately equal to the genetic heterogeneity among populations separated by over 1300km. Those investigators also detected significant allele-frequency variation among year-classes within each of the three microspatial sample sites. Similar patterns of heterogeneity were reported for the limpet *Siphonaria jeanae* (Johnson and Black 1982, 1984ab) and seastar *Acanthaster planei* (Nash et al. 1988, Nishida and Lucas 1988).

Significant microspatial genetic heterogeneity, despite high macrospatial genetic similarity, has been termed "genetic patchiness" (e.g., Johnson and Black 1984b). Such genetic patchiness could be due to either postsettlement natural selection or genetic heterogeneity among groups of recruits that are spatially or temporally separated (Watts et al. 1990). Under both hypotheses, planktonic dispersal is believed to maintain high genetic similarity among populations over broad geographic areas. However, under postsettlement natural selection, one would expect genetic variation among localities to be greater than the temporal variation within localities because of local adaptation. Conversely, under the model of presettlement genetic heterogeneity, spatial and temporal components of genetic variation are expected to be equal because the population structure would result from presettlement events that were independent of the specific localities at which settlement occurred. Under this latter model, spatial heterogeneity among localities would simply reflect the temporal heterogeneity within localities.

Results obtained here for *S. gigas* are most consistent with the presettlement hypothesis of genetic patchiness. Populations of queen conch throughout their geographic range are very similar genetically, yet spatial and temporal components of genetic variation appear significant and approximately equal. Mitton et al. (1989) obtained similar results for macrospatial (among-locality) and microspatial (within-locality) components of genetic variation. These results suggest a dynamic population structure in which allele-frequency heterogeneity may exist among groups of recruits that settle in different years at the same locality or at different localities in the same year. Johnson and Black (1982, 1984ab) and Watts et al. (1990) reached similar conclusions regarding genetic patchiness among populations of limpet and sea urchin, respectively.

Several mechanisms can be invoked to explain genetic patchiness due to presettlement events. Johnson and Black (1984ab) and Watts et al. (1990) suggest that

selective mortality prior to settlement, possibly reflecting stochastic variation in the marine environment (e.g., water temperature, salinity), may be responsible for the "chaotic genetic patchiness" that they observed. Alternatively, temporal variation in the source of recruits for each locality and/or genetic drift resulting from a finite number of breeders could also generate random genetic patchiness on both temporal and spatial scales (e.g., Waples 1989). None of these aforementioned hypotheses can be excluded with the available data.

The effective number of breeders (N_e) contributing to a cohort of larvae that settle together at a particular location is unknown for *S. gigas*. Males and females breed in aggregations at characteristic locations over a 6–9 month period, and each female may produce several egg masses of approximately 310,000–750,000 eggs each during the breeding season (Robertson 1959, Randall 1964, Weil and Laughlin 1984, Berg and Olson 1989). Several females within an aggregation may lay their egg masses simultaneously, and because the rate of embryonic development is temperature-related, hordes of larvae are released synchronously. These larvae can thus be entrained together into the water column and affected simultaneously by marine and oceanic processes. Consequently, hordes of larvae from a finite number of parents could potentially be presented simultaneously to a substrate that would induce settlement and metamorphosis.

Recently, Bucklin et al. (1989) and Bucklin (1991) obtained evidence that ocean currents and related processes (e.g., upwellings, eddies, offshore jets) can spatially and temporally maintain genetically discrete cohorts of zooplankton in the marine environment. For example, Bucklin et al. (1989) concluded that such processes "prevented homogenization of the plankton assemblages during transport" and that "plankton populations in complex flow fields may show patchiness in biological, biochemical, and/or genetic character at small time/space scales." Their results suggest that similar processes could affect significantly the distribution of pelagic larvae following their release into the water column.

The source of *S. gigas* recruits for the Florida Keys is unknown. The Florida Current, which sweeps eastward past the Florida Keys and subsequently forms the Gulf Stream, is created by the massive flow of warm water northward from the Caribbean Sea through the Yucatan Channel. This current could entrain large numbers of larvae from numerous locations prior to flowing eastward past the Florida Keys (Mitton et al. 1989). Stochastic variations in water currents, surface winds, and meteorological events (e.g., tropical storms) could thus affect significantly the source of *S. gigas* recruits for any particular locality. During the course of our study, we attempted to gain permission to collect conch from Cuba and Yucatan, Mexico—two possible sources of recruits for the Florida Keys—but were unable to do so.

One potential shortcoming of our study was that the temporal effects of recruitment were confounded with other population processes; that is, temporal genetic variation was measured among mixed aggregations of conch sampled in different years at the same locality and not among separate year-classes or cohorts. With the exception of the Coffins Patch population or aggregation (see below), all samples consisted of mixed age- and size-classes with new recruits added each year. In addition, some of the temporal genetic variation may have been due to migration of juveniles and adults into and out of the study areas (Hesse 1979, Weil and Laughlin 1984, Stoner et al. 1988, Stoner 1989). Consequently, we cannot separate the temporal effects of recruitment from other population processes. However, our goal was not to estimate temporal genetic variation among cohorts or year-classes *per se*, but rather to provide a measure of within-population (i.e., within-locality) variation by which the significance of genetic variation among localities could be evaluated. Population processes causing temporal genetic variation within localities would similarly affect the genetic variation among localities. Some measure of temporal variation was thus needed before the microevolutionary significance of genetic variation among localities could be ascertained. Alternatively, some form of stratified sampling of year- and/or size-classes would be required to separate recruitment or year-class effects from other potential sources of temporal genetic variation.

Possible evidence that recruitment, migration, or similar population processes may significantly affect the population structure of *S. gigas* was the presence of the *MDH-2*(138)* allele at a frequency of 0.206 in the 1987 sample from Ballast Key but the near absence of this allele in the 1988 sample and elsewhere during our study. Mitton et al. (1989) similarly reported, for the Bermuda population, a frequency of 0.30 for a "fast" *MDH-2** allele that was also rare elsewhere. However, the Bermuda population is believed to be self-sustaining with little planktonic recruitment from the Gulf Stream or elsewhere (Mitton et al. 1989). Conversely, Ballast Key is situated within the Florida Current and is the most upstream locality from which we collected conch for the present study. Two distinct aggregations of *S. gigas* may have been sampled at Ballast Key in 1987 and 1988, respectively.

Anomalous results

Coffins Patch Size distributions suggest that the Coffins Patch population was most likely a single year-class

or cohort that we sampled in three consecutive years (1988–90). This population or cohort presumably resulted from a large recruitment event during the summer and fall of 1987. We estimated that the 1987 aggregation at Coffins Patch consisted of at least 250,000 animals covering an area of approximately 30 hectares (Berg and Glazer, unpubl.).

Although the Coffins Patch aggregation appeared to be a single cohort, we detected a significant allele-frequency variation among years (1988–90) at *MDH-1**. This difference was due to the absence of the *MDH-1* (120)* allele in the 1988 sample (n 100) versus the presence of eight **100/120* heterozygotes in both the 1989 (n 102) and 1990 (n 100) samples. The 1989 sample also had one **120/120* homozygote. Sampling error does not adequately explain those results because the probability of obtaining all **100/100* homozygotes in the 1988 sample was only $(0.955^2)^{100} = 0.0001$ (assuming the true frequency of the **120* allele was 0.045 [mean of 1989 and 1990 samples] and random mating). Similarly, differential mortality among genotypes does not adequately explain those results unless heterozygotes were initially very rare and the subsequent mortality of **100/100* homozygotes was extremely high.

Alternatively, recruitment to the Coffins Patch area in 1987 may have been from more than one source population. This could have resulted in an aggregation that was not distributed randomly. Subsequent mixing and/or possible immigration of juveniles (e.g., Stoner 1989) could thus explain changes in allele frequencies between 1988 and 1989. None of these hypotheses can be excluded with the available data.

Regardless of actual mechanism, the presence of only one highly abundant year-class at Coffins Patch over a 3-year period indicates that recruitment to specific localities in the Florida Keys can be highly variable and unpredictable. This observation thus supports the interpretation that genetic patchiness may simply reflect stochastic events prior to settlement.

DPEP-1* We observed a consistent deficit of heterozygotes (with respect to Hardy-Weinberg expectations) at *DPEP-1** but not at other loci. Similar deficits of heterozygotes have been reported often for marine mollusks (reviewed by Gaffney et al. 1990). Such deficits are frequently associated with positive correlations between body size and individual heterozygosity. We also observed a positive correlation between body size and heterozygosity, but genotypic variation at *DPEP-1** did not contribute to that correlation. These results will be described in detail elsewhere (Campton et al. In press).

PGM-2* One possible point of inconsistency between the study described here and that of Mitton et al. (1989) concerns data for *PGM-2**. Mitton et al. (1989) presented only limited data for this latter locus (9 of 17 populations), but those investigators consistently observed a high frequency (0.57–0.69) polymorphism for a "slow" allele. In contrast, we found *PGM-2** to be fixed for a single allele. Only *PGM-1** and *PGM-2** are expressed in digestive gland tissue, which was the only tissue assayed by Mitton et al (1989). However, we also scored PGM in foot muscle which clearly revealed a third, more cathodal locus (*PGM-3**). We also observed three distinct loci in foot tissue of a second conch species, *S. costatus*.

At least three possibilities could thus account for the apparent difference between our results and those of Mitton et al. (1989) at *PGM-2**: (1) our inability to resolve the variant electromorph at *PGM-2**, (2) the partial expression of the *PGM-3** locus in digestive gland tissue (e.g., Allendorf et al. 1983) of individuals sampled by Mitton et al. (1989), thus giving false readings of heterozygotes at *PGM-2**, or (3) the reported allele-frequency difference between the two groups of populations are indeed real. Of the three possibilities, we believe explanations (1) and (2) are the most likely because of the high consistency of our allele frequencies with those of Mitton et al. (1989) at all other loci. Consequently, we believe that this apparent discrepancy at *PGM-2** most likely reflects laboratory-specific adaptations of basic electrophoretic procedures. In this context, we were able to resolve several loci not resolved by Mitton et al. (1989) and vice-versa.

Conclusions

The major finding of our study was the existence of spatial and temporal genetic patchiness among populations of queen conch in the Florida Keys and Bimini. We suggest that such genetic patchiness most likely results from presettlement stochastic events and processes in the marine environment. Nevertheless, these populations are all very similar genetically, presumably reflecting high levels of gene flow due to larval drift. These interpretations are consistent with the results of Mitton et al. (1989) and also explain similar patterns of "chaotic genetic patchiness" in other taxa of marine invertebrates.

Acknowledgments

We thank R. Estling, A. Kirkley, and W. Schumacher for their assistance in the laboratory.

Citations

Aebersold, P.B., G.A. Winans, D.J. Teel, G.B. Milner, and F.M. Utter
1987 Manual for starch gel electrophoresis: A method for the detection of genetic variation. NOAA Tech. Rep. NMFS 61, 19 p.

Allendorf, F.W., R.F. Leary, and K.L. Knudsen
1983 Structural and regulatory variation of phosphoglucomutase in rainbow trout. Isozymes Curr. Top. Biol. Med. Res. 9:123–142.

Ballantine, D.L., and R.S. Appeldoorn
1983 Queen conch culture and future prospects in Puerto Rico. Proc. Gulf Caribb. Fish. Inst. 35:57–63.

Berg, C.J. Jr., and D.A. Olsen
1989 Conservation and management of queen conch (*Strombus gigas*) fisheries in the Caribbean. *In* Caddy, J.F. (ed.), Marine invertebrate fisheries: Their assessment and management, p. 421–442. John Wiley, NY.

Boyer, S.H., D.C. Fainer, and E.J. Watson-Williams
1963 Lactate dehydrogenase variant from human blood: Evidence for molecular subunits. Science (Wash. DC) 141: 642–643.

Bucklin, A., M.M. Rienecker, and C.N.K. Mooers
1989 Genetic tracers of zooplankton transport in coastal filaments off northern California. J. Geophys. Res. 94(C6: 8277–8288.

Bucklin, A.
1991 Population genetic responses of the planktonic copepod *Metridia pacifica* to a coastal eddy in the California Current. J. Geophys. Res. 96(C8):14,799–14,808.

Campton, D.E., C.J. Berg Jr., L.M. Robison, and R.A. Glazer
In press Deficits of heterozygotes and correlation between size and heterozygosity in the marine mollusk, *Strombus gigas* (Gastropoda: Strombidae). Evolution.

Chakraborty, R., M. Haag, N. Ryman, and G. Stahl
1982 Hierarchical gene diversity analysis and its application to brown trout populations. Hereditas 97:17–21.

Clayton, J.W., and D.N. Tretiak
1972 Amine-citrate buffers for pH control in starch gel electrophoresis. J. Fish. Res. Board Can. 29:1169–1172.

Davis, M., and C. Hesse
1983 Third world level conch mariculture in the Turks and Caicos Islands. Proc. Gulf Caribb. Fish Inst. 35:73–82.

Gaffney, P.M., T.M. Scott, R.K. Koehn, and W.J. Diehl
1990 Interrelationships of heterozygosity, growth rate and heterozygote deficiencies in the coot clam, *Mulinia lateralis*. Genetics 124:687–699.

Hesse, K.O.
1979 Movement and migration of the queen conch, *Strombus gigas*, in the Turks and Caicos Islands. Bull. Mar. Sci. 29: 303–311.

Johnson, M.S., and R. Black
1982 Chaotic genetic patchiness in an intertidal limpet, *Siphonaria* sp. Mar. Biol. (Berl.) 70:157–164.
1984a The Wahlund effect and the geographical scale of variation in the intertidal limpet *Siphonaria* sp. Mar. Biol. (Berl.) 79:295–302.
1984b Pattern beneath the chaos: The effect of recruitment on genetic patchiness in an intertidal limpet. Evolution 38: 1371–1383.

Kinder, T.H., G.W. Hebrun, and A.W. Green
1985 Some aspects of the Caribbean circulation. Mar. Geol. 68:25–52.

Little, C.
1965 Notes on the anatomy of the queen conch, *Strombus gigas*. Bull Mar. Sci. 15:338–358.

Mitton, J.B., C.J. Berg Jr., and K.S. Orr
1989 Population structure, larval dispersal, and gene flow in the queen conch, *Strombus gigas*, of the Caribbean. Biol. Bull. (Woods Hole) 177:356–362.

Morizot, D.C., and M.E. Schmidt
1990 Starch gel electrophoresis and histochemical visualization of proteins. *In* Whitmore, D.H. (ed.), Electrophoretic and isoelectric focusing techniques in fisheries management, p. 23–80. CRC Press, Boca Raton.

Nash, W.J., M. Goddard, and J.S. Lucas
1988 Population genetic studies of the crown-of-thorns starfish, *Acanthaster planci* (L.), in the Great Barrier reef region. Coral Reefs 7:11–18.

Nei, M.
1972 Genetic distance between populations. Am. Nat. 106: 283–292.
1973 Analysis of gene diversity in subdivided populations. Proc. Natl. Acad. Sci. USA 70:3321–3323.

Nishida, M., and J.S. Lucas
1988 Genetic differences between geographic populations of the crown-of-thorns starfish throughout the Pacific region. Mar. Biol. (Berl.) 98:359–368.

Randall, J.E.
1964 Contributions to the biology of the queen conch, *Strombus gigas*. Bull. Mar. Sci. 14:246–295.

Rice, W.R.
1989 Analyzing tables of statistical tests. Evolution 43: 223–225.

Ridgway, G.J., S.W. Sherburne, and R.D. Lewis
1970 Polymorphisms in the esterases of Atlantic herring. Trans. Am. Fish. Soc. 99:147–151.

Robertson, R.
1959 Observations on the spawn and veligers of conchs (*Strombus*) in the Bahamas. Proc. Malacol. Soc. Lond. 33:164–171.

Scheltema, R.S.
1971 Larval dispersal as a means of genetic exchange between geographically separated populations of shallow-water benthic marine gastropods. Biol Bull. (Woods Hole) 140:284–322.
1986 On dispersal and planktonic larvae of benthic invertebrates: An eclectic overview and summary of problems. Bull. Mar. Sci. 39:241–256.

Selander, R.K., M.H. Smith, S.H. Yang, W.E. Johnson, and J.B. Gentry
1971 Biochemical polymorphism and systematics in the genus *Peromyscus*. I. Variation in the old field mouse (*Peromyscus polionotus*). Studies in Genetics VI. Univ. Texas Publ. 7103: 49–90.

Shaklee, J.B., F.W. Allendorf, D.C. Morizot, and G.S. Whitt
1990 Gene nomenclature for protein-coding loci in fish. Trans. Am. Fish. Soc. 119:2–15.

Siciliano, M.J., and C.R. Shaw
1976 Separation and visualization of enzymes on gels. *In* Smith, I. (ed.), Chromatographic and electrophoretic techniques. Vol. II, Zone electrophoresis (4th ed.), p. 185–209. Year Book Med. Publ., Chicago.

Smouse, P.E., and R.H. Ward
1978 A comparison of the genetic infrastructure of the Ye'cuana and the Yanomama: A likelihood analysis of genotypic variation among populations. Genetics 88:611–631.

Sneath, P.H.A., and R.R. Sokal
1973 Numerical taxonomy. W.H. Freeman, San Francisco.

Sokal, R.R., and F.J. Rohlf
1981 Biometry. W.H. Freeman, San Francisco.
Stoner, A.W.
1989 Winter mass migration of juvenile queen conch *Strombus gigas* and their influence on the benthic environment. Mar. Ecol. Prog. Ser. 56:99–104.
Stoner, A.W., R.N. Lipcius, L.S. Marshall Jr., and A.T. Bardales
1988 Synchronous emergence and mass migration in juvenile queen conch. Mar. Ecol. Prog. Ser. 49:51–55.
Waples, R.S.
1989 Temporal variation in allele frequencies: Testing the right hypothesis. Evolution 43:1236–1251.
Watts, R.J., M.S. Johnson, and R. Black
1990 Effects of recruitment on genetic patchiness in the urchin *Echinometra mathaei* in western Australia. Mar. Biol. (Berl.) 195:145–151.
Weil, E.M., and R.G. Laughlin
1984 Biology, population dynamics, and reproduction of the queen conch *Strombus gigas* Linnaeus in the Archipielago de Los Roques National Park. J. Shellfish Res. 4:45–62.

Detecting environmental covariates of Pacific whiting *Merluccius productus* growth using a growth-increment regression model

Martin W. Dorn

Alaska Fisheries Science Center, National Marine Fisheries Service, NOAA
7600 Sand Point Way NE, BIN C15700, Seattle, Washington 98115-0070

Abstract.—The growth patterns of Pacific whiting *Merluccius productus*, also known as Pacific hake, were examined for the period 1978–88 using fishery-based estimates of length-at-age. Mean length-at-age and a delta method variance estimate of mean length-at-age were computed for geographic and temporal strata in the U.S. fishery. These calculations took into account the two-phase sampling design used to sample the catch. A factorial analysis of variance of length found significant differences due to age, year, region, sex, and time-period during the fishery. Length increases with age and season. Pacific whiting found in the north are larger, and females are larger than males. The mean length-at-age began declining in 1978, and reached a minimum in 1984. From 1984 to 1986, there was a slight rebound in length-at-age, but after 1986 length-at-age again declined. To investigate the influence of population density and environmental covariates on annual growth, a generalized form of the von Bertalanffy growth model was developed. Deviations from a baseline model for sex-specific asymptotic growth were significantly correlated with changes in sea-surface temperature and adult biomass. Regression results indicate that a 0.5°C increase in mean summer sea-surface temperature would reduce annual growth by 24% at age 1 and 12% at age 4. In contrast, the effect of adult biomass on annual growth becomes greater with age. An increase of 200,000 metric tons (approximately 10% of the mean population biomass) would reduce annual growth by 5% at age 4 and by 10% at age 7. It is proposed that the effect of population density is greater for the older Pacific whiting because their diet has shifted from euphausiids, whose abundance is closely coupled with environmental processes, towards fish species with multiyear life cycles that can be affected by intense Pacific whiting predation.

Manuscript accepted 18 February 1992.
Fishery Bulletin, U.S. 90:260–275 (1992).

This paper describes research on the growth of Pacific whiting, also known as Pacific hake, a gadoid species that is an important component of the California Current ecosystem (Francis 1983). The coastal population of Pacific whiting is currently the target of a major fishery with an average (1977–88) annual harvest of 147,000 metric tons (t) (Dorn and Methot 1990). Adult Pacific whiting migrate north in spring and summer, feeding in the productive waters along the continental shelf and slope from northern California to Vancouver Island, British Columbia. In late autumn, Pacific whiting migrate south to spawning areas from Point Conception, California, to Baja California (Bailey et al. 1982). The U.S. fishery operates from April to November and in recent years has been conducted primarily under joint-venture arrangements, with U.S. fishing boats delivering fish to processing vessels from the Soviet Union, Poland, Japan, and other nations. The Canadian fishery for Pacific whiting is conducted in similar fashion, except that independent fishing by the foreign fleet still accounts for a significant portion of the catch.

Hollowed et al. (1988) observed that the mean length-at-age of Pacific whiting had declined in recent years, and hypothesized that the disruption of normal circulation and temperature patterns associated with the 1983 El Niño may have been the causative factor. The recruitment of strong 1980 and 1984 year-classes increased the population biomass of Pacific whiting to a maximum in 1986. The decline in the length-at-age could also have been a density-dependent growth response to this increase in population abundance. Since the Pacific whiting resource is managed by setting an annual quota in tons based on a conversion using weight-at-age from a projected yield in numbers (Dorn and Methot 1990), changes in growth must be taken into account when making management recommendations about the resource.

The objective of this paper is to examine the pattern of growth variability displayed by the coastal Pacific whiting population, and, in particular, to determine whether environmental covariates or fluctuations in population density could account for the recent changes in length-at-age. Analysis of variance, while useful as an exploratory technique to identify the sources of variability in length-at-age, is inadequate to describe changes in asymptotic growth. The nonlinear regression model presented in this paper is a simple, biologically realistic model for exploring the environmental determinants of asymptotic growth. Its potential utility is not limited to the application described in this paper, i.e., growth of Pacific whiting.

Methods

The U.S. Foreign Fisheries Observer Program at the Alaska Fisheries Science Center (AFSC) uses a two-phase sampling design to sample the catch of Pacific whiting (French et al. 1981). The first phase consists of obtaining a large initial sample of fish and recording the length and sex. For the second phase of sampling, a subsample of fixed size is selected for each combination of length category and sex. All fish in these subsamples are aged using otoliths.

Typically, each observer samples 2–3 hauls or joint-venture deliveries per day for length and sex, and 150 otoliths (5 per centimeter-length category per sex) are collected over a two-month cruise. The numbers of aged and measured fish from 1978–88 are given in Table 1. This information resides in a data base maintained by the Resource Ecology and Fisheries Management Division (REFM) at the Alaska Fisheries Science Center.

Kimura and Chikuni (1987) point out that, with a two-phase sampling design, estimates of mean length-at-age are biased when obtained simply by averaging the lengths of the aged fish. To avoid this bias, stratified length-at-age estimates were compiled from fishery data for the years 1978–88 using separate age-length keys for each stratum (see Appendix for details). Three spatial strata were defined as: (1) the area from lat. 39°00′N to lat. 43°00N, including part of the International North Pacific Fishery Commission (INPFC) Monterey region and the Eureka INPFC region (EUR); (2) the area from lat. 43°00N north to Cape Falcon (lat. 46°45N) in the southern part of the Columbia INPFC region (SCOL); and (3) the area north of Cape Falcon to the U.S.–Canada border including the northern part of the Columbia INPFC region and the U.S. portion of the Vancouver INPFC region (VNC) (Fig. 1).

Table 1

Number of Pacific whiting *Merluccius productus* sampled from the midwater trawl fishery during the years 1978–88 off Washington, Oregon, and northern California.

	Early period April–June		Middle period July–August		Late period Sept.–Nov.		Annual total	
Year	Aged	Measured	Aged	Measured	Aged	Measured	Aged	Measured
1978	2060	31,819	2801	66,153	978	26,799	5839	124,771
1979	1072	37,678	1552	83,584	500	52,094	3124	173,356
1980	844	15,674	2927	43,038	1565	43,536	5336	102,248
1981	1287	26,961	1928	55,174	1053	53,605	4268	135,740
1982	1913	77,529	1463	66,683	882	27,604	4258	171,816
1983	1480	82,186	1277	70,499	475	14,173	3232	166,858
1984	1344	70,888	1304	108,272	662	64,524	3310	243,684
1985	200	23,329	1690	142,592	550	101,089	2440	267,010
1986	1203	125,542	1393	238,779	474	109,786	3070	474,107
1987	1021	102,191	1414	188,361	740	140,902	3175	431,454
1988	1192	125,714	1349	194,246	502	100,184	3043	420,144
Total	13,616	719,511	19,098	1,257,381	8381	734,296	41,095	2,711,188

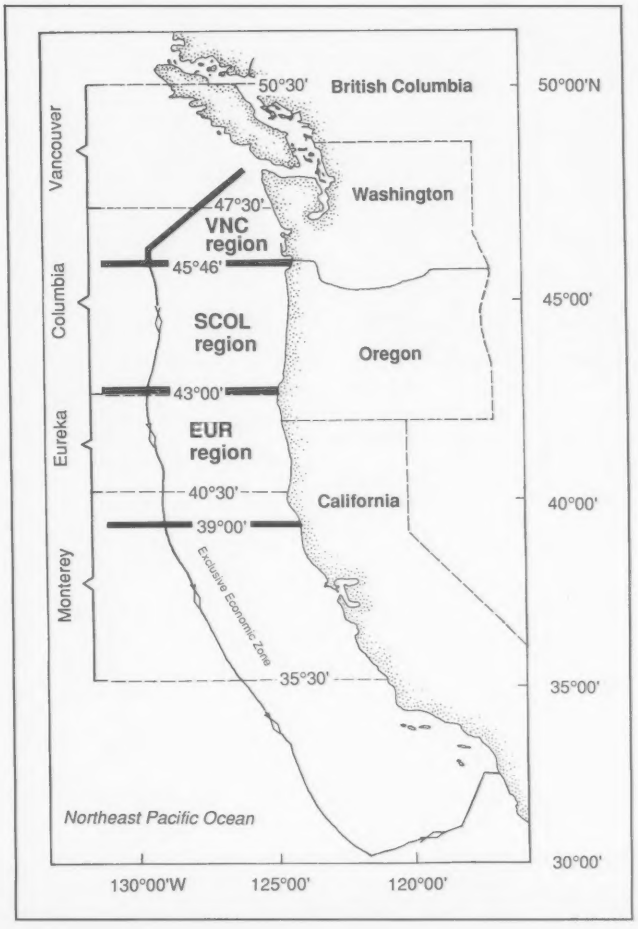

Figure 1

Spatial strata used to compile length-at-age for midwater trawl fishery samples of Pacific whiting *Merluccius productus*.

Each of these geographic regions encloses a center of Pacific whiting abundance and a concentration of fishing activity (Dorn and Methot 1990). Three time-periods were also defined as strata: (1) early (April–June), (2) middle (July–August), and (3) late (September–November). These time-periods divide the fishing season into three roughly equal parts. Over the years 1978–88, 27.9% of the catch came from the early time-period, 47.4% came from the middle time-period, and 24.7% came from the late time-period. In compiling the length-at-age estimates for the spatial and temporal strata, all data collected within that strata were aggregated and assumed to originate from random sampling of the catch within that strata.

Some of the detrimental effects of ageing error bias and low sampling intensity of uncommon age groups—common problems in analyzing fishery length-at-age data—can be reduced if the precision of the length-at-age estimates is known. A delta-method variance estimator of length-at-age for a two-phase sampling plan was derived and implemented for the U.S. fishery samples. Details of this estimator and a procedure for combining the length-at-age from different strata are described in the Appendix.

Two general methods of analyzing the growth in length of fish have been used widely in fishery research. The first method interprets individual observations of length-at-age or mean length-at-age in the population by fitting asymptotic growth curves, most typically the von Bertalanffy (or monomolecular) growth curve (Boehlert and Kappenman 1980, Kimura 1980, Shepherd and Grimes 1983). Using this technique to study environmental effects on growth on an annual scale is difficult because growth curves summarize the growth history of a year-class or a population over the lifespan of the organism. One approach to generalizing growth curves is to include seasonal environmental effects on growth. An example of this is the work of Pauly and Gaschütz (1979); they incorporated a sine wave in the von Bertalanffy growth curve to model the seasonal growth cycle.

The second common approach to analyzing growth data is analysis of variance (ANOVA). Factorial designs have been used to investigate regional growth variability (Francis 1983, Reish et al. 1985). Multiple linear regression is often used to examine the effect of the environment or population density on growth (Kreuz et al. 1982, Ross and Almeida 1986, Peterman and Bradford 1987). A factorial ANOVA of length using age, year, region, sex, and time-period as factors is reported in the Results. It should be recognized, however, that analysis of variance does not account for changes in asymptotic growth, except by fitting interaction terms that tend to obscure the analysis. It is used in this paper only as an exploratory technique to identify the sources of variability in length.

Because asymptotic growth is a universal feature of fish growth, a model to examine the effect of the environment on growth should account for this characteristic. At the same time, such a model must be general enough to allow for covariates to influence annual growth. To meet this objective, a simple extension of the asymptotic von Bertalanffy growth model was developed. The model has a framework similar to analysis of covariance, in that it allows for the possibility of differences in growth between constituent subgroups of the population and differences in growth due to the influence of population density or environmental covariates.

The von Bertalanffy growth model for the mean length l_a of a year-class at age a is given by

$$l_a = l_\infty (1-e^{-k(a-a_0)}),$$

where l_∞ is the asymptotic maximum length, k is a growth coefficient, and a_0 is the hypothetical age at length zero. Subtracting the length at age a+1 from the length at age a gives the first difference of this equation, the annual growth increment from age a to age a+1,

$$l_{a+1} - l_a = l_\infty (1-e^{-k})\, e^{-k(a-a_0)}.$$

Defining $g_0 = \ln[l_\infty(1-e^{-k})]$, and $g_1 = -k$, a simple expression for annual growth is obtained:

$$l_{a+1} - l_a = \exp(g_0 + g_1(a-a_0)).$$

As might be expected, the parameter a_0 becomes redundant in this model for annual growth, since it is confounded with the parameter g_0. One possibility is simply to drop it from the equation. Another alternative, and the one used in this analysis, is to use a_0 to scale chronological age to some initial age for which the growth model is intended to apply. In the Pacific whiting data, there are growth increments from age 1 to age 2, so a_0 is set to 1. In this parameterization, structural growth coefficients, g_0 and g_1, describe simple elements of asymptotic growth: $\exp(g_0)$ is the annual growth increment at age a_0, and g_1 is the exponential decline in the annual growth increment (Fig. 2).

To assess the effect of an environmental covariate, x, this model is augmented with an additional coefficient for that environmental variable,

$$l_{a+1\,t+1\,s} - l_{ats} = \exp[g_0 + \sum_i g_{0i}\, x_i + (g_1 + \sum_j g_{1j}\, x_j)(a-a_0)] + e_{ats},$$

where $e_{ats} \sim N(0, w_{ats}\sigma^2)$. The additional subscripts in this equation are: t for year, s for sex, and i and j to index different environmental variables (e.g., x_i and x_j). The case weights, w_{ats}, are determined by the sum of the estimation variance for the two length-at-age estimates used to calculate the growth increment.

In this regression model, environmental variables can enter as either intercept or slope terms. An intercept coefficient affects g_0 and indicates a constant percent change in the growth increment regardless of age. Slope coefficients affect g_1 and provide flexibility for a varying percent change in the growth increment with age. Together these two types of coefficients, intercept and slope, cover a wide range of different ways that environmental conditions can effect growth at different ages. Note also that in this formulation, it is possible to use indicator variables to parameterize growth differences between different constituent groups of the population; for example, sex differences or geographic differences in growth. This model resembles a linear ANOVA model proposed by Weisberg (1986) to analyze back-calculated fish lengths, though he does not use von Bertalanffy growth to scale the annual growth increments.

The general procedure for fitting a nonlinear regression model in Ratkowsky (1983) was followed using the PAR algorithm in the BMDP statistical package for estimating a nonlinear regression model using weighted least-squares (Dixon 1983). Mean-square error was estimated by fitting a full model consisting of the coefficients g_0 and g_1, and separate intercept and slope coefficients for all environmental covariates (temperature, upwelling, biomass, recruitment strength) assessed in the analysis. Mean-square error was estimated by dividing the residual sum of squares for this model by the degrees of freedom. A full model should account for all the explainable variability, so that the residual error gives an estimate of mean-square error. A P-value of <0.05 was established as the criteria for statistical significance. Because of the presence of negatively-valued growth increments due to measurement error, it was not possible to take the logarithm of the growth increment and analyze the model using linear regression.

The analysis with this model uses the change in mean length of an age-group from the early period of the fishery (April–June) of one year to the early period of the following year. Geographic strata are not used in the analysis because the migratory nature of the coastal population of Pacific whiting would make any conclusions regarding regional growth patterns impossible to defend. It is assumed that the annual increment in growth from one spring to the next is due to conditions prevalent during the summer season of active growth. Although growth increments could be studied for shorter time-periods, this was considered inappropriate for our study because of possible lags between environmental conditions and the growth response of the fish. In addition, the fishery estimates of length-at-

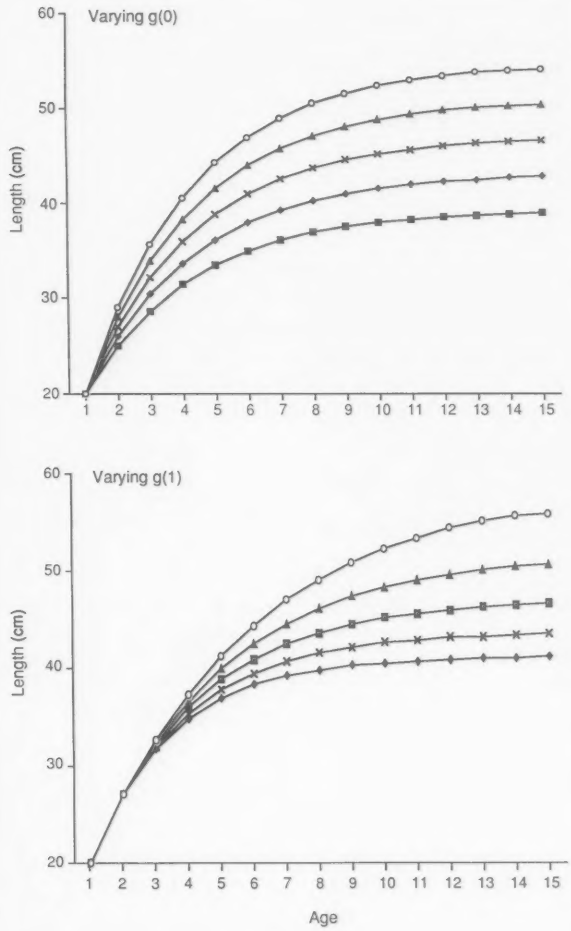

Figure 2

Families of asymptotic von Bertalanffy growth curves parameterized by g_0, the initial growth increment, and g_1, the exponential decline in the annual growth increment with age. All curves were constrained to pass through 20 cm at age 1.

Table 2

Environmental and stock biomass covariates of Pacific whiting *Merluccius productus* growth, assessed using the growth-increment regression model. Mean summer (April–August) sea-surface temperature (°C) is an average over lat. 40–50°N, and from the coast, west to long. 125°W. The Bakun upwelling indices are mean summer coastal upwelling (April–August) from lat. 42–48°N. Stock biomass is measured in millions of tons of age-2 and older fish in the coastal whiting population. Anomalies of temperature, upwelling index, and biomass are calculated as the annual value minus the mean over 1978–87.

Year	Temperature[a] (°C)	Temperature anomaly	Upwelling[b] index	Upwelling anomaly	Biomass[c]	Biomass anomaly
1978	13.1	0.6	49.5	0.3	1.503	−0.268
1979	12.5	0.0	49.2	0.1	1.709	−0.062
1980	12.2	−0.3	67.1	18.0	1.640	−0.131
1981	12.5	0.0	50.0	0.9	1.384	−0.387
1982	12.1	−0.3	55.9	6.7	2.000	0.230
1983	13.4	0.9	31.5	−17.6	1.805	0.035
1984	11.9	−0.5	45.7	−3.4	1.742	−0.029
1985	12.1	−0.4	45.3	−3.8	1.685	−0.086
1986	12.6	0.1	49.6	0.5	2.225	0.455
1987	12.3	−0.2	47.6	−1.5	2.012	0.242
Average 1978–87	12.47		49.15		1.771	

[a] J.G. Norton, Pac. Fish. Environ. Group, P.O. Box 831, Monterey, CA 93942, pers. commun., Aug. 1989.
[b] Mason and Bakun (1986).
[c] Dorn and Methot (1990).

Table 3

Recruitment in billions of age-2 fish to the Pacific whiting *Merluccius productus* population for year-classes 1965–84 (modified from Dorn and Methot 1990). The recruitment anomaly is calculated as the annual number of recruits minus the average over 1965–84.

Year	Recruits	Recruit anomaly
1965	0.692	−0.331
1966	0.786	−0.237
1967	1.110	0.087
1968	0.636	−0.387
1969	0.315	−0.708
1970	3.597	2.574
1971	0.169	−0.854
1972	0.306	−0.717
1973	1.432	0.409
1974	0.139	−0.884
1975	0.220	−0.803
1976	0.094	−0.929
1977	1.716	0.693
1978	0.035	−0.988
1979	0.145	−0.878
1980	4.604	3.581
1981	0.022	−1.001
1982	0.042	−0.981
1983	0.183	−0.840
1984	4.221	3.198
Average 1965-84	1.023	

age are not point estimates in time, but averages over 2 or 3 months. As a result, relating the growth increment to the environment over a short time-period would tend to blur environmentally-determined growth differences.

The environmental variables and stock abundance measures examined in the analysis were intentionally limited to a few variables which would characterize the environment of the population on the largest scale possible. The environmental variables are summer averages over the geographic range of the mature stock. Mean summer (April–August) sea-surface temperature (°C), provided by J.G. Norton (Pac. Fish. Environ. Group, Monterey, CA 93942, pers. commun., Aug. 1989), represents the mean value obtained from ships of opportunity between lat. 40°N and 50°N, and from the North American coast west to long. 125°W (Table 2). The Bakun upwelling indices are a mean of the monthly coastal upwelling indices during April–August from lat. 42–48°N and are in units of metric tons of water transported through the Ekman layer per second per 100 m of coastline (Mason and Bakun 1986). Stock biomass is measured in millions of tons of age-2 and older fish in the coastal whiting population, and is estimated using the stock synthesis model (Dorn and Methot 1990). The estimates of year-class strength in Table 3 come from the same source.

Results

Length analysis of variance

Annual length-at-age estimates by sex for 1978–88 were obtained using the procedures described in the

Appendix for calculating strata estimates of length-at-age, and for combining the strata estimates to produce an annual estimate (Fig. 3). The decline in length-at-age is evident in graphs of both male and female length-at-age.

The factorial analysis of mean length variance is given in Table 4. Weighted analysis of variance was used with the sampling variances as weights. The F-tests for age, year, region, sex, and time-period were all highly significant ($P<0.0001$). Because of the large number of observations (2072), this result is not surprising. The parameter estimates in Table 4 are defined such that the intercept term represents the mean length of a 1-year-old male in the early part of the season in 1978 in the EUR region. Parameter estimates for the other factor levels can be interpreted as the difference between mean length of Pacific whiting identified by that factor level and those identified by the intercept characteristic with all other factors being held constant.

The results of the ANOVA can be summarized as follows. Length increases with age to age 10, then varies irregularly to age 15 (Table 4). Length increases 0.55 cm from the early period (April–June) to the middle period (July–August), and increases an additional 0.46 cm from the middle period to the late period (September–November). There is an increase of 1.36 cm from the EUR region in the south to the VNC region in the north, indicating that the larger Pacific whiting of an age-group migrate farther north. On average, female Pacific whiting are larger than males by 0.55 cm. Since the ANOVA model does not contain a sex-age interaction, this difference in mean length would apply to all ages. In general, these results are consistent with the previously reported findings on the growth of Pacific whiting (Dark 1975, Francis 1983). The ANOVA year coefficients show the decline in length since 1978. Mean length-at-age reached a minimum in 1984. There was a slight rebound in length-at-age from 1984 to 1986, but after 1986 length-at-age began to decline again.

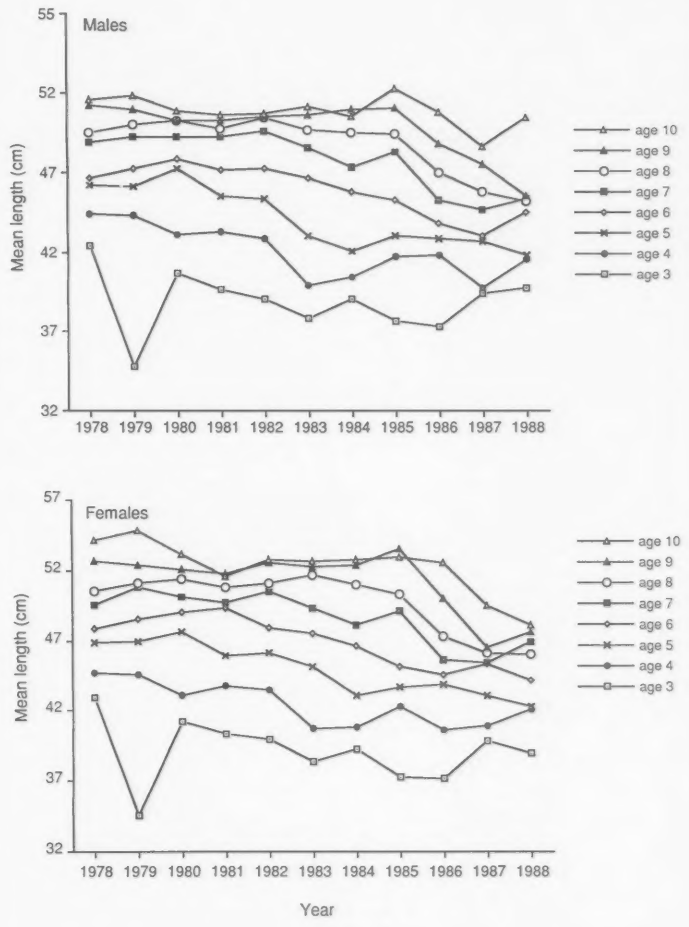

Figure 3

Mean U.S. fishery length-at-age estimates by sex for Pacific whiting *Merluccius productus*, 1978–89. The extremely low estimates of mean length for male and female age-3 fish in 1979 were due to asymmetric error in the ageing of the strong 1977 year-class.

Models containing interaction terms between factors were also analyzed. All the two-way interaction terms were statistically significant, but much less so than the main effects. The addition of more than 200 parameters to describe the two-way interactions would make interpretation difficult. Yet a model with only main effects is clearly inadequate, since it implies, for example, that both the 2-year-old and 12-year-old whiting declined in mean length by the same amount from 1983 to 1984.

Growth increment regression

Before considering the effects of environmental co-

variates, the growth increment model was used to investigate sex differences in growth. This was done by fitting a model with only g_0, g_1, and indicator variables for sex. The P-value for the intercept coefficient for sex was 0.059, but the P-value for the slope term was 0.998. By the criteria established earlier, neither coefficient would be considered statistically significant, although the P-value for the intercept coefficient is close to the critical value. The estimate of the intercept coefficient for sex (0.058) indicates that the females grow approximately 6% ($e^{0.058}$) more than males on an annual basis, regardless of age. A difference of this magnitude is sufficient to account for the greater asymptotic size of the females. Figure 4 shows the fitted sex-specific curves for the annual growth increment. Despite the lack of statistical significance of the intercept term for sex, it was retained in the model while evaluating the significance of environmental covariates on growth. The larger size attained by the female Pacific whiting is compelling evidence that there are sex-specific differences in Pacific whiting growth. Including this term in the baseline model is important because it accounts for this sex-specific variability in growth.

Table 4

Factorial analysis of variance of Pacific whiting *Merluccius productus* length-at-age using midwater trawl fishery samples over 1978–88. The model contains the factors age, year, geographic region, sex, and season. The intercept term estimates the mean length of a 1-year-old male in the early part of the season in 1978 in the EUR region; the other terms estimate the difference in the mean length of fish with that factor level and those with intercept characteristic.

Source	df	SS	Mean square	F-value	$P>F$
Age	14	1,112,327.5	79,452.0	3611.5	<0.001
Year	10	33,126.7	3,312.7	150.6	<0.001
Region	2	5,810.9	2,905.4	132.1	<0.001
Sex	1	2,239.2	2,239.2	101.8	<0.001
Season	2	3,531.0	1,765.5	80.3	<0.001
Error	2042	44,841.1	22.0		

Parameter		Estimate (cm)	SE of estimate
Intercept		26.88	0.211
Age:	2	7.90	0.201
	3	13.22	0.189
	4	17.02	0.147
	5	18.44	0.182
	6	19.39	0.200
	7	20.76	0.205
	8	22.29	0.190
	9	24.04	0.262
	10	29.92	0.308
	11	26.51	0.361
	12	26.07	0.290
	13	27.56	0.528
	14	27.69	0.555
	15	29.94	0.453
Year:	1979	−0.82	0.198
	1980	−0.50	0.174
	1981	−1.54	0.170
	1982	−2.33	0.169
	1983	−3.31	0.187
	1984	−4.64	0.169
	1985	−3.00	0.157
	1986	−2.64	0.175
	1987	−3.03	0.176
	1988	−4.00	0.174
Region:	SCOL	0.57	0.071
	VNC	1.36	0.089
Sex:	Females	0.55	0.052
Season:	Middle	0.53	0.065
	Late	0.99	0.079

Table 5 shows the analysis of variance using the annual growth-increment regression model. The model was built in a forward stepwise fashion, adding the environmental term to the baseline model that resulted in the largest reduction in the residual sum of squares. Temperature and population biomass were significant covariates in the model. Temperature had significant intercept ($P<$ 0.001) and slope terms (P 0.026). For biomass, only the slope term was significant (P 0.002).

The parameter estimates in Table 5 indicate that a 0.5°C increase in mean summer sea-surface temperature will bring about a 24% reduction in the annual growth increment at age 1. At age 4, the same increase in temperature would be expected to produce a 12% reduction in annual growth, and by age 7, the percent reduction would be close to zero. The model predicts an increase in growth due to increasing temperature above age 7, but as annual growth is very slight by this age, the consequences of this prediction are not important. One concern about the reliability of these results is that they may be overdependent on growth during the 1983 El Niño, when sea-surface temperature was the highest during the study. To investigate this possibility, a model was fit to the data excluding the

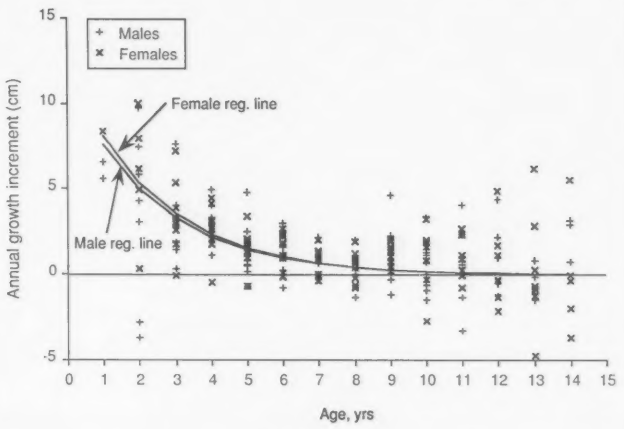

Figure 4

Growth-increment regression curves with different initial growth-increment coefficients (g_0) for male and female Pacific whiting *Merluccius productus*. The distribution of actual growth increments for the years 1978–89 illustrates the saddle-shaped variability of length-at-age statistics based on fishery sampling (N 211). Points represent observed annual growth increments per age-group per year.

Table 5

Analysis of variance of annual length increments using the nonlinear regression model. The coefficient g_0 is an intercept term: $\exp(g_0)$ estimates the growth increment from age 1 to age 2. The coefficient g_1 determines the slope of the exponential decline of the annual growth increment with age under average environmental conditions. Terms relating to covariates are identified as either intercept terms (g_0) or as slope terms (g_1).

Source	df	SS	Mean square	F-value	$P>F$
g_1	1	4067.8	4067.8	1166.5	<0.001
g_0 (sex)	1	12.6	12.6	3.6	0.059
g_0 (temp.)	1	93.5	93.5	26.8	<0.001
g_1 (biomass)	1	36.3	36.3	10.4	0.002
g_1 (temp.)	1	17.4	17.4	5.0	0.026
Error	204	711.4	3.5		

Parameter	Estimate	SE of estimate
g_0	1.995	0.038
g_1	−0.383	0.015
g_0 (sex)	0.058	0.029
g_0 (temp.)	−0.544	0.098
g_1 (biomass)	−0.086	0.027
g_1 (temp.)	0.099	0.043

growth increments from 1983. The parameter estimates followed the same trend as the results in Table 5, with increases in sea-surface temperature associated with large reductions in growth of younger fish, and a decreasing percent reduction with age.

For population biomass, an increase of 200,000t (~10% of the mean population biomass) would cause a 5% reduction in annual growth at age 4, and the percent reduction would increase with age, reaching a 10% reduction at age 7. Because the intercept term for biomass was not significant, growth of the age-1 fish would not be affected by changes in population biomass. During the 10 years studied, range in adult biomass was from 26% above to 22% below the mean of 1.771 million t (1978–87). This lack of contrast in adult biomass makes any interpretation very tentative, but the results do suggest that the effect of population density on growth is relatively small in comparison with the effect of temperature.

None of the other environmental covariates or measures of population density tested in the model were significant. The coefficient for upwelling was highly significant in a model without temperature, but when temperature was included in the regression, upwelling was no longer significant. Because water temperature and the upwelling index are statistically correlated off the coast of Oregon (Kruse and Huyer 1983), the parallel effects of temperature and upwelling index are not unexpected. The same parallel effect was found between year-class abundance and adult biomass. However, adult biomass accounted for more of the variability in annual growth than did year-class abundance. This suggests that the crowding that occurs when a strong year-class recruits to the population is experienced by all the adults, and not just the individuals which make up the strong year-class.

Figure 5 shows the standardized residuals from the final model, plotted against age and year. No trends are evident with respect to age. This plot also shows that the use of the estimation variances as weighting terms in the least-squares fit was successful in stabilizing the error variance with respect to age. However, there still is a noticeable trend in the standardized residuals by year, with positive residuals associated with the earlier years in the time-series (1979 and 1980), and negative residuals with the later years (1985 and 1987). This indicates that the environmental covariates examined thus far are not completely successful in accounting for the decline in mean length-at-age over the past decade.

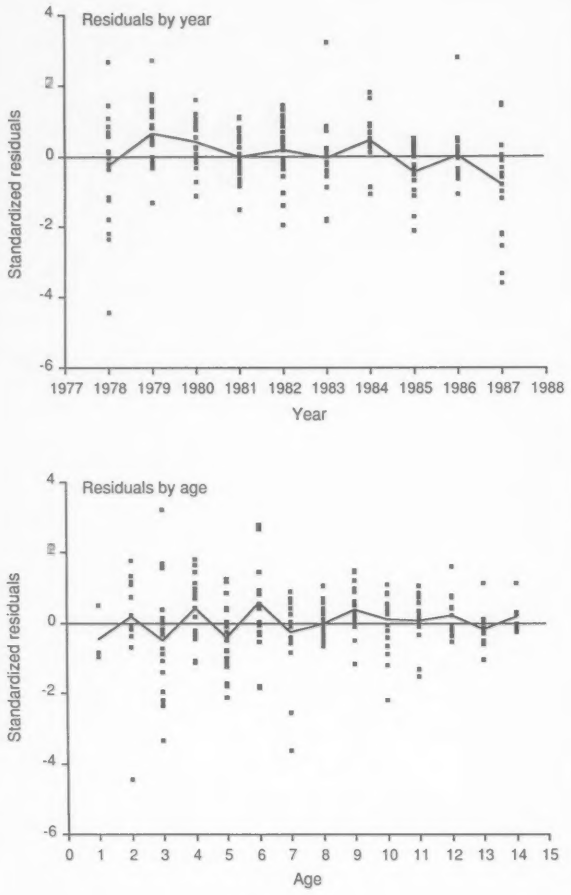

Figure 5

Standardized residuals by age and by year for the final model, which included g_0 and g_1 (coefficients modeling asymptotic growth), and coefficients for sex, sea-surface temperature, and population density. Lines connect averages of the residuals at each cluster of points.

Discussion

Although density-dependent growth has been demonstrated for many fishes (Shepherd and Grimes 1983, Reish et al. 1985, Ware 1985, Ross and Almeida 1986, Peterman and Bradford 1987, Overholtz 1989), few researchers would argue that density-dependent growth is an important characteristic of all fish populations. The age-structured yield models first developed by Beverton and Holt (1957)—currently used to manage many temperate marine fish stocks—use a fixed schedule of weight-at-age to calculate the yield, regardless of the level of population abundance. For a stock of Atlantic mackerel, however, the historically observed variation in weight-at-age attributable to density-dependent growth had a significant effect on the projected yields from the fishery (Overholtz et al. 1991). For Pacific whiting, this potential for changes in weight-at-age to influence yield is taken into account by using the weight-at-age observed in recent years to project the yield for the upcoming year (Dorn and Methot 1990). To obtain a fishing mortality rate that gives the long-term sustainable yield, the average weight-at-age over the history of the fishery is used. This strategy tacitly assumes that the current decline in weight-at-age is not a permanent change in the population.

Parrish et al. (1981) state that the principal resident species of the California Current system do not exhibit density-dependent growth. They contend that the population size of these species is controlled by environmental variability during the larval stages. As a result, the adults are seldom plentiful enough to reach a food-limited carrying capacity.

A contrasting viewpoint is found in Boehlert et al. (1989) who present evidence that the large biomass removals of *Sebastes* spp. in the years 1966–70 off the west coast of the United States resulted in increases in the annual growth of two members of this genus: canary rockfish *S. pinniger* and splitnose rockfish *S. diploproa*. They maintain that the decline in the total abundance of *Sebastes* spp. has had an effect on food availability for individual rockfish species. Although euphausiids are shared by most *Sebastes* species as the principal prey (Brodeur and Percy 1984), they are also a major link in the food chain of the California Current ecosystem, supporting numerous fish and invertebrate populations. For this reason, it is unlikely that changes in the abundance of *Sebastes* spp. alone could have had a substantial impact on the overall abundance of euphausiids in the California Current ecosystem. However, since rockfish are spatially restricted to habitats with limited area, the density-dependent growth displayed by *S. pinniger* and *S. diploproa* may be due to density-dependent changes in the food availability within these habitats. The possibility that cropping by Pacific whiting and other species significantly affects the abundance of euphausiids in the California Current ecosystem at large has not yet been adequately tested, though Mullin and Conversi (1989) were unable to detect any change in the abundance of euphausiids in the California current system after the start of the

large-scale fishery for Pacific whiting *Merluccius productus* in 1966.

Environmental influence on growth has been observed for many marine fish species (Kreuz et al. 1982, Anthony and Fogarty 1985). Because it can be easily measured and is associated with widespread changes in the aquatic environment, water temperature is the covariate most often studied. Water temperature may have a direct physiological effect on the growth of fish, or it may be indirectly linked to growth. For example, decreases in water temperature occur with the onset of upwelling in many coastal marine environments. On the west coast of North America, the availability of coastal upwelling indices on monthly, weekly, and daily time scales (Mason and Bakun 1986) has made it possible to investigate the direct effect of upwelling on growth, although convincing evidence of a link has not yet been found (Kreuz et al. 1982, Francis 1983, Boehlert et al. 1989).

Results from the Pacific whiting growth-increment regression show that an environmental covariate, sea-surface temperature, and population density could explain the deviations from a simple baseline model for asymptotic growth. The effect of temperature was greatest on the youngest ages present in the fishery samples and declined as age increased. In contrast, the effect of population biomass on annual growth increased with age. Temperature was the most important covariate, both in terms of its statistical significance and its effect on growth. This association of enhanced growth and reduced sea temperature is consistent with what is known about the California Current, a major eastern boundary current system. Kreuz et al. (1982) found an identical inverse effect on the growth of English sole *Parophrys vetulus* and Dover sole *Microstomus pacificus* at two locations off the Oregon coast.

Two mechanisms are believed to contribute to the high productivity of the California Current system. Coastal upwelling, generated by wind-driven offshore transport in the surface Ekman layer, brings low temperature, low salinity, and nutrient-rich water to the surface (Bakun and Nelson 1977). A second mechanism is the southward advection of water from the Alaskan Subarctic Gyre. This water is characterized by low temperatures, high nutrient content, and a large standing stock of zooplankton (Roesler and Chelton 1987). Regardless of which mechanism is dominant during a particular year, low mean sea-surface temperature during the summer can be expected to be associated with high productivity.

The diet of Pacific whiting provides the link between primary productivity and growth. The major prey of Pacific whiting are euphausiids, primarily *Thysanoessa spinifera* and *Euphausia pacifica* (Livingston 1983, Rexstad and Pikitch 1986). In summer, the abundance and pattern of distribution of these short-lived species (1–2 yr) are closely tied to upwelling and primary productivity (Simard and Mackas 1989). Rexstad and Pikitch (1986) found that euphausiids comprised 90% by weight of the diet of Pacific whiting 30–44 cm in length collected during a trawl survey in 1983 off the coasts of Oregon and Washington. Above 45 cm, a length which corresponds approximately to ages 5–7, this percentage drops to 20%. In the diet of the older Pacific whiting, euphausiids are largely replaced by small schooling fish and shrimp. These include northern anchovy *Engraulis mordax*, Pacific herring *Clupea harengus pallasi*, eulachon *Thaleichthys pacificus*, pink shrimp *Pandalus jordani*, and rockfish *Sebastes* spp. (Livingston 1983).

This shift in dietary preferences by Pacific whiting may help explain the effect of population biomass on growth. When the biomass of Pacific whiting is high, predation on fish species with multiyear life cycles may become intense enough to reduce their availability to the whiting population. In contrast, euphausiid abundance is closely coupled to annual variations in productivity, so whiting predation would likely have little effect on their abundance.

Some supporting evidence for density-dependent growth of Pacific whiting is found in Dark (1975), who also documented a decline in length-at-age using fishery samples from an earlier period in the fishery, 1964–69. At the time of Dark's research, estimates of population abundance were not available for Pacific whiting. It is now believed that the 1961 year-class was exceptionally strong, nearly the same size as the record 1980 year-class (Dorn and Methot 1990). Consequently, this earlier decline in length-at-age may also be partly attributable to increases in population density as the 1961 year-class moved into the population.

Although weight-at-age is the measure of size typically used in stock assessment models, the analysis in this paper focuses on length rather than weight. A practical reason for this strategy is that most at-sea sampling platforms are not sufficiently stable to obtain accurate individual weights of fish. Indeed, the weights-at-age used in stock assessment models for Pacific whiting are obtained by first estimating length-at-age, then converting to weight using a length-weight relationship (Dorn and Methot 1990). In addition, growth in length has several characteristics that make it amenable for analytical modeling. Except in very rare instances, changes in fish length are always positive or zero. The annual growth increment in length summarizes the growth response of the organism to environmental conditions that are prevalent throughout the year, or are short-term. In contrast, weight-at-age has a seasonal pattern of increase and decline, associated

with spawning, migration, and feeding, which would have to be accounted for in a model before analyzing environmental influences on growth.

Underlying this seasonal pattern of variation in weight is the length-weight relationship characteristic to a species, determined by the overall shape of the fish. Extreme departures from the typical length-weight relationship are unlikely to persist. Fish that are heavy in relation to their length in one year would tend to grow faster in length than average, while underweight fish would tend to experience slower growth in length. Adjustments to an individual's annual reproductive effort can also dampen departures from the typical length-weight relationship (Tyler and Dunn 1976).

During the period covered by this analysis, the length-weight relationship of Pacific whiting has varied from year to year, most noticeably in 1983, when mean weight was extremely low at a given length (Dorn and Methot 1990). The link between anomalies in the length-weight relationship and annual growth increments is best demonstrated by the results of a trial model that used the anomaly in the estimated weight at 45 cm from the annual length-weight regression (Dorn and Methot 1990) as the only predictor variable for the annual growth increment. This variable was highly significant in the model ($P<0.001$), indicating that the annual growth increment is low during years where the length-weight relationship is below average. This result also supports the hypothesis that variation in Pacific whiting length-at-age is caused by environmental processes that affect the availability of food.

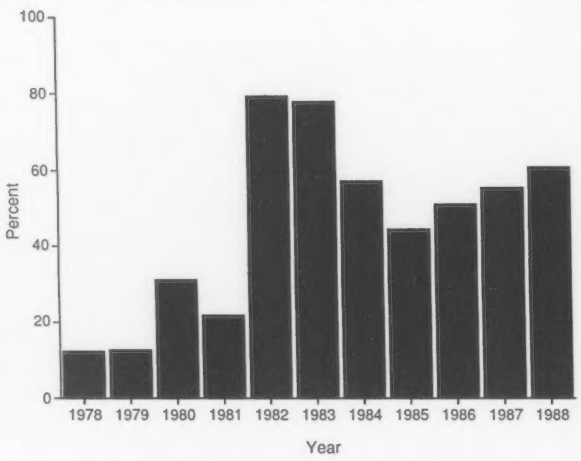

Figure 6

Percent of the Pacific whiting *Merluccius productus* catch biomass taken north of Cape Falcon (lat. 46°45′N) near the mouth of the Columbia River, during 1978–88. Catch of Pacific whiting from the Canadian zone is included in the calculations.

The analysis presented in this paper is based exclusively on fishery data. It should be acknowledged that there are numerous problems associated with the use of fishery statistics to infer growth patterns of fish within a population. Incomplete, size-dependent recruitment to a fishery can make fishery data on length-at-age a biased estimate of population length-at-age. Ageing error can distort the estimates of length-at-age when the year-classes have large differences in abundance. Shifts in the geographic and temporal pattern of the fishery, or shifts in the geographic distribution of the population itself, can cause spurious changes in estimates of length-at-age. The lengths for less abundant age-groups are not estimated as precisely as those for abundant age-groups. This is particularly true of extremely young and old fish, as these age-groups may be represented in fishery samples by only one or two individuals which determine the mean length for that age-group.

The severity of some of these problems can be reduced by using the procedures described in the Appendix for compiling strata estimates of length-at-age and calculating variance estimates. Length-at-age for temporal and geographic strata can be examined separately before being combined to produce annual summary statistics. Length-at-age estimates based on only a few individuals can be discounted in the analysis by using the estimated variances of length-at-age as weights. Nevertheless, some factors affecting growth can only be addressed by modeling fisheries as both a source of information on the stock and a major influence on its dynamics. The growth-increment regression model used in this paper assumes that the fishery samples the population without bias, so it is not the appropriate framework for studying these processes. Models with size-selective fishing mortality and stochastic growth have been developed for exploited fish populations (Deriso and Parma 1988, Parma and Deriso 1990). The practical application of these models is limited by the difficulty of distinguishing between different sources of growth variability using only catch data.

Size-selective mortality may have played a role in causing variation in length-at-age of Pacific whiting over the years covered by this analysis. Since the length ANOVA found a significant increase in length from south to north, a northward shift in the fishery would tend to increase length-at-age in the catch. At the same time, however, the length-at-age of the survivors of the

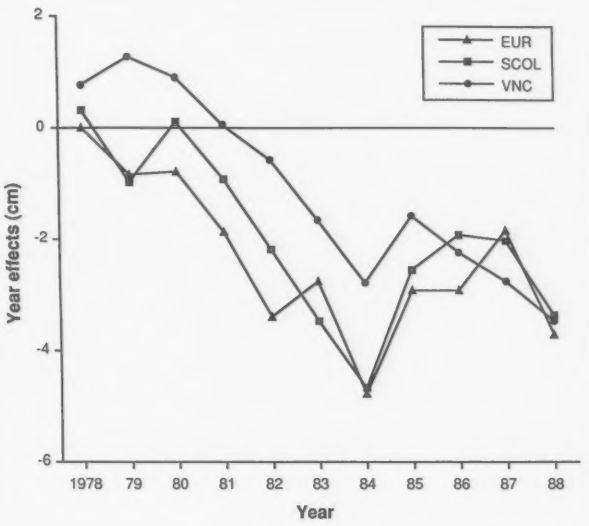

Figure 7

Estimated coefficients for a region-year interaction in a factorial analysis of variance, with the terms age, year, region, sex, season, and region-year interaction, for U.S. fishery length-at-age estimates of Pacific whiting *Merluccius productus* over 1978–88.

fishery would decrease, and this would tend to decrease the length-at-age in the catch in the following year from what it would have been otherwise. From 1978 to 1982, the fraction of the Pacific whiting catch taken north of Cape Falcon (near the mouth of the Columbia River at lat. 46°45′N) increased from 10% to 80%, and was 60% in 1988 (Fig. 6). The lack of fit of the growth-increment regression model with respect to year in Figure 5 may have been a result of this northward shift in fishing mortality.

However, it is difficult to predict the long-term effects of a shift in the geographic pattern of exploitation on length-at-age, because little is known about the extent of mixing from one year to the next of fish migrating from different regions. Without mixing between regions, an increase in fishing in the northern part of the range would reduce the abundance of larger individuals of an age-group, reducing the overall population length-at-age, while length-at-age of the southern fish would be unaffected. A more likely hypothesis is that some inter-regional mixing occurs from year to year. In this case, the length-at-age in all regions would decrease, though the magnitude of the decrease should be greatest in the north where the higher fishing occurred. Ultimately, this would tend to reduce latitudinal variation in length-at-age.

To support this hypothesis, there is some evidence of a change in the degree of latitudinal segregation by size of Pacific whiting. Figure 7 shows the coefficients for a region-year interaction for a length ANOVA with main effects being age, year, region, sex, and season. The absence of interaction between year and region would be identified by parallel year effect lines for each region, and would indicate that size-specific migratory pattern has remained constant. From 1978 to 1985, the region-year interaction does not appear prominent. After 1985, however, the lengths-at-age in the three regions become much closer together; in particular, the lengths of the fish in the VNC region, instead of being 1–2cm larger than the fish in the other regions, are the same size or smaller.

Recently, Smith et al. (1990) examined the length-at-age data from the fishery for Pacific whiting in the Canadian waters over the same years examined by this paper. They used a generalized form of the von Bertalanffy growth model that makes length-at-age a function of length-at-age in the previous year, plus environmental covariates modeled in different ways according to a hypothesized mechanism by which the environmental covariate affects growth or apparent growth. Significant covariates in their model were population biomass, a suite of oceanographic variables measuring the strength of southward advection of water from the Alaskan Subarctic Gyre, and several variables that model size-selective mortality. Since fish younger than age 5 are not common in the Canadian samples, their analysis could not examine the sources of growth variability of the younger fish. Consequently, the analysis presented here on the environmental covariates of Pacific whiting growth in U.S. waters is a necessary complement to the paper by Smith et al. (1990). For example, an inverse relationship between temperature and growth, which is most pronounced for the younger fish, was not detected by Smith et al. (1990), and can partly account for the fact that the fish currently recruiting to Canadian waters at age 5 are much smaller than those recruiting in the late 1970's.

A major contention of Smith et al. (1990) is that expansion of the Canadian fishery is largely responsible for the decline in length-at-age observed since 1976. They used the ratio of the Canadian catch (in biomass) to the total population biomass during the current year as a covariate in their nonlinear regression model, a phenomenological approach that sidesteps the need to model the population dynamics. Although the monotonically increasing Canadian catch of Pacific whiting

since 1976 (except for 1985) and the declining length-at-age over the same period guarantees a statistically significant result, the real role of the Canadian fishery in determining length-at-age can be established only in a wider context that considers the magnitude and the geographic pattern of the fishery for Pacific whiting in U.S. waters. The region-year interaction coefficients in Figure 7 show that, up until 1984, the severity of the decline in length-at-age was similar in all three geographic regions in U.S. waters, extending from California north to the U.S.–Canada border. This is difficult to reconcile with the contention that the Canadian fishery is primarily responsible for the decline in length-at-age.

Both Smith et al. (1990) and this study used growth models that do not take into account the dynamics of the population, and as a consequence both have shortcomings which limit the growth- related phenomena to which they can be applied. An important direction for further research is the development of models for Pacific whiting that simultaneously model the growth and the population dynamics of the stock, including size-specific migratory behavior.

Acknowledgments

I thank Anne Hollowed, Daniel Kimura, Patricia Livingston, and Richard Methot for their comments on a preliminary version of this paper. In addition, suggestions by two anonymous reviewers significantly improved this paper.

Citations

Anthony, V.C., and M.J. Fogarty
1985 Environmental effects on recruitment, growth, and vulnerability of Atlantic herring (*Clupea harengus*) in the Gulf of Maine region. Can. J. Fish. Aquat. Sci. 42(Suppl. 1):158–173.

Bailey, K.M., R.C. Francis, and P.R. Stevens
1982 The life history and fishery of Pacific whiting, *Merluccius productus*. Calif. Coop. Oceanic Fish. Invest. Rep. 23: 81–98.

Bakun, A., and C.S. Nelson
1977 Climatology of upwelling related processes off Baja California. Calif. Coop. Oceanic Fish. Invest. Rep. 19:107–127.

Beverton, R.J.H., and S.J. Holt
1957 On the dynamics of exploited fish populations. Fish. Invest. Minist. Agric. Fish. Food (G.B.) Ser. II(19), 533 p.

Boehlert, G.W., and R.F. Kappenman
1980 Variation of growth with latitude in two species of rockfish (*Sebastes pinniger* and *S. diploproa*) from the northeast Pacific Ocean. Mar. Ecol. Prog. Ser. 3:1–10.

Boehlert, G.W., M.M. Yoklavich, and D.B. Chelton
1989 Time series of growth in the genus *Sebastes* from the northeast Pacific Ocean. Fish. Bull., U.S. 87:791–806.

Brodeur, R.D., and W.G. Pearcy
1984 Food habits and dietary overlap of some shelf rockfishes (genus *Sebastes*) from the northeastern Pacific Ocean. Fish. Bull., U.S. 82:269–294.

Dark, T.A.
1975 Age and growth of Pacific hake, *Merluccius productus*. Fish. Bull., U.S. 73:336–355.

Deriso, R.B., and A.M. Parma
1988 Dynamics of age and size for a stochastic population model. Can. J. Fish. Aquat. Sci. 45:1054–1068.

Dixon, W.J. (editor)
1983 BMDP statistical software. Univ. Calif. Press, Berkeley, 734 p.

Dorn, M.W., and R.D. Methot
1990 Status of the Pacific whiting resource in 1989 and recommendations for management in 1990. NOAA Tech. Memo. NMFS F/NWC-182, Alaska Fish. Sci. Cent., Seattle, 84 p.

Francis, R.C.
1983 Population and trophic dynamics of Pacific hake (*Merluccius productus*). Can. J. Fish. Aquat. Sci. 40:1925–1943.

French, R., R. Nelson Jr., and J. Wall
1981 Results of U.S. observer sampling on Japanese, U.S.S.R., Korean, and Polish fishing vessels, 1979. Int. North Pac. Fish. Comm., Annu. Rep. 1980:96–122.

Hollowed, A.B., S.A. Adlerstein, R.C. Francis, M. Saunders, N.J. Williamson, and T.A. Dark
1988 Status of the Pacific whiting resource in 1987 and recommendations to management in 1988. NOAA Tech. Memo. NMFS F/NWC-138, Alaska Fish. Sci. Cent., Seattle, 54 p.

Kimura, D.K.
1980 Likelihood methods for the von Bertalanffy growth curve. Fish. Bull., U.S. 77:765–776.
1989 Variability in estimating catch in numbers-at-age and its impact on cohort analysis. *In* Beamish, R.J., and G.A. McFarlane (eds.), Effects of ocean variability on recruitment and an evaluation of parameters used in stock assessment models, p. 56–66. Can. Spec. Publ. Fish. Aquat. Sci. 108.

Kimura D.K., and S. Chikuni
1987 Mixtures of empirical distributions: An iterative application of the age-length key. Biometrics 43:23–34.

Kreuz, K.F., A.V. Tyler, G.H. Kruse, and R.L. Demory
1982 Variation in growth of Dover soles and English soles as related to upwelling. Trans. Am. Fish. Soc. 111:180–192.

Kruse, G.H., and A. Huyer
1983 Relationships among shelf temperatures, coastal sea level, and the coastal upwelling index off Newport, Oregon. Can. J. Fish. Aquat. Sci. 40:238–242.

Livingston, P.A.
1983 Food habits of Pacific whiting, *Merluccius productus*, off the west coast of North America, 1967 and 1980. Fish. Bull., U.S. 81:629–636.

Mason, J.E., and A. Bakun
1986 Upwelling index update, U.S. West Coast, 33N–48N latitude. NOAA Tech. Memo. NMFS-SWFC-67, Southwest Fish. Sci. Cent., La Jolla, 81 p.

Mullin, M.M., and A. Conversi
1989 Biomasses of euphausiids and smaller zooplankton in the California current—Geographic and interannual comparisons relative to the Pacific whiting, *Merluccius productus*, fishery. Fish. Bull., U.S. 87:633–644.

Overholtz, W.J.
1989 Density-dependent growth in the northwest Atlantic stock of Atlantic mackerel (*Scomber scombrus*). J. Northwest Atl. Fish. Sci. 9:115–121.

Overholtz, W.J., S.A. Murawski, and W.L. Michaels
1991 Impact of compensatory responses on assessment advice for the Northwest Atlantic mackerel stock. Fish. Bull., U.S. 89:117–128.
Parma, A.M., and R.B. Deriso
1990 Dynamics of age and size composition in a population subject to size-selective mortality: Effects of phenotypic variability in growth. Can. J. Fish. Aquat. Sci. 47:274–289.
Parrish, R.H., C.S. Nelson, and A. Bakun
1981 Transport mechanisms and reproductive success of fishes in the California Current. Biol. Oceanogr. 1(2):175–203.
Pauly, D., and G. Gaschütz
1979 A simple method for fitting oscillating length growth data with a program for pocket calculators. Int. Counc. Explor. Sea CM 1979/G:24.
Peterman, R.M., and M.J. Bradford
1987 Density-dependent growth of age 1 English sole (*Parophrys vetulus*) in Oregon and Washington coastal waters. Can. J. Fish. Aquat. Sci. 44:48–53.
Ratkowsky, D.A.
1983 Nonlinear regression modeling. Marcel Dekker, NY, 276 p.
Reish, R.L., R.B. Deriso, D. Ruppert, and R.J. Carroll
1985 An investigation of the population dynamics of Atlantic menhaden (*Brevoortia tyrannus*). Can. J. Fish. Aquat. Sci. 42(Suppl. 1):147–157.
Rexstad, E.A., and E.K. Pikitch
1986 Stomach contents and food consumption estimates of Pacific hake, *Merluccius productus*. Fish. Bull., U.S. 84: 947–956.
Roesler, C.S., and D.B. Chelton
1987 Zooplankton variability in the California Current, 1951–1982. Calif. Coop. Oceanic Fish. Invest. Rep. 28:107–127.
Ross, M.R., and F.P. Almeida
1986 Density-dependent growth of silver hakes. Trans. Am. Fish. Soc. 115:548–554.
Shepherd, G., and C.B. Grimes
1983 Geographic and historic variations in growth of weakfish, *Cynoscion regalis*, in the Middle Atlantic Bight. Fish. Bull., U.S. 81:803–813.
Simard, Y., and D.L. Mackas
1989 Mesoscale aggregations of euphausiid sound scattering layers on the continental shelf of Vancouver Island. Can. J. Fish. Aquat. Sci. 46:1238–1249.
Singh, B.D., and D. Singh
1965 Some remarks on double sampling for stratification. Biometrika 52:587–590.
Smith, B.D., G.A. McFarlane, and M.W. Saunders
1990 Variation in Pacific hake (*Merluccius productus*) summer length-at-age near southern Vancouver Island and its relationship to fishing and oceanography. Can. J. Fish. Aquat. Sci. 47:2195–2211.
Tyler, A.V., and R.S. Dunn
1976 Ration, growth, and measures of somatic and organ condition in relation to meal frequency in winter flounder, *Pseudopleuronectes americanus*, with hypotheses regarding population homeostasis. J. Fish. Res. Board Can. 33:63–75.
Ware, D.M.
1985 Life history characteristics, reproductive value, and resilience of Pacific herring (*Clupea harengus pallasi*). Can J. Fish. Aquat. Sci. 42(Suppl. 1):127–137.
Weisberg, S.
1986 A linear model approach to backcalculation of fish length. J. Am. Stat. Assoc. 81:922–929.

Appendix: Variance estimates of mean length-at-age using a two-phase sampling procedure

The length and age samples collected by observers in the Pacific whiting fishery are recorded by haul or joint-venture delivery. The position and date of each sampled haul and joint-venture delivery are also recorded. In compiling the length-at-age estimates for spatial and temporal strata, all the data collected within that strata are aggregated and assumed to originate from random sampling from the catch within that strata.

Sampling design

A large initial random sample is obtained from the catch, and the length and sex of each fish is recorded. For the second phase of sampling, a subsample of fixed size is selected for each combination of length category and sex. All fish in these subsamples are aged using otoliths or other ageing structures.

Notation

i = 1,...,I length categories
j = 1,...,J age categories
n' = first-phase sample size
n'_i = number of fish of n' in length category i
q_i = probability that a fish is in length category i
n_i = subsample sizes
n_{ij} = number of the subsample taken from length category i of age j
q'_{ij} = pr(j|i), probability of age j given length i
q_{ij} = pr(i|j), probability of length category i given age j
p_j = pr(j), probability of age j
l_i = midpoint of *ith* length category
$\bar{l}_j$ = mean length of age j fish

To simplify notation, subscripts for males and females are not defined. The variance estimator obtained here is conditional on the first- and second-phase sample sizes. Separate estimates for males and females can be obtained by separating the samples by sex and conditioning on the number of each sex in the first- and second-phase samples. The same variance estimator is appropriate for separate sex estimates.

Sampling distributions

Assuming that the first-phase sample size n' is much smaller than the size of the population being sampled, the distribution of n'_i can be modeled by the multinomial distribution,

$$f(\{n'_i\} \mid n', \{q_i\}) = \left(\frac{n'!}{\prod_i n'_i!} \right) \prod_i q_i^{n'_i},$$

where $\sum_i q_i = 1$. Estimators for $\{q_i\}$ and the elements of the variance-covariance matrix of $\{q_i\}$ are

$$\hat{q}_i = \frac{n'_i}{n'},$$

$$\hat{\text{Var}}(\hat{q}_i) = \frac{\hat{q}_i(1-\hat{q}_i)}{n'},$$

$$\hat{\text{Cov}}(\hat{q}_i, \hat{q}_h) = -\frac{\hat{q}_i \hat{q}_h}{n'}.$$

To obtain a distribution for $\{n_{ij}\}$, it is convenient to condition on the fixed subsamples n_i. As in the case of the first phase of sampling, it is assumed that n_i is much less than the number in the population of that length category, so that a product of multinomial distributions is obtained for the second phase of sampling,

$$f(\{n_{ij}\} \mid \{n_i\}, \{q'_{ij}\}) = \prod_i \left[\left(\frac{n_i!}{\prod_j n_{ij}!} \right) \prod_j q'^{n_{ij}}_{ij} \right],$$

where $\sum_j q'_{ij} = 1$ for all i. Estimators for $\{q'_{ij}\}$ and the elements of the variance-covariance matrix of $\{q'_{ij}\}$ are

$$\hat{q}'_{ij} = \frac{n_{ij}}{n_i},$$

$$\hat{\text{Var}}(\hat{q}'_{ij}) = \frac{\hat{q}'_{ij}(1-\hat{q}'_{ij})}{n_i},$$

$$\hat{\text{Cov}}(\hat{q}'_{ij}, \hat{q}'_{hk}) = -\frac{\hat{q}'_{ij} \hat{q}'_{hk}}{n_i},$$

for i=h and zero otherwise.

A troublesome inconsistency with this approach is that the n_i are assumed to be predetermined quantities. In fact, n_i is necessarily less than or equal to n'_i, the number in the *i*th length category from the first-phase sampling, and n'_i is a random variable that can take values between zero and the min(n', N_i) where N_i is the number of fish of length category i in the total catch. Singh and Singh (1965) address this issue while developing variance estimators for what in this fisheries application would correspond to mean age. While they were able to obtain estimators which correctly modeled the sampling procedures, they also found that their exercise in theoretical rigor did not result in any appreciable difference in practice.

Estimation of mean length-at-age

An unbiased estimate of $\bar{l}_j$ is given by

$$\bar{l}_j = \sum_i l_i q_{ij},$$

where q_{ij} is the probability of length i given age j. An expression for q_{ij} is obtained using Bayes theorem,

$$q_{ij} = \frac{q_i q'_{ij}}{\sum_i q_i q'_{ij}}.$$

A variance approximation for mean length-at-age

Because the above expression for mean length-at-age is nonlinear in the observations $\{n'_i\}$ and $\{n_{ij}\}$, a delta-method approximation is derived. Delta-method estimators can be algebraically complex but all have the same simple structure. For mean length-at-age, a delta-method approximation is given by

$$\text{Var}(\bar{l}_j) \approx \mathbf{d}_j^T \mathbf{V} \mathbf{d}_j,$$

where $\mathbf{d}_j$ is the vector of partial derivatives of $\bar{l}_j$ with respect to $\{q_i\}$ and $\{q'_{ij}\}$, and $\mathbf{V}$ is the variance-covariance matrix of $\{q_i\}$ and $\{q'_{ij}\}$. Defining

$$A_j = \sum_i l_i \hat{q}_i \hat{q}'_{ij},$$

and

$$\hat{p}_j = \sum_i \hat{q}_i \hat{q}'_{ij},$$

the elements of the vector of partial derivatives are given by

$$\frac{\partial \bar{l}_j}{\partial q_i} = \frac{\hat{q}'_{ij}(l_i \hat{p}_j - A_j)}{\hat{p}_j^2}$$

and

$$\frac{\partial \bar{l}_j}{\partial q'_{ij}} = \frac{\hat{q}_i(l_i \hat{p}_j - A_j)}{\hat{p}_j^2}.$$

Combining these expressions with the estimators for the variance-covariance matrix of q_i and q'_{ij} given earlier,

$$\hat{\mathrm{Var}}(\bar{l}_j) = \left[\frac{1}{\hat{p}_j}\right]^4 \left\{\sum_i (l_i\hat{p}_j - A_j)^2 \left(\frac{\hat{q}_i(1-\hat{q}_i)\hat{q}'_{ij}{}^2}{n'} + \frac{\hat{q}'_{ij}(1-\hat{q}'_{ij})\hat{q}_i{}^2}{n_i}\right) - \sum_{i\neq h}\sum \hat{q}_i\hat{q}_h\hat{q}'_{ij}\hat{q}'_{hj}(l_i\hat{p}_j - A_j)\frac{(l_h\hat{p}_j - A_j)}{n'}\right\}.$$

Combining length-at-age from different strata

An estimate of combined mean length-at-age is

$$\bar{l}_j = \sum_h \left(\frac{c_{jh}}{c_j}\right)\bar{l}_{jh},$$

where l_{jh} is the length-at-age in the h*th* stratum, and c_{jh} is the catch-at-age for the same stratum.

Again using a delta-method approximation,

$$\mathrm{Var}(\bar{l}_j) = \sum_h \mathrm{Var}(c_{jh})\left[\frac{(\bar{l}_{jh}\,c_j - \sum_h c_{jh}\,\bar{l}_{jh})}{c_j^2}\right]^2 + \sum_h \mathrm{Var}(\bar{l}_{jh})\left[\frac{c_{jh}}{c_j}\right]^2.$$

The complete expression should include a term involving $\mathrm{Cov}(c_{jh}, \bar{l}_{jh})$. This term was always negligible compared with the other two terms, and depended on the method used to calculate the catch-at-age. Consequently, it is not included here. The variance estimator for combined length-at-age for several strata requires an estimate of the variance of catch-at-age. A method for obtaining this is given in Kimura (1989).

Influence of sectioning otoliths on marginal increment trends and age and growth estimates for the flathead *Platycephalus speculator*

Glenn A. Hyndes
School of Biological and Environmental Sciences, Murdoch University
Murdoch, Western Australia 6150, Australia

Neil R. Loneragan
School of Biological and Environmental Sciences, Murdoch University
Murdoch, Western Australia 6150, Australia
Present address: CSIRO Division of Fisheries
P.O. Box 120, Cleveland, Queensland 4163, Australia

Ian C. Potter
School of Biological and Environmental Sciences, Murdoch University
Murdoch, Western Australia 6150, Australia

Abstract. – Comparisons are made between estimates of ages and growth of the flathead *Platycephalus speculator* Klunzinger, from a temperate Western Australian estuary, using data obtained from whole and sectioned otoliths. The consistent annual trends shown by the width of the opaque zone on the periphery (marginal increment) of sectioned otoliths, irrespective of the number of translucent zones, demonstrate that the translucent zones in these otoliths correspond to annuli. While the marginal increments on whole otoliths also showed a similar marked and consistent annual trend when a single translucent zone was present, they were far less conspicuous when two or more translucent zones were observed. The large sample size and strong trends shown by marginal increments on otoliths exhibiting one translucent zone accounts for the fact that, when data for all whole otoliths are pooled, the marginal increment still shows a consistent annual trend. Sectioning of otoliths enhances the ability to differentiate between the outer opaque and translucent zones, and also often reveals one or more additional inner translucent zones in older fish. The use of whole otoliths frequently underestimated age by one year in 2+ to 4+ fish and two years in 5+ to 10+ fish, and by as much as five or six years in the oldest fish (11+ and 12+). The respective 95% confidence limits for the parameters L_∞, K, and t_0 in the von Bertalanffy growth equations for males, calculated using data from sectioned otoliths, overlapped those calculated from data for whole otoliths, and the same was true for K with females. This similarity in growth curves in particularly the first four years of life can be attributed to the fact that approximately 74 and 65% of the growth of males and females, respectively, occurred in the first three years, when underestimates of age were limited.

Manuscript accepted 18 February 1992.
Fishery Bulletin, U.S. 90:276–284 (1992).

Since assessments of fish stocks often rely on information on age composition, it is crucial that any age estimates used for such assessments are validated (Beamish and McFarlane 1983, Casselman 1987). Validation that growth zones on hard structures, such as otoliths, scales, and spines, are formed annually is often implied by establishing that the pattern of growth on the periphery of these structures follows a consistent annual trend (e.g., Johnson 1983, Maceina et al. 1987, Potter et al. 1988, Beckman et al. 1989). In otoliths of fish in temperate waters, an opaque zone generally starts to form in the spring immediately outside the translucent zone laid down during the preceding winter. The width of this opaque zone usually increases between spring and autumn. Although a subsequent retardation of growth during winter results in formation of the translucent zone at the edge of the otolith, this translucent zone frequently cannot be readily detected until the following spring, when it becomes delineated by the formation of a new opaque zone. The distance outside the outer translucent zone constitutes the marginal increment. Therefore, if the outer opaque and translucent zones are formed annually, the marginal increment should decline only once during the year. Verification that trends shown by the marginal increments follow a pattern consistent with annual growth is an important method for establishing that the alternating translucent and opaque zones each correspond to annuli and are thus appropriate for use in ageing (Brothers 1983).

Many workers have presented data which showed that an annual trend was followed either by the marginal increment, when data for all otoliths in each sample were pooled, or by the overall incidence of otoliths possessing either translucent or opaque zones on their outer edge. When these have shown a consistent annual trend, it has often been concluded that all translucent zones correspond to annuli (e.g., Nel et al. 1985, Reis 1986, Rincon and Lobon-Cervia 1989, Crozier 1990, Hayse 1990). However, trends shown in such pooled data will be strongly influenced by those of the dominant groups, *vis a vis* the number of translucent zones, and may

not be representative of all groups. Furthermore, trends shown by the marginal increment in some long-lived fish become clear only after the otoliths have either been sectioned or broken and burnt (Campana 1984, Collins et al. 1988). This accounts for estimates of age sometimes being lower when whole otoliths have been used than when either sectioned or broken and burnt otoliths were employed (Beamish 1979a, Campana 1984, Collins et al. 1988).

Although the Platycephalidae occurs along the coasts and within estuaries throughout the Indo-west Pacific region, the majority of the 41 species of flathead found in Australia are restricted to its southern waters (Sriramachandra-Murty 1975, Paxton and Hanley 1989). Despite wide distribution and, in some cases, the commercial and recreational importance of the Platycephalidae, estimates of the age and growth of representatives of this family are limited to those obtained for *Platycephalus bassensis*, *P. castelnaui*, and *P. speculator* by Brown (1977) and for *P. richardsoni* by Colefax (1934), Fairbridge (1951), and Montgomery (1985), the populations of which were all located in southeastern Australia. The most abundant species of flathead on the temperate southern coast of Western Australia is *P. speculator*, a species which has been shown to breed within Wilson Inlet, the largest estuary of this region (Hyndes et al. In press).

Previous attempts to age platycephalids have used whole sagittal otoliths (Colefax 1934, Fairbridge 1951, Brown 1977, Montgomery 1985). However, a preliminary investigation of the translucent zones in the sagittal otoliths of *P. speculator* from southwestern Australia showed that the outer opaque and translucent zones on the otoliths of larger fish often became clear only when the otoliths had been sectioned.

The present study was undertaken to determine the age structure and growth of *P. speculator* in Wilson Inlet, where this species is abundant and contributes to the local commercial and recreational estuarine fisheries (Lenanton and Potter 1987). Emphasis has been placed on elucidating the degree to which sectioning the otoliths influences marginal increment trends, age estimates, and growth equations. In addition, marginal increment data were pooled for both whole and sectioned otoliths to examine whether the resultant overall annual marginal increment trends were strongly influenced by that of a group(s) of otoliths with a particular number(s) of translucent zones.

Materials and methods

Sampling locality and regime

Wilson Inlet (117°25′E and 34°50′S) has a narrow entrance channel which opens into a wide basin (48 km^2) supplied by two main tributary rivers. Water depth in the basin is generally less than 2 m. *Platycephalus speculator* was collected monthly from within the basin of Wilson Inlet between September 1987 and April 1989 using beach seines (mesh size in pocket 9.5 mm) during the day and gillnets (six stretched-mesh sizes, 38–102 mm), otter trawls (mesh size in pocket 25 mm) and plankton trawls at night (mesh size 1 mm).

Bottom water temperatures near the entrance channel of Wilson Inlet and 12 km further up the estuary near the top end of the basin were recorded at the time of sampling.

Age determination

Each fish was measured (total length) and weighed to the nearest 1 mm and 0.1 g, respectively. Sex was recorded when the gonad could be identified as either ovary or testis, which was usually possible in fish >100 mm in length. Both of the sagittal otoliths of 1305 juvenile and adult fish were cleaned, dried, and stored in gelatin capsules.

Whole otoliths were placed in methyl salicylate solution and examined microscopically under reflected light against a black background. The marginal increment, i.e., the distance between the outer edge of the outermost translucent zone and the periphery, was measured on one of the otoliths of each fish and expressed either as (1) a proportion of the distance between the focus and the outer edge of the translucent zone when only one translucent zone was present, or (2) as a proportion of the distance between the outer edges of the two outermost translucent zones when two or more translucent zones were present. Measurements were always made along the same axis, to the nearest 0.05 mm (Fig. 1). The number of translucent zones on each otolith was recorded.

These otoliths were later mounted and embedded in black epoxy resin (Bedford 1983, Augustine and Kenchington 1987) and cut into 1.5–2 mm transverse sections using the diamond saw described by Augustine and Kenchington (1987). Sections were mounted on glass slides and their surfaces ground on sequentially finer grades (400–1200) of carborundum paper. Sections were then coated with clear nail polish and examined microscopically under reflected light. Measurements of the marginal increment and counts of the number of translucent zones in these sectioned otoliths were carried out in precisely the same manner as described above for whole otoliths.

Mean marginal increment values were plotted separately for both whole and sectioned otoliths with 1–4 and ≥5 translucent zones to ascertain if they follow a consistent annual trend and thus permit the translucent zones to be considered as annuli. Width and

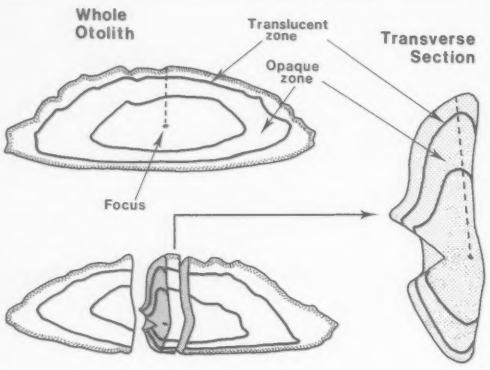

Figure 1
Schematic diagram showing the translucent and opaque zones in a whole and sectioned sagittal otolith of *Platycephalus speculator*. Broken line represents the axis along which measurements were taken.

thickness of the whole otoliths of 123 fish, covering the full range of sizes, were measured to the nearest 0.01 mm to examine the relationship between otolith width and thickness. The number of translucent zones in 140 otoliths, of which up to 20 otoliths came from each age-class (estimated from sectioned otoliths), were counted in whole and sectioned otoliths by a second 'reader' who had no previous experience in examining otoliths of this species. The reproducibility of age estimates for each method was determined by using the coefficient of variation (Sokal and Rohlf 1981, Chang 1982).

Von Bertalanffy growth curves were fitted to individual lengths of males and females at the estimated age-at-capture by a nonlinear technique (Gallucci and Quinn 1979) using a nonlinear subroutine in SPSS (SPSS 1988) and assuming a 'birth date' of 1 January. This date corresponds approximately to the midpoint of the period when, on the basis of gonadosomatic indices and trends shown by oocyte development, *P. speculator* exhibited peak spawning activity in Wilson Inlet (Hyndes et al. In press). The von Bertalanffy equation is $L_t = L_\infty\ [1 - e^{-K(t-t_0)}]$, where L_t is the length at age t (yr), L_∞ is the mean asymptotic length predicted by the equation, K is the growth coefficient, and t_0 is the hypothetical age at which fish would have zero length if growth followed that predicted by the equation. Comparisons have been made between the age estimates and von Bertalanffy growth curves, calculated from data obtained using whole and sectioned otoliths and assuming that, in both cases, the translucent zones correspond to annuli.

Results

Marginal increments

Annual trends in the mean marginal increments for whole and sectioned otoliths with one translucent zone were similar (Fig. 2). However, the sharp decline which occurred in the marginal increment after the winter (June–August) of 1988 was detected earlier in sectioned otoliths (October) than in whole otoliths (December). Although the data for 1987 were not as extensive, they still exhibited a similar marked decrease at the same time of year. In both years, the marginal increment on both whole and sectioned otoliths subsequently rose consistently through the summer, before leveling off in the late autumn and winter (Fig. 2).

Annual trends in mean marginal increments of sectioned otoliths with two, three, and four translucent zones parallel those in sectioned otoliths with one translucent zone, with marginal increments falling sharply in the spring (October) of both 1987 and 1988 (Fig. 2). Although the marginal increment on whole otoliths with two, three, and four translucent zones also declined in spring, the decrease was far less pronounced and the trends less consistent.

Since the number of otoliths with five or more translucent zones was small, values for the marginal increments on all such otoliths were pooled. Although seasonal trends shown by the marginal increment in sectioned otoliths with ≥ 5 translucent zones were slightly less consistent than in those with 1–4 such zones, they still followed a similar annual trend (Fig. 2). Furthermore, the translucent zones were still clearly visible and had the same appearance as those in otoliths with 1–4 translucent zones. No clear annual trend could be seen in the marginal increments of whole otoliths displaying ≥ 5 translucent zones (Fig. 2).

The above trends in marginal increments of sectioned otoliths (with a sharp decline only occurring at one time of the year, i.e., in the spring) show that the first four translucent zones on otoliths of *P. speculator* are laid down annually. Since the same trends were exhibited in pooled data for the fifth and subsequent translucent zones, these zones were presumably also, at least in most of these cases, laid down annually. We thus consider the translucent zone on sectioned otoliths as an annulus which can be used for ageing *P. speculator* from Wilson Inlet. The data also show that the outer opaque zone starts to form when water temperatures are rising from their winter (July) minima of about 11°C towards their summer (December–February) maxima of ~22°C (c.f. Figs. 2,3).

The annual trend shown by the mean marginal increment based on all sectioned otoliths, irrespective of the number of translucent zones, was essentially

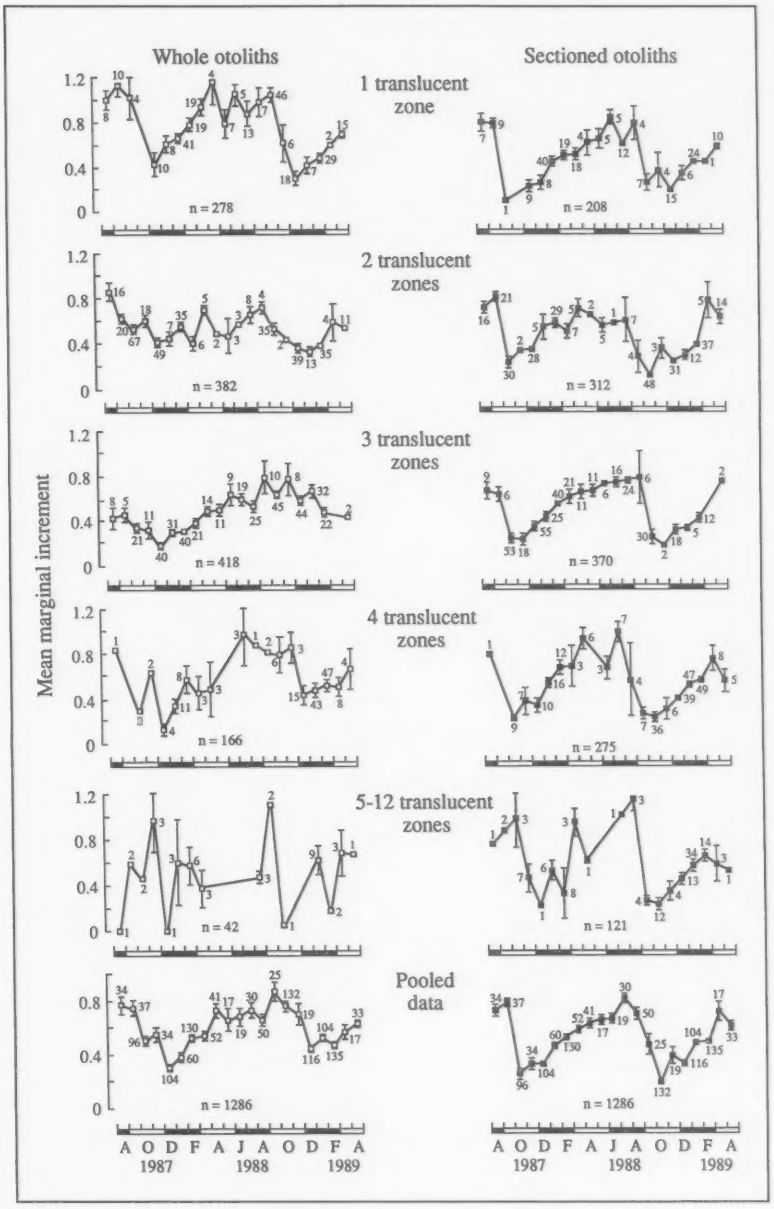

Figure 2
Mean marginal increments ± SE for whole and sectioned sagittal otoliths of *Platycephalus speculator*. Note that the marginal increment is given as a relative value, i.e., as a percentage of the distance between the focus and the outer translucent zone when only one zone was present, or as a percentage of the distance between the outer edges of the two outermost translucent zones when two or more such zones were present. In this Figure and in Figs. 3 and 6, the black bars on the x-axis refer to winter (June–Aug.) and summer (Dec.–Feb.) and the open bars to spring (Sept.–Nov.) and autumn (March–May).

the same as that of otoliths with 1–4 translucent zones (Fig. 2). Mean marginal increments based on all whole otoliths followed similar annual trends, but they were not as pronounced or consistent, and the variation about the means was greater (Fig. 2).

Length-frequency data

Few fish <180 mm in length were caught (Fig. 4), reflecting the fact that smaller individuals of this benthic species did not tend to be collected by seine and gillnets.

The three fish caught in the middle of spring (October) of 1987, which had otoliths with a single translucent zone bounded by a very narrow opaque zone, measured 91–106 mm in length (Fig. 4). This group is assumed to represent the 0+ age-class, i.e., the result of spawning which peaked in early January 1987 and can therefore be referred to as the 1987 year-class. The larger fish, which produced modal length-classes at 325–349 mm and 400–424 mm in October 1987 (Fig. 4), had otoliths with a narrow opaque zone bounding two and three translucent zones, respectively. The groups with two and three translucent zones therefore represent the 1+ and 2+ age-classes, or the 1986 and 1985 year-classes, respectively. Fish with otoliths exhibiting one, two, and three translucent zones in December 1987 and February 1988 are designated as representing the 1987, 1986, and 1985 year-classes, which is consistent with their length distributions (Fig. 4). The marked difference between the lengths of the 1987 year-class in October and December 1987 suggests that this year-class underwent remarkable growth between these months. However, the three fish caught in October were taken by beach seine in the shallows and are thus presumed to represent the lower end of the length range of this year-class, whereas those fish of the

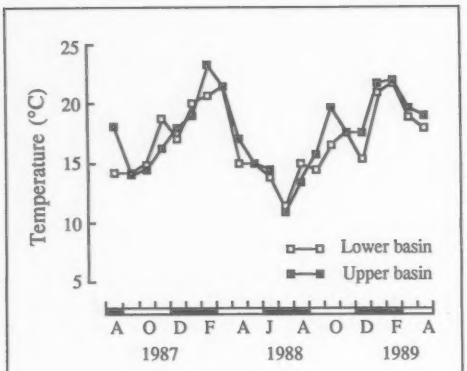

Figure 3
Bottom-water temperatures recorded at sites at lower and upper ends of the basin of Wilson Inlet, Western Australia, August 1987–April 1989.

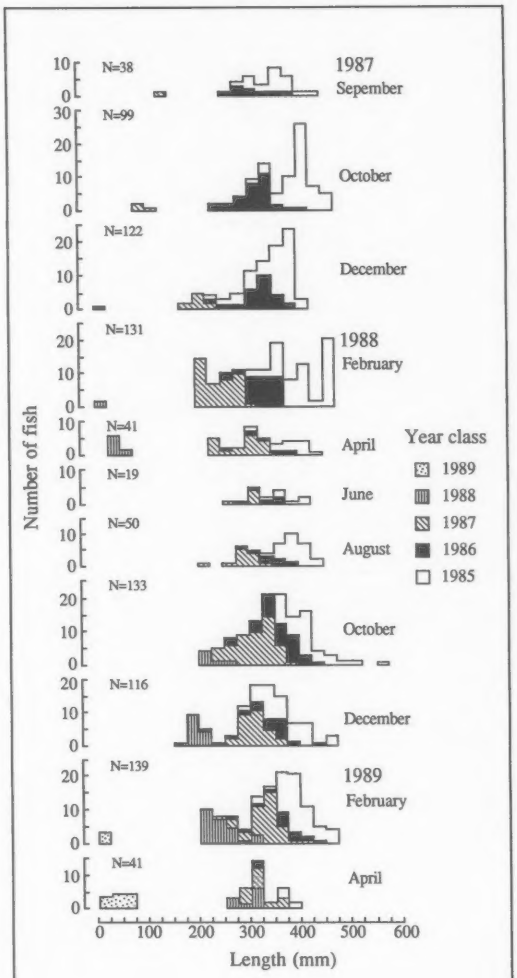

Figure 4
Length-frequency histograms for the 1985–89 year-classes of *Platycephalus speculator*.

corresponding cohort caught in December were taken in gillnets which, because of the mesh sizes of these nets, would have taken only the larger members of that year-class.

Larval *P. speculator*, ranging up to a length of 13 mm, were collected in plankton trawls in December 1987, February 1988, and February and April 1989 (Fig. 4). Otoliths of juveniles caught in April 1988 and 1989, and which from their lengths (23–89 mm) clearly corresponded to the 0+ age-class, did not have a translucent zone. The group of fish representing the 1988 year-class had reached 198–231 mm by December 1988, and 258–323 mm by April 1989. These length ranges are similar to those attained by the previous (1987) year-class in December 1987 and April 1988 (Fig. 4). The modal length of the 1+ age-class in October 1988 (= 1987 year-class) was identical to that of the 1+ age-class in October 1987 (= 1986 year-class). Six year-classes were usually found in samples from each month, and as many as eleven year-classes were present in February 1988 (older year-classes are not shown in Fig. 4). Maximum lengths for each sex were 696 mm for a 10+ female and 545 mm for a 12+ male.

Estimated ages and growth curves using whole and sectioned otoliths

All of the 197 otoliths which showed one translucent zone (= annulus) in sectioned otoliths also displayed a single zone prior to sectioning (Fig. 5). However, 44% of otoliths with two or more translucent zones after sectioning produced underestimates using whole otoliths. Between 23% and 57% of the otoliths with 2–4 annuli each showed one less translucent zone prior to sectioning and thus underestimated ages by 1 year. Discrepancies between the number of translucent zones in sectioned and whole otoliths were even more marked in otoliths with 5 or more translucent zones. Indeed, the numbers of annuli were as many as 5 or 6 less in whole otoliths than the 11 or 12 annuli observed in sectioned otoliths (Fig. 5). The proportion of underestimates using whole otoliths was greatest in spring for those otoliths which showed 2 or 3 translucent zones after sectioning (Fig. 6).

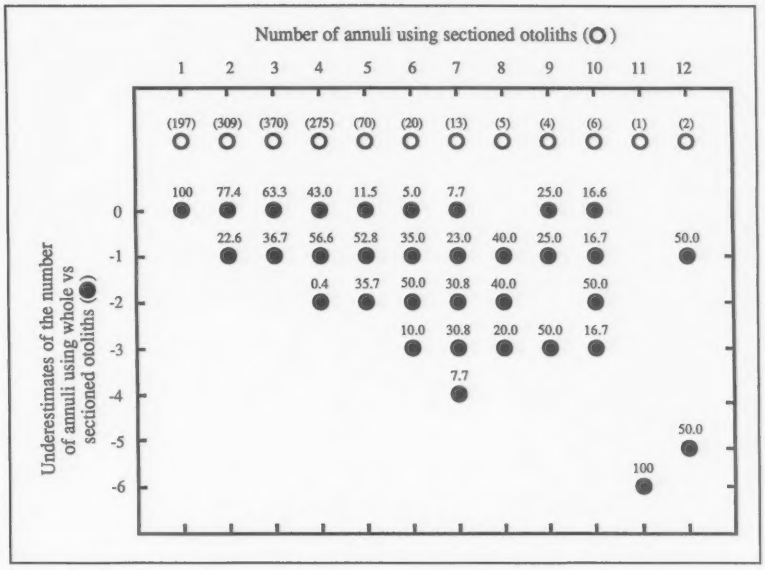

Figure 5
Number of otoliths with 1–12 annuli based on sectioned sagittal otoliths of *Platycephalus speculator*, and underestimates of the number of annuli observed on the same whole sagittal otoliths. Numbers in parentheses indicate the number of fish of different ages based on sectioned otoliths, while numbers above the closed circles indicate the percentage of underestimates using whole otoliths.

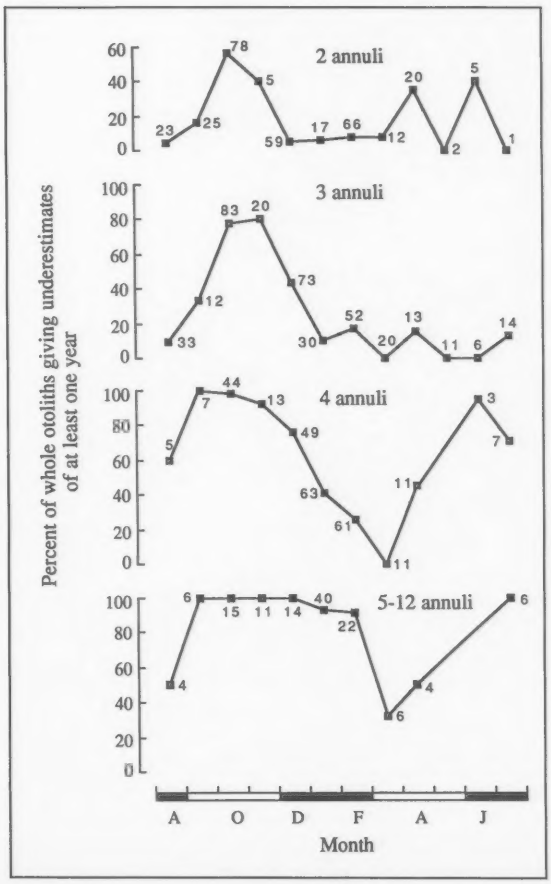
Percent of whole otoliths giving underestimates of at least one year
2 annuli
23 25 78 5 59 17 66 12 20 2 5 1
3 annuli
33 12 83 20 30 73 52 20 13 11 6 14
4 annuli
5 7 44 13 49 63 61 11 11 3 7
5-12 annuli
4 6 15 11 14 40 22 6 4 6
A O D F A J
Month

Figure 6
Seasonal incidence of underestimates by one or more annuli when using whole vs. sectioned sagittal otoliths of *Platycephalus speculator*.

The coefficient of variation for replicate age estimates between readers was far less for sectioned otoliths (1.2%) than for the same otoliths prior to sectioning (8.7%). While the estimated age varied by only 1 year for each of the six sectioned otoliths for which there was disagreement, the estimated ages varied by as much as 3 years for the 53 whole otoliths for which there were discrepancies.

The relationship between width and thickness of sagittal otoliths of *P. speculator* is curvilinear, demonstrating that width does not increase proportionately with thickness (Fig. 7). The relationship between otolith width (W) and otolith thickness (T) is described by the following polynomial equation:

$$W = -0.283 + 4.635T - 1.175T^2 \quad (r^2\ 0.82,\ n\ 123).$$

The von Bertalanffy growth parameters for both male and female flathead were initially determined using individual lengths at estimated age (Table 1). Examination of the length-at-age plots showed that the curve for both sexes fell below the majority of the points for fish >5 years old, i.e., the asymptote was too pronounced to accommodate lengths of the older fish. Individual lengths of the fish were grouped into intervals of 0.1 years and the curves determined again by weighting the data by the inverse of the sample size for each age interval (Beckman et al. 1990). This procedure resulted in a better fit of the curve (Fig. 8). Although the values for t_0 for males and females were shifted slightly away from zero (namely from −0.134 to −0.332 and from −0.056 to −0.423, respectively), differences in the lengths of males and females at

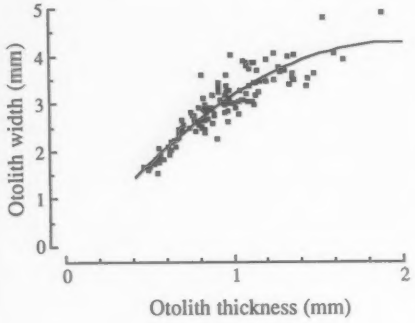

Figure 7
Relationship between width and thickness of the sagittal otoliths of *Platycephalus speculator*.

Table 1
Parameter estimates (95% confidence limits) for the von Bertalanffy growth model fitted to 630 male and 711 female *Platycephalus speculator*, determined from whole and sectioned otoliths using individual lengths-at-age and weighted lengths of each age-group in each month.

Sex	Parameter	Individual lengths Est.	Lower	Upper	Weighted lengths Est.	Lower	Upper
Sectioned otoliths							
Male	L_∞	429.2	419.9	438.5	477.4	468.6	486.2
	K	0.573	0.525	0.621	0.408	0.380	0.437
	t_0	−0.134	−0.201	−0.067	−0.332	−0.411	−0.253
Female	L_∞	481.8	469.4	494.2	601.0	588.2	619.8
	K	0.593	0.547	0.639	0.309	0.283	0.335
	t_0	−0.056	−0.109	−0.003	−0.423	−0.515	−0.331
Whole otoliths							
Male	L_∞	426.9	417.3	436.4	484.9	473.5	496.3
	K	0.700	0.641	0.760	0.466	0.429	0.502
	t_0	−0.068	−0.125	−0.012	−0.244	−0.292	−0.156
Female	L_∞	457.8	445.6	470.0	659.6	626.1	693.2
	K	0.767	0.694	0.840	0.264	0.231	0.296
	t_0	−0.088	−0.148	−0.028	−0.698	−0.837	−0.560

ages 1, 2, 3, and 4 were never altered by more than 22mm and the change was generally less than 12mm. The coefficient of determination (r^2) for the von Bertalanffy curve was 0.85 for both sexes using individual lengths-at-age, and 0.93 for males and 0.89 for females using the weighted procedure.

The respective parameters L_∞, K, and t_0 in the von Bertalanffy growth equations for males determined using weighted data obtained from sectioned otoliths overlapped those when the same approach was employed for whole otoliths, and the same was true for K with females (Table 1, Fig. 8). The von Bertalanffy growth-equation parameters using weighted data from sectioned otoliths show that female *P. speculator* grow towards a larger asymptotic size (L_∞) than males (Table 1, Fig. 8). Individual lengths of *P. speculator* in December–February at the end of their first and second years of life were 190–310mm and 210–370mm, respectively, for males, and 210–300mm and 250–400 mm, respectively, for females (Fig. 8).

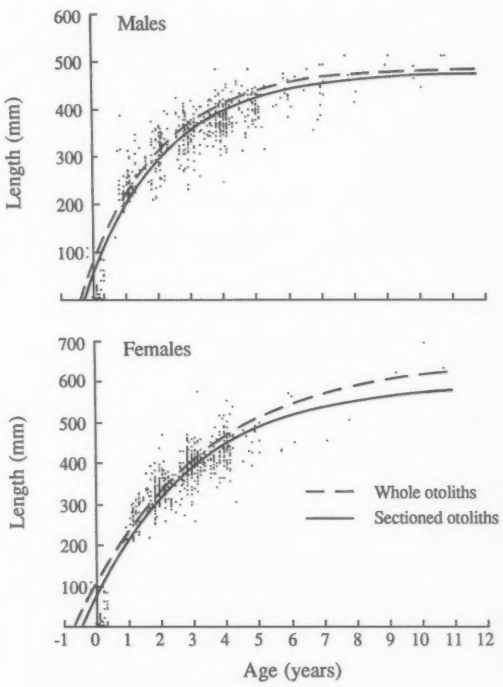

Figure 8
Von Bertalanffy growth curves fitted to length-at-age data, weighted by the inverse of the sample size of each 0.1 year age-group, using whole and sectioned otoliths of male and female *Platycephalus speculator*.

Discussion

Marginal increments

Marginal increments of the otoliths of *P. speculator* with two or more translucent zones exhibited conspicuous trends only after the otoliths were sectioned. This is largely due to the fact that sectioning of otoliths results in more accurate measurement of their peripheral and/or penultimate opaque zones, because one or both of the two outermost translucent zones have become more clearly delineated. This is similar to the situation with starry flounder *Platychthys stellatus*, in which annual trends in the marginal increments of

otoliths with four or more annuli were observed only after otoliths had been broken and burnt (Campana 1984). Likewise, in the case of king mackerel *Scomberomorus cavalla*, the percentage of otoliths with an opaque zone on their edge exhibited an annual trend only after the otoliths were sectioned (Collins et al. 1988).

The consistency in annual trends of marginal increments among sectioned otoliths of *P. speculator*, despite differing numbers of translucent zones, accounts for the clear annual trend in marginal increments when data for all otoliths in each of the monthly samples were pooled. The contrast between the conspicuous trend shown in pooled data for whole otoliths, and the relatively poor trend exhibited in whole otoliths with two or more translucent zones, shows how trends can be unduly influenced by those of a relatively large sample size of otoliths exhibiting a particularly strong annual trend, such as was present with those otoliths having one translucent zone. For validation of the use of translucent zones as annuli, it is thus important to establish that the trends shown by the marginal increments on otoliths with differing numbers of translucent zones each follow a consistent annual trend (Johnson 1983, Maceina et al. 1987, Potter et al. 1988, Beckman et al. 1989).

Age and growth estimates

Our results demonstrate that, while age estimates between sectioned and whole otoliths corresponded when one translucent zone was present, ages of older fish were underestimated by 2–4 years or as much as 5 or 6 years using whole otoliths. Increased resolution of the growth zones after sectioning is reflected in the far lower variability between age estimates made by two independent readers using sectioned otoliths.

Although otoliths with two or three translucent zones frequently yielded counts of one less zone prior to sectioning, many underestimates occurred with the otoliths taken from fish between mid-spring and early summer (October–December). In other words, they were collected during the period when sectioning enabled the new opaque zone to be detected approximately 2 months earlier than was possible with whole otoliths.

Our inability to detect all of the translucent zones in whole otoliths can in part be attributed to the growth pattern of the otolith. Whereas the first translucent zone can be easily detected in whole otoliths, the disproportionate increase in otolith thickness relative to its width results in the translucent zones becoming increasingly more closely apposed and therefore difficult to distinguish from one another. This parallels the situation recorded by Beamish (1979a, b) for Pacific hake *Merluccius productus*, and for several species of rockfish (*Sebastes*), and also by Campana (1984) for starry flounder *Platychthys stellatus*.

Despite the fact that a large proportion of ages were underestimated using whole otoliths, the von Bertalanffy growth curves derived from data using whole otoliths, particularly of males, did not differ markedly from those obtained using sectioned otoliths. This can be attributed to the fact that approximately 74 and 65% of growth for males and females, respectively, occurred in the first 3 years of life when underestimates of age were limited.

Implications for management

The vast majority of male *P. speculator* reach sexual maturity at the end of their first year of life (Hyndes et al. In press).Since males have attained only 190–310 mm by this time (Fig. 8), they will only occasionally have reached 300 mm, the minimum legal length for capture of this species. However, the majority of females do not first attain sexual maturity until they are 2 years old (Hyndes et al. In press), by which time they have reached 250–400 mm. Thus, the females of *P. speculator* can be exploited before they have had the opportunity to spawn.

In summary, this study has demonstrated that, in the case of the flathead *P. speculator*, it is crucial to section its otoliths in order to obtain an accurate estimate of age. Sectioning reduces the problems of distinguishing between peripheral translucent zones which, due to the growth pattern of the otolith, become increasingly more closely apposed with increasing size. While the results presented in this paper refer only to *P. speculator*, they parallel in some respects those obtained for *Platychthys stellatus* and *Scomberomorus cavalla* (Campana 1984, Collins et al. 1988). Such age underestimates have obvious implications in estimating mortalities for use in fisheries management. Our results also demonstrate the importance of plotting marginal increments for otoliths with different numbers of translucent zones, to establish that such zones are laid down annually on the otoliths of fish representing each presumed age-group. Since the females of *P. speculator* are being caught before they have spawned for the first time, there is a case for increasing the minimum legal size for capture.

Acknowledgments

We thank F. Baronie, D. Gaughan, P. Geijsel, P. Humphries, L. Laurenson, and F. Neira for their assistance with sampling. The sectioning saw was kindly provided by S. Blaber of the CSIRO Marine Labora-

tories at Cleveland, Queensland. Helpful discussions were provided by N. Hall, L. Laurenson and L. Pen. L. Pen also estimated the number of translucent zones in otoliths for the precision estimates. Gratitude is expressed to J. Casselman, R. Fletcher, M. Moran, N. Hall, two anonymous referees, and the scientific editor for constructive criticism of our work and this paper. Financial support was provided by the Western Australian Department of Fisheries.

Citations

Augustine, O., and T.J. Kenchington
1987 A low cost saw for sectioning otoliths. J. Cons. Cons. Int. Explor. Mer 43:296–298.

Beamish, R.J.
1979a Differences in the age of Pacific hake (*Merluccius productus*) using whole and sections of otoliths. J. Fish. Res. Board Can. 36:141–151.
1979b New information on the longevity of the Pacific hake (*Sebastes alutus*). J. Fish. Res. Board Can. 36:1395–1400.

Beamish, R.J., and G.A. McFarlane
1983 The forgotten requirement for age validation in fisheries biology. Trans. Am. Fish. Soc. 112:735–743.

Beckman, D.W., C.A. Wilson, and A.L. Stanley
1989 Age and growth of red drum, *Sciaenops ocellatus*, from offshore waters of the northern Gulf of Mexico. Fish. Bull., U.S. 87:17–27.

Beckman, D.W., A.L. Stanley, J.H. Render, and C.A. Wilson
1990 Age and growth of black drum in Louisiana waters of the Gulf of Mexico. Trans. Am. Fish. Soc. 119:537–544.

Bedford, B.C.
1983 A method for preparing sections of large numbers of otoliths embedded in black polyester resin. J. Cons. Cons. Int. Explor. Mer 41:4–12.

Brothers, E.B.
1983 Summary of round table discussions on age validation. *In* Prince, E.D., and L.M. Pulos (eds.), Proceedings, International workshop on age determination of oceanic pelagic fishes: Tunas, billfishes, and sharks, p. 35–44. NOAA Tech. Rep. NMFS 8.

Brown, I.W.
1977 Ecology of three sympatric flatheads (Platycephalidae) in Port Phillip Bay, Victoria. Ph.D. thesis, Monash Univ., Victoria, 304 p.

Campana, S.E.
1984 Comparison of age-determination methods for the starry flounder. Trans. Am. Fish. Soc. 113:365–369.

Casselman, J.M.
1987 Determination of age and growth. *In* Weatherly, A.H., and H.S. Gill (eds.), The biology of fish growth, p. 209–242. Academic Press, London.

Chang, W.Y.B.
1982 A statistical method for evaluating the reproducibilty of age determination. Can. J. Fish. Aquat. Sci. 39:1208–1210.

Colefax, A.N.
1934 A preliminary investigation of the natural history of the tiger flathead (*Neoplatycephalus macrodon*) on the south-eastern Australian coast. I. Distribution and supply; length statistics. Proc. Linn. Soc. N.S.W. 49:71–91.

Collins, M.R., D.J. Schmidt, C.W. Waltz, and J.L. Pickney
1988 Age and growth of the king mackerel, *Scomberomorus cavalla*, from the Atlantic coast of the United States. Fish. Bull., U.S. 87:49–61.

Crozier, W.W.
1990 Age and growth of the angler-fish (*Lophius piscatorius* L.) in the North Irish Sea. Fish. Res. (Amst.) 7:267–278.

Fairbridge, W.S.
1951 The New South Wales tiger flathead, *Neoplatycephalus macrodon* (Ogilby). Aust.J. Mar. Freshwater Res. 2:117–118.

Gallucci, V.F., and T.J. Quinn
1979 Reparameterizing, fitting and testing a simple growth model. Trans. Am. Fish. Soc. 10:14–25.

Hayse, J.W.
1990 Feeding habits, age, growth and reproduction of Atlantic spadefish *Chaetodipterus faber* (Pisces: Ephippidae) in South Carolina. Fish. Bull., U.S. 88:76–83.

Hyndes, G.A., F.J. Neira, and I.C. Potter
In press Reproductive biology and early life history of the marine teleost *Platycephalus speculator* Klunzinger (Platycephalidae) in a temperate Australian estuary. J. Fish Biol.

Johnson, A.G.
1983 Age and growth of yellowtail snapper from South Florida. Trans. Am. Fish. Soc. 112:173–177.

Lenanton, R.C.J., and I.C. Potter
1987 Contribution of estuaries to commercial fisheries in temperate Western Australia and the concept of estuarine dependence. Estuaries 10:28–35.

Maceina, M.J., D.N. Hata, T.L. Linton, and A.M. Landry
1987 Age and growth analysis of spotted seatrout from Galveston Bay, Texas. Trans. Am. Fish. Soc. 116:54–59.

Montgomery, S.S.
1985 Aspects of the biology of the tiger flathead *P. richardsoni* and the associated fishery. Masters thesis, Univ. New South Wales, Sydney, 228 p.

Nel, S.A., I.C. Potter, and N.R. Loneragan
1985 The biology of the catfish *Cnidoglanis macrocephalus* (Plotosidae) in an Australian Estuary. Estuarine Coastal Shelf Sci. 21:895–909.

Paxton, J.R., and J.E. Hanley
1989 Platycephalidae. *In* Walton, D.W., and R. Longmore (eds.), Zoological catalogue of Australia, 7, Pisces, Petromyzontidae to Carangidae, p. 465–472. Brown Prior Anderson, Burwood, Victoria.

Potter, I.C., A.J. Cheal, and N.R. Loneragan
1988 Protracted estuarine phase in the life cycle of the marine pufferfish *Torquigener pleurogramma*. Mar. Biol. (Berl.) 98: 317–329.

Reis, E.G.
1986 Age and growth of the estuarine catfish, *Netuma barba* (Siluriformes, Ariidae), in the estuary of the Patos Lagoon (Brasil). Fish. Bull., U.S. 84:679–686.

Rincon, P.A., and J. Lobon-Cervia
1989 Reproductive and growth strategies of the red roach, *Rutilus arcasii* (Steindachner, 1866), in two contrasting tributaries of the River Duero, Spain. J. Fish Biol. 34:687–705.

Sokal, R.R., and F.J. Rohlf
1981 Biometry, 2d ed. W.H. Freeman, NY, 859 p.

SPSS Inc.
1988 SPSS-X™ user's guide. SPSS Inc, Chicago, 1072 p.

Sriramachandra-Murty, V.
1975 On the fishes of the family Platycephalidae of the seas around India. J. Mar. Biol. Assoc. India 17:679–694.

Abstract.–Morphological changes during metamorphosis of Dover sole *Microstomus pacificus* are described from 2220 larvae and juveniles. Unlike most flounders, initiation of eye migration is uncoupled from metamorphosis and from the habitat change from planktonic to benthic. Dover sole larvae are optically asymmetrical during most of their planktonic life. Major features associated with metamorphosis are reduction in body depth with associated reductions in lengths of neural and hemal spines, increase in relative eye diameter, loss of canine-like teeth coincidental with acquisition of incisor-like teeth, resorption of posterior process of coracoid, development of body scales, change in body pigmentation, and development of the gut loop in the secondary body cavity. From initiation to completion, metamorphosis appears to take about 9 months, during which time there is little increase in body length.

Available evidence indicates that most spawning off Oregon occurs in spring, with April and May as peak hatching months. Settlement from the plankton occurs in winter, with January to March as peak settlement months. Duration of planktonic life appears to be about 2 years, with a minimum duration of about 18 months. Metamorphosing larvae settle over a broad "landing" zone (55–377 m), quantitatively distinct from, but overlapping, the narrower spring nursery zone (40–170 m). As yet, there is no evidence of delayed metamorphosis. Metamorphosis is protracted, seems to be seasonally-triggered, and may involve a significant period during which larvae switch between midwater and bottom habitats.

Manuscript accepted 18 March 1992.
Fishery Bulletin, U.S. 90:285–301 (1992).

Metamorphosis and an overview of early-life-history stages in Dover sole *Microstomus pacificus**

Douglas F. Markle
Phillip M. Harris
Christopher L. Toole

Department of Fisheries and Wildlife, 104 Nash Hall
Oregon State University, Corvallis, Oregon 97331-3803

There is uncertainty about the length of the pelagic life of Dover sole *Microstomus pacificus*. Hagerman (1952) noted that the "pelagic life is prolonged for several months and metamorphosis is delayed." Allen and Mearns (1977) thought a 9-month planktonic stage was "probably not unusual." Pearcy et al. (1977a) examined the early life history in greater detail and concluded that "Dover sole larvae are pelagic for at least a year." Hayman and Tyler (1980), although citing Pearcy et al. (1977a), constructed a time-line indicating a 9-month pelagic larval stage.

There is also little agreement on estimated body length at the end of the first year of life. Pearcy et al. (1977a) estimated growth to be 20–30 mm standard length (SL) during the first year, but also concluded that metamorphosis took place after about 1 year at 30–50 mm SL (the extra 10–30 mm of growth was not explained). Hagerman (1952) and Demory (1972), both limited by small sample sizes, mention lengths of 66–75 mm total length (TL) for nominal 1-year-old specimens.

Uncertainty about duration and growth in the pelagic phase has important implications for age estimates. Whether based on scales or otolith sections, no researcher has documented the age or size at which the first nominal annulus forms (Demory 1972, Chilton and Beamish 1982, Pikitch and Demory 1988, Hunter et al. 1990).

From the large midwater trawl collections made by W.G. Pearcy and colleagues (OSU) from 1961 to 1982, and juvenile bottom-trawl surveys conducted off Oregon from 1988 to 1990, we describe metamorphosis and other stages in the early life history of Dover sole and address questions relating to the duration and timing of these stages.

Materials and methods

Midwater trawl collections

A total of 796 Dover sole larvae were obtained from 425 midwater trawl stations off Oregon. Details of sampling methods are given in Pearcy (1976, 1980) and Pearcy et al. (1977 a, b). Because the midwater trawls were made for a variety of reasons, there are constraints on interpretation of these data. The most important constraints are seasonal, diel, depth, and gear. Seasonal coverage was best from June to September, and poorest in May and October (Table 1). There was a pronounced diel bias. Relatively few samples were collected between 0600 and 2000 hours (Table 2). Most samples were collected at night between 2200 and 0500 hours. The range of collec-

*Technical paper 9837, Oregon State University Agricultural Experiment Station.

Table 1
Distribution of midwater trawl stations by month, 1961–82.

Month	No. of stations	Percent of total
January	94	3.8
February	127	5.1
March	157	6.4
April	174	7.0
May	85	3.4
June	306	12.4
July	397	16.1
August	237	9.6
September	479	19.4
October	74	3.0
November	165	6.7
December	173	7.0
Total	2468	99.9

Table 2
Distribution of midwater trawl stations by time of day, 1961–82.

Hour of set	No. of stations	Percent	Hour of set	No. of stations	Percent
0100	192	7.8	1300	51	2.1
0200	158	6.4	1400	60	2.4
0300	177	7.2	1500	60	2.4
0400	184	7.4	1600	65	2.6
0500	154	6.2	1700	52	2.1
0600	82	3.3	1800	60	2.4
0700	68	2.8	1900	65	2.6
0800	61	2.5	2000	78	3.2
0900	61	2.5	2100	95	3.8
1000	69	2.8	2200	119	4.8
1100	45	1.8	2300	133	5.4
1200	55	2.2	2400	167	6.8

tion depths was 0–6000 m, but 81.8% of the samples were from depths <500 m. Eleven different gear types were used: Tucker trawl, Cobb trawl, 0.9 m Isaacs-Kidd midwater trawl (IKMT), 1.8 m IKMT, 2.4 m IKMT, 3.0 m IKMT, 2.4 m rectangular midwater trawl (RMT), 2.7 m RMT, 1 m^2 multiple plankton sampler, 65 m^2 midwater trawl, and 100 m^2 midwater trawl. Some gears were operated with and without opening-closing devices (Pearcy 1980). Eighty-eight percent of the collections were made with either a 1.8 m or 2.4 m Isaacs-Kidd midwater trawl (IKMT). All specimens were preserved in 10% formalin and transferred to 50% isopropanol.

Juvenile bottom-trawl collections

A bottom-trawl survey of juvenile Dover sole was conducted bimonthly, January to November 1989, in three areas off Oregon (Fig. 1). In March 1988 and 1990, a more limited survey was conducted in the central (Foulweather) area. Each area was 10 miles wide and oriented to the coast such that the depth range of 50–400 m could be covered in the shortest distance. Each area was subdivided into six strata bounded by isobaths at 50, 80, 100, 120, 160, 220 and 400 m. Trawl stations were randomly chosen such that a minimum of three 5-minute trawls were attempted in each stratum. When time permitted, additional stations were added in strata with highest concentrations of Dover sole (100–119 and 120–159 m). All trawling was conducted from the FV *Olympic* during daylight hours. The gear was a commercial, 34.9 mm mesh, two-seam shrimp trawl with a 27.4 m headrope, rigged with a 28.5 m footrope and tickler chain. The posterior 3/4 of the codend had a 6.4 mm liner. The catch was sorted on board, all fish species were counted and measured, and all Dover sole <200 mm SL were frozen or fixed in 10% formalin and returned to the laboratory for morphological analysis. All formalin-fixed specimens were preserved in 50% isopropanol before measurement.

Morphological analysis

All measurements reported herein were made in the laboratory on defrosted or formalin-fixed, isopropanol-preserved specimens. We found no significant differences (P 0.93) between measurements of 39 defrosted juvenile Dover sole (46.9–71.0 mm SL) when remeasured over a year after fixation and preservation.

Measurements were taken on 2220 larvae, juveniles, and adults. Using the staging system developed herein, the numbers examined in each stage were: Stage 1, 811; Stage 2, 29; Stage 3, pelagic captures, 12; Stage 3, benthic captures, 409; Stage 4, pelagic captures, 1; Stage 4, benthic captures, 461; and Stage 5, 497. On all specimens returned to the laboratory, we measured TL, SL, body depth at anus (BD1A), maximum body depth, snout to posterior extent of intestine length (SINT), and body weight. Length measurements were taken to the nearest 0.1 mm using an ocular micrometer on specimens <20 mm SL and dial calipers on larger specimens. Body weight was determined to the nearest 0.001 g for Stages 1 and 2 and to the nearest 0.1 g for Stages 3, 4, and 5 (see staging description below). Weights were taken from undamaged, pat-dried individuals. Weight loss in isopropanol-preserved larvae was as great as 10% after 2 minutes of air exposure due to alcohol evaporation. Although specimens were exposed for less time before weighing, a 10% weighing error was

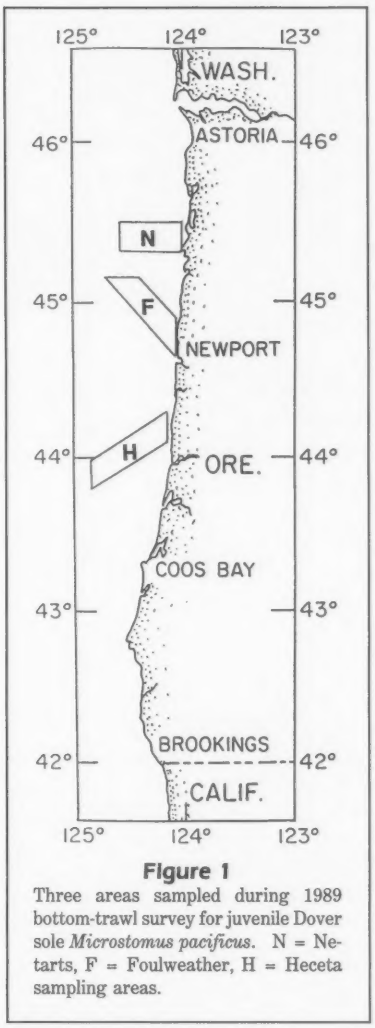

Figure 1
Three areas sampled during 1989 bottom-trawl survey for juvenile Dover sole *Microstomus pacificus*. N = Netarts, F = Foulweather, H = Heceta sampling areas.

assumed for this study. Considering the change in weight of three orders of magnitude between 10 and 50 mm SL, the weighing error was considered acceptable for this study.

A smaller subset of 201 specimens was examined to describe metamorphosis in greater detail, and all were deposited in the Oregon State University Fish Collection (OS). These specimens were either cleared and differentially stained with alizarin red S and alcian blue (Potthoff 1984), radiographed, or both. This subset included only postflexion Stage-1, most Stage-2, and representatives of Stages 3–5 larvae. In addition to routine measurements listed above, we measured right eye diameter, interorbital width, right upper jaw length, length of gastrointestinal tract as measured from anus to most posterior part of intestinal loop, length of first caudal neural spine, length of dorsal fin pterygiophore anterior to first caudal neural spine, length of dorsal fin pterygiophore posterior to first caudal neural spine, length of first hemal spine, length of anal fin pterygiophore anterior to first caudal hemal spine, and length of anal fin pterygiophore posterior to caudal hemal spine. Counts of vertebrae and rays of dorsal, anal, caudal, pectoral, and pelvic fins also were made.

A staging system describing Dover sole ontogeny was developed following the suggestions of Youson (1988). Our terminology deviates from Balon (1979, 1984) and Youson (1988) in our use of five numbered stages for early development, rather than numbered stages for metamorphosis only. Dover sole have a protracted metamorphosis, and our stages can be related, generally, to flatfish metamorphosis. We suggest terminology for each stage that incorporates traditional concepts of larval and juvenile periods as well as the metamorphic phase of the larval period. Metamorphosis occurs in Stages 2–4.

We were especially concerned with describing the beginning of metamorphosis, the initiation event, and the completion of metamorphosis, the climax event (Youson 1988). The initiation event was described based on six characters that reach the adult state during the plankton-to-benthos transition (see Results below). Another character, body scale formation, could be documented only in cleared and stained specimens and was concordant with completion of the six initiation-event characters. Development of the intestinal loop in the secondary body cavity, quantified by SINT, is the last character to change in Dover sole metamorphosis. The climax event was described based on the rate of change of the ratio of natural logarithms of two measurements (SINT and SL). Both initiation and climax events are further corroborated by body shape changes.

We use the concept of competency, as developed in the marine invertebrate developmental literature, as part of our definition of stages. The term regrettably has become a synonym for metamorphosis, as in the phrase "competent to metamorphose" (Pechenik 1986). Doyle (1975), using the term "delay" stage, noted that the onset of competency included both developmental criteria (strict metamorphosis as used herein) and a behavioral criterion, the ability to settle. In some invertebrates, attachment to a substrate is a prerequisite to metamorphosis; thus settlement must occur prior to metamorphosis. In fishes there is not necessarily a connection between metamorphosis (Youson 1988) and competence. However, Cowen (1991) applied the terms to fish and kept the marine invertebrate connection intact. Competency has been defined more narrowly

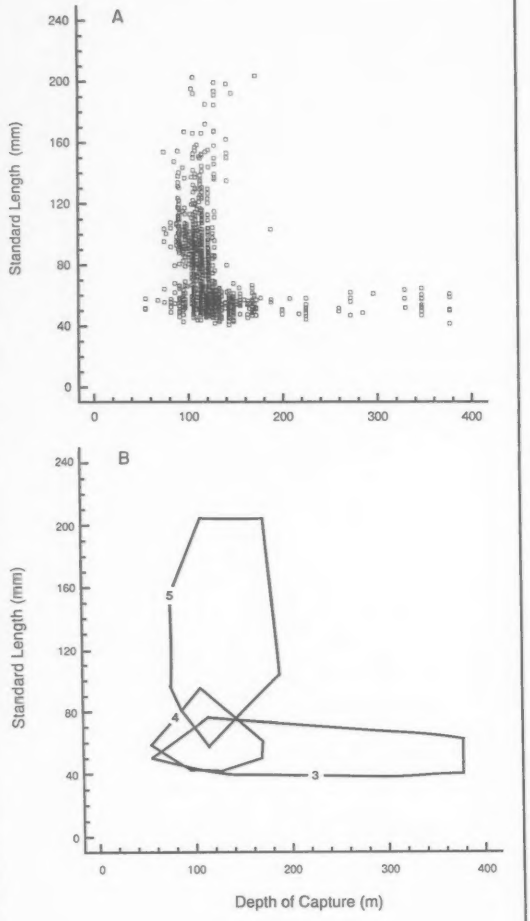

Figure 2
Relationship between body depth at anus and standard length in Dover sole *Microstomus pacificus*: (A) scatterplot of data points, Stages 1–5; (B) polygons circumscribing areas bounded by specimens in Stages 1–5.

Table 3
Characters used to quantify metamorphosis in Dover sole *Microstomus pacificus*.

Character	Character state
Teeth	0 Canines 1 Canines, incisors developing 2 Incisors
Eye position	0 Left side of head or dorsal ridge 1 Right side of head, adult position
Position of dorsal fin	0 First ray posterior to left eye 1 First ray equal with posterior margin or anterior to left eye
Posterior process of coracoid	0 Straight, angled posteriorly 1 Resorption beginning, tip curled into hook 2 Resorption complete, process absent
Pectoral fin shape	0 Round, paddlelike shape, < adult shape complement of rays, no radials formed 1 Intermediate shape, adult complement of rays, cartilaginous radials 2 Adult morphology
Pigmentation	0 Planktonic coloration 1 Benthic coloration

as the ability to settle (Jackson and Strathmann 1981), a conceptual improvement that removes predefined connections to metamorphosis. We identify precompetent, competent, and postcompetent stages during metamorphosis of Dover sole.

Time-series analysis

Two approaches were used to construct a time-line of early development: modal progression analysis (MPA, Bhattacharya 1967) and an analysis of seasonality of stages. MPA was facilitated using the computer program ELEFAN (Pauly 1987), but its utility was limited by sample sizes. Analysis of seasonality of stages was corroborated partly by monitoring growth of a single metamorphosing individual held in the laboratory at 13°C. The Stage-3 specimen was 57.7 mm SL when captured on 20 March 1989. It was measured regularly and progressed completely through Stage 4 to an early Stage 5, when it was sacrificed on 15 June 1989.

Results

Morphology and development

Stage 1 (premetamorphic larvae), 6.1–58.5 mm SL
For convenience and because of our emphasis on metamorphosis, all premetamorphic planktonic specimens are referred to as Stage 1. However, the premetamorphic phase of the larval period could be usefully divided into two intervals, the first approximating Stage I of Pearcy et al. (1977a). A transition from the first interval to the second occurs around 10–15 mm SL, during which eye migration begins, body depth increases (Fig. 2), the first dorsal and anal fin rays form, and caudal fin flexion begins. During the second interval, specimens acquire the adult numbers of vertebrae, and dorsal, anal, caudal, and pelvic fin rays; the stomach and intestine coil; 3–4 pyloric cecae develop; and a pigmentation pattern of dashes develops into a solid

Figure 3
Jaw dentition during metamorphosis in Dover sole *Microstomus pacificus*, left lateral views: (A) OS12578, Stage 1 with canine teeth; (B) OS11377, Stage 2 with canine and developing incisor teeth; and (C) OS11288, Stage 5 with developed incisor teeth.

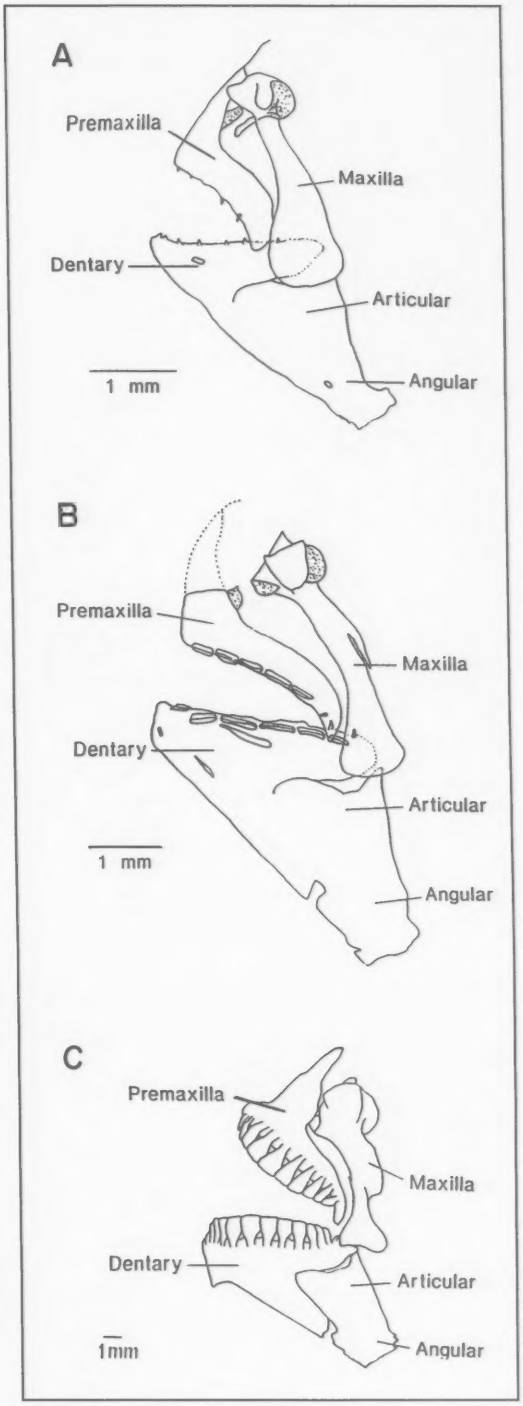

outline at the base of the dorsal and anal fins around 35–40 mmSL (Pearcy et al. 1977a).

Stage 2 (metamorphic precompetent larvae), 42.3–60.4 mmSL Six morphological characters that define the initiation event of metamorphosis are, in their approximate order of development: jaw dentition, completion of eye migration, position of anterior margin of dorsal fin, position or presence of posterior process of the coracoid, pectoral fin morphology, and beginning of asymmetrical coloration. Numerical scores given to the two or three states of each character are shown in Table 3. A metamorphosing presettlement individual can have a metamorphic score of 1 to 8. A score of 9 defines Stage 3, metamorphic competent larvae.

Dover sole larvae have canine-like teeth on left and right jaws (Fig. 3A). During Stage 2, incisor-like teeth develop on the left premaxilla and dentary (Fig. 3B). The canine-like teeth are lost from both jaws coincident with eruption of incisors in the left jaw (Fig. 3C).

In Stage 1 larvae, anterior dorsal-fin pterygiophores and fin rays are posterior to the orbit of the left eye which is located on the dorsal ridge of the cranium (Fig. 4A). During Stage 2, these pterygiophores move anterior to the orbit of the left eye (Fig. 4B).

The posterior process of the coracoid in larvae is a long, slender element that projects posteriorly above the visceral cavity, underneath the skin (Fig. 5A). During metamorphosis the process is resorbed. At the beginning of resorption, during Stage 2, the distal end of the process curls anteriorly into a hook (Fig. 5B). In our samples there is some indication that the process deteriorates (poor staining with alcian blue), but there is no gradual reduction in length or thickness of the process. Specimens either have the process or have lost it (Fig. 5C).

The pectoral fin in Stage-1 larvae is a paddle-shaped membrane with a thin, fleshy base and without radials. During Stage 2, a fleshy rectangular base, cartilaginous radials, and the adult complement of fin rays form (Fig. 5).

The Stage-1 larval color pattern consists of little or no pigment on the midlateral areas. A transitional pattern, in which melanophores aggregate along myosepta, is followed by the first indication of melanophores aggregating in two approximately circular groups anteriorly and posteriorly along the lateral line (Fig. 6). We score larval

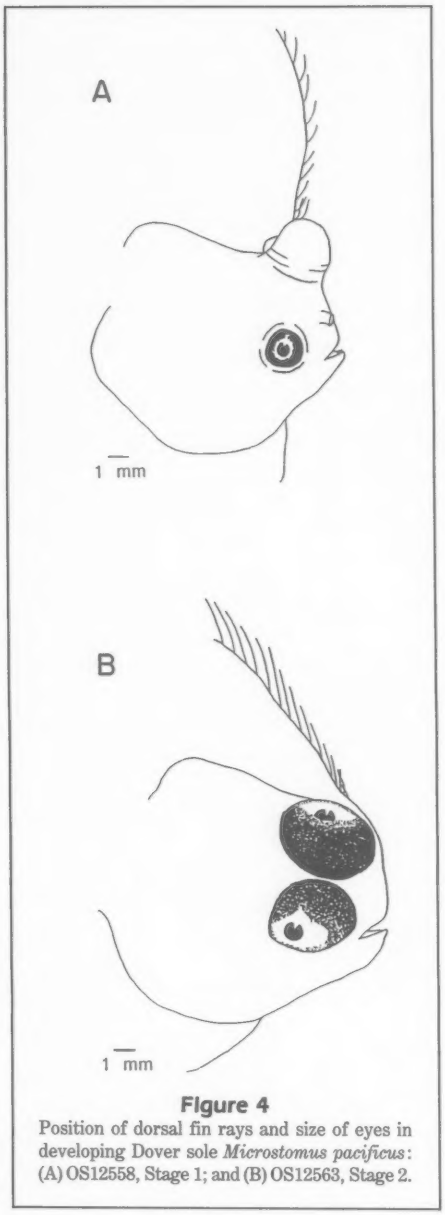

Figure 4
Position of dorsal fin rays and size of eyes in developing Dover sole *Microstomus pacificus*: (A) OS12558, Stage 1; and (B) OS12563, Stage 2.

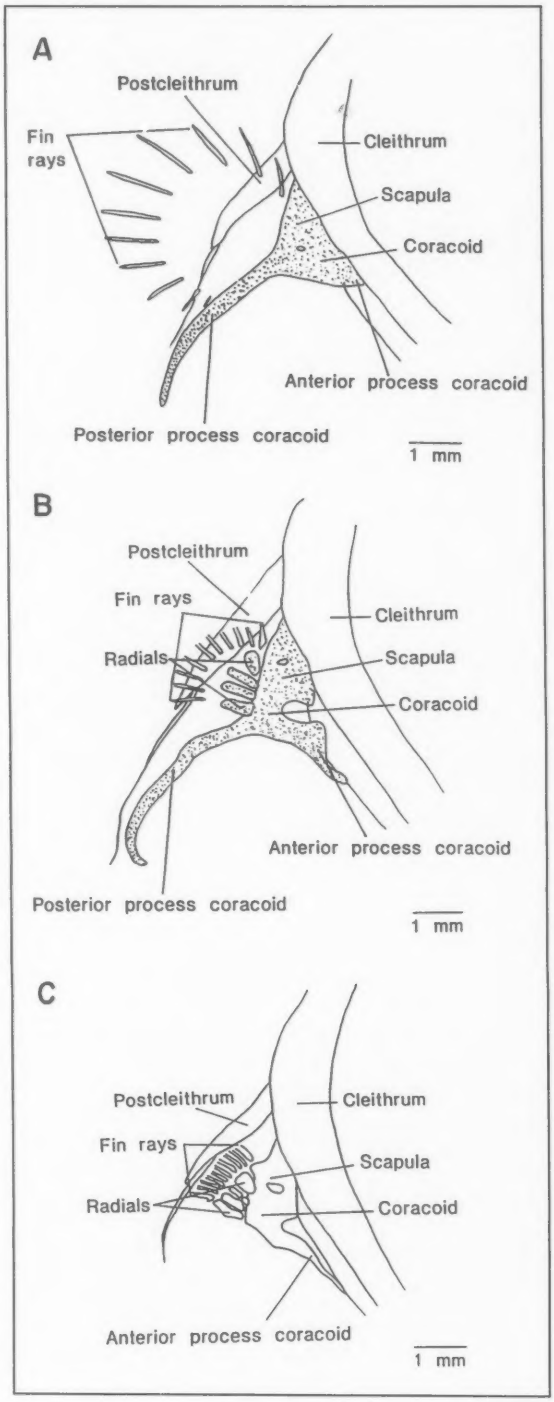

Figure 5
Pectoral fin development in Dover sole *Microstomus pacificus*: (A) OS12558, Stage 1 with straight ventral process of coracoid; (B) OS11377, Stage 2 with hooked tip on ventral process of coracoid; and (C) OS12563, Stage 3 after resorption of ventral process of coracoid.

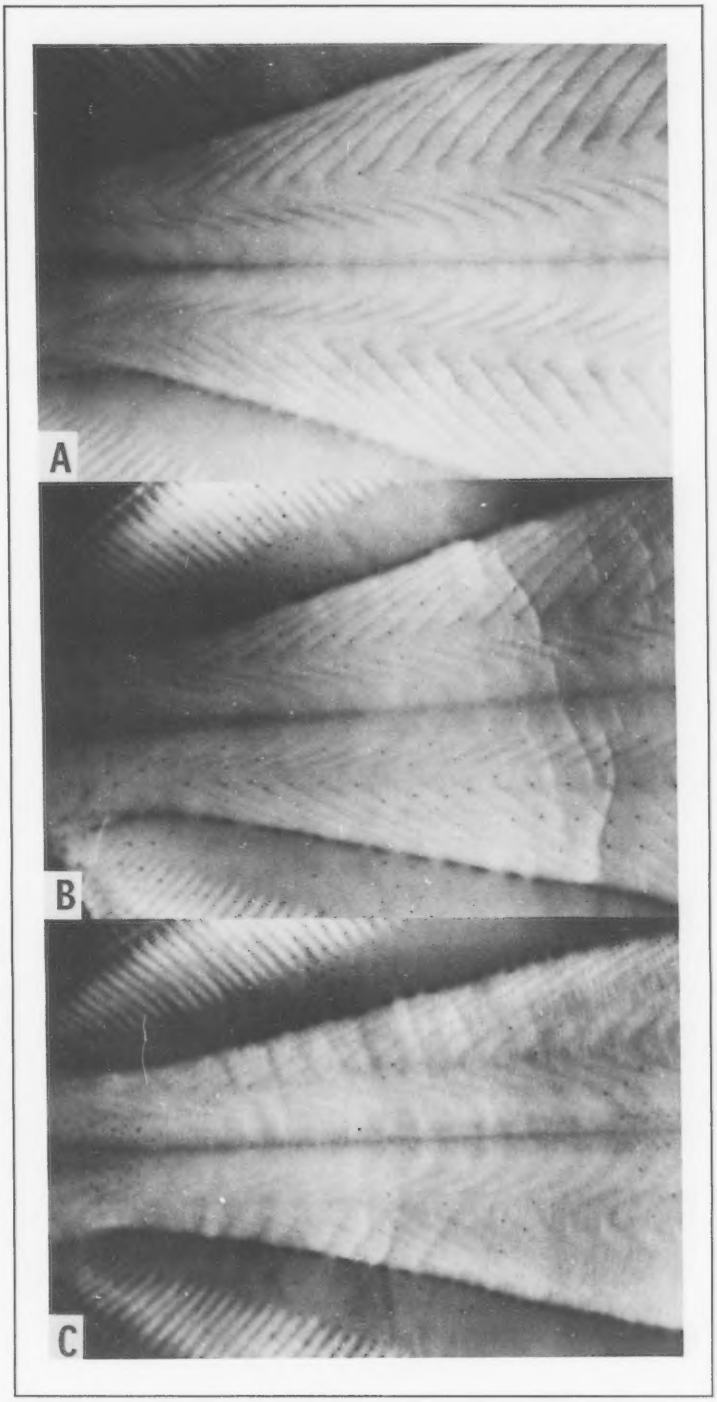

Figure 6
Right-side midlateral pigmentation patterns during development in Dover sole *Microstomus pacificus*: (A) OS13115, Stage 2, developmental score 5, larval pattern of no melanophores on myomeres; (B) OS13118, Stage 2, developmental score 8, transitional pattern of melanophores on myosepta; and (C) OS13117, Stage 3, aggregated pattern of melanophores in circular area on caudal peduncle and anterior trunk.

and transitional patterns equally and consider the circular aggregations as the first indication of asymmetrical coloration.

Coincident with changes in these six features are changes in features that are not easily coded: gradual loss of otic spines, reduction in body depth (Figs. 3 and 8), reduction in interorbital width (Fig. 7), increase in right eye diameter (Fig. 7), and increase in right upper jaw length (Fig. 3). Development of body scales also begins in Stage-2 specimens with metamorphic scores of 7 or 8. Body scales first form above and below the lateral line, anteriorly near the pectoral fin base, and on the caudal peduncle.

Stage 3 (metamorphic competent larvae), 40.7–74.9 mm SL Stage-3 specimens have a metamorphic score of 9, indicating that all six initiation-event features have either begun or reached the adult state. These specimens have a translucent appearance, intermediate between the earlier transparent stages and later opaque stages. Stage-3 specimens have asymmetrical coloration, retain the coiled, larval gut configuration, and have resorbed the posterior process of the coracoid. Some morphometric features initiated in Stage 2, such as increasing right eye diameter and shrinkage in body depth, continue in Stage 3 (Fig. 2). Ossification of pelvic-fin rays and radials is initiated in Stage 3, apparently after settlement (1 of 10 pelagic specimens and 4 of 4 benthic Stage-3 specimens have ossified pelvic fin rays and radials).

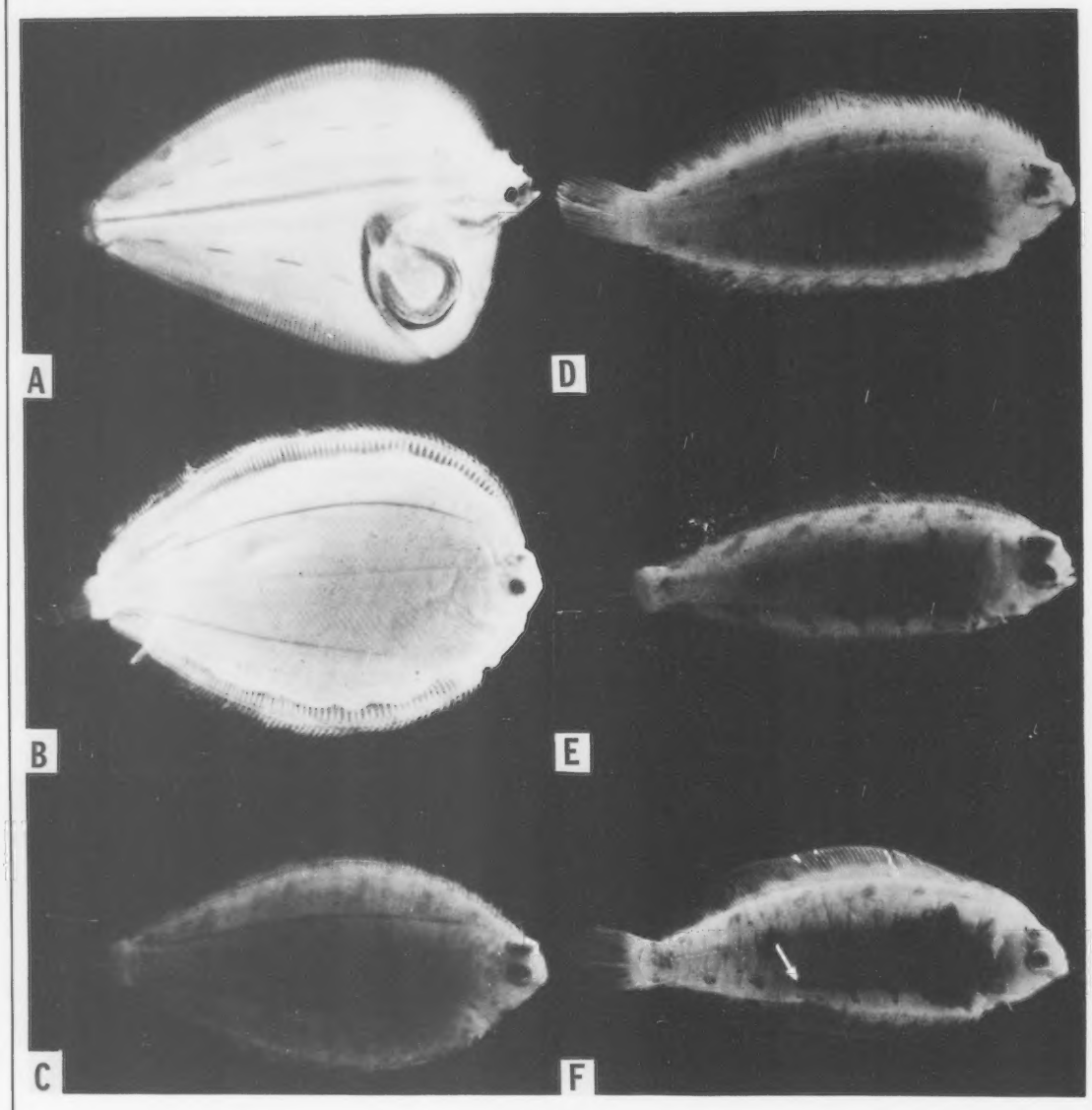

Figure 7

Dover sole *Microstomus pacificus* right lateral view: (A) OS13214, Stage 1, 20.4 mm SL; (B) OS11377, Stage 2, 54.5 mm SL; (C) OS13202, Stage 3 benthic capture, 52.4 mm SL; (D) OS13202, early Stage 4, 61.5 mm SL (intestinal loop is dark area above anal fin); (E) OS13203, late Stage 4, 58.4 mm SL; (F) OS13204, early Stage 5, 78.4 mm SL, arrow points to posterior end of intestinal loop.

Stage 4 (metamorphic postcompetent larvae), 41.7–79.3 mm SL Adult Dover sole have a long intestinal loop in the secondary body cavity above anal fin pterygiophores (Hagerman 1952). This intestinal loop (Fig. 7) forms after settlement, and its initiation is the defining feature of Stage 4. Continuous metamorphic changes in morphology, such as shrinkage in body depth, are completed during Stage 4 (Fig. 2).

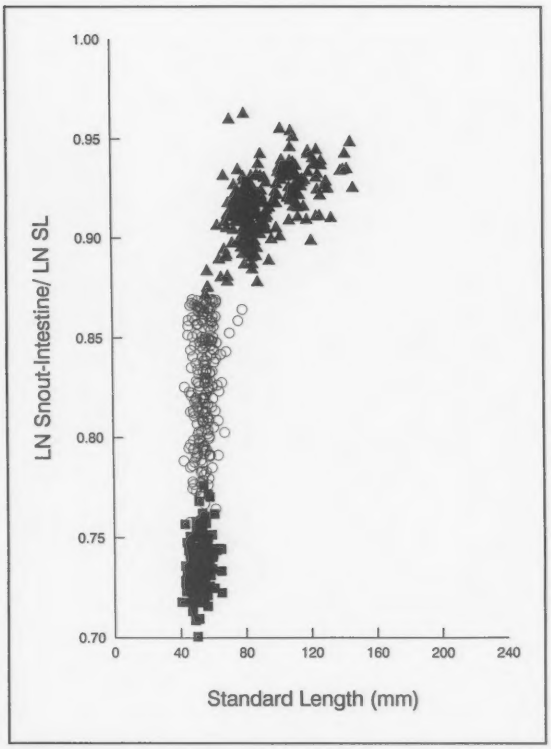

Figure 8
Relationship between the ln SINT/ln SL ratio and standard length during development of Dover sole *Microstomus pacificus*. Symbols represent Stage 3 (■), Stage 4 (O), and Stage 5 (▲).

Stage 5 (juvenile), 48.9 mm SL to sexual maturity
We define the climax event, and Stage 5, as the point at which length of the intestinal loop attains adult proportions. The continuous nature of this process is illustrated in the logarithm ratios of SINT/SL (Fig. 8). We chose a cut-off ratio by calculating the ratio for 2 mm SL increments and examining the rate at which the ratio changes over length. The greatest rate of change occurs between 67 and 69 mm SL, during which the mean ratio changes from 0.85 to 0.89. We chose the midpoint of these ratios and therefore define Stage 5 as those individuals with a ratio of ln (SINT)/ln (SL) > 0.87. Coincident with this change is an overall darkening of body color such that Stage 5 specimens look like small adults.

General features of early development and metamorphosis

Unlike most flounders, initiation of eye migration in Dover sole is uncoupled from the change in habitat from planktonic to benthic, as well as from the process of metamorphosis (as defined herein). Eyes are symmetrical up to a maximum size of only 13.4 mm SL, and the left eye can be on the midline in specimens as small as 9.5 mm SL (Pearcy et al. 1977a). Eye migration in Dover sole is arrested during planktonic growth, with the left eye stopping at the dorsal margin of the cranium at 15–20 mm SL (Fig. 4A). It remains in this position until metamorphosis. Thus, during most of their planktonic life, the eyes of Dover sole are asymmetrical.

There is a complex relationship between body depth and SL (Fig. 2), including (1) an interval of rapid increase from about 10 mm to at least 60.4 mm SL in some individuals, (2) a compensatory shrinkage phase over the size range 40.7–74.9 mm SL, and (3) a more typical linear growth phase that may begin in specimens as small as 41.7 mm SL. Body depth reduction is a regressive process (Youson 1988) in which lengths of neural and hemal spines and pterygiophores are reduced (Fig. 9). Two- and three-fold reductions occur in lengths of first caudal neural and hemal spines and their immediate anterior and posterior pterygiophores. Consequently, metamorphosing Stage-3 specimens 40–50 mm SL have neural and hemal elements comparable in length to those of 20–30 mm SL Stage-1 larvae. Neural and hemal elements and dorsal and anal pterygiophores in Stage-1 larvae are cartilaginous or weakly ossified, and vertebral centra lack zygopophyses. Complete ossification of neural and hemal elements and formation of zygopophyses occurs in Stages 2 and 3.

During most of metamorphosis, especially in Stages 2 and 3, body length appears to be arrested (Fig. 10). Although the sample size of Stage-2 larvae limits our confidence in further analysis, the data show little indication of growth between Stages 2 and 3 (Fig. 10). Because metamorphosis occurs over a broad range of sizes, similarity in size minima and maxima between stages also suggests little or no growth in body length. For example, the minimum sizes for Stages 2, 3, and 4 are almost identical (42.3, 40.7 and 41.7 mm SL, respectively). During Stage 4 there is finally some indication of growth because the smallest Stage-5 juvenile is 48.9 mm SL, more than 7 mm larger than the smallest Stage-4 larva. Yet, even this juvenile is 26 mm smaller than the largest metamorphosing Stage-3 larva.

There is an apparent loss in body weight during metamorphosis because of a decrease in mean weight from 2.6 to 2.4 g from Stage 2 to Stage 4 (Fig. 11). However, the small sample size of Stage 2 and our measuring error preclude attaching significance to the

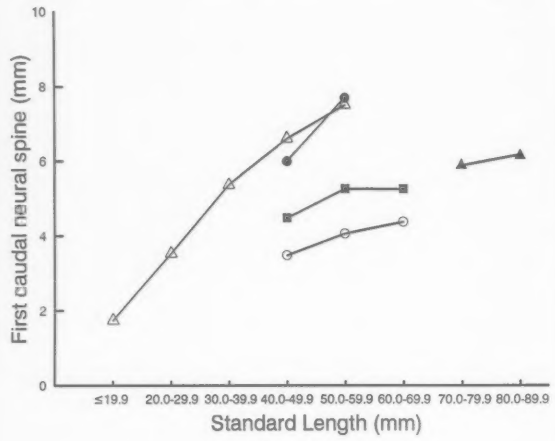

Figure 9
Change in length of first caudal neural spine during development of Dover sole *Microstomus pacificus*. Symbols represent Stage 1 (△), Stage 2 (●), Stage 3 (■), Stage 4 (○), and Stage 5 (▲).

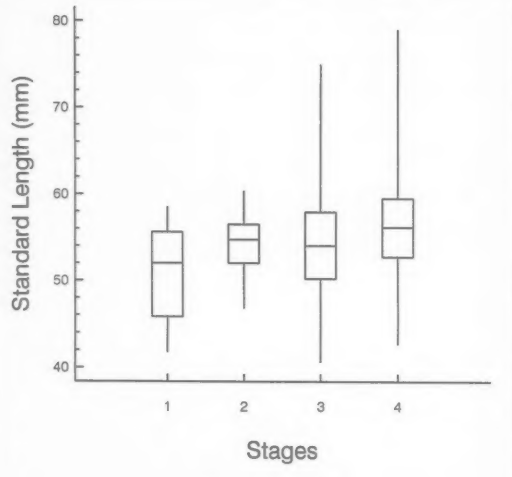

Figure 10
Mean standard length (horizontal line), size interval for 50% of observations (box), and size range for Stage-1 specimens >40 mm, all Stage-2 specimens, and all January and March Stage-3 and Stage-4 specimens of Dover sole *Microstomus pacificus*.

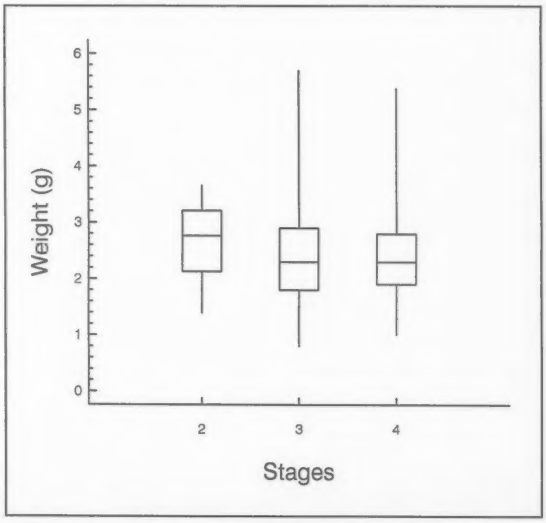

Figure 11
Mean weight (horizontal line), weight interval for 50% of observations (box), and weight range for Stages 2–4 in Dover sole *Microstomus pacificus*.

apparent loss. During the second year of life in the plankton (see next section), body weight increases an order of magnitude from a mean of about 0.30 g for Stage 1 in February to 2.0–4.0 g for Stage 2. All individuals that reach a size of 40 mm SL are at least 0.74 g; Stage-2 specimens are at least 1.39 g; Stage 3, at least 0.80 g; and Stage 4, at least 1.0 g. Because our sample size for Stage 3 is relatively large, our best estimate of a weight threshold for metamorphosis is ~0.8 g. However, if the suggestion of weight loss during metamorphosis is not an artifact (Fig. 11), the weight threshold may be closer to the minimum weight of Stage 2. Further complicating an estimate of that threshold is the observation that our lightest Stage-2 specimen (42.6 mm SL and 1.39 g) was caught in January with a developmental score of 7, and presumably may already have lost weight.

Because SINT increases during metamorphosis and BD1A decreases, the SINT/BD1A ratio provides an additional means of visualizing the relationship between the metamorphic process and developmental stages (Fig. 12).

Timing and duration of stages

Temporal change in size of Stage-1 larvae <40 mm SL was analyzed using MPA (Fig. 13). Small larvae, about 6–8 mm, were found from February to June. The smallest identifiable mode was in April, and from November to March modes were level around 22–25 mm. Two notable features of these data are apparent accelerated growth in June and reduced availability of larger

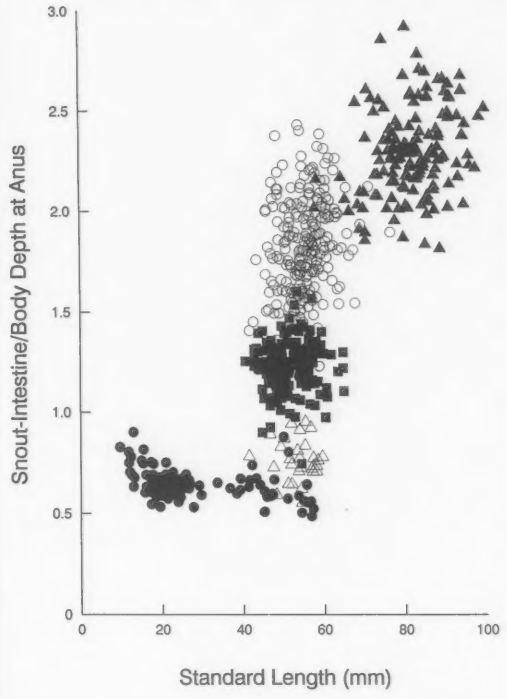

Figure 12
Relationship between the SINT/BD1A ratio and standard length during development of Dover sole *Microstomus pacificus*. Symbols represent Stage 1 (●), Stage 2 (△), Stage 3 (■), Stage 4 (○), and Stage 5 (▲).

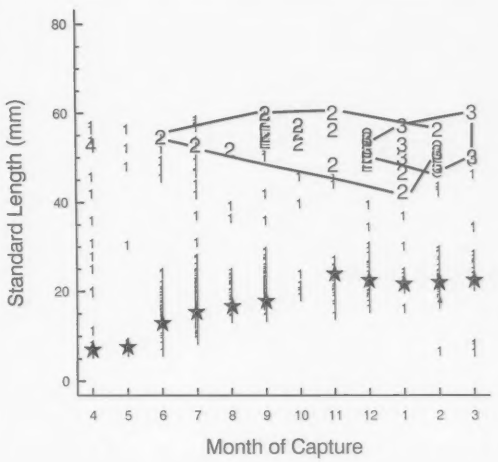

Figure 13
Relationship between standard length and month of capture for Dover sole *Microstomus pacificus*, Stages 1–4 collected in midwater trawls. Stars indicate modes determined by modal progression analysis in larvae <40 mm SL. Stage-2 and -3 specimens are circumscribed by lines.

Table 4
Seasonal catch-per-effort for planktonic Stage-2 and Stage-3 Dover sole *Microstomus pacificus* larvae off Oregon. *N* = number of trawls.

Month of collection	*N*	No. of Stage 2 based on metamorphic score								No. of Stage 3
		1	2	3	4	5	6	7	8	
January	128	—	—	—	—	—	—	2	—	2
February	167	—	—	—	—	—	—	—	2	4
March	147	—	—	—	—	—	—	—	—	2
April	201	—	—	—	—	—	—	—	—	0
May	106	—	—	—	—	—	—	—	—	0
June	278	1	—	—	—	—	—	—	—	0
July	291	—	—	—	—	—	1	—	—	0
August	303	1	1	—	—	—	—	—	—	0
September	217	—	1	—	4	2	1	—	—	0
October	129	—	—	—	—	1	1	—	1	0
November	217	—	—	—	—	—	—	2	1	0
December	126	—	—	—	—	—	—	2	6	2

specimens after March (Fig. 13). All small larvae (<10 mm SL) were collected on one day, 12 June 1971, between 50 and 67 km offshore, whereas larger larvae from June were collected considerably further offshore, 108–275 km on various dates. There appears to be little or no coherent size progression after the 24.5 mm mode in March. Specimens >30 mm are found in every month, and weakly-defined modes can be visualized around 50 mm in June, July, and September. Accelerated growth in April and May would seem to be required if the modal size were to double from about 25 mm in March to 50 mm in the second summer of life. Paradoxically, April is a time when micronekton biomass is normally low (Pearcy 1976).

Stage-2 specimens were caught from June to February (Table 4). The coherent progression of metamorphic scores for Stage-2 larvae indicates that metamorphosis begins as early as June; Stage-3 larvae are present as early as December and as late as March. About 6 months seems to be required to progress through Stage 2.

The seasonal distribution of Stage-3 larvae in benthic samples was consistent with their planktonic distribution (Table 5). During bimonthly sampling in 1989, 98.5% of Stage-3 specimens were caught in January or March. Five Stage-3 specimens were caught in May, and most new settlers appear to be in Stage 5 by July

Table 5
Seasonal distribution of Dover sole *Microstomus pacificus* stages in bottom-trawl samples off Oregon, 1989.

Month of collection	*N*	Number (%)		
		Stage 3	Stage 4	Stage 5
January	371	177 (48)	12 (3)	182 (49)
March	655	155 (24)	347 (53)	153 (23)
May	222	5 (2)	113 (51)	104 (47)
July	60	0	11 (18)	49 (82)
September	154	0	5 (3)	149 (97)
November	267	0	3 (1)	264 (99)

(Table 5). Individuals appear to require about 45 days to progress through Stage 3. Our laboratory-held specimen progressed through Stage 4 in 43 days. Overall, the progression through Stages 2–4 appears to require about 1 year for the population as a whole and about 9 months for an individual.

The length and weight of benthic Stage 3 larvae were compared between January and March 1989. Mean length in March (51.5 mm SL) was significantly smaller than the mean length in January (56.3 mm SL, $P<0.00001$). March specimens were also significantly lighter (2.0 g) than January specimens (2.7 g, $P<0.0001$). A similar pattern (earliest individuals in a stage being largest) was seen in Stage-2 larvae. The mean length of Stage-2 larvae captured between January and March (late in the season, Table 4) was smaller (53.0 mm vs. 54.3 mm SL) and lighter (2.4 vs. 2.8 g) than Stage-2 larvae captured between June and December (early in the season, Table 4), but the differences were not significant (length $P<0.4642$; weight $P<0.1227$).

Habitat of stages

On average, Stage-1 specimens were caught in nets fished to a maximum depth of 338 m, Stage-2 specimens in nets fished to 538 m, and planktonic Stage-3 specimens in nets fished to 293 m. All planktonic Stage-3 larvae were caught at night, between 1835 and 0544 hours, and 93% of Stage-2 larvae were caught at night, between 1802 and 0748 hours. Sampling effort was also greatest at night (Table 1; opening-closing nets collected 516 Dover sole but most (509) were Stage 1). The minimum depth of capture in the discrete depth samples was <100 m for 82%, and <300 m for 95%, of Stage-1 specimens. Only six Stage-2 specimens were caught in discrete depth samples, and only two of these in nets not fishing the surface. One Stage-2 larva was caught at 100–150 m and the other at 400–500 m. The single Stage-3 larva collected in a discrete depth sample was collected at 0–330 m.

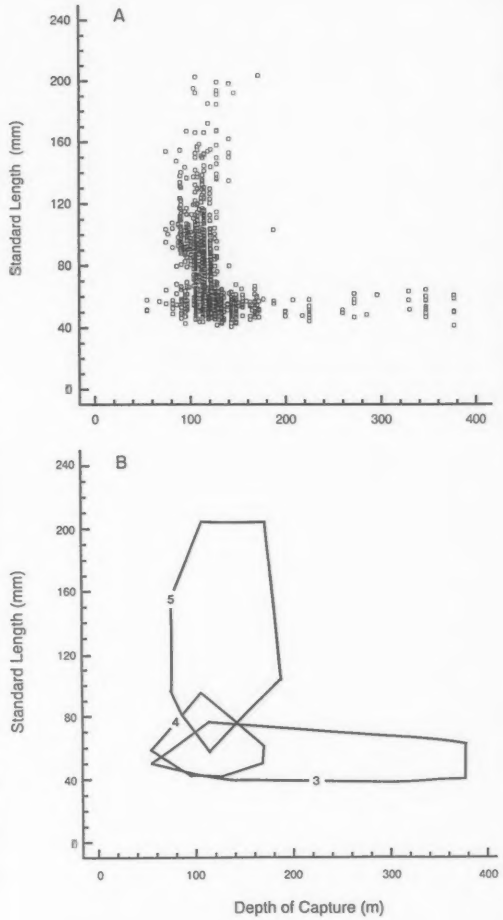

Figure 14
Relationship between standard length and depth of capture of developing Dover sole *Microstomus pacificus*, caught in bottom trawls off Oregon, January and March 1989: (A) scatterplot of data points, Stages 3–5; (B) polygons circumscribing areas bounded by specimens in Stages 3–5.

Benthic specimens were caught at depths shallower than the maximum depth fished by non-closing midwater nets. Based on our stratified sampling, a comparison of depth of capture of stages shows that Stage-3 specimens were caught at an average depth of 146 m (SE 2.65, range 55–377 m), Stage-4 specimens in January and March at an average depth of 118 m (SE 0.68, range 40–170 m), and Stage-5 specimens in January and March at an average depth of 110 m (SE

0.48, range 75–188 m). Compared with Stages 4 and 5, the greater average depth and variance of benthic Stage-3 larvae indicate a much broader depth distribution (Fig. 14).

Stage-3 larvae occupy a transitional "landing" zone quantitatively distinct from, but overlapping, the late-larval and juvenile nurserygrounds. Although Stage-3 larvae caught in bottom trawls quickly take to the bottom when placed in aquaria (pers. observ.), their nighttime capture in midwater trawls and daytime capture in bottom trawls suggest they may be engybenthic (nearbottom) or benthopelagic, rather than exclusively benthic.

Behavior associated with metamorphosis presumably includes some short-term (hours to days) switching between midwater and bottom habitats. In one individual in our data set, the behavior continued into Stage 4. A 53.0 mm Stage-4 specimen was caught 19 April 1963 off the mouth of the Columbia River at 0411 hours in a midwater trawl fished to 73 m over a bottom depth of about 125 m. Its gut loop was well developed and contained sand grains. Additional evidence is provided by midwater Cobb trawl samples collected by W. Lenarz and colleagues (NMFS Southwest Fish. Sci. Cent., Tiburon, CA 94920) between Monterey and San Francisco, California, from 28 March to 2 April 1990. In eight nighttime (2235–0447 hour) samples, fished at 0–110 m (most 0–30 m) over bottom depths of 33–1462 m, they collected 14 Stage-3 larvae (40.4–51.2 mm SL) and 16 Stage-4 larvae (42.4–53.4 mm SL). Stage-3 larvae were collected over bottom depths of 73–1462 m, and Stage-4 larvae were collected over bottom depths of 33–91 m. Thus, settling Stage-3 larvae were found in a "landing" zone at 55–377 m and in a wedge of the water column above and seaward of that zone.

Discussion

Time-line

Dover sole spawn in deep water in winter, December to February, according to Hagerman (1952), and November to April according to the circumstantial evidence of Harry (1959). Yoklavich and Pikitch (1989) provide evidence that smaller Dover sole have an earlier, shorter spawning season than larger fish, and that Dover sole now mature at significantly smaller sizes than reported by Hagerman (1952) or Harry (1959). These observations suggest the possibility that size-selective exploitation might have shifted the spawning season to earlier dates.

However, other observations suggest that peak hatching of Dover sole off Oregon is later, not earlier, than indicated by Hagerman (1952) or Harry (1959). Results of sampling the commercial Dover sole catch off southern Oregon (43°N) from March 1990 to September 1991 indicate running ripe females were caught from February through July with a peak in April (Mike Hosie, Oreg. Dep. Fish Wildl., Charleston, OR 97420, pers. commun.). Spent females increased from less than 10% of all females in April to 100% by early August. However, these observations may be biased towards later-spawning fish because the commercial catch is culled of small fish (Yoklavich and Pikitch 1989). Experiments performed in 1972 by S. Williams at Newport, Oregon, showed that hatching took 18 days at 12.5°C, 27 days at 10.0°C, and 38 days at 7.5°C (Mike Hosie, pers. commun.). In agreement with these observations, small larvae (<10 mm SL) in this study were collected from February to July, with most caught in April and May (Fig. 13, Pearcy et al. 1977a). In ten NMFS ichthyoplankton cruises conducted at 40–48°N from 1980 to 1987, high densities of Dover sole eggs were found in each of six cruises conducted in March, April, or May; none or trace amounts were found in four cruises conducted in August, November, or January (Urena 1989; M. Doyle, NMFS Alaska Fish. Sci. Cent., Seattle, WA 98115, pers. commun.). Finally, "spawning" adults off Alaska have been collected primarily in May and June (Hirschberger and Smith 1983), and eggs are collected in June (Kendall and Dunn 1985). Thus, the weight of evidence seems to indicate that most Dover sole off Oregon hatch from February (Fig. 13) to August (Urena 1989), with a peak in April and May (see also the time-line in Hayman and Tyler 1980).

Settlement is restricted to the period from January to March or April (Table 5), whereas metamorphosis requires a protracted period of up to one year, occurs at sizes >40 mm SL (Fig. 3), includes little growth in body length, and may include loss of weight. Cessation in growth of body length before and during metamorphosis has been documented in other flounders (Fukuhara 1986, 1988). If the modal size of Stage-1 larvae is ~25 mm in March, then the average duration of the planktonic period of Dover sole is about 21 months (Fig. 15). However, the timing of settlement has a size component; larger larvae tend to settle before smaller larvae. It seems reasonable that larger larvae are those that grow faster, but it is also possible that they are slow growers or have otherwise delayed metamorphosis and, therefore, are more than 2 years old (see Discussion below).

Distribution and relative abundance of metamorphic planktonic stages provide additional insight. Larger planktonic specimens were generally rare in midwater trawl collections (Fig. 13). However, Stage-2 larvae, with developmental scores of 7 and 8, and Stage-3 larvae were the most abundant of all metamorphic stages found in midwater (Table 4), even though they

were collected in months with few samples (Table 1). Planktonic Stage-2 larvae were caught in nets fished deeper than either Stage-1 or planktonic Stage-3 larvae. The rarity of larger planktonic and early metamorphic stages may reflect movement deeper into the mesopelagic zone and lower relative sampling effort in deeper water. Late in Stage 2 (developmental scores 7 and 8) and in Stage 3 this trend appears to be reversed, as these stages were caught more frequently. If metamorphosis is a time of increased vulnerability, deeper water may provide a predation refuge. Alternatively, the behavior may place metamorphosing specimens in a water mass that facilitates late larval transport.

Settlement seems remarkably gradual, coincides with the downwelling season, ends with the spring transition in the oceanographic regime (Huyer et al. 1979), and occurs over a very broad "landing" zone (Fig. 14). Stage-3 larvae settling outside the nursery zone may experience differential mortality, or their broad depth distribution may reflect a process of testing the habitat in search of the preferred nurseryground. Capture of Stage-3 and -4 specimens in both nighttime midwater and daytime bottom trawls suggests a diel vertical search pattern.

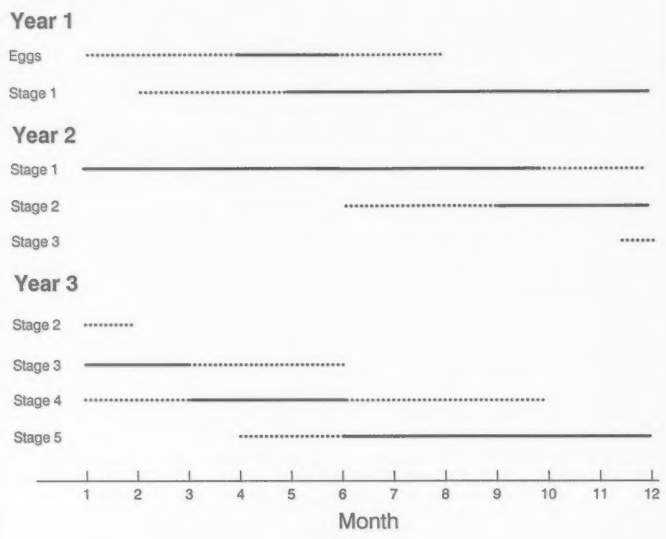

Figure 15

Hypothetical time-line of development for a cohort of Dover sole *Microstomus pacificus*, off Oregon. Solid lines represent presumed peak times for the different stages, and dotted lines represent the ranges.

Egg and larval drift

A proposed recruitment mechanism for Dover sole (Hayman and Tyler 1980, Parrish et al. 1981) focuses on inshore-offshore transport. The long planktonic period of Dover sole implies that alongshore transport also may be important. Our data allow some first-order generalizations about the distribution of early-life-history stages and may give further insight into the recruitment mechanism.

Urena (1989) found that greatest abundances of Dover sole eggs were in neuston samples collected beyond the 200 m isobath. In April and May in the upper 50 m, the current flows southward at about 10–15 cm/second at the 200 m isobath (Huyer 1977, fig. 9; Huyer et al. 1979) and is even weaker further offshore (Huyer and Smith 1978). At 10 cm/second, eggs could be transported 260 km southward in 30 days, assuming that their transport was not interrupted by offshore jets or gyres. Onshore-offshore transport of eggs should be variable. During upwelling, the upper 20 m may experience an average offshore velocity of 2–5 cm/second (Huyer 1983), and the upper 5 m may experience an average offshore velocity of 15 cm/second (Peterson et al. 1979). The short duration of the egg stage, restricted area of high offshore velocity, and the return inshore of water masses during relaxation after upwelling (Peterson et al. 1979) suggest that average offshore transport of eggs should be slow, but nontrivial. Deepwater spawning may help reduce both alongshore and onshore-offshore transport.

Stage-1 larvae also are found beyond the 200 m isobath (Pearcy et al. 1977a) and, like eggs, would be vulnerable to the southward flow of the California Current. In fact, the large surface area of the body of Dover sole larvae might facilitate such transport. Although there are important seasonal changes in direction (Huyer et al. 1979), on an annual basis the average surface current around 100 km offshore is ~0.5–1.0 cm/second to the south (Hickey 1979, fig. 8b). If Stage 1 lasts an average of 15 months, and assuming a mean flow of 0.75 cm/second, these larvae would travel an additional 295 km southward.

We suggest that early Stage-2 larvae move into deeper water. The California Undercurrent is a northward-flowing countercurrent located below 200 m and

influencing an area up to 500 km off the shelf (McLain and Thomas 1983). Its velocity is <10 cm/second over the continental slope north of Cape Mendocino (Hickey 1979) and weaker seaward of the slope. Somewhat further south, between Pt. Arena and Pt. Reyes, the current is 3–10 cm/second from July to October and <1 cm/second from October to January (Huyer et al. 1989). If eggs and Stage-1 larvae are displaced, on average, 555 km (260 + 295) southward of their spawning site, a northward-flowing undercurrent of 3.25 cm/second would be sufficient to return Stage-2 larvae to the vicinity of their spawning site in 6 months. This does not seem to be an unreasonable average velocity for the undercurrent from July to January.

The depth range of the Stage 3 "landing" zone (55–377 m) corresponds with the northward undercurrent located at 200–300 m (Huyer and Smith 1985). However, these larvae appear to need a mechanism to bring them shoreward. The surface Ekman layer, 0–20 m, within which wind-driven transport occurs (Huyer 1983), could be reached if larvae moved up in the water column during storms. Diel offbottom migrations could be part of this mechanism. Alternatively, as the body surface area is reduced during this stage, larvae may become less passive and move actively inshore.

Delayed metamorphosis and settlement

The protracted process of metamorphosis in Dover sole is contrary to expectations based on the ideas of saltatory ontogeny (Balon 1981). In general, ontogenetic transformations are expected to occur rapidly because intermediate forms are presumed to be maladapted. For example, loss of teeth from the right side of the jaw and development of incisors on the left side seem to hold no advantage for a planktonic larva, yet this is the situation in Dover sole for several months during the precompetent Stage 2. Delayed metamorphosis is also related to the concept of saltatory ontogeny; because the transition is assumed to be quick, an organism without the proper cues simply delays metamorphosis and settlement. In other words, it keeps the morphology appropriate for the habitat. Typically, field researchers identify a minimum threshold size or developmental stage for metamorphosis and assume that planktonic specimens greater than the threshold size or in the threshold stage have delayed metamorphosis (Pechenik 1986). Others have used a minimum age as a threshold (Cowen 1991).

Pearcy et al. (1977a) suggested that larger "holdover" Dover sole larvae (>50 mm SL) delayed metamorphosis and few successfully recruited to the benthic juvenile stage. Delayed metamorphosis is predicted for coastal organisms subjected to offshore transport (Jackson and Strathmann 1981) and there is some evidence for delayed metamorphosis in fishes (Victor 1986, Cowen 1991). An advantage of delayed metamorphosis is extension of the settlement season beyond what would be expected based on the spawning season (Victor 1986). Contrary to this expectation, the duration of Dover sole settlement is seasonally restricted and, off Oregon, no greater than the duration of the spawning season. Because precompetent larvae are probably a great distance from their settlement site, cues for metamorphosis are likely to be seasonal rather than site-related.

Experimental studies focusing on flounders have shown (1) fast-growing individuals metamorphose at smaller sizes, (2) fast-growing individuals retain their faster growth rate for at least several weeks after metamorphosis, (3) age at metamorphosis (defined by eye migration) is more variable than size at metamorphosis, and (4) a target size or threshold must be reached prior to metamorphosis (Policansky 1982, Chambers and Leggett 1987, Chambers et al. 1988). Other fishes and organisms may have age-triggered, size-triggered, or age- and size-triggered metamorphosis (Policansky 1983). Policansky (1983) points out that a size threshold would be expected when there is a size difference in available food between different habitats or a minimum energy requirement to successfully function at a certain stage.

We suggest two contrasting interpretations of the early life history of Dover sole. If size and age at metamorphosis are positively correlated, as is the case in winter flounder (Chambers et al. 1988), then larger, earlier settlers are older and slower-growing than smaller, later settlers. The difference in age could be the difference between early and late spawners or between different years of spawning. Alternatively, variation in size at metamorphosis may simply reflect differential growth rates operating for a long time, probably at least 2 years. As a consequence, larger, earlier settlers would be the faster growers rather than slower growers. One could distinguish between these alternatives and demonstrate delayed metamorphosis by documenting different year-classes among settlers.

In terms of life-history strategies, delayed metamorphosis and protracted metamorphosis may confer similar advantages. Extension of settlement through delayed metamorphosis allows for adaptive responses to short-term oceanographic variability and avoidance of settling during unfavorable conditions. If metamorphosis and settlement are cued to favorable seasons, protracted metamorphosis and the ability of competent metamorphosing individuals (Stage-3 larvae) to spend several months moving between midwater and bottom habitats should also compensate for any short-term unfavorable oceanographic conditions.

Acknowledgments

This study was funded, in part, by Oregon Sea Grant with funds from NOAA, Office of Sea Grant, Department of Commerce, under grant NA85AA-D-SG095 (project R/OPF-29) and from appropriations made by the Oregon State Legislature; by the Pacific Outer Continental Shelf Region of the Minerals Management Service, U.S. Department of the Interior, Washington, D.C., under Contract 14-12-0001-30429; and by National Marine Fisheries Service contract NA-87-ABH-00014. Some ship time was generously donated by T.N. Thompson. C. Ridgley, D. Nelson, S. Banks, and R. Melendez helped collect data. Shipboard work was made as pleasant as circumstances permitted by T.N. Thompson and the crew of FV *Olympic*. A. Kendall (NMFS, Seattle, WA), W. Lenarz (NMFS, Tiburon, CA), and G. Moser and J. Butler (NMFS, La Jolla, CA) shared results of ongoing research. W. Pearcy, D. Stein, and collaborators saved, documented, and made available 20 years of planktonic and midwater trawl collections that were invaluable for this study.

Citations

Allen, M.J., and A.J. Mearns
1977 Life history of the Dover sole. Annu. Rep. South Calif. Coastal Water Res. Proj. 77-1, El Segundo, p. 223–228.

Balon, E.K.
1979 The theory of saltation and its application to the ontogeny of fishes: Steps and thresholds. Environ. Biol. Fishes 4: 97–101.
1981 Saltatory processes and altricial to precocial forms in the ontogeny of fishes. Am. Zool. 21:573–596.
1984 Reflections on some decisive events in the early life of fishes. Trans. Am. Fish. Soc. 113:178–185.

Bhattacharya, C.G.
1967 A simple method for resolution of a distribution into Gaussian components. Biometrics 23:115–135.

Chambers, R.C., and W.C. Leggett
1987 Size and age at metamorphosis in marine fishes: An analysis of laboratory-reared winter flounder (*Pseudopleuronectes americanus*) with a review of variation in other species. Can. J. Fish. Aquat. Sci. 44:1936–1947.

Chambers, R.C., W.C. Leggett, and J.A. Brown
1988 Variation in and among early life history traits of laboratory-reared winter flounder *Pseudopleuronectes americanus*. Mar. Ecol. Prog. Ser. 47:1–15.

Chilton, D.E., and R.J. Beamish
1982 Age determination methods for fishes studied by the groundfish program at the Pacific Biological Station. Can. Spec. Publ. Fish. Aquat. Sci. 60, 102 p.

Cowen, R.K.
1991 Variation in the planktonic larval duration of the temperate wrasse *Semicossyphus pulcher*. Mar. Ecol. Prog. Ser. 69:9–15.

Demory, R.L.
1972 Scales as a means of aging Dover sole (*Microstomus pacificus*). J. Fish. Res. Board Can. 29:1647–1650.

Doyle, R.W.
1975 Settlement of planktonic larvae: A theory of habitat selection in varying environments. Am. Nat. 109:113–126.

Fukuhara, O.
1986 Morphological and functional development of Japanese flounder in early life stage. Bull. Jpn. Soc. Sci. Fish. 52:81–91.
1988 Morphological and functional development of larval and juvenile *Limanda yokohamae* (Pisces: Pleuronectidae) reared in the laboratory. Mar. Biol. (Berl.) 99:271–281.

Hagerman, F.B.
1952 The biology of the Dover sole. Calif. Dep. Fish Game, Fish. Bull. 85:1–48.

Harry, G.Y. Jr.
1959 Time of spawning, length at maturity, and fecundity of the English, Petrale, and Dover soles (*Parophrys vetulus*, *Eopsetta jordani*, and *Microstomus pacificus*, respectively). Oreg. Fish Comm. Res. Briefs 7:5–13.

Hayman, R.A., and A.V. Tyler
1980 Environment and cohort strength of Dover sole and English sole. Trans. Am. Fish. Soc. 109:54–70.

Hickey, B.M.
1979 The California Current System—Hypotheses and facts. Prog. Oceanogr. 8:191–279.

Hirschberger, W.A., and G.B. Smith
1983 Spawning of twelve groundfish species in the Alaska and Pacific Coast regions, 1975–81. NOAA Tech. Memo. NMFS F/NWC-44, Northwest Fish. Sci. Cent., Seattle, WA 98112, 50 p.

Hunter, J.R., J.L. Butler, C. Kimbrell, and E.A. Lynn
1990 Bathymetric patterns in size, age, sexual maturity, water content, and caloric density of Dover sole, *Microstomus pacificus*. Calif. Coop. Oceanic Fish. Invest. Rep. 31:132–144.

Huyer, A.
1977 Seasonal variation in temperature, salinity and density over the continental shelf off Oregon. Limnol. Oceanogr. 22:442–453.
1983 Coastal upwelling in the California Current system. Prog. Oceanogr. 12:259–284.

Huyer, A., and R.L. Smith
1978 Physical characteristics of Pacific northwestern coastal waters. *In* Krauss, R. (ed.), The marine plant biomass of the Pacific Northwest coast, p. 37–55. Oregon State Univ. Press, Corvallis.
1985 The signature of El Niño off Oregon, 1982–1983. J. Geophys. Res. 90:7133–7142.

Huyer, A., E.J.C. Sobey, and R.L. Smith
1979 The spring transition in currents over the Oregon continental shelf. J. Geophys. Res. 84:6995–7011.

Huyer, A., P.M. Kosro, S.J. Lentz, and R.C. Beardsley
1989 Poleward flow in the California Current system. *In* Neshyba, S.J., Ch.N.K. Mooers, R.L. Smith, and R.T. Barber (eds.), Poleward flows along eastern ocean boundaries, p. 144–159. Springer-Verlag, NY.

Jackson, G.A., and R.R. Strathmann
1981 Larval mortality from offshore mixing as a link between precompetent and competent periods of development. Am. Nat. 118:16–26.

Kendall, A.W. Jr., and J.R. Dunn
1985 Ichthyoplankton of the continental shelf near Kodiak Island, Alaska. NOAA Tech. Rep. NMFS 20, 89 p.

McLain, D.R., and D.H. Thomas
1983 Year-to-year fluctuations of the California Countercurrent and effects on marine organisms. Calif. Coop. Oceanic Fish. Invest. Rep. 24:165–181.

Parrish, R.H., C.S. Nelson, and A. Bakun
1981 Transport mechanisms and reproductive success of fishes in the California Current. Biol. Oceanogr. 1(2):175–203.

Pauly, D.
1987 A review of the ELEFAN system for analysis of length-frequency data in fish and aquatic invertebrates. *In* Pauly, D., and G. Moran (eds.). Length-based methods in fisheries research, p. 7–34. Int. Cent. Living Aquat. Res. Manage., Manila.

Pearcy, W.G.
1976 Seasonal and inshore-offshore variations in the standing stocks of micronekton and macrozooplankton off Oregon. Fish. Bull., U.S. 74:70–80.
1980 A large, opening-closing midwater trawl for sampling oceanic nekton, and comparison of catches with an Isaacs-Kidd midwater trawl. Fish. Bull., U.S. 78:529–534.

Pearcy, W.G., M.J. Hosie, and S.L. Richardson
1977a Distribution and duration of pelagic life of larvae of Dover sole, *Microstomus pacificus*; Rex sole, *Glyptocephalus zachirus*; and Petrale sole, *Eopsetta jordani*, in waters off Oregon. Fish. Bull., U.S. 75:173–183.

Pearcy, W.G., E.E. Krygier, R. Mesecar, and F. Ramsey
1977b Vertical distribution and migration of oceanic micronekton off Oregon. Deep-Sea Res. 24:223–245.

Pechenik, J.A.
1986 Field evidence for delayed metamorphosis of larval gastropods: *Crepidula plana* Say, *C. fornicata* (L.), and *Bittium alternatum* (Say). J. Exp. Mar. Biol. Ecol. 97:313–319.

Peterson, W.T., C.B. Miller, and A. Hutchinson
1979 Zonation and maintenance of copepod populations in the Oregon upwelling zone. Deep-Sea Res. 26A:467–494.

Pikitch, E.K., and R.L. Demory
1988 An assessment of scales as a means of aging Dover sole. Trans. Am. Fish. Soc. 117:345–349.

Policansky, D.
1982 Influence of age, size, and temperature on metamorphosis in the starry flounder, *Platichthys stellatus*. Can J. Fish. Aquat. Sci. 39:514–517.
1983 Size, age and demography of metamorphosis and sexual matuartion in fishes. Am. Zool. 23:57–63.

Potthoff, T.
1984 Clearing and staining techniques. *In* Moser, G., et al. (eds.), Ontogeny and systematics of fishes, p. 35–37. Spec. Publ. 1, Am. Soc. Ichthyol. Herpeteol. Allen Press, Lawrence, KS.

Urena, H.M.
1989 Distribution of the eggs and larvae of some flatfishes (Pleuronectiformes) off Washington, Oregon and Northern California, 1980–1983. Unpubl. M.S. thesis, Oregon State Univ., Corvallis, 192 p.

Victor, B.C.
1986 Delayed metamorphosis with reduced larval growth in a coral reef fish (*Thalassoma bifasciatum*). Can. J. Fish. Aquat. Sci. 43:1208–1213.

Yoklavich, M.M., and E.K. Pikitch
1989 Reproductive status of Dover sole, *Microstomus pacificus*, off northern Oregon. Fish. Bull., U.S. 87:988–995.

Youson, J.H.
1988 *First metamorphosis. In Hoar*, W.S., and D.J. Randall (eds.), Fish physiology, vol. XI. The physiology of developing fish, Part B. Viviparity and posthatching juveniles, p. 135–196. Academic Press, San Diego.

Estimating stock abundance from size data

Michael L. Parrack

Miami Laboratory, Southeast Fisheries Science Center
National Marine Fisheries Service, NOAA
75 Virginia Beach Drive, Miami, Florida 33149-1099

Abstract.—The projection of resource production and the effect of removals on fisheries populations are based on abundance estimates, particularly estimates of the most current abundance. Monte Carlo methods were used to investigate a size-based method of estimating abundance for instances where the age of caught fish cannot be established, but where size samples and a growth schedule exist. Neither process variability (recruitment dates, growth rates, and unobserved change rates) nor sampling error (catch estimation, growth rate estimation, and relative abundance sampling) adversely affected estimation, although low sampling intensities often decreased precision. Abundances of recently recruited fish too small to occur in relative abundance samples more than once were estimated with large uncertainty. Inappropriately wide size-class widths caused uncertain abundance estimates of larger size-classes. However, if size-classes were of suitable width, the abundance of fish large enough to occur in abundance samples more than once were accurately and precisely estimated even in cases of high process variability and small sample sizes. Sampling gear efficiency (catchability) coefficients were often estimated without large bias but imprecisely. The exponent of the unobserved change rate (including natural mortality) was estimated precisely, but estimates were often biased. High correlations between estimates of the unobserved change rate and sampling gear efficiencies were not often observed. Estimation characteristics were unlike those based on virtual population analysis calculations. Maximum-likelihood estimates of the most recent abundances were accurate and precise, yet calculations of historical abundances were biased and extremely imprecise.

Manuscript accepted 9 March 1992.
Fishery Bulletin, U.S. 90:302–325 (1992).

Most often, the objective of fisheries regulations is to insure that stock abundance does not decrease or, if abundance is low, to increase it. The welfare of the entire stock may be of concern, or only a part of it such as the adult portion (spawning stock). These objectives are obtained by limiting yields (weight caught) to stock growth or, in instances were abundance is low, to less than stock growth. Abundance estimates are the bases for this regulation strategy. An opinion as to whether stock abundance is currently depressed or not is based on a comparison of an estimate of current abundance with estimates of previous abundances. Stock production (growth) in the immediate future is projected from the estimate of current abundance. Since the production projection is the basis for the yield limit, the estimate of current abundance determines the yield limit. Because it is a critical element of regulatory responsibility, abundance estimation methodology is of major interest.

Most estimation methods are based on age data. These methods specify that the population is entirely composed of unique groups of fish of equal age (cohorts) and that all members of a cohort grow into the first exploitable size (recruit) instantaneously before fishing begins once each year. These two requirements rarely, if ever, occur. Most populations spawn during several months, or sometimes throughout the entire year, so that annual or even monthly cohorts do not really exist. The growth of the young fish to sizes large enough to be caught is a continuous process so that recruitment is typically an ongoing phenomena. These biological realities are often ignored, and age-based analysis methods are used anyway.

Since the primary data element of age-based methods is the number of caught fish of each age, the ages of caught fish must be determined. Sometimes this requirement is difficult to satisfy. Major circuli from differing bone densities or the chemical composition of skeletal structures (scales, fin spines, or otoliths) have been validated as age marks in only 3.4% of age determination studies (Beamish and McFarlane 1983). Even in cases where indirect evidence of validation seems ample (Kreuz et al. 1982), direct measurement of growth from mark and recapture data can document a very different reality (Pikitch and Demory 1988). Collecting and processing samples can be so difficult and time consuming that large data voids occur. Frequent molting and the absence of bony tissue preclude the possibility of using hardpart ageing methods for many invertebrates, and the technology to determine age from somatic tissue does not currently exist.

These problems can be avoided by methods that model populations in terms of size and time rather than age and years (or months). Size-based methods need not require that the population be composed of age-specific cohorts nor that recruitment be an instantaneous, one-time event. The first size-based methods, however, are not so constructed.

The original technique to assess fish stocks from size instead of age data is a stepwise double-estimation procedure (see Pauly et al. 1987 for an example). Size-specific catches are first transformed to age-specific catches by using an inverted growth equation (Ricker 1975:221) or statistical estimators based on growth data (Clark 1981, Bartoo and Parker 1982, Shepherd 1985, Hoenig and Heisey 1987, Kimura and Chikuni 1987) so that the stock is assumed to be composed of age-specific cohorts. Size-to-age transformation methods that require size-frequencies only (i.e., growth data are not required) are available (Macdonald and Pitcher 1979, Pauly 1982, Fournier et al. 1990), but Monte Carlo tests have shown pronounced weaknesses in these methods (Hampton and Majkowski 1987, Rosenberg and Beddington 1987, Basson et al. 1988). Virtual population analysis (Ricker 1948, Fry 1949, Jones 1961, Gulland 1965, Murphy 1965) is then applied to the transformed catch, but the system of cohort-specific catch equations is underdetermined (Agger et al. 1971, Doubleday 1975, Ulltang 1977, Pope and Shepherd 1982). The inclusion of auxiliary data (total fishing effort, catch effort, or other relative abundance samples) using any of several statistical procedures (Laurec and Bard 1980; Paloheimo 1980; Anon. 1981b, 1983, 1984, 1986; Parrack 1981, 1986; Collie and Sissenwine 1983; Deriso 1985; Pope and Shepherd 1985; Mendelssohn 1988) eliminates that problem, so abundances can be estimated. If based on actual age data, virtual population analysis using auxiliary information does estimate stock abundances and fishing mortality rates reasonably well if the natural mortality rate is known (Deriso 1985, Pope and Shepherd 1985), but if the method is used without actual age data, its statistical characteristics are unknown. If the population is not composed of true age-specific cohorts or if the ageing of caught fish is problematic, the method is not appropriate. Spawning often is too protracted to establish cohorts and fish cannot be aged with reasonable certainty; yet because it is simple and tractable, this method is used anyway.

Several size-based abundance estimation methods do not employ data auxiliary to catches (Jones 1974 and 1981, Brethes and Desrosiers 1981, Lai and Gallucci 1988). Instead of using fishing effort or relative abundance samples to overcome the determination problem, they assume that the size-frequency of the catch, and thus of the stock (and recruitment magnitudes), is constant (in steady state). That assumption greatly restricts the usefulness of these methods.

Three items seem important when considering stock-abundance estimators. First, the data an estimator requires often may preclude its use if such data is not usually available. Next, since the likelihood procedure requires one, often a sampling distribution for an observed statistic is assumed even though support for the assumption cannot be offered. The resulting estimator thus might be entirely based on an inappropriate probability expression. Last, the statistical properties of an estimator are of concern. An estimator may be too imprecise to be useful unless sample sizes are unrealistically large, or its bias may be too large to ignore during estimation.

Since the method of least squares is not based on probability theory, statistical characteristics of such estimators are very uncertain. The likelihood procedure tends to generate estimators with superior statistical characteristics, but success is not guaranteed. Commonly, estimators of parameters of nonlinear models are problematic. They cannot be written in closed form so their expectations, which lead to bias and variance expressions, cannot be derived analytically. Since the estimator's performance characteristics cannot be predicted, they must be established from Monte Carlo studies. If such studies do not exist, the estimator's usefulness is unknown.

The first size-based procedure, a least-squares estimator, was developed (Beddington and Cooke 1981) and applied to sperm whales (Anon. 1981a, Cooke and Beddington 1982, Cooke et al. 1983b, Shirakihara and Tanaka 1983, de la Mare and Cooke 1984) to assess the northwestern Pacific stock (Beddington et al. 1983, Cooke and de la Mare 1983b, Shirakihara and Tanaka 1983). It is based entirely on size-specific catches and assumes a known adult-progeny ratio instead of using fishing effort or other auxiliary data. The statistical characteristics of the estimator were established with extensive Monte Carlo studies (Cooke et al. 1983a, Cooke and de la Mare 1983a, Shirakihara and Tanaka 1984, de la Mare and Cooke 1985 and 1987, Shirakihara et al. 1985, de la Mare 1988).

The method of Fournier and Doonan (1987) was derived by the likelihood method by assuming that catch and effort are each lognormal random variables and that the first four moments of length-frequencies are normal random variables. Monte Carlo tests established the estimator's ability to predict optimal long-term fishing effort, but the errors of the stock-abundance estimates are not described. The maximum-likelihood method of Schnute et al. (1989) assumes that the annual ratio of total yield to total effort is a normal random variable. The statistical characteristics of the estimator are not described.

The method of Sullivan et al. (1990) is a least-squares estimator based on catches, but Kalman filter methodology also may be used to obtain estimates (Sullivan 1989). The method does not require data other than catches even though it is well known that, in the case of age-based (VPA) methods, the system of catch equations without auxiliary data is not determined (Agger

et al. 1971, Doubleday 1975, Ulltang 1977, Pope and Shepherd 1982). Sullivan et al. (1990) suggest expanding the number of terms in the sum of squares to include effort and abundance indices if meaningful weights for these auxiliary data can be found (guidance for finding such weights is not provided). The statistical characteristics of the estimator are not yet described.

The lack of Monte Carlo tests of the performance of these estimators is a particular concern because, without knowledge of their statistical behavior, little certainty can be placed on the resulting estimates. Some of the estimators were developed by the likelihood method, but the justification for assuming the chosen sampling distributions often seems weak or lacking. The usefulness of those estimators that require total fishing effort seem limited, since that statistic is often estimated from catch and effort samples rather than enumerated. Most of the methods estimate the parameters of individual growth as part of the solution vector. This seems questionable in view of findings in a study of the separation of central moments of individual distributions from distribution mixtures (Hasselbald 1966), studies of the magnitude of correlation between estimates of growth-equation parameters (Gallucci and Quinn 1979), and of the performance of methods that estimate growth parameters from size distributions (Hampton and Majkowski 1987, Rosenberg and Beddington 1987, Basson et al. 1988). Also, most of the methods are based on elaborate population models, a characteristic that leads to two problems. First, such models often include deterministic stock-recruitment functions, and such functions are regarded as unrealistic representations of the dynamics of fish stocks. Second, since the population model is extensive, it includes a large number of parameters that must be estimated. It is well known that an exact representation of a real-world system is not possible; hence, a suitably parsimonious model that is a useful approximation with an informative structure is superior (Box 1979). The most germane variables are the current size-specific abundances since they will determine stock production in the immediate future.

The object of this study was to develop an abundance estimator that would be appropriate in almost all cases, whether or not the population is composed of cohorts, or whether or not age data is available. Effort was taken to write the estimation model as parsimonious as possible, to base estimation on data commonly collected from most fisheries, and to insure that the correct sampling distribution was used in the likelihood procedure. The bulk of the study was directed at describing the statistical characteristics of the estimator over a broad range of conditions from Monte Carlo simulations.

Methods

Abundance estimator

An abundance estimator was developed that uses a model of individual growth, size-specific catches and catch dates, and size-specific abundance observations (sighting data, research cruise catch-per-tow, etc.). The estimator makes three assumptions:

(1) Unobserved phenomena that change stock abundance (immigration, emigration, unrecorded catch, predation, and disease) are a (continuous) Poisson process with combined rate z,
(2) the size of an individual on a date is a known deterministic function of size on another date, and
(3) the sample average of relative abundance observations is a normally-distributed random variable with an expectation equal to a portion of absolute abundance.

The estimator uses a growth model to relate sizes and dates and an abundance model to project abundance from observed catches scaled to relative abundance observations.

Consider T time-periods, not necessarily of equal duration, so that $0 \leqslant t \leqslant T$. Within period t, relative abundance was observed on date y_t, then a catch occurred on date c_t. The number of fish caught on date c_t was C_t. Abundance on the date of the relative abundance observation (date y_t) is of interest; let this abundance (numbers of fish) be N_t. From assumption (1),

$$N_{t+1} = [N_t\, e^{-z_t(c_t - y_t)} - C_t]\, e^{-z_t(y_{t+1} - c_t)}.$$

Abundance on the date of the final abundance sample (i.e., N_T) is of most interest because stock production in the immediate future depends on it. Writing the above equation in terms of N_T as a time-series gives a simple forward projection of abundance on each relative abundance sampling date:

$$N_t = N_T\, e^{\sum_{k=t}^{T-1} z_k(y_{k+1} - y_k)} + \sum_{k=t}^{T-1} C_k\, e^{z_k(c_k - y_k) + \sum_{i=t}^{k-1} z_i(y_{i+1} - y_i)}.$$

If the unobserved change rate is assumed temporally invariant, this simplifies to

$$N_t = N_T\, e^{z(y_T - y_t)} + \sum_{k=t}^{T-1} C_k\, e^{z(c_k - y_t)}.$$

Each catch is subtracted separately; catching is not assumed to occur continuously at a constant rate. Abundance changes due to unobserved events are, however, assumed to occur continuously at a constant rate.

The model suggested by Chapman (1961) and Richards (1959) may be used to include growth. Letting A, m, b, and k be parameters, s the size, and t the time from birth, the general model

$$s_t = (A^{1-m} - b\, e^{-k \cdot t})^{\frac{1}{1-m}}$$

is the "logistic" function of Verhulst if m=2, the Brody (monomolecular, von Bertalanffy) model if m=0, and it approaches the Gompertz function as m approaches unity. Using the rationale of Fabens (1965) where s_1 is the size at time t_1 and s_2 is the size at time t_2, the above growth model leads to

$$s_2 = (A^{1-m} - (A^{1-m} - s_1{}^{1-m})\, e^{-k(t_2-t_1)})^{\frac{1}{1-m}}. \qquad (1)$$

This satisfies assumption (3), without reference to the actual age of individuals, by expressing size as a continuous function of time, but if growth is intermittent or has changed, a specialized model is most appropriate. From (1), or a more suitable model, let

- l' = the size of a fish on date y_T that was size s on date y_t,
- u' = the size of a fish on date y_T that was size s+1 on date y_t,
- a' = the size of a fish on date c_k that was size s on date y_t, and
- b' = the size of a fish on date c_k that was size s+1 on date y_t,

where l', u', a', and b' fall in size-classes l, u, a, and b. Including size in the abundance equation gives

$$N_{t,s} = \qquad (2)$$

$$\int_{l'}^{u'} N_{T,w}\, dw\, e^{z(y_T - y_t)} + \sum_{k=t}^{T-1} \int_{a'}^{b'} C_{k,w}\, dw\, e^{z(c_k - y_t)}.$$

If size-classes are suitably narrow, the frequency of size within size-classes tends to be proportional to size. The frequency of size within a class is therefore approximated by a trapezoid (i.e., trapezoidal integral approximation). The number of fish within the size class is

$$F_s = \int_s^{s+1} f_w\, dw = \tfrac{1}{2}(s+1-s)\,(f_s + f_{s+1})$$

$$= \tfrac{1}{2}(f_s - f_{s+1}),$$

where s is a size class, f_s is the frequency at size s, and F_s is the number within size-class s. Let the largest fish fall in class S:

$$f_S = \tfrac{1}{2}F_S \text{ because } f_{S+1} = 0.$$

Rewriting gives $f_S = 2\,F_S$.

Proceeding to smaller sizes,

$$F_{S-1} = \tfrac{1}{2}(f_{S-1} + f_S) \quad = \tfrac{1}{2}(f_{S-1} + 2F_S)$$

$$\text{so } f_{S-1} = 2(F_{S-1} - F_S).$$

$$F_{S-2} = \tfrac{1}{2}(f_{S-2} + f_{S-1}) = \tfrac{1}{2}(f_{S-2} + 2F_{S-1} + 2F_S)$$

$$\text{so } f_{S-2} = 2(F_{S-2} - F_{S-1} + F_S).$$

$$\vdots \qquad\qquad \vdots$$

$$F_s = \tfrac{1}{2}(f_s + f_{s+1})$$

$$= \tfrac{1}{2}(f_s + 2F_{s+1} - 2F_{s+2} + \ldots \pm 2F_S).$$

Rearrangement gives the general expression for the frequency at size-class bounds:

$$f_s = 2(F_s - F_{s+1} + F_{s+2} - F_{s+3} + \ldots \pm F_S).$$

The frequency of any size, s, within class s is also required:

$$f_{s'} = f_s + \frac{f_{s+1} - f_s}{s+1-s}(s'-s) = f_s + (s'-s)\,(f_{s+1} - f_s).$$

The approximate integrals for equation (2) are thus:

$$\text{If } u = l\text{:} \int_{l'}^{u'} N_{t,w}\, dw =$$

$$\tfrac{1}{2}(u'-l)\,(\eta_l + (l'-l)(\eta_{l+1} - \eta_l) + (u'-l)(\eta_{l+1} - \eta_l),$$

or

$$\text{if } u > l\text{:} \int_{l}^{u'} N_{t,w}\, dw =$$

$$\tfrac{1}{2}(l+1-l')(\eta_l + (l'-l)(\eta_{l+1} - \eta_l) + \eta_{l+1}) + \ldots$$

$$\ldots \tfrac{1}{2}(u'-u)(2\eta_u + (u'-u)(\eta_{u+1} - \eta_u))$$

$$+ \sum_{i=l+1}^{u-1} N_{T,i},$$

and

$$\text{if } b = a: \int_{a'}^{b'} C_{k,w}\, dw =$$

$$\tfrac{1}{2}(b'-a')(\varsigma_a+(a'-a)(\varsigma_{a+1}-\varsigma_a)+\varsigma_b$$

$$+(b'-b)(\varsigma_{b+1}-\varsigma_b)),$$

or

$$\text{if } b < a: \int_{a'}^{b'} C_{k,w}\, dw =$$

$$\tfrac{1}{2}(a+1-a')(\varsigma_a+(a'-a)(\varsigma_{a+1}-\varsigma_a)+\varsigma_{a+1})+\ldots$$

$$\ldots\tfrac{1}{2}(b'-b)(2\varsigma_b+(b'-b)(\varsigma_{b+1}-\varsigma_b)),$$

where $\eta_s = 2(N_{T,s}-N_{T,s+1}+N_{T,s+2}-N_{T,s+3}+\ldots\pm N_{T,S}$,

and $\varsigma_s = 2(C_{k,s}-C_{k,s+1}+C_{k,s+2}-C_{k,s+3}+\ldots\pm C_{k,S}$.

On a sampling date, r measures are recorded and sample mean calculated for each size class:

$$Y_{t,s} = \sum_{k=1}^{r} \frac{Y_{t,s,k}}{r}.$$

According to assumption (3), the expectation of relative abundance is

$$E[Y_{t,s}] = f[\beta|Y,C] = q_s\, N_{t,s},$$

where β contains the sampling-gear efficiency coefficients (the q_s), the unobserved change rate (z), and the abundance of each size-class on date y_T (the $N_{T,s}$). $N_{t,s}$ is as defined by (2), Y indicates a matrix of relative abundance observations and C catches. Since it is a mean, clearly

$$Y_{t,s} \sim N\left(f[\beta|Y,C], \frac{\sigma^2[Y_{t,s}]}{r}\right)$$

(assumption 3). This implies the likelihood,

$$L(\beta) = \prod_{t,s}^{n} (2\pi)^{-\frac{1}{2}}\, \sigma[Y_{t,s}]^{-1}\, e^{-\frac{1}{2}(Y_{t,s}-f[\beta|Y,C])^2+\sigma^2[Y_{t,s}]},$$

where n is the product of the number of size-classes and sampling dates. Maximizing its logarithm (constant terms ignored),

$$-\sum_{t}^{T}\sum_{s}^{S}(Y_{t,s}-f[\beta|Y,C])^2 \div \sigma^{||}[Y_{t,s}] \qquad (4)$$

with respect to β yields maximum-likelihood estimates of the q_s, the $N_{T,s}$, and z. Maximization was achieved by minimizing the negative of (4) by the "Marquardt" method (Morrison 1960, Marquardt 1963, Conway et al. 1970, Gallant 1975, Press et al. 1986).

This estimator is equivalent to common least-squares if size and date variances are equal, but that restriction seems unlikely. Since

$$\sigma^2[Y_{t,s}] = N_{t,s}^2\, \mathrm{Var}[q_s], \qquad (5)$$

abundance is the dominant term. Abundance is dependent on reproductive success and a mortality history. Both are time-variant, so an assumption of equal variances is inappropriate.

This abundance estimator possesses few restrictions. Relative-abundance measures and catches can occur on any date. Any number of catches, or none at all, can occur between relative abundance samples or visa versa. The period of data collection may be short; the time-series may be brief. Individual growth can follow any form. Most important, recruitment to the exploited stock can occur continuously so that breeding (spawning) and birth (hatching) need not happen just once during each period. Reproduction may be continuous so age-specific cohorts need not exist. This estimator is not a cohort analysis, but it uses similar data.

Monte Carlo tests

Each test was designed to collect a history of estimator performance over many applications of the method in similar circumstances. Each test was composed of several trials. On each trial, a new exploited population was simulated, followed by relative abundance sampling, growth rate estimation, and catch estimation. Next, β was estimated by (4) from the data collected in the second step. Last, estimation error for each element of $\hat{\beta}$ was calculated. The familiar measure of error, $e = (\hat{\beta}-\beta)$, where β is the vector of population parameters estimated by $\hat{\beta}$, was not appropriate because β changed from one simulation to the next. Error was measured by the sufficient statistic $\in = \hat{\beta} \div \beta$. The bias of each element of β was estimated as the average $\in$ over the n trials (Monte Carlo samples). If a particular estimate was unbiased, then $\mu[\in] = 1$ for that parameter. The estimated error variance of each parameter, $s^2[\in]$, was also calculated.

A significance level for bias larger than 10% was found by computing the probability of the standard normal random variable as follows:

$$\text{significance level } \begin{pmatrix} \text{HO: } \mu[\in] \geq 0.9 \\ \text{HA: } \mu[\in] < 0.9 \end{pmatrix} =$$

$$\int_{-\infty}^{Z} f_p \, dp, \; Z = (\bar{\in} - 0.9) \div [s(\in)/\sqrt{n}].$$

$$\text{significance level } \begin{pmatrix} \text{HO: } \mu[\in] \leq 1.1 \\ \text{HA: } \mu[\in] > 1.1 \end{pmatrix} =$$

$$\int_{Z}^{\infty} f_p \, dp = 1.0 - \int_{-\infty}^{Z} f_p \, dp, =$$

$$(\bar{\in} - 1.1) \div [S(\in)/\sqrt{n}].$$

The results between tests were statistically compared by placing confidence intervals on the difference between the biases (Law and Kelton 1982:319) and using the variance ratio test (*F* test) to compare error variances.

In each Monte Carlo test, the intent was to complete trials until the estimate of bias was within a given bound with a prescribed probability (Law and Kelton 1982). Several parameters were estimated, so several biases were involved. It was too costly to confirm that all bias estimates were trustworthy and many parameters were not of primary interest, so the error of last-period total stock size ($\in[N(T.)]$) was used as the reference statistic. Trials were completed until

$$1.96^2 \cdot s^2(\in[N(T.)]) \div n \leq \Phi^2,$$

where Φ was usually small. The 95% confidence bound half-lengths for all parameters were computed to indicate how well bias was estimated for each parameter.

The method of Schrage (1979) was used to generate uniform random variables because it is portable and known to perform well (Law and Kelton 1982:227–228). Normal random variables were generated by the polar method (Law and Kelton 1982:259). The method of Scheuer and Stoller (1962) was used to generate correlated bivariate normal random numbers.

In most trials, the lives of 20,000 fish were individually simulated over 20 time-periods. A history of abundance and catch was created, then abundance sampling, catch estimation, and growth parameter estimation was simulated. Each fish possessed a unique growth pattern and recruitment date and independently encountered unobserved events and fishing death. The result of these encounters, growth rates, and recruitment dates were tabulated into size-class and date-specific matrices of numerical abundance and catch. The sequence of events of the population simulation is diagrammed in Appendix 1. A detailed description of the simulation and justification of control variable levels is given by Parrack (1990).

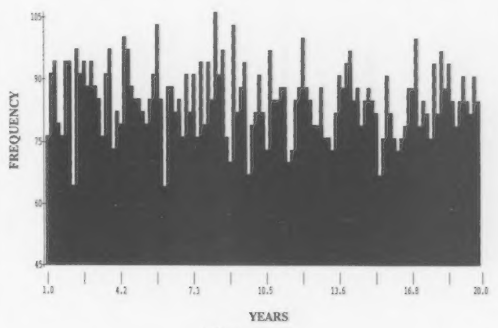

Figure 1

Frequency of recruitment dates from one trial of uniform recruitment simulations.

Von Bertalanffy growth was simulated by fixing m of equation (1) null. For each fish, A and k of (1) were drawn as normal random variables. The expectations were set near those estimated for many stocks, including Pacific cod (N.J.C. Parrack 1986), and their coefficients of variation (cv) were set as high or higher than common in other studies (≤ 0.4).

Two kinds of recruitment were considered, uniform and seasonal. The uniform pattern (Fig. 1) simulated continuous recruitment of constant magnitude. The date each fish recruited to the minimum size category was drawn as a U(1,20) random variable. Seasonal recruitment dates were drawn from normal distributions so that recruitment magnitudes varied U(1,20) between periods and so that a typical "pulse" of young fish recruited once each period, with some recruitment occurring continuously. The recruitment peak was simulated to occur randomly during April, May, and June by drawing the expected recruitment date for each period U(0.25, 0.50). Protracted and contracted seasonal recruitment patterns were considered. Seasonal protracted recruitment was simulated by drawing the standard deviation of recruitment dates U(0.20, 0.33) so that 80% of recruitment occurred randomly within ±3–5 months of the peak (Fig. 2). Seasonal contracted recruitment was simulated by drawing the standard deviation U(0.13, 0.26) so that 80%

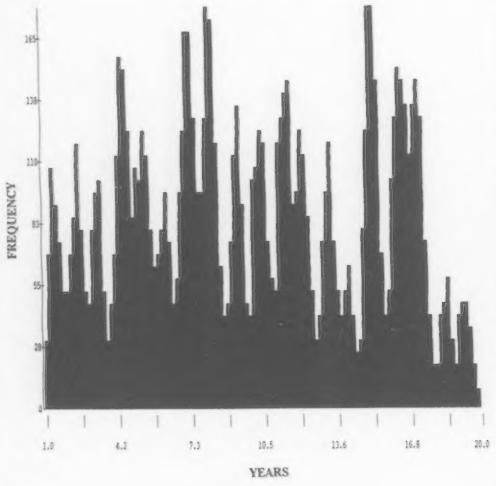

Figure 2

Frequency of seasonal, protracted recruitment dates from one trial. Peak recruitment occurs 1 April–1 June, 80% occurs within 3–5 months of the peak, and recruitment levels vary.

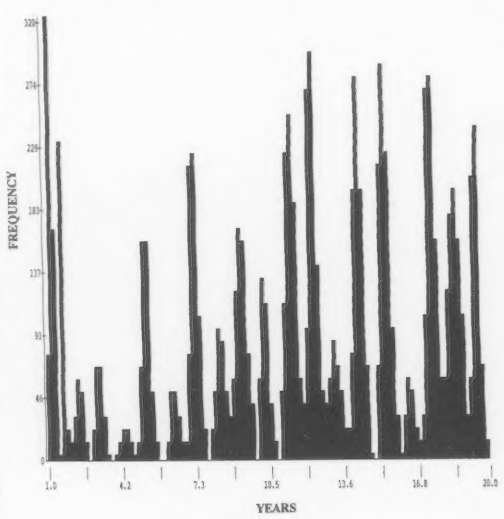

Figure 3

Frequency of seasonal, contracted recruitment dates from one trial. Peak recruitment occurs 1 April–1 July, 80% occurs within 2–4 months of the peak, and recruitment levels vary 20-fold between time periods.

of recruitment occurred randomly within ±2–4 months of the peak (Fig. 3).

The unobserved change rate was simulated both temporally invariant and variant. If variant, then $z_t \sim U(z_1, z_2)$ on each new trial; z_1 and z_2 were simulation control variables. Catching was simulated either as a single event that occurred once each midperiod or as a continuous event in each period. Fishing mortality was not imposed until period 6 so that the stock would accumulate as soon as possible after simulation initialization. In most tests the fishing mortality rate was drawn $U(F_1, F_2)$ on each new trial; F_1 and F_2 were control variables. Period-specific rates were set constant over all trials in two tests to guarantee a stock depletion caused by a rapid increase in fishing levels.

Sampling simulation included the generation of catch estimates, growth parameter estimates, and relative abundance measures. Populations and catches were generated over 20 time-periods. Relative abundance samples and catch estimates were simulated in the last four periods only, but catches were considered to be removed after the date of abundance samples so catch in the last period was irrelevant to estimation (and thus was not computed).

Size-class and date-specific catch estimates were drawn from a Gaussian distribution with catches from the simulator as the expectations and with variances specified by a cv. The estimator of catches was thus unbiased, and estimation errors (estimator variances) were proportional to catches.

A complete simulation of growth sampling and estimation was deemed too costly, so a reasonable proxy of unbiased estimation was used. Let A_i be a growth parameter of fish i such that $A_i \sim N(A, \sigma^2[A])$. Defining the uniqueness in growth of fish i as $\tau_i = A_i - A$, $\sigma^2[A] = \Sigma\tau_i^2/N$. Let A_i be unbiasedly measured by a_i with normal error so that $a_i = A_i + e_i$, $e_i \sim N(0, \sigma^2[e])$. Since $e_i = a_i - A_i$, $\sigma^2[e] = \Sigma e_i^2/N$, $\sigma^2[a_i] = E\{a_i - E[a_i]\}^2 = \sigma^2[A] + \sigma^2[e] + 2\sigma[\tau,e]$ where the last term is null because τ and e are independent. Using the sample mean of g fish to estimate A, $\sigma^2[A] = (\sigma^2[A] + \sigma^2[e])/g$, so that growth-parameter estimation variance is separated into two parts, that of inherent variability from fish to fish and that of growth measurement error. CV's were used as simulation control input instead of variances, so growth parameter estimates were $N(A, A^2(cv[A]^2 + cv[e]^2)/g)$ random variables. In reality, all growth parameters are estimated simultaneously. As a rule, growth parameter estimates are highly negatively correlated (Gallucci and Quinn 1979, Knight 1968, Burr 1988) with correlation coefficients often −0.90 or less. Estimates of k and A of (1) were drawn as normal random correlated variables (Rubinstein 1981:86) with a correlation coefficient of −0.95. The

number of fish sampled for growth (g) was specified in the simulation indirectly as a probability level and limit of a confidence bound. For a $1-\alpha$ level confidence interval on A of bound length $2\Phi A$,

$$\Phi A = Z(1-\alpha/2)\,\sigma[\hat{A}]$$

$$= Z(1-\alpha/2)\sqrt{A^2(cv[\hat{A}]^2+cv[e]^2)/g},$$

so

$$g = Z^2\left(1-\frac{\alpha}{2}\right)(cv[\hat{A}]^2 + cv[e]^2) \div \Phi^2.$$

On each sampling date r, relative abundance samples, $1 \leqslant k \leqslant r$, were simulated as

$$Y_{t,s} = \sum_{k=1}^{r} Y_{t,s,k} \div r = \sum_{k=1}^{r} q_{s,k}\, N_{t,s} \div r,$$

$$q_{s,k} \sim N\,(q_s,\ cv[q]^2\, q_s^2),$$

where cv[q] and the q_s were simulation constants. The q_s were 0.025, 0.05, 0.175, 0.225, 0.2425, and 0.25 (smallest to largest size-class) in most simulations. Several other variations were tried, and it was found that these constants did not affect results at all. Cv's of q were 0.4 or less. The observation and its variance were calculated as the maximum likelihood estimates,

$$Y_{t,s} = \sum_{k}^{r} Y_{t,s,k}/r$$

$$s^2[Y_{t,s}] = \sum_{k}^{r} (Y_{t,s,k}-Y_{t,s})^2/(r^2-r).$$

The sample size (r) was fixed indirectly by two control variables, the probability level and confidence-bound width for $Y_{t,s}$ where $\sigma^2[Y_{t,s}]$ is as (5). If a $1-\alpha$ level confidence interval on $Y_{t,s}$ was to be of bound length $2 \bullet \Phi \bullet N_{t,s} \bullet q_s$ then:

$$\Phi\, N_{t,s}\, q_s = \left(1-\frac{\alpha}{2}\right)\sigma[Y_{t,s}],$$

$$r = Z^2(1-\alpha/2)\ cv[q]^2 \div \Phi^2.$$

Sampling error entered the simulation as variation in q_s, not as variation in the $Y_{t,s}$; the variance of the abundance index was not an input.

These simulations encompassed many possibilities, but not all. Random variation was simulated in all process variables (z, growth parameters and recruitment magnitude, duration, and timing), but time trends were not. A different unobserved change rate was drawn for each time-period ($z_t \sim N(\mu_z,\ \sigma^2[z])$), but the expectation and variance were constant over time and size. Different growth parameters were drawn for each fish, but the expectations and variances were the same for all fish. Recruitment magnitudes for each time-period were drawn from a uniform distribution so time trends were not simulated. A different recruitment peak (i.e., the expectation of recruitment date) was drawn for each time-period from a common expectation and variance. A duration of recruitment (i.e., variance of recruitment date) was drawn for each time-period, but with the same expectation and variance. Random variation was simulated in sampling variables (catch estimates, growth parameter estimates, and the q_s), but biased estimates were not simulated. Although a different vector of sampling efficiencies (the q_s) were drawn for each sampling date, the expectation and variance for each size was temporally constant.

Results

The Monte Carlo tests fall into two categories: those that investigate the influence of population process variability on estimation errors, and those that test the effects of sampling and data estimation. Process variability includes recruitment phenomena, growth rates, and unobserved change due to emigration, immigration, natural death, and unrecorded catch. Sampling variation and data estimation includes four topics: catch estimation error, unrecorded dates of catch, growth parameter estimation error, and variability in sampling-gear efficiency coefficients, and thus in the abundance indices. Each of these items were studied separately in 14 tests.

Population process variability

For these tests, catches, dates of catch, and population growth parameters were considered to be known, and sampling gear efficiencies (the q's) invariant so that all sampling variation was absent. Catches were taken at midperiod. The probability of death due to catching in each period was an U(0.05, 0.2) random variable, and asymptotic size was 11.95 units (i.e., 119.5 cm, with 10 cm intervals).

Recruitment patterns Uniform recruitment test results (Table 1) show little bias and high precision in estimates of abundance and q's. Significance levels for the hypothesis of bias = 1.0 (unbiased) versus bias ≠ 1.0 (biased) were < 0.00005 in almost every case, but bias

Table 1

Monte Carlo tests of populations processes. Catches, dates of catch, and population growth parameters were assumed known. Sampling gear efficiencies (q) were invariant. The probability of death due to catching in each period was a U(0.05, 0.2) random variable. Catches occurred at midperiod. Asymptotic size (i.e., μ[A]) was 11.95.

	Recruitment patterns				Variable growth	Variable, rapid	Variable, slow
	Uniform	Protracted	Contracted	z variable	Test 1	growth - Test 2	growth - Test 3
μ[k]	0.17	0.17	0.17	0.17	0.17	0.34	0.085
cv[A & k]	0.00	0.00	0.00	0.00	0.40	0.40	0.40
Loss rate z	0.10	0.10	0.10	U(0.1,0.4)	0.10	0.10	0.10
Recruit levels	constant	U(1,20)	U(1,20)	U(1,20)	U(1,20)	U(1,20)	U(1,20)
Recruit dates	U(1,20)	$N(\mu,\sigma^2)$	$N(\mu,\sigma^2)$	$N(\mu,\sigma^2)$	$N(\mu,\sigma^2)$	$N(\mu,\sigma^2)$	$N(\mu,\sigma^2)$
$\mu(t)$		U(0.25, 0.5)	U(0.25, 0.5)	U(0.25,0.5)	U(0.247, 0.5)	U(0.247, 0.5)	U(0.247, 0.5)
$\sigma(t)$		U(0.2, 0.33)	U(.13, 0.26)	U(0.2, 0.33)	U(0.2, 0.33)	U(0.2, 0.33)	U(0.2, 0.33)
95% CI of bias of N(T.)							
½ width achieved	0.0024	0.0114	0.0160	0.0139	0.0434	0.0457	0.0498
Number of trials	1010	210	775	105	109	327	32

Variable	Bias	$s^2[\epsilon]$	Bias	$s^2[\epsilon]$	Bias	$s^2[\epsilon]$	Bias	$s^2[\epsilon]$	Bias	$s^2[\epsilon]$	Bias	$s^2[\epsilon]$	Bias	$s^2[\epsilon]$
N(T, 3)	0.9711	0.0032	1.1319	0.0333	1.3138	0.2460	1.1569	1.0508	0.7575	0.0204	0.8594	0.0319	0.8542	0.0456
N(T, 4)	0.9923	0.0152	0.9140	0.2824	0.9780	1.5205	0.9833	0.0955	1.0697	0.0588	0.7410	0.0152	0.8815	0.0379
N(T, 5)	0.9986	0.0055	0.9710	0.0527	0.9802	0.1454	1.0191	0.0364	0.9596	0.0134	0.9087	0.0168	0.9745	0.0044
N(T, 6)	0.9941	0.0010	1.0271	0.0078	1.0632	0.0165	1.0511	0.0341	0.9964	0.0010	1.0168	0.0101	1.0051	0.0036
N(T, 7)	0.9989	0.0016	0.9651	0.0072	0.9383	0.0133	0.9742	0.0046	0.9850	0.0010	0.9892	0.0041	0.9989	0.0036
N(T, 8)	1.0049	0.0005	1.0044	0.0012	1.0018	0.0041	0.9925	0.0017	1.0041	0.0003	0.9899	0.0013	1.0364	0.0043
N(T, 9)	0.9912	0.0008	0.9933	0.0024	0.9940	0.0036	1.0003	0.0024	0.9924	0.0004	0.9911	0.0004	1.0219	0.0100
N(T,10)	1.0084	0.0009	0.9916	0.0036	0.9905	0.0087	0.9735	0.0122	1.0200	0.0007	0.9991	0.0004	1.0836	0.0241
N(T,11)	0.9752	0.2291	0.6789	1.5190	0.4585	2.1818	0.2999	5.7229	1.0590	0.4399	1.2595	0.1852	1.9661	1.5290
N(T,12)									2.3825	2.7796	3.2020	1.3185	3.7363	5.9230
N(T,13)									2.9063	5.4646	3.8776	2.0041	5.5877	13.3879
N(T,14)									3.3177	8.3135	4.8876	1.9756	9.0415	77.7329
N(T,15)									3.9400	19.2576	6.3783	2.9742	11.3780	166.9735
N(T,16)									4.4074	45.0368	8.3752	6.7119	14.2365	403.7108
N(T,17)									5.5771	120.2284	11.3020	27.2042	14.9405	905.7713
N(T,18)									5.1845	203.8775	15.4323	50.7470	18.1915	903.7181
N(T,19)									9.6012	870.1467	23.3307	358.9141	26.6017	1253.4483
N(T,20)									1.3244	222.7073	26.9926	486.5381	11.0799	640.3803
N(T,21)									4.1712	169.5628	38.8813	2180.3053	24.4425	2117.6233
N(T,22)									-1.5598	53.1271	40.2471	3481.6977	2.3077	9.6225
N(T,23)									1.9878	41.6990	48.5059	4438.4966		
N(T,24)									-8.5990	2.7742	33.4447	6841.2892		
N(T,25)											32.0736	4537.5995		
N(T,26)											1.6141	5790.4488		
N(T.)	0.9908	0.0015	1.0064	0.0071	1.0491	0.0516	1.0245	0.0053	1.0988	0.0535	1.8714	0.1781	1.1147	0.0206
q(3)	1.0331	0.0039	0.9010	0.0209	0.8103	0.0410	0.8891	0.0268	1.3544	0.0543	1.2201	0.0676	1.4094	0.1195
q(4)	1.0178	0.0036	0.8844	0.0085	0.7299	0.0185	0.8728	0.0091	1.1304	0.0161	1.3772	0.0487	1.1669	0.0297
q(5)	0.9977	0.0030	0.9787	0.0067	0.9292	0.0181	0.9581	0.0058	1.0987	0.0118	1.2252	0.0325	1.0611	0.0064
q(6)	1.0090	0.0012	1.0212	0.0033	1.0177	0.0091	1.0161	0.0043	1.0478	0.0031	1.1014	0.0104	1.0094	0.0043
q(7)	0.9870	0.0011	1.0758	0.0062	1.1436	0.0137	1.0855	0.0073	1.0110	0.0023	1.0738	0.0063	0.9641	0.0025
q(8)	1.0133	0.0015	0.9290	0.0046	0.8422	0.0100	0.8780	0.0157	0.9706	0.0056	1.0444	0.0033	0.9198	0.0114
q(9)	1.0311	0.0039	1.0462	0.0199	1.0381	0.0275	0.9848	0.0437	0.9363	0.0100	1.0057	0.0044	0.9531	0.0258
q(10)	0.9717	0.0190	0.9655	0.1925	0.9282	0.2356	0.7786	0.3357	0.8790	0.0230	0.9282	0.0058	0.8257	0.0304
q(11)	0.7365	0.1902	0.6016	1.5307	0.8387	1.7031	0.1939	2.5069	0.5449	0.3805	0.4157	0.0087	0.4976	0.0643
q(12)									0.4371	0.0403	0.3132	0.0056	0.3373	0.0272
q(13)									0.3349	0.0263	0.2554	0.0047	0.2187	0.0129
q(14)									0.2587	0.0174	0.1940	0.0588	0.1427	0.0084
q(15)									0.1777	0.0124	0.1510	0.0221	0.0983	0.0038
q(16)									0.1242	0.0051	0.1171	0.0049	0.0654	0.0019
q(17)									0.0887	0.0036	0.0822	0.0029	0.0437	0.0015
q(18)									0.0589	0.0020	0.0580	0.0012	-0.2827	2.9493
q(19)									0.0394	0.0022	0.0365	0.0009	0.7259	13.8313
q(20)									-0.0925	1.0754	0.0247	0.0003	-0.1340	0.1934
q(21)									0.2614	2.9476	0.0165	0.0001	-0.0174	0.0165
q(22)									-0.1324	0.5450	0.0200	0.0473	-9.6131	278.5656
q(23)									-0.3803	3.0233	0.5313	53.3122		
q(24)									0.0163	0.0000	0.0122	0.2028		
q(25)									0.0177	0.0001	-0.0096	0.0421		
q(26)											-2.1688	167.9745		
z	1.5847	0.0715	1.6436	0.1442	1.8264	0.2772			1.9012	0.3023	2.7344	0.5514	0.9394	0.1280
exp(z)	1.0608	0.0008	1.0676	0.0017	1.0877	0.0034			1.0959	0.0036	1.1926	0.0075	0.9946	0.0013

was not large; the significance levels for the hypotheses of bias $\leq 10\%$ were >0.99995 for all estimates. Precision was not a problem, although error variances were not zero.

Since sampling variation was zero and the estimation model encompassed all of the population characteristics simulated, the estimation bias and imprecision were unexpected. The only possible source of that error are the integral approximations required in estimation.

The estimate of the unobserved change rate (z) was biased high by about 60% and its error variance was large. It entered estimation in an exponent, so the term in the model was the exponent of z (the reciprocal of "survival" from unobserved change), not z. The error term was again computed on the exponent of the estimate of z instead of z. The estimated bias was ten times lower and the error variance was several orders of magnitude less. This result proved consistent in all tests of population processes.

Partial correlation coefficients between parameter estimates did not exhibit meaningful trends. Although some adjoining abundance estimates were correlated (probably because the abundances were), evidence of other correlations were absent. Estimates of z were not correlated with the estimates of the q's or abundances; estimates of the q's were not correlated with abundance estimates. This result proved consistent. The correlation matrices for this and following tests are not shown for the sake of brevity but are presented in Parrack (1990).

The two seasonal recruitment tests (protracted and contracted patterns) show increased bias and imprecision. As the recruitment frequency contracted, bias and error variance-of-abundance estimates of the smallest and largest size-classes increased. This problem was worst for the largest size-class. Estimates of the q's also degraded.

Unobserved change rate The estimator assumes that the rate of change due to phenomena that cannot be observed (natural death, migration, unrecorded catch) is constant over periods. Since the assumption is undoubtedly false, estimation errors resulting from assigning a U(0.1,0.4) random variable to z for each period were investigated. Other simulation characteristics were as in the seasonal protracted recruitment test. The 95% confidence intervals on the difference of abundance estimation bias between this test and the protracted recruitment test included zero for size-classes 3 and 4, most others, and total abundance. Error variances were likely equal for size-classes 3, 4, and total abundance (SL 0.005, SL<0.000, SL<0.000). Correlations between estimates were low. A fourfold random variability in z did not affect estimation at all.

Growth Three tests consider highly variable growth. The cv's of asymptotic size and k were 0.4. Test 1 simulated the same growth parameters as the protracted recruitment test (k 0.17), test 2 considered growth twice as rapid (k 0.34), and test 3 growth twice as slow (k 0.085). All other simulation control variables are the same as the protracted recruitment test, so the results are comparable.

The results of all three tests were very similar. All reflected the high variation of asymptotic size: the parameter vector included size-classes larger than the asymptote. Abundance and q estimates of these classes (12 and larger) were worthless; huge bias and imprecision occurred. Abundances of smaller size-classes in all three tests were more precise than in the protracted recruitment test where growth was not variable. Biases and error variances of abundance and q estimates for size-class 11 and smaller were very similar in the three tests; performance seemed unaffected by growth rates. The exponent of z was again estimated much better than z in all three tests; estimates were precise although significant bias was present in the case of rapid, variable growth. Evidence of correlated estimates was absent. The introduction of an extremely high level of variation on individual growth parameters did not negatively affect estimates.

Data estimation and sampling

Errors attributable to sampling and the compilation of various input statistics were studied in seven tests. Catches are rarely censused as assumed by the estimator; estimates are usually the available statistics. The estimator models the dates of each catch, yet catch statistics are usually summed over an interval of dates. Growth rates are assumed to be known, but that is never possible; growth parameters must be estimated. Last, the variability in sampling-gear efficiency coefficients, and thus in the abundance indices, is also a source of uncertainty.

Most of the simulation control variables in these seven tests were the same as in the protracted recruitment test. Asymptotic size was 11.95, growth k was 0.17, the unobserved loss rate (z) was fixed at 0.1, and the seasonal, protracted recruitment pattern was employed; thus recruitment levels varied 20-fold between periods. Catching was simulated differently than in the protracted recruitment test. Catching was continuous (see Appendix 1, step 4) instead of a single subtraction at midperiod, and the fishing mortality rate (F) was a U(0.1,0.4) random variable.

Catch dates A single scenario was used to investigate the importance of recording each catch date and modeling each catch separately. The summed catch over each period was assumed to be known, but not

Table 2

Monte Carlo tests for the effects of sampling variation. $\mu[A]=11.95$, $\mu[k]=0.17$, $z=0.1$, and seasonal, protracted recruitment was simulated. Catching was simulated as a continuously occurring event. The instantaneous rate of fishing mortality was a U(0.1, 0.4) random variable.

			Growth parameter measurement error			Relative abundance	
	Unknown catch date	Catch estimation error	40% Error	15% Error	with process variance	cv[q] 0.4, r3	cv[q] 0.2, r16
cv[A & k]	0.00	0.00	0.00	0.00	0.20	0.00	0.00
Catch estimation							
catch dates	absent	absent	absent	absent	absent	absent	absent
cv[C(t, s)]	0.00	0.40	0.00	0.00	0.00	0.00	0.00
Growth estimation							
cv[error]	0.00	0.00	0.40	0.15	0.15	0.00	0.00
precision level	—	—	—	—	0.02	—	—
probability level	—	—	—	—	0.95	—	—
fish sampled, g	1	1	1	1	601	1	1
Sampling efficiency							
cv[q(s)]	0.00	0.00	0.00	0.00	0.00	0.40	0.10
precision level	—	—	—	—	—	0.50	0.05
probability level	—	—	—	—	—	0.95	0.95
sample size, r	1	1	1	1	1	3	16
95% CI of bias of N(T.)							
½width achieved	0.0155	0.0197	0.4789	0.0210	0.0198	0.0354	0.0198
Number of trials	101	84	192	198	79	200	52

Variable	$\bar{\epsilon}$	$s^2[\epsilon]$	$\bar{\epsilon}$	$s^2[\epsilon]$	$\bar{\epsilon}$	$s^2[\epsilon]$	$\bar{\epsilon}$	$s^2[\epsilon]$	$\bar{\epsilon}$	$s^2[\epsilon]$	$\bar{\epsilon}$	$s^2[\epsilon]$	$\bar{\epsilon}$	$s^2[\epsilon]$
N(T, 3)	1.1081	0.0295	1.1817	0.0646	1.8710	217.1297	1.1439	0.1424	0.9947	0.0355	1.3381	5.2758	1.0972	0.0768
N(T, 4)	0.9710	0.3532	1.0314	0.2057	1.0034	3.4342	0.9228	1.0249	1.0184	0.0767	0.9247	3.0564	0.9288	0.0823
N(T, 5)	1.0009	0.0253	0.9350	0.0398	1.1353	3.4290	1.0028	0.1066	1.0026	0.0108	0.8733	0.2110	0.9128	0.0471
N(T, 6)	1.0162	0.0052	1.0197	0.0034	1.3096	6.9835	1.0375	0.0511	0.9902	0.0011	1.0156	0.0289	1.0092	0.0056
N(T, 7)	0.9740	0.0051	0.9660	0.0055	1.3544	12.7702	0.9675	0.0170	0.9953	0.0009	0.9530	0.0430	0.9191	0.0119
N(T, 8)	1.0000	0.0010	0.9956	0.0079	1.6209	17.9277	1.0437	0.0598	1.0019	0.0010	1.0243	0.0194	1.0239	0.0045
N(T, 9)	1.0003	0.0007	0.9939	0.0061	1.5861	11.9433	1.0458	0.0952	0.9959	0.0008	0.9703	0.0079	0.9688	0.0024
N(T,10)	0.9914	0.0045	0.9973	0.0012	2.6909	26.6738	1.3480	1.1729	1.0096	0.0019	1.0077	0.0112	1.0021	0.0004
N(T,11)	0.8191	3.9963	0.7914	1.2824	3.4334	111.2210	1.2774	5.3882	1.1619	0.3091	1.1734	1.1168	0.9568	0.1516
N(T,12)									2.3955	1.6866				
N(T,13)									3.4498	5.9767				
N(T,14)									3.2299	16.5785				
N(T,15)									3.6964	41.8706				
N(T,16)									0.4291	92.2468				
N(T,17)									6.5117	174.0005				
N(T,18)									1.5430	10.9191				
N(T,19)									18.1902	768.6451				
N(T.)	1.0242	0.0063	1.0259	0.0086	1.4105	11.4628	1.0416	0.0226	1.0542	0.0081	1.0345	0.0653	0.9799	0.0053
q(3)	0.9180	0.0200	0.8754	0.0291	1.3725	9.3538	0.9143	0.0715	1.0346	0.0290	0.9655	0.1063	0.9661	0.0460
q(4)	0.8578	0.0062	0.8729	0.0126	1.5114	25.7585	0.8825	0.0451	1.0391	0.0157	0.8933	0.0776	0.9397	0.0124
q(5)	0.9715	0.0051	0.9725	0.0103	2.0644	87.9064	1.0305	0.3386	1.0472	0.0098	1.0162	0.0709	1.0402	0.0091
q(6)	1.0046	0.0043	1.0141	0.0065	1.9815	47.7841	1.0593	0.1689	1.0315	0.0021	1.0467	0.0553	1.0629	0.0045
q(7)	1.0783	0.0059	1.0679	0.0065	2.0977	54.6183	1.0887	0.0294	1.0112	0.0022	1.1524	0.0767	1.1242	0.0159
q(8)	0.9093	0.0058	0.9342	0.0061	1.5326	20.5395	0.9387	0.0249	0.9900	0.0058	0.9596	0.0590	0.9590	0.0075
q(9)	1.0159	0.0190	1.0447	0.0239	1.7836	46.8489	1.0023	0.0620	0.9735	0.0082	1.1949	0.1016	1.1582	0.0194
q(10)	1.0151	0.1572	1.0147	0.0816	1.4402	25.2990	0.8819	0.1195	0.9388	0.0293	1.0083	0.1004	0.9874	0.0182
q(11)	0.5695	0.8583	0.8320	1.4223	1.4677	34.9181	0.9667	0.5829	0.6416	0.0701	0.9200	0.6084	0.8700	0.1365
q(12)									0.3774	0.0303				
q(13)									0.2138	0.0091				
q(14)									0.1017	0.0042				
q(15)									0.0488	0.0012				
q(16)									−3.1478	425.1308				
q(17)									0.0866	0.0670				
q(18)									−0.0707	0.0967				
q(19)									1.2251	4.4242				
$\bar{z}$	0.8137	0.1022	1.6881	0.2587	0.2301	25.5499	1.0396	0.0219	0.1835	0.0000	0.8525	1.0626	0.8542	0.2896
exp(z)	0.9820	0.0010	1.0736	0.0031	0.9828	0.0416	1.0527	0.0067	1.0898	0.0022	0.9913	0.0104	0.9869	0.0029

the dates of the catches. The accumulated catch each period was assigned to the midpoint of each period for estimation. The results (Table 2) were almost identical with those of the protracted recruitment test (Table 1). The 95% confidence interval (Welch 1938) on the difference between total-abundance estimation bias of the protracted recruitment test and this test included zero (−0.0014 to 0.0372). The error variances were very similar (0.0072 and 0.0063). Estimates were not correlated. The absence of exact catch dates did not affect estimation.

Catch estimation error The effects of estimating catches rather than enumerating them were investigated by drawing size-class-specific catch estimates as normal random variables with expectation $C(t,s)$ and variance $(cv[C] \cdot C(t,s))^2$. This simulated unbiased catch estimation and estimation error proportional to catches. A large degree of catch estimation uncertainty was imposed ($cv[C]=0.40$). Simulation control variables were the same as in the catch date test and the protracted recruitment test. Results were also similar. The bias of total abundance estimates was about the same for all three tests and the error variances were nearly so. Correlated estimates were not evident. Confidence intervals (95%) on the difference in bias between this test and the protracted recruitment test included zero for all size-classes and total abundance. The error variance for size-class 3 was different ($SL<0.0005$) and might have been different for size-class 4 (SL 0.052), but probably not for total abundance (SL 0.142) and all others. Imprecise catch estimates did not impact bias or error variance.

Growth parameter estimation error The effect of imprecise growth parameter estimates was also considered. Estimates of growth parameters were simulated as normal correlated random variables with expectations equal to those of the population. As explained in the Monte Carlo methods section, the variance of a growth parameter estimate is composed of two parts: process variation due to variant individual growth, and growth measurement error. Simulation control constants were therefore the cv of A and of k, the growth measurement error cv, the two constants required to compute the sample size used to estimate the growth parameters, and the correlation coefficient between estimates (−0.95). Simulation constants were as in the catch date test except those related to growth parameter estimation.

Three tests were carried out, two without process variation. First, the effect of two measurement error cv's was studied in the absence of growth variability. The sample size was set at one fish in these two tests so affects due to measurement error would be magnified. Then, the combined effect of process variation and estimation error was considered.

In the first test with extremely imprecise growth parameter estimates (cv 0.4), Monte Carlo trials were carried out until it became obvious that little more information would be gained with further computations. Error variances were huge (Table 2). Only the exponent of z was reasonably estimated. Many estimates were correlated, particularly those of z with those of sampling-gear efficiency coefficients. Even without individually variant growth rates (an unlikely prospect), large growth-parameter measurement error created significant uncertainty.

The second test simulated 15% measurement error. A 95% confidence interval on the difference between the bias of total abundance estimates between this and the protracted recruitment test included zero, but the error variances were probably different ($SL<0.0001$); most error variances were higher. Bias was unaffected although error variance approximately doubled. The estimates did not seem correlated. The introduction of a 15% growth measurement error increased error variances but did not affect bias.

The third test simulated both process error (cv 0.2) and 15% growth measurement error, but with a sample size such that 95% confidence intervals on the estimate of the expectation of growth parameters were with precision ±2% ($g=601$ fish). The 95% confidence interval on the difference in bias of total abundance estimates between this test and the protracted recruitment test included zero (−0.0220 to 0.0238) although error variances perhaps differed ($SL\approx0.05$). Estimates were not correlated. Apparently 15% (or less) measurement error, even with natural growth variation, minimally affects estimation.

Gear efficiency variability The estimator is derived from the density function of relative abundance observations (Y), but the effect of Y variability on estimation error was not of large interest. The variance of Y is $\sigma^2[Y_{t,s}]=N_{t,s}^2 cv[q]^2$. The dominant term is the square of abundance, so as abundance increases, $\sigma^2[Y_{t,s}]$ increases. This may be dampened a bit by an increase in q with size, but the dominant factor in the variance expression for the observations is abundance. Abundance levels cannot be controlled or anticipated beforehand, so knowledge of the effect of Y variability is of little value. Knowledge of the effect of q variability is useful, however, since care may be taken in the selection and design of sampling gear.

Studies that document the statistics necessary to calculate the variability of relative abundance sampling-gear efficiencies are not common. Studies of commerical fishery statistics offer different but useful information. Yield is a portion of biomass; the pro-

portion is the product of fishing effort and q for the fishing method. Since yield is the product of q, effort, and biomass, then yield-per-effort equals the product of q and biomass and q is yield-per-effort divided by biomass. It then follows that the cv's of q and yield-per-effort are equal. The cv of yield-per-effort of the Pacific halibut longline fishery is estimated to be 0.02 (Quinn et al. 1982), and that of Newfoundland flounder trawlers on the Grand Bank (Smith 1980) is estimated to be about the same. The levels used in these simulations (0.4 and 0.2) are about an order of magnitude higher than those.

Effects of the variability in q on estimation errors were investigated in three tests. All simulation constants were as in the protracted recruitment test except those related to abundance sampling. Simulation control constants were cv[q] and the two constants required to compute the sample size. Although they were probably unrealistically large, a cv[q] of 0.4 was used in the first test and 0.2 was used in the second.

First, the impact of extreme variability (cv 0.4) and extremely light sampling was tested. The sample size (r 3) was such that a 95% confidence interval on relative abundance was within ±50% of the expectation. The extremely high cv[q] and low relative-abundance sample size were not reflected in error variances as much as expected (Table 2), but error variances were higher than those of the protracted recruitment test. Most abundance estimates were biased by less than 10%. Estimates were not correlated.

Next, the cv[q] was reduced to 0.1 and the sample size was increased so that a 95% confidence interval on relative abundance was within ±5% of the expectation (r 16). The result was very similar to those of the first test except error variances were much lower. Biases of abundance estimates were ±10% or less and estimates were not correlated.

There was no evidence that high variation in the q_s biased abundance estimates even if sample sizes were insufficient, but error variances were affected. Error variance was considerably reduced with reasonable sample sizes.

Bias

The results of these experiments (Tables 1 and 2) show that abundances and gear efficiencies (q's) of the smallest and largest size-classes were often biased. Bias did not occur with uniform, constant recruitment and no sampling variation, but as process and sampling variation increased, bias in estimates of the smallest and largest sizes became pronounced.

Each expected value is a proportion of calculated abundance. The abundance calculation sums future catches (data), last-period abundance (estimates), and an amount for unobserved changes (estimate). Future catches and terminal abundance are thus the major components of each projection. Both catch and final abundance must be integrated over size. The integration of catch over size at each catch date following the date of the expected value is required. The integration of abundance over size on the date of the final relative abundance sample is also necessary. All integrals are approximated, so these calculations are the source of the bias. The amount of error incurred at each integration depends on how well the trapezoidal rule approximates the size distribution. Since the size frequency within a size-class is never smooth, the approximation will be in error with the amount depending on the degree of smoothness within the size-class. If growth is variable or the number of fish is small, clumps in size frequencies can result from chance alone, but the major factor is the growth and recruitment pattern combination.

Narrowing the size-classes eliminates this problem. If they are narrowed enough to eliminate clumping caused by the particular recruitment frequency contraction, the size frequency within size-classes will be smooth and the trapezoidal approximation will be accurate. The seasonal contracted pattern of recruitment test 3 was again used to demonstrate this. An asymptotic size of 120 cm was simulated with recruitment occurring at 20 cm. First, it was assumed that the data were collected in 20 cm intervals so that the asymptotic size was 6 and the recruitment size was class 1. In the second case, it was assumed that data were collected in 2 cm groups so that the asymptotic size was 60 and the recruitment size was class 10. The unobserved change rate was set at 0.2 in both tests, and all other simulation control variables were as in the contracted recruitment test.

Ninety-two trials were required to obtain a 95% confidence interval half-length of 0.05 on the bias of total abundance in bias test 1 with 20 cm interval data. Estimates of the smallest and largest size-class abundances were biased and the error variances were very large (Table 3), particularly for the largest size-class. The estimate of the survival from unobserved change (z) was, however, reasonably accurate and precise.

Only 16 trials were required to obtain a 95% confidence interval half-length of 0.03 on the bias of total abundance in bias test 2 with two-unit size-interval data because the error variances were very low. Estimates of the first three size groups were probably biased by 10% or more, but the rest were not. Only six of the 47 estimates were probably biased at all (0.95 level). The estimate of the exponent of z was also not biased. Although the matrix was too large to be included (194 rows and columns), there was no evidence that estimates were correlated.

Table 3

Biases for 20 cm size-class width data (bias test 1, 92 trials) versus biases for 2 cm size-class width data (bias test 2, 16 trials).

Bias test	Variable	Estimates: Bias	Estimates: $s^2[\in]$	Bias 95% CI ½-width	Significance levels: HO:Bias≥0.9 HA:Bias<0.9	Significance levels: HO:Bias≤1.1 HA:Bias>1.1
1	N(20–39)	1.2941	0.1332	0.0746	1.0000	0.0000
2	N(20–21)	1.8093	0.5273	0.3558	1.0000	0.0000
2	N(22–23)	1.5883	0.2529	0.2464	1.0000	0.0001
2	N(24–25)	1.5190	0.3576	0.2930	1.0000	0.0025
2	N(26–27)	1.1204	0.0790	0.1377	0.9991	0.3856
2	N(28–29)	0.9746	0.0578	0.1178	0.8927	0.9815
2	N(30–31)	0.8908	0.0124	0.0545	0.3699	1.0000
2	N(32–33)	1.0826	0.0440	0.1028	0.9997	0.6303
2	N(34–35)	0.9963	0.0002	0.0073	1.0000	1.0000
2	N(36–37)	1.0142	0.0032	0.0276	1.0000	1.0000
2	N(38–39)	0.9924	0.0005	0.0109	1.0000	1.0000
1	N(40–59)	1.0071	0.0234	0.0313	1.0000	1.0000
2	N(40–41)	1.0052	0.0003	0.0089	1.0000	1.0000
2	N(42–43)	1.0009	0.0000	0.0032	1.0000	1.0000
2	N(44–45)	1.0013	0.0001	0.0041	1.0000	1.0000
2	N(46–47)	0.9977	0.0001	0.0042	1.0000	1.0000
2	N(48–49)	1.0060	0.0008	0.0136	1.0000	1.0000
2	N(50–51)	0.9966	0.0004	0.0097	1.0000	1.0000
2	N(52–53)	1.0022	0.0000	0.0030	1.0000	1.0000
2	N(54–55)	0.9985	0.0001	0.0046	1.0000	1.0000
2	N(56–57)	0.9998	0.0000	0.0013	1.0000	1.0000
2	N(58–59)	0.9969	0.0001	0.0047	1.0000	1.0000
1	N(60–79)	0.9741	0.0288	0.0347	1.0000	1.0000
2	N(60–61)	1.0046	0.0001	0.0045	1.0000	1.0000
2	N(62–63)	0.9975	0.0002	0.0077	1.0000	1.0000
2	N(64–65)	0.9998	0.0000	0.0018	1.0000	1.0000
2	N(66–67)	0.9998	0.0001	0.0059	1.0000	1.0000
2	N(68–69)	1.0026	0.0002	0.0062	1.0000	1.0000
2	N(70–71)	0.9959	0.0002	0.0071	1.0000	1.0000
2	N(72–73)	1.0034	0.0001	0.0060	1.0000	1.0000
2	N(74–75)	1.0025	0.0001	0.0050	1.0000	1.0000
2	N(76–77)	1.0039	0.0003	0.0081	1.0000	1.0000
2	N(78–79)	1.0004	0.0001	0.0049	1.0000	1.0000
1	N(80–99)	1.0517	0.0745	0.0558	1.0000	0.9553
2	N(80–81)	0.9982	0.0003	0.0080	1.0000	1.0000
2	N(82–83)	1.0009	0.0001	0.0045	1.0000	1.0000
2	N(84–85)	1.0037	0.0002	0.0067	1.0000	1.0000
2	N(86–87)	1.0013	0.0000	0.0010	1.0000	1.0000
2	N(88–89)	0.9995	0.0000	0.0016	1.0000	1.0000
2	N(90–91)	0.9992	0.0001	0.0054	1.0000	1.0000
2	N(92–93)	0.9994	0.0000	0.0009	1.0000	1.0000
2	N(94–95)	0.9963	0.0001	0.0041	1.0000	1.0000
2	N(96–97)	0.9989	0.0000	0.0017	1.0000	1.0000
2	N(98–99)	0.9974	0.0000	0.0022	1.0000	1.0000
1	N(100–119)	6.4942	254.5641	3.2603	0.9996	0.0006
2	N(100–101)	1.0003	0.0000	0.0007	1.0000	1.0000
2	N(102–103)	0.9997	0.0003	0.0091	1.0000	1.0000
2	N(104–105)	0.9979	0.0003	0.0105	1.0000	1.0000
2	N(106–107)	0.9997	0.0000	0.0005	1.0000	1.0000
2	N(108–109)	1.0009	0.0000	0.0005	1.0000	1.0000
2	N(110–111)	0.9981	0.0000	0.0035	1.0000	1.0000
2	N(112–113)	1.0000	0.0000	0.0005	1.0000	1.0000
1	N(T.)	1.1808	0.0592	0.0497	1.0000	0.0007
2	N(T.)	1.0388	0.0049	0.0342	1.0000	0.9998

Bias test	Variable	Estimates: Bias	Estimates: $s^2[\in]$	Bias 95% CI ½-width	Significance levels: HO:Bias≥0.9 HA:Bias<0.9	Significance levels: HO:Bias≤1.1 HA:Bias>1.1
1	q(20–39)	0.8296	0.0207	0.0294	0.0000	1.0000
2	q(20–21)	0.6373	0.0560	0.1160	0.0000	1.0000
2	q(22–23)	0.6924	0.0504	0.1101	0.0001	1.0000
2	q(24–25)	0.7464	0.0621	0.1221	0.0068	1.0000
2	q(26–27)	0.9410	0.0465	0.1057	0.7766	0.9984
2	q(28–29)	1.0818	0.0616	0.1216	0.9983	0.6151
2	q(30–31)	1.1408	0.0234	0.0749	1.0000	0.1431
2	q(32–33)	0.9545	0.0300	0.0849	0.8959	0.9996
2	q(34–35)	0.7751	0.0463	0.1055	0.0101	1.0000
2	q(36–37)	0.6608	0.0531	0.1129	0.0000	1.0000
2	q(38–39)	0.7494	0.0379	0.0954	0.0010	1.0000
1	q(40–59)	1.0050	0.0125	0.0228	1.0000	1.0000
2	q(40–41)	0.9352	0.0099	0.0487	0.9216	1.0000
2	q(42–43)	1.0218	0.0205	0.0701	0.9997	0.9856
2	q(44–45)	1.0357	0.0093	0.0473	1.0000	0.9961
2	q(46–47)	0.8792	0.0154	0.0608	0.2513	1.0000
2	q(48–49)	0.7148	0.0542	0.1141	0.0007	1.0000
2	q(50–51)	0.7373	0.0333	0.0894	0.0002	1.0000
2	q(52–53)	0.8691	0.0090	0.0464	0.0960	1.0000
2	q(54–55)	1.0389	0.0438	0.1025	0.9961	0.8786
2	q(56–57)	1.0358	0.0056	0.0365	1.0000	0.9997
2	q(58–59)	0.8082	0.0187	0.0670	0.0036	1.0000
1	q(60–79)	0.9049	0.0193	0.0284	0.6333	1.0000
2	q(60–61)	0.6377	0.0760	0.1351	0.0001	1.0000
2	q(62–63)	0.8143	0.0401	0.0982	0.0434	1.0000
2	q(64–65)	0.9890	0.0204	0.0700	0.9936	0.9991
2	q(66–67)	1.0381	0.0257	0.0785	0.9997	0.9388
2	q(68–69)	0.8908	0.0447	0.1036	0.4306	1.0000
2	q(70–71)	0.7287	0.0583	0.1183	0.0023	1.0000
2	q(72–73)	1.0168	0.0152	0.0604	0.9999	0.9965
2	q(74–75)	1.0449	0.0163	0.0626	1.0000	0.9577
2	q(76–77)	0.8313	0.0415	0.0998	0.0886	1.0000
2	q(78–79)	0.7050	0.0727	0.1321	0.0019	1.0000
1	q(80–99)	0.7632	0.2257	0.0971	0.0029	1.0000
2	q(80–81)	0.9684	0.0392	0.0970	0.9167	0.9961
2	q(82–83)	1.0334	0.0214	0.0717	0.9999	0.9657
2	q(84–85)	0.6644	0.0478	0.1071	0.0000	1.0000
2	q(86–87)	0.9742	0.0679	0.1277	0.8727	0.9732
2	q(88–89)	0.7991	0.0914	0.1481	0.0909	1.0000
2	q(90–91)	0.7715	0.0667	0.1266	0.0233	1.0000
2	q(92–93)	0.9841	0.0515	0.1148	0.9244	0.9761
2	q(94–95)	0.7314	0.1194	0.1749	0.0294	1.0000
2	q(96–97)	0.8420	0.0390	0.1000	0.1279	1.0000
2	q(98–99)	0.9202	0.1227	0.1835	0.5856	0.9726
1	q(100–119)	0.1117	0.5453	0.1509	0.0000	1.0000
2	q(100–101)	0.7954	0.1388	0.1952	0.1467	0.9989
2	q(102–103)	0.9848	1.5099	0.6680	0.5983	0.6323
2	q(104–105)	1.0579	0.0507	0.1224	0.9943	0.7497
2	q(106–107)	0.8840	0.0867	0.1923	0.4350	0.9862
2	q(108–109)	0.8992	0.0936	0.2682	0.4976	0.9289
2	q(110–111)	1.0052	0.1531	0.3835	0.7047	0.6860
2	q(112–113)	1.0121	0.0004	0.0238	1.0000	1.0000
1	exp(z)	0.9716	0.0135	0.0237	1.0000	1.0000
2	exp(z)	0.9783	0.0169	0.0637	0.9920	0.9999

Estimates of the first three size-classes were both biased and imprecise. Poor estimates of the smallest few size-classes were expected. These classes lacked a catch history at the time of the last sample, so these estimates of abundance (at the time of the last relative abundance sample) were a function of the last-period relative abundance sample only.

Examples

Two tests were used to discover what might be expected when assessing populations with no periodicity in recruitment at all; recruitment dates were completely protracted uniformly through time (Fig. 1). Most control variables were the same in the two tests. Data were assumed to be available in two-unit size intervals. A 120-unit asymptotic size fell in size-class 60, and a 30-unit recruitment size in class 15. The growth parameter k was left at 0.17. Continuous fishing was simulated; the fishing mortality rate (F) for each period was drawn from a U(0.3, 0.8) distribution. The expectations of sampling efficiencies (q_s) were arbitrarily chosen so that their regression on size was sigmoid, reaching an asymptote at size-class 30 (0.028, 0.031, 0.033, 0.038, 0.044, 0.053, 0.069, 0.101, 0.153, 0.190, 0.218, 0.234, 0.242, 0.247, 0.249, and 0.250). Catch estimates were simulated to be imprecise (cv 0.4). A 10% growth measurement error was simulated. Sampling intensities were the same in both tests; sample sizes for growth parameter estimates and for relative abundance observations were such that a 95% CI was of width ±5%.

Although the levels of population processes were the same in both tests, the amount of process variability was much higher in test 2. Normal growth variability was simulated in test 1 and extreme variability in test 2. The rate of unobserved change in test 1 was constant, but varied three-fold in test 2. The variance of sampling efficiencies was set one order of magnitude larger than that observed for commercial fishing gear in test 1 and twice that in test 2.

Error variances-of-abundance estimates were very low in the case of normal process variability (Table 4). Estimates of all but the smallest six size-classes were biased by 10% or less, if at all, and were precise. Bias (more than 10%) and imprecision of the smallest six size-class estimates was expected because the smaller fish were barely represented in the catch and appeared in the relative abundance samples just once. Estimates of the sampling efficiencies (the q_s) tended to be imprecise. Some were biased from 20% to 30% and a few even more. The estimate of survival from unobserved change was biased low (about 15%), yet precise. Estimates did not tend to be correlated. The correlations between the estimate of the unobserved change rate (z) and other estimates (Table 5), particularly of the q_s, were of interest because other studies found corre-

Table 4

Monte Carlo test results for two examples of constant, uniform recruitment.

	Example 1, Normal process variability	Example 2, High process variability
Loss rate z	0.20	U(0.2, 0.6)
Growth cv[A & k]	0.20	0.40
Growth estimation		
cv[error]	0.10	0.10
precision level	0.05	0.05
probability level	0.95	0.95
fish sampled, g	77	262
Sampling efficiency		
cv[q(s)]	0.20	0.40
precision level	0.05	0.05
probability level	0.95	0.95
sample size, r	62	246
95% CI of bias of N(T.)		
½ width achieved	0.0149	0.024
Number of trials	97	64

	Example 1, Normal process variability					Example 2, High process variability				
	Estimates		Bias 95% CI	Significance levels		Estimates		Bias 95% CI	Significance levels	
	Bias	Variance	½ width	HO:Bias≥0.9 HA:Bias<0.9	HO:Bias≤1.1 HA:Bias>1.1	Bias	Variance	½ width	HO:Bias≥0.9 HA:Bias<0.9	HO:Bias≤1.1 HA:Bias>1.1
N(T,15)	0.7669	0.0368	0.0382	0.0000	1.0000	0.5605	0.0273	0.0405	0.0000	1.0000
N(T,16)	0.7556	0.0520	0.0454	0.0000	1.0000	0.6660	0.0633	0.0616	0.0000	1.0000
N(T,17)	0.8022	0.0718	0.0533	0.0002	1.0000	0.7294	0.0567	0.0583	0.0000	1.0000
N(T,18)	0.9012	0.0960	0.0617	0.5157	1.0000	0.7382	0.0765	0.0678	0.0000	1.0000
N(T,19)	0.8423	0.0689	0.0522	0.0152	1.0000	0.7538	0.0754	0.0673	0.0000	1.0000

Table 4 (continued)

	Estimates		Bias 95% CI ½ width	Significance levels HO:Bias≥0.9 HA:Bias<0.9	Significance levels HO:Bias≤1.1 HA:Bias>1.1	Estimates		Bias 95% CI ½ width	Significance levels HO:Bias≥0.9 HA:Bias<0.9	Significance levels HO:Bias≤1.1 HA:Bias>1.1
	Bias	Variance				Bias	Variance			
N(T,20)	0.8227	0.0662	0.0512	0.0015	1.0000	0.7826	0.0722	0.0658	0.0002	1.0000
N(T,21)	0.9475	0.0440	0.0418	0.9871	1.0000	0.8975	0.0738	0.0666	0.4702	1.0000
N(T,22)	1.0006	0.0001	0.0019	1.0000	1.0000	0.9982	0.0003	0.0042	1.0000	1.0000
N(T,23)	1.0007	0.0001	0.0020	1.0000	1.0000	1.0012	0.0004	0.0051	1.0000	1.0000
N(T,24)	0.9973	0.0001	0.0024	1.0000	1.0000	0.9993	0.0005	0.0053	1.0000	1.0000
N(T,25)	0.9992	0.0001	0.0019	1.0000	1.0000	0.9979	0.0002	0.0037	1.0000	1.0000
N(T,26)	0.9995	0.0001	0.0020	1.0000	1.0000	0.9946	0.0003	0.0040	1.0000	1.0000
N(T,27)	0.9979	0.0000	0.0012	1.0000	1.0000	0.9938	0.0002	0.0038	1.0000	1.0000
N(T,28)	0.9984	0.0000	0.0013	1.0000	1.0000	0.9970	0.0001	0.0022	1.0000	1.0000
N(T,29)	0.9992	0.0000	0.0012	1.0000	1.0000	0.9944	0.0004	0.0050	1.0000	1.0000
N(T,30)	0.9973	0.0000	0.0013	1.0000	1.0000	0.9944	0.0002	0.0032	1.0000	1.0000
N(T,31)	1.0008	0.0001	0.0016	1.0000	1.0000	0.9948	0.0002	0.0038	1.0000	1.0000
N(T,32)	0.9965	0.0001	0.0016	1.0000	1.0000	0.9956	0.0001	0.0028	1.0000	1.0000
N(T,33)	0.9984	0.0000	0.0010	1.0000	1.0000	0.9954	0.0001	0.0030	1.0000	1.0000
N(T,34)	0.9973	0.0000	0.0014	1.0000	1.0000	0.9951	0.0005	0.0055	1.0000	1.0000
N(T,35)	0.9987	0.0001	0.0015	1.0000	1.0000	0.9948	0.0002	0.0034	1.0000	1.0000
N(T,36)	0.9950	0.0002	0.0026	1.0000	1.0000	0.9944	0.0004	0.0051	1.0000	1.0000
N(T,37)	0.9974	0.0001	0.0017	1.0000	1.0000	0.9960	0.0001	0.0029	1.0000	1.0000
N(T,38)	0.9977	0.0001	0.0020	1.0000	1.0000	0.9980	0.0002	0.0034	1.0000	1.0000
N(T,39)	0.9984	0.0000	0.0011	1.0000	1.0000	0.9989	0.0001	0.0029	1.0000	1.0000
N(T,40)	0.9984	0.0001	0.0014	1.0000	1.0000	0.9946	0.0002	0.0035	1.0000	1.0000
N(T,41)	0.9980	0.0001	0.0016	1.0000	1.0000	0.9964	0.0001	0.0029	1.0000	1.0000
N(T,42)	0.9975	0.0001	0.0016	1.0000	1.0000	0.9983	0.0001	0.0019	1.0000	1.0000
N(T,43)	0.9988	0.0001	0.0015	1.0000	1.0000	0.9991	0.0000	0.0017	1.0000	1.0000
N(T,44)	0.9985	0.0001	0.0016	1.0000	1.0000	0.9971	0.0001	0.0026	1.0000	1.0000
N(T,45)	0.9996	0.0000	0.0006	1.0000	1.0000	0.9977	0.0001	0.0026	1.0000	1.0000
N(T,46)	0.9997	0.0000	0.0006	1.0000	1.0000	0.9995	0.0000	0.0009	1.0000	1.0000
N(T,47)	0.9997	0.0000	0.0014	1.0000	1.0000	1.0041	0.0016	0.0113	1.0000	1.0000
N(T,48)	1.0000	0.0000	0.0000	1.0000	1.0000	1.0475	0.0902	0.0931	0.9990	0.8655
N(T,49)	0.9984	0.0001	0.0022	1.0000	1.0000	0.9992	0.0000	0.0016	1.0000	1.0000
N(T,50)	1.0245	0.0480	0.0579	1.0000	0.9947	1.2121	1.1789	0.3952	0.9392	0.2892
N(T,51)	0.9994	0.0000	0.0011	1.0000	1.0000	1.0000	0.0000	0.0000	1.0000	1.0000
N(T,52)	0.9744	0.0256	0.0503	0.9981	1.0000	1.0000	0.0000	0.0000	1.0000	1.0000
N(T,53)	0.9152	0.2376	0.1663	0.5709	0.9853	1.2839	0.9669	0.5151	0.9280	0.2420
N(T,54)	1.0519	0.0840	0.1093	0.9968	0.8060	0.9500	0.0250	0.0980	0.8413	0.9987
N(T,55)	1.0000	0.0000	0.0000	1.0000	1.0000	0.8944	0.1003	0.2069	0.4790	0.9743
N(T,56)	1.0000	0.0000	0.0000	1.0000	1.0000	0.8500	0.1350	0.2940	0.3694	0.9522
N(T,57)	1.0000	0.0000	0.0000	1.0000	1.0000	1.2500	0.2500	0.4900	0.9192	0.2743
N(T,58)	0.9000	0.0400	0.1960	0.5000	0.9772	2.0500	2.2050	2.0580	0.8633	0.1828
N(T,59)	0.6500	0.3675	0.6860	0.2375	0.9007	1.4500	0.0050	0.0980	1.0000	0.0000
N(T,60)	0.1000	0.6050	1.0780	0.0729	0.9655					
N(T.)	0.9023	0.0056	0.0149	0.6165	1.0000	0.7959	0.0096	0.0240	0.0000	1.000
q(15)	1.3860	0.1273	0.0710	1.0000	0.0000	1.9296	0.3080	0.1360	1.0000	0.0000
q(16)	1.4553	0.2337	0.0962	1.0000	0.0000	1.7558	0.6789	0.2019	1.0000	0.0000
q(17)	1.4210	0.3804	0.1227	1.0000	0.0000	1.4925	0.1753	0.1026	1.0000	0.0000
q(18)	1.2625	0.2663	0.1027	1.0000	0.0010	1.6064	0.6341	0.1951	1.0000	0.0000
q(19)	1.3163	0.2459	0.0987	1.0000	0.0000	1.5429	0.4501	0.1644	1.0000	0.0000
q(20)	1.3521	0.2433	0.0982	1.0000	0.0000	1.4564	0.4088	0.1566	1.0000	0.0000
q(21)	1.1274	0.0701	0.0527	1.0000	0.1544	1.2697	0.1354	0.0901	1.0000	0.0001
q(22)	1.0136	0.0295	0.0342	1.0000	1.0000	1.0701	0.0400	0.0490	1.0000	0.8842
q(23)	1.0494	0.0236	0.0306	1.0000	0.9994	1.0805	0.0313	0.0434	1.0000	0.8113
q(24)	1.0770	0.0349	0.0372	1.0000	0.8875	1.0460	0.0401	0.0491	1.0000	0.9846
q(25)	1.0515	0.0266	0.0324	1.0000	0.9983	1.0328	0.0437	0.0512	1.0000	0.9949
q(26)	1.0264	0.0288	0.0338	1.0000	1.0000	0.9658	0.0560	0.0580	0.9870	1.0000
q(27)	0.9990	0.0386	0.0391	1.0000	1.0000	1.0400	0.0476	0.0534	1.0000	0.9861
q(28)	1.0209	0.0333	0.0363	1.0000	1.0000	0.9478	0.0739	0.0666	0.9202	1.0000
q(29)	0.9869	0.0450	0.0422	1.0000	1.0000	0.9101	0.0623	0.0611	0.6264	1.0000
q(30)	0.9408	0.0390	0.0393	0.9790	1.0000	0.9330	0.0487	0.0540	0.8843	1.0000
q(31)	0.9596	0.0434	0.0415	0.9976	1.0000	0.8261	0.0839	0.0710	0.0206	1.0000
q(32)	0.9150	0.0425	0.0410	0.7631	1.0000	0.9050	0.0622	0.0611	0.5634	1.0000
q(33)	0.9620	0.0444	0.0419	0.9981	1.0000	0.8922	0.0814	0.0699	0.4138	1.0000
q(34)	0.9051	0.0598	0.0486	0.5808	1.0000	0.8964	0.0935	0.0749	0.4623	1.0000
q(35)	0.9179	0.0619	0.0495	0.7603	1.0000	0.8245	0.0933	0.0748	0.0240	1.0000
q(36)	0.8685	0.0924	0.0605	0.1537	1.0000	0.7950	0.1000	0.0775	0.0039	1.0000
q(37)	0.8611	0.0802	0.0563	0.0883	1.0000	0.7620	0.0863	0.0720	0.0001	1.0000
q(38)	0.8240	0.0971	0.0620	0.0082	1.0000	0.7804	0.1357	0.0903	0.0047	1.0000
q(39)	0.7925	0.0791	0.0560	0.0001	1.0000	0.7502	0.1244	0.0871	0.0004	1.0000

Table 4 (continued)

	Estimates		Bias 95% CI ½ width	Significance levels HO:Bias≥0.9 HA:Bias<0.9	Significance levels HO:Bias≤1.1 HA:Bias>1.1	Estimates		Bias 95% CI ½ width	Significance levels HO:Bias≥0.9 HA:Bias<0.9	Significance levels HO:Bias≤1.1 HA:Bias>1.1
	Bias	Variance				Bias	Variance			
q(40)	0.8476	0.1304	0.0722	0.0775	1.0000	0.7426	0.0887	0.0747	0.0000	1.0000
q(41)	0.7956	0.0730	0.0546	0.0001	1.0000	0.7352	0.4793	0.1737	0.0315	1.0000
q(42)	0.6863	1.5698	0.2546	0.0500	0.9993	0.7424	0.1202	0.0885	0.0002	1.0000
q(43)	0.8525	0.1842	0.0882	0.1455	1.0000	0.8617	0.1037	0.0829	0.1827	1.0000
q(44)	0.8133	0.0973	0.0648	0.0044	1.0000	0.8777	0.1561	0.1044	0.3375	1.0000
q(45)	1.0254	2.2033	0.3119	0.7846	0.6804	0.8420	0.0913	0.0799	0.0774	1.0000
q(46)	0.8358	0.1309	0.0774	0.0519	1.0000	1.0564	0.9370	0.2606	0.8803	0.6284
q(47)	0.3470	25.6967	1.1397	0.1708	0.9023	63.2003	<99999.99	121.9043	0.8417	0.1590
q(48)	0.8576	0.6898	0.1974	0.3370	0.9919	1.0744	0.3067	0.1716	0.9768	0.6152
q(49)	0.7220	0.4331	0.1638	0.0166	1.0000	0.0008	75.0753	3.0502	0.2817	0.7600
q(50)	0.9710	3.3934	0.4868	0.6124	0.6983	2.7969	115.6154	3.9135	0.8290	0.1977
q(51)	−0.3572	73.2005	2.4998	0.1621	0.8734	0.7113	2.1593	0.6141	0.2735	0.8926
q(52)	−3.7106	632.0744	12.6793	0.2380	0.7715	0.8225	0.6106	0.3610	0.3370	0.9340
q(53)	1.0422	0.3956	0.2146	0.9031	0.7011	1.7977	6.0280	1.2861	0.9144	0.1438
q(54)	1.0498	0.3516	0.2237	0.9054	0.6700	2.2403	8.9080	1.8499	0.9222	0.1135
q(55)	0.0243	7.1499	1.2023	0.0767	0.9602	3.6459	67.4526	5.3658	0.8421	0.1762
q(56)	4.1165	89.6428	6.1858	0.8459	0.1696	3.2914	12.9452	2.8790	0.9482	0.0679
q(57)	0.8978	0.0700	0.2116	0.4919	0.9694	0.9321	0.0669	0.2536	0.5980	0.9028
q(58)	−3.1313	74.4663	8.4568	0.1751	0.8366	0.6640	0.2346	0.6713	0.2454	0.8985
q(59)	−5.6513	172.1638	14.8479	0.1936	0.8136	0.7438	0.0005	0.0294	0.0000	1.0000
q(60)	−0.3459	7.3840	3.7661	0.2584	0.7741					
exp(z)	0.6422	0.0084	0.0182	0.0000	1.0000					

Table 5

Correlation coefficients between estimates of the unobserved change rate (z) and all other estimates.

Estimate	Rho	Estimate	Rho	Estimate	Rho	Estimate	Rho
N(T,15)	0.46	N(T,38)	0.08	q(15)	−0.53	q(38)	−0.18
N(T,16)	0.34	N(T,39)	0.11	q(16)	−0.30	q(39)	0.09
N(T,17)	0.45	N(T,40)	0.21	q(17)	−0.36	q(40)	−0.03
N(T,18)	0.20	N(T,41)	0.22	q(18)	−0.24	q(41)	0.02
N(T,19)	0.27	N(T,42)	0.22	q(19)	−0.18	q(42)	−0.09
N(T,20)	0.23	N(T,43)	0.15	q(20)	−0.18	q(43)	−0.14
N(T,21)	0.23	N(T,44)	0.08	q(21)	−0.22	q(44)	−0.01
N(T,22)	0.11	N(T,45)	0.31	q(22)	−0.22	q(45)	−0.07
N(T,23)	0.27	N(T,46)	0.20	q(23)	−0.16	q(46)	0.03
N(T,24)	0.22	N(T,47)	0.04	q(24)	−0.15	q(47)	0.11
N(T,25)	0.21	N(T,48)	0.19	q(25)	−0.27	q(48)	0.11
N(T,26)	0.10	N(T,49)	0.13	q(26)	−0.31	q(49)	0.08
N(T,27)	0.19	N(T,50)	0.26	q(27)	−0.26	q(50)	0.12
N(T,28)	0.22	N(T,51)	0.22	q(28)	−0.10	q(51)	0.02
N(T,29)	0.29	N(T,52)	0.11	q(29)	−0.35	q(52)	−0.11
N(T,30)	0.09	N(T,53)	0.16	q(30)	−0.10	q(53)	0.15
N(T,31)	0.17	N(T,54)	0.12	q(31)	−0.43	q(54)	0.15
N(T,32)	0.19	N(T,55)	0.21	q(32)	0.09	q(55)	0.02
N(T,33)	0.21	N(T,56)	0.16	q(33)	−0.17	q(56)	−0.05
N(T,34)	0.25	N(T,57)	0.06	q(34)	−0.19	q(57)	0.15
N(T,35)	0.18	N(T,58)	0.03	q(35)	−0.02	q(58)	−0.11
N(T,36)	0.08	N(T,59)	0.06	q(36)	0.04	q(59)	−0.11
N(T,37)	0.23	N(T,60)	−0.03	q(37)	−0.01	q(60)	−0.06

lations (Paloheimo 1980, Collie and Sissenwine 1983). These estimates do not seem highly correlated.

The unobserved change rate was a random variable in the second test, so its estimation error was not computed. Error characteristics-of-abundance estimates were extremely similar to those of example one; apparently high process variability does not adversely affect estimation even in the presence of sampling variance.

The contracted seasonal recruitment pattern (Fig. 3), conventionally interpreted as age-specific cohorts, was used in the last two examples. Growth parameters were the same as the two previous examples and growth variation was moderate (cv 0.1). Sampling efficiencies were also unchanged and their variability set at that of example 1 (cv[q]=0.2). The unobserved change rate randomly varied five-fold ($z_t \sim U(0.05, 0.25)$). Catching was continuous so each period's catch was assigned to midperiod for estimation. Overfishing was simulated by rapidly increasing exploitation enough to decrease stock abundance 36% during the four periods of sampling (last four). The fishing mortality rates for periods 6–19 were: 0.05, 0.1, 0.15, 0.2, 0.25, 0.3, 0.6, 0.4, 0.5, 0.8, 0.6, 0.8, 1.0, and 1.2. Example 3 simulated very low sampling levels and example 4, high levels. It was of interest to find if abundance would be correctly estimated during overfishing under either sampling condition.

Example 3 was the limited-data case. The growth measurement error was large (cv 0.20) and the sample size for growth parameter estimation was moderate (95% CI of width ±5%, 77 fish). The precision of catch estimates was low (cv[C] = 0.4) and relative abundance sampling was meager (95% CI of width ±30%, two samples each period).

Error variances of the smallest seven size class abundance estimates were very large (Table 6), but error variances were low for size-classes 25 and larger. Usefully narrow confidence intervals on the bias of these estimates were obtained with few trials. Significance levels suggested that abundance estimates of size-classes 17–21 might not have been biased and unbiased estimation seemed likely for size-classes 22 and larger. Estimates of sampling gear efficiencies (q(s)) also seemed accurate although error variances were high.

Example four simulated sufficient sampling. A growth parameter measurement error (cv 0.05) and sample size (99% CI of width ±1%, 829 fish) more characteristic of databases for heavily sampled fisheries were used. Catches were precisely estimated (cv[C] = 0.2) and relative abundance sampling was at a very sufficient level (99% CI of width ±3%, 295 samples each period).

Biases (Table 6) were very similar to those of example 3. Abundance estimates for the smaller size-classes that appeared in relative abundance samples just once were probably biased by more than 10%, but the rest were not. Estimates of q for the smallest 10 size-classes were biased by more than 10% and the rest were probably not. Most error variances for stocksize estimates were several times smaller than those of example 3, and some were an order of magnitude smaller. Likewise, the error variance of q estimates was also smaller. As may be expected, sufficient sampling levels increased precision but did not affect bias. Abundance estimates of sizes that appeared in abundance samples more than once were estimated accurately when overfishing occurred, whether or not sampling levels were sufficient or not.

Estimates of historical stock sizes are usually used to find out if stock abundance is increasing or decreasing. Errors of virtual population analysis back-calculations of cohort- specific abundances converge as dates decrease (Agger et al. 1971, Pope 1972, Jones 1981). Conventional wisdom is thus that abundance estimates for the last period are extremely uncertain, but due to the convergence, estimated abundance trends are reliable. For this size-based estimator, (2) provides abundance calculations before date y(T) from the estimates available at the solution of (4).

Error characteristics of historical abundance estimates (Table 7) were unexpected. Bias and error variance increased as dates decreased. Last-period

Table 6

Examples for seasonal, contracted recruitment and overfishing.

	Example 3, Limited sampling					Example 4, Sufficient sampling				
Catch estimation										
catch dates	absent					absent				
cv[C(t,s)]	0.40					0.20				
Growth estimation										
cv[error]	0.20					0.05				
precision level	0.05					0.01				
probability level	0.95					0.99				
fish sampled, g	77					829				
Sampling efficiency										
cv[q(s)]	0.20					0.20				
precision level	0.30					0.03				
probability level	0.95					0.99				
sample size, r	2					295				
Number of trials	83					128				
	Estimates		Bias 95% CI ½ width	Significance levels HO:Bias≥0.9 HA:Bias<0.9	HO:Bias≤1.1 HA:Bias>1.1	Estimates		Bias 95% CI ½ width	Significance levels HO:Bias≥0.9 HA:Bias<0.9	HO:Bias≤1.1 HA:Bias>1.1
	Bias	Variance				Bias	Variance			
N(T,15)	9.3261	759.7793	5.9301	0.9973	0.0033	12.8103	1297.3179	6.2399	0.9999	0.0001
N(T,16)	8.3623	546.7384	5.0304	0.9982	0.0023	8.3910	128.6375	1.9649	1.0000	0.0000
N(T,17)	2.0437	320.3240	3.8505	0.7198	0.3155	3.4678	49.7123	1.2215	1.0000	0.0001
N(T,18)	1.8321	42.6741	1.4054	0.9032	0.1536	1.2202	1.3293	0.1997	0.9992	0.1191
N(T,19)	0.9011	1.3723	0.2520	0.5033	0.9391	0.7992	0.3075	0.0961	0.0199	1.0000
N(T,20)	1.1948	1.6789	0.2788	0.9809	0.2525	0.8677	0.3403	0.1011	0.2657	1.0000

Table 6 (continued)

	Estimates		Bias 95% CI ½ width	Significance levels HO:Bias≥0.9 HA:Bias<0.9	Significance levels HO:Bias≤1.1 HA:Bias>1.1	Estimates		Bias 95% CI ½ width	Significance levels HO:Bias≥0.9 HA:Bias<0.9	Significance levels HO:Bias≤1.1 HA:Bias>1.1
	Bias	Variance				Bias	Variance			
N(T,21)	1.3401	5.0248	0.4823	0.9632	0.1646	1.7942	1.3107	0.1983	1.0000	0.0000
N(T,22)	0.9265	0.1610	0.0863	0.7262	1.0000	0.8043	1.2599	0.1945	0.1673	0.9986
N(T,23)	0.9335	0.4053	0.1370	0.6840	0.9914	0.8082	0.7830	0.1533	0.1203	0.9999
N(T,24)	0.9017	0.7664	0.1895	0.5072	0.9799	0.9673	0.1843	0.0744	0.9619	0.9998
N(T,25)	0.9988	0.0606	0.0533	0.9999	0.9999	1.0007	0.0106	0.0179	1.0000	1.0000
N(T,26)	0.9540	0.0476	0.0472	0.9875	1.0000	1.0021	0.0032	0.0098	1.0000	1.0000
N(T,27)	0.9890	0.0186	0.0295	1.0000	1.0000	0.9898	0.0055	0.0129	1.0000	1.0000
N(T,28)	0.9865	0.0129	0.0246	1.0000	1.0000	0.9855	0.0109	0.0181	1.0000	1.0000
N(T,29)	0.9596	0.0341	0.0400	0.9983	1.0000	0.9795	0.0174	0.0230	1.0000	1.0000
N(T,30)	1.0184	0.0600	0.0530	1.0000	0.9987	0.9979	0.0235	0.0269	1.0000	1.0000
N(T,31)	0.9606	0.0254	0.0349	0.9997	1.0000	0.9916	0.0084	0.0161	1.0000	1.0000
N(T,32)	0.9922	0.0073	0.0188	1.0000	1.0000	0.9945	0.0029	0.0094	1.0000	1.0000
N(T,33)	1.0158	0.0266	0.0359	1.0000	1.0000	0.9861	0.0022	0.0082	1.0000	1.0000
N(T,34)	0.9851	0.0117	0.0240	1.0000	1.0000	0.9824	0.0040	0.0112	1.0000	1.0000
N(T,35)	0.9700	0.0138	0.0260	1.0000	1.0000	0.9846	0.0025	0.0090	1.0000	1.0000
N(T,36)	0.9908	0.0339	0.0411	1.0000	1.0000	0.9921	0.0008	0.0052	1.0000	1.0000
N(T,37)	0.9852	0.0071	0.0195	1.0000	1.0000	0.9988	0.0004	0.0038	1.0000	1.0000
N(T,38)	0.9807	0.0027	0.0126	1.0000	1.0000	0.9992	0.0006	0.0048	1.0000	1.0000
N(T,39)	0.9874	0.0116	0.0278	1.0000	1.0000	0.9957	0.0003	0.0037	1.0000	1.0000
N(T,40)	0.9841	0.0024	0.0132	1.0000	1.0000	0.9986	0.0004	0.0042	1.0000	1.0000
N(T,41)	0.9992	0.0010	0.0090	1.0000	1.0000	1.0001	0.0001	0.0028	1.0000	1.0000
N(T,42)	1.0102	0.0314	0.0549	1.0000	0.9993	1.0002	0.0000	0.0013	1.0000	1.0000
N(T,43)	0.9924	0.0012	0.0115	1.0000	1.0000	0.9987	0.0001	0.0025	1.0000	1.0000
N(T,44)	0.9798	0.0101	0.0452	0.9997	1.0000	0.9986	0.0001	0.0027	1.0000	1.0000
N(T,45)	0.9833	0.0012	0.0158	1.0000	1.0000	1.0000	0.0000	0.0000	1.0000	1.0000
N(T,46)	0.9854	0.0006	0.0141	1.0000	1.0000	1.0000	0.0000	0.0000	1.0000	1.0000
N(T,47)	1.0000	0.0010	0.0253	1.0000	1.0000	1.0000	0.0000	0.0000	1.0000	1.0000
N(T,48)	0.8000	0.0200	0.1960	0.1587	0.9987	1.0000	0.0000	0.0000	1.0000	1.0000
N(T,49)						1.0000	0.0000	0.0000	1.0000	1.0000
N(T.)	1.1369	32.0777	1.2185	0.6484	0.4763	1.1493	29.8091	0.9459	0.6973	0.4593
q(15)	0.3282	0.1186	0.0741	0.0000	1.0000	0.2474	0.0501	0.0388	0.0000	1.0000
q(16)	0.3998	0.2084	0.0982	0.0000	1.0000	0.2984	0.0519	0.0395	0.0000	1.0000
q(17)	0.7850	0.7019	0.1802	0.1055	0.9997	0.6889	0.2424	0.0853	0.0000	1.0000
q(18)	1.3854	0.9594	0.2107	1.0000	0.0040	1.2926	0.6908	0.1440	1.0000	0.0044
q(19)	1.9397	2.7953	0.3597	1.0000	0.0000	1.6785	0.6126	0.1356	1.0000	0.0000
q(20)	1.3499	0.6184	0.1692	1.0000	0.0019	1.4341	0.3226	0.0984	1.0000	0.0000
q(21)	0.9199	0.4187	0.1392	0.6104	0.9944	0.6845	0.0844	0.0503	0.0000	1.0000
q(22)	0.6958	0.2367	0.1047	0.0001	1.0000	0.5667	0.0730	0.0468	0.0000	1.0000
q(23)	0.7353	0.2491	0.1074	0.0013	1.0000	0.6515	0.0753	0.0475	0.0000	1.0000
q(24)	0.9467	0.5200	0.1561	0.7213	0.9729	0.7885	0.0992	0.0546	0.0000	1.0000
q(25)	1.0306	0.3424	0.1266	0.9784	0.8584	0.9317	0.0882	0.0515	0.8861	1.0000
q(26)	1.0431	0.2997	0.1185	0.9910	0.8266	1.0073	0.0575	0.0415	1.0000	1.0000
q(27)	1.0743	0.3260	0.1236	0.9971	0.6583	0.9851	0.0475	0.0377	1.0000	1.0000
q(28)	1.0729	0.4116	0.1389	0.9927	0.6489	0.9155	0.0586	0.0419	0.7658	1.0000
q(29)	1.0112	0.3553	0.1290	0.9545	0.9113	0.9105	0.0767	0.0482	0.6652	1.0000
q(30)	0.9345	0.4927	0.1519	0.6719	0.9836	0.9002	0.0721	0.0471	0.5027	1.0000
q(31)	1.0777	0.5119	0.1568	0.9869	0.6096	0.8955	0.0796	0.0495	0.4297	1.0000
q(32)	1.0668	0.3685	0.1339	0.9927	0.6864	0.9643	0.1123	0.0587	0.9841	1.0000
q(33)	1.0548	0.2669	0.1139	0.9961	0.7818	1.0293	0.1086	0.0578	1.0000	0.9918
q(34)	1.0891	0.4220	0.1442	0.9949	0.5588	0.9230	0.1037	0.0569	0.7862	1.0000
q(35)	1.2517	1.4470	0.2670	0.9951	0.1327	0.9907	0.1106	0.0597	0.9985	0.9998
q(36)	1.0885	0.5550	0.1664	0.9868	0.5537	1.0126	0.1046	0.0591	0.9999	0.9981
q(37)	1.0643	0.3099	0.1286	0.9939	0.7066	1.0658	0.1899	0.0814	1.0000	0.7950
q(38)	1.2725	1.2458	0.2713	0.9964	0.1064	0.9944	0.0895	0.0589	0.9992	0.9998
q(39)	0.9949	0.7569	0.2239	0.7970	0.8211	1.0445	0.2018	0.0923	0.9989	0.8806
q(40)	1.1630	0.5160	0.1934	0.9962	0.2617	0.9748	0.1302	0.0806	0.9656	0.9988
q(41)	1.3898	1.4057	0.3320	0.9981	0.0435	0.9666	0.2227	0.1130	0.8761	0.9896
q(42)	1.4005	2.9713	0.5342	0.9668	0.1351	1.0596	0.2525	0.1316	0.9913	0.7265
q(43)	1.0215	0.2530	0.1643	0.9263	0.8256	−0.7903	123.8881	3.4933	0.1715	0.8556
q(44)	0.9185	0.2248	0.2132	0.5674	0.9524	1.1289	0.8725	0.3051	0.9293	0.4263
q(45)	4.0163	137.2726	5.4127	0.8704	0.1455	1.4194	2.0954	0.5674	0.9636	0.1350
q(46)	1.2540	0.3985	0.3572	0.9740	0.1990	1.0488	0.0964	0.1396	0.9816	0.7639
q(47)	1.2032	0.2502	0.4002	0.9312	0.3067	1.9698	5.6933	1.4101	0.9315	0.1133
q(48)	1.1792	0.2007	0.6210	0.8109	0.4013	1.0484	0.0029	0.0473	1.0000	0.9839
q(49)						0.9818	0.0718	0.2626	0.7291	0.8113

Table 7
Error statistics of historical abundance estimates from example 4.

Variable	n	Error variance	Bias estimate	Variable	n	Error variance	Bias estimate	Variable	n	Error variance	Bias estimate
N(1,15)	128	115.5114	5.9596	N(1,27)	128	0.1871	0.9173	N(1,39)	91	0.4743	0.7745
N(2,15)	128	86.8395	6.0680	N(2,27)	128	0.1899	0.8982	N(2,39)	91	0.5662	0.9049
N(3,15)	128	119.8275	5.3517	N(3,27)	128	0.4459	1.0290	N(3,39)	91	0.4302	1.0320
N(4,15)	128	1296.6914	12.8388	N(4,27)	128	0.0056	0.9896	N(4,39)	91	0.0003	0.9957
N(1,16)	128	30.4340	4.2588	N(1,28)	128	0.4354	0.9534	N(1,40)	77	1.1408	0.9088
N(2,16)	128	184.7422	7.4660	N(2,28)	128	0.2830	1.0502	N(2,40)	77	0.7205	1.0607
N(3,16)	128	68.0011	6.3408	N(3,28)	128	0.4060	1.1279	N(3,40)	77	0.4176	0.9065
N(4,16)	128	128.6176	8.3893	N(4,28)	128	0.0109	0.9854	N(4,40)	77	0.0004	0.9986
N(1,17)	128	10.8289	1.7620	N(1,29)	127	0.3800	0.9685	N(1,41)	67	0.8746	1.0508
N(2,17)	128	50.7792	2.9860	N(2,29)	127	0.6222	1.2014	N(2,41)	67	0.7359	0.9693
N(3,17)	128	6.3308	2.2878	N(3,29)	127	0.6897	1.1322	N(3,41)	67	0.6803	1.1584
N(4,17)	128	49.7113	3.4675	N(4,29)	127	0.0174	0.9794	N(4,41)	67	0.0001	1.0001
N(1,18)	128	0.5225	0.8387	N(1,30)	125	1.3161	1.1217	N(1,42)	56	0.2236	0.5534
N(2,18)	128	1.8065	1.0217	N(2,30)	125	0.6497	1.1361	N(2,42)	56	0.9773	0.8919
N(3,18)	128	1.3119	1.1786	N(3,30)	125	0.6635	1.1661	N(3,42)	56	0.8370	1.0048
N(4,18)	128	1.3292	1.2202	N(4,30)	125	0.0234	0.9971	N(4,42)	56	0.0000	1.0002
N(1,19)	128	0.2076	0.5674	N(1,31)	125	0.4402	0.9570	N(1,43)	39	0.3770	0.7205
N(2,19)	128	0.6367	0.7745	N(2,31)	125	0.7042	1.1035	N(2,43)	39	0.7222	1.0594
N(3,19)	128	0.2891	0.8107	N(3,31)	125	1.2571	1.1914	N(3,43)	39	0.5246	0.9171
N(4,19)	128	0.3074	0.7989	N(4,31)	125	0.0084	0.9916	N(4,43)	39	0.0001	0.9987
N(1,20)	128	0.3131	0.6707	N(1,32)	125	0.4139	0.8962	N(1,44)	36	0.3870	0.8145
N(2,20)	128	0.7200	0.8515	N(2,32)	125	0.4712	1.0943	N(2,44)	36	0.3686	0.8018
N(3,20)	128	0.4237	0.9559	N(3,32)	125	0.6876	1.1207	N(3,44)	36	0.2355	0.8025
N(4,20)	128	0.3411	0.8679	N(4,32)	125	0.0029	0.9944	N(4,44)	36	0.0001	0.9986
N(1,21)	128	1.3938	1.2717	N(1,33)	125	0.2451	0.7301	N(1,45)	25	0.4571	0.8148
N(2,21)	128	0.9207	1.3560	N(2,33)	125	0.4089	1.0021	N(2,45)	25	0.3210	0.8143
N(3,21)	128	1.5664	1.6328	N(3,33)	125	0.6057	1.1316	N(3,45)	25	0.1735	0.7110
N(4,21)	128	1.3111	1.7941	N(4,33)	125	0.0022	0.9864	N(4,45)	25	0.0000	1.0000
N(1,22)	128	3.4192	1.7054	N(1,34)	123	0.7671	0.8896	N(1,46)	19	0.3338	0.6204
N(2,22)	128	6.9873	2.0668	N(2,34)	123	0.5906	0.9968	N(2,46)	19	0.3380	0.5746
N(3,22)	128	7.5242	2.6186	N(3,34)	123	0.9354	1.1637	N(3,46)	19	0.1914	0.8296
N(4,22)	128	1.2599	0.8042	N(4,34)	123	0.0040	0.9824	N(4,46)	19	0.0000	1.0000
N(1,23)	128	1.1626	1.6450	N(1,35)	119	0.2867	0.8088	N(1,47)	11	0.1290	0.4227
N(2,23)	128	1.6512	1.5052	N(2,35)	119	0.6020	1.0950	N(2,47)	11	0.2434	0.4377
N(3,23)	128	8.1272	2.3806	N(3,35)	119	0.7955	1.1538	N(3,47)	11	0.0694	0.9398
N(4,23)	128	0.7830	0.8082	N(4,35)	119	0.0025	0.9846	N(4,47)	11	0.0000	1.0000
N(1,24)	128	1.2296	1.3307	N(1,36)	115	0.2635	0.6926	N(1,48)	5	0.1338	0.4633
N(2,24)	128	2.6137	1.3469	N(2,36)	115	0.4223	0.9411	N(2,48)	5	0.0132	1.0800
N(3,24)	128	23.1672	1.9363	N(3,36)	115	0.7491	1.0997	N(3,48)	5	0.1087	0.7000
N(4,24)	128	0.1842	0.9673	N(4,36)	115	0.0008	0.9921	N(4,48)	5	0.0000	1.0000
N(1,25)	128	0.5672	0.9923	N(1,37)	110	0.2637	0.6720	N(1,49)	4	0.1558	0.3750
N(2,25)	128	0.7867	0.9758	N(2,37)	110	0.5350	0.8555	N(2,49)	4	0.4950	1.1000
N(3,25)	128	5.6842	1.4490	N(3,37)	110	0.6735	1.0410	N(3,49)	4	0.0050	0.9500
N(4,25)	128	0.0106	1.0005	N(4,37)	110	0.0004	0.9986	N(4,49)	4	0.0000	1.0000
N(1,26)	128	0.2515	0.8747	N(1,38)	99	0.8277	0.8260				
N(2,26)	128	0.8233	0.9564	N(2,38)	99	0.2681	0.7480				
N(3,26)	128	3.1000	1.2203	N(3,38)	99	0.8225	1.2851				
N(4,26)	128	0.0032	1.0024	N(4,38)	99	0.0006	0.9989				

abundance estimates were accurate, but those of preceding periods were not. Error variances of estimates before the last period tended to be one to two orders of magnitude higher than those of the last period. This implies that abundance trends estimated in this manner probably will be wrong. In this example, the problem is large enough to mask much of the 36% decrease in abundance; the downward abundance trend would not be clear in calculations of historical stock sizes.

Discussion

These Monte Carlo tests show that size-based methods can be accurate and precise estimators of stock abundance. Population characteristics need not conform to the restrictive assumptions of traditional VPA methods. Any sort of fish stock can be successfully addressed with size-based techniques, an important aspect when assessing populations where ageing is impossible or where recruitment is not periodic.

These results imply that little will be gained from the extensive age sampling programs that are the foundation of VPA-based methods. They are not needed if size-based methods are used; only size samples and the rate of growth are required. Light, periodic growth sampling is sufficient to monitor possible growth rate changes through time. Also, since growth rates are required instead of ages, mark-recapture methods can be used to obtain growth measures if hardpart interpretations (age is not observed on hardparts; instead, characteristic marks are interpreted as annular occurrences) are difficult or expensive to obtain.

The method of abundance estimation developed in this study, a meticulous bookkeeper of size data as is the method of Beddington and Cook (1981), is primitive compared with other size-based methods (Fournier and Doonan 1987, Schnute et al. 1989, Sullivan 1989, Sullivan et al. 1990). Its degree of success in estimating abundance suggests that complete population-model structures are unnecessary. Estimates were usefully accurate and precise even with very high process variability. Very pronounced individual growth variation did not cause estimation problems. These results show that precise, accurate abundance estimates are possible with any recruitment pattern imaginable. It was a particular surprise to find that temporally variant (fourfold) unobserved change rates ("natural mortality" of Ricker (1948) but including migration and unrecorded catch) did not affect estimation at all. That result is reassuring, since the rate is probably extremely variable in nature.

Sampling problems did not seem to degrade estimation either. The level of catch estimation error proved unimportant and there was no indication that exact catch dates need to be recorded. Highly variable sampling efficiencies (q_s) did not cause estimation problems, particularly when sample sizes were adequate. Highly variable individual growth rates (20%) and significant growth measurement error (15%) did not adversely affect abundance estimation when sampling was sufficient. Very large growth-parameter measurement error (40%) and small sample size destroyed performance; although bias was not a problem, extreme error variances and correlated estimates were.

It is of particular interest that this was the only test where estimates of the unobserved change rate (z) and sampling efficiencies (q) were highly correlated. The lack of a pronounced correlation between sampling gear efficiencies and the unobserved change rate in all other tests except this one was unexpected; similar studies of VPA-based methods (Paloheimo 1980, Collie and Sissenwine 1983) found such correlation a major characteristic. It thus seems possible that ageing errors, or the violation of a connected VPA assumption, contributed to correlation in those studies.

Abundances of most size-classes were estimated precisely with little or no bias, but biased and imprecise abundance estimates occurred in three circumstances. First, abundances of very small fish that were recruited between the next-to-last and last relative abundance sample were estimated poorly. A recruitment group had to be present in the relative abundance samples twice to be estimated with a useful degree of certainty. In practice, this problem is easily fixed if obtaining certain estimates of recent recruitment of small fish is important enough to justify the cost of additional samples during the last period. Since the estimator is not based on equal time units, only dates, additional sample(s) will monitor the size-classes of interest several times instead of just once. Second, wide size-classes caused bias and imprecision, particularly for larger sizes. This bias was easily eliminated by narrowing size-classes. Last, calculations of historical abundances were in large error. It is well known that VPA calculations are poor for the most recent period of data and improve as dates decrease. Though they are not germane to current production levels, estimates of the oldest stock sizes are the most certain ones in VPA. The exact opposite is true for this size-based method. Estimates of historical abundances obtained in the solution calculation should not be used; error variances of these computations are very large. Since the estimates of the final-period abundances are accurate and precise, this is probably not a problem even if historical stock-size estimates are needed. Although the procedure was not tested, these estimates might be obtained by starting with the initial four periods of data, estimating the fourth period abundance vector, and then progressing forward one period at a time. Abundance in the first three periods cannot be estimated but subsequent abundances can. The relation between the number of periods in the data and estimation errors was not investigated, but the authors- experience with VPA-based methods indicates little, if any, would be gained with a longer time-series.

This study shows that *a priori* knowledge of the unobserved change rate (z) is not required to accurately and precisely estimate abundance with this size-based method, yet it is well known (Paloheimo 1980, Collie and Sissenwine 1983, Deriso 1985, Pope and Shepherd 1985) that such knowledge is necessary when applying VPA-based procedures.

This study suggests that the unobserved change rate (z) will often be estimated with bias, yet z should be included in the vector of estimates anyway. Monte Carlo tests of the Beddington and Cook model established that simultaneous estimation of a natural mortality schedule (analogous to the unobserved change rate in this study) is necessary to avoid biased abundance estimates (de la Mare 1988). If z is fixed instead

of estimated, abundance estimation bias is assured because stock size is a function of that rate. It thus seems prudent to include the rate in the vector of estimates to avoid abundance estimation bias even if it is not useful. When necessary, Monte Carlo methods can be used to establish interval estimates on e^{-z}. This study indicates that estimates of e^{-z} are often biased, yet precise. The estimate of error variance over the 97 trials of example 1 was 0.0084, so the 95% CI width is $\pm 1.96\sqrt{(0.0084 \div 97)}$ or ± 0.0182, and the bias adjustment is 0.6422.

Acknowledgments

I express very sincere appreciation to Douglas G. Chapman for his knowledgeable and diligent guidance of this research and William G. Clark whose critical suggestions and encouragement significantly broadened the scope of this study. I am indebted to Bradford E. Brown, of the Southeast Fisheries Center of the National Marine Fisheries Service, who provided computer resources and other critical support. I especially thank Nancie J. Parrack for many helpful suggestions as the study progressed and Stephen B. Mathews for technical recommendations as well as a critical review of the original manuscript.

Citations

Agger, P., I. Boetius, and H. Lassen
1971 On errors in virtual population analysis. Int. Counc. Explor. Sea Doc. CM 1971/H:16, 10 p.

Anonymous
1981a Report of the sub-committee on sperm whales (Appendix II). Rep. Int. Whaling Comm. 31:100–101.
1981b Report of the ad hoc working group on the use of effort data in assessments. Int. Counc. Explor. Sea Doc. CM 1981/G:5, 65 p.
1983 Report of the working group on methods of fish stock assessment. Int. Counc. Explor. Sea Doc. CM 1983/Assess:17, 73 p.
1984 Report of the working group on methods of fish stock assessments. Int. Counc. Explor. Sea Doc. CM 1984/Assess: 19, 56 p.
1986 Report of the ad hoc multispecies assessment working group. Int. Counc. Explor. Sea Doc. CM 1986, 10 p.

Bartoo, N.W., and K.R. Parker
1982 Stochastic age-frequency estimation using the von Bertalanffy growth equation. Fish. Bull., U.S. 81:91–96.

Basson, M., A.A. Rosenberg, and J.R. Beddington
1988 The accuracy and reliability of two new methods for estimating growth parameters from length-frequency data. J. Cons. Cons. Int. Explor. Mer 44:277–285.

Beamish, R.J., and G.A. McFarlane
1983 The forgotten requirement for age validation in fisheries biology. Trans. Am. Fish. Soc. 112:735–743.

Beddington, J.R., and J.G. Cooke
1981 Development of an assessment technique for male sperm whales based on the use of length data from the catches, with special reference to the North-west Pacific stock. Rep. Int. Whaling Comm. 31:747–760.

Beddington, J.R., J.G. Cooke, and W.K. de la Mare
1983 Estimations of the western North Pacific sperm whale population using the length distribution of catches. Rep. Int. Whaling Comm. 33:747–749.

Box, G.E.P.
1979 Robustness in the strategy of scientific model building. *In* Launer, R.L., and G.N. Wilkinson (eds.), Robustness in statistics, p. 201–236. Academic Press, NY.

Brethes, J.F., and G. Desrosiers
1981 Estimation of potential catches of an unexploited stock of soft-shell clam (*Mya arenaria*) from length composition data. Can. J. Fish. Aquat. Sci. 38:371–374.

Burr, R.L.
1988 Inferring the distribution of the parameters of the von Bertalanffy growth model from length moments. Can. J. Fish. Aquat. Sci. 45:1779–1788.

Chapman, D.G.
1961 Statistical problems in dynamics of exploited fisheries populations. *In* Proc., 4th Berkeley symp. math. stat. and probability. Contrib. Biol. and Probl. Med. 4:153–168. Univ. Calif. Press.

Clark, W.G.
1981 Restricted least-squares estimates of age composition from length composition. Can J. Fish. Aquat. Sci. 38:297–307.

Collie, J.S., and M.P. Sissenwine
1983 Estimating population size from relative abundance data measured with error. Can. J. Fish. Aquat. Sci. 40:1871–1879.

Conway, G.R., N.R. Glass, and J. C. Wilcox
1970 Fitting nonlinear models to biological data by Marquardt's algorithm. Ecology 51(3):503–507.

Cooke, J.G., and J.R. Beddington
1982 Further development of an assessment technique for male sperm whales based on length data from the catches. Rep. Int. Whaling Comm. 32:239–241.

Cooke, J.G., and W.K. de la Mare
1983a Description of and simulation studies on the length-specific sperm whale assessment technique. Rep. Int. Whaling Comm. 33:741–745.
1983b Further analyses for the location of the possible stock boundary for the North-West Pacific sperm whale based on length distributions of males. Rep. Int. Whaling Comm. 33: 275–277.

Cooke, J.G., W.K. de la Mare, and J.R. Beddington
1983a Some aspects of the reliability of the length data for the western North Pacific stock of sperm whales. Rep. Int. Whaling Comm. 33:265–267.
1983b An extension of the sperm whale model for the simulation of the male population by length and age. Rep. Int. Whaling Comm. 33:731–733.

de la Mare, W.K.
1988 Extended sensitivity trials on the length-specific method for estimating the size of exploited sperm whale populations. Rep. Int. Whaling Comm. 38:243–248.

de la Mare, W.K., and J.G. Cooke
1984 A new model for the female sperm whale incorporating aspects of the reproductive cycle. Rep. Int. Whaling Comm. 34:251–254.
1985 Analyses of the sensitivity of the length-specific estimation procedure to some departures from underlying assumptions. Rep. Int. Whaling Comm. 35:193–197.

1987 Further sensitivity trials in the length specific method for estimating the size of exploited sperm whale populations. Rep. Int. Whaling Comm. 37:219–222.

Deriso, R.B.
1985 Catch-age analysis with auxiliary information. Can. J. Fish. Aquat. Sci. 42:815–824.

Doubleday, W.G.
1975 A least squares approach to analyzing catch at age data. Int. Comm. Northwest Atl. Fish. Res. Doc. 75/35, 22 p.

Fabens, A.J.
1965 Properties and fitting the von Bertalanffy growth curve. Growth 29:265–289.

Fournier, D.A., and I.J. Doonan
1987 A length-based assessment method utilizing a generalized delay-difference model. Can. J. Fish. Aquat. Sci. 44:422–437.

Fournier, D.A., J.R. Sibert, J. Majkowski, and J. Hampton
1990 MULTIFAN: A likelihood-based method for estimating growth parameters and age composition from multiple length-frequency data sets illustrated using data for southern bluefin tuna. Can. J. Fish. Aquat. Sci. 47:301–317.

Fry, F.E.J.
1949 Statistics of a lake trout fishery. Biometrics 5:27–67.

Gallant, A.R.
1975 Nonlinear regression. Am. Stat. 29(2):73–81.

Gallucci, V.F., and T.J. Quinn II
1979 Reparameterization, fitting, and testing a simple growth model. Trans. Am. Fish. Soc. 108:14–25.

Gulland, J.A.
1965 Estimation of mortality rates. Annex to Rep. Arctic Fish. Working Group, Int. Counc. Explor. Sea Doc. CM 1965(3), 9 p.

Hampton, J., and J. Majkowski
1987 An examination of the accuracy of the Elefan computer programs for length based stock assessment. *In* Pauly, D., and G.P. Morgan (eds.), Length-based methods in fisheries research, p. 203–216. ICLARM (Int. Cent. Living Aquat. Resour. Manage.) Conf. Proc. 13, Manila.

Hasselblad, V.
1966 Estimation of parameters for a mixture of normal distributions. Technometrics 8:431–444.

Hoenig, J.M., and D.M. Heisey
1987 Use of a log-linear model with the EM algorithm to correct estimates of stock composition and to convert length to age. Trans. Am. Fish. Soc. 116:232–243.

Jones, R.
1961 The assessment of long-term effects of changes in gear selectivity and fishing effort. Mar. Res. (Scotl.) 1961(2):1–19.
1974 Assessing the long term effects of changes in fishing effort and mesh size from length composition data. Int. Counc. Explor. Sea Doc. CM 1974/F:33, 13 p.
1981 The use of length composition data in fish stock assessments (with notes on VPA and cohort analysis). FAO Fish. Circ. 734, 60 p.

Kimura, K.K., and S. Chikuni
1987 Mixtures of empirical distributions: An iterative application of the age-length key. Biometrics 43:23–35.

Knight, W.
1968 Asymptotic growth: An example of nonsense disguised as mathematics. J. Fish. Res. Board Can. 25:1303–1307.

Kreuz, K.F., A.V. Tyler, and G.H. Kruse
1982 Variation in growth of Dover soles and English soles as related to upwelling. Trans. Am. Fish. Soc. 111:180–192.

Lai, H.L., and V.F. Gallucci
1988 Effects of parameter variability on length-cohort analysis. J. Cons. Cons. Int. Explor. Mer 45:82–92.

Laurec, A., and F.X. Bard
1980 Analyse multicohorte sur deux classes d'age. Int. Com. Cons. Atl. Tunas Collect. Vol. Sci. Pap XV (SCRS-1979):1–20.

Law, A.M., and W.D. Kelton
1982 Simulation modeling and nalysis. McGraw-Hill, NY, 400 p.

Macdonald, P.D.M., and T.J. Pitcher
1979 Age groups from size frequency data: A versatile and efficient method of analyzing distributing mixtures. J. Fish. Res. Board Can. 36:987–1001.

Marquardt, D.W.
1963 An algorithm for least-squares estimation of non-linear parameters. J. Soc. Ind. Appl. Math 11(2):431–441.

Mendelssohn, R.
1988 Some problems in estimating population sizes from catch-at-age data. Fish. Bull., U.S. 86:617–630.

Morrison, D.D.
1960 Methods for nonlinear least squares problems and convergence proofs, tracking programs, and orbit determination. Proc. Jet Propul. Lab. Sem. (1960):1–9.

Murphy, G.I.
1965 A solution of the catch equation. J. Fish. Res. Board Can. 9:450–491.

Paloheimo, J.E.
1980 Estimation of mortality rates in fish populations. Trans. Am. Fish. Soc. 109:378–386.

Parrack, M.L.
1981 An assessment of the Atlantic bluefin tuna resource. Int. Com. Cons. Atl. Tunas Collect. Vol. Sci. Pap. XV:259–272.
1986 A method of analyzing catches and abundance indices from a fishery. Int. Com. Cons. Atl. Tunas Collect. Vol. Sci. Pap. XXIV:209–221.
1990 Estimating stock abundance from size data. Ph.D. diss., School Fish., Univ. Wash., Seattle, 116 p.

Parrack, N.J.C.
1986 Aspects of Pacific cod biology and population dynamics in the North Pacific. M.S. thesis, Univ. Wash., Seattle, 157 p.

Pauly, D.
1982 Studying single species dynamics in a tropical multispecies context. *In* Pauly, D., and G.I. Murphy (eds.), Theory and management of tropical fisheries, p. 33–70. ICLARM (Int. Cent. Living Aquat. Resour. Manage.) Conf. Proc. 9, Manila.

Pauly, D., M.L. Palomares, and F.C. Gayanilo
1987 VPA estimates of monthly population length composition, recruitment, mortality, biomass and related statistics of Peruvian anchoveta, 1953 to 1981. *In* Pauly, D., and I. Tsukayama (eds.), The Peruvian anchoveta and its upwelling ecosystem: Three decades of change, p. 142–166. ICLARM (Int. Cent. Living Aquat. Resour. Manage.) Stud. Rev. 15, Manila.

Pikitch, E.K., and R.L. Demory
1988 Assessment of scales as a means of aging Dover sole. Trans. Am. Fish. Soc. 117:345–349.

Pope, J.G.
1972 An investigation of the accuracy of virtual population analysis using cohort analysis. Int. Comm. Northwest Atl. Fish. Res. Bull. 9:65–74.

Pope, J.G., and J.G. Shepherd
1982 A simple method for the consistent interpretation of catch-at-age data. J. Cons. Cons. Int. Explor. Mer 40:176–184.
1985 A comparison of the performance of various methods for tuning VPAs using effort data. J. Cons. Cons. Int. Explor. Mer 42:129–151.

Press, W.H., B.P. Flannery, S.A. Teukolsky, and W.T. Vetterling
1986 Numerical recipes, the art of scientific computing. Cambridge Univ. Press, Cambridge, 818 p.

Quinn, T.J., S.H. Hoag, and G.M. Southward
1982 Comparison of two methods of combining catch-per-unit-effort data from geographic regions. Can. J. Fish. Aquat. Sci. 39:837–846.

Richards, F.J.
1959 A flexible growth function for empirical use. J. Exp. Botany 10(29) 290–300.

Ricker, W.E.
1948 Methods of estimating vital statistics of fish populations. Indiana Univ. Publ. Sci. Ser. 15, 101 p.
1975 Computation and interpretation of biological statistics of fish populations. Bull. Fish. Res. Board Can. 191, 382 p.

Rosenberg, A.A., and J.R. Beddington
1987 Monte Carlo testing of two methods for estimating growth from length frequency data, with general conditions for their applicability. *In* Pauly, D., and G.P. Morgan (eds.), Length-based methods in fisheries research, p. 283–289. ICLARM (Int. Cent. Living Aquat. Resour. Manage.) Conf. Proc. 13, Manila.

Rubinstein, R.Y.
1981 Simulation and the Monte Carlo method. John Wiley, NY, 278 p.

Scheuer, E.M., and D.S. Stoller
1962 On the generation of normal random vectors. Technometrics 4:278–281.

Schnute, J.T., L.J. Richards, and A.J. Cass
1989 Fish survival and recruitment: Investigations based on a size-structured model. Can. J. Fish. Aquat. Sci. 46:743–769.

Schrage, L.
1979 A more portable Fortran random number generator. ACM (Assoc. Comput. Machines) Trans. Math. Software 5: 132–138.

Shepherd, J.G.
1985 Deconvolution of length compositions. Int. Counc. Explor. Sea Methods Working Group, Working paper, 7 p.

Shirakihara, K., and S. Tanaka
1983 An alternative length-specific model and population assessment for the western North Pacific sperm whales. Rep. Int. Whaling Comm. 33:287–294.
1984 Simulation studies on length-specific population assessment techniques for western North Pacific sperm whales. Rep. Int. Whaling Comm. 34:259–264.

Shirakihara, K., S. Tanaka, and T. Nakano
1985 Further simulation studies on length-specific population assessment techniques for western North Pacific sperm whales. Rep. Int. Whaling Comm. 35:199–203.

Smith, S.J.
1980 Comparison of two methods of estimating the variance of the estimate of catch per unit effort. Can. Fish. Aquat. Sci. 37:2346–2351.

Sullivan, P.J.
1989 Kalman filter approach to catch at length analysis. Ph.D. diss., Univ. Wash., Seattle, 160 p.

Sullivan, P.J., H.L. Lai, and V.F. Gallucci
1990 A catch-at-length analysis that incorporates a stochastic model of growth. Can. J. Fish. Aquat. Sci. 47:184–198.

Ulltang, O.
1977 Sources of errors in and limitations of virtual population analysis (cohort analysis). J. Cons. Cons. Int. Explor. Mer 37:249–260.

Welch, B.L.
1938 The significance of the difference between two means when the population variances are unequal. Biometrika 25:350–362.

Appendix: Simulation steps of Monte Carlo tests

Control variables are F_1, F_2, z_1, p_t, μ_1, μ_2, σ_1, σ_2, μ_k, cv[k], μ_A, cv[A], cv[q], cv[C]

Compute the following once each trial for $1 \leqslant t \leqslant\leqslant T$:

1 If the F_t are variable, $F_t \sim U(F_1, F_2)$

2 If the z_t are variable, $z_t \sim U(z_1, z_2)$

3 If a single catch occurs once each period, then

- A probability of unobserved events (z) during y_t to c_t is $Pr[z']_t = 1 - e^{-z_t(c_t - y_t)}$,
- B probability of being caught (on date c_t) is $Pr[C]_t = F_t$,
- C probability of unobserved events (z) during c_t to y_{t+1} is $Pr[z']_t = 1 - e^{-z_t(y_{t+1} - c_t)}$, or

4 If catching is continuous, then

- A probability of death during y_t to y_{t+1} is $Pr[D]_t = 1 - e^{-(z_t + F_t)(y_{t+1} - y_t)}$, and
- B $Pr[z]_t = Pr[D]_t \; z_t \div (z_t + F_t)$.

5 If recruitment is seasonal, then

- A $p_t \sim U(1,20)$ where p_t is the proportion recruited during period t,
- B $\delta_t = \sum_{i=1}^{t} p_i \sum_{j=1}^{T-1} p_j$ = the accumulative frequency,
- C $\mu_t \sim U(\mu_1, \mu_2)$, and
- D $\sigma_t \sim U(\sigma_1, \sigma_2)$.

Compute the following once for each fish:

6 Draw growth parameters k and A such that

- A $k \sim N(\mu_k, (\mu_k \; cv[k])^2)$,
- B $A \sim N(\mu_A, (\mu_A \; cv[A])^2)$.

7 Draw a recruitment data, t_1, such that

- A if recruitment is uniform, then $t_1 \sim U(1,20)$, or
- B if recruitment is seasonal,
  - (1) draw t with probability specified by δ,
  - (2) draw $t_1 \sim N(\mu_t, \sigma^2_t)$.

8 If fishing is continuous, then

- A for the time period of recruitment draw u where $u \sim U(0,1)$.
  - (1) If $u \leqslant z_{t1}(1 - e^{-(z_{t1} + F_{t1})(y_{t1+1} - t_1)}) \div (z_{t1} + F_{t1})$, the fish exited of unobserved causes; STOP.
  - (2) If not, but if $u \leqslant 1 - e^{-(z_{t1} + F_{t1})(y_{t1+1} - t_1)}$, the fish was caught; go to step 8C(2)(a).
  - (3) If neither occurred, the fish lived through the time period of recruitment; continue.
- B Add a fish to the abundance matrix.
  - (1) $t = t+1$.
  - (2) $t_1 = y_t$.
  - (3) s_1 = the lower bound of the minimum size-class.
  - (4) Compute the size-class from equation (1).
  - (5) $N_{t,s2} = N_{t,s2} + 1$.
  - (6) If $t = T$, STOP.
- C Draw u where $u \sim U(0,1)$.
  - (1) If $u \leqslant Pr[z]_t$, the fish exited dur to unobserved events; STOP.
  - (2) If not, but if $u \leqslant Pr[D]_t$, the fish was caught.
    - (a) Draw u where $u \sim U(0,1)$.
    - (b) $t_2 = t + u$.
    - (c) Compute the size-class equation (1).
    - (d) Add to the catch matrix: $C_{t,s} = C_{t,s} + 1$; STOP.

(3) If neither occurred, the fish survived; go to step 8B.

9 If fishing occurs just once each period, then

A If $t_1 < c_{t1}$, the fish recruited before the catch.
(1) Draw u where $u \sim U(0,1)$.
(2) If $u \leqslant 1 - e^{-z_{t1}(c_{t1} - t_1)}$, the fish exited unobserved events before date c_t; STOP.
(3) If not, the fish survived to the catch date; go to step 9F.

B If $t_1 = c_{t1}$, the fish recruited on the catch date; go to step 9F.

C If $t_1 > c_{t1}$, the fish recruited after the catch.
(1) Draw u where $u \sim U(0,1)$.
(2) If $u \leqslant 1 - e^{-z_{t1}(y_{t1+1} - t_1)}$, the fish exited due to unobserved events before the next abundance sample (date y_{t+1}); STOP.
(3) If not, the fish survived fishing and so was alive on the next sampling date: $t = t+1$.

D Add a fish to the abundance matrix.
(1) $t_2 = y_t$.
(2) s_1 = lower bound of the minimum size-class.
(3) Compute the size-class from equation (1).
(4) $N_{t,s2} = N_{t,s2} + 1$.
(5) If $t = T$, STOP.

E Draw u where $u \sim U(0,1)$. If $u \leqslant Pr[z']_t$, the fish exited due to unobserved events before the date of catch; STOP.

F Draw u where $u \sim U(0,1)$. If $u \leqslant Pr[C]_t$, the fish was caught on date c_t.
(1) $t_2 = c_t$.
(2) s_1 = lower bound of the minimum size-class.
(3) Compute the size-class when caught from equation (1).
(4) $C_{t,s2} = C_{t,s2} + 1$.
(5) STOP.

G Draw u where $u \sim U(0,1)$.
(1) If $u \leqslant Pr[z']_t$, the fish exited due to unobserved events before the next abundance sampling date; STOP.
(2) If not, the fish survived to the next relative abundance sample date.
(a) $t = t+1$.
(b) Go to step 9D.

Collect samples once each trial:

10 Draw an extimate of the growth parameters such that
$\rho[\hat{A}, \hat{k}] = -0.95$,
$\hat{k} \sim N(\mu_k, \mu_k^2(cv[k]^2 + cv[e_k]^2)$divg, and
$\hat{A} \sim N(\mu_A, \mu_A^2(cv[A]^2 + cv[e_A]^2) \pm g$.

11 Draw an extimate of catch for all t and s where $\hat{C}_{t,s} \sim N(C_{t,s}, C_{t,s}\, cv[C]^2)$.

12 For each t and s draw $q_{t,s,k} \sim N(q_s, (q_s\, cv[q]^2)$ for $1 \leqslant k \leqslant r$.

13 Calculate $Y_{t,s}$ and $s^2[Y_{t,s}]$.

14 Determine the largest sampled size-class.

Biology of two co-occurring tonguefishes, *Cynoglossus arel* and *C. lida* (Pleuronectiformes: Cynoglossidae), from Indian waters

Arjuna Rajaguru

Systematics Laboratory, National Marine Fisheries Service, NOAA
National Museum of Natural History, Washington, DC 20560

Abstract.—Feeding ecology, age and growth, length-weight relationships, and reproductive biology of two species of tonguefishes, *Cynoglossus arel* and *C. lida*, from Porto Novo, southeast coast of India, were studied during October 1981–September 1982. These tonguefishes are benthophagus; adults feed primarily on polychaetes, while juveniles more often consume smaller prey such as hyperiid amphipods and copepods. A negative correlation between spawning activity and gastrosomatic index/hepatosomatic index was noted for *C. arel*. In *C. lida*, a higher percentage of empty stomachs was observed in males than in females.

Age and growth of these tonguefishes were determined by three methods, viz, (1) Petersen method, (2) probability plot, and (3) von Bertalanffy's equation. Rate of growth from the time of hatching through the first year is higher than that of older year-classes. Both species reach commercial size during their 2d and 3d year, and have a life-span of 3–4 years. Value of L_∞ (theoretical maximum attainable length) is 570 mm for male and 615 mm for female *C. arel*, and 335 mm for male and 340 mm for female *C. lida*.

Analyses of the length-weight relationship showed a significant difference in length-weight slopes of male and female *C. arel*. Due to gonad development, mature female *C. lida* deviated significantly from the 'cube law.'

Cynoglossus arel and *C. lida* have prolonged spawning periods of 10 months, with a spawning peak in January and September, respectively. Individuals spawn only once during each season. Both sexes of both species attain first sexual maturity during the 2d year. In male *C. lida*, higher values of the gonadosomatic index (GSI) in September indicate the occurrence of fully-mature specimens during this period. A rise in Kn values (relative condition factor) corresponds with a rise in gonadal activity in female *C. arel*. The correlation coefficient shows that fecundity in *C. arel* is correlated with total length, total weight, ovary length, and ovary weight, whereas in *C. lida* it is correlated only with ovary length and ovary weight.

Manuscript accepted 4 March 1992.
Fishery Bulletin, U.S. 90:328–367 (1992).

Out of 77 species of flatfishes occurring along the east and west coasts of India (Rajaguru 1987), only one species, viz, the Malabar sole *Cynoglossus macrostomus*, constitutes an important fishery along the Malabar coast (west coast of India) (Bal and Rao 1984). The Indian halibut *Psettodes erumei*, because of its larger size and delicious flesh, fetches a high value in fish markets (Pradhan 1969); however, it does not comprise a high value fishery. Other species of flatfishes which contribute to fisheries along the Indian coasts are: *Cynoglossus macrolepidotus*, *C. arel*, *C. dubius*, *C. lida*, *C. puncticeps*, *C. bilineatus*, *C. lingua*, *Paraplagusia* spp., *Solea* spp., and *Pseudorhombus* spp. (Seshappa 1973, Ramanathan 1977, Rajaguru 1987). However, none of these species comprises a single-species fishery. Separate statistics are not reported for these species; all flatfish species are jointly reported as 'soles' (CMFRI 1969, Fischer and Bianchi 1984). Average landings of flatfishes along the Indian coast is about 2% of the total marine fish catches (Ramanathan 1977, Rajaguru 1987). Most of these flatfish species became prominent in the landings only after the introduction of trawlers (Devadoss and Pillai 1973). These species, except the malabar sole *Cynoglossus macrostomus*, are generally not the target species, but are taken incidentally in the penaeid shrimp fishery. Along the Porto Novo Coast, of the 47 flatfish species (Rajaguru 1987), only *Psettodes erumei*, *Pseudorhombus arsius*, *Cynoglossus arel*, and *C. lida* occur throughout the year. The latter two species are taken in a fishery throughout the year, even during the northeast monsoon period, when other marine fish are generally absent.

The biology of these two tonguefishes is poorly known, except for work on age and growth of 138 *C. lida* from the west coast of India (Seshappa 1978). The present study examines various aspects of biology, including feeding ecology, age, growth, length-weight relationships, and reproductive biology of *C. arel* and *C. lida* in Porto Novo coastal waters.

Objectives of the study on the feeding ecology of these two species of tonguefishes are to determine (a) the diet of juveniles and adults, (b) differences in diet between seasons, and (c) relationships between feeding morphology, digestive morphology, and diet. An age and growth study was also undertaken to (a) evaluate differences in growth patterns between males and females, (b) determine age of recruitment to the Porto Novo fishery, and (c) determine longevity of these two tonguefishes. The objective of the studies on length-weight relationships is to determine if there is a significant deviation from the cube law of length-weight relationship related to ontogeny and gonadal development. The final aspect

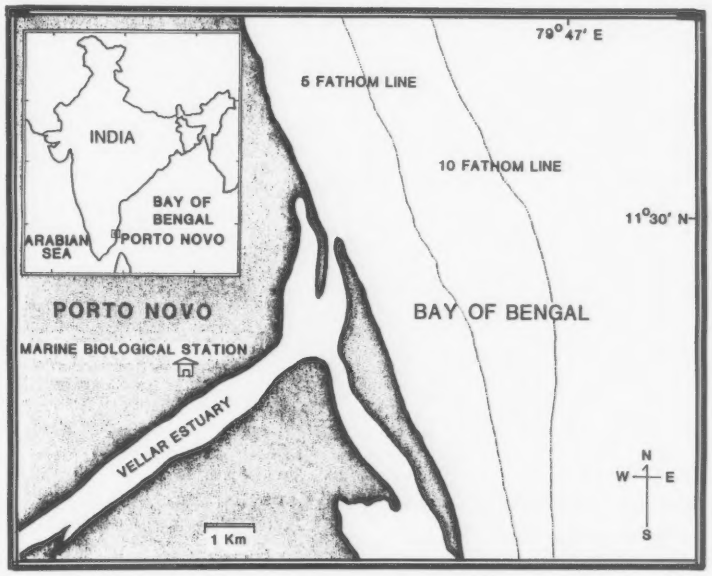

Figure 1
Map showing 5- and 10-fathom lines off Porto Novo coast, India.

of the study is reproductive biology. The objectives are to (1) determine the spawning season, spawning periodicity, age and size at first maturity, and (2) examine relationships between fecundity and total length, total weight, ovary length and ovary weight.

Materials and methods

Samples of large-scaled tonguefish *Cynoglossus arel* (Bloch and Schneider 1801) and shoulder-spot tonguefish *C. lida* (Bleeker 1851) were collected twice weekly (a total of 96 collections) from commercial fish catches landed in Porto Novo, southeast coast of India (11°29′N, 79°46′E; Fig. 1), from October 1981 to September 1982. Fishing operations were confined to the upper continental shelf, to a depth of 18–22 m, up to 4 km from the coast.

A total of 1220 specimens of *C. arel* (627 males, 569 females, 24 juveniles) and 1382 specimens of *C. lida* (718 males, 640 females, 24 juveniles) were collected for stomach analyses. For the age and growth study, a total of 1203 specimens of *C. arel* (634 males and 569 females), and 1374 specimens of *C. lida* (724 males and 650 females) were utilized; since juveniles were available only for 4 months, they were not included in the age and growth study. Length-weight equations were computed using data of 1281 specimens of *C. arel* (655 males, 599 females, and 27 juveniles) and 1519 specimens of *C. lida* (768 males, 723 females, and 28 juveniles). A total of 1196 specimens of *C. arel* (627 males and 569 females) and 1358 specimens of *C. lida* (718 males and 640 females) were examined for the reproductive biology studies. Some specimens were used for all four studies. Size range of the specimens was as follows: *C. arel* (males 95–360 mm TL, females 99–435 mm TL, juveniles 83–128 mm TL) and *C. lida* (males 97–248 mm TL, females 98–242 mm TL, juveniles 81–125 mm TL). Total length (TL) of each fish was measured to the nearest 1 mm; total weight (TW) was recorded to the nearest 0.1 g. Sex, maturity stages, TL, and TW were noted in fresh-caught fish. Size of monthly samples utilized for various analyses is given in Appendix.

Feeding ecology

Stomachs were removed and preserved in 5% formalin. Some empty stomachs were shrunken and contained mucus, while others were expanded but completely empty; the latter type is believed to occur in fish which have recently regurgitated (Daan 1973). Regurgitated stomachs, as well as fish with food remains in their mouths, were discarded.

Gastrosomatic index (GI) and hepatosomatic index (HI) were calculated to examine monthly variations in feeding intensity and to correlate these variations with breeding cycles, using the following formulae:

$$\text{Gastrosomatic index} = \frac{\text{Weight of gut (including contents)} \times 100}{\text{Weight of fish}}$$

$$\text{Hepatosomatic index} = \frac{\text{Weight of liver} \times 100}{\text{Weight of fish}}$$

For stomach analysis, the Index of Relative Importance (IRI) (Pinkas et al. 1971) was used. It incorporates percentage by number (N), volume (V), and frequency of occurrence (F) in the formula

$$IRI = (\%N + \%V) \times \%F.$$

The percentage IRI was calculated for the entire data set of juveniles, males, and females, and by length intervals (45 mm interval for *C. arel*, and 21 mm for *C. lida*).

Stomach contents were sorted, identified to the lowest possible taxa, and enumerated. Appendages and remains of the unidentified crustaceans are classified as "crustacean fragments." Volume of each taxonomic group of prey was measured by water displacement. To determine ontogenetic variations in feeding habits, stomach contents of juveniles were analyzed separately from those of adults.

Age and growth

Length measurement data were grouped into size-classes at intervals of 15 mm for *C. arel* and 7 mm for *C. lida*. Percentage frequencies were calculated by month. Sexes were treated separately, to determine whether there were differences in growth patterns between males and females. The Petersen method, probability plot method, and von Bertalanffy's equation were used to determine age and growth. Attempts to detect growth layers in hard parts (scales, otoliths, opercular bones, and supraoccipital crests) were not successful.

Petersen method This method of growth analysis is based on the assumption that the lengths of individuals of the same age in a population are distributed normally. When there are distinct intra-annual spawning periods, the length-frequency distribution may be multimodal, representing successive age-groups. The rate of growth slows with age (Ford 1933), and as a result the modes overlap, making interpretation difficult. In the case of fishes, such as tonguefishes, which have a prolonged spawning period, various broods entering the fishery overlap. In this case, it is necessary to trace a size-group for as many months as possible after it enters the commercial fishery and to find the average monthly growth rate for different size-classes. Approximate values of average size at different ages may then be calculated.

Probability plot method Plots of cumulative percentages of length distribution on probability paper provide estimates of the length ranges of fish in each age-group (Harding 1949, Cassie 1954). Hence fish lengths were used to obtain an approximation of the length-at-age structure. One difficulty in this method is the uncertainty surrounding whether the deviations represent virtual inflexion points of the lines. Another difficulty is locating each inflexion point, since any bend in the line is considered an inflexion point. Following this procedure, the line was divided into separate parts and for each (Cassie 1954), partial straight lines were drawn from which, a mean length was calculated for each age-group.

von Bertalanffy's equation The most widely accepted growth model is that of von Bertalanffy (1938),

$$L_t = L_\infty (1 - e^{-k(t-t_0)})$$

where L_t = length at age t,
L_∞ = theoretical maximum attainable (asymptotic) length,
k = a constant, expressing the rate of change in length increments with respect to t,
t_0 = hypothetical age at zero length, and
e = base of Naparian or natural logarithm.

The value of t_0 was calculated as follows:

$$-t_0 = 1/k\,[\log_e (L_\infty) - \log_e (L_\infty - L_t)] - t.$$

Walford's (1946) procedure was used to substitute L_t+1 for L_t. The equation now can be written as

$$L_t + 1 = L_\infty (1 - e^{-k}) + L_t\, e^{-k}.$$

Length-weight relationship

Length-weight curves were obtained by using the equation $W = aL^b$. The least-squares regression of the logarithmic transformation,

$$\log_{10} W = \log_{10} a + b \log_{10} L,$$

where $\log_{10} W = Y$, $\log_{10} a = a$, $\log_{10} L = X$, $b = n$, was used for estimating the values of a and b (Snedecor 1956). This linear equation was fitted separately for males, females, and unsexed juveniles of *C. arel* and *C. lida* from monthly data.

To determine whether increased weight at a given length was caused by increased gonad weight in mature fish, the length-weight relationship was compared between different stages of maturity. Adults of both sexes of *C. arel* and *C. lida* were classified into three stages (Rajaguru 1987):

Immature (Stage I for both sexes): *n* 56 male and 47 female *C. arel*; 105 male and 54 female *C. lida*;
Maturing (Stage II for males, Stages II–III pooled for females): *n* 221 male and 224 female *C. arel*; 259 male and 342 female *C. lida*; and
Mature (Stage III for males, Stages IV–VI pooled for females): *n* 359 male and 292 female *C. arel*; 363

male and 254 female *C. lida*. (Refer to section on Reproductive biology, for Stages I–VI.)

The significance of variation in the estimate of b, from the expected value B (=3) for an ideal fish was tested by the *t*-test in both sexes of *C. arel* and *C. lida* (James 1967):

$$t = \frac{b - B}{Sb}$$

where B = hypothetical b (=3), and Sb = standard error of b.

Analysis of covariance (Snedecor 1956) was used for all comparisons.

Reproductive biology

Tonguefishes have no secondary sexual characters to distinguish the sexes. In females with gonads in advanced stages of maturity, ovaries can be seen easily through the body wall when the fish is held against light. In earlier stages of maturity, sexes are distinguishable only after dissection. Extension of gonads into body cavity, and their color, shape, and size, were noted after dissection. Ovary length was measured to the nearest mm, while weight of testis/ovary was recorded to the nearest mg. Ovaries were fixed in modified Gilson's fluid (Simpson 1951) for ova diameter studies.

To investigate the distribution pattern of ova in different regions of the ovary, ova were taken from anterior, middle, and posterior regions of eyed-side and blind-side lobes of ovaries in different stages of maturity (Clark 1934, Hickling and Rutenberg 1936, de Jong 1940). Ova diameter measurements in each part were noted separately. Results showed a uniform distribution of ovum size in different parts of both ovarion lobes. Hence to study development of ova, random samples of ~500 ova per ovary were measured from ovaries representing Stages I–VI (a total of 108 ovaries, at 18 ovaries/stage in *C. arel*, and a total of 168 ovaries, at 28 ovaries/stage in *C. lida*), using an ocular micrometer at a magnification which gave a value of 12.5 μ (0.0125 mm) to each micrometer division (m.d.). Ova diameter-frequency polygons were drawn after grouping the ova into 3 m.d. (0.04 mm) class-intervals.

Spawning seasons in both species were determined from percentage occurrence of different maturity stages during various months of the year.

Generally, gonad weight depends on size and stage of gonadal development. To account for effects of differential body size on gonad size, gonad weight was expressed as a percentage of body weight (Nikolsky 1963). This ratio,

$$\frac{\text{Weight of gonad} \times 100}{\text{Weight of fish}},$$

is termed gonadosomatic index (GSI). To determine the spawning season, GSIs for various months were calculated.

Relative condition factor (Kn) was calculated for individual fish of both sexes from the formula (Le Cren 1951),

$$Kn = W/\bar{W}$$

where, W = observed weight, and $\bar{W}$ = calculated weight ($\bar{W} = a + bx$). Monthly mean values of Kn were also calculated to confirm the spawning season.

To determine minimum length-at-first-maturity (i.e., Lm or L_{50} = length at which 50% of fish are mature), specimens of *C. arel* and *C. lida* were grouped into 15 mm and 7 mm class-intervals, respectively. Sexes were treated separately. Percentage occurrence of immature and mature fish of various length-groups was determined, and then percentage occurrence of mature fish was plotted for both sexes.

Fecundity was determined by the gravimetric method. For this study, 26 ovaries of *C. arel* (from specimens 200–439 mm TL) and 19 of *C. lida* (161–201 mm TL) were used. Since some ova might already have been shed, ovaries with oozing ova were not used. Ovaries were removed, measured to the nearest mm, and weighed to the nearest mg. From each ovary, three subsamples (each ~50 mg) were taken and weighed after removing excess moisture, and fixed in modified Gilson's fluid. From each of these subsamples, yolked ova were separated and counted. Mean number of ova from three subsamples was multiplied by the ratio of subsample weight: ovary weight to obtain an estimation of the total number of mature ova in the ovary. Numbers of ova per mm body length, per g body weight, per mm ovary length, and per mg ovary weight were also calculated. Fecundity of *C. arel* and *C. lida* was related to total length (TL), total weight (TW), ovary length (OL), and ovary weight (OW) using linear regression. Statistical comparisons (Snedecor 1956) of fecundity to TL, TW, OL, and OW were made.

To determine the differential distribution of sexes during the spawning migration, as well as during aggregation, the sex ratio was calculated for each month. To test the homogeneity in distribution of males and females, the chi-square formula was used.

Classification of maturity stages

Maturity stages were indexed for both sexes of *C. arel* and *C. lida*, following the ICES scale (Lovern and Wood 1937), with the following modifications. Color, shape, and extension of the ovary into the body cavity,

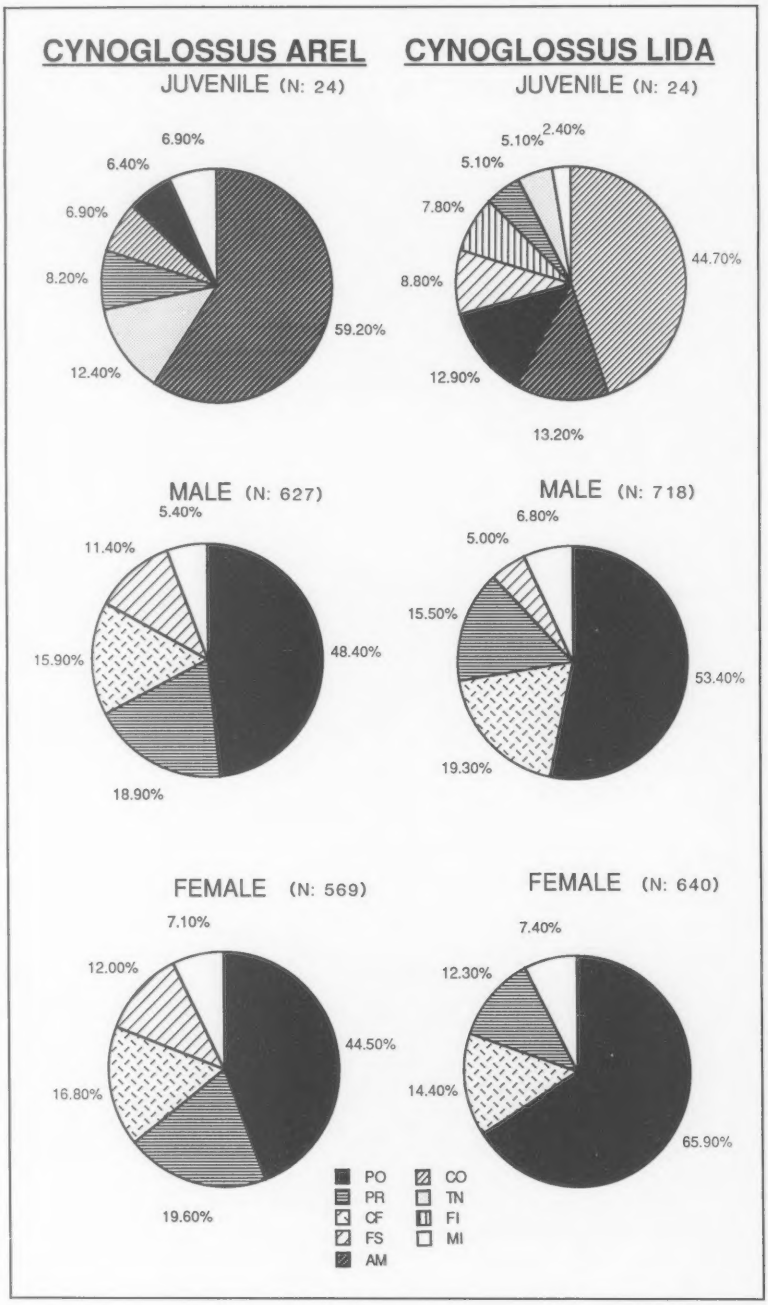

Figure 2
Percentage contribution of food items to the diet of juvenile, male, and female *Cynoglossus arel* and *C. lida* caught commercially off Porto Novo, India, October 1981–September 1982. Only values >5% IRI are individually shown; values <5% IRI are clumped together into a single category, the unshaded wedge of the pie chart. PO = polychaetes, PR = prawns; CF = crustacean fragments, FS = fish scales, AM = amphipods, CO = copepods, TN = tintinnids, FI = fishes, MI = miscellaneous.

as well as color and shape of ova, were considered to define stage of maturity in females. Degree of transparency of the ovary was also used as a criterion, since it is one of its characteristic features during early as well as fully-mature phases. Color and size of testis were used to determine the stage of maturity in males. In both species, testes were divided into four stages, and ovaries into seven stages as follows:

Males:

Stage I (Immature) Testis minute, pale white.

Stage II (Maturing) Testis slightly enlarged, sac-like, creamy white; no milt oozes out on pressure.

Stage III (Mature) Testis enlarged, sac-like, creamy white; whitish milt running from vent on slight pressure.

Stage IV (Spent) Not found during the present study.

Females:

Stage I (Immature) Ovary very small, thread-like and transparent; under microscope, yolkless and transparent ova seen with prominent nuclei in the center; ova invisible to naked eye.

Stage II (Virgin maturing) Ovary slightly thicker, translucent and yellowish; occupying 1/3 to 1/2 of body cavity; ova invisible to naked eye; under a microscope, translucent ova seen with yolk granules around nucleus.

Stage III (Maturing) Ovary yellowish, granular, extending to more than 1/2 the length of body cavity, with vascularization; ova small; under microscope, opaque; nucleus hidden by yolk.

Stage IV (Mature) Ovary creamy yellow, with

Table 1

Percent IRI of various food items of male *Cynoglossus arel* caught commercially off Porto Novo, India, October 1981–September 1982. *N* = number of stomachs analyzed; Crustacean fr. = crustacean fragments; UI = unidentified. (Data presented to one decimal point; 0.0 denotes value of <0.05, and dash denotes absence of food item.)

	Jan.	Feb.	Mar.	Apr.	May	June	July	Aug.	Sep.	Oct.	Nov.	Dec.	Total	
Food items *N*	53	24	54	46	56	35	69	44	56	75	86	29	627	%
Polychaetes	28.0	0.3	62.2	52.4	25.2	60.4	57.9	75.6	70.1	73.2	56.1	19.1	580.5	(48.4)
Prawns	19.1	21.0	12.5	12.5	58.7	25.4	23.9	13.4	22.0	11.2	5.2	1.8	226.7	(18.9)
Crustacean fr.	23.5	15.6	14.0	25.2	10.9	9.6	8.1	3.6	0.6	4.3	4.2	70.9	190.5	(15.9)
Fish scales	26.6	53.1	10.4	2.8	1.4	2.7	2.3	1.8	4.9	3.7	26.7	0.3	136.7	(11.4)
Amphipods	0.4	0.2	0.7	1.0	3.3	0.6	7.5	5.1	0.0	2.4	2.2	3.4	26.9	(2.2)
Fish bone	1.3	–	–	–	–	–	–	–	–	–	5.2	0.6	7.1	(0.6)
Fish spine	–	5.8	–	–	0.0	–	0.0	–	–	–	–	–	5.8	(0.5)
Bivalves	0.1	0.3	0.1	0.1	0.0	0.3	0.1	0.1	0.0	4.2	0.3	–	5.7	(0.5)
Lingula sp.	–	–	–	5.4	0.0	–	–	–	–	–	–	0.0	5.4	(0.5)
Fishes	–	3.1	0.1	–	0.4	–	0.1	–	0.1	–	0.0	0.3	4.1	(0.3)
Crabs	0.9	0.4	0.0	0.4	0.1	0.8	0.1	0.1	0.4	0.2	0.1	–	3.6	(0.3)
Isopods	–	0.1	0.0	–	–	–	–	0.0	1.7	0.4	0.0	0.0	2.3	(0.2)
Algae	–	–	–	–	–	–	–	–	0.0	0.0	0.0	2.2	2.2	(0.2)
Fish eggs	–	–	0.0	–	–	–	–	–	0.0	0.1	–	1.3	1.4	(0.1)
Copepods	0.1	–	0.0	–	0.0	0.0	0.0	0.3	–	0.0	–	–	0.4	(0.0)
Gastropods	–	–	0.0	–	–	–	–	0.0	0.0	0.2	0.0	0.1	0.3	(0.0)
Squilla sp.	–	0.1	–	–	0.0	0.1	–	–	–	–	0.0	–	0.2	(0.0)
Coscinodiscus	–	–	–	–	–	–	–	–	0.2	–	–	–	0.2	(0.0)
Brittle star	–	–	–	0.1	–	–	0.0	–	–	–	–	–	0.1	(0.0)
Medusae	–	–	–	–	–	–	–	–	0.0	0.0	0.0	–	0.0	(0.0)
Egg mass (UI)	–	–	–	–	–	–	–	–	–	–	–	0.0	0.0	(0.0)
Nematode	0.0	–	0.0	–	–	–	0.0	0.0	–	–	–	–	0.0	(0.0)
Sand dollar	–	–	–	–	–	–	–	–	–	–	0.0	–	0.0	(0.0)
Echinoderm (UI)	–	–	–	–	–	–	–	–	0.0	–	–	–	0.0	(0.0)

prominent blood vessels; occupying 2/3 of body cavity; ova visible to naked eye and rich with yolk.

Stage V (Ripe) Ovary resembling Stage IV, but occupying more than 2/3 of the body cavity; under a microscope, ova slightly translucent with yolk granules; ova not running out of genital aperture on application of gentle pressure.

Stage VI (Oozing) Ovary yellowish and transparent, occupying entire length of body cavity; ripe ova running out through genital aperture on application of gentle external pressure on ovary; under a microscope, ova transparent.

Stage VII (Spent) Not found during the study.

Results

Feeding ecology

Food composition In *Cynoglossus arel*, polychaetes made up the bulk (44.5–48.4% IRI) of the diet of adults (Tables 1–2, Fig. 2). At least 11 species of polychaetes, viz, *Nephtys polybranchia, N. oligobranchia, Clymene annandalei, Phyllodoce* sp., *Ancistrosyllis constricta, Nereis chilkaensis, Diopatra* sp., *Onuphis* sp., *Eunice* sp., *Terebellides stroemi*, and *Sternaspis* sp., were consumed. The next most important prey items were prawns (18.9–19.6% IRI), crustacean fragments (15.9–16.8% IRI), and fish scales (11.4–12.0% IRI). The prey species which were consumed in smaller quantities included bivalves (represented by *Amussium* sp., *Placenta* sp., *Arca* sp., and *Pinna* sp.), gastropods (by *Umbonium* sp., *Turritella* sp., and *Dentalium* sp.), and fishes (by gobiids and *Cynoglossus monopus*) (Tables 1–2).

In adult *C. lida*, polychaetes (same species as in *C. arel*) dominated (53.4–65.9% IRI) (Tables 3–4, Fig. 2), while crustacean fragments (14.4–19.3% IRI) and prawns (12.3–15.5% IRI) ranked next in importance. The prey species which were consumed in smaller quantities included bivalves (represented by *Placenta* sp.), gastropods (by *Umbonium* sp. and *Turritella* sp.), and fishes (by gobiids and *Cynoglossus monopus*) (Tables 3–4).

Food of juveniles and adults Differences can be seen in stomach contents between juveniles and adults of both species (Tables 1–5, Fig. 2). Larger tonguefishes ate larger individuals of food species than did

Table 2

Percent IRI of various food items of female *Cynoglossus arel* caught commercially off Porto Novo, India, October 1981–September 1982. See Table 1 for abbreviations.

Food items	*N*	Jan. 39	Feb. 45	Mar. 49	Apr. 55	May 54	June 40	July 56	Aug. 54	Sep. 35	Oct. 54	Nov. 54	Dec. 34	Total 569	%
Polychaetes		4.6	10.7	25.2	74.4	19.6	36.4	60.7	71.9	71.6	72.9	37.4	48.3	533.7	(44.5)
Prawns		30.8	17.9	26.4	9.5	41.0	41.1	19.0	3.3	10.8	14.3	12.7	8.7	235.5	(19.6)
Crustacean fr.		28.0	35.1	25.4	11.8	33.6	17.6	5.1	2.1	4.6	2.4	7.6	28.7	202.0	(16.8)
Fish scales		21.6	23.2	14.3	2.0	0.7	1.5	8.0	20.9	1.1	9.0	40.5	0.7	143.5	(12.0)
Amphipods		0.2	0.7	1.3	1.4	2.1	1.8	5.4	0.9	—	0.3	0.8	3.2	18.1	(1.5)
Fish bone		13.9	—	—	—	—	—	—	—	—	0.2	0.0	—	14.1	(1.2)
Fish spine		—	7.9	2.6	—	—	—	0.0	0.0	—	—	—	—	10.5	(0.9)
Crabs		0.7	0.0	1.6	0.2	2.6	1.4	0.1	0.0	0.7	0.1	0.4	2.6	10.4	(0.9)
Isopods		0.1	—	0.0	—	—	0.0	0.0	0.0	7.3	0.0	—	0.0	7.4	(0.6)
Fish eggs		—	0.0	—	—	—	—	—	—	—	0.0	0.0	6.1	6.1	(0.5)
Bivalves		0.1	1.6	1.0	0.1	0.0	0.0	0.0	0.0	1.7	0.1	0.2	0.5	5.3	(0.4)
Fishes		—	2.3	0.4	—	—	0.1	0.4	0.9	0.7	0.1	0.2	—	5.1	(0.4)
Lingula sp.		—	—	1.8	0.6	—	—	—	0.0	—	—	—	—	2.4	(0.2)
Gastropods		0.0	—	0.0	0.0	0.0	—	—	—	1.2	0.0	0.1	0.7	2.0	(0.2)
Lucifer		—	—	—	—	—	—	1.2	—	0.0	—	—	0.1	1.3	(0.1)
Copepods		—	0.6	—	—	0.4	—	0.0	0.0	—	0.0	—	0.0	1.0	(0.1)
Ciliates (UI)		—	—	—	—	—	—	—	—	—	0.5	—	—	0.5	(0.0)
Algae		—	—	—	—	—	—	—	—	0.0	0.0	0.0	0.4	0.4	(0.0)
Coscinodiscus		—	—	—	—	—	—	—	—	0.3	—	—	—	0.3	(0.0)
Squilla sp.		—	—	—	0.0	0.0	—	0.0	—	—	—	0.1	0.0	0.1	(0.0)
Brittle star		—	—	—	—	—	—	—	0.0	—	0.1	—	—	0.1	(0.0)
Medusae		—	—	—	—	—	—	0.1	—	0.0	—	—	—	0.1	(0.0)
Sand dollar		—	—	—	—	—	0.1	—	—	—	—	—	—	0.1	(0.0)
Nematode		0.0	0.0	0.0	—	0.0	—	—	0.0	—	—	—	0.0	0.0	(0.0)
Egg mass (UI)		—	—	—	0.0	—	—	—	0.0	—	—	0.0	0.0	0.0	(0.0)
Tube-like worm		—	—	—	—	—	—	—	—	0.0	—	—	—	0.0	(0.0)
Jelly fish		—	—	—	—	—	—	0.0	—	—	—	—	—	0.0	(0.0)
Sepia		—	—	—	—	—	0.0	—	—	—	—	—	—	0.0	(0.0)

smaller tonguefishes. In *C. arel*, amphipods (59.2% IRI) dominated diets of juveniles, followed by tintinnids (12.4% IRI). Smaller-sized prawns (8.2% IRI), copepods (6.9% IRI), and polychaetes (6.4% IRI) were next in importance. Fish remains, isopods, smaller crabs, and nematodes were found in decreasing order of importance and never composed more than 5% of the IRI. Breadth of the diet is much smaller in juveniles than adults (compare Tables 1–4 and 5). Only 10 types of food items occurred in stomachs of relatively few juveniles examined, whereas 29 different types of prey were noted in stomachs of adult *C. arel* (Tables 1–2, 5). In adult stomachs, fewer amphipods and more polychaetes were found than in juvenile stomachs. Prawns were the third most important prey in the diet of the juveniles, whereas in adults they were the second most important. Algal filaments were found only in stomachs of adults, while tintinnids were found only in stomachs of juveniles.

Juvenile *C. lida* fed on only 10 types of prey items and usually smaller sizes, whereas adults consumed 24 types of relatively large-sized prey items (Tables 3–5). Copepods (44.7% IRI) were preyed upon predominantly by juveniles of *C. lida* (Fig. 2), while polychaetes were dominant in the diet of adults. Hyperiid amphipods (13.2% IRI), which were of secondary importance and abundant in the diet of juveniles, occurred in smaller quantities in adult stomachs. Crustacean fragments were the second most important food item for adults. Other food items of juveniles are listed in Table 5.

However, the sample sizes for the juveniles of both tonguefishes are quite smaller than those of the adults. Therefore, the differences in number of prey in adults and juveniles may reflect differences in sample sizes.

Food of males and females A total of 76% of males and females of *C. arel*, and 65% of males and 73% of females of *C. lida*, had identifiable prey in their stomachs. In *C. lida*, females consumed 19 types of food items and males consumed 24 types (Tables 3–4). Polychaetes were relatively more abundant (Fig. 2) in the diet of females than males (65.9% vs. 53.4% IRI).

Table 3

Percent IRI of various food items of male *Cynoglossus lida* caught commercially off Porto Novo, India, October 1981–September 1982. See Table 1 for abbreviations.

	Jan.	Feb.	Mar.	Apr.	May	June	July	Aug.	Sep.	Oct.	Nov.	Dec.	Total	
Food items *N*	32	59	64	84	38	56	25	43	46	83	160	28	718	%
Polychaetes	5.4	42.3	31.2	89.4	21.4	67.6	27.8	93.8	87.4	83.0	89.2	2.8	641.3	(53.4)
Crustacean fr.	64.5	12.6	26.4	1.0	16.5	4.9	18.2	0.1	2.5	0.7	1.6	83.1	232.1	(19.3)
Prawns	17.5	9.6	26.6	3.8	57.3	21.5	23.3	3.6	8.0	6.2	5.1	3.8	186.3	(15.5)
Fish scales	6.4	20.4	12.7	0.8	2.7	0.2	3.8	0.2	0.5	6.5	0.6	5.2	60.0	(5.0)
Amphipods	0.6	2.4	0.2	3.2	1.9	5.7	24.7	2.0	—	3.4	3.3	0.2	47.6	(4.0)
Algae	5.2	4.3	—	—	—	—	—	0.0	0.0	—	—	4.4	13.9	(1.2)
Medusae	—	8.3	—	—	—	—	—	—	—	—	0.0	—	8.3	(0.7)
Lucifer	0.0	—	—	—	0.1	—	2.1	—	0.1	—	—	—	2.3	(0.2)
Copepods	0.0	—	2.0	0.0	—	—	—	0.0	0.0	—	—	0.1	2.1	(0.2)
Lingula sp.	—	0.0	0.2	1.6	—	—	—	—	—	—	0.0	—	1.8	(0.2)
Crabs	—	0.1	0.4	0.1	0.1	0.1	—	0.1	0.0	—	0.0	0.1	1.0	(0.1)
Isopods	0.3	0.0	0.3	—	—	—	—	—	0.3	—	—	0.0	0.9	(0.1)
Fishes	—	—	—	0.1	—	—	—	—	0.7	—	—	—	0.8	(0.1)
Fish eggs	0.1	0.1	—	—	—	—	—	—	—	—	—	0.3	0.5	(0.0)
Gastropods	—	0.0	—	—	—	—	—	0.1	0.2	—	0.1	—	0.4	(0.0)
Coscinodiscus	—	—	—	—	—	—	—	—	0.3	—	—	—	0.3	(0.0)
Bivalves	—	0.0	—	—	—	—	—	0.1	0.0	0.2	0.1	—	0.4	(0.0)
Nematode	0.0	0.0	—	—	—	—	—	—	0.0	—	—	0.0	0.0	(0.0)
Brittle star	—	—	—	0.0	—	—	—	—	—	—	—	—	0.0	(0.0)
Squilla sp.	—	0.0	—	—	—	—	—	—	—	—	0.0	—	0.0	(0.0)
Fish spine	—	—	—	0.0	—	—	—	—	—	—	0.0	—	0.0	(0.0)
Octopus sp.	—	0.0	—	—	—	—	—	—	—	—	—	—	0.0	(0.0)
Tape worm	—	—	—	0.0	—	—	—	—	—	—	—	—	0.0	(0.0)
Egg mass (UI)	—	0.0	—	—	—	—	—	—	—	—	—	—	0.0	(0.0)

Table 4

Percent IRI of various food items of female *Cynoglossus lida* caught commercially off Porto Novo, India, October 1981–September 1982. See Table 1 for abbreviations.

	Jan.	Feb.	Mar.	Apr.	May	June	July	Aug.	Sep.	Oct.	Nov.	Dec.	Total	
Food items *N*	42	16	18	51	31	59	25	62	25	76	207	28	640	%
Polychaetes	17.7	58.8	58.1	84.5	60.8	73.4	63.3	95.0	93.4	87.9	94.2	4.0	791.1	(65.9)
Crustacean fr.	48.5	12.5	7.7	2.0	5.2	5.0	10.3	0.6	1.2	0.8	0.3	78.7	172.8	(14.4)
Prawns	26.5	13.6	17.3	7.6	31.3	20.3	16.7	1.8	2.9	4.2	2.5	2.5	147.2	(12.3)
Amphipods	0.3	12.0	8.2	4.1	2.4	0.9	7.9	2.6	—	0.9	2.8	0.0	42.1	(3.5)
Fish scales	4.4	—	1.2	0.0	0.2	0.4	1.4	0.0	—	6.0	0.0	2.6	16.2	(1.4)
Fish eggs	0.4	0.1	0.3	—	—	—	—	—	0.9	—	—	7.5	9.2	(0.8)
Lingula sp.	—	—	6.7	1.8	—	—	—	0.0	—	—	—	—	8.5	(0.7)
Algae	1.3	1.2	—	—	—	—	—	—	—	—	—	4.6	7.1	(0.6)
Crabs	0.1	1.0	—	—	0.1	—	—	0.0	—	—	0.0	0.1	1.3	(0.1)
Isopods	0.0	0.1	0.2	0.0	0.0	0.0	—	—	0.9	0.1	0.0	—	1.3	(0.1)
Bivalves	0.3	—	—	—	—	0.0	0.3	—	0.3	0.1	0.2	—	1.2	(0.1)
Squilla sp.	0.1	0.5	—	—	—	0.0	—	—	—	—	—	—	0.6	(0.1)
Nematode	0.3	0.1	—	—	—	—	—	—	0.0	0.0	0.0	0.0	0.4	(0.0)
Copepods	0.0	—	0.2	—	—	0.0	0.1	—	—	0.0	0.0	—	0.3	(0.0)
Gastropods	0.0	0.1	—	—	—	—	—	—	0.3	—	0.0	—	0.4	(0.0)
Coscinodiscus	—	—	0.1	—	—	—	—	—	0.1	—	—	—	0.2	(0.0)
Medusae	0.1	—	—	—	—	—	—	—	—	—	—	—	0.1	(0.0)
Egg mass (UI)	0.0	—	—	—	—	—	—	—	—	—	—	—	0.0	(0.0)
Fish spine	—	—	—	—	—	—	—	0.0	—	—	—	—	0.0	(0.0)

Table 5

Percent IRI of various food items of juvenile *Cynoglossus arel* and *C. lida* caught commercially off Porto Novo, India, October 1981–September 1982. See Table 1 for abbreviations. (Data presented to one decimal point; dash denotes absence of food item.)

		C. arel						*C. lida*				
		Mar.	June	Oct.	Nov.	Total		Apr.	Nov.	Dec.	Total	
Food items	*N*	6	5	7	6	24	%	8	9	7	24	%
Amphipods		50.0	83.0	60.4	43.5	236.9	(59.2)	3.0	32.8	3.9	39.7	(13.2)
Copepods		7.6	—	0.1	19.9	27.6	(06.9)	75.9	1.7	56.4	134.0	(44.7)
Tintinnids		11.1	—	16.4	21.9	49.4	(12.4)	—	12.0	3.3	15.3	(5.1)
Polychaetes		17.1	8.5	—	—	25.6	(6.4)	13.3	18.7	6.7	38.7	(12.9)
Prawns		—	1.3	20.4	10.9	32.6	(8.2)	2.5	12.7	—	15.2	(5.1)
Fish scales		1.0	1.6	1.2	3.0	6.8	(1.7)	1.7	18.4	6.3	26.4	(8.8)
Fishes		—	—	—	—	—	—	—	—	23.4	23.4	(7.8)
Crustacean fr.		11.1	5.1	—	—	16.2	(4.1)	—	0.8	—	0.8	(0.3)
Isopods		2.2	—	0.8	0.8	3.8	(1.0)	—	—	—	—	—
Ciliates (UI)		—	—	—	—	—	—	3.6	—	—	3.6	(1.2)
Nematode		—	0.3	0.1	0.1	0.5	(0.1)	—	3.0	—	3.0	(1.0)
Crabs		—	—	0.6	—	0.6	(0.2)	—	—	—	—	—

In *C. arel*, males consumed 24 types of food and females had 28 types of prey (Tables 1–2). Polychaetes were slightly more important in diets of males (48.4% IRI) than in females (44.5% IRI) (Tables 1–2, Fig. 2). The difference in numbers of identified prey in males and females is due to rare species occurring in some individuals.

Table 6

Percent frequency of occurrence (%F), percent of total number (%N), percent of total volume (%V), and index of relative importance (IRI) for food items of male and female *Cynoglossus arel* caught off Porto Novo, India, October 1981–September 1982. Size groups: 95–139 mm TL (*n* 10 ♂, *n* 15 ♀), and 140–184 mm TL (*n* 122 ♂, *n* 96 ♀) combined. *n* = number of stomachs analyzed; Crustacean fr. = crustacean fragments; UI = unidentified. (Data presented to one decimal point; 0.0 denotes value of <0.05, and dash denotes absence of food item.)

	Male (*n* 132)					Female (*n* 111)				
Food items	%F	%V	%N	IRI	%IRI	%F	%V	%N	IRI	%IRI
Polychaetes	27.7	62.8	30.7	2590.0	66.3	24.8	52.7	27.8	1996.4	62.7
Crustacean fr.	15.8	12.5	24.4	583.0	15.0	16.1	15.0	31.5	748.7	23.5
Prawns	14.9	15.9	10.4	391.9	10.0	11.2	10.7	7.5	203.8	6.4
Fish scales	10.9	1.7	17.0	203.8	5.2	9.9	0.4	3.8	41.6	1.3
Amphipods	12.4	0.9	8.6	117.8	3.1	11.8	0.7	7.5	96.8	3.0
Bivalves	2.0	1.5	1.4	5.8	0.2	3.8	2.2	2.3	17.1	0.5
Gastropods	2.0	0.1	0.6	1.4	0.0	2.5	0.2	1.5	4.3	0.1
Isopods	1.5	0.5	0.5	1.5	0.0	1.2	0.4	0.4	1.0	0.0
Copepods	1.5	0.0	0.6	0.9	0.0	2.5	0.0	1.3	3.3	0.1
Crabs	1.5	0.6	0.5	1.7	0.0	3.2	2.1	1.5	11.5	0.4
Fish	0.5	2.0	0.2	1.1	0.0	1.2	11.9	1.0	15.5	0.5
Fish bone	0.5	0.0	0.2	0.1	0.0	—	—	—	—	—
Fish spine	1.0	0.0	0.5	0.5	0.0	—	—	—	—	—
Fish egg	1.9	0.1	1.1	2.3	0.1	3.8	0.4	7.7	30.8	1.0
Squilla	—	—	—	—	—	0.6	0.0	0.2	0.1	0.0
Lingula sp.	1.0	0.5	1.1	1.6	0.0	1.2	1.5	2.9	5.3	0.2
Nematode	0.5	0.0	0.2	0.1	0.0	1.2	0.1	0.8	1.1	0.0
Algae	2.4	0.1	1.1	2.9	0.1	3.1	0.1	1.3	4.3	0.1
Brittle star	1.0	0.4	0.5	0.9	0.0	—	—	—	—	—
Echinoderm (UI)	0.5	0.2	0.2	0.2	0.0	—	—	—	—	—
Egg mass (UI)	0.5	0.2	0.2	0.2	0.0	—	—	—	—	—
Lucifer	—	—	—	—	—	1.9	1.6	1.0	4.9	0.2

Table 7

Percent frequency of occurrence (%F), percent of total number (%N), percent of total volume (%V), and index of relative importance (IRI) for food items of male and female *Cynoglossus arel* caught off Porto Novo, India, October 1981–September 1982. Size group: 185–229 mm TL (*n* 338 ♂, *n* 229 ♀). See Table 6 for abbreviations.

	Male (*n* 338)					Female (*n* 229)				
Food items	%F	%V	%N	IRI	%IRI	%F	%V	%N	IRI	%IRI
Polychaetes	28.2	57.5	30.5	2481.6	60.5	22.2	58.8	33.6	2051.3	58.8
Prawns	19.3	25.6	18.1	843.4	20.5	20.7	22.1	16.8	805.2	23.1
Crustacean fr.	14.7	8.6	18.2	394.0	9.6	14.2	7.9	18.0	367.8	10.5
Fish scales	13.6	1.7	18.1	269.3	6.6	12.4	0.6	7.1	95.5	2.8
Amphipods	11.6	0.7	7.3	92.8	2.3	12.4	0.8	9.3	125.2	3.6
Bivalves	3.3	1.4	1.5	9.6	0.2	2.3	3.5	4.0	17.3	0.5
Gastropods	0.4	0.0	0.1	0.0	0.0	1.2	0.3	2.6	3.5	0.1
Isopods	1.5	0.5	0.4	1.4	0.0	1.6	0.5	0.6	1.8	0.1
Copepods	1.3	0.0	0.4	0.5	0.0	1.2	0.0	0.3	0.4	0.0
Crabs	3.1	1.5	1.0	7.8	0.2	3.5	1.8	1.3	10.9	0.3
Fish	0.2	0.6	0.1	0.1	0.0	0.4	1.2	0.1	0.5	0.0
Fish egg	0.7	0.0	0.4	0.3	0.0	1.4	0.1	3.3	4.8	0.1
Squilla	—	—	—	—	—	0.4	0.2	0.1	0.1	0.0
Lingula sp.	0.6	1.6	3.4	3.0	0.1	0.8	0.2	0.5	0.5	0.0
Nematode	0.2	0.0	0.1	0.0	0.0	0.4	0.0	0.1	0.0	0.0
Algae	0.7	0.0	0.2	0.1	0.0	1.0	0.0	0.6	0.5	0.0
Egg mass (UI)	—	—	—	—	—	0.4	0.1	0.1	0.1	0.0
Lucifer	—	—	—	—	—	1.9	0.9	0.7	3.0	0.1
Sepia	—	—	—	—	—	0.2	0.1	0.1	0.0	0.0
Sand dollar	—	—	—	—	—	0.2	0.5	0.1	0.1	0.0
Tube-like worm	0.6	0.3	0.2	0.3	0.0	0.8	0.2	0.3	0.4	0.0
Jelly fish	—	—	—	—	—	0.2	0.1	0.1	0.0	0.0
Coscinodiscus	—	—	—	—	—	0.2	0.0	0.3	0.1	0.0

Food vs. fish size In *C. arel*, the dominant size-group in both sexes is 185–229 mm TL (54% of males, and 40% of females). Females in this size-group had eaten 23 types of prey, while males consumed only 16 types (Table 7). In the remaining size-groups of both sexes, there is no obvious difference in the number of prey types consumed (Tables 6, 8–9). In both sexes of *C. arel*, fish <275 mm TL preyed predominantly on polychaetes (55.1–66.3% IRI in males, 53.4–62.7% IRI in females), whereas in fish >275 mm TL the polychaetes were of lesser importance (10.5% IRI in females, <5.0% IRI in males), with fish remains being the most abundant (54.5% IRI in males, and 48.9% IRI in females) (Tables 6–9, and Fig. 3).

In both sexes of *C. lida*, fewer prey types were consumed by fish >200 mm TL (8–9 prey types) and by fish <136 mm TL (10–13 types), compared with fish 137–199 mm TL (16–19 types). Among fish <200 mm TL, polychaetes were the most abundant prey in both sexes (67.2–89.0% IRI in females, 61.0–81.5% IRI in males) (Tables 10–13, Fig. 4). Among the fish >200 mm TL, polychaetes were the most abundant prey only in females (90.2% IRI), whereas polychaetes were the second-most important prey in males (28.2% IRI) and prawns the most abundant prey (52.6% IRI) (Table 14, Fig. 4).

Seasonal variations in diet composition In male *C. arel*, polychaetes were dominant, except in February, May, and December (Table 1). During these 3 months, other prey items, viz, prawns (in May), crustacean fragments (in December), and fish remains (in February) were more important in the diet. In females, polychaetes also formed the primary food during 6 months (April, July, August, September, October, and December). In other months, prawns (January, March, May, and June), crustacean fragments (February), and fish remains (November) were the primary food consumed (Table 2).

In male *C. arel*, prawns were the secondary prey item for 6 months (February, June, July, August, September, and October), with polychaetes in May and December, crustacean fragments in March and April, and fish remains in January and November. In females, crustacean fragments were the secondary prey item for 5 months (January, March, April, May, and December), prawns for 3 months (July, September, and October), polychaetes for 2 months (June and November), and fish remains for 2 months (February and August). The tertiary food group in the diet of

Table 8

Percent frequency of occurrence (%F), percent of total number (%N), percent of total volume (%V), and index of relative importance (IRI) for food items of male and female *Cynoglossus arel* caught off Porto Novo, India, October 1981–September 1982. Size group: 230–274 mm TL (*n* 136 ♂, *n* 182 ♀). See Table 6 for abbreviations.

	Male (*n* 136)					Female (*n* 182)				
Food items	%F	%V	%N	IRI	%IRI	%F	%V	%N	IRI	%IRI
Polychaetes	23.2	46.8	21.7	1589.2	55.1	23.7	50.1	25.8	1798.8	53.4
Prawns	18.8	20.0	12.4	609.1	21.1	18.0	24.9	17.0	756.0	22.4
Crustacean fr.	14.8	10.0	18.6	423.3	14.7	17.3	11.9	24.5	629.7	18.7
Fish scales	10.3	0.5	3.6	42.2	1.5	10.7	0.5	4.9	57.8	1.7
Amphipods	11.8	1.1	6.3	87.3	3.0	10.5	0.4	3.8	44.1	1.3
Bivalves	3.3	3.0	2.8	19.1	0.7	2.7	1.0	1.0	5.4	0.2
Gastropods	2.6	0.1	0.6	1.8	0.1	1.6	0.0	0.3	0.5	0.0
Isopods	1.8	1.3	1.2	4.5	0.2	1.8	0.8	0.8	2.9	0.1
Copepods	1.5	0.0	0.3	0.5	0.0	–	–	–	–	–
Crabs	3.7	2.2	1.3	13.0	0.4	5.9	5.5	3.8	54.9	1.6
Fish	1.5	3.9	0.3	6.3	0.2	0.9	2.0	0.2	2.0	0.1
Fish bone	2.2	9.6	29.7	86.5	3.0	0.2	0.0	0.1	0.0	0.0
Fish spine	–	–	–	–	–	0.9	0.1	0.5	0.5	0.0
Fish egg	0.7	0.0	0.2	0.1	0.0	0.9	0.1	1.4	1.4	0.0
Squilla	1.1	0.6	0.2	0.9	0.0	0.9	0.5	0.3	0.7	0.0
Lingula sp.	0.4	0.0	0.1	0.0	0.0	0.9	1.3	3.0	3.9	0.1
Nematode	0.4	0.0	0.1	0.0	0.0	0.5	0.0	0.1	0.1	0.0
Algae	1.1	0.0	0.4	0.0	0.0	0.5	0.1	0.2	0.2	0.0
Egg mass (UI)	–	–	–	–	–	0.9	0.1	11.8	10.7	0.4
Lucifer	–	–	–	–	–	0.5	0.1	0.1	0.1	0.0
Sand dollar	0.4	0.8	0.1	0.4	0.0	–	–	–	–	–
Tube-like worm	0.4	0.1	0.1	0.1	0.0	–	–	–	–	–
Coscinodiscus	–	–	–	–	–	0.2	0.0	0.1	0.0	0.0
Brittle star	–	–	–	–	–	0.5	0.6	0.3	0.5	0.0

Table 9

Percent frequency of occurrence (%F), percent of total number (%N), percent of total volume (%V), and index of relative importance (IRI) for food items of male and female *Cynoglossus arel* caught off Porto Novo, India, October 1981–September 1982. Size groups: 275–319 mm TL (*n* 12 ♂, *n* 24 ♀); 320–364 mm TL (*n* 9 ♂, *n* 8 ♀); 365–409 mm TL (*n* 0 ♂, *n* 9 ♀), and 410–454 mm TL (*n* 0 ♂, *n* 6 ♀) combined. See Table 6 for abbreviations.

	Male (*n* 21)					Female (*n* 47)				
Food items	%F	%V	%N	IRI	%IRI	%F	%V	%N	IRI	%IRI
Fish scales	13.9	31.2	66.3	1355.3	54.5	15.3	23.4	60.8	1288.3	48.9
Prawns	20.8	19.2	2.7	455.5	18.3	18.5	16.9	2.9	366.3	13.9
Crustacean fr.	25.0	11.6	4.9	412.5	16.6	16.1	19.6	10.2	479.8	18.2
Polychaetes	11.1	8.4	0.9	103.2	4.2	14.5	16.9	2.2	277.0	10.5
Amphipods	5.6	4.5	0.2	26.3	1.1	4.0	0.1	0.2	1.2	0.0
Bivalves	–	–	–	–	–	3.3	0.5	0.1	2.0	0.1
Gastropods	–	–	–	–	–	1.6	0.0	0.0	0.0	0.0
Isopods	4.2	0.7	0.2	3.8	0.2	0.8	0.1	0.0	0.1	0.0
Copepods	–	–	–	–	–	1.6	0.1	3.0	5.0	0.2
Crabs	5.5	1.5	0.2	9.4	0.0	6.5	2.0	0.3	15.0	0.6
Fish	4.2	10.1	0.2	43.3	1.8	7.3	10.8	0.3	81.0	3.1
Fish bone	1.4	5.0	10.8	22.1	1.0	2.4	0.1	0.1	0.5	0.0
Fish spine	2.7	7.5	12.7	54.5	2.2	4.0	9.5	19.8	117.2	4.5
Fish egg	–	–	–	–	–	0.8	0.0	0.0	0.0	0.0
Squilla	1.4	0.3	0.0	0.4	0.0	–	–	–	–	–
Nematode	1.4	0.0	0.0	0.0	0.0	3.3	0.0	0.1	0.3	0.0
Algae	1.4	0.0	0.0	0.0	0.0	–	–	–	–	–
Coscinodiscus	1.4	0.0	0.9	1.3	0.1	–	–	–	–	–

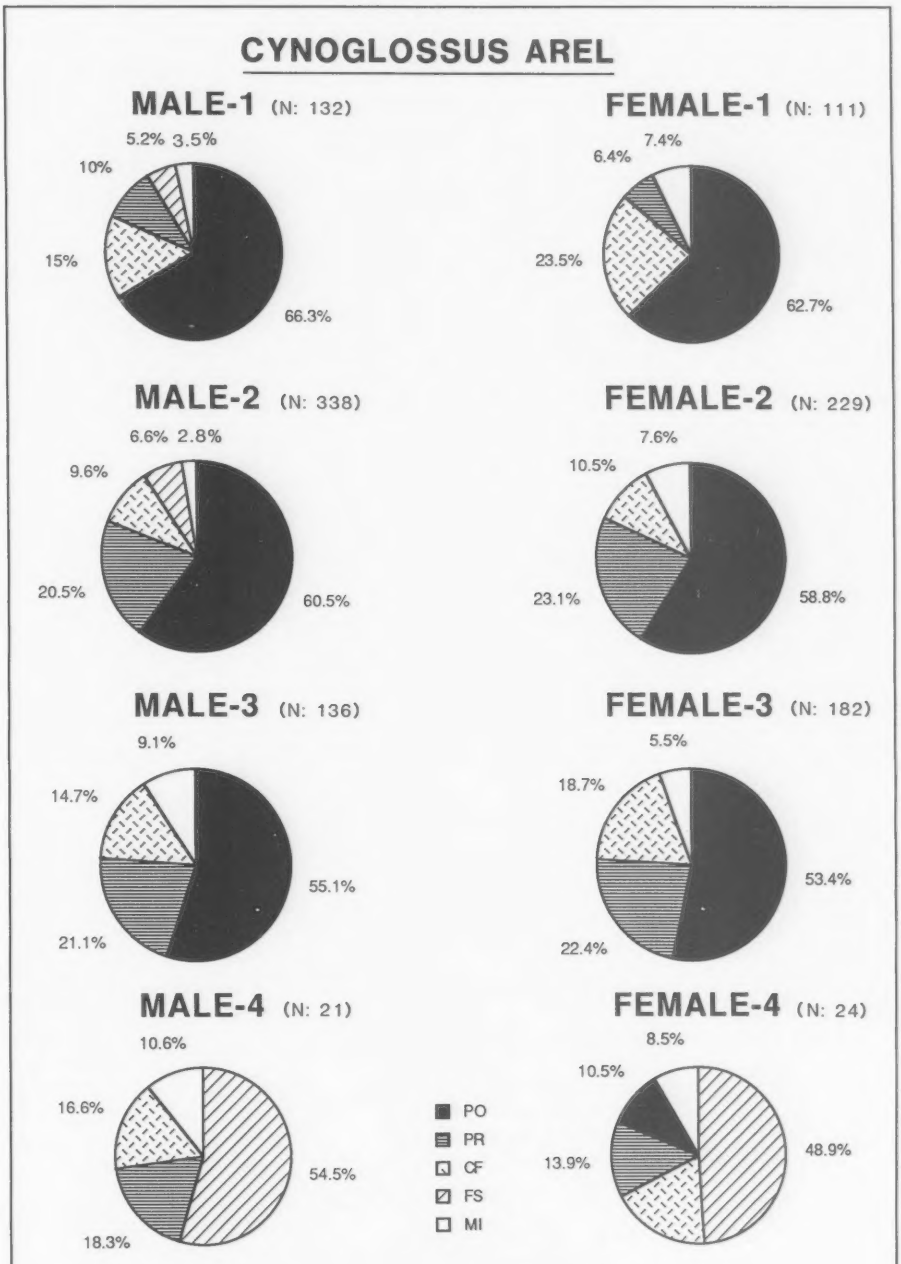

Figure 3

Percentage contribution of food items to the diet of various size groups of male and female *Cynoglossus arel* caught commercially off Porto Novo, India, October 1981–September 1982. Male-1 (*n* 132) and Female-1 (*n* 111) = size group 95–184 mm TL; Male-2 (*n* 338) and Female-2 (*n* 229) = 185–229 mm TL; Male-3 (*n* 136) and Female-3 (*n* 182) = 230–274 mm TL; Male-4 (*n* 21) = 275–364 mm TL; and Female-4 (*n* 47) = 275–454 mm TL. Only values >5% IRI are individually shown; values <5% IRI are clumped together into a single category, the unshaded wedge of the pie chart. PO = polychaetes, PR = prawns, CF = crustacean fragments, FS = fish scales, MI = miscellaneous.

Table 10

Percent frequency of occurrence (%F), percent of total number (%N), percent of total volume (%V), and index of relative importance (IRI) for food items of male and female *Cynoglossus lida* caught off Porto Novo, India, October 1981–September 1982. Size groups: 95–115 mm TL (*n* 6 ♂, *n* 13 ♀), and 116–136 mm TL (*n* 85 ♂, *n* 56 ♀) combined. *n* = number of stomachs analyzed; Crustacean fr. = crustacean fragments. (Data presented to one decimal point; 0.0 denotes value of <0.05, and dash denotes absence of food item.)

	Male (*n* 91)					Female (*n* 69)				
Food items	%F	%V	%N	IRI	%IRI	%F	%V	%N	IRI	%IRI
Polychaetes	29.0	73.4	42.6	3364.0	81.5	30.4	66.2	35.4	3088.6	70.2
Prawns	16.9	10.9	8.5	327.9	8.0	17.4	13.8	9.9	412.4	9.4
Crustacean fr.	8.9	8.4	19.6	249.2	6.1	13.0	16.2	34.5	659.1	15.0
Fish scales	13.0	0.8	9.0	22.1	0.5	10.9	0.4	4.3	51.2	1.2
Amphipods	13.0	0.6	6.7	94.9	2.3	17.4	0.8	8.1	154.9	3.5
Bivalves	—	—	—	—	—	1.1	0.3	0.3	0.7	0.0
Isopods	1.6	0.5	0.5	1.6	0.0	1.1	0.3	0.3	0.7	0.0
Copepods	1.6	0.0	0.5	0.8	0.0	—	—	—	—	—
Crabs	2.4	1.7	1.3	7.2	0.2	—	—	—	—	—
Fish egg	2.4	0.1	1.3	3.4	0.1	1.1	0.0	0.9	1.0	0.0
Lingula sp.	4.0	2.2	5.0	28.8	0.7	3.3	1.9	4.1	19.8	0.5
Algae	5.6	0.2	4.2	24.6	0.6	4.3	0.1	2.2	9.9	0.2
Lucifer	0.8	0.3	0.3	0.5	0.0	—	—	—	—	—
Brittle star	0.8	0.9	0.5	1.1	0.0	—	—	—	—	—

Table 11

Percent frequency of occurrence (%F), percent of total number (%N), percent of total volume (%V), and index of relative importance (IRI) for food items of male and female *Cynoglossus lida* caught off Porto Novo, India, October 1981–September 1982. Size group: 137–157 mm TL (*n* 211 ♂, *n* 136 ♀). See Table 10 for abbreviations.

	Male (*n* 211)					Female (*n* 136)				
Food items	%F	%V	%N	IRI	%IRI	%F	%V	%N	IRI	%IRI
Polychaetes	25.5	61.7	28.4	2297.6	61.0	30.0	62.0	29.9	2757.0	67.2
Crustacean fr.	15.3	16.7	30.7	725.2	19.2	15.5	16.5	31.8	748.7	18.3
Prawns	15.6	13.6	8.3	341.6	9.1	14.5	17.0	10.9	404.6	9.9
Fish scales	16.3	1.4	12.8	231.5	6.1	11.4	0.5	5.2	65.0	1.6
Amphipods	12.3	1.1	10.5	142.7	3.9	13.6	0.6	5.5	83.0	2.0
Bivalves	1.8	0.8	0.7	2.7	0.1	1.8	0.7	0.7	2.5	0.1
Gastropods	0.3	0.0	0.1	0.0	0.0	0.9	0.0	0.2	0.2	0.0
Isopods	0.9	0.4	0.4	0.7	0.0	1.4	0.4	0.4	1.1	0.0
Copepods	0.9	0.0	0.6	0.5	0.0	0.9	0.0	0.3	0.3	0.0
Crabs	1.3	0.7	0.4	1.4	0.0	0.9	0.7	0.5	1.1	0.0
Fish	0.3	1.1	0.1	0.4	0.0	—	—	—	—	—
Fish spine	0.3	0.0	0.2	0.1	0.0	—	—	—	—	—
Fish egg	0.6	0.0	0.2	0.1	0.0	2.3	0.5	9.7	23.5	0.6
Squilla	—	—	—	—	—	0.4	0.2	0.1	0.1	0.0
Lingula sp.	0.9	1.0	2.0	2.7	0.1	1.4	0.7	1.3	2.8	0.1
Nematode	0.3	0.0	0.1	0.0	0.0	1.4	0.0	0.5	0.7	0.0
Algae	5.3	0.2	3.3	18.6	0.5	3.2	0.2	2.9	9.9	0.2
Lucifer	0.9	0.4	0.2	0.5	0.0	—	—	—	—	—
Coelenterate	0.9	0.7	0.9	1.4	0.0	—	—	—	—	—
Coscinodiscus	—	—	—	—	—	0.4	0.0	0.1	0.0	0.0
Tape worm	0.3	0.2	0.1	0.1	0.0	—	—	—	—	—

Table 12

Percent frequency of occurrence (%F), percent of total number (%N), percent of total volume (%V), and index of relative importance (IRI) for food items of male and female *Cynoglossus lida* caught off Porto Novo, India, October 1981–September 1982. Size group: 158–178 mm TL (*n* 284 ♂, *n* 260 ♀). See Table 10 for abbreviations.

	Male (*n* 284)					Female (*n* 260)				
Food items	%F	%V	%N	IRI	%IRI	%F	%V	%N	IRI	%IRI
Polychaetes	29.0	61.2	28.4	2598.4	67.4	32.2	75.9	47.4	3970.3	81.3
Crustacean fr.	11.2	16.2	30.1	518.6	13.5	10.7	8.2	20.4	306.0	6.3
Prawns	16.2	14.9	9.2	390.4	10.1	18.3	12.5	10.4	419.1	8.6
Fish scales	14.9	1.4	12.7	210.1	5.6	8.9	0.4	4.4	42.7	0.8
Amphipods	9.7	0.8	7.1	76.6	2.0	14.7	0.6	8.1	127.9	2.6
Bivalves	0.5	0.4	0.4	0.4	0.0	2.5	0.7	0.9	4.0	0.1
Gastropods	2.6	0.2	1.2	3.6	0.1	1.4	0.1	0.5	0.8	0.0
Isopods	–	–	–	–	–	0.5	0.1	0.1	0.1	0.0
Copepods	0.8	0.0	0.2	0.2	0.0	0.8	0.0	0.3	0.2	0.0
Crabs	1.3	0.6	0.4	1.3	0.0	1.3	0.3	0.3	0.8	0.0
Fish spine	0.3	0.0	0.2	0.1	0.0	–	–	–	–	–
Fish egg	1.3	0.0	0.5	0.7	0.0	1.4	0.1	3.1	4.5	0.1
Squilla	0.5	0.5	0.2	0.4	0.0	1.0	0.4	0.3	0.7	0.0
Lingula sp.	0.5	0.1	0.2	0.2	0.0	0.8	0.4	1.0	1.1	0.0
Nematode	0.8	0.0	0.2	0.2	0.0	1.0	0.0	0.5	0.5	0.0
Algae	7.2	0.3	4.7	36.0	0.9	3.6	0.1	2.0	7.6	0.2
Egg mass (UI)	0.3	0.1	0.1	0.1	0.0	0.3	0.1	0.1	0.1	0.0
Coelenterate	2.1	3.2	3.9	14.9	0.4	0.3	0.1	0.1	0.1	0.0
Coscinodiscus	0.5	0.0	0.2	0.1	0.0	0.3	0.0	0.1	0.0	0.0
Octopus sp.	0.3	0.1	0.1	0.1	0.0	–	–	–	–	–

Table 13

Percent frequency of occurrence (%F), percent of total number (%N), percent of total volume (%V), and index of relative importance (IRI) for food items of male and female *Cynoglossus lida* caught off Porto Novo, India, October 1981–September 1982. Size group: 179–199 mm TL (*n* 111 ♂, *n* 144 ♀). See Table 10 for abbreviations.

	Male (*n* 111)					Female (*n* 144)				
Food items	%F	%V	%N	IRI	%IRI	%F	%V	%N	IRI	%IRI
Polychaetes	31.8	60.0	33.7	2979.7	70.8	35.7	82.4	56.5	4958.7	89.0
Prawns	20.6	16.9	12.6	607.7	14.4	14.9	9.1	8.3	259.3	4.7
Crustacean fr.	11.2	12.8	28.8	465.9	11.1	10.0	5.4	14.9	203.0	3.6
Fish scales	10.6	0.5	6.0	68.9	1.6	10.0	0.3	3.5	38.0	0.7
Amphipods	10.0	0.4	4.7	51.0	1.2	13.1	0.5	6.6	93.0	1.7
Bivalves	1.2	0.4	0.5	1.1	0.2	2.3	0.5	0.6	2.5	0.0
Gastropods	0.6	0.0	0.2	0.1	0.0	1.4	0.2	1.5	2.4	0.0
Isopods	1.2	0.3	0.3	0.7	0.0	3.2	0.5	0.7	3.8	0.1
Copepods	1.2	0.0	0.3	0.4	0.0	0.4	0.0	0.1	0.0	0.0
Crabs	1.2	0.4	0.3	0.8	0.0	1.4	0.3	0.3	0.8	0.0
Fish	0.5	1.8	0.2	1.0	0.0	–	–	–	–	–
Fish spine	–	–	–	–	–	0.4	0.0	0.2	0.1	0.0
Fish egg	1.8	0.0	0.5	0.9	0.0	2.3	0.1	2.8	6.7	0.1
Lingula sp.	–	–	–	–	–	0.4	0.6	1.8	1.0	0.0
Nematode	1.2	0.0	0.3	0.4	0.0	0.9	0.0	0.2	0.2	0.0
Algae	4.7	0.1	2.8	13.6	0.3	2.7	0.1	1.6	4.6	0.1
Lucifer	0.5	0.4	0.3	0.4	0.0	–	–	–	–	–
Coelenterate	1.2	6.0	8.3	17.2	0.4	–	–	–	–	–
Coscinodiscus	0.5	0.0	0.2	0.1	0.0	0.9	0.0	0.4	0.4	0.0

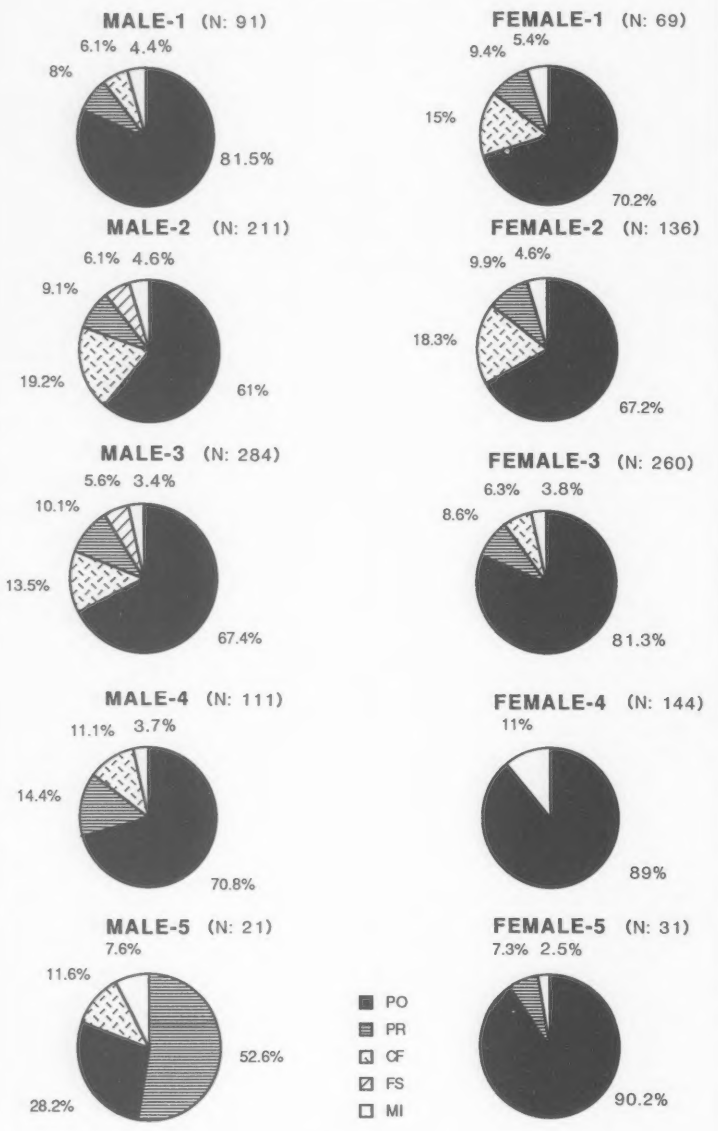

Figure 4

Percentage contribution of food items to the diet of various size groups of male and female *Cynoglossus lida* caught commercially off Porto Novo, India, October 1981–September 1982. Male-1 (n 91) and Female-1 (n 69) = size group 95–136 mm TL; Male-2 (n 211) and Female-2 (n 136) = 137–157 mm TL; Male-3 (n 284) and Female-3 (n 260) = 158–178 mm TL; Male-4 (n 111) and Female-4 (n 144) = 179–199 mm TL; and Male-5 (n 21) and Female-5 (n 31) = 200–262 mm TL. Only values >5% IRI are individually shown; values <5% IRI are clumped together into a single category, the unshaded wedge of the pie chart. PO = polychaetes, PR = prawns, CF = crustacean fragments, FS = fish scales, MI = miscellaneous.

male and female *C. arel* is shown in Figure 5. All other food items occurred sporadically (Tables 1–2).

In male *C. lida*, polychaetes were the dominant prey for 9 months (Table 3). In the remaining months, crustacean fragments (January and December) and prawns (May) dominated. In females, polychaetes were the primary food item for every month, except in January and December when crustacean fragments were the most important prey item (Table 4).

Prawns were next in importance in both sexes of *C. lida*. In males, prawns formed the secondary prey item except in February, May, July, October, and December. During these 5 months, fish remains (February, October, and December), polychaetes (May), and amphipods (July) were the secondary prey. In females, prawns were the secondary food, except in August and October–December. During these 4 months, amphipods (August and November), fish remains (October), and fish eggs (December) were consumed by females. The tertiary food group in the diet of male and female *C. lida* is shown in Figure 5. Organisms of lesser importance are listed in Tables 3–4.

Gastro- (GI) and hepatosomatic (HI) indices and occurrence of empty stomachs in relation to spawning In male *C. arel*, a peak occurrence of empty stomachs (Fig. 6) occurred in January, which is the peak spawning period. Lowest gastro- and hepatosomatic indices were also observed in January (Fig. 6). However, over the rest of the year, these factors did not appear to be related. The gastro- and hepatosomatic indices did not track the percentage occurrence of empty stomachs throughout the year.

Table 14

Percent frequency of occurrence (%F), percent of total number (%N), percent of total volume (%V), and index of relative importance (IRI) for food items of male and female *Cynoglossus lida* caught off Porto Novo, India, October 1981–September 1982. Size groups: 200–220 mm TL (*n* 19 ♂, *n* 27 ♀); 221–241 mm TL (*n* 1 ♂, *n* 3 ♀), and 242–262 mm TL (*n* 1 ♂, *n* 1 ♀) combined. See Table 10 for abbrevations.

	Male (*n* 21)					Female (*n* 31)				
Food items	%F	%V	%N	IRI	%IRI	%F	%V	%N	IRI	%IRI
Polychaetes	25.0	25.7	16.4	1052.5	28.2	39.1	84.8	70.8	6084.0	90.2
Prawns	25.0	42.5	36.1	1965.0	52.6	21.7	10.7	11.9	490.4	7.3
Crustacean fr.	10.0	12.2	31.1	433.0	11.6	10.9	1.8	6.2	87.2	1.3
Fish scales	10.0	0.3	3.4	37.0	1.0	8.7	0.1	2.3	20.9	0.3
Amphipods	15.0	0.6	8.2	132.0	3.4	8.7	0.3	4.2	39.2	0.5
Bivalves	—	—	—	—	—	4.3	2.1	3.4	23.7	0.4
Isopods	5.0	1.3	1.6	14.5	0.4	—	—	—	—	—
Copepods	—	—	—	—	—	2.2	0.0	0.4	0.9	0.0
Crabs	5.0	2.0	1.6	18.0	0.5	—	—	—	—	—
Fish	5.0	15.4	1.6	85.0	2.3	—	—	—	—	—
Lingula sp.	—	—	—	—	—	2.2	0.2	0.4	1.3	0.0
Nematode	—	—	—	—	—	2.2	0.0	0.4	0.9	0.0

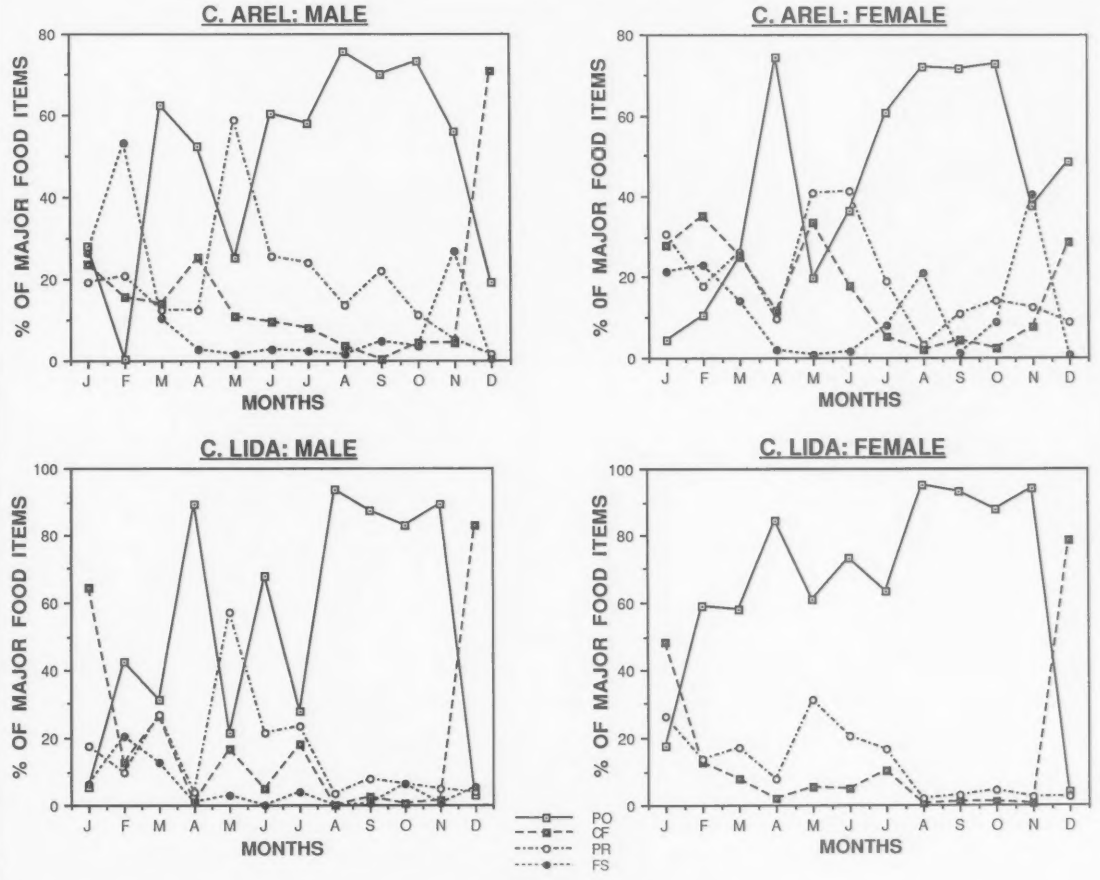

Figure 5

Seasonal variations in percentage contribution of major food items to the diet of male and female *Cynoglossus arel* and *C. lida* caught commercially off Porto Novo, India, October 1981–September 1982. Only values >5% IRI value are graphed. (Refer to Appendix for monthly sample size). PO = polychaetes, CF = crustacean fragments, PR = prawns, FS = fish scales.

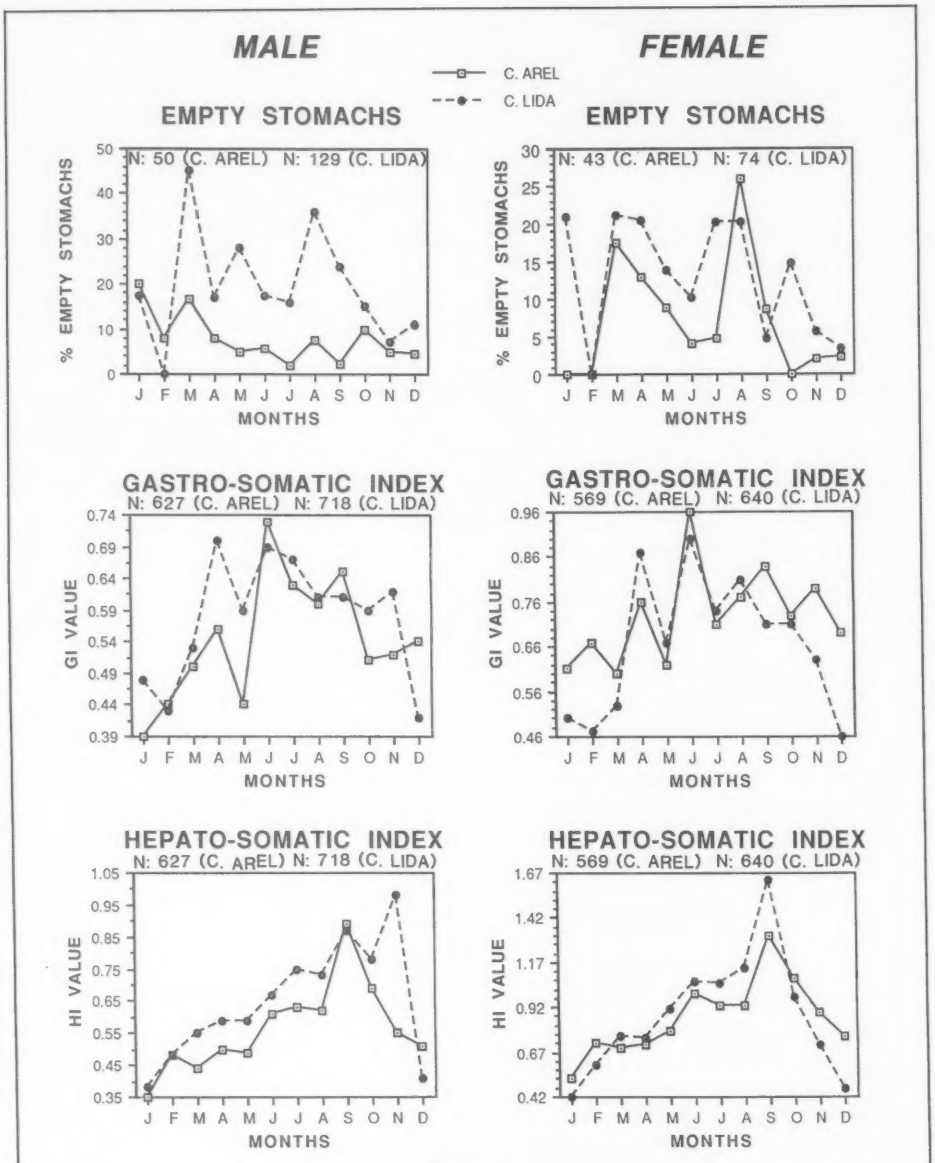
MALE
FEMALE
C. AREL
C. LIDA
EMPTY STOMACHS
N: 50 (C. AREL) N: 129 (C. LIDA)
N: 43 (C. AREL) N: 74 (C. LIDA)
% EMPTY STOMACHS
GASTRO-SOMATIC INDEX
N: 627 (C. AREL) N: 718 (C. LIDA)
N: 569 (C. AREL) N: 640 (C. LIDA)
GI VALUE
HEPATO-SOMATIC INDEX
HI VALUE
J F M A M J J A S O N D
MONTHS

Figure 6

Seasonal variations in the percentage occurrence of empty stomachs, gastrosomatic index (GI), and hepatosomatic index (HI) for male and female *Cynoglossus arel* and *C. lida* caught commercially off Porto Novo, India, October 1981–September 1982. (Refer to Appendix for monthly sample size).

In female *C. arel*, occurrence of empty stomachs did not correspond with spawning. However, the lowest values of gastro- and hepatosomatic indices were recorded (Fig. 6) only during the peak spawning period (in January).

In both sexes of *C. lida*, gastro-/hepatosomatic indices and the occurrence of empty stomachs did not reveal any relationship (Fig. 6) with peak spawning activities (in September) of this species.

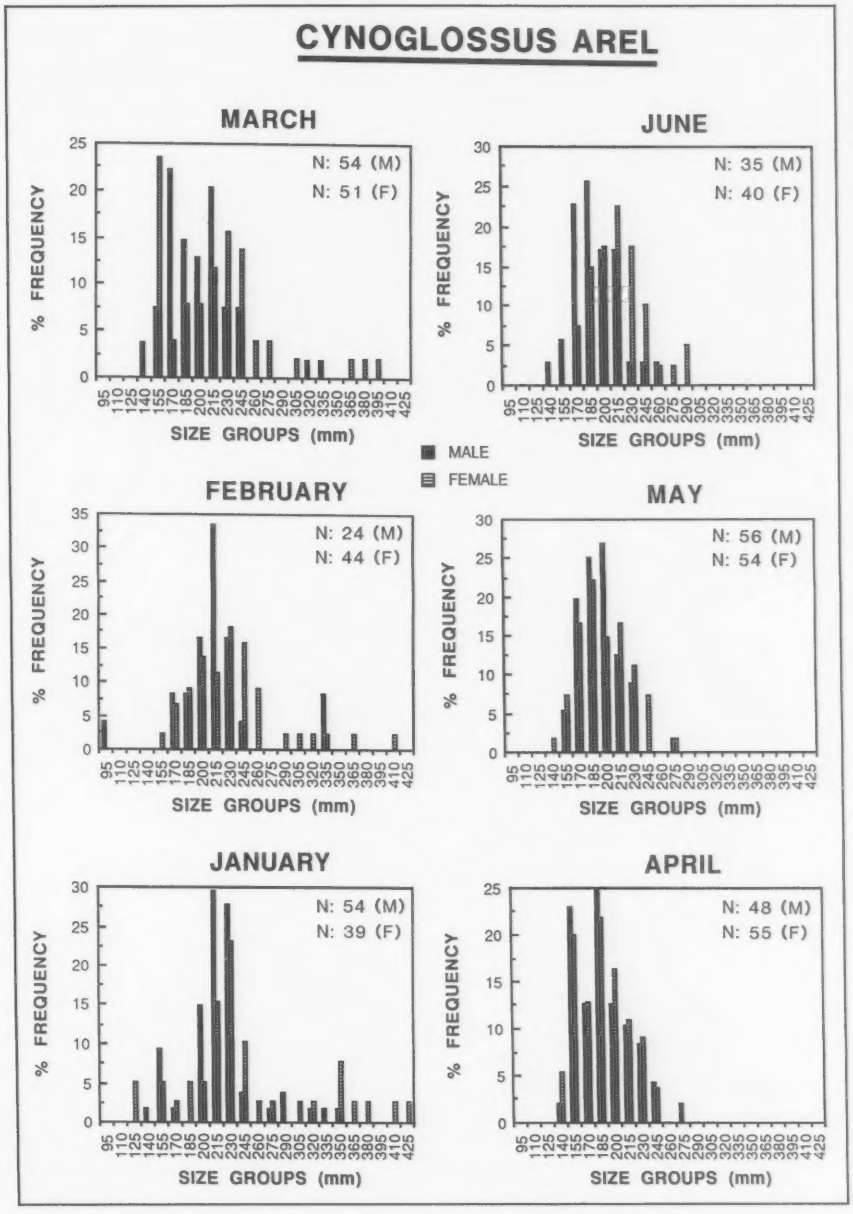

Figure 7A
Size-frequency histograms for male (M) and female (F) *Cynoglossus arel* (January–June) caught commercially off Porto Novo, India, October 1981–September 1982.

Age and growth

Petersen method Progression of modes in the length-frequency data could be traced for both sexes of *C. arel* and *C. lida* (Figs. 7,8).

In male *C. arel* (Fig. 7), the first mode was the 155–169 mm length-group in January. A progressive shift during subsequent months until October, to the 290–304 mm length-group, indicated a growth of 135 mm in 9 months. Assuming the same rate of growth, a fish would attain a length of 180 mm in the first year. Beyond November, it was not possible to trace length-groups.

In female *C. arel* (Fig. 7), the first mode was the 125–139 mm length-group in September. A progressive shift during subsequent months until March, to the 230–240 mm length-group, indicated a growth of 105 mm in 6 months. Groups could not be traced beyond April. At the same rate of growth, a fish would have

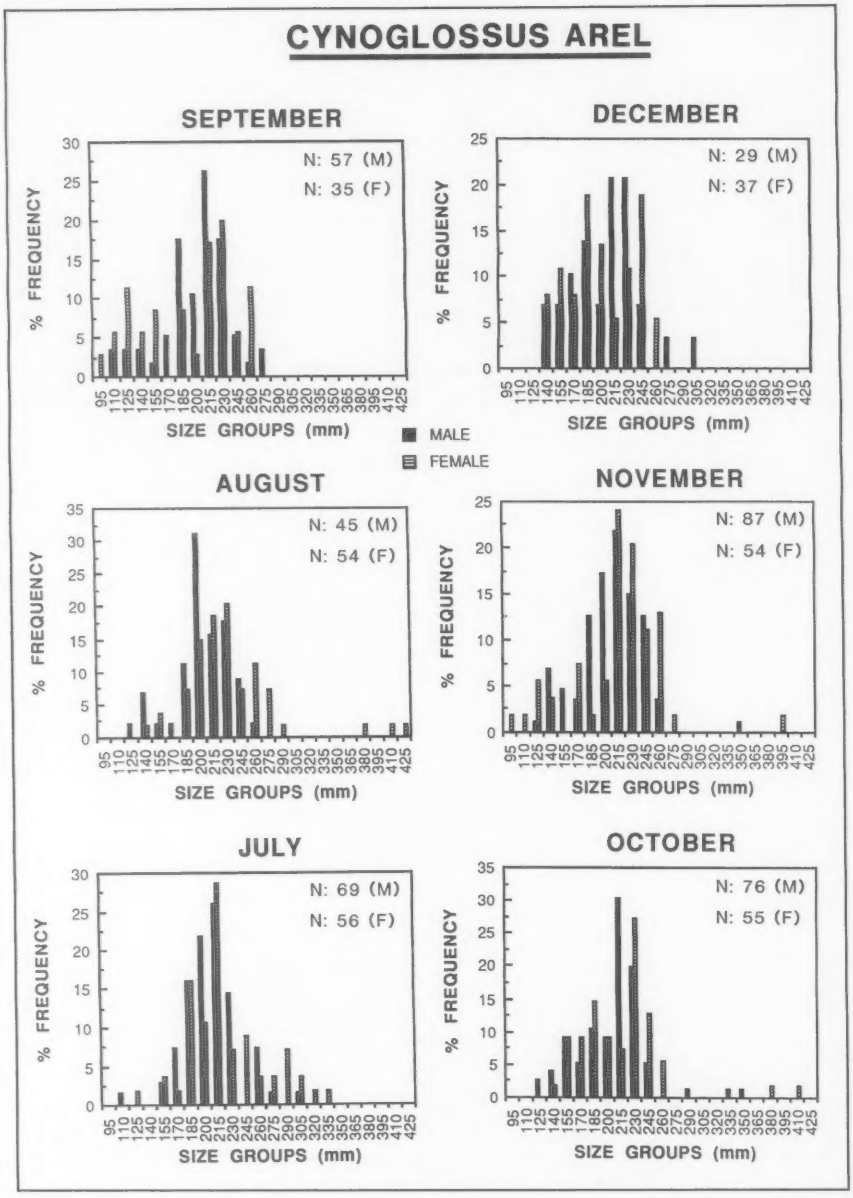

Figure 7B
Size-frequency histograms for male (M) and female (F) *Cynoglossus arel* (July–December) caught commercially off Porto Novo, India, October 1981–September 1982.

attained a length of 210 mm in the first year. There was another mode at the 200–214 mm length-group during February. A progressive shift of this mode during subsequent months until November, to the 260–274 mm length-group, indicated a growth of 60 mm in 9 months. Groups could not be traced beyond December. Based on this rate of growth, a fish would reach 290 mm at the end of the second year. Because of poorer representation in older size-groups, later modes were not traced.

In male *C. lida* (Fig. 8), the first mode was the 102–108 mm size-group in November. This was traced to the 179–185 mm size-group in May, 77 mm of growth in 6 months. Length-groups could not be traced beyond June. At this rate, a fish would be 154 mm at the end of the first year. The mode at the 151–157 mm size-group in March was traced to the 179–185 mm size-group in November, 28 mm growth in 8 months. At this rate of growth, a fish at the end of the second

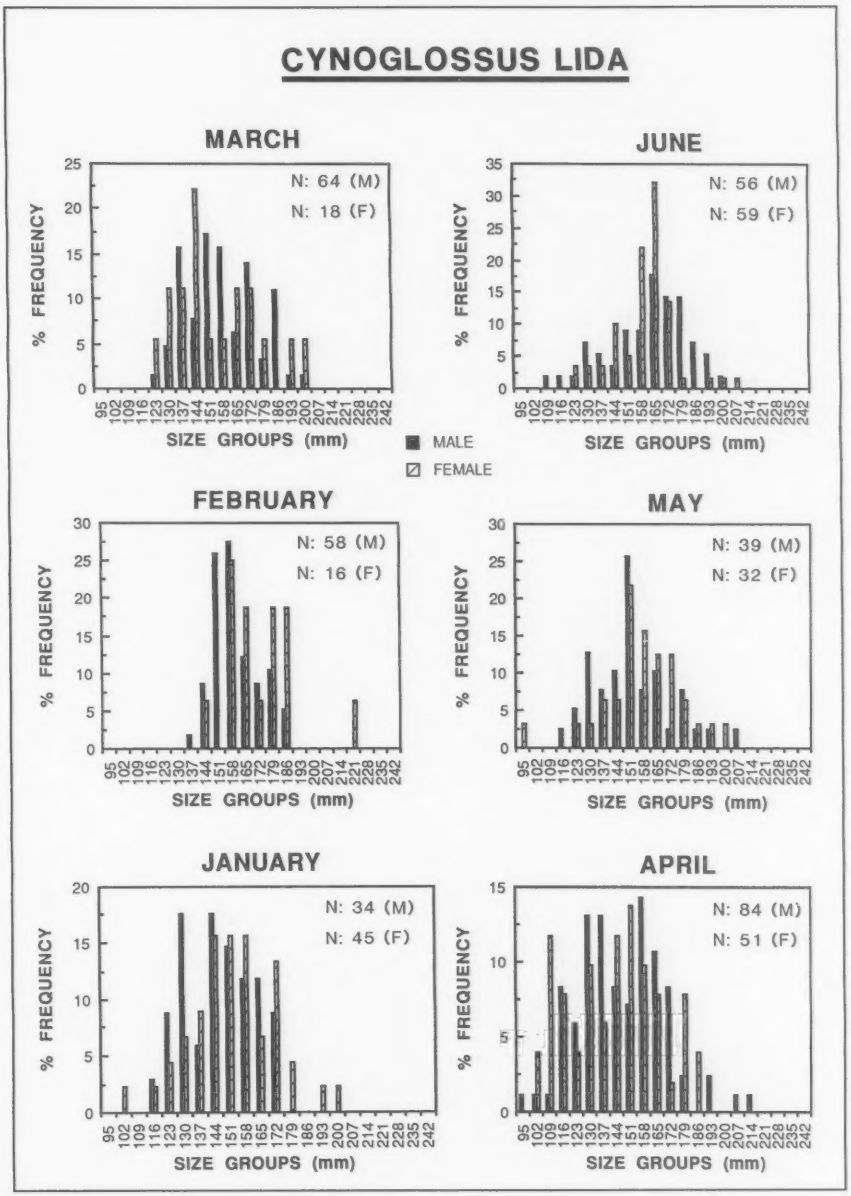

Figure 8A
Size-frequency histograms for male (M) and female (F) *Cynoglossus lida* (January–June) caught commercially off Porto Novo, India, October 1981–September 1982.

year would be 196mm. Further modes could not be traced.

In female *C. lida* (Fig. 8), the first mode was the 102–108mm size-group in November. This was traced to the 193–199mm size-group in June, 91mm growth in 7 months. At this rate, a fish would be 156mm in the first year. The mode at the 151–157mm size-group in January was traced back to the 193–199mm size-group in January, 42mm growth in 12 months. A fish would be 198mm at the end of the second year. The mode at the 193–199mm size-group in May was traced to the 207–213mm size-group in December, 14mm growth in 7 months. At this rate, a fish at the end of the third year would be 222mm.

The rate of growth from the time of hatching and throughout the first year would be more rapid than that of the older year-classes.

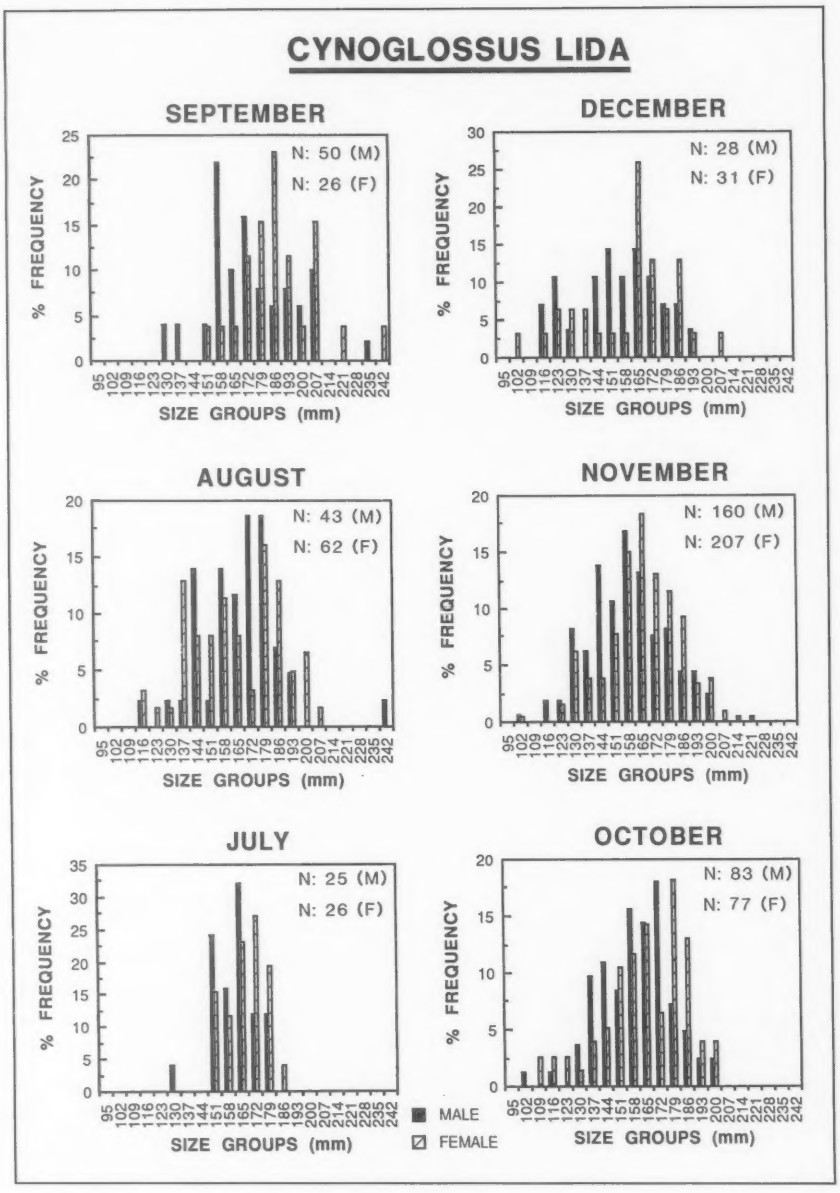

Figure 8B
Size-frequency histograms for male (M) and female (F) *Cynoglossus lida* (July–December) caught commercially off Porto Novo, India, October 1981–September 1982.

Probability plot method Cumulative percentage distribution of lengths was calculated for *C. arel* and *C. lida*, and plotted against the midpoints of length-groups on probability paper (Fig. 9I, J). These points formed approximately straight lines, but slight deviations could be recognized. Based on the probability plots, male *C. arel* attained 194 mm, 272 mm, and 333 mm in the 1st, 2d, and 3d years, respectively, while females reached 201, 312, and 393 mm for these years. In *C. lida*, males attained 151, 188, and 218 mm, while females reached 153, 188, and 216 mm, in the 1st, 2d, and 3d years, respectively.

von Bertalanffy's equation Plots of L_t+1 against L_t, showing a straight-line relationship for *C. arel* and *C. lida*, were drawn. A least-square line was then fitted and an estimate of L_∞ was obtained (Fig. 9A, C, E, G). By this Ford-Walford graph, L_∞ was 570 mm for male

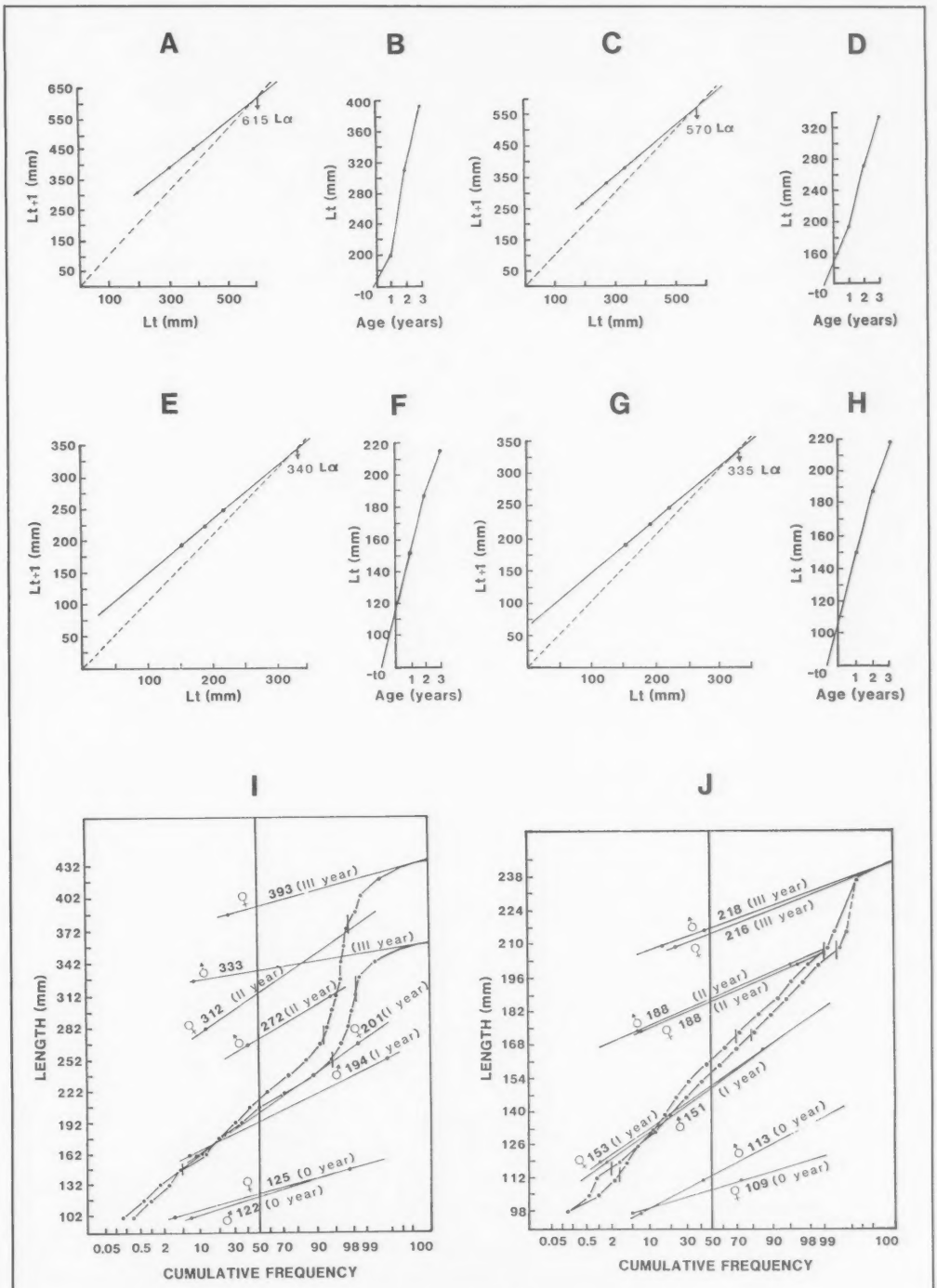

Figure 9

Age and growth of *Cynoglossus arel* and *C. lida* caught commercially off Porto Novo, India, October 1981–September 1982. Ford-Walford plot for female (A) and male (C) *C. arel*, and for female (E) and male (G) *C. lida*; theoretical growth curve for female (B) and male (D) *C. arel*, and female (F) and male (H) *C. lida*; probability plot for male and female *C. arel* (I) and *C. lida (J)*.

and 615 mm for female *C. arel*; 335 mm for male and 340 mm for female *C. lida*.

Based on values obtained, the von Bertalanffy's equations are:

C. arel

Male $L_t = 570(1-e^{-0.2376(t+0.7753)})$

Female $L_t = 615(1-e^{-0.3151(t+0.2645)})$

C. lida

Male $L_t = 335(1-e^{-0.2326(t+1.6348)})$

Female $L_t = 340(1-e^{-0.2231(t+1.8029)})$

Male *C. arel* reached 194, 272, and 333 mm in the 1st, 2d, and 3d years, respectively (Fig. 9D), while females attained a length of 201, 312, and 393 mm for the 1st, 2d, and 3d years, respectively (Fig. 9B). Male *C. lida* reached 151, 188, and 218 mm (Fig. 9H), while females attained lengths of 153, 188, and 216 mm in the 1st, 2d, and 3d years, respectively (Fig. 9F).

Estimates of age and growth, based on the three different methods, are presented in Table 15.

Length-weight relationships

The linear relationships in logarithmic values of length and weight for males, females, and juveniles are shown in Figure 10A. These were typical length-weight relationships in which length increase is rapid initially, but later slows down with a corresponding increase in weight. Correlation coefficient values (r) are highly significant as follows:

Table 15

Mean length (mm) attained in different years of life (per 3 methods) by *Cynoglossus arel* and *C. lida* caught commercially off Porto Novo, India, October 1981–September 1982.

Species		Year	Method: Petersen	Method: Probability plot	Method: von Bertalanffy
Cynoglossus arel	Male	I	180	194	194
		II	–	272	272
		III	–	333	333
	Female	I	210	201	201
		II	290	312	312
		III	–	393	393
Cynoglossus lida	Male	I	154	151	151
		II	196	188	188
		III	–	218	218
	Female	I	156	153	153
		II	198	188	188
		III	222	216	216

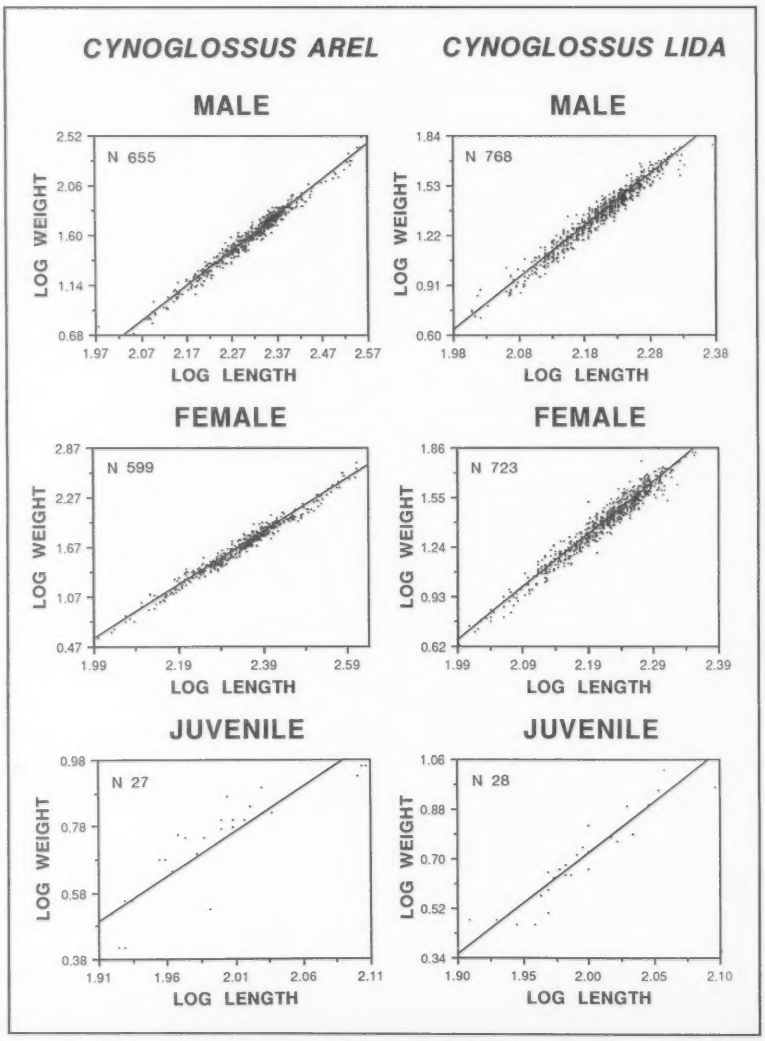

Figure 10A

Length-weight relationships for male, female, and juvenile *Cynoglossus arel* and *C. lida* caught commercially off Porto Novo, India, October 1981–September 1982.

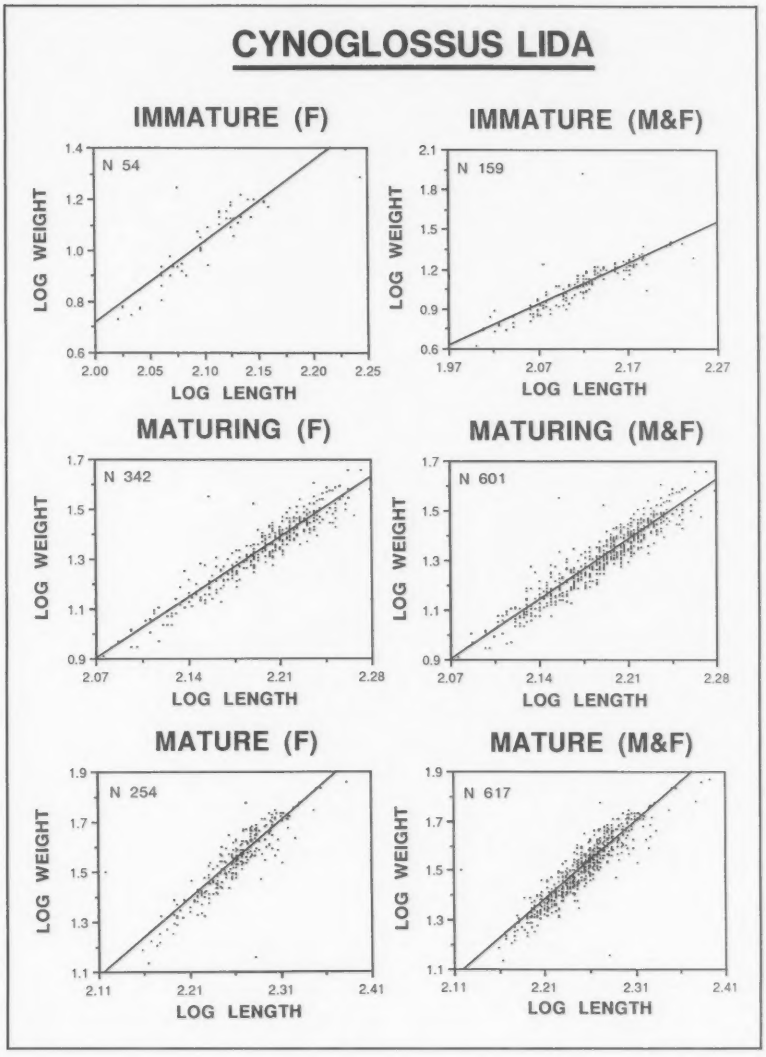

Figure 10B
Length-weight relationships for immature, maturing, and mature females (F), and pooled sexes (M&F) of *Cynoglossus lida* caught commercially off Porto Novo, India, October 1981–September 1982.

differences noted for the remaining 8 months (Table 17). In *C. lida*, no significant differences were observed in regression coefficients of length and weight between males and females.

Analysis of covariance was employed to determine whether growth patterns differed significantly between stages of maturity (immature, maturing, and mature) in males and females. No significant differences were noted for *C. arel* ($P>0.05$). Hence immature, maturing, and mature male and female *C. arel* were combined irrespective of sexes. As there was no significant difference in the regression of Y and X between maturity stages irrespective of sexes, the data for male, female, and juvenile *C. arel* were pooled for the entire year, irrespective of months and maturity stages, and the linear equation was fitted for males, females, and juveniles. Analysis of covariance was again employed for the pooled data to test whether growth patterns differed significantly between sexes of *C. arel*. Significant differences were obtained in the b value between male, female, and juvenile *C. arel*. On comparing males and females, males and juveniles, and females and juveniles, significant values were obtained. Since the growth rates of males, females, and juveniles differed significantly from one another, three separate equations, relating log W to log L, are presented for *C. arel* as follows,

C. arel Male $\log W = -5.9551 + 3.2665 \log L$
Female $\log W = -5.8231 + 3.2100 \log L$
Juvenile $\log W = -4.8615 + 2.7901 \log L$,

and the parabolic equations are

Male $W = 0.0000011\ L^{3.2665}$
Female $W = 0.0000015\ L^{3.2100}$
Juvenile $W = 0.0000138\ L^{2.7901}$.

C. arel Male 0.9870 ($P<0.001$)
Female 0.9905 ($P<0.001$)
Juvenile 0.8747 ($P<0.001$)

C. lida Male 0.9782 ($P<0.001$)
Female 0.9756 ($P<0.001$)
Juvenile 0.9409 ($P<0.001$).

Calculated b, a, r values, and observed F values are presented in Tables 16 and 17.

Linear equations were computed separately for males and females of each month to examine variations in growth patterns. In *C. arel*, significant differences were observed in regression coefficients during January, February, May, and July, with no significant

Table 16

Results of linear regressions of length-weight relations in *Cynoglossus arel* and *C. lida* caught off Porto Novo, India, October 1981–September 1982. r* = all r values were significant at 0.1% level.

	Cynoglossus arel				*Cynoglossus lida*			
Sample	*N*	r*	a	b	*N*	r*	a	b
				By months				
Male								
January	52	0.9920	−5.6785	3.1411	24	0.9900	−6.4285	3.5199
February	34	0.9902	−4.9278	2.8233	48	0.9872	−5.8703	3.2715
March	51	0.9785	−5.7827	3.1860	85	0.9822	−6.4397	3.5300
April	46	0.9834	−5.5809	3.0970	86	0.9878	−5.4470	3.0715
May	57	0.9813	−6.3448	3.4326	62	0.9823	−5.6679	3.1747
June	44	0.9887	−6.3781	3.4432	54	0.9705	−5.6760	3.1793
July	70	0.9868	−5.8109	3.1991	37	0.9677	−6.0573	3.3573
August	54	0.9951	−6.0999	3.3202	45	0.9860	−5.6693	3.1758
September	59	0.9913	−5.9119	3.2575	62	0.9809	−5.2038	2.9803
October	81	0.9907	−6.1854	3.3770	83	0.9678	−5.5118	3.1283
November	70	0.9922	−6.1151	3.3468	135	0.9823	−5.4126	3.0827
December	37	0.9930	−6.0433	3.3060	47	0.9879	−5.7740	3.2354
Total	655	0.9870	−5.9551	3.2665	768	0.9782	−5.7717	3.2315
Female								
January	49	0.9959	−5.9501	3.2687	31	0.9899	−6.1744	3.4089
February	52	0.9913	−5.6840	3.1432	45	0.9935	−5.8431	3.2598
March	47	0.9926	−5.7543	3.1782	38	0.9866	−6.1015	3.3718
April	58	0.9825	−5.3251	2.9920	54	0.9893	−5.6817	3.1849
May	52	0.9812	−5.6617	3.1412	43	0.9703	−5.7400	3.2157
June	41	0.9831	−6.0536	3.3047	54	0.9624	−5.1232	2.9342
July	55	0.9807	−5.0773	2.8787	44	0.9601	−5.9178	3.2983
August	66	0.9969	−6.2004	3.3643	64	0.9886	−5.6065	3.1489
September	39	0.9955	−5.8507	3.2361	37	0.9533	−5.2175	2.9923
October	57	0.9928	−5.9232	3.2654	80	0.9739	−5.7639	3.2454
November	45	0.9870	−5.8994	3.2511	168	0.9680	−5.7278	3.2335
December	38	0.9921	−6.0110	3.2960	65	0.9898	−5.9707	3.3277
Total	599	0.9905	−5.8231	3.2100	723	0.9756	−5.9084	3.2987
Juvenile								
All months	27	0.8747	−4.8615	2.7901	28	0.9409	−6.5983	3.6579
				By maturity stages				
Male								
Immature	56	0.9524	−4.7589	2.7205	105	0.8264	−5.5077	3.1101
Maturing	221	0.8111	−5.4998	3.0714	259	0.9260	−5.8584	3.2713
Mature	359	0.8909	−5.4090	3.0404	363	0.9328	−5.5189	3.1182
Female								
Immature	47	0.9266	−4.5468	2.6221	54	0.8867	−5.0851	2.9124
Maturing	224	0.9463	−4.8001	2.7575	342	0.9392	−6.2651	3.4629
Mature	292	0.9104	−4.9627	2.8516	254	0.8054	−5.5588	3.1443
Male and female								
Immature	103	0.9391	−4.6496	2.6699	159	0.8542	−5.3162	3.0209
Maturing	445	0.8725	−5.0463	2.8687	601	0.9399	−6.2280	3.4439
Mature	651	0.9089	−5.1071	2.9122	617	0.8726	−5.6599	3.1843

In *C. lida*, the tests made to check the relationship between length and weight during various stages of maturity (immature, maturing, and mature) in males and females showed significant differences between the three maturity stages in females alone and in pooled sexes, whereas males showed no significant differences. Hence logarithmic equations for immature, maturing, and mature females, as well as pooled sexes of *C. lida*, are presented as follows,

C. lida

Female alone

Immature logW = −5.0851+2.9124 logL

Maturing logW = −6.2651+3.4629 logL

Mature logW = −5.5588+3.1443 logL

Pooled sexes

Immature logW = −5.3162+3.0209 logL

Maturing logW = −6.2280+3.4439 logL

Mature logW = −5.6599+3.1843 logL.

The linear relationships in logarithmic values of length and weight for immature, maturing, and mature female, as well as pooled sexes of *C. lida*, are shown in Figure 10B.

Although female maturity exhibited a significant effect on the length-weight relationship, all data for male, female, and juvenile *C. lida* were treated separately, irrespective of month and maturity stage. Analysis of covariance was used to find variations in the growth patterns of males, females, and juveniles. Significant differences were observed in regression coefficients of males, females, and juveniles. While comparing males and juveniles, a significant difference was noted; however, no significant differences were observed in comparing males and females, and females and juveniles. Hence two logarithmic equations, one common equation for adults (male and female) and another for juveniles, are presented for *C. lida* as follows,

C. lida

Male & female logW = −5.8643+3.2761 logL

Juveniles logW = −6.5983+3.6579 logL,

and the parabolic equations are

Table 17
Observed F values and their significance in length-weight relationships of *Cynoglossus arel* and *C. lida* caught commercially off Porto Novo, India, October 1981–September 1982. *$P<0.05$.

Samples		*C. arel*	*C. lida*
Comparison between male, female, and juvenile			
January	Male × Female	8.0000*	1.8571
February	Male × Female	12.2941*	0.0000
March	Male × Female	0.0000	1.6923
April	Male × Female	1.1667	1.8182
May	Male × Female	5.5000*	12.0000
June	Male × Female	1.1429	2.1765
July	Male × Female	10.1667*	0.0000
August	Male × Female	1.8333	9.0000
September	Male × Female	8.0000	0.0000
October	Male × Female	2.3125	1.1875
November	Male × Female	1.0625	3.1333
December	Male × Female	0.0000	1.1250
All months			
Male × Female × Juvenile		4.8571*	3.7368*
Male × Female		4.2500*	3.3889
Male × Juvenile		6.8000*	5.5882*
Female × Juvenile		4.6522*	3.1905
Comparison between maturity stages			
Male			
Immature × Maturing × Mature		1.5915	1.2727
Immature × Maturing		2.1798	1.3333
Immature × Mature		3.5556	0.0000
Maturing × Mature		24.6667	2.1176
Female			
Immature × Maturing × Mature		1.0303	4.3913*
Immature × Maturing		1.0625	11.6296*
Immature × Mature		1.2826	1.4038
Maturing × Mature		1.6098	4.6000
Male and female combined			
Immature × Maturing × Mature		1.7971	7.2162*
Immature × Maturing		2.2131	13.6765*
Immature × Mature		3.4789	1.4000
Maturing × Mature		5.0714	8.6452*

Male and female $W = 0.0000014\ L^{3.2761}$
Juvenile $W = 0.0000003\ L^{3.6579}$

The *t*-test was employed, and the calculated b value was found to differ significantly from the hypothetical B value (=3), at 5% level, in male and female *C. arel* and in adult and juvenile *C. lida*, whereas juvenile *C. arel* showed no significant difference:

C. arel Male $t = 12.8125$
Female $t = 11.5385$
Juvenile $t = -0.6788$

C. lida Male & female $t = 14.8441$
Juvenile $t = 2.5470$

Hence it is clear that the cubic formula is not a proper representation of length-weight relationship in male and female *C. arel* and in adult and juvenile *C. lida*.

Reproductive biology

Seasonal occurrence of maturity stages Female *C. arel* with Stage-I ovaries occurred throughout the year, with a peak in September (Fig. 11). Stage-II ovaries were also present during all months, with higher percentages in April and October. Individuals with Stage-III ovaries occurred throughout the year, with higher proportions during March–May and July. Specimens with Stage-IV (mature ovaries) were present throughout the year, with a peak in November. Stage-V (ripe ovaries) were also noted during all months of the year, but maximum abundance was observed in November and December. Specimens with Stage-VI (oozing ovaries) were collected in all months except April and May. High incidence of oozing ovaries was observed in January and February. This indicates that the spawning occurs for up to 10 months (June–March). Occurrence of Stage-VI specimens, with a peak in January, indicates that the maximum number of individuals may spawn during January, which is the post-(northeast) monsoon period in Porto Novo.

In male *C. arel* (Fig. 12), immature (Stage-I), maturing (Stage-II), and mature (Stage-III) individuals occurred throughout the year. High percentages of individuals with Stage-I testes occurred in March and October–December. Maturing specimens (Stage II) were abundant from February to September. Occurrence of mature males (Stage III) showed a peak in January. Occurrence of a higher percentage of fully-mature specimens in January indicated that even though the spawning probably occurred year-round, the majority of individuals might spawn during the post-(northeast) monsoon period (January) in Porto Novo.

Female *C. lida* (Fig. 11) with Stage-I (immature) ovaries occurred for 9 months (absent in February, March, and July), with a peak in April. Stage-II (virgin maturing) individuals were present during all months except February and March, with a peak in December. Stage-III (maturing) ovaries were present throughout the year, with abundance in January, March, June, November, and December. Stage-IV (mature) specimens were present during all months of the year, with higher proportions during February, March, May, and July. Stage-V (ripe) individuals occurred throughout the year, except in December, with maximum abundance in February and September–October. Specimens with Stage-VI (oozing) ovaries were noted for 10 months (absent in January and December), with a peak in September. This indicates that the spawning period lasts for 10 months (February–November), while a

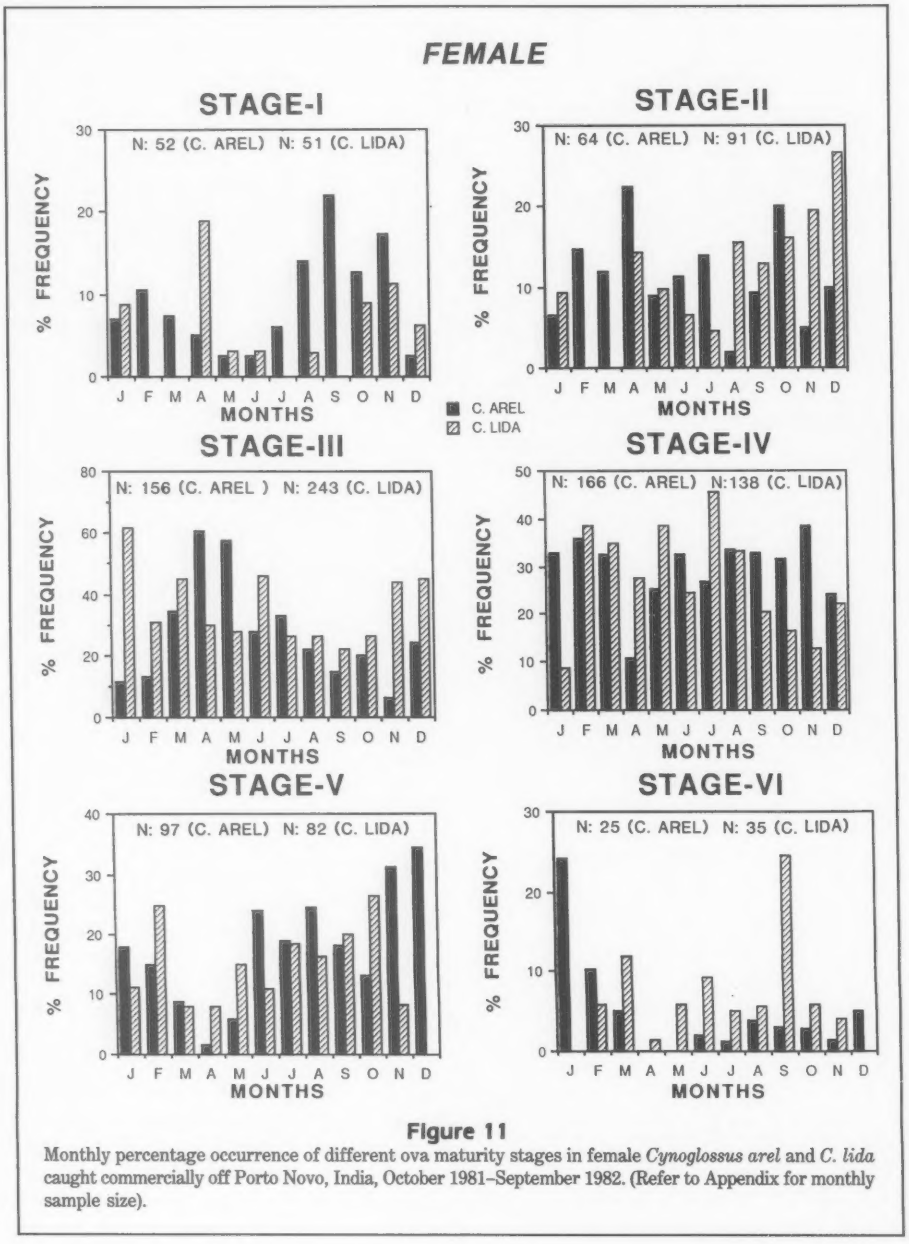
FEMALE
STAGE-I
N: 52 (C. AREL) N: 51 (C. LIDA)
STAGE-II
N: 64 (C. AREL) N: 91 (C. LIDA)
STAGE-III
N: 156 (C. AREL) N: 243 (C. LIDA)
STAGE-IV
N: 166 (C. AREL) N:138 (C. LIDA)
STAGE-V
N: 97 (C. AREL) N: 82 (C. LIDA)
STAGE-VI
N: 25 (C. AREL) N: 35 (C. LIDA)
% FREQUENCY
MONTHS
J F M A M J J A S O N D
C. AREL
C. LIDA

Figure 11

Monthly percentage occurrence of different ova maturity stages in female *Cynoglossus arel* and *C. lida* caught commercially off Porto Novo, India, October 1981–September 1982. (Refer to Appendix for monthly sample size).

maximum number of individuals spawn in September, which is the pre- (northeast) monsoon period in Porto Novo.

In male *C. lida* (Fig. 12), immature (Stage-I) specimens occurred throughout the year, except July and September, with a peak in January. Specimens at Stage II (maturing) were observed throughout the year, with high percentages at all months, except August and September. Stage-III (mature) males were available throughout the year, with a peak in September. This indicates that spawning occurs throughout the year, but a maximum number of males also seemed to spawn during September. Maximum occurrence of mature males in September corresponds with maximum occurrence of oozing females in the same period, and supports this view.

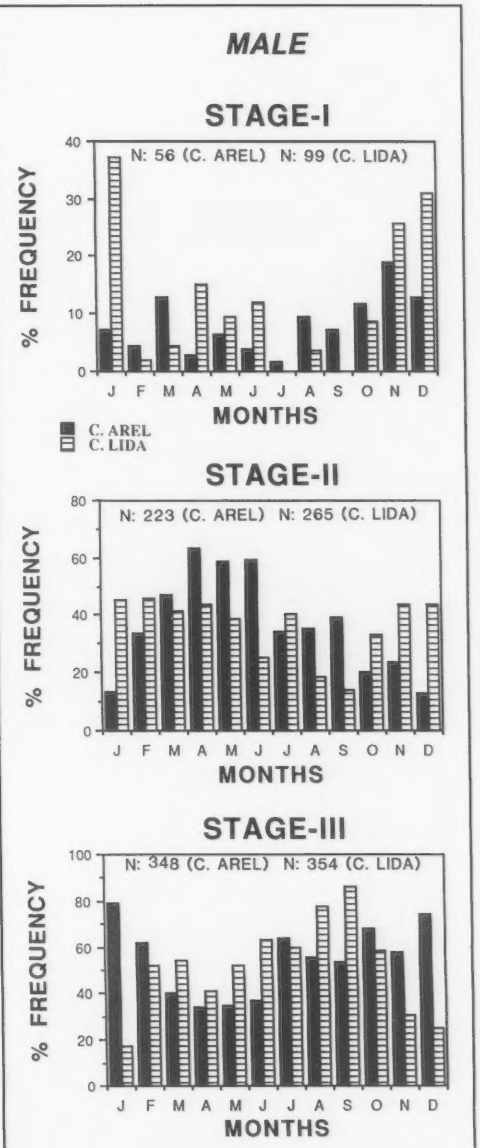

Figure 12
Monthly percentage occurrence of different testis maturity stages in male *Cynoglossus arel* and *C. lida* caught commercially off Porto Novo, India, October 1981–September 1982. (Refer to Appendix for monthly sample size).

Ova diameter Ova diameter frequencies, from ovaries of Stage I–VI, are shown in Figure 13 for *C. arel* and *C. lida*. Since immature, transparent, and microscopic ova (≤0.11 mm) outnumbered the maturing ova during all stages of maturity, only ova >0.11 mm were taken into consideration, from Stage II onwards. Progressive maturation to spawning condition was evident from increasing ova diameters of the most advanced mode at each stage.

For *C. arel* (Fig. 13) in Stage I, maximum number of ova measured 0.01–0.04 mm; however, a few relatively larger ova (0.09–0.11 mm) were also recorded. In Stage II, a mode was discernible with a stock of ova (0.16–0.19 mm) separated from immature stock. In Stage III, the previous mode (at 0.16–0.19 mm) shifted to 0.24–0.26 mm. In Stage IV, a mode made by opaque ova was observed at 0.36–0.38 mm. In Stage V, two modes were found, one with a peak at 0.43–0.45 mm, and another at 0.50–0.53 mm. In Stage VI, the preceding two modes formed jointly a single mode, with fully mature, transparent, and large-sized ova of 0.54–0.56 mm.

For *C. lida* (Fig. 13) in Stage I, immature ova measured 0.01–0.04 mm. In addition, a few relatively larger ova (0.09–0.11 mm) were also seen. In Stage II, a mode was discernible with a stock of ova at 0.09–0.11 mm, which was separated clearly from immature ova. In Stage III, the previous mode was shifted to 0.20–0.23 mm. In Stage IV, a mode of opaque ova was located at 0.31–0.34 mm. In Stage V, a mode of ripe ova was noted at 0.35–0.38 mm. In Stage VI, fully mature, transparent, and large-sized ova formed a mode at 0.39–0.41 mm.

Results indicate that individuals of *C. arel* and *C. lida* spawn only once during each season. Further, mature modes were wide-based (0.49–0.83 mm in *C. arel*, and 0.34–0.64 mm in *C. lida*); therefore, the spawning period of these species must be extended.

Gonadosomatic index In male *C. arel* (Fig. 14), the highest GSI peak was in March, and the lowest GSI value was observed in January. In female *C. arel* (Fig. 14), the highest GSI peak was observed in November, and the lowest value was in January. In both sexes of *C. arel*, the peak values of GSI did not correspond with the observed spawning period in that year.

In male *C. lida* (Fig. 14), the highest GSI peak occurred in September, and the lowest value was in January, November, and December. In female *C. lida* (Fig. 14), the highest GSI peak was observed in May, while the lowest value was in December. Only in male *C. lida* did the high GSI peak coincide with the observed peak spawning period in September.

Relative condition factor (Kn) In male *C. arel* (Fig. 14), the highest Kn value peak was observed in February, and the lowest value was in October. In female *C. arel* (Fig. 14), the highest Kn peak was observed in January, and the lowest value was in November. Only

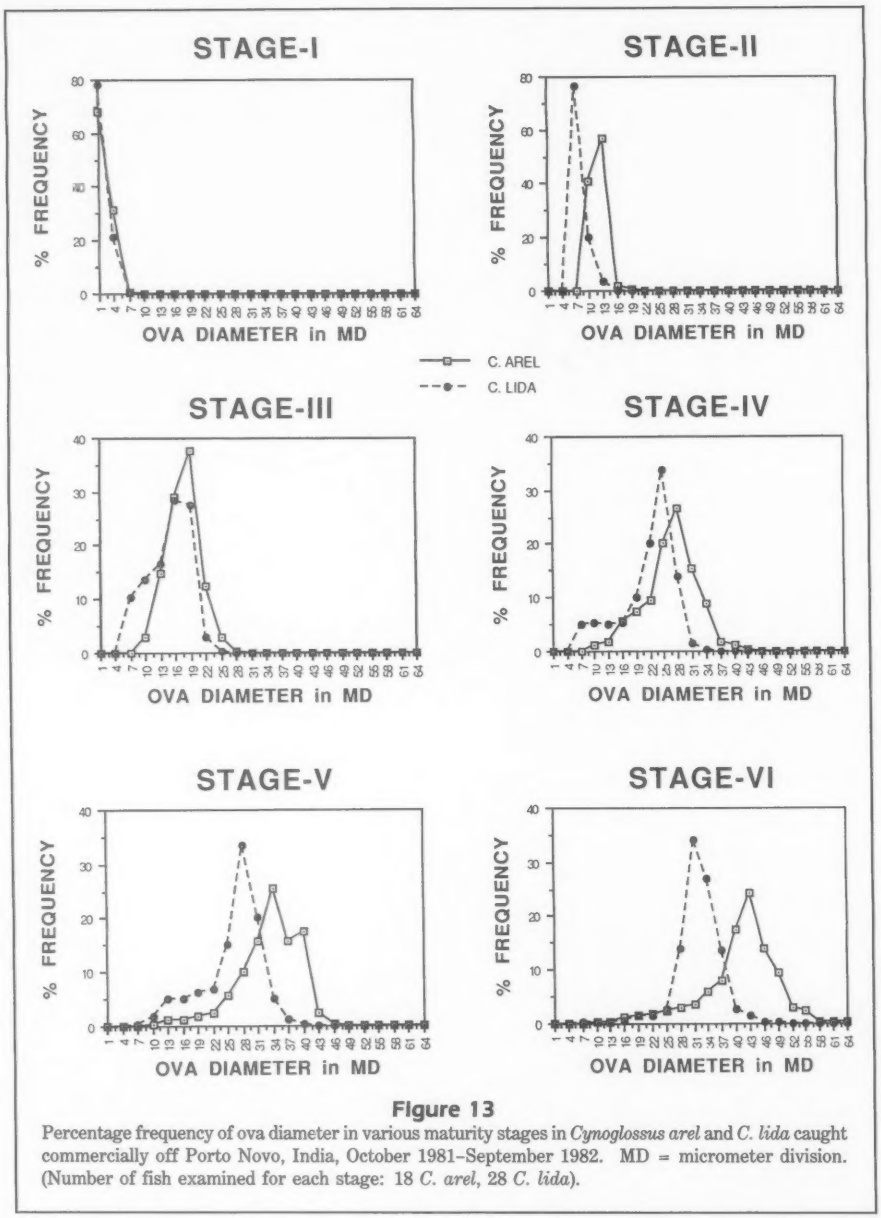

Figure 13

Percentage frequency of ova diameter in various maturity stages in *Cynoglossus arel* and *C. lida* caught commercially off Porto Novo, India, October 1981–September 1982. MD = micrometer division. (Number of fish examined for each stage: 18 *C. arel*, 28 *C. lida*).

in female *C. arel* did a rise in Kn value correspond with a rise in gonadal activity, indicating the spawning period (in January).

In male *C. lida* (Fig. 14), the highest Kn peak was seen in January and the lowest value was in February. In females of *C. lida* (Fig. 14), the highest Kn peaks were seen in January, July, and December, and the lowest value in May. In both sexes of *C. lida*, a rise in Kn value did not indicate the spawning period.

Size-at-first-maturity Both sexes of *C. arel* began to mature after the 140–154 mm size-group (Fig. 15). From the 155–169 mm size-group onwards, percentage occurrence of mature males and females increased steadily. Maturity reached 100% in the 245–259 mm size-group in males, and in the 275–289 mm size-group

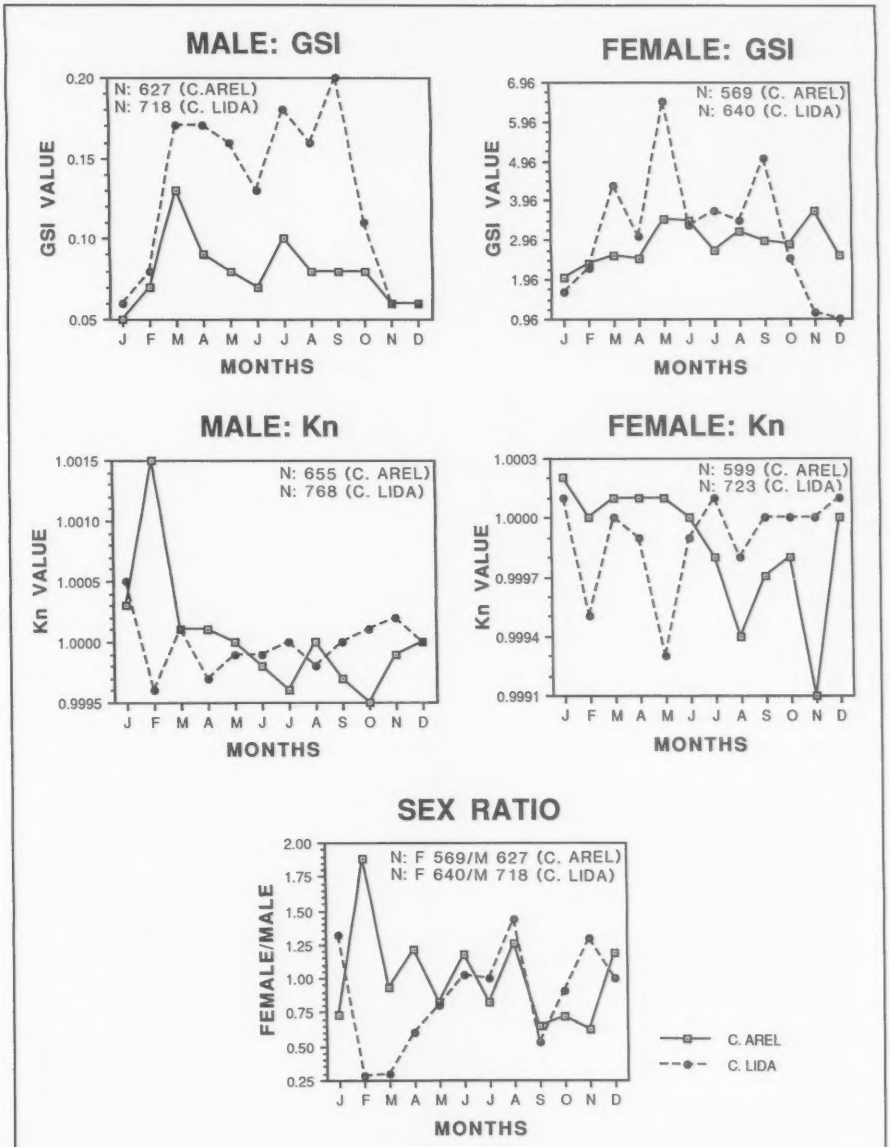

Figure 14

Relative condition factor (Kn), gonadosomatic index (GSI), and sex ratio (female/male) in *Cynoglossus arel* and *C. lida* caught commercially off Porto Novo, India, October 1981–September 1982. (Refer to Appendix for monthly sample size).

in females. The calculated Lm for *C. arel* was 217 mm for males and 225 mm for females.

In *C. lida*, no specimen of either sex was mature until the 137–143 mm size-group, and the percentage occurrence of mature specimens increased gradually from then on (Fig. 15). All male fish were mature at the 186–192 mm size-group, and females at the 193–199 mm size-group. In *C. lida*, Lm ($=L_{50}$) was calculated as 167 mm for males and 179 mm for females. In both species, males mature at a smaller size than females.

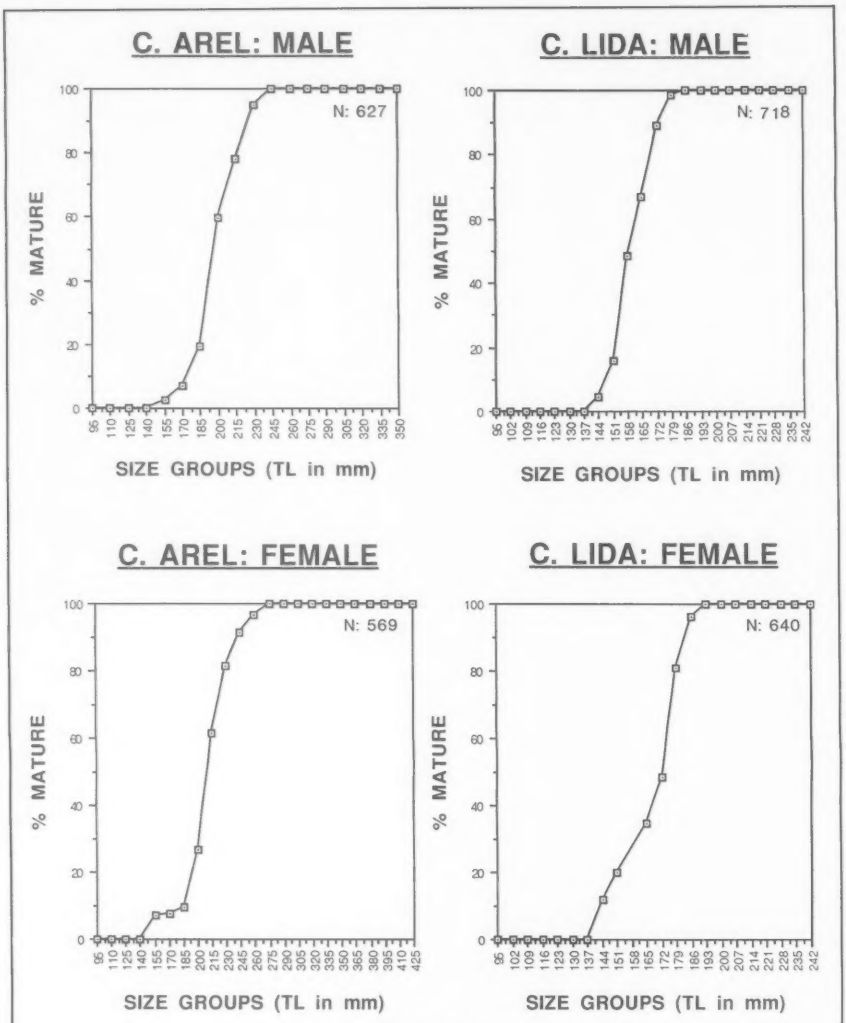

Figure 15
Size-at-first-maturity in male and female *Cynoglossus arel* and *C. lida* caught commercially off Porto Novo, India, October 1981–September 1982.

Age-at-first-maturity In their first year, males of *C. arel* grow to 180 mm according to the Petersen method, and to 194 mm according to the probability plot method and von Bertalanffy's equation (Rajaguru 1987). Female *C. arel* reached 201 mm as per the probability plot method and von Bertalanffy's equation, and 210 mm according to the Petersen method, at the end of their first year of life (Rajaguru 1987). Hence it appears that 50% of male and female *C. arel* attain first maturity at the beginning of their second year of life.

Male *C. lida*, at the end of their first year of life, would grow to 151–154 mm based on all three methods (Rajaguru 1987). Females of *C. lida* reach 153 mm according to von Bertalanffy's equation and the probability plot method, and 156 mm according to the Petersen method, at the end of the first year of their life (Rajaguru 1987). Therefore, 50% of male and female *C. lida* attain first sexual maturity during the second year of their life.

Fecundity Fecundity varied from 14,972 to 127,001 eggs/ovary in *C. arel*, and 11,267 to 81,004 eggs/ovary

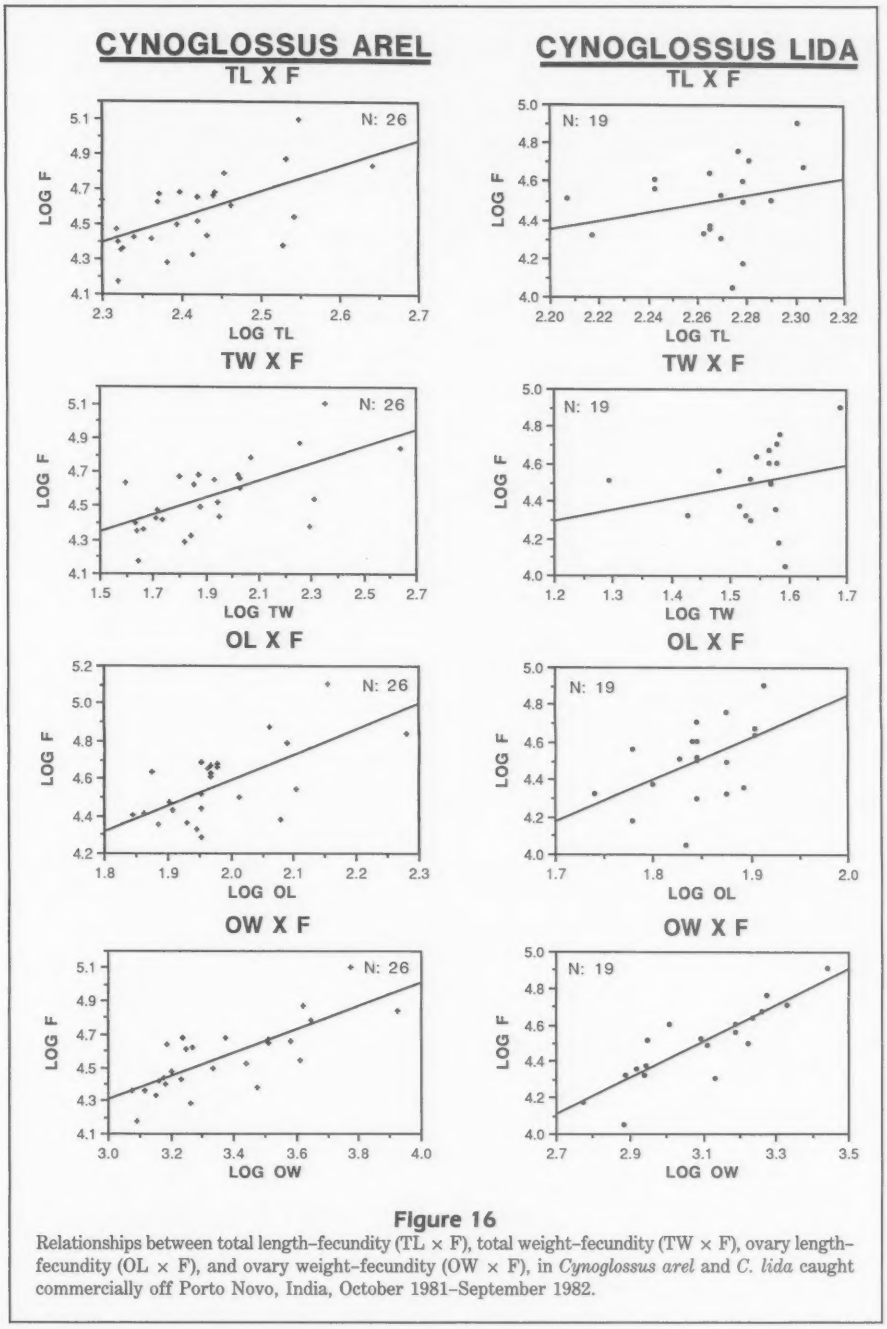

Figure 16

Relationships between total length–fecundity (TL × F), total weight–fecundity (TW × F), ovary length–fecundity (OL × F), and ovary weight–fecundity (OW × F), in *Cynoglossus arel* and *C. lida* caught commercially off Porto Novo, India, October 1981–September 1982.

in *C. lida*. Number of ova/g body weight was 124–1096 ($\bar{x}$ 464) in *C. arel*, and 287–1664 ($\bar{x}$ 988) in *C. lida*. Scatter diagrams of fecundity (F) against TL, TW, OL, and OW are shown in Figure 16.

Fecundity was found to increase with TL (Fig. 16). The calculated equation for F against TL is,

C. arel $\log F = 1.0629 + 1.4459 \log TL$

C. lida $\log F = -0.4923 + 2.2006 \log TL$.

The correlation coefficient (r) for this relationship in *C. arel* is 0.6043 ($P<0.001$) and is statistically significant; in *C. lida*, it is 0.2579 ($P>0.05$) and is not statistically significant.

Fecundity against TW showed a linear relationship (Fig. 16), and equations for the transformed data are,

C. arel $\log F = 3.5907 + 0.4995 \log TW$

C. lida $\log F = 3.5536 + 0.6108 \log TW.$

The correlation coefficient (r) for this relationship in *C. arel* is 0.6345 and is highly significant ($P<0.001$); in *C. lida*, the correlation coefficient of 0.2302 ($P>0.05$) did not indicate a significant correlation between these two variables.

Ovary length showed a straight-line relationship with fecundity (Fig. 16). In logarithmic form, the relationships between F and OL can be expressed as follows;

C. arel $\log F = 1.8472 + 1.3693 \log OL$

C. lida $\log F = 0.3206 + 2.2630 \log OL.$

The correlation coefficient in *C. arel* is 0.6632 ($P< 0.001$) and is statistically significant; in *C. lida*, it is 0.4990 ($P< 0.05$), showing a high degree of correlation.

Fecundity plotted against OW showed a linear relationship (Fig. 16) and equations for these two variables are,

C. arel $\log F = 2.1858 + 0.7050 \log OW$

C. lida $\log F = 1.3909 + 1.0038 \log OW.$

The correlation coefficient in *C. arel* is 0.7729 ($P< 0.001$), indicating a high degree of correlation between these two variables. In *C. lida*, the correlation coefficient of 0.8606 ($P<0.001$) is highly significant.

In the present study, the exponential value (b) for total length–fecundity was higher than for total weight–fecundity. Similarly, the b value for ovary length–fecundity was higher than for ovary weight–fecundity.

Sex ratio The sex ratio was about 1:1 for both species (Table 18, Fig. 14). However, the ratio varied in monthly samples, and chi-square values showed a significant deviation from the expected 1:1 ratio for 3 months (February, September, and November) in *C. arel*, and during February–April, September, and November in *C. lida*. Since data were pooled for one year, the chi-square value conformed to the expected 1:1 ratio in *C. arel*; whereas in *C. lida*, it deviated significantly from the expected 1:1 ratio. The deviation may be due to multiple testing.

Discussion

Feeding ecology

Cynoglossus arel and *C. lida* feed predominantly on polychaetes and crustaceans, followed by other phyla such as molluscs, echinoderms, and coelenterates. These similarities in diets indicate common feeding strategies within the tonguefishes and soles (Seshappa and Bhimachar 1955, Kuthalingam 1957, de Groot 1971, Braber and de Groot 1973ab, Stickney 1976, Pearcy and Hancock 1978, Langton and Bowman 1981, Wakabara et al. 1982, Langton 1983, Honda 1984).

Table 18

Sex ratio of *Cynoglossus arel* and *C. lida* caught commercially off Porto Novo, India, October 1981–September 1982. F = Probability.

	Cynoglossus arel							*Cynoglossus lida*						
Months	♂ *N*	♀ *N*	♂ %	♀ %	♂:♀	χ^2	F	♂ *N*	♀ *N*	♂ %	♀ %	♂:♀	χ^2	F
Jan.	53	39	57.6	42.4	1.4:1.0	2.1304	>0.05	32	42	43.2	56.8	0.8:1.0	1.3514	>0.050
Feb.	24	45	34.8	65.2	0.5:1.0	6.3913	<0.05	59	16	78.7	21.3	3.7:1.0	24.6533	<0.001
Mar.	54	49	52.4	47.6	1.1:1.0	0.2427	>0.05	64	18	78.0	22.0	3.6:1.0	25.8049	<0.001
Apr.	46	55	45.5	54.5	0.8:1.0	0.8020	>0.05	84	51	62.2	37.8	1.7:1.0	8.0667	<0.010
May	56	45	55.4	44.6	1.2:1.0	1.1980	>0.05	38	31	55.1	44.9	1.2:1.0	0.7101	>0.050
June	35	40	46.7	53.3	0.9:1.0	0.3333	>0.05	56	59	48.7	51.3	0.9:1.0	0.0783	>0.050
July	69	56	55.2	44.8	1.2:1.0	1.3520	>0.05	25	25	50.0	50.0	1.0:1.0	0.0000	—
Aug.	44	54	44.9	55.1	0.8:1.0	1.0204	>0.05	43	62	41.0	59.0	0.7:1.0	3.4381	>0.050
Sep.	56	35	61.5	38.5	1.6:1.0	4.8462	<0.05	46	25	64.8	35.2	1.8:1.0	6.2113	<0.050
Oct.	75	54	58.1	41.9	1.4:1.0	3.4186	>0.05	83	76	52.2	47.8	1.1:1.0	0.3082	>0.050
Nov.	86	54	61.4	38.6	1.6:1.0	7.3143	<0.01	160	207	43.6	56.4	0.8:1.0	6.0191	<0.050
Dec.	29	34	46.0	54.0	0.9:1.0	0.3968	>0.05	28	28	50.0	50.0	1.0:1.0	0.0000	—
Total	627	560	52.8	47.2	1.1:1.0	3.7818	>0.05	718	640	52.9	47.1	1.1:1.0	4.4801	<0.050

Diet of fishes is related not only to their feeding behavior, but also to their digestive morphology and mouth structure (Stickney et al. 1974). In *C. arel* and *C. lida*, jaws are asymmetrical so that the mouth points to the bottom when opened, aiding feeding upon benthic prey. Flatfishes that feed on benthose usually have asymmetrical jaws (Pearcy and Hancock 1978). *Cynoglossus arel*, *C. lida*, and other tonguefishes are, in general, polychaete feeders. These fishes have small stomachs (not highly demarcated) and long intestines, and lack gillrakers and pyloric caecae.

Although there were similarities in food items, importance of prey species differed between adults and juveniles. Juveniles of *C. arel* and *C. lida*, probably owing to their very small mouths, fed predominantly on smaller prey such as amphipods and copepods, and ingested fewer types (only 10) of food items. Adults of both species, in contrast, had eaten 24 and 29 types, respectively, of relatively large-sized prey, primarily polychaetes, prawns, crustacean fragments, and fish remains. Mouth size severely limits the size of prey which can be ingested (Stickney 1976). According to Honda (1984), the extent of food demand and ability for food acquisition increase with growth and development of fish. Lande's (1976) findings on the dab *Limanda limanda* revealed that larger fish consumed large-sized prey compared with smaller fish. Pearcy and Hancock (1978) studied feeding habits of Dover sole *Microstomus pacificus*, rex sole *Glyptocephalus zachirus*, slender sole *Lyopsetta exilis*, and Pacific sanddab *Citharichthys sordidus* off Oregon, and concluded that the number and size of prey taxa generally increased with size in these flatfishes, due to the ability of larger fish to consume a larger range of prey sizes than smaller fish.

During the present investigation, fewer empty stomachs were noted in female than male (11.6% vs. 18.0%) *C. lida*. A similar trend was observed by Langton (1983) for yellow-tail flounder *Limanda ferruginea* off the northeastern United States. In female and male *C. arel*, the percentage occurrence of empty stomachs was similar (7.7% vs. 8.0%).

Sexual differences in food and feeding habits of flatfishes have not been reported. In this study, there was some indication of differences in prey between males and females. The primary food group (polychaetes) was the same in both sexes of *C. lida*; however, polychaetes were somewhat more important in females (IRI 65.9%) than males (IRI 53.4%). Moreover, the breadth of the diet was somewhat less in females which fed upon only 19 food types, in contrast to males in which 24 prey types were consumed.

The present analysis on feeding intensity reveals that in males of *C. arel*, the peak occurrence of empty stomachs had a positive correlation with peak spawning activity (in January). Spawning fish contained the least amounts of prey, or had empty stomachs. This result is consistent with the findings of Ramanathan and Natarajan (1980) on Indian halibut *Psettodes erumei* and flounder *Pseudorhombus arsius*, and with those of Langton (1983) on yellowtail flounder *Limanda ferruginea*. However, in female *C. arel* and both sexes of *C. lida*, the occurrence of empty stomachs had no obvious relationship with spawning activities. Seshappa and Bhimachar (1955) also reported that in Malabar sole *C. semifasciatus*, feeding intensity was not interrupted by increased reproductive activity.

Male and female *C. arel* showed an inverse relationship between gastrosomatic/hepatosomatic indices and breeding cycle, with the lowest values observed during peak spawning (in January). This indicates that gut/liver energy reserves may be used for gonadal recrudescence. Such a correlation was observed by Ramanathan (1977) for the Indian halibut *Psettodes erumei* and flounder *Pseudorhombus arsius*. Wingfield and Grimm (1977) found HI to be highest in the prespawning season and lowest in the postspawning period of the Irish Sea plaice *Pleuronectes platessa*. However, *C. lida* did not show a relationship between gastrosomatic/hepatosomatic indices and breeding cycle.

Although the primary diet of these two demersal flatfishes consisted of benthic prey such as polychaetes, prawns, echinoderms, and molluscs, it was surprising to find that pelagic amphipods ($\leq$59.2% IRI) and copepods ($\leq$44.7% IRI) were also relatively important in their diets, especially in juveniles. *Cynoglossus arel* and *C. lida* are demersal flatfishes that have never been caught in the pelagic waters off Porto Novo, either during day or night. These tonguefishes are not known to undergo vertical feeding migrations. Based on the present study, it is speculated that these tonguefishes ingested pelagic prey such as hyperiid amphipods and copepods when these prey organisms approached or contacted the bottom during vertical migrations through the water column. Hyperiid amphipods have been reported to undertake extensive vertical migrations (Bowman et al. 1982, Roe et al. 1984, Clark et al. 1989). Isaacs and Schwartzlose (1965) and Pereyra et al. (1969) have reported that in the eastern North Pacific Ocean, demersal fishes feed on pelagic prey, when such prey approach the bottom along the edge of the continental shelf.

Polychaetes, prawns, amphipods, copepods, crustaceans, and fishes were important prey for both *Cynoglossus arel* and *C. lida*. These tonguefishes shared 25 different food items as prey (out of 30 food types in *C. arel*, and out of 26 in *C. lida*). High overlap in diet may reflect abundant prey resources, reducing competition. Lande (1976) observed such a high prey

abundance for Norwegian flatfishes. However, during the present study, some individuals had full and gorged stomachs, filled only with either polychaetes or prawns. This might indicate either greater availability or patchy distribution of the major food items. Seshappa and Bhimachar (1955) reported for Malabar sole *Cynoglossus semifasciatus*, from the west coast of India, that during certain months the guts were gorged with only one prey, mostly polychaetes.

During the present investigation, most stomachs of *C. arel* and *C. lida* were found to contain considerable quantities of sediment (sand and mud). In some specimens, the entire stomach was filled with sediment. Algal filaments were also found in some stomachs. Sediment and algal filaments were probably ingested accidentally with bottom-living polychaetes and other infauna. Since demersal fishes browse near the sea bottom, some amount of sediment may frequently be in their gut. This has been reported for other flatfishes, such as Malabar sole *Cynoglossus semifasciatus* (Seshappa and Bhimachar 1955) and *C. lingua* (Kuthalingam 1957), and for other demersal fishes (Sedberry and Musick 1978). Stickney (1976) stated that the high percentage occurrence of sand in the stomachs of blackcheek tonguefish *Symphurus plagiusa* might be due to ingestion of a significant quantity of detrital material in its feeding activities. It is unknown if sediment ingestion in *C. arel* and *C. lida* is accidental or represents a deliberate feeding action. *In situ* or aquarium studies on feeding habits would be required to answer this question.

Nematodes, present in stomachs of several specimens of *C. arel* and *C. lida*, were not attached to the stomach wall but, rather, appeared to be free-living species.

Age and growth

In the present study, distinct annual markings were not seen in scales, otoliths, opercular bones, and supraoccipital crests of *C. arel* and *C. lida*. Struhsaker and Uchiyama (1976) have stated that tropical and subtropical fishes are difficult to age, because they generally experience little seasonal and environmental changes and so do not develop annual rings clearly.

It was observed in *C. arel* and *C. lida* that after very rapid growth during the first year, there is a considerable reduction in the growth rate during the years when sexual maturity sets in; afterwards, the growth rate decreases slightly with age. This observation is consistent with the findings of Ford (1933) and Devold (1942).

Females of *C. arel* show faster growth, compared with males, and also live longer. According to Pitt (1966, 1967), since males mature earlier than females, it seems likely that energy is diverted at an earlier age from growth to reproduction, so that the rate of growth in males is reduced at an earlier age than in females. Results of age and growth studies on yellowtail flounder *Limanda ferruginea* from New England (Lux and Nichy 1969), *Limanda herzensteini* from Japan (Wada 1970a), Agulhas sole *Austroglossus pectoralis* from South Africa (Zoutendyk 1974a), and *Solea solea* from Spain (Ramos 1982) are also consistent with Pitt's view. In contrast to the above view, no significant difference was observed between the growth patterns in males and females of *C. lida*.

It is important to know at what age fishes are recruited to the fishery. The present study reveals that *C. arel* and *C. lida* reach commercial size during their 2d and 3d year. Botha et al. (1971) stated that Agulhas sole *Austroglossus pectoralis* off South Africa reached commercial size during their 3d–5th years, and at certain times their 2d–4th years. Lux and Nichy (1969) observed that yellowtail flounder *Limanda ferruginea* of the New England fishing grounds recruited to the commercial fishery during their 3d and 4th years. According to Seshappa and Bhimachar (1955), the bulk of commercial catches of Malabar sole *Cynoglossus semifasciatus* consisted of 2d-year individuals.

Cynoglossus arel and *C. lida* have a life-span of a little over 3 years in the southeast coast of India. The longevity for *C. lida* from the west coast of India has also been reported to be 3–4 years (Seshappa 1978). Longevity in most tropical fish species is relatively shorter and seldom exceeds 2–3 years (Qasim 1973b). However, temperate flatfishes were reported to have a longevity of 6–30 years (Devold 1942, Arora 1951, Pitt 1967, Lux and Nichy 1969, Lux 1970, Wada 1970a, Zoutendyk 1974a, Smith and Daiber 1977).

Length-weight relationships

During the present analyses, *C. arel* showed differences in characteristic length-weight slopes for males and females. Similar observations were made by Ketchen and Forrester (1966) and Powles (1967), while analyzing the length-weight relationships of Petrale sole *Eopsetta jordani* and American plaice *Hippoglossoides platessoides*, respectively. However, *C. lida* showed no significant differences in characteristic length-weight slopes for males and females. Zoutendyk (1974b) on Agulhas sole *Austroglossus pectoralis*, and Smith and Daiber (1977) on summer flounder *Paralichthys dentatus*, did not report significant differences in length-weight characteristics of males and females.

Cynoglossus arel and *C. lida* showed significant regression coefficients (b-values), which differed significantly from the hypothetical B value (=3). Webb (1972) made similar observations for yellow-bellied flounder *Rhombosolea leporina*.

Significant deviation from the 'cube law' was observed in mature females of *C. lida* due to gonad development. Similar findings were observed by Dawson (1962) in hogchokers *Trinectes maculatus*, and by Lux (1969) in yellowtail flounder *Limanda ferruginea*.

In male and female *C. arel*, and male, female, and juvenile *C. lida*, the exponent values are >3, indicating that the weight increase is more in relation to length. But the exponent value for juveniles of *C. arel* is <3, indicating that an increase in weight is less compared with length.

During the present investigation, specimens <83 mm TL in *C. arel* and <81 mm TL in *C. lida* were not available from the continental shelf off Porto Novo. Arora (1951) reported such an absence of juveniles in the commercial catches for California sand dab *Citharichthys sordidus*. Non-availability of juveniles in commercial catches might be due to the gears operated or due to their occurrence in deeper waters, since spawning of cynoglossines in inshore waters has not been reported (Seshappa and Bhimachar 1955).

Reproductive biology

Spawning periods of *C. arel* and *C. lida* were prolonged, lasting for 10 months. The present study agrees with Qasim's (1973a) view that in Indian waters many fish species may be prolonged breeders. Seshappa and Bhimachar (1955) reported that the spawning season in the Malabar sole *Cynoglossus semifasciatus* off the west coast of India was prolonged (8 months).

In *C. arel* and *C. lida*, ova in different maturity stages taken from anterior, middle, and posterior regions of both lobes of ovaries showed no variation in their mean diameter. It is therefore concluded that the development of ovarian eggs proceeds uniformly throughout the ovary. Such a distribution of ova has been reported for Indian halibut *Psettodes erumei* and flounder *Pseudorhombus arsius* (Ramanathan and Natarajan 1979).

Male *C. arel* and *C. lida* attained maturity earlier than females. Pitt (1966) observed that males of American plaice *Hippoglossoides platessoides* were obviously smaller than females at first maturity. Results obtained by Lux and Nichy (1969) for yellowtail flounder *Limanda ferruginea* (New England), by Wada (1970b) for *Limanda herzensteini* (Japan), by Zoutendyk (1974a) for Agulhas sole *Austroglossus pectoralis* (South Africa), and by Ramos (1982) for *Solea solea* (Spain) were similar to the present findings.

The GSI is used widely as an index of gonadal activity and as an index for spawning preparedness. In male and female *C. arel* and in female *C. lida*, GSI did not accurately reflect gonadal activity; the relation of gonadal weight to body weight did not change with stage of gonadal development. de Vlaming et al. (1982) stated that the GSI is widely and consistently used for gonadal size and activity without verification of its validity. According to de Vlaming et al. (1982), the GSI is not always the best way of expressing gonadal activity, and so this index should not be applied without validation. Chrzan (1951) concluded that the ratio of gonad weight to body weight, which normally characterizes sexual maturity, could not be determined exactly. According to Delahunty and de Vlaming (1980), the exponential relationship between ovarian weight and body weight did not change with the phase of oocyte development. However, in male *C. lida*, higher values of GSI indicated the occurrence of fully-mature specimens during this period, and a sudden fall in GSI value after September appeared to be due to spawning. Such a relationship between GSI and gonadal activity was reported for Indian halibut *Psettodes erumei* and flounder *Pseudorhombus arsius* (Ramanathan and Natarajan 1979).

In male *C. arel* and male and female *C. lida*, a rise in Kn value did not correspond with a rise in gonadal activity. Webb (1973) observed no significant variation in body condition, with onset of spawning, in sand flounder *Rhombosolea plebeia* and yellow-bellied flounder *R. leporina* off New Zealand. However, in female *C. arel*, a rise in Kn value corresponded with a rise in gonadal activity, and thus showed a positive correlation.

A linear relationship between fecundity and other variables (total length, total weight, ovary length, and ovary weight) was observed in *C. arel* and *C. lida*. The result agrees with those of Hoda (1976). The correlation coefficient between fecundity and total length, total weight, ovary length, and ovary weight showed a high positive degree of correlation in *C. arel*. In *C. lida*, the correlation coefficient between fecundity and ovary length and ovary weight showed a high positive degree of correlation; whereas the correlation coefficient between fecundity and total length and total weight did not show significant correlations. Hence in *C. lida*, fecundity was dependent only on ovary length and ovary weight.

In *C. arel* and *C. lida*, fecundity was better correlated with total length and ovary length than with total weight and ovary weight. According to Colman (1973), in sand flounder *Rhombosolea plebeia* and yellow-bellied flounder *R. leporina* off New Zealand, fecundity increased at a rate greater than the cube of length, and more than proportionately to weight; fecundity was probably slightly less proportional to ovary weight. Colman (1973) suggested that this might be due to large ovaries containing either great quantities of ovarian fluid or connective tissue or a high proportion of nondeveloping eggs.

In *C. arel* and *C. lida*, age of fish had no effect on the number of eggs. Among fish of the same length, older ones did not contain more eggs than younger ones. This result is consistent with the findings of Simpson (1951) and Bagenal (1957).

More fecund *C. lida* (relative fecundity 287–1664, $\bar{x}$ 988) laid smaller eggs (≤0.6250 mm d.m.), while less fecund *C. arel* (relative fecundity 124–1096, $\bar{x}$ 464) laid larger eggs (≤0.8125 mm d.m.). Dahl (1918) and Svärdson (1949) also found that more fecund species lay smaller eggs.

In *C. arel* and *C. lida*, males outnumbered females and were relatively smaller in size than females. The present finding is inconsistent with Qasim's (1966) view that the sex which outnumbers the other attains a much bigger size.

Chi-square values showed a significant deviation from the expected 1:1 ratio for 3 months in *C. arel* and for 5 months in *C. lida*. Such a deviation could be due to a partial segregation of mature forms through habitat preference (Reynolds 1974), due to migration (Collignon 1960) or behavioral differences between sexes (Polonsky and Tormosova 1969), thus rendering one sex to be more easily caught than another.

During the present investigation, spent individuals of *C. arel* and *C. lida* were not found throughout the study period, since spawning of tonguefishes appears to take place mainly in deeper waters, as observed by Seshappa and Bhimachar (1955) for Malabar sole *Cynoglossus semifasciatus*. This is a gap in the reproductive biology of these tonguefishes. Deep-sea fishing is needed to confirm this type of spawning behavior by the tonguefishes.

For *C. arel*, the spawning peak was in January which is the post-(northeast) monsoon period along the southeast coast of India. Monsoonal floods end by this time, and food resources (like copepods and amphipods, which are essential food items of juveniles) are abundant; this season would appear to be a favorable time for spawning. The spawning peak of *C. lida* was in September, which is the pre-(northeast) monsoon period along the southeast coast of India; this period coincides with the most active southwest monsoon period along the west coast of India. Most of the rivers originating in the west receive floodwaters through the southwest monsoon and empty them into the Bay of Bengal, which thus gets rich primary food resources at this time. This period would also appear to be a favorable time for spawning, because of food abundance.

Thus *C. arel* and *C. lida*, though co-occurring sympatrically in the continental shelf waters off Porto Novo, share available food resources and appear to avoid competition for food and space for their juveniles by exhibiting spawning peaks during different periods (pre-/post-northeast monsoon).

Acknowledgments

I am indebted to Dr. Bruce B. Collette, Systematics Laboratory, for his many helpful suggestions in the modification of this manuscript for publication, and for providing the facilities of the Systematics Laboratory. My sincere thanks to Dr. Thomas Munroe for critically reviewing part (food and feeding) of the manuscript. Comments made by the editor, and two anonymous reviewers helped in modifying this manuscript. Special thanks go to Ms. Ruth E. Gibbons, for her suggestions regarding computer graphics. Grateful acknowledgement is extended to the University Grants Commission, New Delhi, to Dr. R. Natarajan, and to the authorities of Annamalai University, India, for offering financial support and necessary facilities to carry out this study as a part of my Ph.D. program. I thank Dr. K. Sriraman, Tamil Nadu Fisheries, Porto Novo, for his help in the statistics. My sister, Miss G. Shantha, helped me in processing the data. Computer help extended by Mr. H.A. Kurt Luginbyhl, Dr. Jeffrey Williams, Mr. Tom Orrell, and Mr. Jeffrey Howe is greatly appreciated.

Citations

Arora, H.L.
1951 An investigation of the California sand dab, *Citharichthys sordidus* (Girard). Calif. Fish Game 37(1):3–42.

Bagenal, T.B.
1957 The breeding and fecundity of the long rough dab *Hippoglossoides platessoides* (Fabr.) and the associated cycle in condition. J. Mar. Biol. Assoc. U.K. 36(2):339–375.

Bal, D.V., and V. Rao
1984 Marine fisheries. Tata McGraw-Hill, New Delhi, 470 p.

Botha, L., D.K. Lucks, and D.S. Chalmers
1971 Mesh selectivity experiments on the east coast sole. S. Afr. Ship. News & Fishing Ind. Rev. 26(10):50–57.

Bowman, T.E., A.C. Cohen, and M.M. McGuiness
1982 Vertical distribution of *Themisto gaudichaudii* (Amphipoda:Hyperiidea) in deep-water dumpsite 106 off the mouth of Delaware Bay. Smithson. Contrib. Zool. 351, 24 p.

Braber, L., and S.J. deGroot
1973a On the morphology of the alimentary tract of flatfishes (Pleuronectiformes). J. Fish. Biol. 5(2):147–153.
1973b The food of five flatfish species (Pleuronectiformes) in the southern North Sea. Neth. J. Sea Res. 6(1–2):163–172.

Cassie, R.M.
1954 Some uses of probability paper in the analysis of size frequency distributions. Aust. J. Mar. Freshwater Res. 5(3): 513–522.

Chrzan, F.
1951 Studies on the biology of the cod in the Gulf of Gdansk. Rep. Sea Fish. Inst. (Gdynia, Poland) 6:1–28.

Clark, F.N.
1934 Maturity of the California sardine (*Sardina caerulea*) determined by ova diameter measurements. Calif. Dep. Fish. Game Fish Bull. 42, 49 p.

Clark, M.R., K.J. King, and P.J. McMillan
1989 The food and feeding relationships of black oreo, *Allocyttus niger*, smooth oreo, *Pseudocyttus maculatus*, and eight other fish species from the continental slope of the south-west Chatham Rise, New Zealand. J. Fish. Biol. 35(4):465–484.

CMFRI
1969 Marine fish production in India, 1950–1968. Bull. Cent. Mar. Fish. Res. Inst. 13, Cochin, India, 144 p.

Collignon, J.
1960 Contribution à la connaissance des *Otolithus* des côtes d'Afrique Equatoriàle. Bull. Inst. Études Centrafracaines Brazzaville, N.S. 19–20:55–84.

Colman, J.A.
1973 Spawning and fecundity of two flounder species in the Hauraki Gulf, New Zealand. N.Z. J. Mar. Freshwater Res. 7(1&2):21–43.

Daan, N.
1973 A quantitative analysis of the food intake of North Sea cod, *Gadus morhua*. Neth. J. Sea Res. 6(4):479–517.

Dahl, K.
1918 Studies of trout and trout waters in Norway. Salmon Trout Mag. 17:58–79.

Dawson, C.E.
1962 Length-weight and standard length-total length relationships of South Carolina hogchokers, *Trinectes maculatus*. Trans. Am. Fish. Soc. 91(1):89–90.

deGroot, S.J.
1971 On the interrelationships between morphology of the alimentary tract, food and feeding behaviour in flatfishes (Pisces:Pleuronectiformes). Neth. J. Sea Res. 5(2):121–196.

de Jong, J.K.
1940 A preliminary investigation of the spawning habits of some fishes of Java Sea. Treubia Buitenzorg 17(4):307–330.

Delahunty, G., and V.L. deVlaming
1980 Seasonal relationships of ovary weight, liver weight and fat stores with body weight in the gold fish, *Carassius auratus* (L.). J. Fish. Biol. 16(1):5–13.

Devadoss, P., and P.K.M. Pillai
1973 Observations on the food of juveniles of *Psettodes erumei* (Bloch). Indian J. Fish. 20(2):664–667.

deVlaming, V., G. Grossman, and F. Chapman
1982 On the use of the Gonadosomatic Index. Comp. Biochem. Physiol. 73A(1):31–39.

Devold, F.
1942 Plaice investigations in Norwegian waters. Rep. Norw. Fish. Mar. Invest. VII(3), 83 p.

Fischer, W., and G. Bianchi
1984 FAO species identification sheets for fishery purposes. II. W. Indian Ocean–Fishing area 51. FAO, Rome.

Ford, E.
1933 An account of the herring investigations conducted at Plymouth during the years from 1924–'33. J. Mar. Biol. Assoc. U.K. 19(1):305–384.

Harding, J.P.
1949 The use of probability paper for the graphical analysis of polymodal frequency distributions. J. Mar. Biol. Assoc. U.K. 28(1):141–153.

Hickling, C.F., and E. Rutenberg
1936 The ovary as an indicator of the spawning period in fishes. J. Mar. Biol. Assoc. U.K. 21(1):311–317.

Hoda, S.M.S.
1976 Reproductive biology and length-weight relationship of *Thryssa dussumieri* (Val.) of the Pakistan coast. J. Mar. Biol. Assoc. India 18(2):272–287.

Honda, H.
1984 Food acquisition patterns in some demersal teleosts. Tohoku J. Agric. Res. 35(1):33–54.

Isaacs, J.D., and R.A. Schwartzlose
1965 Migrant sound scatterers: Interaction with the sea floor. Science (Wash. DC) 150(3705):1810–1813.

James, P.S.B.R.
1967 The ribbonfishes of the family Trichiuridae of India. Mem. Mar. Biol. Assoc. India 1, 226 p.

Ketchen, K.S., and C.R. Forrester
1966 Population dynamics of the Petrale sole, *Eopsetta jordani*, in waters off western Canada. Bull. Fish. Res. Board Can. 153, 195 p.

Kuthalingam, M.D.K.
1957 Life history and feeding habits of *Cynoglossus lingua* (Ham. Buch.). J. Zool. Soc. India 9(2):208–215.

Lande, R.
1976 Food and feeding habits of the dab (*Limanda limanda* [L.]) in Borgenfjorden, north Trondelag, Norway. Norw. J. Zool. 24(3):225–230.

Langton, R.W.
1983 Food habits of yellow-tail flounder, *Limanda ferruginea* (Storer), from off the northeastern United States. Fish. Bull., U.S. 81(1):15–22.

Langton, R.W., and R.E. Bowman
1981 Food of eight northwest Atlantic pleuronectiform fishes. NOAA Tech. Rep. NMFS-SSRF 749,16 p.

Le Cren, E.D.
1951 The length-weight relationship and seasonal cycle in gonad weight and condition in the perch (*Perca fluviatilis*). J. Anim. Ecol. 20(2):201–219.

Lovern, J.A., and H. Wood
1937 Variations in the chemical composition of herring. J. Mar. Biol. Assoc. U.K. 22(1):281–293.

Lux, F.E.
1969 Length-weight relationships of six New England flatfishes. Trans. Am. Fish. Soc. 98(4):617–621.
1970 Note on growth of American plaice, *Hippoglossoides platessoides* (Fabr.) in ICNAF Subarea 5. Int. Comm. Northwest Atl. Fish. Spec. Publ. 7:5–7.

Lux, F.E., and F.E. Nichy
1969 Growth of yellowtail flounder, *Limanda ferruginea* (Storer), on three New England fishing grounds. Int. Comm. Northwest Atl. Fish. Res. Bull. 6:5–25.

Nikolsky, G.V.
1963 The ecology of fishes. Academic Press, NY, 352 p.

Pearcy, W.G., and D. Hancock
1978 Feeding habits of dover sole, *Microstomus pacificus*; rex sole, *Glyptocephalus zachirus*; slender sole, *Lyopsetta exilis*; and Pacific sand dab, *Citharichthys sordidus*, in a region of diverse sediments and bathymetry off Oregon. Fish. Bull., U.S. 76(3):641–651.

Pereyra, W.T., W.G. Pearcy, and F.E. Carvey Jr.
1969 *Sebastes flavidus*, a shelf rockfish feeding on mesopelagic fauna, with consideration of the ecological implications. J. Fish. Res. Board Can. 26:2211–2215.

Pinkas, L., M.S. Oliphant, and I.L.K. Iverson
1971 Food habits of albacore, bluefin tuna and bonito in Californian waters. Calif. Fish Game 152, 105 p.

Pitt, T.K.
1966 Sexual maturity and spawning of American plaice, *Hippoglossoides platessoides* (Fabricius), from Newfoundland and Grand Bank areas. J. Fish. Res. Board Can. 23(5):651–672.
1967 Age and growth of American plaice, *(Hippoglossoides platessoides)* in the Newfoundland area of the Northwest Atlantic. J. Fish. Res. Board Can. 24(5):1077–1099.

Polonsky, A.S., and I.D. Tormosova
1969 The spawning of the jack-mackerel of the northeast Atlantic and the distribution of its eggs and larvae. Trudy Atl. Nauchno-Issled. Inst. Rybn. Khoz. Okeanogr. 23:27–48 [in Russian].

Powles, P.M.
1967 Length-weight relationships for American plaice, witch, and yellowtail, in ICNAF Subarea 4. Int. Comm. Northwest Atl. Fish. Res. Bull. 4:121–123.

Pradhan, M.J.
1969 Fishery and biology of *Psettodes erumei* (Schneider) an Indian Ocean flatfish. Bull. Natl. Inst. Sci. India 38, Part II. Proc., Symp. Indian Ocean, Sect. IV, Fisheries, p. 885–894.

Qasim, S.Z.
1966 Sex ratio in fish population as a function of sexual differences in growth rate. Curr. Sci. (Bangalore) 35(6):140–142.
1973a An appraisal of the studies on maturation and spawning in marine teleosts from Indian waters. Indian J. Fish. 20(1):166–181.
1973b Some implications of the problem of age and growth in marine fishes from the Indian waters. Indian J. Fish. 20(2):351–371.

Rajaguru, A.
1987 Studies on taxonomy of Indian flatfishes (Teleostei: Pleuronectiformes) and biology of two species of *Cynoglossus* Ham. Buch., 1822 (Cynoglossidae) from Porto Novo. Unpubl. Ph.D. diss., Annamalai Univ., Tamil Nadu, India, 301 p.

Ramanathan, N.
1977 Studies in flatfishes of Porto Novo waters (Teleostei: Pleuronectiformes). Unpubl. Ph.D. diss., Annamalai Univ., Tamil Nadu, India, 250 p.

Ramanathan, N., and R. Natarajan
1979 Breeding biology of *Psettodes erumei* (Bloch. and Schn.) and *Pseudorhombus arsius* (Ham. Buch.) (Pisces:Pleuronectiformes), along Porto Novo coast (S. India). Aquaculture 18(3):269–282.
1980 Food and feeding habits of *Psettodes erumei* (Bloch and Schn.) and *Pseudorhombus arsius* (Ham. Buch.). Matsya (Bull. Indian Soc. Ichthyol.) 6:39–42.

Ramos, J.
1982 Estudio de la edad y crecimiento del lenguado, *Solea solea* (Linneo, 1758) (Pisces:Soleidae). Invest. Pesq. 46 (1):15–28.

Reynolds, J.D.
1974 Biology of small pelagic fishes in the new Volta Lake in Ghana. Part III: Sex and reproduction. Hydrobiologia 45(4): 489–508.

Roe, H.S.J., P.T. James, and M.H. Thurston
1984 The diel migrations and distributions within a mesopelagic community in the north east Atlantic. 6. Medusae, ctenophores, amphipods and euphausiids. Prog. Oceanogr. 13: 425–460.

Sedberry, G.R., and J.A. Musick
1978 Feeding strategies of some demersal fishes of the continental slope and rise off the mid-Atlantic coast of the USA. Mar. Biol. (Berl.) 44:357–375.

Seshappa, G.
1973 The flatfish resources of the west coast of India. Proc., Symp. Living Resour. Seas around India, CMFRI (Cochin, India), p. 470–482.
1978 Some observations on the size distribution and the occurrence of growth rings in the scales of three species of *Cynoglossus* at Calicut. Indian J. Fish. 25 (1&2):188–196.

Seshappa, G., and B.S. Bhimachar
1955 Studies on the fishery and biology of the Malabar sole, *Cynoglossus semifasciatus* Day. Indian J. Fish. 2(1):180–230.

Simpson, A.C.
1951 The fecundity of the plaice. Fish. Invest. Minist. Agrl. Fish. U.K. Ser. II, 17(5), 27 p.

Smith, R.W., and F.C. Daiber
1977 Biology of the summer flounder, *Paralichthys dentatus*, in Delaware Bay. Fish. Bull., U.S. 75(4):823–830.

Snedecor, G.W.
1956 Statistical methods, 5th ed. Iowa State Coll. Press, Ames, 534 p.

Stickney, R.R.
1976 Food habits of Georgia estuarine fishes. II. *Symphurus plagiusa* (Pleuronectiformes:Cynoglossidae). Trans. Am. Fish. Soc. 105(2):202–207.

Stickney, R.R., G.L. Taylor, and R.W. Heard III
1974 Food habits of Georgia estuarine fishes. I. Four species of flounders (Pleuronectiformes:Bothidae). Fish. Bull., U.S. 72:515–525.

Struhsaker, P., and J.H. Uchiyama
1976 Age and growth of the nehu, *Stolephorus purpureus* (Pisces: Engraulidae), from the Hawaiian islands as indicated by daily growth increments of sagittae. Fish. Bull., U.S. 74:9–17.

Svärdson, G.
1949 Natural selection and egg number in fish. Rep. Inst. Freshwater Res., Drottningholm 29:115–122.

von Bertalanffy, L.
1938 A quantitative theory of organic growth. Hum. Biol. 10(2):181–213.

Wada, K.
1970a Studies on the population biology of the flatfish, *Limanda herzensteini* Jordan et Snyder in Niigata Region. Bull. Jpn. Sea Reg. Fish. Res. Lab. 22:31–43.
1970b Studies on the population biology of the flatfish, *Limanda herzensteini* Jordan et Snyder in Niigata Region. II. Maturity and spawning. Bull. Jpn. Sea Reg. Fish. Res. Lab. 22: 45–57.

Wakabara, V., E.K. deRezende, and A.S. Tararam
1982 Amphipods as one of the main food components of three pleuronectiforms from the continental shelf of South Brazil and North Uruguay. Mar. Biol. (Berl.) 68:67–70.

Walford, L.A.
1946 A new graphic method of describing growth of animals. Biol. Bull. (Woods Hole) 90(2):141–147.

Webb, B.F.
1972 Fish populations of the Avon-Heathcote estuary. 1. General ecology, distribution, and length-frequency. N.Z. J. Mar. Freshwater Res. 6(4):570–601.
1973 Fish populations of the Avon-Heathcote estuary. 2. Breeding and gonad maturity. N.Z. J. Mar. Freshwater Res. 7(1&2):45–66.

Wingfield, J.C., and N.S. Grimm
1977 Seasonal changes in plasma cortisol, testosterone and oestradiol-17β in the plaice, *Pleuronectes platessa* L. Gen. Comp. Endocrinol. 31:1–11.

Zoutendyk, P.
1974a The biology of the Agulhas sole, *Austroglossus pectoralis*, Part-2. Age and growth. Trans. R. Soc. S. Afr. 41(1):33–41.
1974b The biology of the Agulhas sole, *Austroglossus pectoralis*, Part-3. Length-weight relationships. Trans. R. Soc. S. Afr. 41(2):99–108.

Appendix

Monthly sample sizes (n) for various studies on biology of *Cynoglossus arel* and *C. lida* caught commercially off Porto Novo, India, October 1981–September 1982. GI = gastrosomatic index; HI = hepatosomatic index; GSI = gonadosomatic index; L-W = length-weight relationships; Kn = relative condition factor.

	GI/HI/GSI/Sex ratio				L-W/Kn				Age and growth			
	C. arel		*C. lida*		*C. arel*		*C. lida*		*C. arel*		*C. lida*	
Months	♂	♀	♂	♀	♂	♀	♂	♀	♂	♀	♂	♀
January	53	39	32	42	52	49	24	31	54	39	34	45
February	24	45	59	16	34	52	48	45	24	44	58	16
March	54	49	64	18	51	47	85	38	54	51	64	18
April	46	55	84	51	46	58	86	54	48	55	84	51
May	56	54	38	31	57	52	62	43	56	54	39	32
June	35	40	56	59	44	41	54	54	35	40	56	59
July	69	56	25	25	70	55	37	44	69	56	25	26
August	44	54	43	62	54	66	45	64	45	54	43	62
September	56	35	46	25	59	39	62	37	57	35	50	26
October	75	54	83	76	81	57	83	80	76	55	83	77
November	86	54	160	207	70	45	135	168	87	54	160	207
December	29	34	28	28	37	38	47	65	29	37	28	31
Total	627	569	718	640	655	599	768	723	634	569	724	650

Abstract.—The inverse method for mortality and growth estimation (IMMAGE) is a new approach to obtain unbiased estimates of mortality and growth parameters for larval fishes from length-frequency data biased by the size selectivity of plankton nets. The performance of IMMAGE is compared with methods which attempt to eliminate selection bias from sampled length-frequencies. Using Monte Carlo simulations, IMMAGE estimates growth and mortality parameters that are more accurate and precise than those produced by other methods.

Inverse method for mortality and growth estimation: A new method for larval fishes

David A. Somerton

Honolulu Laboratory, Southwest Fisheries Science Center
National Marine Fisheries Service, NOAA
2570 Dole Street, Honolulu, Hawaii 96822-2396
Present address: Alaska Fisheries Science Center
National Marine Fisheries Service, NOAA
7600 Sand Point Way NE, Seattle, Washington 98115-0070

Donald R. Kobayashi

Honolulu Laboratory, Southwest Fisheries Science Center
National Marine Fisheries Service, NOAA
2570 Dole Street, Honolulu, Hawaii 96822-2396

Estimation of the growth and mortality rates of larval fishes is complicated by the sampling biases that can result from the size selectivity of plankton nets. Size selectivity due to net avoidance by larvae, for example, results in an underestimation of larval abundance that progressively increases with increasing larval length. This bias leads to an underestimation of mean length-at-age and therefore growth rate, because larger larvae in each age-class are underrepresented relative to smaller larvae. Such bias also leads to an overestimation of mortality rate, because older larvae are underrepresented relative to younger larvae. Size selectivity due to extrusion of larvae results in an underestimation of larval abundance that progressively decreases with increasing larval length and likewise leads to bias in estimates of growth and mortality rates.

Growth studies rarely address such size selection, and when they do, the approach taken is usually to devise a sampling procedure that provides unbiased length-frequencies (Methot and Kramer 1979, Yoklavich and Bailey 1990). Mortality studies, by comparison, almost always address size selection and do so after the fact by taking one of several approaches to eliminate the selection bias from the sampled length-frequencies. One approach taken by mortality studies is to divide the sampled length-frequencies by length-specific estimates of capture probability. Such capture probabilities have been obtained from field studies and estimated as (1) catch ratios of large to small mesh nets (Lenarz 1972, Leak and Houde 1987), (2) catch ratios of day to night sampling (Houde 1977, Zweifel and Smith 1981, Morse 1989, Somerton and Kobayashi 1989), or (3) catch ratios of plankton nets to purse seines (Murphy and Clutter 1972, Leak and Houde 1987). Capture probabilities have also been based on theoretical escapement models (Ware and Lambert 1985). A second approach taken by mortality studies is to simply eliminate the biased portions of the length distribution. Such elimination may exclude only small (Morse 1989) or large larvae (Houde 1977, Methot and Kramer 1979) or both (Essig and Cole 1986). Elimination of biased length-frequencies also has been combined with the use of capture probabilities (Houde 1977, Morse 1989).

Manuscript accepted 9 March 1992.
Fishery Bulletin, U.S. 90:368–375 (1992).

Although the various approaches may differ in the specifics of their application, all are based on the premise that length-frequency data must first be corrected for selection bias before they can be utilized to estimate growth and mortality. Here we introduce a new approach which reorders and joins the processes of data correction and parameter estimation. This approach, which is based on a stock assessment technique known as synthesis modeling (Methot 1989, 1990), will herein be referred to as the inverse method for mortality and growth estimation (IMMAGE). The use of IMMAGE is examined to estimate growth and mortality rates from biased length-frequency data. Additionally, the performance of IMMAGE, using Monte Carlo simulation, is compared with approaches used to correct selection bias in length-frequency data prior to parameter estimation.

Materials and methods

IMMAGE vs. bias correction

To understand how IMMAGE works and why it is an inverse method for obtaining estimates of growth and mortality parameters, the bias-correction approach should first be examined (Fig. 1a–d). One variant of the bias-correction approach might include (1) estimating the unbiased length-frequency distribution (Fig. 1b) by dividing the observed length-frequency distribution (Fig. 1a) by length-specific estimates of capture probability; (2) converting the unbiased length-frequency distribution to an age-frequency distribution (Fig. 1c) using age and length information; and (3) estimating the instantaneous mortality rate (M) as the slope of a straight line fit to the logarithms of numbers at age (Fig. 1d).

The IMMAGE approach, if applied to the same data, would include (1) choosing initial values for M and the number of day-0 larvae (N_0); (2) estimating an unbiased age-frequency distribution (Fig. 1e) based on the values of M and N_0; (3) estimating the unbiased length-frequency distribution (Fig. 1f) from the age-frequency distribution using age and length information; (4) estimating the observed (i.e., biased) length-frequency distribution (Fig. 1g) by multiplying the unbiased length-frequency distribution by estimates of capture probability; and (5) iteratively varying M and N_0, and repeating steps 2–4, until the best fit is achieved between the estimated and observed length-frequency distributions.

Thus both approaches estimate M by fitting a mortality model. However, in the bias correction approach, the model is fit to numbers-at-age derived from the observed length-frequencies; while in the IMMAGE approach, the model is fit to the observed length-frequencies themselves. Growth parameters are estimated by IMMAGE in a similar manner, except a growth model rather than a mortality model is fit to the length-frequencies.

To estimate the observed length distribution, IMMAGE requires specification of a process model and ancillary data. The process model contains parameters that are iteratively varied to achieve the best fit to the observed length-frequency distribution; the ancillary data are parameters assumed to be known. For growth estimation, the process model consists of a growth function describing the mean length-at-age and a variance function describing the variance in length-at-age. Ancillary data include estimates of the capture probability at each length. For mortality estimation, the process model consists of a mortality function describing the instantaneous mortality rate at age or length. Ancillary data include the mean and variance in length-at-age, and the capture probability at each length. Growth and mortality process models are not restricted to any particular form and may include linear or nonlinear functions.

The performance of IMMAGE and several of the bias correction approaches to parameter estimation was examined by using a Monte Carlo simulation model. For growth parameter estimation, bias correction approaches were not examined because no application to larval fishes could be found in the literature. For mortality parameter estimation, three bias correction approaches were examined: (1) elimination of the biased portions of the observed length-frequency distribution, (2) division of the observed length-frequency distribution by estimates of capture probability (correction), and (3) elimination of the biased ages from a corrected age distribution.

Monte Carlo model

The Monte Carlo simulation model is designed to mimic the sequence of steps typically used in growth and mortality studies. A central feature of this model is the simulated collection of three types of data: length-frequency samples, selection samples, and ageing samples.

Length-frequency samples are either unbiased, representing random samples drawn from a larval fish population, or biased, representing samples collected with a plankton net. Selection samples are two independent length-frequency samples, one biased and the other unbiased, used to estimate length-specific capture probabilities. Such samples represent those that might be produced by an experiment to estimate the length-selection characteristics of a plankton net (i.e., day to night catch comparisons). Ageing samples are length-frequency samples in which each length mea-

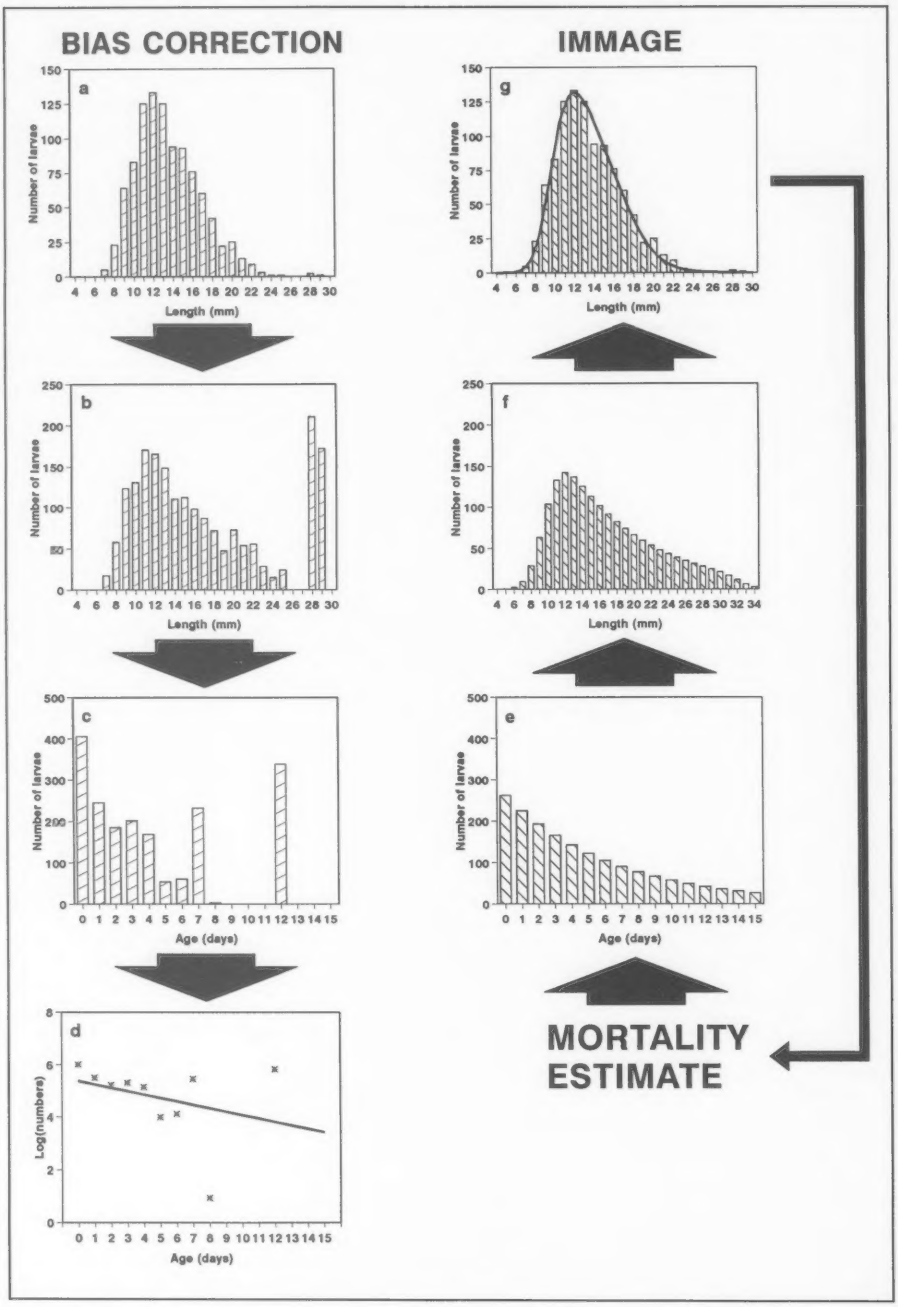

Figure 1
Comparison of the bias-correction and IMMAGE approaches to estimating instantaneous mortality rate (M) from selection-biased length-frequency data. Bias correction (left column) begins by dividing (a) the observed length-frequency distribution by estimates of capture probability to estimate (b) the unbiased length distribution. The unbiased length distribution is then converted to (c) an age distribution, and M is estimated with (d) linear regression. IMMAGE (right column) begins by creating (e) an unbiased age distribution using initial estimates of M and the number of day-0 larvae, N_0. The unbiased age distribution is converted to (f) an unbiased length distribution using the ageing sample. (g) The unbiased length distribution is multiplied by the capture probabilities to estimate the sampled length distribution (solid line), then mortality estimates are varied iteratively to minimize the residual sum of squares between the observed (histogram) and the estimated length distributions.

surement is associated with an age. Ageing samples are considered biased when used in growth parameter estimation but are considered unbiased when used in mortality parameter estimation. This distinction is made because mortality parameters can be influenced by selection bias in ageing samples as well as by selection bias in the length-frequency samples. To simplify interpretation of the results and avoid compounding the effects of the two sources of bias, bias in the ageing samples has been ignored in the mortality estimation.

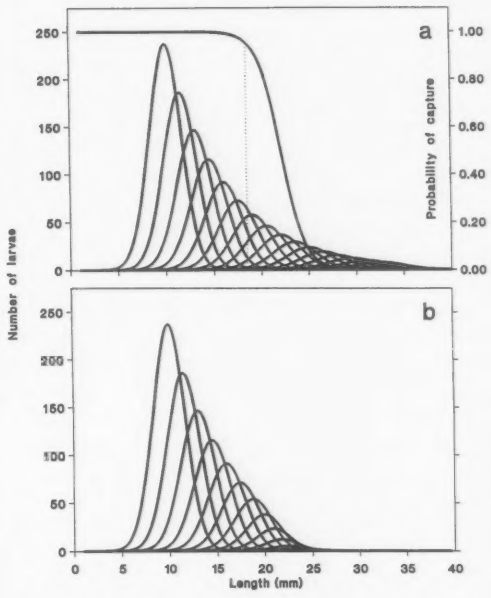

Figure 2

(a) Unbiased length distribution and relative abundance of each age-class in the simulated population of larvae, and the assumed values of capture probability (solid line) and the length of 95% selection (dotted line). With the length elimination method of bias corrector, all lengths to the right of the 95% selector line are eliminated. (b) Length distribution and relative abundance of each age-class within a sample collected with a size-selective plankton net. This distribution is created by multiplying the length distribution shown in (a) by the capture probabilities.

Unbiased length-frequency samples for these three types of data were generated by simulating the random sampling of a larval fish population (Fig. 2a) with a constant daily recruitment, a constant instantaneous daily mortality rate (M) of 0.20, and a length distribution at each age conforming to a normal probability distribution. Mean (l_t) and variance ($Var(l_t)$) of length-at-age were chosen, for simplicity, to be linear functions of age:

$$l_t = 10.00 + 1.50t, \text{ and} \quad (1)$$

$$Var(l_t) = 2.50 + 0.25t, \quad (2)$$

where t is age (in days) and l_t is length (in millimeters). Samples were drawn from the cumulative length probability distribution of this population that was constructed by dividing each of the population length-frequencies by the total sample size, then cumulatively summing across all lengths. Individual lengths within a sample were chosen by determining which category in the cumulative length probability distribution just exceeded the value of a generated uniform random number.

Biased length-frequency samples were generated by simulating the sampling of the model population by using a plankton net, which allowed zero extrusion and produced capture probabilities ($P_{c,l}$) described by an inverse logistic function:

$$P_{c,l} = 1 - \frac{1}{1 + 9.00 \times 10^7 \, e^{-2.61\,l}}, \quad (3)$$

where l is length (in mm) [Fig. 2a; parameters in Eq. (1–3) were chosen arbitrarily and were not intended to represent any particular species or sampling gear]. Samples were drawn by using the same procedure as used for unbiased samples except the population length distribution was multiplied by the capture probabilities (Fig. 2b).

Ageing samples were generated similar to length-frequency samples, but after each length was drawn, an associated age was also drawn by using the cumulative age probability distribution at each length and an additional uniform random number. The sample sizes used in the simulations [1000 length-frequency samples, 300 ageing samples, 600 selection samples, with the biased sample size set equal to the unbiased sample size × the average probability of capture determined from Equation (3)] were arbitrarily chosen but were similar to those used in Somerton and Kobayashi (1989, unpubl. data).

Growth simulations

Growth simulations examining the performance of IMMAGE consisted of 1000 repetitions of the following sequence. First, a biased ageing sample and a selection sample were generated. Second, capture probabilities were estimated from the selection sample by fitting an inverse logistic function of length, using nonlinear regression, to the ratios of the biased to the unbiased length-frequencies. Third, initial parameter estimates for the growth process model [Eq. (1) and (2)] were obtained from the ageing sample by fitting straight lines to length-at-age and variance of length-at-age. Fourth, the unbiased length distribution of each age-class was estimated as a normal distribution with mean and variance predicted from Eq. (1) and (2) evaluated at the current parameter estimates. Fifth, the biased length-frequency distribution of each age-class was estimated by multiplying the unbiased length-frequency distribution by the estimated capture probabilities. Sixth, parameter estimates for Eq. (1) and (2)

were iteratively varied, and steps 4 and 5 were repeated, until the minimum residual sum of squares (RSS) was achieved. The RSS was defined as

$$\sum_j \sum_i (F_{ij} - \hat{F}_{ij})^2, \quad (4)$$

where F_{ij} and $\hat{F}_{ij}$ are the observed and estimated frequency within the ith length interval and the jth age-class.

Mortality simulations

Mortality simulations examined the performance of IMMAGE and three bias-correction approaches: length elimination, division by capture probabilities, and age elimination. Each of the 1000 repetitions of a simulation began by generating a biased length-frequency sample, an unbiased ageing sample, and a selection sample. For all simulations, except those examining IMMAGE, mortality estimation began with an attempt to derive an unbiased age distribution. If length elimination was used, this was accomplished in two stages. First, an unbiased length-frequency distribution was estimated by eliminating all length categories with a capture probability of <0.95 [based on capture probabilities defined by Equation (3), length-classes 3–18 were retained; Fig. 2a]; a probability of 0.95 was used instead of 1.00 because it is better defined. Second, the age-frequency distribution was estimated from the unbiased length-frequency distribution by using the ageing sample and a procedure known as age-slicing (Mesnil and Shepherd 1990). To do this, lengths from the ageing sample were regressed on the ages, and the fitted linear regression equation was evaluated to determine the length corresponding to each age boundary (i.e., 0.5, 1.5, 2.5 days, and so on). Age-frequencies were then estimated by summing length-frequencies between age boundaries.

If division by capture probabilities was used, the age-frequency distribution was estimated by first dividing the observed length-frequency distribution by estimates of capture probability, then converting the length-frequencies to age-frequencies using age-slicing. If age elimination was used, age-classes with a capture probability of <0.95 at the mean length also were eliminated from the age-frequency distribution (age-classes 0–5 days were retained; Fig. 2a). For all three cases, instantaneous mortality rate was then estimated as the slope of an unweighted linear regression to the natural logarithm of numbers-at-age (Ricker 1975).

For simulations examining IMMAGE, mortality estimation proceeded as follows. First, initial values of M and N_0 were obtained from the ageing sample by fitting a straight line to the logarithm of numbers-at-age. Second, values of l_t and $\mathrm{Var}(l_t)$ were estimated from the ageing sample by fitting straight lines to length-at-age and $\mathrm{Var}(l_t)$-at-age, using linear regression, and then evaluating the fitted regression equations at each t. Third, capture probabilities were estimated from the selection sample. Fourth, the unbiased age distribution was estimated as $N_t = N_0 e^{-Mt}$. Fifth, the unbiased length distribution of each age-class was estimated as N_t times a normal probability distribution with a mean equal to l_t and a standard deviation equal to the square root of $\mathrm{Var}(l_t)$. The unbiased length distribution for the population was then estimated by summing the age-specific length distributions over all age-classes. Sixth, the biased (observed) length distribution was estimated by multiplying the unbiased population length distribution by the estimated capture probabilities. Seventh, N_0 and M were iteratively varied, and steps 4–6 repeated, until the minimum RSS was achieved. The RSS was defined as

$$\sum_j (F_j - \hat{F}_j)^2, \quad (5)$$

where F_j and $\hat{F}_j$ are the observed and estimated frequencies within the jth length interval.

The IMMAGE application used in the simulations (i.e., one that assumes linear growth and constant mortality) is available from the authors as a stand-alone program (IMMAGE, written in Microsoft QuickBasic) designed to run on IBM-compatible microcomputers.

Results and discussion

Growth

The type of size selection examined in the simulations (i.e., a decrease in the probability of capture with increasing larval length) complicates the estimation of growth and mortality in slightly different ways. For growth estimation, the primary effect is that the largest larvae in each age-class are undersampled relative to the smallest larvae, and the mean lengths-at-age are therefore underestimated (Fig. 2b). Since the bias progressively increases with age, plots of mean length against age are curvilinear and falsely indicate a declining growth rate (Fig. 3). Such curvilinear or even asymptotic growth patterns are often reported in studies of wild-caught larvae (Bailey 1982, Laroche et al. 1982, Lough et al. 1982, Thorrold 1988, Warlen 1988). Although there may be biological reasons to expect such a pattern, especially for species with pronounced ontogenetic changes in body form, length-selective sampling may be a contributing factor.

IMMAGE estimates of the slope (1.499 ± 0.005; $\bar{x}$ 1000 replicates ± 2 SE) and intercept (10.002 ± 0.012)

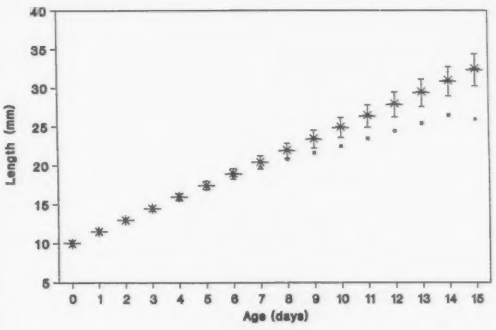

Figure 3

Mean length-at-age in the simulated population (•), mean length-at-age estimated without correction for size selection (■), and mean length-at-age (±2 SE) estimated with IMMAGE (vertical bars).

of the linear growth function [cf. Eq. (1)] were both unbiased, as were all of the estimates of mean length-at-age over the entire age range (Fig. 3). This indicates that, at least for linear growth, IMMAGE provides unbiased estimates of growth parameters from biased length and age samples.

Mortality

For mortality estimation, the primary effect of the decrease in capture probability with increasing larval length is that relative abundance is progressively underestimated with increasing age (Fig. 2b). If ignored, such a progressive underestimation would result in positively biased mortality estimates. In the simulated population, for example, mortality estimates obtained from the observed length-frequency samples ($M = 0.450 \pm 0.004$) had a highly significant positive bias of 125% (Fig. 4a).

Elimination of the biased length-frequencies was only partially effective in reducing the bias in estimated mortality rates, because the mortality estimates ($M = 0.364 \pm 0.007$) still had a highly significant positive bias of 80% (Fig. 4b). In practice, length elimination is likely to be even less effective than it appears here, because it is usually applied to cases where the capture probabilities are crudely known, whereas exact knowledge is assumed in the simulations.

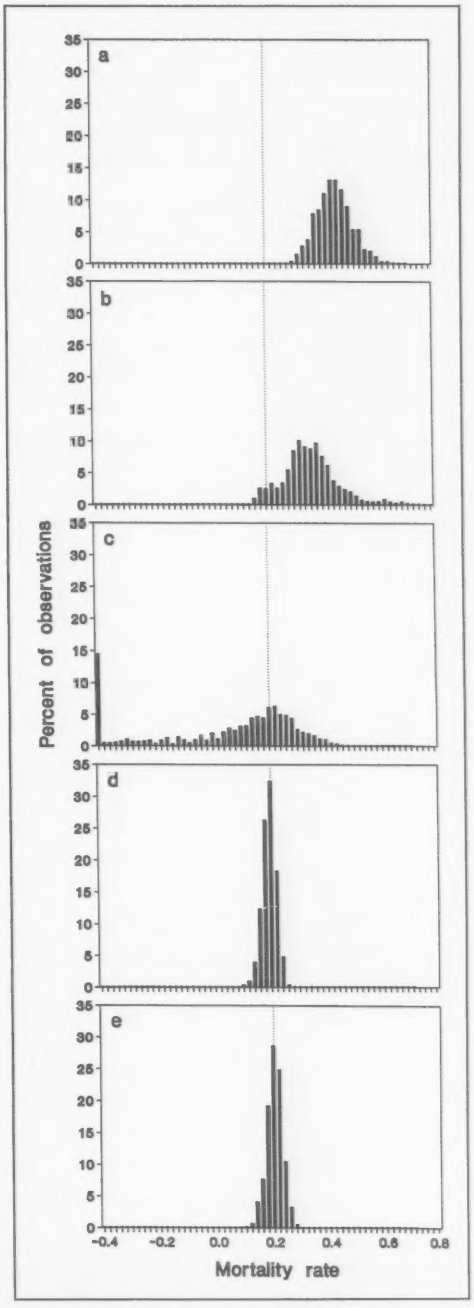

Figure 4 (right)

Frequency distribution of 1000 simulated estimates of instantaneous mortality rate computed from (a) observed length-frequency data, (b) observed length-frequency data after eliminating all length-frequencies with a capture probability of < 0.95, (c) observed length-frequency data divided by estimates of capture probability, (d) corrected age-frequency data after eliminating all age-frequencies with a capture probability of < 0.95, and (e) observed length-frequency data using IMMAGE.

Dividing the observed length-frequency distribution by estimates of capture probability was as ineffective because the mortality estimates (-0.035 ± 0.030) had a highly significant negative bias of 83% (Fig. 4c). The negative bias and the strong negative skew in the frequency distribution are due to the infrequent generation of large larvae. When such larvae occur in a sample, their relative abundance is greatly magnified by their extremely small capture probabilities. The overestimation of large length-classes results in a corresponding overestimation of old age-classes. Because the overestimated age-frequencies are at the extreme of the age range, they exert considerable influence on the slope of the mortality regression and thereby result in the underestimation of M.

Elimination of the biased age-frequencies nearly eliminates this problem and results in mortality estimates (0.192 ± 0.002) with a significant but small negative bias of 4% and a considerable reduction in variance (Fig. 4d). The apparently greater effectiveness of age elimination compared with length elimination is a function of the variance in length-at-age within the larval fish population. For example, when length elimination is applied to the simulated population, essentially all of the undersampled lengths are removed. However, this creates a new bias in the age distribution, because some age-classes experience greater elimination than others (Fig. 2a). Clearly, if no variation exists in length-at-age, length elimination will be identical to age elimination. To our knowledge, the use of age elimination has not been reported in the literature.

Mortality estimates produced by IMMAGE (0.201 ± 0.002) are unbiased and, along with age elimination, have the smallest variance (Fig. 4e). This superior performance is achieved because, unlike length or age elimination, IMMAGE uses all of the sampled length-frequency data and, unlike correction, uses capture probability multiplicatively and therefore avoids magnifying the sampling error.

Practical application of IMMAGE

The application of IMMAGE using the Monte Carlo simulation has been chosen because of its simplicity. Although linear growth, constant mortality, and monotonically increasing size selection may not always be suitable for a particular application, the IMMAGE procedure is extremely adaptable in the way growth, mortality, and size selection can be specified. For example, growth could be specified as an exponential or a Laird-Gompertz function, and size selection could be specified as a double logistic function (Somerton and Kobayashi 1989) describing extrusion and avoidance simultaneously. Mortality could be specified as either a stage-specific function, where the mortality rates of yolksac and feeding larvae differ, or an inverse function of age (Lo 1986). More importantly perhaps, mortality could also be specified as a function of length.

Although mortality rates of larvae likely decline with length for many species (Pepin 1991), length-dependent mortality rates are difficult to estimate because such mortality induces a progressive bias in mean length-at-age (if the largest larvae in an age-class survive better than the smallest, the apparent growth rate is positively biased; Methot and Kramer 1979). This problem can be circumvented with IMMAGE by estimating the size-selected length-frequency distribution using a length-based population model (Somerton and Kobayashi 1990) which mimics the growth and survival of individual members of an age-class over time. Using such an approach, the likelihood of size-dependent mortality could be tested against constant or age-dependent mortality based on goodness-of-fit to the observed length-frequencies.

Several variations on the application of IMMAGE described herein may be more appropriate in other cases. First, the estimation of growth and mortality parameters could be accomplished simultaneously rather than separately by allowing the mortality process model to include growth parameters as variables rather than as known quantities. Second, the objective function used for parameter estimation could be specified as a likelihood function rather than a sum-of-squares function. This would be especially appropriate in cases where the errors about the observed length-frequencies are not normally distributed. Third, prior estimates of some parameters could be included in the growth and mortality process models rather than estimating all parameters directly from the three samples (i.e., ageing, length-frequency, and selection samples).

We believe the best way of estimating parameter variances for an IMMAGE application is to use a sample reuse technique known as boot-strapping (Efron and Tibshirani 1991), because all sources of sampling variability can be included. Boot-strapping IMMAGE, however, is computationally intensive and potentially time-consuming. To facilitate variance estimation on slow computers, we have therefore included in the IMMAGE program an approximate technique that is based on the inverse of the information matrix (Ratkowsky 1983).

When obtaining larval fish samples free of selection bias is difficult, IMMAGE can still obtain unbiased estimates of growth and mortality parameters. Not only does IMMAGE provide estimates that are more accurate and precise than other approaches, its greater flexibility in form allows estimation of length-dependent mortality rates that are perhaps biologically more realistic than the constant rates now estimated.

Acknowledgments

We thank George Boehlert, Ed DeMartini, Chyan Huei Lo, Sue Picquelle, and Tim Ragen for reviewing the manuscript and offering helpful suggestions. In addition, we thank Rick Methot who gave us the original idea of the inverse estimation procedure.

Citations

Bailey, K.M.
1982 The early life history of Pacific hake *Merluccius productus*. Fish Bull., U.S. 80:589–598.

Efron, B., and R. Tibshirani
1991 Statistical analysis in the computer age. Science (Wash. DC) 253:390–395.

Essig, R.J., and C.F. Cole
1986 Methods of estimating larval fish mortality from daily increments in otoliths. Trans. Am. Fish. Soc. 115:34–40.

Houde, E.D.
1977 Abundance and potential yield of the round herring, *Etrumeus teres*, and aspects of its early life history in the eastern Gulf of Mexico. Fish. Bull., U.S. 75:61–89.

Laroche, J.L., S.L. Richardson, and A.A. Rosenberg
1982 Age and growth of a pleuronectid, *Parophrys vetulus*, during the pelagic larval period in Oregon coastal waters. Fish. Bull., U.S. 80:93–104.

Leak, J.C., and E.D. Houde
1987 Cohort growth and survival of bay anchovy *Anchoa mitchilli* larvae in Biscayne Bay, Florida. Mar. Ecol. Prog. Ser. 37:109–122.

Lenarz, W.
1972 Mesh retention of larvae of *Sardinops caerulea* and *Engraulis mordax* by plankton nets. Fish. Bull., U.S. 70: 789–798.

Lo, N.
1986 Modeling life-stage-specific instantaneous mortality rates, an application to northern anchovy *Engraulis mordax* eggs and larvae. Fish. Bull., U.S. 84:395–407.

Lough, R.G., M. Pennington, G.R. Bolz, and A.A. Rosenberg
1982 Age and growth of larval Atlantic herring, *Clupea harengus*, in the Gulf of Maine–Georges Bank region based on otolith growth increments. Fish. Bull., U.S. 80:187–199.

Mesnil, B., and J.G. Shepherd
1990 A hybrid age- and length-structured model for assessing regulatory measures in multiple-species, multiple-fleet fisheries. J. Cons. Cons. Int. Explor. Mer 47:115–132.

Methot, R.D.
1989 Synthetic estimates of historical abundance and mortality for northern anchovy. *In* Edwards, E.F., and B. Megrey (eds.), Mathematical analysis of fish stock dynamics, p. 66–82. Am. Fish. Soc. Symp. 6, Bethesda.
1990 Synthesis model: An adaptable framework for analysis of diverse stock assessment data. *In* Low, L.L. (ed.), Proceedings, Symposium on application of stock assessment techniques to gadids, p. 259–277. Int. North Pac. Fish. Comm. Bull. 50.

Methot, R.D., and D. Kramer
1979 Growth of northern anchovy larvae, *Engraulis mordax*, in the sea. Fish. Bull., U.S. 77:413–423.

Morse, W.W.
1989 Catchability, growth and mortality of larval fish. Fish. Bull., U.S. 87:417–446.

Murphy, G.I., and R.I. Clutter
1972 Sampling anchovy larvae with a plankton purse seine. Fish. Bull., U.S. 70(3S):789–798.

Pepin, P.
1991 Effect of temperature and size on development mortality and survival of marine fish. Can. J. Fish. Aquat. Sci. 48: 503–518.

Ratkowsky, D.A.
1983 Nonlinear regression modeling. Marcel Dekker, NY, 276 p.

Ricker, W.E.
1975 Computation and interpretation of biological statistics of fish populations. Bull. Fish. Res. Board Can. 191, 382 p.

Somerton, D.A., and D.R. Kobayashi
1989 A method for correcting catches of fish larvae for the size selection of plankton nets. Fish. Bull., U.S. 87:447–455.
1990 Robustness of the Wetherall length-based method to population disequilibrium. Fish. Bull., U.S. 89:307–314.

Thorrold, S.
1988 Estimating some early life history parameters in a tropical clupeid, *Herklotsichthys castelnaui*, from daily growth increments in otoliths. Fish. Bull., U.S. 87:73–83.

Ware, D.M., and T.C. Lambert
1985 Early life history of Atlantic mackerel (*Scomber scombrus*) in the southern Gulf of St. Lawrence. Can. J. Fish. Aquat. Sci. 42:577–592.

Warlen, S.M.
1988 Age and growth of larval gulf menhaden, *Brevoortia patronsis*, in the northern Gulf of Mexico. Fish. Bull., U.S. 86:77–90.

Yoklavich, M.M., and K.M. Bailey
1990 Hatching period, growth and survival of young walleye pollock *Theragra chalcogramma* as determined from otolith analysis. Mar. Ecol. Prog. Ser. 64:12–23.

Zweifel, J., and P. Smith
1981 Estimates of abundance and mortality of larval anchovies (1951–75): Application of a new method. Rapp. P.-V. Réun. Cons. Int. Explor. Mer 178:248–259.

Seasonal distribution of river herring *Alosa pseudoharengus* and *A. aestivalis* off the Atlantic coast of Nova Scotia

Heath H. Stone
Brian M. Jessop

Department of Fisheries and Oceans, Biological Science Branch
P.O. Box 550, Halifax, Nova Scotia B3J 2S7, Canada

Abstract.—The seasonal distribution and relative abundance of river herring *Alosa pseudoharengus* and *A. aestivalis* off Nova Scotia is examined using Canadian Department of Fisheries and Oceans data from bottom-trawl surveys (1970–89) and the International Observer Program (1980–89). River herring occurred throughout the year in regions characterized by strong tidal mixing and upwelling in the Bay of Fundy and off southwestern Nova Scotia. During spring, river herring were most abundant in the warmer, deeper waters of the central Scotian Shelf, particularly between Emerald and Western Banks, and in areas of warm slope water intrusion along the Scotian Slope, the western and southern edges of Georges Bank, and in the eastern Gulf of Maine–Bay of Fundy. Most catches occurred at bottom temperatures of 7–11°C offshore at mid-depths in spring (101–183 m), in shallower nearshore waters in summer (46–82 m) and in deeper offshore waters in fall (119–192 m). Diel variation in catch occurred during summer and fall but not during spring, with largest catches during daylight. Seasonal distribution patterns of small (<19 cm FL) and large (>19 cm FL) river herring overlapped geographically. Small fish preferred shallow regions (<93 m) during spring and fall, while large fish occurred in deeper areas (>93 m) during all seasons. The temporal and spatial distribution of river herring off the coast of Nova Scotia is likely influenced by zooplankton concentrations and occurrence of bottom temperatures >5°C. The pattern of seasonal movement is generally inshore and northward during spring, and offshore and southward in the fall.

Manuscript accepted 6 March 1992.
Fishery Bulletin, U.S. 90:376–389 (1992).

River herring (a collective term for the alewife *Alosa pseudoharengus* and the blueback herring *A. aestivalis*) are anadromous clupeids native to the Atlantic coast of North America. These closely-related species are remarkably similar in morphology and life history and differ only slightly in terms of meristics, morphometrics, growth parameters and time of spawning (Bigelow and Schroeder 1953, Leim and Scott 1966, Messieh 1977, Loesch 1987). Alewives and blueback herring are sympatric; alewife range from Newfoundland to North Carolina, and blueback herring from the Gulf of St. Lawrence to Florida (Bigelow and Schroeder 1953). They are fished commercially in the Maritime provinces of Canada and Atlantic coastal United States during their spring spawning migrations and are often marketed together as alewife, gaspereau, or river herring, depending on local convention.

Both species often co-occur in freshwater (Loesch et al. 1982, Jessop and Anderson 1989), estuarine (Stone and Daborn 1987), and marine (Neves 1981) habitats. While the freshwater life histories of alewives and blueback herring have been well documented (reviewed by Loesch 1987), less information is available on their distribution and movements at sea, particularly in Canadian coastal areas. Off the Atlantic coast of Nova Scotia, bottom trawls have caught river herring on the western Scotian Shelf, with alewives collected during spring and fall (Vladykov 1936, Neves 1981, Vinogradov 1984) and blueback herring in spring and summer (Netzel and Stanek 1966, Neves 1981). In the inner Bay of Fundy, river herring aggregate during summer in the turbid estuarine waters of Minas Basin (Rulifson 1984, Stone and Daborn 1987) and Cumberland Basin (Dadswell et al. 1984). In the outer Bay of Fundy, alewives and blueback herring have been captured during summer and autumn in herring weirs, purse seines (Jessop 1986), and during bottom-trawl surveys (Neves 1981). Neves (1981) examined the marine distribution and seasonal movements of river herring along the continental shelf from Cape Hatteras, North Carolina, to southwestern Nova Scotia. In this paper, we describe the seasonal marine distribution and relative abundance of river herring off Nova Scotia based on 20 years of combined alewife and blueback herring catch data from Canadian research vessel surveys, thereby extending northward the analysis by Neves (1981) of their distribution off the Atlantic coast of the United States. Offshore distributions are interpreted in relation to water depth and temperature within the survey area.

Although marine exploitation of alewives and blueback herring in the Maritime provinces by incidental

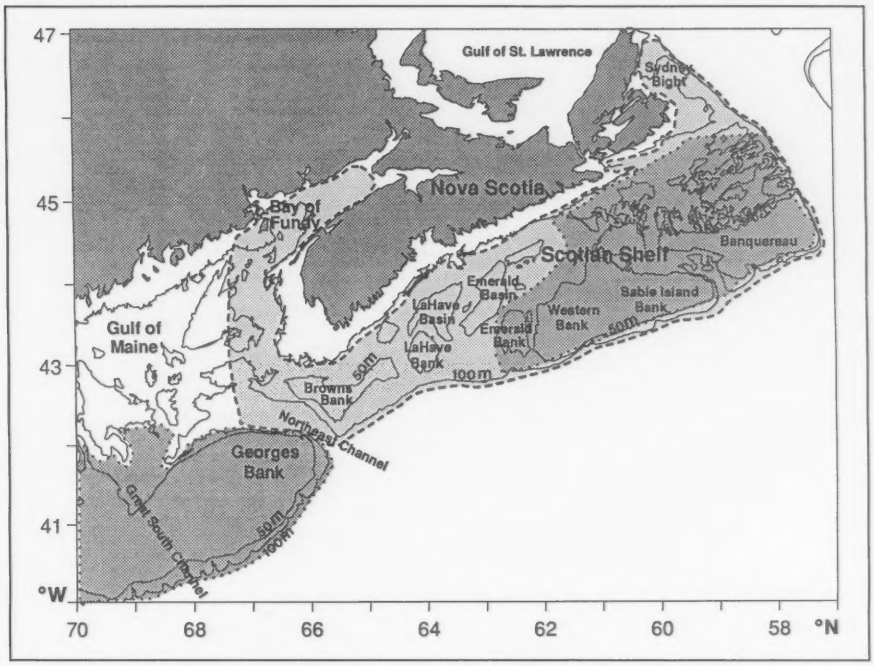

Figure 1
Topographical map of Canadian groundfish survey areas (1970–89) and geographic features mentioned in text. Spring (1979–85), summer (1970–89), and fall (1978–84) survey coverage of the Scotian Shelf and Bay of Fundy (- - -) is shaded light-gray. Spring (1986–89) survey coverage of the eastern shelf and Georges Bank (. . .) is shaded dark-gray. Offshore banks are delineated by the 100 m depth contour; basins and the outer edge of the continental shelf are delineated by the 200 m depth contour.

catches in offshore bottom-trawl fisheries from 1984 to 1989 has averaged 1,400 t, which is <17% of the freshwater exploitation (Statistics Branch, Dep. Fish. Oceans, P.O. Box 550, Halifax, Nova Scotia B3J 2S7), only a limited amount of information on marine distribution is available from commercial fishing operations. More comprehensive information comes from the bycatch of the annual bottom trawl surveys of the Scotian Shelf–Bay of Fundy region conducted by the Canadian Department of Fisheries and Oceans (DFO) to monitor temporal changes in the abundance of commercially exploited groundfish species and associated environmental conditions (Halliday and Koeller 1981). Additional information on river herring distribution was obtained from 10 years of bycatch data from foreign and domestic fishing operations compiled by the DFO International Observer Program.

Description of survey area

The survey area, which includes the Scotian Shelf, eastern Gulf of Maine, Bay of Fundy, and, recently, Georges Bank, is topographically and hydrographically complex (Fig. 1). The oceanographic and biological characteristics of this area influence the distribution of other species (Sinclair 1988) and are assumed to do so for river herring.

The Scotian Shelf is characterized by deep central basins (>200 m) and shallow offshore banks (<50 m). Over the deeper parts of the shelf, three distinct vertical layers occur: a surface mixed layer with seasonal temperature changes, an intermediate layer with temperatures <5°C regardless of season, and a warm bottom layer derived from cross-shelf intrusions of slope water (Hatchey 1942, Smith et al. 1978). The coldest water at any depth occurs in the northeastern Shelf and the warmest in the bottom waters of the central Shelf (also termed the Scotian Gulf) where intrusion of warm slope water to adjacent Emerald and LaHave Basins is a persistent feature (McLellan 1954). Nutrient-rich upwellings along the shelf-slope interface sustain high levels of biological productivity (Fournier et al. 1977). Consequently, pelagic fish production on the shelf-slope is much higher than on the shelf (Mills and Fournier 1979).

The Bay of Fundy and eastern Gulf of Maine regions are vertically well mixed due to the action of strong tidal currents (Greenburg 1984). Strong, persistent summertime fronts in sea-surface temperature occur near the mouth of the Bay and off southwestern Nova Scotia (Loder and Greenburg 1985). The upwelling of nutrient-rich deep water from the Gulf of Maine and Scotian Shelf supports high biological productivity during spring and summer (Fournier et al. 1984). Secondary production in the outer Bay of Fundy occurs

Table 1

Summary of river herring (*Alosa* spp.) catch (in numbers) and effort for spring, summer, and fall groundfish surveys conducted off Nova Scotia by the Canadian Department of Fisheries and Oceans, 1970–89. Parentheses enclose percentages of total numbers of sets containing catch. SD = sample standard deviation.

Season	Year	No. of surveys	No. of sets	Catch-per-set $\bar{x}$	Catch-per-set SD	Total no. of fish	Sets with catch
Spring (Feb–Apr)	1979–89	11	1231	6.6	73.85	8117	268 (21.8)
Summer (June–July)	1970–89	20	1892	2.0	18.05	3703	214 (11.3)
Fall (Sept–Dec)	1978–84	7	982	1.6	9.47	1537	120 (12.3)
Total	1970–89	38	4105	3.3	42.53	13357	602 (14.7)

predominantly within the water column and provides forage to pelagic fish species (Emerson et al. 1986).

On Georges Bank, frontal regions generated by tidal mixing along the northern and southern edges are highly productive due to advection of nutrients from deeper waters on both sides of the bank (Cohen et al. 1982). Intrusions of warm, saline slope water occur into the southern Gulf of Maine through the Great South Channel (Mountain et al. 1989) and the Northeast Channel (Ramp and Wright 1979).

Materials and methods

Survey design and sampling

River herring catch and length-frequency data were obtained from 38 bottom-trawl surveys conducted between 1970 and 1989 (Table 1). The main study area (Scotian Shelf, eastern Gulf of Maine, and Bay of Fundy; Fig. 1) was surveyed at least once annually during this period. A single summer (June–July) survey was conducted annually between 1970 and 1977; spring (February–April), summer, and fall (September–December) surveys were made from 1978 to 1984; and spring and summer surveys from 1985 to 1989. Changing research requirements shifted spring survey effort to Georges Bank and the eastern Scotian Shelf in 1986, thereby excluding the western shelf region and the Bay of Fundy (Fig. 1). Recent (1987–89) summer surveys also included some coverage of northeastern Georges Bank.

All surveys used a stratified random design with trawl stations allocated to depth strata in proportion to stratum area and randomly positioned within strata. Stratum depth ranges were 0–92 m (0–50 fm), 93–183 m (51–100 fm), and 184–366 m (101–200 fm). Before 1981, summer cruises used a No. 36 Yankee bottom trawl with a 10 mm stretched-mesh liner in the cod end; all other cruises used a Western IIA trawl with a 10- or 20 mm stretched-mesh liner. Tows at each sampling station were for 30 minutes. Halliday and Koeller (1981) and Smith (1988) give further details of Canadian groundfish survey methods.

Total number and weight (kg) of river herring in the catch were recorded for each tow as was bottom-water temperature (°C), tow deployment time (Atlantic Standard Time), latitude, longitude, and bottom depth (m). Fork lengths (FL) were measured (to nearest cm) for all fish in catches of <250 fish; otherwise, catches were subsampled (no fixed procedure) for length. Alewife and blueback herring were not differentiated and sex was not determined.

Catches of river herring in Canadian surveys probably consist mainly of alewives since both species tend to be vertically separated by depth. Blueback herring frequent upper levels; alewives frequent mid-depths (Neves 1981) where they are more available to capture in bottom-trawl gear. All of the river herring catch from 1990 spring and summer groundfish surveys (n 1048) were confirmed by examination to be alewives. However, because river herring were not identified to species during the 1970–89 surveys, upon which our analysis is based, we cannot exclude the possibility that the catch included a small proportion of blueback herring captured incidentally when setting or hauling the gear.

Data analysis

Catch-per-set was standardized to a tow length of 1.75 nm with no adjustment for differences between gear types. Only cruises with catches of one or more fish were analyzed; 17 cruises on the eastern Scotian Shelf with no catches were omitted. River herring >33 cm FL were excluded from the data set (<0.5% of all fish measured), since they exceed the maximum fork lengths recorded for alewife and blueback herring (Loesch 1987) and are believed to be incorrectly identified American shad *Alosa sapidissima*.

Seasonal distributions of relative abundance were obtained from plots of average catch-per-set data (including zero catches) aggregated by 20-minute rectangles of latitude and longitude. Seasonal, rather than monthly, distributions gave a more complete picture of offshore distribution patterns. The locations of 2, 5, and 10°C isotherms, generated from plots of the mean bottom-water temperature in 20-minute rectangles, were superimposed on seasonal distribution plots. Differences in the seasonal distribution of two size-groups of river herring (i.e., ≤19 cm and >19 cm FL) were examined by plotting the capture locations of each group. The size-at-first-spawning of Saint John River blueback herring (Jessop et al. 1982), which mature at a smaller size than alewife, was used as the separation criterion.

Approximate randomization tests, with 1000 permutations (Edgington 1987) were used to examine the following relationships: (a) effects of season (spring, summer, fall) and depth (<93 m, 93–183 m, >183 m) on mean catch-per-set (including sets with no catches), (b) diel variability in seasonal catch-per-set (day and night, based on gear deployment times in relation to monthly morning and evening civil twilight times for the appropriate geographic location), and (c) mean fork length by season and depth. All comparisons used catch or fork-length data from a 6-year time-series (1979–84) in which annual sampling occurred during spring, summer, and fall. Each dependent comparison (i.e., depth effect within season, season effect within depth), used a Bonferroni significance level (α 0.05, divided by the number of dependent comparisons) (Day and Quinn 1989).

Randomization procedures were used for the analysis because statistically significant heteroscedasticity in the variances of (a) transformed ($\ln X+1$) catch per set data by season and depth (Cochran's $C=0.372$, $P<0.0001$, df 239, 9), (b) transformed ($\ln X+1$) diel catch-per-set by season (Cochran's $C=0.365$, $P<0.0001$, df 359, 6), and (c) fork length by season and depth (Cochran's $C=0.293$, $P<0.0001$, df 637, 9) violates an assumption of parametric statistics. This violation is compounded by unequal sample sizes.

Bycatch data

Set locations and fork lengths of river herring bycatch in foreign and domestic commercial groundfish operations (1980–89) obtained from the DFO International Observer Program database were compared with research survey data. Catch locations were plotted for spring (February–May) and summer (June–August), when fishing effort and bycatch were highest. Fork length distributions were truncated at 33 cm due to assumed misclassification (4% of fish measured exceeded this length). Annual landings of alewife in metric tons (t) for the Scotian Shelf–Bay of Fundy region (4VWX) from 1970 to 1989 were obtained from Northwest Atlantic Fisheries Organization (NAFO) Statistical Bulletins and correlated (Spearman rank) with catch indices from research vessel surveys. The analysis was conducted to determine if survey indices (i.e., mean number and mean weight per set · season^{-1} · year^{-1}) were consistent with bycatch landings as an indicator of relative abundance.

Results

Seasonal distribution and abundance

A total of 13,357 river herring were captured in 602 (15%) of 4105 bottom-trawl sets conducted between 1970 and 1989 (Table 1). Spring survey catches were the highest and most variable, followed by summer. The proportion of sets with river herring from spring surveys was nearly double that from the other two seasons. A maximum catch of 2292 river herring occurred on 17 March 1980 in the Scotian Gulf region, south of Emerald Basin.

During spring surveys, river herring dominated in three regions: the Scotian Gulf, southern Gulf of Maine, and off southwestern Nova Scotia from the Northeast Channel north to the central Bay of Fundy (Fig. 2). Catches also occurred along the southern edge of Georges Bank and in the canyon between Banquereau and Sable Island Banks. Relative abundance was highest in the Scotian Gulf between Emerald and Western Banks, and on the southern slope of Georges Bank. Most catches of river herring occurred where bottom temperatures exceeded 5°C (Fig. 2), although in the Bay of Fundy, captures occurred at lower temperatures.

Summer distributions of river herring were less extensive than in spring and were limited mainly to the eastern Gulf of Maine (off southwestern Nova Scotia) and the Bay of Fundy, with a few occurrences nearshore in the central Shelf region (Fig. 2). Catches were highest along the northern shore of the Bay of Fundy, with very few fish captured in the Scotian Gulf and on the eastern Scotian Shelf. Bottom temperatures exceeded 5°C at all capture locations.

Fall distributions of river herring were more extensive than in summer (Fig. 2). Moderate to large catches were obtained from southwestern Nova Scotia to the Bay of Fundy, the central Scotian Shelf, and Sydney Bight. As in the case of spring and summer surveys, very few fish were captured on the eastern half of the Scotian Shelf. All catches occurred at bottom temperatures exceeding 5°C.

Bycatch of river herring from foreign fishing fleets (1980–89) occurred mainly during spring in a narrow

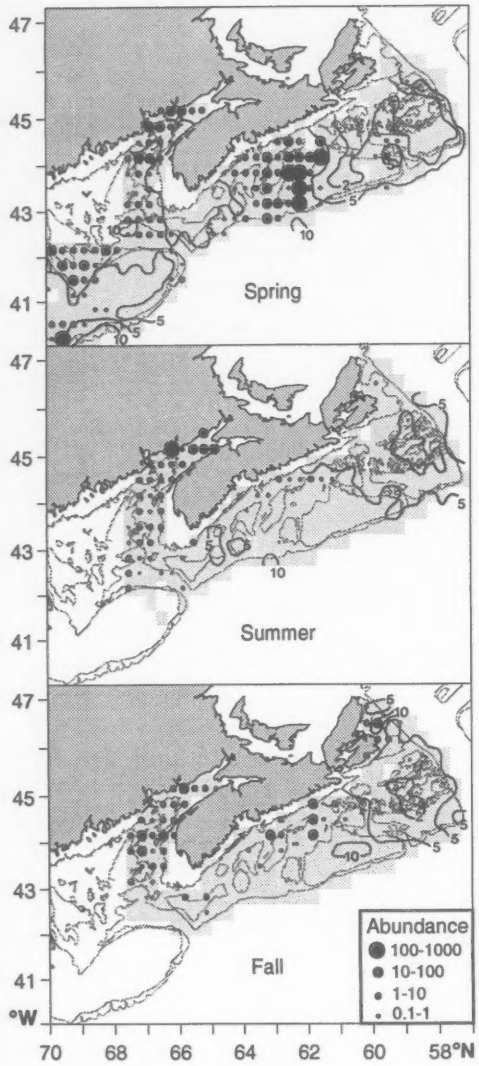

Figure 2

Distribution and relative abundance ($\bar{x}$ catch per 20-min square) of river herring from spring (1979–89), summer (1970–89), and fall (1978–84) groundfish surveys conducted off the Atlantic coast of Nova Scotia. Area sampled is indicated by shading, and mean catch (n/tow) for each 20-min square is represented by a solid circle, scaled to catch level. Isotherms for 2, 5, and 10°C of bottom temperature are also indicated.

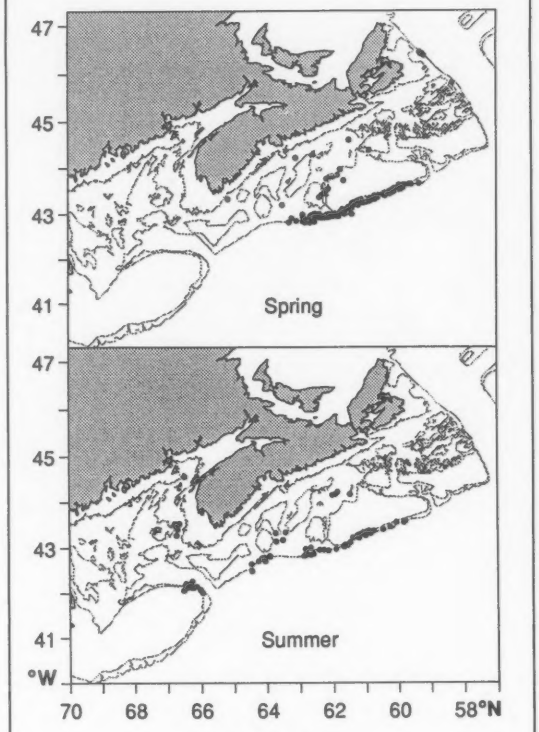

Figure 3

Spring and summer set locations of river herring bycatch from foreign and domestic fishing operations on the Scotian Shelf recorded by Canadian International Observers, 1980–89.

band along the edge of the Scotian Shelf from Emerald Bank east to Sable Island Bank (Fig. 3). This distribution reflects the location of the Soviet and Cuban silver hake fishery (M. Showell, Bedford Inst. Oceanogr., Dartmouth, N.S. B2Y 4A2, pers. commun., Jan. 1991) and indicates a more widespread occurrence of river herring along the shelf break than was apparent from bottom-trawl surveys. Bycatch from domestic fishing operations during spring occurred on the edge of Western and Emerald Banks and corresponds with catch locations from spring groundfish surveys.

Summer bycatch locations were similar to spring but extended further south and west along the shelf edge, with clusters of catches on the northern edge of Georges Bank, off southwestern Nova Scotia, and in the mouth of the Bay of Fundy (Fig. 3). River herring distribution along the shelf break, as indicated from spring and summer bycatches in the silver hake fishery, reflects the spatial distribution of that fishery. The number of summer observations from a reduced foreign fishing effort (n 86) was much less than spring (n 460). In both seasons, most bycatches occurred in

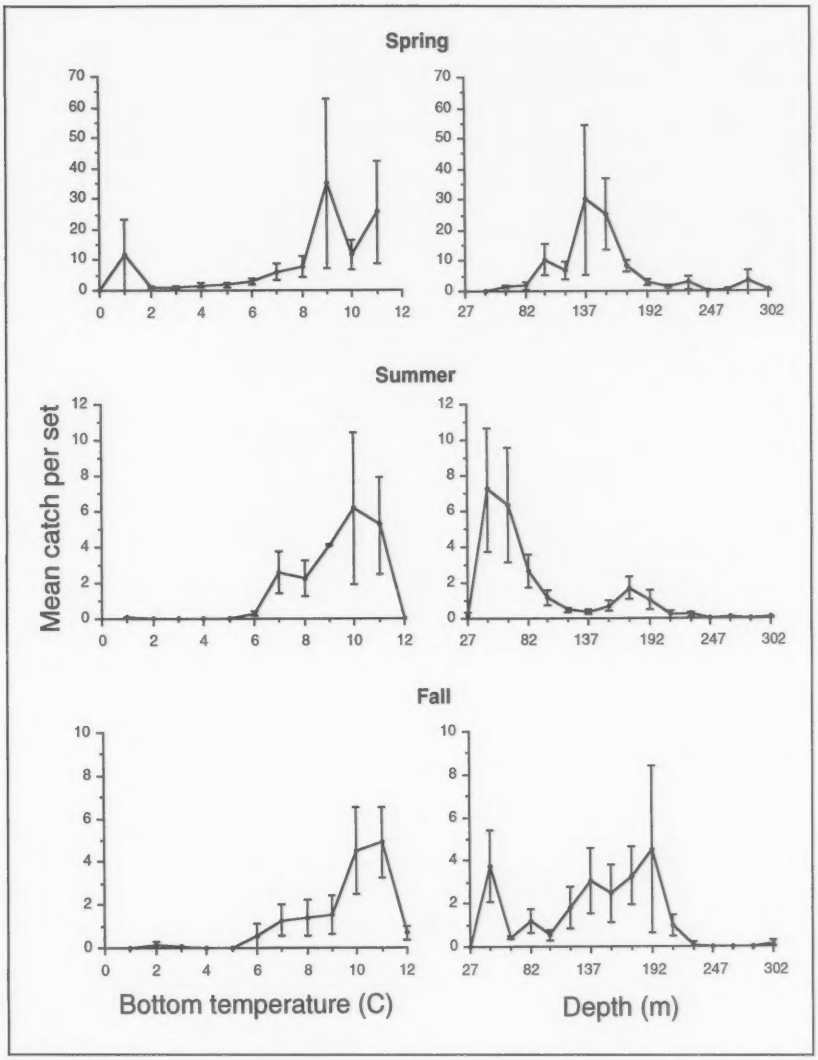

Figure 4
Mean catch-per-set of river herring within 1°C intervals of bottom temperature and 18.2 m (10 fm) depth intervals from spring, summer, and fall groundfish surveys, 1979–84, conducted off the Atlantic coast of Nova Scotia. Vertical bars represent ±1 SE. Sample sizes are ⩾10 sets for each temperature and depth interval.

regions where bottom temperatures from groundfish surveys exceeded 5°C.

Temperature, depth, and diel effects on catch

The relationship between catch, bottom temperature, and depth was examined by plotting mean catch-per-set by season for intervals of 1°C and 18.3 m (10 fm) (Fig. 4). Despite much variability in the data, most catches occurred within the 7–11°C range regardless of season, with maximum catches within 9–11°C from spring through fall. An exception is the moderate catches at bottom temperatures <2°C during spring surveys in the Bay of Fundy (Figs. 2 and 4). The depth distribution of catches was more variable; spring catches occurred mainly at intermediate depths of 101–174 m, summer catches in shallow areas (46–82 m), and fall catches at mixed depths (i.e., 46 m, 119–192 m).

Mean catch-per-set of river herring for annual (1979–84) spring, summer, and fall surveys varied significantly by season and depth (Table 2, Fig. 5). Season effects within depth strata were significant for depths of <93 m and 93–183 m, but not for depths >183 m where all catches were low. Catches were highest within the <93 m strata during summer and within the 93–183 m depth strata during spring. Depth-within-season interaction was significant only during

Table 2

Summary of results from approximate randomization tests used to examine the following relationships: (a) effects of season and depth on mean catch-per-set, (b) diel variability in seasonal catch-per-set, and (c), mean fork length (FL) by season and depth. All comparisons used catch and fork-length data from Canadian groundfish surveys conducted 1979–84. Interaction effects with an asterisk are significant at the adjusted Bonferroni significance level of $P \leq 0.017$.

	Catch by season and depth		Catch by season and time		FL by season and depth	
Source	n	P	n	P	n	P
Main effects						
Season	2157	0.002	2157	0.006	5739	0.001
Depth	2157	0.010	—	—	5739	0.001
Time	—	—	2157	0.80	—	—
Interactions						
Season effect within depth						
<93 m	800	0.008*	—	—	1564	0.001*
93–183 m	836	0.001*	—	—	3769	0.001*
>183 m	521	0.027	—	—	406	0.001*
Depth effect within season						
spring	788	0.002*	—	—	3807	0.001*
summer	565	0.028	—	—	1114	0.001*
fall	804	0.060	—	—	818	0.001*
Season effect within time						
day	—	—	1231	0.228	—	—
night	—	—	926	0.033	—	—
Time effect within season						
spring	—	—	788	0.043	—	—
summer	—	—	565	0.001*	—	—
fall	—	—	804	0.017*	—	—

spring when the range in catches was greatest; summer and fall catches were similar at all depths (Table 2).

Mean catch-per-set of river herring varied significantly by season but not by time-period (Table 2, Fig. 6). Interactions of season effect within time-period were nonsignificant for day and night; interactions of time effect within season were significant for summer and fall but not for spring. For summer and fall surveys, catches from sets conducted during daylight were significantly higher than those conducted at night. While night catches from spring surveys tended to be higher than day catches (but not significantly so), they were extremely variable ($\bar{x}$ 13.4, sample SD 131.32). The proportion of sets with catch during day and night showed a seasonal pattern similar to that for mean catch, i.e., similar in spring (20% vs. 24%) and higher during the day in summer (15% vs. 5%) and fall (16% vs. 9%).

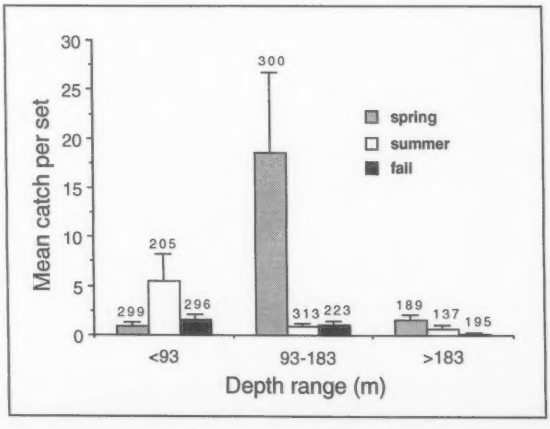

Figure 5

Mean catch-per-set of river herring by depth strata from spring, summer, and fall groundfish surveys, 1979–84, conducted off the Atlantic coast of Nova Scotia. Vertical bars represent +1 SE. Number of tows is indicated above error bars.

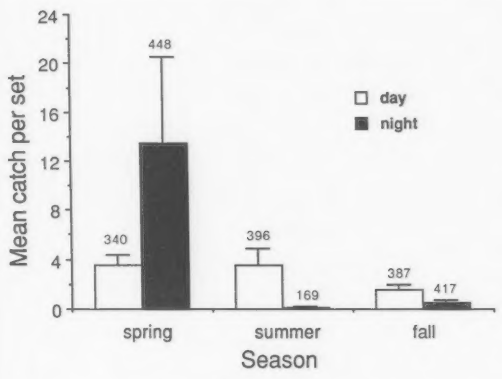

Figure 6

Mean catch-per-set of river herring in day and night collections from spring, summer, and fall groundfish surveys, 1979–84, conducted off the Atlantic coast of Nova Scotia. Vertical bars represent +1 SE. Number of tows is indicated above error bars.

Survey catch indices and NAFO landings

Seasonal catch indices (annual mean number and weight of river herring per set) from research vessel surveys were uncorrelated with NAFO bycatch data for the Scotian Shelf–Bay of Fundy area (4VWX) (Table 3). However, landings from the central and eastern shelf (4VW) were significantly correlated with spring (1979–89) survey indices. The relationship between mean weight index and 4VW NAFO landings (Fig. 7) gave the highest Spearman rank correlation coefficient (r_s 0.74).

Table 3

Spearman rank correlation coefficients for river herring (*Alosa* spp.) catch indices from spring (1979–89), summer (1970–89), and fall (1978–84) groundfish surveys vs. NAFO landings from the Scotian Shelf–Bay of Fundy (4VWX) and the central and eastern Scotian Shelf (4VW). (n = number of years; * significant at $P<0.05$; ** significant at $P<0.01$).

NAFO areas	Spring (n 11)	Summer (n 20)	Fall (n 7)
Mean catch/set · yr^{-1}			
4VWX	−0.23	−0.15	−0.07
4VW	0.60*	−0.01	−0.18
Mean weight/set · yr^{-1}			
4VWX	−0.19	−0.17	−0.29
4VW	0.74**	−0.05	−0.09

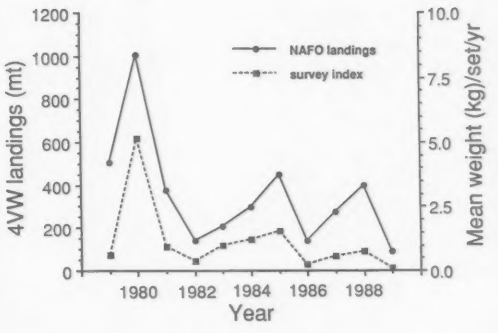

Figure 7

Annual landings in metric tons (t) reported to the Northwest Atlantic Fisheries Organization for the central and eastern Scotian Shelf (4VW), and spring survey catch index (kg/set · yr^{-1}) for 1979–89.

Seasonal length-composition and distribution

River herring from bottom-trawl collections measured 5–33 cm FL ($\bar{x}$ 23.7 cm; Table 4). Mean fork length in spring catches was less than in summer or fall. Fork lengths of river herring from foreign and domestic fisheries were 22–33 cm ($\bar{x}$ 29.6 cm) and were of comparable size in spring and summer sample collections. The larger size of bycatch fish compared with those from bottom-trawl surveys is probably due to the larger cod end mesh size (6 cm stretched) of commercial gear permitting escapement of smaller fish.

In all seasons, large river herring (>19 cm FL) were more abundant than small (≤19 cm) fish (Fig. 8). Polymodal length-frequency distributions indicated the

Table 4

River herring (*Alosa* spp.) fork-length statistics by season from groundfish surveys conducted by the Canadian Department of Fisheries and Oceans and from foreign and domestic bycatches recorded by Canadian International Observers. All fork lengths were truncated at 33 cm (see 'Materials and methods' for explanation). SD = sample standard deviation.

Season	Years	Fork length (cm) n	$\bar{x}$	SD	range
Groundfish survey data					
Spring (Feb–Apr)	1979–89	7543	22.7	5.08	5.0–33.0
Summer (June–July)	1970–89	3167	25.4	3.77	9.0–33.0
Fall (Sept–Dec)	1978–84	1512	24.8	4.92	5.0–33.0
Combined	1970–89	12213	23.7	4.91	5.0–33.0
Bycatch data					
Spring (Feb–May)	1980–89	1754	29.4	2.14	20.0–33.0
Summer (June–Aug)	1980–89	249	30.4	1.45	26.0–33.0
Combined	1980–89	2032	29.6	2.13	20.0–33.0

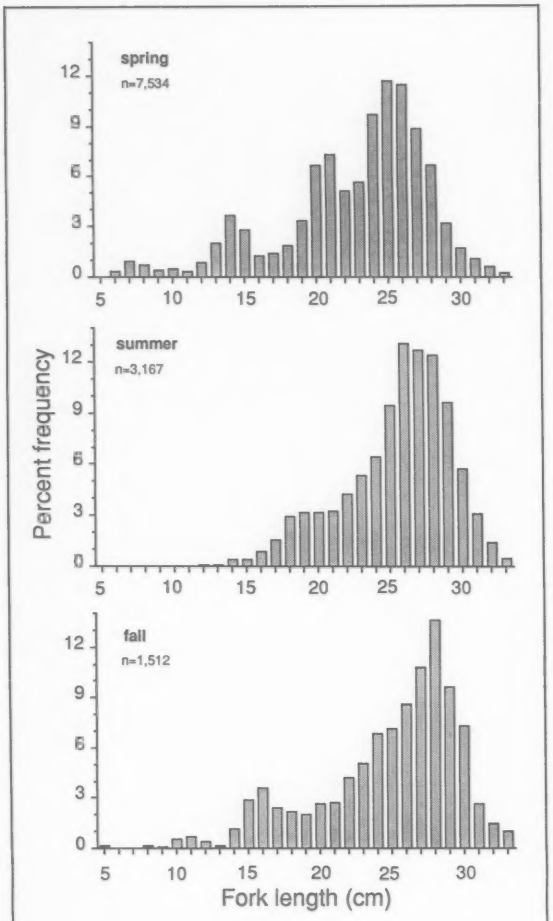

Figure 8
Length-frequency distributions of river herring from spring (1979–89), summer (1970–89), and fall (1978–84) groundfish surveys conducted off the Atlantic coast of Nova Scotia.

presence of at least three year-classes in the fall and four in the spring. Smaller individuals (≤19 cm FL) represented a larger proportion of the overall length composition in spring and fall than in summer.

River herring >19 cm FL were more densely and extensively distributed in all seasons than smaller fish. During summer and fall, most river herring ≤19 cm long were captured within the Bay of Fundy, although a few occurred in the central Shelf region and in Sydney Bight (fall only) (Fig. 9). The greatest overlap in the spatial distribution of both size-groups was during spring, especially in offshore regions (i.e., central Scotian Shelf, southern Gulf of Maine).

The mean fork length of trawl-caught (1979–84) river herring varied significantly by season of capture and depth (Table 2, Fig. 10). Interactions of season effect within depth strata and depth effect within season were all significant. Smaller fish were caught more frequently at depths <93 m during spring and fall. Larger fish occurred at all depths during summer (more numerously at <93 m depth) and at depths ≥93 m during spring and fall. In all three depth strata, river herring from spring surveys averaged smaller in length than those captured in summer and fall because of the greater occurrence of fish ≤19 cm throughout the survey area during spring (Fig. 9).

Discussion

Canadian groundfish survey data indicate persistent patterns in the temporal and spatial distribution of river herring off the Atlantic coast of Nova Scotia which appear to be greatly influenced by oceanographic features. In spring, river herring were most abundant in the warmer, deeper waters of the Scotian Gulf, particularly along the edges of Emerald and Western Banks and within the channel separating them, and in regions of warm slope-water intrusion along the Scotian Slope, the western and southern edges of Georges Bank, and the eastern Gulf of Maine. In all seasons, river herring occurred in the Bay of Fundy and off southwestern Nova Scotia, regions characterized by strong tidal mixing and upwelling, but were rarely present on the eastern Scotian Shelf.

Water temperature evidently influences temporal and spatial patterns in river herring depth distribution. In all seasons, most catches occurred within the 7–11°C range but shifted from mid-depths offshore in spring (101–183 m) to shallower, nearshore waters in summer (46–82 m), and to deeper offshore waters in fall (119–192 m). River herring were not present in colder regions on the eastern and western Scotian Shelf. Catches of river herring along the U.S. continental shelf were most frequent at bottom temperatures of 4–7°C and depths <92 m (Neves 1981). Spring catches of river herring at bottom temperatures <5°C in the Bay of Fundy indicate some flexibility in thermal selection, as might be expected of a migratory anadromous fish. American shad, which are closely related to alewives and blueback herring, can remain for extended periods in temperatures outside their usual range (7–13°C) and migrate rapidly between areas with different temperature regimes (Dadswell et al. 1987).

Seasonal shifts in zooplankton abundance, which are influenced by local oceanographic features, may also influence river herring distribution patterns off Nova Scotia. Both alewives and blueback herring are zoo-

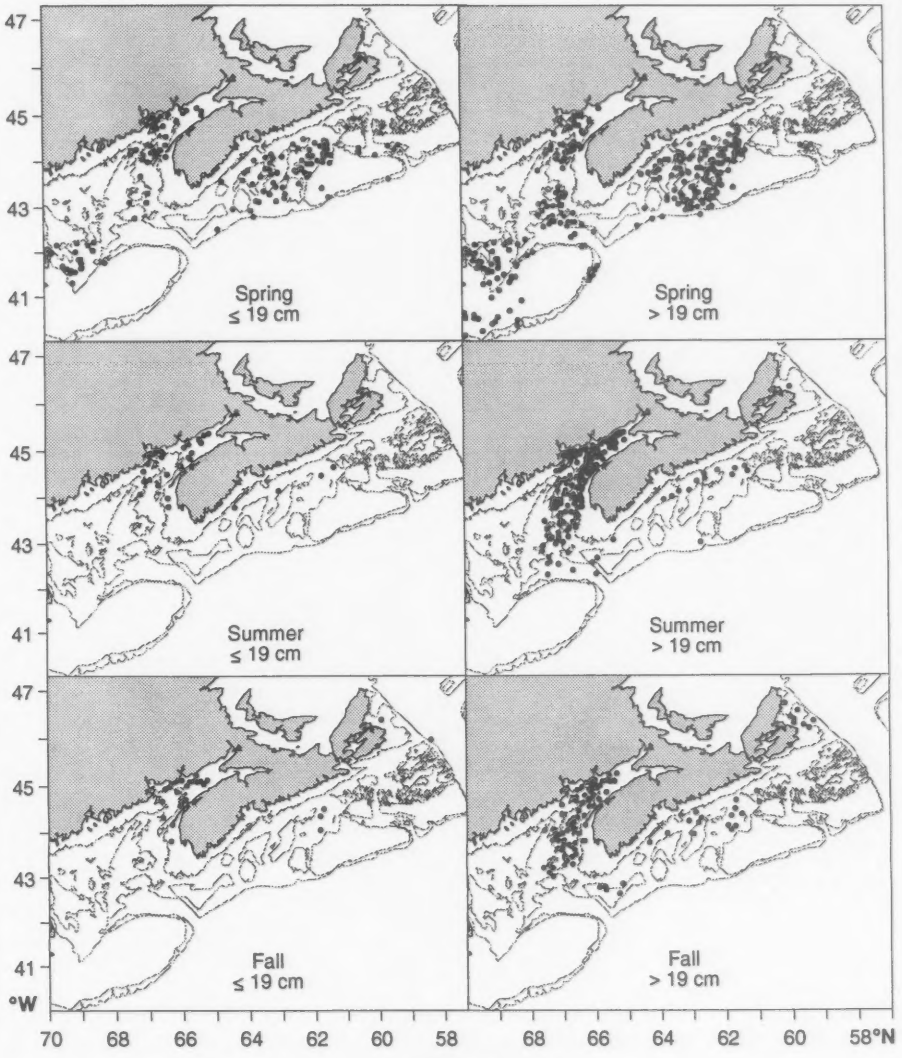

Figure 9

Set locations for catches of river herring ≤ 19 cm FL and > 19 cm FL from spring (1979–89), summer (1970–89), and fall (1978–84) groundfish surveys conducted off the Atlantic coast of Nova Scotia.

planktivores. Stomach contents of river herring collected on Georges Bank and the Scotian Shelf consisted mainly of euphausiids and calanoid copepods (Vinogradov 1984). These prey items are concentrated during winter and spring in deep basins of the Scotian Shelf (Sameoto and Herman 1989, Herman et al. 1991) as well as the outer Shelf and Shelf Slope (Sameoto 1982). Calanoid copepods dominate zooplankton production on Georges Bank during spring (Sherman et al. 1987) and are abundant during summer and fall in the eastern Gulf of Maine–outer Bay of Fundy region (Emerson et al. 1986) along with large populations of euphausiids (Kulka et al. 1982). Aggregations of river herring during spring on the central Shelf, Shelf Slope, and Georges Bank, during summer in the Bay of Fundy–eastern Gulf of Maine, and during fall in the

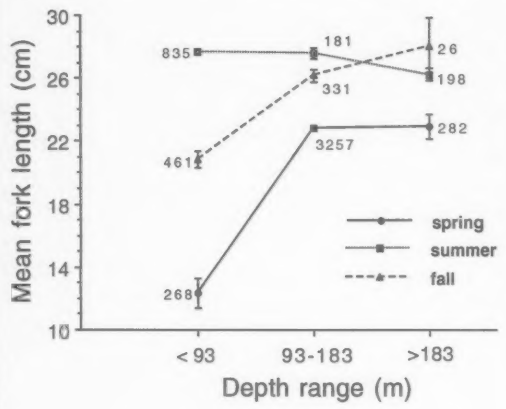

Figure 10

Mean fork length (cm) of river herring by depth strata from spring, summer, and fall groundfish surveys, 1979–84, conducted off the Atlantic coast of Nova Scotia. Vertical bars represent 95% CI. The number of fish in each category is adjacent to symbols.

outer Bay of Fundy and central Scotian Shelf coincide with high secondary productivity and an abundance of prey. River herring may move inshore in summer and offshore in winter in order to exploit seasonally available food resources.

The diurnal pattern of vertical migration by river herring accounts for the higher catches and proportion of sets with catches during daylight hours in summer and fall. Alewives and blueback herring that are closer to the bottom during the day are more susceptible to capture in bottom-trawling gear (Neves 1981, Loesch et al. 1982). Diel migrations, involving an upward movement at dusk followed by a downward movement at dawn, occur in landlocked adult alewives (Janssen and Brandt 1980), as well as anadromous juvenile (Jessop 1990) and adult river herring (Neves 1981). While spring catches did not follow this pattern, the presence of a cold (<5°C) intermediate water mass over warmer, deeper waters on the Scotian Shelf (Hatchey 1942), where the largest catches occurred, may have restricted the extent of vertical migration resulting in more captures at night. Our study indicates that few river herring are captured in areas where bottom temperatures are <5°C during spring; therefore, vertical migrations may be confined by a water temperature inversion.

Catch indices by number and weight from spring groundfish surveys (when relative abundance is greatest) both appear to be useful indicators of river herring bycatch in foreign and domestic trawl fisheries on the eastern and central shelf regions (4VW). Poor correlations, obtained when the Bay of Fundy–eastern Gulf of Maine bycatch landings (NAFO area 4X) were included in the analysis, were puzzling. Survey data indicate the presence of river herring in this area from spring through fall. Underreporting of river herring bycatches in domestic fishing operations (i.e., bottom trawl, gillnet, purse seine) may explain the poor correlations when landings from 4X and 4VW were combined. Catches from the central and eastern shelf region (4VW) are largely bycatches from the silver hake fishery. The frequent presence of DFO observers aboard these vessels may reduce the incidence of misreporting. Another possibility is the seasonal immigration of American-origin river herring into the Bay of Fundy–eastern Gulf of Maine region (Rulifson et al. 1987) which would increase the variability in the NAFO landings for area 4X.

The small proportion of fish ≤19 cm in summer collections, relative to spring and fall collections, may reflect their movement outside the survey area into coastal embayments and estuarine habitats in Maine and the inner Bay of Fundy. These areas serve as important summer feeding areas for river herring (Stone and Daborn 1987) and other anadromous fish species (Haedrich and Hall 1976). Summer resident river herring generally leave the inner Bay of Fundy in autumn when secondary production declines (Stone 1985).

Both large (>19 cm FL) and small (≤19 cm FL) river herring occurred nearshore from spring through fall, but were widely distributed offshore during spring (i.e., southern Gulf of Maine, Scotian Gulf). Most river herring ≤19 cm FL are sexually immature while those >19 cm FL are generally mature fish which have spawned previously or are maturing to spawn for the first time. Smaller, immature river herring evidently migrate offshore seasonally as do larger, mature fish. Size-related differences in depth distribution were such that small river herring occurred in shallow regions (<93 m) during spring and fall, while larger fish occurred in deeper areas (≥93 m) in all seasons. Janssen and Brandt (1980) reported that the nocturnal depth distribution of adult landlocked alewife differed by size-class, with the smaller fish at shallower depths.

Both Canadian and American marine survey data provide evidence of distinct seasonally and geographically separate aggregations of river herring. Off the Atlantic coast of the United States, the Middle Atlantic Bight is an important overwintering area for river herring, while in summer they concentrate further north in the Nantucket Shoals and on Georges Bank (Neves 1981). Aggregations of river herring in spring and fall on the central Scotian Shelf and in the eastern Gulf of Maine–Bay of Fundy suggest that these areas are important overwintering sites off Nova Scotia,

although the Scotian Shelf has not been surveyed during winter months (i.e., November–February). The main summer concentration extends northward from southwestern Nova Scotia into the Bay of Fundy.

Other members of the clupeid family also exhibit spatial and temporal discontinuity in marine distribution patterns. American shad winter off Florida, the mid-Atlantic Bight, and in the Scotian Shelf–Bay of Fundy region (Neves and Depres 1979, Dadswell et al. 1987), while summer concentrations occur off Newfoundland and Labrador (Hare and Murphy 1974), the inner Gulf of St. Lawrence (Dadswell et al. 1987), the Gulf of Maine (Neves and Depres 1979), and in the inner Bay of Fundy (Dadswell et al. 1983). Atlantic herring populations in the Gulf of Maine–Scotian Shelf region have several geographically separate areas for summer feeding (southwest Nova Scotia, Georges Bank, Bay of Fundy) and overwintering (Long Island Sound, Chedabucto Bay) (Sinclair and Isles 1985).

Seasonal movement patterns of river herring inferred from American and Canadian survey data involve a north-south progression and an inshore-offshore movement similar to that described for American shad populations along the Atlantic coast of North America (Neves and Depres 1979, Dadswell et al. 1987). During spring, river herring from the Middle Atlantic Bight move north as far as the Nantucket Shoals, Georges Bank, coastal Gulf of Maine and even the inner Bay of Fundy for the summer, then return south to the mid-Atlantic coast in winter and early spring (Neves 1981, Rulifson et al. 1987). The spring aggregation of mature river herring observed in Canadian survey catches from the southern Gulf of Maine likely consists of fish which will move inshore to spawn in rivers along the eastern seaboard of the United States, although some may enter Canadian rivers. A large component of the overwintering population on the Scotian Shelf moves inshore during spring to spawn in rivers along the Atlantic coast of Nova Scotia, the Bay of Fundy, and perhaps the Gulf of Maine. American shad tagged in rivers in Nova Scotia (Melvin et al. 1986) and in Quebec (Vladykov 1956) were recaptured on the Scotian Shelf in winter. The large aggregation of river herring in the eastern Gulf of Maine, apparent during spring surveys, may include fish in transit from overwintering areas on the Shelf to spawning rivers along the Bay of Fundy–Gulf of Maine coast. Considering their preference for water temperatures above 5°C, the migration route would occur along the Shelf Slope and into the eastern Gulf of Maine through the Northeast Channel. Postspawning river herring probably feed during summer in the Bay of Fundy–eastern Gulf of Maine before returning offshore to the central Shelf in the fall to overwinter. Some may move offshore soon after spawning, as indicated by the presence of large fish ($\bar{x}$ FL 30.4 cm) in the summer bycatch from the silver hake fishery along the shelf slope. Another component of the Shelf overwintering population may move north around Cape Breton to the Gulf of St. Lawrence in spring to spawn in natal rivers, returning in autumn to the Scotian Shelf to overwinter. This hypothesis is supported by the fall concentration of river herring in the Sydney Bight area and movement of an alewife accidently tagged in the Sydney Bight fall fishery for Atlantic herring, to the Margaree River (southern Gulf of St. Lawrence) where it was recaptured the following spring (Jessop, unpubl. data).

Most river herring overwintering on the Scotian Shelf probably originate in the Canadian Maritime Provinces and U.S. Gulf of Maine region. Some river herring of Canadian Maritime origin evidently migrate south to overwinter off the Middle Atlantic Bight as do American shad (Melvin et al. 1986, Dadswell et al. 1987). The tagging of over 50,000 river herring in the Saint John River, New Brunswick, produced two recaptures off North Carolina the following spring and other recoveries along the intervening coast (Jessop, unpubl. data). In another study, most recaptures from over 19,000 river herring tagged during summer and fall in the upper Bay of Fundy occurred in spring fisheries in Nova Scotia rivers, but one occurred off Massachusetts and several came from North Carolina (Rulifson et al. 1987). Summer aggregations of river herring in the Bay of Fundy–eastern Gulf of Maine may therefore consist of a mixture of stocks from the entire Atlantic coast, as do similar aggregations of American shad (Dadswell et al. 1987).

An understanding of the seasonal movements, stock composition, and exploitation of river herring populations which overwinter on the Scotian Shelf may help fishery managers to explain high variability in the returns of spawning fish regionally and to particular river systems. Stock composition and migratory routes remain to be examined.

Acknowledgments

We thank M. Dadswell and K. Frank for critically reviewing earlier drafts of the manuscript. We also wish to thank J. McMillan and C. Harvie for their assistance in data analysis and G. Black for helping with the offshore distribution plots. The constructive comments of the anonymous reviewers are also appreciated.

Citations

Bigelow, H.B., and W.C. Schroeder
1953 Fishes of the Gulf of Maine. Bull. U.S. Fish. Wildl. Serv. 74, 577 p.

Cohen, E.B., M.D. Grosslein, and M.P. Sissenwine
1982 Energy budget of Georges Bank. *In* Mercer, M.C. (ed.), Multispecies approaches to fisheries management advice, p. 95–107. Can. Spec. Publ. Fish. Aquat. Sci. 59.

Dadswell, M.J., G.D. Melvin, and P.J. Williams
1983 Effect of turbidity on the temporal and spatial utilization of the inner Bay of Fundy by American shad (*Alosa sapidissima*) (Pisces: Clupeidae) and its relationship to local fisheries. Can. J. Fish. Aquat. Sci. 40(Suppl. 1):322–330.

Dadswell, M.J., R. Bradford, A.H. Leim, D.J. Scarratt, G.D. Melvin, and R.G. Appy
1984 A review of research on fishes and fisheries in the Bay of Fundy between 1976 and 1983 with particular reference to its upper reaches. *In* Gordon, D.C., and M.J. Dadswell (eds.), Update on the marine environmental consequences of tidal power development in the upper reaches of the Bay of Fundy, p. 163–294. Can. Tech. Rep. Fish. Aquat. Sci. 1256, 686 p.

Dadswell, M.J., G.D. Melvin, P.J. Williams, and D.E. Themelis
1987 Influences of origin, life history and chance on the Atlantic coast migration of American shad. *In* Dadswell, M.J., et al. (eds.), Common strategies of anadromous and catadromous fishes, p. 313–330. Am. Fish. Soc., Bethesda.

Day, R.W., and G.P. Quinn
1989 Comparisons of treatments after an analysis of variance in ecology. Ecol. Monogr. 59:433–463.

Edgington, E.S.
1987 Randomization tests. Marcel Dekker, NY.

Emerson, C.W., J.C. Roff, and D.J. Wildish
1986 Pelagic-benthic energy coupling at the mouth of the Bay of Fundy. Ophelia 26:165–180.

Fournier, R.O., J. Marra, R. Bohrer, and M. Van Det
1977 Plankton dynamics and nutrient enrichment of the Scotian Shelf. J. Fish. Res. Board. Can. 34:1001–1018.

Fournier, R.O., M. Van Det, N.B. Hargraves, J.S. Wilson
1984 Physical factors controlling summer distribution of chlorophyll *a* off southwestern Nova Scotia. Limnol. Oceanogr. 29:517–526.

Greenburg, D.A.
1984 A review of the physical oceanography of the Bay of Fundy. *In* Gordon, D.C., and M.J. Dadswell (eds.), Update on the marine environmental consequences of tidal power development in the upper reaches of the Bay of Fundy, p. 9–30. Can. Tech. Rep. Fish. Aquat. Sci. 1256, 686 p.

Haedrich, R.L., and C.A.S. Hall
1976 Fishes and estuaries. Oceanus 19:55–63.

Halliday, R.G., and P.A. Koeller
1981 A history of Canadian groundfish trawling surveys and data usage in ICNAF divisions 4TVWX. *In* Doubleday, W.G., and D. Rivard (eds.), Bottom trawl surveys. Can. Spec. Publ. Fish. Aquat. Sci. 58:27–41.

Hare, G.M., and H.P. Murphy
1974 First record of American shad (*Alosa sappidissima*) from Labrador waters. J. Fish. Res. Board Can. 31:1536–1537.

Hatchey, H.B.
1942 The waters of the Scotian Shelf. J. Fish. Res. Board Can. 5:377–397.

Herman, A.W., D.D. Sameoto, C. Shunnian, M.R. Mitchell, B. Petrie, and N. Cochrane
1991 Sources of zooplankton on the Nova Scotia Shelf and their aggregations within deep shelf basins. Continental Shelf Res. 11:211–238.

Janssen, J., and S.W. Brandt
1980 Feeding ecology and vertical migration of adult alewives (*Alosa pseudoharengus*) in Lake Michigan. Can. J. Fish. Aquat. Sci. 37:177–184.

Jessop, B.M.
1986 Alewife and blueback herring in the Gulf of Maine area. Can. Atl. Fish. Sci. Adv. Comm. Res. Doc. 67, 7 p.
1990 Diel variation in density, length composition, and feeding activity of juvenile alewife, *Alosa pseudoharengus* Wilson, and blueback herring, *A. aestivalis* Mitchill, at near-surface depths in a hydroelectric dam impoundment. J. Fish. Biol. 37: 813–822.

Jessop, B.M., and W.E. Anderson
1989 Effects of heterogeneity in the spatial and temporal pattern of juvenile alewife (*Alosa pseudoharengus*) and blueback herring (*A. aestivalis*) density on estimation of an index of abundance. Can. J. Fish. Aquat. Sci. 46:1564–1574.

Jessop, B.M, A.H. Vromans, and W.E. Anderson
1982 Life-history data on alewife and blueback herring, Mactaquac Dam, 1975–81. Can. Data Rep. Fish. Aquat. Sci. 367, 43 p.

Kulka, D.W., S. Corey, and T.D. Isles
1982 Community structure and biomass of euphausiids in the Bay of Fundy. Can. J. Fish. Aquat. Sci. 39:326–334.

Leim, A.H., and W.B. Scott
1966 Fishes of the Atlantic Coast of Canada. Bull. Fish. Res. Board Can. 155, 485 p.

Loder, J.W., and D.A. Greenburg
1985 Predicted positions of tidal fronts in the Gulf of Maine. Continental Shelf Res. 4:397–414.

Loesch, J.G.
1987 Overview of life history aspects of anadromous alewife and blueback herring in freshwater habitats. *In* Dadswell, M.J., et al. (eds.), Common strategies of anadromous and catadromous fishes, p. 89–103. Am. Fish. Soc., Bethesda.

Loesch, J.G., W.H. Kriete, and E.J. Foell
1982 Effects of light intensity on the catchability of juvenile anadromous *Alosa* species. Trans. Am. Fish. Soc. 111:41–44.

McLellan, H.J.
1954 Bottom temperatures on the Scotian Shelf. J. Fish. Res. Board Can. 11:404–418.

Melvin, G.D., M.J. Dadswell, and J.D. Martin
1986 Fidelity of American shad, *Alosa sapidissima* (Clupeidae), to its river of previous spawning. Can. J. Fish. Aquat. Sci. 43:640–646.

Messieh, S.N.
1977 Population structure and biology of alewives (*Alosa pseudoharengus*) and blueback herring (*A. aestivalis*) in the Saint John River, New Brunswick. Environ. Biol. Fishes 2:195–210.

Mills, E.L., and R.O. Fournier
1979 Fish production and the marine ecosystems of the Scotian Shelf, eastern Canada. Mar. Biol. 54:101–108.

Mountain, D.G., M. Pastuszak, and D. A. Busch
1989 Slope water intrusion to the Great South Channel during autumn, 1977–85. J. Northwest Atl. Fish. Sci. 9:97–102.

Netzel J., and E. Stanek
1966 Some biological characteristics of blueback, *Pomolbus aestivalis* (Mitchell) and alewife, *Pomolbus pseudoharengus* (Wilson), from Georges Bank, July and October, 1964. Int. Comm. North Atl. Fish. Bull. 3:106–110.

Neves, R.J.
1981 Offshore distribution of alewife, *Alosa pseudoharengus* and blueback herring, *A. aestivalis*, along the Atlantic coast. Fish. Bull., U.S. 79:473–485.

Neves, R.J., and L. Depres
1979 The oceanic migration of American shad, *Alosa sapidissima*, along the Atlantic coast. Fish. Bull., U.S. 77: 199–212.

Ramp., S.R., and W.R. Wright
1979 Northeast Channel flow: The view after one year's measurements. Int. Counc. Explor. Sea CM 1979/C:54.

Rulifson, R.A.
1984 Tagging studies of river herring (*Alosa pseudoharengus* and *A. aestivalis*) in Bay of Fundy, Nova Scotia. N.C. Dep. Nat. Resour. Comm. Develop., Div. Mar. Fish., Completion Rep. AFC-22, E. Carolina Univ., Greenville, 26 p.

Rulifson, R.A., S.A. McKenna, and M.L. Gallagher
1987 Tagging studies of striped bass and river herring in upper Bay of Fundy, Nova Scotia. N.C. Dep. Nat. Resour. Comm. Develop., Div. Mar. Fish., Completion Rep. AFC-28-1, E. Carolina Univ., Greenville, 175 p.

Sameoto, D.D.
1982 Zooplankton and micronekton abundance in acoustic scattering layers on the Nova Scotian slope. Can. J. Fish. Aquat. Sci. 39:760–777.

Sameoto, D.D., and A.W. Herman
1989 Life cycle and distribution of *Calanus finmarchicus* in deep basins on the Nova Scotia shelf and seasonal changes in *Calanus* spp. Mar. Ecol. Prog. Ser. 66:225–237.

Sherman, K., W.G. Smith, J.R. Green, E.B. Cohen, M.S. Berman, K.A. Marti, and J.R. Goulet
1987 Zooplankton production and the fisheries of the northeastern shelf. *In* Backus, R.H., and D.W. Bourne (eds.), Georges Bank, p. 268–282. MIT Press, Cambridge.

Sinclair, M.
1988 Marine populations: An essay on population regulation and speciation. Univ. Wash. Press, Seattle, 252 p.

Sinclair, M., and T.D. Isles
1985 Atlantic herring (*Clupea harengus*) distributions in the Gulf of Maine–Scotian Shelf area in relation to oceanographic features. Can. J. Fish. Aquat. Sci. 42:880–887.

Smith, P.C., B. Petrie, and C.R. Mann
1978 Circulation, variability, and dynamics of the Scotian Shelf and Slope. J. Fish. Res. Board Can. 35:1067–1083.

Smith, S.J.
1988 Abundance indices from research survey data. *In* Rivard, D. (ed.), Collected papers on stock assessment methods, p. 16–43. Can. Atl. Fish. Sci. Adv. Comm. Res. Doc. 61.

Stone, H.H.
1985 Composition, morphometric characteristics and feeding ecology of alewives (*Alosa pseudoharengus*) and blueback herring (*A. aestivalis*) (Pisces: Clupeidae) in Minas Basin. MSc. thesis, Acadia Univ., Wolfville, N.S., 191 p.

Stone, H.H., and G.R. Daborn
1987 Diet of alewives, *Alosa pseudoharengus* and blueback herring, *A. aestivalis* (Pisces: Clupeidae) in Minas Basin, Nova Scotia, a turbid, macrotidal estuary. Environ. Biol. Fishes 19:55–67.

Vinogradov, V.I.
1984 Food of silver hake, red hake and other fishes on Georges Bank and adjacent waters, 1968–1974. NAFO (Northwest Atl. Fish. Organ.) Sci. Counc. Stud. 7:87–94.

Vladykov, V.D.
1936 Occurrence of three species of anadromous fishes on the Nova Scotian banks during 1935 and 1936. Copeia 1936:168.
1956 Distant recaptures of shad tagged in Quebec. Naturaliste Canadien (Quebec) 83:235–248.

Long-term coded wire tag retention in juvenile *Sciaenops ocellatus*

Britt W. Bumguardner
Robert L. Colura

Texas Parks and Wildlife Department, Perry R. Bass Marine Fisheries Research Station
HC 2, Box 385, Palacios, Texas 77465

Gary C. Matlock

Texas Parks and Wildlife Department, Fisheries and Wildlife Division
4200 Smith School Road, Austin, Texas 78744

Red drum *Sciaenops ocellatus*, a popular sport fish in the Gulf of Mexico and associated estuarine systems, have been subjected to increasing fishing pressure in recent years which has led to declining population size in Texas (Matlock 1982) and poor annual survival in Texas bays (Green et al. 1985). Commercial harvest of both inshore stocks of red drum in Texas prior to 1981 (Matlock 1982) and offshore stocks in the Gulf of Mexico prior to 1987 (Goodyear 1987) contributed to the apparent population decline in red drum. Documented commercial landings in the Gulf of Mexico were less than 50% of estimated recreational harvest prior to 1984. However, documented commercial landings increased to more than double the estimated recreational harvest from 1984 to 1986, primarily due to expansion of an oceanic purse seine fishery which began in 1978 (Goodyear 1987).

In Texas, reported commercial landings of red drum were more than double estimated recreational landings for 1976–77, then declined to slightly more than recreational landings for 1978–80. Estimated recreational landings were relatively stable, with a general downward trend, during 1976–80 (Matlock 1982). The sale of red drum harvested from Texas public waters was prohibited by legislative action as of 1 September 1981 (Maddux et al. 1989), while the purse seine fishery for offshore stocks of adult red drum was closed by the Gulf of Mexico Fisheries Management Council in 1986. Increasing sportfishing pressure and catastrophic freezes, which caused extensive fish kills in bays along the northern Gulf of Mexico (Maddux et al. 1989), have also contributed to imposition of increasingly restrictive sport bag and size limits for red drum in Texas.

Development of controlled spawning and pond culture techniques for red drum has allowed large-scale production and stocking of red drum fingerlings to enhance declining populations (Colura et al. 1976, Arnold et al. 1977, McCarty et al. 1986). Over 68 million red drum fingerlings have been stocked for population enhancement in Texas coastal waters since 1975, with the majority of fingerlings stocked since 1983 (Dailey 1990). Development of a reliable method for identifying stocked fish would allow evaluation of this stocking program. The fish, which are typically <50 mm total length (TL) when stocked (Dailey 1990), are frequently released in spring and summer when no small red drum (≤100 mm TL) occur naturally in bays (McEachron and Green 1986), as red drum spawn in the fall (Comyns et al. 1991). Survival of fish stocked in spring and summer can be monitored by analysis of length-frequencies for about 9 months, at which time variation in growth masks the initial length differences. Fish stocked in fall cannot be monitored by length-frequency methods due to onset of the spawning season and resultant confusion of stocked and wild fish of similar size (Dailey and McEachron 1986, Matlock et al. 1986).

For stocking to be considered successful, hatchery fish must survive long enough to be recruited to the fishery and then to offshore schools of mature red drum. When evaluation of stocking success is based on recapture of tagged fish which must grow large enough to enter the fishery, determination of long-term tag retention and detection rates is necessary for accurate evaluation of fingerling stocking success. Appreciable tag loss or nondetection would result in underestimation of the proportion of hatchery fish in the population (Heimbach et al. 1990).

Tagging of hatchery fish has had little success (Matlock et al. 1984 and 1986, Gibbard and Colura 1980, Bumguardner et al. 1990). Only 10 of 5942 hatchery-reared red drum ($\bar{x}$ 452 mm TL) tagged with monel jaw tags on the opercula were recaptured within 8 months of release (Matlock et al. 1984). Three fish from over 38,000 fingerlings (40–120 mm TL) tagged in the snout with coded wire microtags and released in St. Charles Bay, Texas, were recaptured (Matlock et al. 1986). The low recapture rate of microtagged fish was probably due to tag loss. Gibbard and Colura (1980) reported 27% retention of coded wire tags placed in the nose of red drum fingerlings (50 mm mean TL) after 1 year. Bumguardner et al. (1990) conducted a short-term study (114 days) of red drum fingerlings ($\bar{x}$ 52 mm TL) tagged in the adductor mandibularis (cheek

Manuscript accepted 9 March 1992.
Fishery Bulletin, U.S. 90:390–394 (1992).

muscle) with coded wire microtags. Loss of coded wire tags was initially high (32.7% after 24 hours), but the rate of tag loss declined substantially 23 days post-tagging.

Tag retention by the same group of fish initially tagged by Bumguardner et al. (1990) was monitored 115–464 days post-tagging to determine if additional tag loss occurred. Tag detection rates using two methods of tag detection—a Northwest Marine Technology Field Sampling Device, and examination of X-ray negatives—were also determined and contrasted with tag detection rates reported for the two methods by Bumguardner et al. (1990). Our primary objective was to determine if tag retention rates declined between 114 and 464 days post-tagging, and to what extent tag loss and nondetection affected estimates of tag retention rates. While Bumguardner et al. (1990) considered mortality a component of tag loss and reported differential mortality between tagged and untagged fish, we limited the scope of this project to investigation of tag loss and nondetection rates. We did not consider mortality a component of tag loss because the facilities to maintain a group of control fish were not available.

Table 1

Coded wire microtag retention for red drum *Sciaenops ocellatus* through 464 days post-tagging, determined with the NMT Field Sampling Device.

Activity	No. fish	Interval (days)	No. fish examined	No. fish retaining tags	Tag retention (%)	Cumulative tag retention (%)
Tagged	2124	0–1	220[a]	148	67.3	67.3
Stocked in 0.1-ha ponds	1500	2–23	844[b]	397	69.8[c] ±31.2	47.0[c] ±20.2
Restocked in 0.2-ha ponds	599	24–114	238[b]	108	96.6[c] ±25.8	45.4[c] ±12.1
Held in tank[d]	52	115–285	33[b]	31	93.9	42.6 (93.9)[e]
Stocked in 0.4-ha pond	32	286–464	31[b]	26	89.3	38.0 (83.9)[f]

[a] Fish selected randomly from the total number of fish tagged.
[b] Number of fish surviving at the end of the interval.
[c] Reported as weighted average for three ponds with standard error.
[d] First 52 fish encountered while monitoring tag retention were overwintered in indoor tanks.
[e] Cumulative percent tag retention for days 115–285 used to calculate percent tag retention for 286–464 day interval.
[f] Cumulative percent tag retention for days 115–464 used to calculate percent tag retention for 286–464 day interval.

Materials and methods

Coded-wire microtag retention for red drum was monitored from tagging to 464 days post-tagging. About 2100 red drum fingerlings ($\bar{x}$ 52 mm TL) were tagged with coded wire microtags on 13 July 1987. Tags (1.07 × 0.25 mm) were inserted horizontally in the cheek muscle using a Northwest Marine Technology (NMT) Model MK2A tagging unit (Northwest Mar. Technol., Shaw I., WA) equipped with a plastic side mold to orient fish for consistent tag placement. An NMT Quality Control Device was used to magnetize tags and separate tagged from untagged fish.

Tagged fish were held in a 3.0 × 0.6 × 0.6 m tank for 24 hours, stocked in three 0.1-ha ponds at 500 fish/pond for 23 days, then transferred to three 0.2-ha ponds for 91 days (Table 1). Surviving fish harvested from each 0.1-ha pond were restocked as a group in separate 0.2-ha ponds. Fish were fed a commercially-prepared trout feed daily while in ponds. Tag retention was determined at 24 hours (prestocking), 23 days (harvest from 0.1-ha ponds), and 114 days (harvest from 0.2-ha ponds) post-tagging with an NMT Field Sampling Device (FSD) (Bumguardner et al. 1990). Fish were harvested from 0.2-ha ponds 114 days post-tagging, and 52 fish ($\bar{x}$ 220 mm TL) confirmed by the FSD as retaining tags were placed in a 4200 L circular fiberglass tank on 11 October 1987 for overwintering. As available tank space was limited, overwintering was restricted to 52 fish confirmed as retaining tags. Experience has shown indoor overwintering is required to insure survival of red drum in hatcheries during episodic freezing conditions on the Texas coast. Fish were fed 300 g chopped fish and shrimp daily. Fish were treated with a 0.25 mg/L Cu^{++} bath on four occasions for a protozoan parasite infestation tentatively identified as *Amyloodinium* sp. Fish were immersed in a 20 mg/L oxytetracycline HCl bath, and about 10 mL of injectable oxytetracycline solution (50 mg oxytetracycline HCl/mL solution) was placed in chopped shrimp and fish offered as feed to combat a bacterial infection. Surviving fish (n 33) were removed from the tank on 22 April 1988 (285 days after tagging), measured and checked for tag presence with the FSD.

The 33 surviving fish ($\bar{x}$ 352 mm TL) were placed in a 0.4-ha pond, with the exception of one fish that had lost the caudal fin, presumably as the result of a bacterial infection. These fish were fed a a 35% protein

floating fish ration (Texas Farm Products, Nacogdoches, TX), 0.45kg/day, 5 days/week, as a supplement to natural forage available in the pond. Fish were harvested on 11 October 1988, 464 days post-tagging. Microtag retention was determined with the FSD, fish were measured ($\bar{x}$ 473mmTL), and 10 of 31 surviving fish were selected at random and preserved in 50% formalin for X-ray analysis of tag retention. X-ray negatives of the preserved fish were visually inspected to confirm the presence or absence of tags as determined by the FSD.

Tag retention was determined for each interval, and overall or cumulative tag retention was determined at the end of each interval. As mortality was not considered tag loss in this study, cumulative tag retention reflects only the percentage of tag losses from shedding and nondetection of tags. A problem encountered in the course of this program was the calculation of tag retention rates when fish which had shed tags were not removed from the group at the end of the interval (2–23 days, 24–114 days, and 286–464 days). The percent decrease in cumulative tag retention was selected as an estimate of the percentage of fish losing tags in these intervals. Conversely, when fish that had lost tags were removed from the group, determination of tag retention for that interval (days 115–285) was simple (no. fish with tags/total no. fish examined), but cumulative tag retention had to be calculated. Tag retention for the interval in question was multiplied by cumulative tag retention from the previous interval to determine cumulative tag retention for the interval. The relationship used in these calculations was

$$TR_i = \frac{CTR_i}{CTR_{i-1}} \times 100,$$

where TR_i is percent tag retention for interval i, CTR_i is percent cumulative tag retention for interval i, and CTR_{i-1} is percent cumulative tag retention for the interval prior to interval i. Percent tag retention and percent cumulative tag retention for 1–23 and 24–114 day intervals for fish from individual ponds were used to calculate weighted means reported in Table 1. The weighting factor used was the number of fish harvested from each pond.

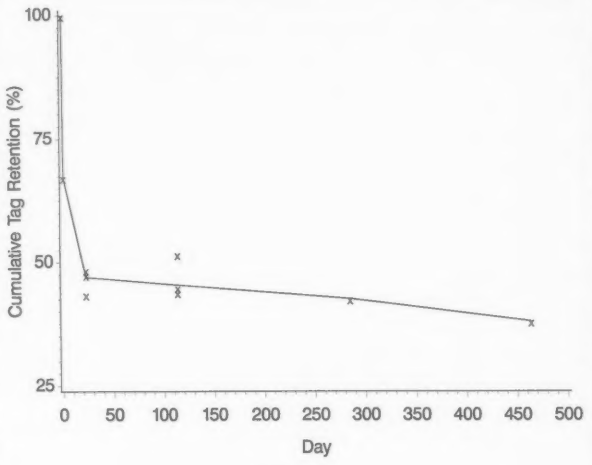

Figure 1
Observed values (X) of cumulative tag retention for microtagged red drum *Sciaenops ocellatus* fingerlings through 464 days post-tagging.

Results and discussion

Tag retention for surviving fish at 115–464 days post-tagging was 83.9%. Tag retention was 93.9% at 115–285 days post-tagging, and 89.3% at 286–464 days post-tagging (Table 1). Cumulative retention of coded wire microtags for red drum was 38.0% at 464 days post-tagging (Table 1, Fig. 1). Lack of replication at all intervals prevented statistical comparison of tag retention for different intervals. However, tag retention values of 96.6% for 24–114 days, 93.9% for 115–285 days, and 89.3% for 286–464 days post-tagging indicate cumulative tag retention decreased in the interval 24–464 days post-tagging, although at a slower rate than for the period 0–23 days (Table 1). Numerous authors (Gibbard and Colura 1980, Klar and Parker 1986, Fletcher et al. 1987, Williamson 1987, Bumguardner et al. 1990, and Dunning et al. 1990) have reported that the majority of coded-wire tag losses occur within a relatively short period (14–90 days) post-tagging. Our results agree with this generalization, but indicate tag losses may continue at a much reduced rate for extended periods after tagging. While our results are based on a small unreplicated sample (n 31 fish at study end), we believe they indicate long-term tag loss may be important when estimating the contribution of hatchery fish to a population. Accounting for this continued tag loss would prevent underestimation of the proportion of tagged fish occurring in the population (Heimbach et al. 1990).

Although Bumguardner et al. (1990) reported the FSD failed to detect tags present in 9% of live fish 114 days after tagging as determined by examination of X-ray negatives (n 186), no difference in tag detection between the FSD and X-ray negatives was found in this

study. Both X-ray negatives and the FSD indicated that 3 of 10 preserved fish lost tags. The criteria used to select fish for this study, i.e., confirmation of tag presence by the FSD, may have biased the comparison by eliminating fish with weakly magnetized tags.

Inserting coded wire tags horizontally in the cheek musculature of red drum fingerlings resulted in low tag retention. The site of tag insertion and tag orientation may affect tag retention. Tags implanted in striped bass *Morone saxatilis* and largemouth bass *Micropterus salmoides* cheek musculature resulted in higher retention rates than tags placed in snouts of striped bass and largemouth bass (Klar and Parker 1986, Fletcher et al. 1987, Williamson 1987). Changing the plane of tag insertion in the cheek muscle may increase tag retention. Dunning et al. (1990) reported coded-wire microtag retention in striped bass (65–100 mm TL) was greater when tags were inserted vertically rather than horizontally in the cheek muscle. A possible explanation of poor retention and high initial loss of wire microtags implanted horizontally in the cheek muscle of small fish may be the small margin of error in depth placement of the tag, due to size and thickness of the target area. Tags may be implanted too deeply, penetrate the muscle, and lodge in the buccal cavity. Anesthetized fish could retain the tag in the buccal cavity while passing through the Quality Control Device which magnetizes the tag and confirms tag presence, but then eject the tag after regaining equilibrium in the recovery tank. Changing tag orientation in the cheek muscle from horizontal to vertical would provide a thicker target for tag insertion and may be responsible for higher reported retention of microtags inserted vertically rather than horizontally in the cheek muscle of small fish.

Stocked red drum fingerlings are typically harvested at about 25 mm TL. Attempts to tag red drum of that size with wire microtags have resulted in high mortality (Gene McCarty, Texas Parks Wildl. Dep., Austin, unpubl. data). Tagging larger fish might improve retention rates and would reduce tagging mortality, but the fish would not be representative of the size of fish normally stocked. These factors would complicate any attempt to evaluate the effectiveness of stocking hatchery-reared red drum fingerlings using fish tagged with coded wire microtags.

Acknowledgments

We would like to acknowledge the assistance of Maxine Kubecka, D.V.M., Linda Kocurek, and the staff of the Palacios Veterinary Clinic in obtaining X-ray negatives. We also thank Paul Hammerschmidt for reviewing the manuscript. This study was conducted with partial funding from the U.S. Department of the Interior, Fish and Wildlife Service, under DJ 15.605 (Project F-36-R).

Citations

Arnold, C.R., T.D. Williams, W.H. Bailey, and J.L. Lasswell
1977 Laboratory spawning and rearing of red drum and southern flounder. Proc., Annu. Conf., Southeast. Assoc. Fish Wildl. Agencies 31:437–440.

Bumguardner, B.W., R.L. Colura, A.F. Maciorowski, and G.C. Matlock
1990 Tag retention, survival and growth of red drum fingerlings marked with coded wire tags. Am. Fish. Soc. Symp. 7:286–292.

Colura, R.L., B.T. Hysmith, and R.E. Stevens
1976 Fingerling production of striped bass (*Morone saxatilis*), spotted seatrout (*Cynoscion nebulosus*), and red drum (*Sciaenops ocellatus*) in saltwater ponds. Proc. World Maricult. Soc. 7:79–92.

Comyns, B.H., J. Lyczkowski-Schultz, D.L. Nieland, and C.A. Wilson
1991 Reproduction of red drum, *Sciaenops ocellatus*, in the north central Gulf of Mexico: Seasonality and spawner biomass. *In* Hoyt, R. (ed.), Larval fish recruitment and research in the Americas, p. 17–26. NOAA Tech. Rep. NMFS 95.

Dailey, J.A.
1990 Fish stocking in Texas Bays: 1975–1989. Manage. Data Ser. 49, Texas Parks Wildl. Dep., Fish. Div., Coastal Fish. Br., Austin, 32 p.

Dailey, J.A., and L.W. McEachron
1986 Survival of unmarked red drum stocked into two Texas bays. Manage. Data Ser. 116, Texas Parks Wildl. Dep., Coastal Fish. Br., Austin, 8 p.

Dunning, D.J., Q.E. Ross, B.R. Friedman, and K.L. Marcellus
1990 Coded wire tag retention by, and tagging mortality of, striped bass reared at the Hudson River hatchery. Am. Fish. Soc. Symp. 7:262–266.

Fletcher, D.H., F. Haw, and P.K. Bergman
1987 Retention of coded wire tags implanted into cheek musculature of largemouth bass. N. Am. J. Fish. Manage. 7: 436–439.

Gibbard, G.L., and R.L. Colura
1980 Retention and movement of magnetic nose tags in juvenile red drum. Proc., Texas Chap. Am. Fish. Soc. 3:22–29.

Goodyear, C.P.
1987 Status of the red drum stocks of the Gulf of Mexico. Contr. CRD 86/87-34, NMFS Southeast Fish. Sci. Cent., Miami, 121 p.

Green, A.W., H.R. Osburn, G.C. Matlock, and H.E. Hegen
1985 Estimated survival rates for immature red drum in northwest Gulf of Mexico bays. Fish. Res. (Amst.) 3:263–277.

Heimbach, D.G., D.J. Dunning, H. Wilson, and Q.E. Ross
1990 Sample-size determination for mark-recapture experiments: Hudson River case study. Am. Fish. Soc. Symp. 7: 684–690.

Klar, G.T., and N.C. Parker
1986 Marking fingerling striped bass and blue tilapia with coded wire tags and microtaggants. N. Am. J. Fish. Manage. 6:439–444.

Maddux, H.R., H.R. Osburn, D.L. Trimm, and K.W. Spiller
1989 Trends in finfish landings by sport-boat fishermen in Texas marine waters, May 1974–May 1988. Manage. Data Ser. 8, Texas Parks Wildl. Dep., Fish Div., Coastal Fish. Br., Austin, 496 p.

Matlock, G.C.
1982 The conflict between user groups of red drum and spotted seatrout in Texas. *In* Stroud, R. (ed.), Proc., 7th Annu. Mar. Rec. Fish. Symp. p. 101–109. Sport Fish. Inst., Wash., DC.

Matlock, G.C., B.T. Hysmith, and R.L. Colura
1984 Returns of tagged red drum stocked into Matagorda Bay, Texas. Manage. Data Ser. 63, Texas Parks Wildl. Dep., Coastal Fish. Br., Austin, 6 p.

Matlock, G.C., R.J. Kemp Jr., and T.J. Heffernan
1986 Stocking as a management tool for a red drum fishery, a preliminary evaluation. Manage. Data Ser. 75, Texas Parks Wildl. Dep., Coastal Fish. Br., Austin, 27 p.

McCarty, C.E., J.E. Geiger, L.N. Sturmer, B.A. Gregg, and W.P. Rutledge
1986 Marine finfish culture in Texas: A model for the future. *In* Stroud, R. (ed.), Fish culture in fishery management, p. 249–262. Am. Fish. Soc., Fish Cult. Fish. Manage. Sec., Bethesda.

McEachron, L.W., and A.W. Green
1986 Trends in relative abundance and size of selected finfish in Texas bays: November 1975–June 1984. Manage. Data Ser. 91, Texas Parks Wildl. Dep., Coastal Fish. Br., Austin, 271 p.

Williamson, J.H.
1987 Evaluation of wire nosetags for marking largemouth bass. Prog. Fish-Cult. 49:156–158.

Growth and mortality of *Lutjanus vittus* (Quoy and Gaimard) from the North West Shelf of Australia

Tim L.O. Davis
Grant J. West
CSIRO Division of Fisheries, Marine Laboratories
GPO Box 1538, Hobart, Tasmania 7001, Australia

The tropical waters of the North West Shelf of Australia are highly productive (Tranter 1962) and support a diverse fish fauna (Sainsbury et al. 1985). A significant multispecies trawl fishery has developed in the region, its total catch peaking in 1973 at 37,000 t, although this had decreased to 2700 t in 1989 (Jernakoff and Sainsbury 1990). *Lutjanus vittus* is an important and highly valued fish in this trawl fishery, comprising about 4% of the total catch (Jernakoff and Sainsbury 1990).

Assessment of fish yields of the North West demersal trawl fishery is based mainly on a Beverton and Holt dynamic pool model (Sainsbury 1987), which requires estimates of mortality and growth parameters for each species. In this paper we investigate the age, growth, population structure, and mortality of *L. vittus* collected from random trawl surveys of the North West Shelf during 1982–83.

Materials and methods

Field collection

Material was obtained from the CSIRO North West Shelf program (Young and Sainsbury 1985), which surveyed the shelf waters within latitudes 116–119°E about every two months between August 1982 and October 1983 (Fig. 1). Fish were caught with a Frank and Bryce trawl (30.5 m foot rope and a 20 mm cod-end liner) towed at 3.5–4.5 knots for 30 minutes during the day. Demersal tows were made at computer-generated random positions in 13 strata defined by water depth (10–50 m, 50–120 m, and 120–210 m), sediment type (nominally shelly sand, sand, sandy silt, and silt), and two geographical zones in which different fishing regimes were planned in the future (Table 1). Sixty-two trawl positions were produced for each sampling survey, with effort being allocated according to the mean and variance of catches determined by preliminary surveys and the area of each stratum. On average, 58 trawls were completed each survey.

At each random station the total weight of *L. vittus* and the fork length by 10 mm classes of each *L. vittus* was recorded. A subsample of 20–40 fish, approximately representing the size/frequency composition of the total catch (Kimura 1977) was then selected from each station for further analysis. Fork length was measured to the nearest mm and total weight to the nearest g, and sex were recorded. Sagittal otoliths and urohyals were collected for age determination.

Manuscript accepted 18 February 1992.
Fishery Bulletin, U.S. 90:395–404 (1992).

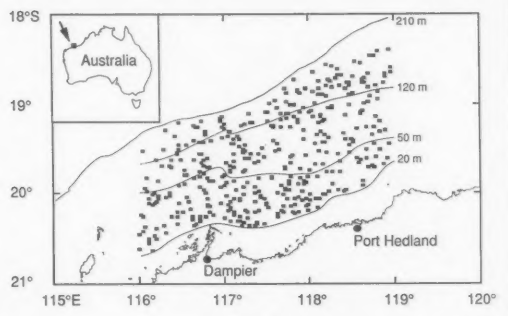

Figure 1
Distribution of 407 random stations sampled during seven cruises on the North West Shelf, September 1982–October 1983. The 20, 50, 120, and 200 m depth contours used to stratify sampling are shown.

Table 1
Stratified random trawl survey on the North West Shelf. The 13 strata sampled during each survey based on depth, geographical zones, and sediment type. Area (km^2) of each stratum and number of random trawls made in each stratum (in parenthesis) on each survey are shown.

	Sand	Shelly-sand	Silt	Sandy-silt
20–49 m				
116°E–117°30′E	3278(6)	3123(4)		
117°30′E–119°E	6309(6)	1732(4)		
50–119 m				
116°E–117°30′E	6123(7)	2381(4)		5505(5)
117°30′E–119°E	9679(7)	2381(4)		1423(5)
120–200 m				
116°E–117°30′E			4577(4)	
117°30′E–119°E		4886(4)	2412(2)	

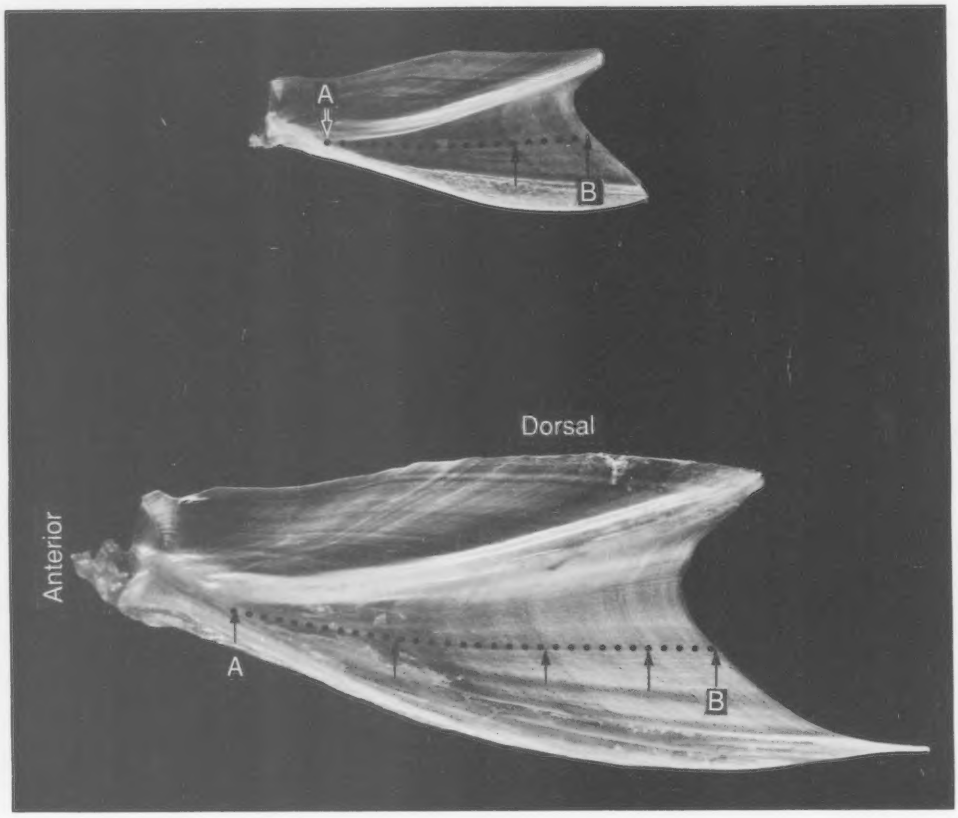

Figure 2
Urohyal bone of *Lutjanus vittus* with one check (129 mm FL) and three checks (242 mm FL). A–B taken as line of measurement.

Age determination

A preliminary examination of the sagittal otoliths, urohyals, scales, and vertebrae from 60 *L. vittus* indicated that checks were more clearly defined in otoliths and urohyals than in other hard parts. Due to their thickness and opacity, otoliths in older fish required sectioning because inner checks were obscured. As urohyals required little preparation before reading, they were chosen as the primary ageing structure; their only disadvantage being that checks in older fish were represented by a cluster of bands, so that determining the point at which the check was formed was somewhat subjective. Otoliths were referred to only when interpretation of urohyals was difficult. Urohyals were frozen and the flesh later removed by dipping in boiling water for 5 minutes, scrubbing, rinsing, and air drying before long-term storage.

Urohyals were examined dry on a black surface under incident light using a dissecting microscope. Checks under this lighting appeared as dark (hyaline) bands (Fig. 2). The distance from the origin to each check and the outer margin of the urohyal was measured along the axis indicated in Figure 2. The periodicity of check formation was determined from analysis of the temporal pattern of marginal increment development (distance from the outermost check to the outer margin of the urohyal) calculated as the index of completion (C) using the formula of Tanaka et al. (1981):

$$C = W_n / W_{n-1}, \quad (1)$$

where W_n = marginal increment, and W_{n-1} = previous complete increment. Analysis of variance was

used to test for significant differences in this index with time of year after arcsine square-root transformation.

Growth analysis

Two forms of length-at-age data were available: lengths were back-calculated to the last annulus (Whitney and Carlander 1956, Carlander 1981) to provide length-at-age data unconfounded by differences in the time of year of sampling. Absolute age-at-observed-length was also assigned, using an artificial January 1 birthdate.

The von Bertalanffy growth curve parameters were fitted to both sets of length-at-age data by direct non-linear least-squares estimation. The null hypothesis that there was no difference between males and females in the three growth-curve parameters was tested using the extra sum-of-squares principle (Draper and Smith 1981, Ratkowsky 1983). The mean lengths at the last annulus of fish aged 1–6 years were also compared between sexes using analysis of variance.

Population structure and mortality

Sex-specific length-frequency distributions and sex-specific age-length keys were obtained from the subsamples from each random station, pooled for each sampling period. It was assumed that neither the sex ratio nor the sex-specific growth rate varied in some systematic way between the different strata. The log-likelihood ratio χ^2 was used to test for departures from a 1:1 sex ratio.

For each sampling period in 1983, the length frequency of the total population was determined using the following equation (K.J. Sainsbury, CSIRO Div. Fish., pers. commun. 1991):

$$F_i = \sum_{j=1}^{j=13} f_{ij} A_j / n_j, \qquad (2)$$

where F_i is the relative frequency of size-class i in the population, f_{ij} is the frequency of size-class i in stratum j, A_j is the area of stratum j, and n_j is the number of trawls in stratum j. These length frequencies were then broken down by sex, using sex-specific length-frequency distribution determined for each sampling period in 1983. The sex-specific age structure at each sampling period was then calculated using the sex-specific age-length keys determined for each sampling period (Ricker 1975, Kimura 1977). A catch curve for each sex was then constructed (Gulland 1969) and total instantaneous mortality estimated by least-squares linear regression of the descending right-hand of the catch curve. Equality of mortality rates between the sexes was determined by analysis of covariance.

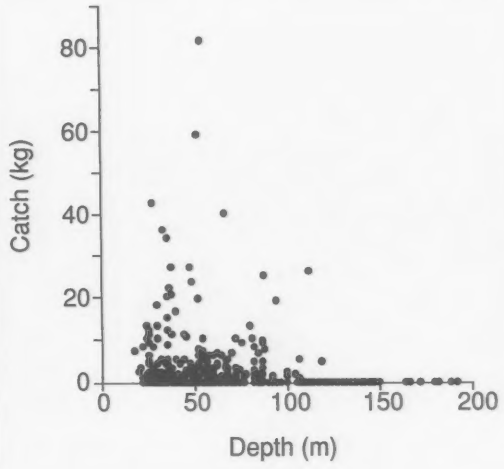

Figure 3
Catch per trawl of *Lutjanus vittus* by water depth on the North West Shelf of Australia, 1982–83.

Results

Depth distribution

Lutjanus vittus were caught in depths from 20 m (the shallowest depth sampled) to 120 m, with the largest catches being at 30–70 m (Fig. 3). There was a positive correlation between individual fish lengths and depth (r 0.337, t 24.7, df 4754, $P<0.001$). While almost the full size-range was encountered at most depths, there was a marked absence of fish <200 mm at depths >90 m (Fig. 4).

Length/weight relationship

In the regression of log weight/log length, the test for homogeneity of slopes between sexes was found to be not significant (ANCOVA, F 0.318, df 1, 2604, P 0.57) and, assuming a common slope, there was no significant difference in the intercepts for the two sexes (ANCOVA, F 1.76, df 1, 2605, P 0.19). Both sexes and juveniles whose sex could not be determined were then combined and a general relation between length (L in mm) and weight (W in g) for *L. vittus* was determined:

$$W = 9.99 \times 10^{-6} L^{3.086}$$

(F 367248, df 1, 2797, $P<0.001$).

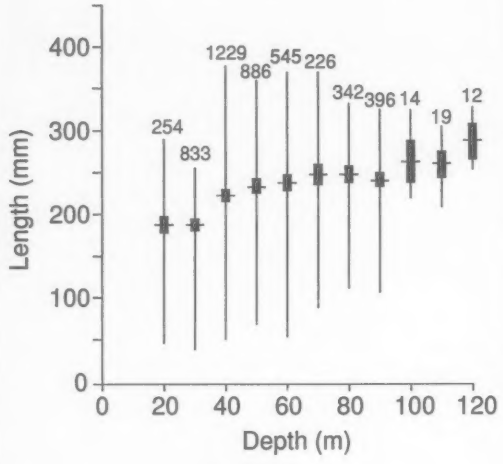

Figure 4

Mean length, 95% confidence limits (vertical bars), length range. and sample size of *Lutjanus vittus* by 10 m depth intervals.

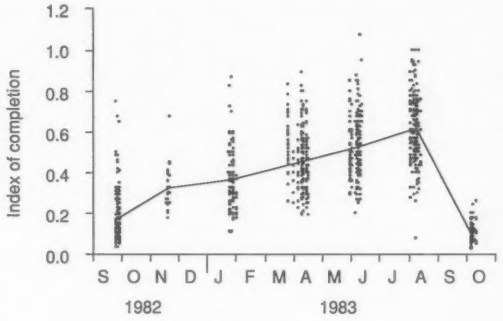

Figure 5

Seasonal change in the index of completion (amount of bone growth since the last check was formed) in *Lutjanus vittus* urohyals with 1–6 checks. Individual indices are plotted against day of sampling, and the line links the mean index for each sampling period.

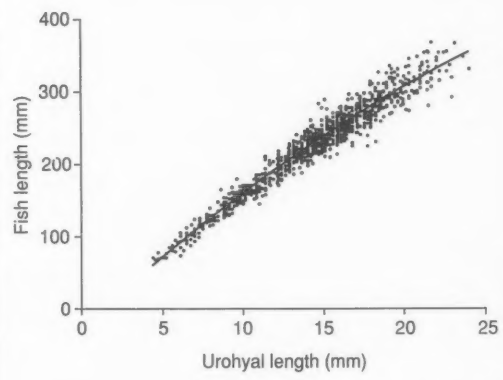

Figure 6

Curvilinear relationship between urohyal length and fish length in *Lutjanus vittus*.

Annulus formation

Evidence that checks are formed annually was obtained by examining the index of completion at about 2-month intervals throughout one season. The index of completion is a measure of the amount of bone growth since the last check was formed, expressed as a proportion of the previous growth increment. The indices of completion for fish aged 1–6 years were combined after each age-group was observed to follow the same seasonal changes in the index (Fig. 5). There were significant ($P<0.001$) differences in this index with time of year for urohyals having one, two, three, four, five and six checks (ANOVA, F 31.4, df 4, 172; F 80.1, df 6, 246; F 100.7, df 6, 263; F 40.0, df 6, 141; F 15.5, df 6, 69; F 88.8, df 5, 233, respectively). While there was considerable variation in this index at any one sampling period, there was a steady increase in the mean index from October to August, followed by a marked drop between August and October. It appears that checks are laid down some time between August and October.

Back-calculation

Lengths were back-calculated to the last annulus, using a proportional method based on the regression of fish length on urohyal length—the body proportional hypothesis (BPH) of Francis (1990). A quadratic equation best described the relationship between body length (L in mm) and urohyal length (U in mm) (Fig. 6):

$$L = -25.48 + 20.485U - 0.193U^2 \quad (r^2\ 0.95,\ \text{df}\ 1102).$$

The mean absolute difference between using BPH and SPH (regression of fish length on urohyal length) was 1.6 mm; BPH back-calculated smaller lengths in fish <150 mm and larger lengths in fish >200 mm.

Growth

Von Bertalanffy growth curves were fitted to length-at-age data for each sex separately. Fish whose sex

Table 2

Mean lengths back-calculated to the last annulus, 95% confidence limits, and sample number (n) at each age (years) for male and female *Lutjanus vittus*.

Age (yr)	Mean length (mm)	95% CL	n
Males			
1	90	87–93	92
2	164	160–167	104
3	214	210–217	122
4	261	256–266	66
5	295	288–302	52
6	313	304–322	22
7	338	330–347	14
Females			
1	89	87–92	92
2	167	163–170	148
3	216	214–219	159
4	251	247–253	115
5	276	271–282	45
6	291	284–298	17

could not be identified (104 juveniles) presented a problem, because excluding them created a bias since fish that could be sexed in age-class 1 (40 males and 40 females) were larger animals. There were significant differences ($P<0.001$) in back-calculated and observed lengths between age-class 1 males, females, and juveniles (one-way ANOVA, F 50.7, df 2, 181; F 89.0, df 2, 181, respectively). Multiple comparison by the Tukey test indicated that age-class 1 fish that could be sexed were significantly larger than juveniles by about 17 mm for back-calculated lengths and 33 mm for observed lengths. To eliminate this bias, juveniles were ranked by size. The smallest was randomly assigned a sex, and then each juvenile in order was assigned to alternate sexes. The mean lengths back-calculated to the last annulus at each age for male and female (including assigned sexes in age-class 1) are presented in Table 2 and Figure 7.

Back-calculated length-at-age data minimize the effects of seasonal growth but do not completely eliminate it, because the time of check formation ranges over several months (Fig. 5). Assigning an absolute age using an arbitrary birthdate will only compensate for growth differences between fishes caught at different times of the year when there is little seasonal variation in growth rate. However, assigning absolute ages does enable age-class 0 data to be used in determining growth curves (Fig. 8). While back-calculated lengths cannot use age-class 0 data, they do enable a more realistic time-scale parameter (t_0) to be estimated.

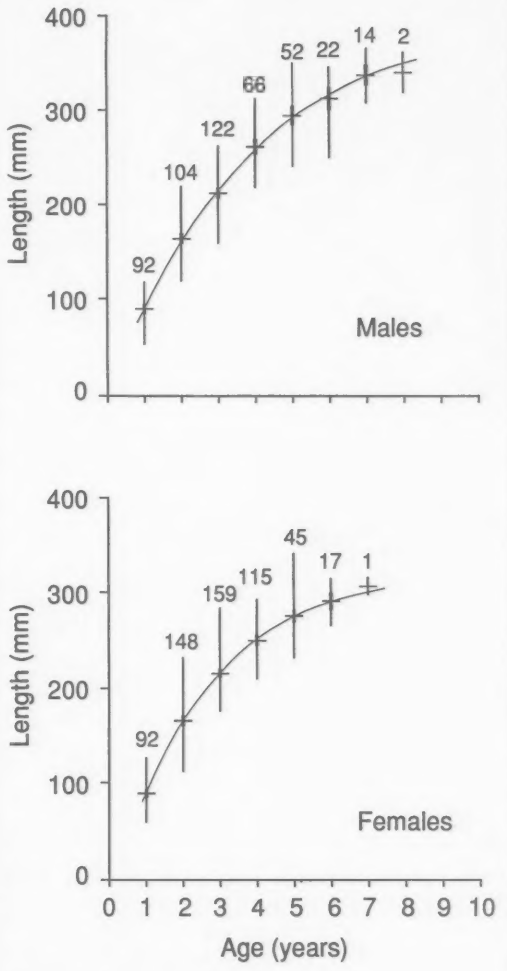

Figure 7

Growth of male and female *Lutjanus vittus*. Mean back-calculated lengths to the last annulus, 95% confidence limits (vertical bars), range, and sample size have been plotted. Von Bertalanffy growth curves were fitted to individual observations.

The least-squares estimates of the von Bertalanffy growth curve parameters are quite different between the sexes for both forms of length-at-age data (Table 3). Independent of any assumed growth curve, there were significant differences in mean back-calculated lengths between sexes for age-classes 4–6 years (ANOVA, F 42.1, df 1, 311, $P<0.001$) but age-classes 1–3 were not significantly different (F 0.32, df 1, 605, P 0.569). Only fish whose sex was determined

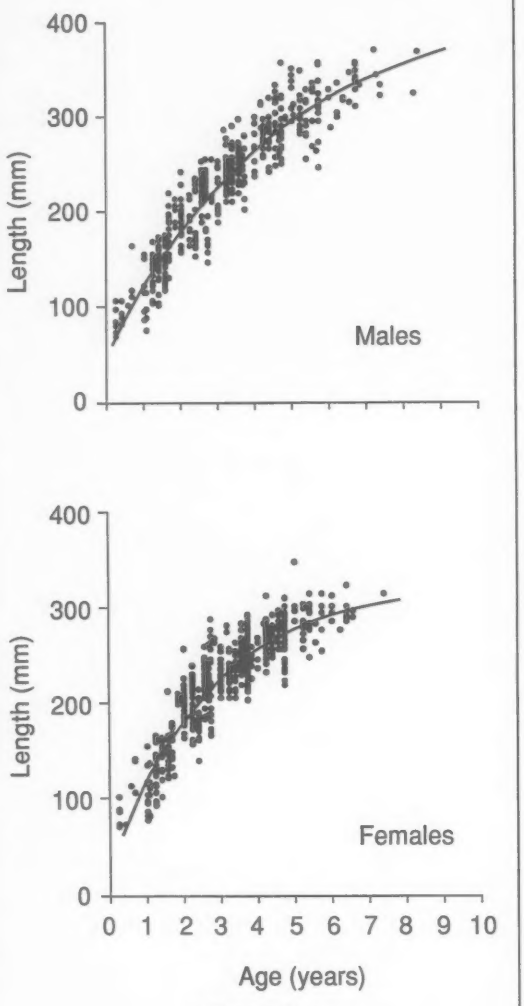

Figure 8
Growth of male and female *Lutjanus vittus* assigned an absolute age assuming a 1 January birthdate.

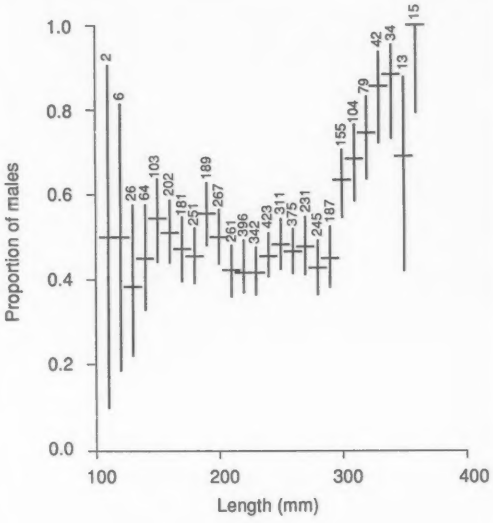

Figure 9
Proportion of males by 10 mm length-class. Means, 95% binomial confidence limits (vertical lines), and sample size are plotted.

were used in this analysis. Both males and females grow at the same rate for the first three years, after which females grow at a markedly slower rate than males.

Sex ratio

There was a marked departure from a 1:1 sex ratio (Fig. 9; likelihood ratio χ^2 152.1, df 29, $P<0.001$) which can be attributed to different growth rates between the sexes. Below 300 mm, sex ratios did not differ from 1:1 (likelihood ratio χ^2 23.3, df 18, P 0.18) but in all larger size groups there was a predominance of males.

Table 3
Estimated parameters (± SE) of the von Bertalanffy growth curve for *Lutjanus vittus*.

	Growth curve parameters				*F* test of parameter estimates		
	df	L_∞ (mm)	K	t_0 (yr)	*F*	df	*P*
Back-calculated length-at-age							
Males	473	403(10.4)	0.26(0.01)	0.02(0.05)	21.7	3, 1045	<0.001
Females	578	323(6.6)	0.39(0.02)	0.17(0.04)			
Length at absolute age							
Males	486	422(15.9)	0.22(0.02)	−0.56(0.09)	19.9	3, 1066	<0.001
Females	586	325(7.7)	0.37(0.03)	−0.23(0.08)			

Length-frequency distributions

Length-frequency distributions of the population were determined separately for males and females (Fig. 10). Each length-class was separated into age-classes based on the urohyal data. There was a jump in age-class between samples taken in August and October because a new check was formed in the intervening period. While

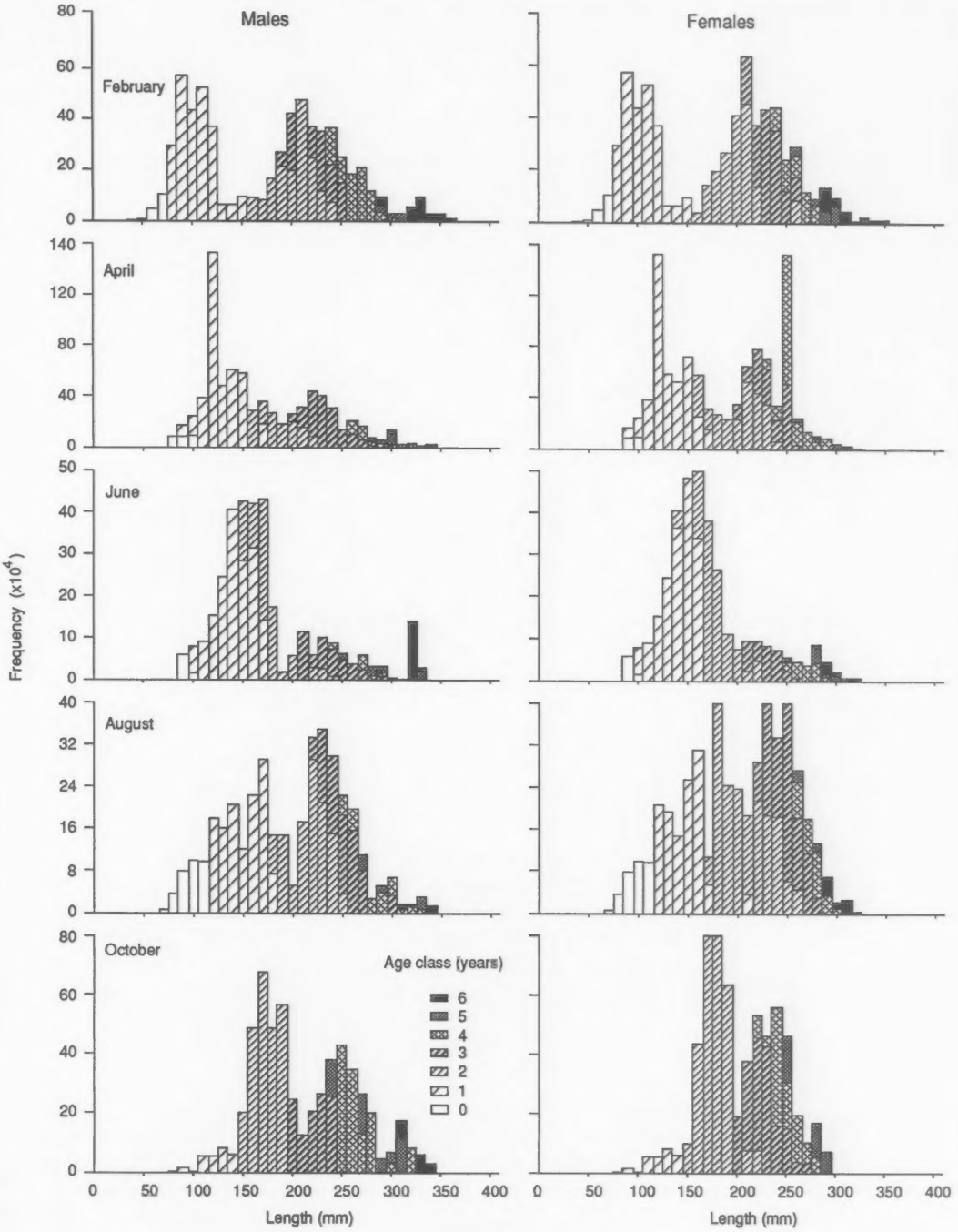

Figure 10

Total population length-frequency distribution of male and female *Lutjanus vittus* at each sampling period in 1983. Hatching within each distribution indicates the age-class structure determined from urohyal ageing. All age-groups increment by 1 year, August–September, due to check formation.

separation of sexes would have reduced variance in the length-frequency distribution of the older age-classes due to growth differences between sexes, there was still considerable size overlap of age-classes and difficulty in identifying modes after age 2 (Fig. 10). There was a clear progression in the length of age-classes 1 and 2 through the year, although age-class-2 fish of both sexes were somewhat larger than expected in February based on the progression in length of this age-class in subsequent months.

Mortality

The relative abundance of each age-class by sex was determined for the five periods sampled in 1983 (Fig. 11). A line was fitted by least squares to the descending limb of the catch curve. Fish not considered to be fully recruited to the sampling gear (circled points) were excluded. There was no significant difference in the slopes of the lines for males and females (ANCOVA, F 0.85, df 1, 47, P 0.36) and no significant sex effect (ANCOVA, F 1.23, df 1, 47, P 0.27) so a catch curve was fitted to the combined data. The instantaneous rate of annual mortality (Z) for males and females was estimated to be 0.98 (SE 0.076).

Discussion

Lutjanus vittus was caught at depths of 20 m (the shallowest depth sampled) to 120 m, with larger fish tending to inhabit deeper waters. This tendency has also been observed in other shallow-water lutjanids such as *L. aya* (Moseley 1966), *L. griseus* (Starck 1971), and *L. bohar* (Wright et al. 1986).

Most ageing studies on lutjanids have relied on otoliths as the principal structure (see review by Manooch 1987).However, a few authors (i.e., Reshetnikov and Claro 1976, Pozo and Espinosa 1982, Claro 1983, Palazón and González 1986) have used urohyals. Reshetnikov and Claro (1976) had difficulty determining the boundaries of the annual increment after the second or third annulus in urohyals because the annuli were made up of multiple bands. It was our experience that, despite this problem, increments were still easier to measure on urohyals than on whole otoliths, and preparation was far less time-consuming.

Our preliminary investigation indicated that the same number of checks were formed on a variety of hard structures, including urohyals. Data on marginal increments in urohyals showed a seasonal pattern with one check being formed each year, consistent with most other studies on lutjanids in tropical waters. However, studies on two lutjanid species from Cuban shelf waters have suggested that checks are formed twice a year

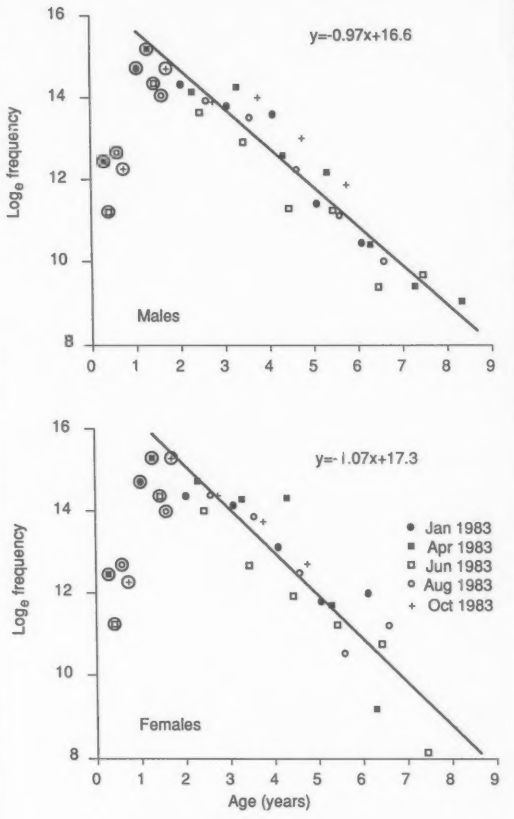

Figure 11

Log$_e$ frequency against absolute age for male and female *Lutjanus vittus*. Data for fish <2 years old (circled) were excluded from the regressions, as they were incompletely recruited age-classes.

(Espinosa and Pozo 1982, Pozo and Espinosa 1982).

The growth of male and female *L. vittus* was significantly different after 3 years of age, with females growing markedly slower than males. There are few documented cases of growth rates differing between sexes in lutjanids. However, female *L. vittus* in New Caledonia were found to grow at a slower rate, and slight growth differences were found in *L. amabilis* in New Caledonia (Loubens 1980) and *L. synagris* in Trinidad (Manickchand-Dass 1987). All mature females observed were 3 years of age or older (unpubl. data), and it seems likely that females grow more slowly than males at this stage because they expend proportionally more energy on gamete production than do males. Stunting in females from a sexually precocious population of *Lates calcarifer* was also attributed

to channeling energy into gonadal growth at the expense of somatic growth at a relatively early age (Davis 1984).

Length-frequency distributions did not show the modal structure one would expect knowing the age structure of the population. The length-frequencies showed three modes, whereas direct ageing suggested there should be at least six. Length-based methods of ageing work best with fish that spawn over a short period of time, have short life spans, and are fast growing; characteristics not typical of lutjanids (Manooch 1987).

A preponderance of females at larger sizes has been reported in studies of other lutjanids, e.g., *L. synagris* (Rodriguez Pino 1962, Erhardt 1977), *Etelis carbunculus* (Everson 1984), *E. coruscans*, *Aprion viriscens* (Everson et al. 1989), and *Rhomboplites aurorubens* (Grimes and Huntsman 1980). The latter authors attributed the preponderance to differential mortality and longevity. *L. vittus* goes against this trend: males predominate the larger size-classes, as is the case for *Lutjanus amabilis* (Loubens 1980) and *Lutjanus buccanella* (Thompson and Munro 1983). The preponderance of males at larger sizes appears to be due largely to a reduction in growth rates of mature females.

No significant differences were found in the instantaneous rate of annual mortality (Z) between male and female *L. vittus*. One of the assumptions of estimating mortality using the catch curve method of Gulland (1969) is that the mortality rate is constant for all years used in the estimation. This may not be the case for female *L. vittus* after 6 years of age. However, the data points in the oldest age-groups are based on smaller sample sizes, so the mortality curve at this stage should be interpreted with caution. Using the relationship between natural mortality (M) and the growth coefficient (K) for snappers and groupers determined by Ralston (1987) from published data provides us with estimates for M of 0.59 for males and 0.92 for females. The value for males seems reasonable, but that for females is unlikely if total mortality is about 0.98. Clearly, regression methods to produce estimates of M such as those used by Pauly (1980) and Ralston (1987) should be applied with caution.

Acknowledgments

This paper is dedicated to the memory of Mr. Otto Augustine, a technician with the CSIRO Division of Fisheries. He was responsible for the ageing of many fish species in the Division's programs from the late sixties up until his death in 1990. He determined the age and marginal increment data used in this paper. We wish to thank W. Thomas for laboratory assistance and all people who assisted in the fieldwork on the Northwest Shelf Program. We are grateful to K.J. Sainsbury for providing length-frequency and catch data from his research program, and K. Haskard for statistical advice. S. Blaber and J.S. Gunn reviewed the manuscript.

Citations

Carlander, K.D.
1981 Caution on the use of the regression method of back-calculating lengths from scale measurements. Fisheries (Bethesda) 6:2–4.

Claro, R.
1983 Ecologia y ciclo de vida del caballerote, *Lutjanus griseus* (Linnaeus), en la plataforma Cubana: 2. Edad y crecimiento, estructura de las poblaciones, pesquerias. Rep. Invest. Inst. Oceanol. Acad. Cienc. Cuba 8, 26 p.

Davis, T.L.O.
1984 A population of sexually precocious barramundi, *Lates calcarifer*, in the Gulf of Carpentaria, Australia. Copeia 1984: 144–149.

Draper, N.R., and H. Smith
1981 Applied regression analysis, 2d ed. Wiley, NY, 407 p.

Erhardt, H.
1977 Beitrage zur biologie von *Lutjanus synagris* (Linnaeus 1758) an der Kolumbianischen Atlantikkuste. Int. Rev. Gesamten Hydrobiol. 62:161–171.

Espinosa, L., and E. Pozo
1982 Edad y crecimento del sesí (*Lutjanus buccanella* Cuvier, 1828) en la plataforma suroriental de Cuba. Rev. Cubana Invest. Pesq. 7(1):80–100.

Everson, A.R.
1984 Spawning and gonadal maturation of the ehu, *Etelis carbunculus*, in the Northwestern Hawaiian Islands. *In* Grigg, R.W., and K.Y. Tanoue (eds.), Proc., Second symposium on resource investigations in the northwestern Hawaiian Islands, vol. 2, p. 128–148. UNIHI-SEAGRANT-MR-84-01, Univ. Hawaii, Honolulu.

Everson, A.R., H.A. Williams, and B.M. Ito
1989 Maturation and reproduction in two Hawaiian eteline snappers, uku, *Aprion virescens*, and onaga, *Etelis coruscans*. Fish. Bull., U.S. 87:877–888.

Francis, R.I.C.C.
1990 Backcalculation of fish length: A critical review. J. Fish Biol. 36:883–902.

Grimes, C.B., and G.R. Huntsman
1980 Reproductive biology of the vermilion snapper, *Rhomboplites aurorubens*, (Cuvier) from North and South Carolina waters. Fish. Bull., U.S. 78:137–146.

Gulland, J.A.
1969 Manual of methods for fish stock assessment. Part 1. Fish population analysis. FAO Man. Fish. Sci. 4:1–154.

Jernakoff, P., and K.J. Sainsbury
1990 CSIRO's northern demersal finfish stock assessments: 1980 to 1990. Bur. Rural Resour., Dep. Primary Ind. Energy Aust. Inf. Pap. IP/6/90, Canberra, A.C.T., Aust., 169 p.

Kimura, D.K.
1977 Statistical assessment of the age-length key. J. Fish. Res. Board Can. 34:317–324.

Loubens, G.
1980 Biologie de quelques espèces de poissons du lagon néocaldonien. II. Sexualité et reproduction. Cah. Indo-Pac. II(1):41–72.

Manickchand-Dass, S.
1987 Reproduction, age and growth of the lane snapper, *Lutjanus synagris* (Linnaeus), in Trinidad, West Indies. Bull. Mar. Sci. 40 (1):22–28.

Manooch, C.S. III
1987 Mortality rates of snappers and groupers. *In* Polovina, J.J., and S. Ralston (eds.), Tropical snappers and groupers: Biology and fisheries management, p. 329–373. Westview Press, Boulder.

Mori, K.
1984 Early life history of *Lutjanus vitta* (Lutjanidae) in Yuya Bay, the Sea of Japan. Jpn. J. Ichthyol. 30(4):374–392.

Moseley, F.N.
1966 Biology of the red snapper, *Lutjanus aya* Bloch, of the Northwestern Gulf of Mexico. Publ. Inst. Mar.Sci. Univ. Tex. 11:90–101.

Pauly, D.
1980 On the interrelationships between natural mortality, growth parameters, and mean environmental temperature in 175 fish stocks. J. Cons. Perm. Int. Explor. Mer 39:175–192.

Palazón, J.L., and L.W. González
1986 Edad y crecimiento del pargo cebal, *Lutjanus analis* (Cuvier, 1828) (Teleostei: Lutjanidae) en la isla de Margarita y alrededores, Venezuela. Invest. Pesq. 50(2):151–165.

Pozo, E., and L. Espinosa
1982 Estudio de la edad y el crecimento del pargo del alto (*Lutjanus vivanus* Cuvier, 1828) en la plataforma suroriental de Cuba. Rev. Cubana Invest. Pesq. 7(2):1–23.

Ralston, S.V.D.
1987 Mortality rates of snappers and groupers. *In* Polovina, J.J., and S. Ralston (eds.), Tropical snappers and groupers: Biology and fisheries management, p. 375–404. Westview Press, Boulder.

Ratkowsky, D.A.
1983 Nonlinear regression modeling: A unified practical approach. Marcel Dekker, NY, 276 p.

Reshetnikov, Y.S., and R.M. Claro
1976 Cycles of biological processes in tropical fishes with reference to *Lutjanus synagris*. J. Ichthyol. 16:711–723.

Ricker, W.E.
1975 Computation and interpretation of biological statistics of fish populations. Bull. Fish. Res. Board Can. 191, 382 p.

Rodriguez Pino, Z.
1962 Estudios estadísticos y biológicos sobre la biajaiba (*Lutjanus synagris*). Cent. Invest. Pesq., Notas Sobre Invest. 4:1–91.

Sainsbury, K.J.
1987 Assessment and management of the demersal fishery on the continental shelf of northwestern Australia. *In* Polovina, J.J., and S. Ralston (eds.), Tropical snappers and groupers: Biology and fisheries management, p. 465–503. Westview Press, Boulder.

Sainsbury, K.J., P.J. Kailola, and G.G. Leyland
1985 Continental shelf fishes of northern and northwestern Australia. Clouston & Hall and Peter Pownall Fish. Inf. Serv., Canberra, Aust., 375 p.

Starck, W.A. II
1971 Biology of the gray snapper, *Lutjanus griseus*. *In* Starck, W.A. II, and R.E. Schroeder (eds.), Investigations on the gray snapper, *Lutjanus griseus*, p. 1–150. Stud. Trop. Oceanogr. (Miami) 10, Univ. Miami Press.

Tanaka, K., Y. Mugiya, and J. Yamada
1981 Effects of photoperiod and feeding on the daily growth patterns in otoliths of juvenile *Tilapia nilotica*. Fish. Bull., U.S. 79:459–465.

Thompson, R., and J.L. Munro
1983 The biology, ecology and bionomics of the snappers, Lutjanidae. *In* Munro, J.L. (ed.), Caribbean coral reef fishery resources, p. 94–109. ICLARM Stud. Rev. 7, Int. Cent. Living Aquat. Resour. Manage., Manila.

Tranter, D.J.
1962 Zooplankton abundance in Australian waters. Aust. J. Mar. Freshwater Res. 13:106–129.

Whitney, R.R., and K.D. Carlander
1956 Interpretation of body-scale regression for computing body length of fish. J. Wildl. Manage. 20:21–27.

Wright, A., P.J. Dalzell, and A.H. Richards
1986 Some aspects of the biology of the red bass, *Lutjanus bohar* (Forsskal), from the Tigak Islands, Papua New Guinea. J. Fish Biol. 28:533–544.

Young, P.C., and K.J. Sainsbury
1985 CSIRO's North West Shelf program indicates changes in fish populations. Aust. Fish. 44(3):16–20.

Correlation of winter temperature and landings of pink shrimp *Penaeus duorarum* in North Carolina

William F. Hettler

Beaufort Laboratory, Southeast Fisheries Science Center
National Marine Fisheries Service, NOAA, Beaufort, North Carolina 28516-9722

In habitats where low water temperature is not a limiting factor, pink shrimp *Penaeus duorarum* production has been related to rainfall and surface-water inflow (Browder 1985, Sheridan 1991). In contrast, North Carolina landings of pink shrimp were correlated with water temperature during the previous winter, but not to rainfall (Hettler and Chester 1982). In that study, the average water temperature of the two coldest consecutive weeks of each year recorded at a single temperature station located at the Beaufort Laboratory was a predictor of spring landings (through July) for the entire North Carolina fishery. Fifteen years of temperature records and landings were used to determine this relationship. Since the last year reported (1981), 10 additional years of temperature and landings data have become available. This note presents these new data and uses the resulting 25-year time-series to report that average minimum winter water temperature remains a reliable basis for forecasting landings of this species.

The temperature/landings relationship previously published (Hettler and Chester 1982) was recalculated after adding the 1982–91 temperature and landings data (Table 1, Fig. 1). No evidence of curvilinearity in the relationship could be found by fitting higher-order polynomial models. A time-series model was not appropriate because pink shrimp are 'annuals' and their annual population levels generally show low autocorrelation as suggested by the 1962–91 North Carolina pink shrimp heads-off landings data (Fig. 1). Thus the simple linear model was retained. The new regression to determine spring pink shrimp landings in North Carolina was

$$\text{Landings (kg)} = 83747(T) - 245208,$$

where T was the average temperature of the two coldest consecutive weeks (°C). The relationship was significant ($P<0.001$, r^2 0.803). The more general relationships of average winter water temperature (Dec–Mar) or average midwinter water temperature (Jan–Feb) did not correlate with landings over the 25-year time-series.

Predicted landings of pink shrimp were calculated and averaged within 25% of the actual landings for the recent 10-year period. Landings in 1991 were within >0.1% of the prediction. Possible causes of the relatively large deviations in some years' landings from the predicted are discussed in Hettler and Chester (1982) and include errors in the process of estimating landings, year-to-year changes in fishing effort, and, in addition, possible local thermal anomalies.

These new data continue to support the hypothesis that reduced pink shrimp landings in North Carolina are probably a result of cold kill of overwintering shrimp caused by cold water temperatures. In the coldest years (1963, 1977, 1978, and 1990) when spring landings were less than 100,000 kg, lethal cold water probably penetrated all but the most highly protected overwintering estuarine habitat. North Carolina is the northern limit in the range of pink shrimp, thus this species is more likely to encounter low temperature stress in this location than in more southerly locations. The linearity of the model is perhaps a consequence of these shrimp's inherent vulnerability to cold water temperatures interact-

Table 1

Actual and predicted landings (heads-off) of pink shrimp *Penaeus duorarum* in the North Carolina spring fishery, February–July, based on average water temperature of the two coldest consecutive weeks of the preceding winter.

Year	Temp. °C	Landings (kg)		Percent over (+) or under (−)
		Actual	Predicted	
1982	5.0	197,630	173,527	+13.9
1983	8.8	451,163	491,765	−8.3
1984	5.9	184,380	248,899	−25.9
1985	5.4	126,797	207,025	−38.7
1986	6.9	307,514	332,646	−7.6
1987	8.3	551,521	449,892	+22.6
1988	6.1	433,125	265,648	+63.0
1989	8.1	639,166	433,142	+47.5
1990	3.7	66,853	64,656	+3.4
1991	10.0	592,381	592,262	<+0.1

Manuscript accepted 20 March 1992.
Fishery Bulletin, U.S. 90:405–406 (1992).

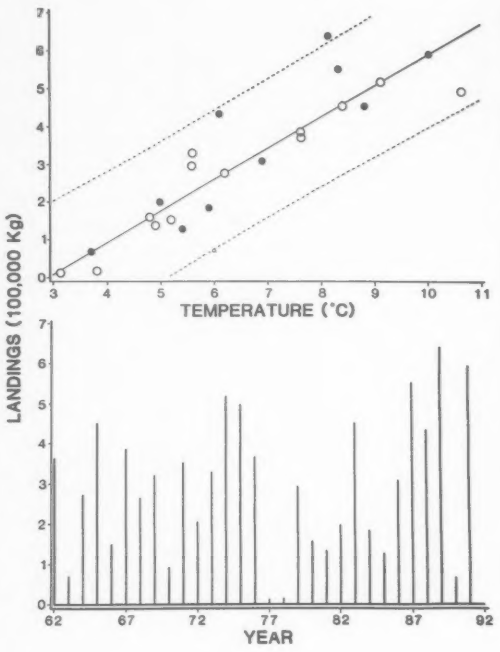

Figure 1

(Upper) Regression and 95% confidence limits for 25 years of temperatures and landings (heads-off) of pink shrimp *Penaeus duorarum*. Open circles represent years before 1982 reported by Hettler and Chester (1982); closed circles represent the years 1982–91. (Bottom) Spring landings (heads-off) of pink shrimp in North Carolina since 1962.

ing with the geographical/spatial distribution and availability of habitats that respond differently to dropping temperatures. The safest habitats would include favorable sediments for deep burrowing, deep water, and physiologically isosmotic salinity.

Acknowledgment

Landings data for 1982–91 were provided by the North Carolina Division of Marine Fisheries, NC/NMFS Cooperative Regional Statistics Program.

Citations

Browder, J.A.
1985 Relationship between pink shrimp production on the Tortugas grounds and water flow patterns in the Florida Everglades. Bull. Mar. Sci. 37:839–856.

Hettler, W.F., and A.J. Chester
1982 The relationship of winter temperature and spring landings of pink shrimp, *Penaeus duorarum*, in North Carolina. Fish. Bull., U.S. 80:761–768.

Sheridan, P.F.
1991 Tortugas pink shrimp forecast. *In* Baxter, K.N. (ed.), Shrimp resource review, briefing book, p. 39. NMFS Southeast Fish. Sci. Cent., Galveston, TX.

Growth of five fishes in Texas bays in the 1960s

Gary C. Matlock
Texas Parks and Wildlife Department
4200 Smith School Road, Austin, Texas 78744

The estuarine sport and commercial fish fisheries in Texas have historically relied upon five species: black drum *Pogonias cromis*, red drum *Sciaenops ocellatus*, sheepshead *Archosargus probatocephalus*, southern flounder *Paralichthys lethostigma*, and spotted seatrout *Cynoscion nebulosus*. Regulation of these fisheries dramatically increased as human demand for fish generally increased through the 1980s. For example, the sale of red drum and spotted seatrout caught in Texas was prohibited in 1981, use of nets in coastal waters was prohibited in 1988, and size, bag, and possession limits were imposed for each species by 1988. Growth information was used in selecting appropriate regulations for optimizing yield and sustaining recruitment. However, comprehensive, coastwide growth rates were available only for red drum, black drum, and spotted seatrout caught in the late 1970s and 1980s when exploitation was extremely high (Doerzbacher et al. 1988, Green et al. 1990). Potential yields may be underestimated when based on growth rates obtained when fishing mortality is high. Tagging data from which growth parameters could be estimated for those species had been collected sporadically from the late 1950s through the early 1970s (Green 1986) when fishing effort was presumably lower than in the 1980s, but these data have not been examined. The objective of this study was to describe quantitatively the growth of black drum, red drum, sheepshead, southern flounder, and spotted seatrout tagged in the 1960s.

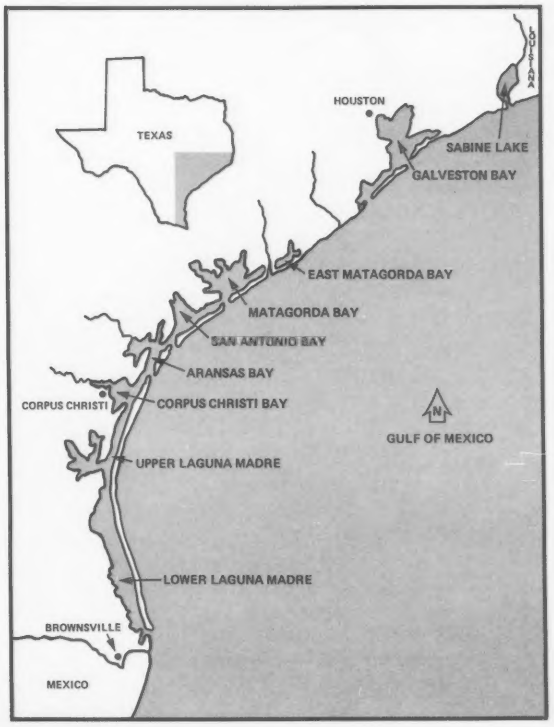

Figure 1
Location of Texas bay systems.

Methods

Data on total length (TL, mm) at tagging and recapture, and the number of days free until recapture for five fishes—black drum, red drum, sheepshead, southern flounder, and spotted seatrout—tagged by the Texas Parks and Wildlife Department (TPWD) in Texas bays (Fig. 1) and recaptured during the period 1950–75 were obtained from Green (1986). No length data were available for fish tagged in the Matagorda Bay system, however. Data resulted from a variety of projects designed to obtain life history information on fishes, mainly red drum and spotted seatrout. Fish for tagging were obtained using rod and reel, trotlines, and trammel and gill nets. Monel strap tags and internal abdominal tags were primarily used. The release of tagged fish and requests for information concerning recaptured fish were advertised through the news media and posters placed in areas frequented by fishermen. Non-monetary rewards of various types were usually offered for returned tags. Additional details are contained in Green (1986). The mean daily growth rate (G) was used to examine the suitability of the von Bertalanffy model for describing growth of each species. The growth rate was calculated as follows:

Manuscript accepted 9 March 1992.
Fishery Bulletin, U.S. 90:407–411 (1992).

$$G = (l_r - l_m)/d,$$

where l_r = TL at recapture,
l_m = TL at tagging, and
d = time in days between tagging and recapture.

A plot of mean daily growth rate versus TL at tagging for each species suggested asymptotic growth, since growth rate generally declined as size-at-tagging increased. Therefore, the von Bertalanffy growth model was chosen as an empirically-based description of growth (Moreau 1987) to which these tagging data were fit. Of the currently available estimating procedures for using tag data to describe growth following the von Bertalanffy growth equation, Fabens' (1965) method provides the most accurate estimates (Sundberg 1984). Data were analyzed using the Fishery Science Application System (Saila et al. 1988) and Fabens' (1965) iterated least-squares method for estimating K and L_∞ in the von Bertalanffy growth equation,

$$l_r = l_m + (L_\infty - l_m)[1 - \exp(-Kd)]$$

where l_r, l_m , and d are defined as above, and
L_∞ = the average TL in a population of fish allowed to grow indefinitely following the von Bertalanffy growth function, and
K = Brody's growth coefficient (per day).

Before analysis, data were screened following procedures of Doerzbacher et al. (1988) to eliminate outliers. Fish with growth rates >3 mm/day or <−3 mm/day were eliminated from the data set. The mean ±3 SD for the remaining data were then calculated, and fish with growth rates outside this range were also eliminated from the data set. Sufficient data were available to analyze tagged red drum separately by bay system (except for Sabine Lake and Matagorda Bay). Data for each of the other species were analyzed for all tagging locations combined.

The measure of effectiveness (P) used by Phares (1980) which is similar to the multiple correlation coefficient of linear regression (R^2) was used to determine how well the von Bertalanffy model fit the data:

$$P = (SSL - SSE)/SSL,$$

where SSL is the sum of squares of $(l_r - l_m)$, and SSE is the residual sum of squares of the model,

$$SSE = (l_r' - l_r)^2,$$

where l_r' is the model's predicted length-at-recapture, and n is the number of recaptured tagged fish (after data screening). The value of l_r' for each tagged fish was calculated following Parrack (1979):

$$l_r' = L_\infty - (L_\infty - l_m)\, e^{-K(d)}).$$

Standard errors of each estimated K and L_∞ were estimated using 10-fold cross-validation technique (a form of jackknife resampling) described by Verbyla and Litvaitis (1989). For each data set, the original data were randomly partitioned into ten subsamples, nine of which each contained 10% of the data, and one which contained the remainder. The first subsample was excluded from the data set, and K and L_∞ were reestimated. The first subsample was recombined with the data set, and the second subsample was excluded, and so on, until all 10 subsamples had been excluded. The standard error of each parameter of the original data set is approximated by the standard deviation of the mean of the 10 separate estimates made after removing each subsample.

Results and discussion

Most of the data reported for recaptured tagged fish during the 1960s were included in the analyzed data set (i.e., few outliers were found). Of 1630 recaptured fish, only 72 (4.4%) fish were excluded from the analyses (Table 1). Red drum from the lower Laguna Madre had the greatest proportion of outliers (13 of 69 fish). However, the size range at tagging of the remaining 56 fish was comparable to the range of red drum tagged in other bays. These results are similar to those of Doerzbacher et al. (1988) for red drum and black drum, and are supported by Ferguson et al. (1984) who demonstrated that red drum lengths reported by sportfishermen were accurate.

Mean daily growth rates of tagged fish during the time between release and recapture were about 0.2 mm/day for all species, except red drum which averaged about 0.4–0.7 mm/day (Table 1). These means mainly represent the growth of smaller fish within each range because the size data were skewed toward small fish. For example, of 254 recaptured black drum, over 250 were <300 mm TL at tagging and recapture. However, the estimates of daily growth for black drum, red drum, sheepshead, and spotted seatrout in this study were within the ranges of those reported by Colura et al. (1984), Cornelius (1984), Beckman et al. (1988, 1990, 1991), Doerzbacher et al. (1988), Murphy and Taylor (1989), Matlock (1990), and Green et al. (1990).

The estimated L_∞ for black drum, red drum, southern flounder, and spotted seatrout tagged in Texas

Table 1

Size, time free, and growth rate of five fishes tagged and released in Texas bays and recaptured by sport and commercial fishermen during the period 1950–75. Outliers were removed (screened) before anaylsis following the procedures described by Doerzbacher et al. (1988).

					TL (mm) at release		TL (mm) at recapture		Time free (days)		Growth rate (mm/day)	
Species	Bay system	No. tagged	No. in analysis	No. screened	Range	Mean (SD)	Range	Mean (SD)	Range	Mean (SD)	Range	Mean (SD)
Black drum	All bays	28,423	254	6	160–750	317 (101)	175–965	373 (116)	4–4143	273 (467)	−1.167–1.438	0.187 (0.125)
Red drum	Galveston	1370	73	2	155–620	342 (104)	241–762	453 (123)	2–1079	204 (200)	−0.500–1.667	0.624 (0.395)
	San Antonio	1272	101	4	220–720	397 (96)	220–915	506 (120)	11–2432	204 (259)	−0.679–1.847	0.569 (0.343)
	Aransas	3061	435	7	175–615	360 (85)	230–838	473 (107)	2–784	206 (169)	−0.378–1.729	0.565 (0.365)
	Corpus Christi	835	58	4	185–520	322 (93)	280–762	462 (123)	3–692	199 (142)	0–1.686	0.733 (0.396)
	Upper Laguna Madre	2857	147	5	133–693	426 (121)	203–774	544 (110)	6–831	250 (177)	0.600–1.526	0.416 (0.316)
	Lower Laguna Madre	2202	56	13	151–685	326 (122)	171–1016	440 (146)	11–5078	412 (824)	−0.274–0.938	0.395 (0.267)
Sheepshead	All bays	6530	56	6	200–555	313 (74)	210–555	336 (75)	1–630	148 (119)	−0.085–0.779	0.167 (0.209)
Southern flounder	All bays	3176	21	0	255–505	337 (78)	250–560	394 (84)	1–546	197 (169)	0–0.647	0.223 (0.192)
Spotted seatrout	All bays	20,517	357	25	192–762	373 (90)	192–762	406 (98)	1–1315	173 (196)	−0.786–1.220	0.171 (0.276)

bays was about 840–950 mm TL, whereas the sheepshead estimate was about 470 mm (Table 2). Daily growth coefficients (K) were about 0.0005 (0.183 annualized) for black drum, southern flounder, and spotted seatrout, and about 0.001 (0.365 annualized) for red drum and sheepshead (Table 1). The 1960s estimates of L_∞ for black drum, red drum, sheepshead, and spotted seatrout in Texas were generally higher than comparable estimates made in the 1980s. Red drum L_∞ in the 1960s ranged from 879 mm in the upper Laguna Madre to 1177 mm in the Aransas Bay system; L_∞ was 918 mm in the 1980s (Doerzbacher et al. 1988). Values for black drum, sheepshead, and spotted seatrout were as follows (1960s vs. 1980s): 844 mm vs. 798 mm (Doerzbacher et al. 1988); fork length (FL) 478 mm vs. 419 mm (males) and 447 mm (females) (Beckman et al. 1991); and 836 mm vs. 691 mm (Green et al. 1990), respectively. No estimates were available for southern flounder in the 1980s.

Red drum growth varied among bays. Estimates of L_∞ for red drum in each bay system approximated 930 mm, except in Aransas Bay where L_∞ was 1177 mm, and K (annualized) varied between 0.3 and 0.5. Reasons for the interbay variation in L_∞ and K for red drum in the 1960s are unknown. However, factors affecting growth (e.g., fishing mortality, food supply, red drum density, and environmental conditions like salinity and temperature) varied among bays (Matlock 1984).

The estimated values of L_∞ for black drum and red drum from fish tagged in the 1960s and 1980s appear to be underestimates because the data include few adult fish which reside mostly in the Gulf of Mexico (Matlock 1987, 1991). The addition of older adults would probably increase L_∞ and reduce K for both species, but the change in parameter estimates would depend on the average maximum age and size actually reached relative to the largest fish included in the analysis. Parameter estimates (standard error) for the von Bertalanffy model for black drum (0–58 years old) growth in Florida were 1172 mm (±9 mm) and 0.124 mm (±0.0003 mm), respectively. When the von Bertalanffy growth equation was fit to length and age (from otoliths) data for adults off Louisiana, the estimate for L_∞ was 1000 mm FL (Beckman et al. 1991); recall, L_∞ for Texas black drum was 844 mm TL. However, Beckman et al. (1991) questioned the biological significance of their L_∞ estimates because an asymptotic

Table 2

Estimates of parameters (daily K and L_∞) in the von Bertalanffy growth equation for five fishes tagged in Texas bays during the period 1950–75 (N = number of fish used in analysis). Approximate standard errors (SE) were estimated using ten-fold validation (Verbyla and Litvaitis 1989). Annualized K and associated SE were estimated by multiplying daily K and daily SE by 365 days. Measure of effectiveness (P) reflects how well the von Bertalanffy model fit the data (Phares 1980).

Species	Bay system	N	K (±1 SE) Daily	K (±1 SE) Annual	L_∞ (mm) (±1 SE)	P (%)
Black drum	All bays	254	0.00048 (0.000039)	0.175 (0.014)	844 (40)	77.7
Red drum	Galveston	73	0.00116 (0.000118)	0.423 (0.043)	900 (61)	91.7
	San Antonio	101	0.00112 (0.000119)	0.409 (0.043)	978 (77)	88.3
	Aransas	435	0.00075 (0.000036)	0.274 (0.013)	1177 (33)	90.2
	Corpus Christi	58	0.00138 (0.000210)	0.504 (0.077)	940 (82)	90.0
	Upper Laguna Madre	147	0.00127 (0.000085)	0.464 (0.031)	879 (27)	90.0
	Lower Laguna Madre	56	0.00075 (0.000221)	0.274 (0.810)	957 (88)	87.0
Sheepshead	All bays	56	0.00098 (0.000289)	0.358 (0.105)	478 (36)	43.9
Southern flounder	All bays*	21	0.00063 (0.000066)	0.230 (0.024)	848 (32)	80.4
Spotted seatrout	All bays	357	0.00045 (0.000040)	0.164 (0.015)	836 (36)	63.0

*Convergence criteria (successive estimates differ by $<2\times10^{-6}$) was not met after 25 iterations.

size was not attained within the size range sampled and growth was practically linear beyond age 5. Further, neither the von Bertalanffy nor power model accurately described the growth of black drums younger than age 5. A similar result was found for red drum when the von Bertalanffy model was fit to data from fish from the Gulf of Mexico (Beckman et al. 1989). The estimates for L_∞ were 909 mm FL for males and 1013 mm FL for females, but estimates for K (0.137 for males and 0.088 for females) were smaller than published estimates based primarily on young fish (Beckman et al. 1989). They suggested that separate models may be necessary to describe growth of young red drum from estuarine areas or old fish from offshore.

The estimates for spotted seatrout growth are probably more accurate than those for the other four species. The sample size is large, and fish of all sizes are well represented in the data set, including adult spotted seatrout which generally reside in the bays (Perret et al. 1980). Estimates for L_∞ and K using published length-at-age data collected from spotted seatrout in the Gulf of Mexico sporadically during 1929–84 were 655 mm and 0.2 mm, respecitvely (Condrey et al. 1985).

The L_∞ estimate for southern flounder (848 mm TL) may be an overestimate, whereas L_∞ for sheepshead (478 mm TL) may be an underestimate. State records for southern flounder and sheepshead caught in Texas salt waters are 711 mm and 641 mm, respectively (Anonymous 1989). Reasons for the apparent bias are unknown but may be related to the few recaptures of tagged southern flounder (21 fish) and the few large sheepshead recaptured. Only one sheepshead was >500 mm TL.

Citations

Anonymous
1989 Texas state fish records. Tex. Parks Wildl. Dep. PWD-L-9000-5-3/89, Austin, 1 p.

Beckman, D.W., A.L. Stanley, J.H. Render, and C.A. Wilson
1990 Age and growth of black drum in Louisiana waters of the Gulf of Mexico. Trans. Am. Fish. Soc. 119:537–544.
1991 Age and growth-rate estimation of sheepshead *Archosargus probatocephalus* in Louisiana waters using otoliths. Fish. Bull., U.S. 89:1–8.

Beckman, D.W., G.R. Fitzhugh, and C.A. Wilson
1988 Growth rates and validation of age estimates of red drum, *Sciaenops ocellatus*, in a Louisiana salt marsh impoundment. Contrib. Mar. Sci. (Suppl.) 30:93–98.

Beckman, D.W., C.A. Wilson, and A.L. Stanley
1989 Age and growth of red drum, *Sciaenops ocellatus*, from offshore waters of the northern Gulf of Mexico. Fish. Bull., U.S. 87:17–28.

Colura, R.L., C.W. Porter, and A.F. Maciorowski
1984 Preliminary evaluation of the scale method for describing age and growth of spotted seatrout (*Cynoscion nebulosus*) in the Matagorda Bay system, Texas. Manage. Data Ser. 57, Tex. Parks Wildl. Dep., Coastal Fish. Br., Austin, 17 p.

Condrey, R.E., G. Adkins, and M.W. Wascom
1985 Yield-per-recruit of spotted seatrout. Gulf Res. Rep. 8(1):63–67.

Cornelius, S.E.
1984 Contribution to the life history of black drum and analysis of the commercial fishery of Baffin Bay, Vol. II. Tech. Rep. 6, Caesar Kleberg Wildl. Res. Inst., Kingsville, TX, 241 p.

Doerzbacher, J.F., A.W. Green, and G.C. Matlock
1988 A temperture compensated von Bertalanffy growth model for tagged red drum and black drum in Texas bays. Fish. Res. (Amst.) 6:135–152.

Fabens, A.J.
1965 Properties and fitting of the von Bertalanffy growth curve. Growth 25:265–289.

Ferguson, M.O., A.W. Green, and G.C. Matlock
1984 Evaluation of the accuracy and precision of volunteered size data from tagged red drum returns. N. Am. J. Fish. Manage. 4:181–185.

Green, A.W., L.W. McEachron, G.C. Matlock, and H.E. Hegen
1990 Use of abdominal streamer tags and maximum-likelihood techniques to estimate spotted seatrout survival and growth. Am. Fish. Soc. Symp. 7:286–292.

Green, L.
1986 Fish tagging on the Texas coast, 1950–1975. Manage. Data Ser. 99, Tex. Parks Wildl. Dep., Coastal Fish. Br., Austin, 206 p.

Matlock, G.C.
1984 A basis for the development of a management plan for red drum in Texas. Ph.D. diss., Texas A&M Univ., College Station, 287 p.
1987 Maximum total length and age of red drum off Texas. Northeast Gulf Sci. 9:49–52.
1990 The life history of red drum. *In* Chamberlain, G.W., R.J. Miget, and M.G. Haby (compilers), Red drum aquaculture, p. 1–22. TAMU-SG-90-603, Texas A&M Univ. Sea Grant Coll. Prog., College Station.
1991 Maximum total length and age of black drum off Texas. Northeast Gulf Sci. 11:171–174.

Moreau, J.
1987 Mathematical and biological expression of growth in fishes: Recent trends and further developments. *In* Summerfelt, R.C., and G.E. Hall (eds.), The age and growth of fish, p. 81–113. Iowa State Univ. Press, Ames.

Murphy, M.D., and R.G. Taylor
1989 Reporduction and growth of black drum, *Pogonias cromis*, in northeast Florida. Northeast Gulf Sci. 10:127–137.

Parrack, M.L.
1979 Aspects of brown shrimp, *Penaeus aztecus*, growth in the northern Gulf of Mexico. Fish. Bull., U.S. 76:827–836.

Perret, W.S., J.E. Weaver, R.O. Williams, P.L. Johansen, T.D. McIlwain, R.C. Raulerson, and W.M. Tatum
1980 Fishery profiles of red drum and spotted seatrout. Gulf States Mar. Fish. Comm. 6, Ocean Springs, MS, 60 p.

Phares, P.L.
1980 Temperature associated growth of white shrimp in Louisiana. NOAA Tech. Memo. NMFS-SEFC-56, Southeast Fish. Sci. Cent., Galveston, TX, 19 p.

Saila, S.B., C.W. Recksiek, and M.H. Prager
1988 Basic fishery science programs, a compendium of microcomputer programs and maual of operation. Dev. Aquacult. Fish. Sci. 18, Elsevier Sci. Publ. Co., NY, 178 p.

Sundberg, P.
1984 A Monte Carlo study of three methods for estimating the parameters in the von Bertalanffy growth equation. J. Cons. Cons. Int. Explor. Mer 41:248–258.

Verbyla, D.L. and J.A. Litvaitis
1989 Resampling methods for evaluating classfication accuracy of wildlife habitat models. Environ. Manage. 13:783–787.

A mortality model for a population in which harvested individuals do not necessarily die: The stone crab

Victor R. Restrepo

University of Miami, Rosenstiel School of Marine and Atmospheric Science
Cooperative Institute for Marine and Atmospheric Studies
4600 Rickenbacker Causeway, Miami, Florida 33149

Stone crabs *Menippe mercenaria* support a valuable commercial fishery in the Gulf of Mexico, with most of the catch occurring near southwest Florida. Florida landings increased from about 400,000 lbs per fishing season (15 October–15 May) in the early 1960s to an average 2.7 million lbs since 1988. The 1990 landings were valued at over $15 million.

The stone crab fishery is unique in that only the crabs' claws can be harvested, provided that the claws are of legal size (70 mm in propodus length); declawed crabs must be returned to the ocean. Stone crabs can regenerate their massive claws which contain much of the crabs' edible meat (a large claw can weigh 250 g). In a sense, stone crabs are a "reusable resource" because claw regeneration by previously declawed crabs accounts for 1–10% of the annual landings (Savage et al. 1975, Ehrhardt and Restrepo 1989).

The main difficulty associated with estimating mortality rates in this unique fishery is that existing models are not applicable to the crabs' population dynamics. Traditional fisheries models are usually based on the equation (see Beverton and Holt 1957),

$$\frac{dN}{dt} = -(F+M)\,N_t,$$

where N is the population size, t is time, and F and M are the instantaneous fishing and natural mortality rates. An implication of this model is that all harvested animals die. Up to 50% of harvested stone crabs may survive, depending on fishing practices such as the amount of time animals are exposed to air and on the extent of the injury caused by declawing (Davis et al. 1979). Therefore, the above model is not appropriate for this fishery or others like it. In this paper I develop a mortality model that accounts for the possibility that harvested individuals may survive. The model can be used to estimate fishing mortality rates for stone crabs.

The model

Consider a closed population of large-sized individuals (large enough to lose both claws to fishing upon capture), in which catches are monitored for a short period of time. This time-period should be sufficiently short to ensure that declawed crabs will not have time to regenerate their claws. Claw regeneration in large stone crabs takes one year or more (Restrepo 1990), so this should not be a major constraint. The population dynamics during this time-period can be modeled by subdividing the population into harvestable and unharvestable crabs (those with and without legal-sized claws, respectively). Harvestable crabs may become unharvestable if they survive fishing; unharvestable crabs may not become harvestable within the time-interval, since it is assumed that claw regeneration does not occur.

Let

^{h}N, ^{n}N = population sizes (in numbers) of harvestable and unharvestable crabs,

F = rate of capture (assumed to be the same for both types of crabs),

^{h}M, ^{n}M = natural mortality rates for harvestable and unharvestable crabs, and,

S = fraction of harvestable crabs that survive claw removal and release ($0 \leqslant S \leqslant 1$).

For simplicity, assume that harvest and natural mortality rates remain fixed during the time-period. Note also that unharvestable crabs are immediately returned to the water upon capture so that their mortality due to capture is negligible. The differential equations describing the two-compartment model are

$$\frac{d^{h}N_t}{dt} = -(^{h}M + FS + F(1-S))^{h}N_t$$

$$= -(^{h}M + F)^{h}N_t, \text{ and} \quad (1a)$$

$$\frac{d^{n}N_t}{dt} = -{}^{n}M\,{}^{n}N_t + FS\,{}^{h}N_t. \quad (1b)$$

Equation (1a) is the standard mortality model and simply shows that crabs disappear from the population due to fishing and natural mortality. Losses due to fishing are $F\,{}^{h}N_t$. Of these, a fraction $(1-S)$ actually die, and a fraction (S) become part of the unharvestable population (Eq. 1b). Thus, F is a true fishing mortality only when $S=0$.

Equation (1a) has the general solution

$$^{h}N_t = {}^{h}N_0\, e^{-(F+{}^{h}M)t}, \quad (2)$$

Manuscript accepted 11 March 1992.
Fishery Bulletin, U.S. 90:412–416 (1992).

where ${}^hN_0$ is the population size at the beginning of the time-period (t=0). This solution can be substituted into Equation (1b) to solve it since, without claw regeneration, ${}^hN_t$ is independent of ${}^nN_t$ (i.e., by assumption, there is no transfer from the nonharvestable into the harvestable population):

$$\frac{d{}^nN_t}{dt} = - {}^nM {}^nN_t + FS {}^hN_0 e^{-(F+{}^hM)t}. \quad (3)$$

This is a first-order linear differential equation that can be solved with the integrating factor

$$e^{\int {}^nM\,dt} = e^{{}^nMt}.$$

Multiplying (3) throughout by this factor gives

$$\frac{d[e^{{}^nMt}\,{}^nN_t]}{dt} = FS {}^hN_0 e^{-(F+{}^hM-{}^nM)t}.$$

Integrating and letting ${}^nN_t={}^nN_0$ at t=0 gives the solution to Equation (3):

$${}^nN_t = \quad (4)$$

$$\frac{FS {}^hN_0 (1-e^{-(F+{}^hM-{}^nM)t})\, e^{-{}^nMt}}{F+{}^hM-{}^nM} + {}^nN_0 e^{-{}^nMt}.$$

The dynamics explained by Equations (2) and (4) depend on six parameters (${}^hN_0$, ${}^nN_0$, ${}^hM$, ${}^nM$, S, and F). The main usefulness of these two equations lies in simulation modeling (e.g., for yield-per-recruit analyses) in which parameters are given as inputs rather than estimated from fitting the equations to data. However, as shown below, the number of parameters can be reduced to three by taking the ratio $R={}^nN_t/{}^hN_t$. Note that the ratio of the two population types is largely independent of the level of sampling intensity, provided that the availabilities of harvestable and unharvestable crabs to the sampling gear do not change. Obtaining estimates of either ${}^nN_t$ or ${}^hN_t$ alone would be a more difficult task which could involve tagging or detailed survey statistics (see Seber 1982 for a discussion on the estimation of abundance). Dividing Equation (4) by Equation (2) gives

$$R_t = a e^{bt} - c, \quad (5)$$

where $R_t = \frac{{}^nN_t}{{}^hN_t}$,

$$a = \frac{FS}{F+{}^hM-{}^nM} + \frac{{}^nN_0}{{}^hN_0},$$

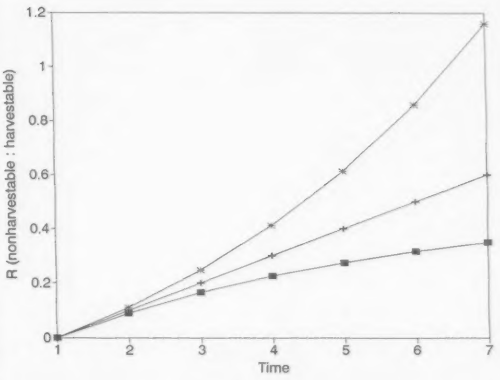

Figure 1

Expected trends in the ratio R (number of nonharvestable: harvestable stone crabs *Menippe mercenaria*) for three values of b in Eq. (5). Lower curve: b is negative and the trend exhibits convex curvature. Middle curve: b approaches zero and the trend is a straight line. Upper curve: b is positive and the trend is concave-upwards.

$$b = F+{}^hM-{}^nM, \text{ and}$$

$$c = \frac{FS}{F+{}^hM-{}^nM}.$$

Equation (5) shows that in a closed population and in the absence of claw regeneration, the ratio of nonharvestable to harvestable crabs should change exponentially with a concave, convex, or straight trend depending on the value of b. Consider a hypothetical population in which ${}^hN_0=1000$, ${}^nN_0=0.0$, S=0.5, F=0.2 per month, and ${}^hM=0.2$ per month. When ${}^nM=0.6$, $b=-0.2$, and R increases with convex curvature (Fig. 1, filled squares). When ${}^nM$ approaches 0.4, b approaches zero, and R increases linearly (Fig. 1, crosses). When ${}^nM=0.2$ (${}^nM={}^hM$), b is positive and the trend in R is a concave-upwards curve (Fig. 1, asterisks). In practice, some of the model's assumptions may not be always met. For instance, if ${}^nM=0.2$ per month and 250 crabs recruit to the harvestable stock at the beginning of months 5, 6, and 7, then the trend in R decreases starting in month 5, while fishing is still ongoing (Fig. 2).

Application of the model to a data set

No studies have been carried out in which the data necessary for the model have been collected. For this reason the estimates presented below are meant to

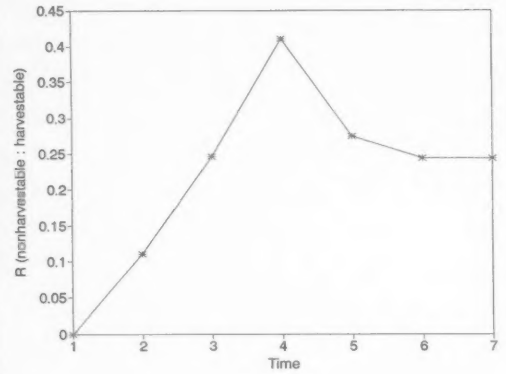

Figure 2

Trend in the ratio R (number of nonharvestable:harvestable stone crabs *Menippe mercenaris*) when the assumption of a closed population is not met. The value of b is positive, as in the upper curve in Fig. 1, but recruitment of harvestable crabs occurs in months 5, 6, and 7.

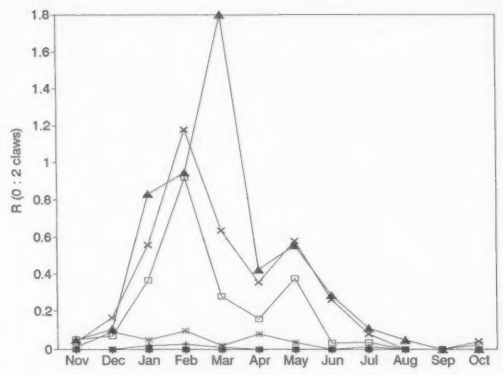

Figure 3

Observed values of the ratio of male stone crabs *Menippe mercenaria* without claws to those with two normal (not regenerated) claws, by size-group. Data from Sullivan (1979).

illustrate how the model can be applied. The data set I used (Sullivan 1979) was collected during 1975 and 1976 in an area where the fishery has been traditionally most intense. This data set contains detailed information on every individual captured, including carapace size, claw sizes, and claw status (presence/absence, regeneration stage, etc.).

The first step in analyzing the data is to define exactly how to categorize crabs in order to meet the assumption that unharvestable crabs do not become harvestable due to claw regeneration during the study period. One way to do so is as follows (Restrepo 1990): "Harvestable" crabs are those with two normal, legal-sized claws (normal claws are defined as those that have no signs of regeneration); "nonharvestable" are those without claws.

With this definition, all harvestable crabs that are caught will likely lose both claws and hence become part of the nonharvestable population if they survive. Conversely, crabs without any claws will not quickly become part of the harvestable population because it would take several regenerative molts (years) before their claws looked normal. Note that the definition above excludes from the analysis all crabs that have either one or two sublegal claws which could, through molting, become part of the harvestable population. In terms of meeting the model's assumptions, the above definition still poses a problem in that crabs with only one claw of legal size (which are relatively uncommon), whether normal or not, may become part of the nonharvestable stock upon declawing.

Figure 3 shows the observed trend in the ratio R [0 claws:2 normal claws] of male stone crabs from Sullivan's (1979) data, for several size-groups. (Female crabs are also harvested, but they are excluded from this analysis because few of them reach sizes at which both claws are of legal size.) Note that R is relatively constant and near zero for crabs <90 mm in carapace width (CW) (Fig. 3). Based on claw size—carapace width relationships (Restrepo 1990), the smaller of the crabs' claws (the "pincer") becomes harvestable only when the carapace reaches 90 mm in width. Thus males with two normal claws are not expected to lose both claws to fishing at sizes <90 mm CW, a fact which is corroborated by Figure 3. Otherwise, R values for the smaller crabs would show larger deviations from the zero line in Figure 3. For this reason, the analyses were conducted with crabs >90 mm CW (Fig. 4).

The trend in the observed R values (Fig. 4, filled squares) is reminiscent of that in Figure 2: it appears to increase concavely upwards from November to February, suggesting that ${}^{n}M < {}^{h}M + F$, and it then decreases starting in March. This decline is possibly a consequence of recruitment of large crabs with normal claws into the fishing grounds, suggesting a failure of the closed-population assumption. Empirical evidence for a similar recruitment peak of large males in the spring was found by Ehrhardt et al. (1990) in Everglades National Park. In addition to recruitment, the decline in R after February could also be attributed to declawed crabs being removed from the study site in greater numbers after this month (some vessels may remove the claws at the end of the day as they travel from the fishing grounds to port). Because of these

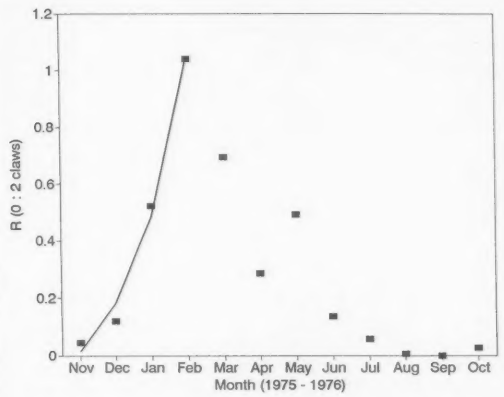

Figure 4

Grouped values from Fig. 3 for crabs ≥ 90 mm CW (symbols). Solid line: fit of Eq. (5) to the first four observations (estimates of fitted parameters are given in Table 1).

Table 1

Parameter estimates and correlation matrix obtained by fitting Equation (5) to Sullivan's (1979) data on stone crab *Menippe mercenaria*.

			Correlation with		
Parameter	Estimate	SE	$\hat{a}$	$\hat{b}$	$\hat{c}$
a	0.191	0.175	1.000		
b	0.618	0.252	−0.994	1.000	
c	0.175	0.229	0.972	−0.949	1.000

problems, only the first four data points in the series were used to estimate the parameters in Equation (5).

The least-squares parameter estimates, standard errors and correlation matrix are given in Table 1 (fit shown in Fig. 4). Note that the errors and correlations are extremely high, owing to the small amount of data used (4 data points to estimate 3 parameters). From these estimates, the following are obtained:

$$\frac{{}^{n}N_0}{{}^{h}N_0} = \hat{a} - \hat{c} = 0.016$$

$$FS = \hat{c}\,\hat{b} = 0.109$$

$$F + {}^{h}M - {}^{n}M = \hat{b} = 0.618.$$

Thus by fitting Equation (5) to the data, the relevant parameters that are estimated are the initial ratio (which could be measured directly, anyway) and the product FS. Due to the indeterminacy in the estimates of FS and $F + {}^{h}M - {}^{n}M$, auxiliary information is required before the harvest rate (F) can be deduced. One possibility is to assume that the natural mortalities of clawed and clawless crabs are identical. If so, then $F = \hat{b}$ and $S = \hat{c}$. This would result in F = 0.618/month and S = 17.6%; instantaneous mortality due to fishing would be F(1 − S) = 0.51/month. If ${}^{n}M > {}^{h}M$ as suggested by Bert et al. (1978), then the value of F will be less than that estimated by $\hat{b}$. Note that $F = \hat{b} =$ 0.618/month translates into about 4.3/year (during a 7-month fishing season), which appears to be unreasonably high, giving indirect support to Bert et al.'s (1978) contention.

Conclusions

An application of the model to estimate current exploitation rates has not been carried out. As shown in the previous section, the data required to do so are relatively simple (crab size, number of claws, and type of claws) but cannot be obtained from the fishery landing statistics. Therefore, a research sampling program would have to be set up to monitor the population and obtain an estimate using the model. Such a sampling program should give consideration to the following requirements:

1 The areal coverage should be large enough to ensure that declawed crabs are not removed from the study site by the fishing vessels.

2 Time-periods when recruitment, immigration, or emigration take place should not be included in the analyses.

3 Counts of both harvestable and nonharvestable individuals should be made periodically (e.g., weekly) so the counts represent the number of individuals at a particular time, rather than the average number of individuals during a long time-period as was done in the preceding section.

4 To avoid imprecision and parameter correlations such as those in Table 1, a large number of R values should be available for parameter estimation.

Acknowledgments

I am grateful to Nelson Ehrhardt, David Die, and Clay Porch for their discussions and to an anonymous reviewer for helpful comments. Special thanks are due to the Marine Research Lab of the Florida Department of Natural Resources for allowing me the use of their data. Financial support for this study was provided by

the Florida Sea Grant College Program under project No. R/LR-b-24, and through the Cooperative Institute for Marine and Atmospheric Studies by the National Oceanic and Atmospheric Administration Cooperative Agreement No. NA90-RAH-0075.

Citations

Bert, T.M., R.E. Warner, and L.D. Kessler
1978 The biology and Florida fishery of the stone crab *Menippe mercenaria* (Say) with emphasis on southwest Florida. Fla. Sea Grant Tech. Rep. 9, Univ. Fla. Sea Grant Prog., Gainesville, 82 p.

Beverton, R.J.H., and S. Holt
1957 On the dynamics of exploited fish populations. Fish. Invest. Minist. Agric. Fish. Food U.K. (Ser. 2), 19, 533 p.

Davis, G.E., D.S. Baughman, J.D. Chapman, D. MacArthur, and A.C. Pierce
1979 Mortality associated with declawing stone crabs, *Menippe mercenaria*. Rep. SFRC T-552, Natl. Park Serv., South Fla. Res. Cent., Homestead, 23 p.

Ehrhardt, N.M., and V.R. Restrepo
1989 The Florida stone crab fishery: A reusable resource? *In* Caddy, J.F. (ed.), Marine invertebrate fisheries: Their assessment and management, p. 225–240. Wiley, NY.

Ehrhardt, N.M., D.J. Die, and V.R. Restrepo
1990 Abundance and impact of fishing on a stone crab (*Menippe mercenaria*) population in Everglades National Park, Florida. Bull. Mar. Sci. 46:311–323.

Restrepo, V.R.
1990 Population dynamics and yield-per-recruit assessment of southwest Florida stone crabs, *Menippe mercenaria*. Ph.D. thesis, Univ. Miami, Coral Gables, 225 p.

Savage, T., J.R. Sullivan, and C.E. Kalman
1975 An analysis of stone crab (*Menippe mercenaria*) landings on Florida's west coast, with a brief synopsis of the fishery. Fla. Dep. Nat. Resour. Mar. Res. Lab. Publ. 13, St. Petersburg, 37 p.

Seber, G.A.F.
1982 The estimation of animal abundance, 2d ed. Charles Griffin, London.

Sullivan, J.R.
1979 The stone crab, *Menippe mercenaria*, in the southwest Florida fishery. Fla. Dep. Nat. Resour. Mar. Res. Publ. 36, St. Petersburg, 37 p.

Optimal course by dolphins for detection avoidance

Carlos A.M. Salvadó
Pierre Kleiber
Andrew E. Dizon

Southwest Fisheries Science Center, National Marine Fisheries Service, NOAA
P.O. Box 271, La Jolla, California 92038-0271

One of the assumptions of line transect sampling is that movement of animals being counted is not in response to the approaching vessel before the animals are detected (Burnham et al. 1980). By observing from a helicopter the reaction of dolphins to an approaching survey vessel, Au and Perryman (1982) and Hewitt (1985) demonstrated that dolphin schools can detect the approach and maneuver to attempt to avoid detection. Because it may be that dolphin exhibit forms of optimal behavior (Au and Weihs 1980), it is of interest to determine whether there is a direction the dolphin should take that maximizes their distance to the vessel at the point of closest approach and, if there is such a direction, to determine whether dolphin use it. If this is so, this may be the way of determining through aerial means when dolphin first react to an approaching vessel and whether it is after they are detected by a shipboard observer.

Since the advent of purse-seine fishing in the eastern tropical Pacific in 1959, dolphin that associate with yellowfin tuna (i.e., primarily *Stenella attenuata*, *S. longirostris*, and *Delphinus delphis*) are chased, caught in nets, and sometimes drowned (Perrin 1968, 1969). Stuntz and Perrin (1979) reported that these species of dolphin are more difficult to capture in areas where purse-seine-vessel fishing effort has been greatest, implying that evasive behavior may be learned. It has also been reported by Au and Perryman (1982) that evasive maneuvers by dolphin upon approach of a vessel sometimes begin at a distance that is approximately the shipboard observer's horizon. Because the visual horizon of even a leaping dolphin is shorter than that of a shipboard observer, it is likely that they are reacting to the vessel sound. It is therefore plausible that by experiencing repeatedly the approach of such vessels, dolphin not only have learned to evade but do so optimally by choosing through trial and error the direction of escape, if it exists, in which the noise amplitude increases the least. Because the attenuation of sound is proportional to the distance transversed by it, escaping from a sound source in the direction where the amplitude increases the least is the same direction that maximizes the distance between a uniformly-moving source and receiver at the point of closest approach.

Here, we formulate the following problem: Upon detecting the approach of a vessel, a dolphin attempts to avoid detection by retreating. If the velocity of the vessel is V_B and that of the dolphin is V_D, is there a direction in which a dolphin can escape to maximize its distance from the vessel at the point of closest approach (Fig. 1)? And if so, what direction is it? We will show that there is such a direction: If α is the angle between V_B and V_D, the angle $\alpha = \arccos(V_D/V_B)$, where V_B and V_D are, respectively, the speeds of the vessel and the dolphin, will maximize the distance

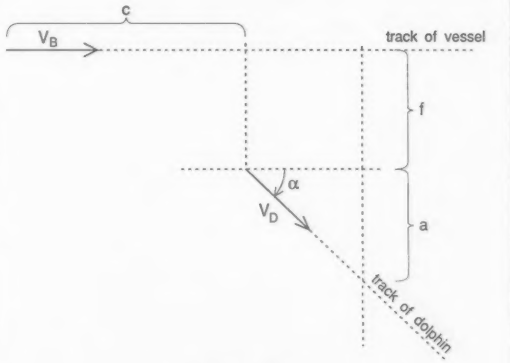

Figure 1
The vessel traveling at speed V_B and the dolphin traveling at V_D as seen in the stationary frame of reference. The direction α is the one chosen by the dolphin. Distance f is the perpendicular distance between the initial position of the dolphin and the projected path of the vessel, while a+f is the distance between vessel and dolphin when the dolphin is abeam.

Manuscript accepted 5 February 1992.
Fishery Bulletin, U.S. 90:417–420 (1992).

between vessel and dolphin at the point of closest approach.

Finally, to ease the task of data analysis by whoever makes the necessary observations, we have derived the expressions that relate dolphin speed and direction to their range and bearing from the vessel. In a cartesian coordinate system let V_x and V_y be, respectively, the x and y components of the dolphin velocity minus, respectively, the x and y components of the vessel velocity. Both V_x and V_y are constructed using range and bearing measurements of the dolphin from the vessel. Then $V_D=[(V_x+V_B)^2+V_y^2]^{1/2}$ and $\alpha=\arctan[V_y/(V_x+V_B)]$.

Problem solution

As stated in the formulation above, the problem makes sense only for the case $V_D \leqslant V_B$. With reference to Figure 2, to maximize the distance between vessel and dolphin at the point of closest approach, we must find the maximum value of r_{min} with respect to angle $0 \leqslant \alpha \leqslant \pi$.

For the purpose of the following exposition, we define initial position to be that position of the vessel (or the dolphin) at the time when the dolphin detects the approaching vessel and begins evasion. Initial time is the time corresponding to the initial position.

In Figure 2, at the point of closest approach the distance between vessel and dolphin is given by

$$r_{min} = (a+f)\cos\beta, \quad (1)$$

where $0 \leqslant \beta \leqslant \pi/2$, f is the perpendicular distance between the initial position of the dolphin and the projected path of the vessel, and (a+f) is the distance between vessel and dolphin when the dolphin is abeam. The vector diagram of Figure 2 shows that the apparent track of the dolphin as seen from the vessel is a function of α, the direction of escape of the dolphin. Therefore, to solve the problem as posed, we must find the extreme value of Eq. (1) with respect to angle α.

By computing the derivative with respect to α of Eq. (1), we find that r_{min} is rendered an extreme value when

$$\frac{dr_{min}}{d\alpha} = \cos\beta\frac{da}{d\alpha} - (a+f)\sin\beta\frac{d\beta}{d\alpha} \quad (2)$$

vanishes. Depending on the functional dependence of a and β on α, an equation of the form of Eq. (2), could vanish either term by term or by cancellation of the terms. For the former case, each term could vanish trivially (i.e., a and β are independent of α), or non-trivially (i.e., both a and β are rendered extreme values with respect to α simultaneously).

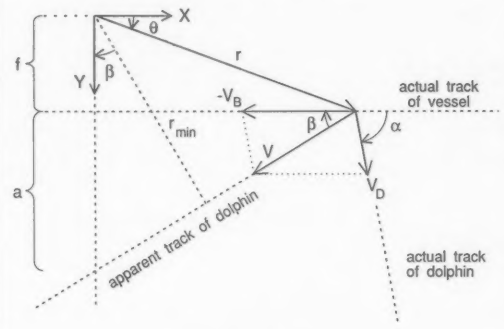

Figure 2

The apparent motion of the dolphin as seen in the moving frame of reference of the vessel. The apparent velocity **V** of the dolphin is the resultant of the vector addition of $-\mathbf{V}_B$ and $\mathbf{V}_D$. Distance f is the perpendicular distance between the initial position of the dolphin and the projected path of the vessel, while a+f is the distance between vessel and dolphin when the dolphin is abeam.

In Figure 1, c is the distance along the projected path of the vessel between the vessel's initial position and the point that is abeam of the dolphin's initial position. Let t_c be the time it takes the vessel to transverse distance c, and t that time from the initial time until the vessel has the dolphin abeam. From the application of the Pythagorean Theorem we can deduce

$$(V_D t)^2 = a^2 + [V_B(t-t_c)]^2. \quad (3)$$

Because

$$a = V_D t \sin\alpha, \quad (4)$$

it can then be shown by substitution of Eq. (4) into Eq. (3) that

$$t = \frac{t_c}{1-(V_D/V_B)\cos\alpha}. \quad (5)$$

By substituting Eq. (5) into Eq. (4), we find that as a function of α, a is given by

$$a = \frac{V_D t_c \sin\alpha}{1-(V_D/V_B)\cos\alpha}. \quad (6)$$

Because at least a is a function of α, we can conclude that in general Eq. (2) does not vanish trivially. However, β is also a function of α as can be deduced by the application of the Law of Sines to Figure 2:

$$\beta = \arctan\left[\left(\frac{V_D}{V_B}\right)\frac{\sin\alpha}{1-(V_D/V_B)\cos\alpha}\right]. \quad (7)$$

Next we investigate whether Eq. (2) vanishes nontrivially. Computing the derivative with respect to α of Eq. (6), we get

$$\frac{da}{d\alpha} = \frac{V_D t_c[\cos\alpha-(V_D/V_B)]}{[1-(V_D/V_B)\cos\alpha]^2}. \quad (8)$$

which vanishes only if

$$\alpha = \arccos\left(\frac{V_D}{V_B}\right) = \alpha_0. \quad (9)$$

Noting the similarity between a and β given respectively in Eq. (6) and (7), we can easily and simply express one in terms of the other. Writing

$$\beta = \arctan\left[\frac{a}{V_B t_c}\right], \quad (10$$

the derivative of β with respect to α is given by

$$\frac{d\beta}{d\alpha} = \frac{\cos^2\beta}{V_B t_c}\frac{da}{d\alpha}. \quad (11)$$

Substituting into Eq. (2) the equivalence of Eq. (11), we find that

$$\frac{dr_{min}}{d\alpha} = \cos\beta\left[1-\frac{(a+f)\sin\beta\cos\beta}{V_B t_c}\right]\frac{da}{d\alpha}, \quad (12)$$

which allows us to conclude that r_{min} is extreme at the point $\alpha=\alpha_0$ because, as we found in Eq. (8), a is extreme at that point. However, as can be appreciated in Eq. (12), there may be other points where r_{min} is extreme. We now investigate whether r_{min} is extreme for values of α other than α_0.

Other extreme values of r_{min} may be attained if

$$\cos\beta = 0 \quad (13)$$

or

$$(a+f)\sin\beta\cos\beta = V_B t_c \quad (14)$$

are physically realizable. Eq. (13) is satisfied for $\beta = n\pi/2$ ($n=1,3,5,...$), and of these only $\beta=\pi/2$ concerns us. It corresponds to the upper limit of the physically realizable range of $0\leqslant\beta\leqslant\pi/2$, and represents the uninteresting case $V_D=V_B$ (i.e., $\alpha_0=0$) which is the trivial special case of this problem: r_{min} is rendered constant when $V_D=V_B$ (i.e., the dolphin swims with the same velocity as the vessel), so the vanishing of Eq. (2) is trivially satisfied.

In Eq. (14) let $f=0$. This limit will not diminish the generality of the solution. The direction a dolphin should take to maximize its distance to the vessel at the point of closest approach will not depend on how close the dolphin is initially to the projected path of the vessel. So without loss of generality we investigate if there is a physically realizable angle β such that

$$a\sin\beta\cos\beta = V_B t_c \quad (15)$$

is satisfied. With the result from Eq. (10) and the identity $\tan\beta=\sin\beta\cos^{-1}\beta$, Eq. (15) can be expressed as the condition $\sin\beta=\pm1$ which is satisfied by the same uninteresting case that satisfies Eq. (13). Therefore, we can conclude that the nontrivial extreme value attained by r_{min} at $\alpha=\alpha_0$ is unique in the interval $0\leqslant\alpha\leqslant\pi$.

We only have left to show that the extreme value attained by r_{min} at $\alpha=\alpha_0$ is a maximum. Let a_0 and β_0 be the respective values of a and β at $\alpha=\alpha_0$. The second derivative of r_{min} with respect to α evaluated at $\alpha=\alpha_0$ is given by

$$\frac{d^2 r_{min}}{d\alpha^2}\Big|_{\alpha_0} = \cos\beta_0\left[1-\frac{a_0\sin\beta_0\cos\beta_0}{V_B t}\right]\frac{d^2a}{d\alpha^2}\Big|_{\alpha_0}. \quad (16)$$

Because the second derivative of a with respect to α evaluated at $\alpha=\alpha_0$ is

$$\frac{d^2a}{d\alpha^2}\Big|_{\alpha_0} = \frac{-V_D t_c}{[1-(V_D/V_B)^2]^{3/2}} < 0, \quad (17)$$

to determine whether Eq. (16) is negative we must show that

$$a_0\sin\beta\cos\beta_0 < V_B t_c. \quad (18)$$

We have shown already that Eq. (15) can only be satisfied for an angle $\beta=\pi/2$. Then Eq. (18) is satisfied for $0\leqslant\beta<\pi/2$. We have seen already that $\beta=\pi/2$ when $\alpha=0$, so $da/d\alpha=0$ at that point also. Therefore, we can also conclude that the nontrivial extreme value achieved by r_{min} at $\alpha=\alpha_0$, unique in the interval $0\leqslant\alpha\leqslant\pi$, is a maximum. Because Eq. (2) vanishes term by term, the same result is achieved by finding the extreme value with respect to α of either β or a.

In conclusion, a dolphin escaping at speed V_D at an angle α relative to the velocity V_B of an approaching vessel will maximize its distance to the vessel at the point of closest approach if $\alpha=\arccos(V_D/V_B)$.

Determination of dolphin velocity from range and bearing measurements

In this section we relate the dolphin velocity to practical *in situ* measurements. We will derive a relationship between dolphin speed and direction to its range $0 \leqslant r < \infty$ and bearing $0 \leqslant \theta \leqslant 2\pi$ from the vessel that triggers the dolphin to flight.

For the times $\{t_i: i=1,2,...,n\}$ we perform the corresponding measurements $\{r_i, \theta_i: i=1,2,...,n\}$. It is not necessary that the measurements be made from the vessel, but with reference to it (e.g., aerial measurements). However, it is necessary that there be no other vessel in the vicinity that perturbs the measurements by reaction of the dolphin to its presence.

The measurements of range and bearing of the dolphin from the vessel are equivalent to the cylindrical coordinates of the dolphin with respect to the moving frame of reference of the vessel. The cartesian coordinates $-\infty < x < \infty$ and $-\infty < y < \infty$ with respect to the same frame of reference are determined from

$$x = r \cos \theta \text{ and } y = r \sin \theta. \quad (19)$$

Let Δx, Δy, and Δt be, respectively, the increments of the variables x, y, and t. For each of the $(n-1)$ consecutive intervals, we can compute the average speeds in the x and y directions by

$$V_x = \frac{\Delta x}{\Delta t} \text{ and } V_y = \frac{\Delta y}{\Delta t}. \quad (20)$$

These are the components of the dolphins' apparent velocity **V** in the frame of the moving vessel (Fig. 2). We can express the dolphin velocity in the moving frame as a function of its speed and direction in the stationary frame by

$$V_x = V_D \cos \alpha - V_B \text{ and } V_y = V_D \sin \alpha, \quad (21)$$

which are a system of two coupled, nonlinear equations with V_D and α as unknowns. The solution to this set of equations is given by

$$V_D = \sqrt{V_x + V_B + V_y^2}, \quad (22)$$

where we have chosen the positive root, and

$$\alpha = \arctan\left(\frac{V_y}{V_x + V_B}\right). \quad (23)$$

With these results we can compare the $(n-1)$ time-intervals the direction α taken by the dolphin given Eq. (23), with the optimal direction given in Eq. (9) computed from the result given Eq. (22).

Acknowledgments

We gratefully acknowledge the valuable suggestions by Dave Au and Bill Perrin, and a correction of an erroneous definition by Tim Gerrodette.

Citations

Au, D., and W. Perryman
1982 Movement and speed of dolphin schools responding to an approaching ship. Fish. Bull., U.S. 80:371–379.

Au, D., and D. Weihs
1980 At high speeds dolphins save energy by leaping. Nature 284(5756):548–560.

Burnham, K.P., D.R. Anderson, and J.L. Laake
1980 Estimation of density from line transect sampling of biological populations. Wildl. Monogr. 72, 202 p.

Hewitt, R.P.
1985 Reaction of dolphins to a survey vessel: Effects on census data. Fish. Bull., U.S. 83:187–193.

Perrin, W.F.
1968 The porpoise and the tuna. Sea Frontiers 14:166–174.
1969 Using porpoise to catch tuna. World Fishing 18(6): 42–45.

Stuntz, W.E., and W.F Perrin
1979 Learned evasive behavior by dolphins involved in the eastern tropical Pacific tuna purse seine fishery. *In* Abstracts from presentations at the Third Biennial Conference of the Biology of Marine Mammals, Seattle, Oct. 7–11, 1979, p. 58. [Avail. Library, Natl. Mar. Mammal Lab., Seattle 98115.]

Effects of microprobe precision on hypotheses related to otolith Sr:Ca ratios

Christopher L. Toole

Department of Fisheries and Wildlife, Oregon State University
104 Nash Hall, Corvallis, Oregon 97331-3803
Present address: Environmental and Technical Services Division
National Marine Fisheries Service, NOAA
911 NE 11th Street, Suite 620, Portland, Oregon 97232

Roger L. Nielsen

College of Oceanography, Oregon State University
Ocean Administration 104, Corvallis, Oregon 97331-5503

Several recent studies have used the electron microprobe to infer environmental temperature at the time of otolith formation from the concentration ratio of strontium and calcium. Sr/Ca ratios of otoliths from fish held at constant temperature or collected at known temperature were examined using atomic absorption spectrophotometry (Radtke 1984, 1989) or wavelength dispersive electron microprobe analysis (Townsend et al. 1989, Kalish 1989, Radtke et al. 1990). These studies, with the exception of Kalish (1989), concluded that there is a negative linear relation between environmental temperature and otolith Sr/Ca ratio. This relationship, coupled with assignment of age to each microprobe sample site, has been used to infer the relative temperature histories of wild-caught fish (Radtke 1984,1987,1989; Radtke and Targett 1984; Radtke and Morales-Nin 1989; Townsend et al. 1989; Radtke et al. 1990). The most ambitious application of the method used otolith Sr/Ca ratios to contrast the calculated temperature histories of different subpopulations of larval herring in the Gulf of Maine (Townsend et al. 1989).

Using the electron microprobe to calculate individual fish temperature histories from otolith Sr/Ca ratios is potentially a useful technique for fisheries biologists. However, precision of back-calculated temperature estimates should be examined in greater detail. Previous studies do not explicitly state confidence limits for mean responses or prediction limits for new observations. The scatter of points in Radtke (1989), Townsend et al. (1989), and Radtke et al. (1990) suggest that widths of 95% prediction limits may be on the order of one to several °C for most levels of Sr/Ca examined. While this might be acceptable for studies of fish which are exposed to wide variations in environmental temperature, it is of less use for species which experience more subtle temperature changes.

Future validation experiments may improve the predictive capabilities of the Sr/Ca vs. temperature relationship by examining effects of other variables. For instance, the regression model might be expanded to include growth rate (Kalish 1989) and some measure of physiological stress (Townsend et al. 1989), since these also appear to influence the Sr/Ca ratio.

However, one component of the variation not likely to change in future experiments employing the electron microprobe is the model error term associated with measurement. Usually measurement error is considered insignificant in relation to other sources of variation and is incorporated into the total error term:

$$Y = a + b*X + \epsilon_{Total}$$

where $\epsilon_{Total} = \epsilon_{Measurement} + \epsilon_{Other}$. Measurement error can be thought of as a lower bound to the variation associated with the regression model when other sources of error are minimized.

We suspect that measurement error may be nontrivial when deriving Sr/Ca vs. temperature relationships. Sr/Ca ratios associated with a 1°C change in environmental temperature were approximately 0.00013–0.00036 in previous studies (Table 1). It is difficult to evaluate the significance of these small values without more information on the analytical precision of Ca and Sr detection in fish otoliths using the electron microprobe. Of the studies cited above, only Kalish (1989) reported analytical precision for representative values of Sr and Ca. In that study, measurement error associated with Sr was 3.5% and that associated with Ca was 0.5% for an Sr/Ca ratio of 0.002.

One purpose of the present study was to examine the precision associated with measuring Sr/Ca ratios in fish otoliths, and to demonstrate how this error affects temperature estimates derived from published regressions. Our approach was to intensively sample one otolith from one fish at three beam-power densities and four counting times. By using one otolith, between-fish effects could be ignored. Within-fish Sr/Ca effects were minimized by referencing samples to the same growth zones, leaving the different analytical techniques as the primary source of variation.

Manuscript accepted 15 January 1992.
Fishery Bulletin, U.S. 90:421–427 (1992).

Table 1
Published Sr/Ca vs. temperature relationships.

Source and species examined	Equation
Radtke et al. (1990)	T = 19.172 − 2.955 * (Sr/Ca * 1000)
Clupea harengus	1°C = 0.000338 (Sr/Ca)
Atlantic herring	Sr/Ca range 0.002–0.0045
Townsend et al. (1989)	T = 12.6 − 2.81 (Sr/Ca * 1000)
Clupea harengus	1°C = 0.000356 (Sr/Ca)
Atlantic herring	Sr/Ca range 0.001–0.0045
Radtke (1989)	(Sr/Ca * 1000) = 16.371 − 0.219 * T
Fundulus heteroclitus	1°C = 0.000219 (Sr/Ca)[a]
Mummichog	Sr/Ca range 0.009–0.013
Radtke (1984)	(Sr/Ca * 1000) = 4.19 − 0.13 * T[b]
Gadus morhua	1°C = 0.000130 (Sr/Ca)[a]
Atlantic cod	Sr/Ca range 0.0028–0.0038

[a]Assumes that slope of Sr/Ca on temperature (T) will also predict T on Sr/Ca.
[b]Not stated explicitly in Radtke (1984), but later reported in Kalish (1989).

A second purpose was to determine the effect of beam exposure on the constancy of Sr/Ca ratios. This was necessary because analytical techniques, such as increasing the counting time, will improve the precision of an analysis but may reduce its accuracy through beam damage to the specimen (e.g., Smith 1986, Potts 1987). This problem is encountered in the analysis of other carbonates, but is particularly severe for otoliths, which contain organic material in addition to $CaCO_3$ (Degens et al. 1969). CO_2 is lost during electron beam exposure and, because it is not actually measured by the microprobe but assumed to occur on a 1:1 basis with cations such as Sr and Ca, concentrations of those elements will increase with increasing beam damage. However, if Sr and Ca are not fractionated from one another by beam damage, their ratio should remain unchanged. Absence of change would indicate that methods which improve precision can be implemented without affecting the accuracy of Sr/Ca ratio determinations.

Methods

Dover sole *Microstomus pacificus* is a common Pacific coast flatfish. Juvenile Dover sole 54–104 mm SL were captured by trawling off the Oregon coast on 17 March 1990 and immediately injected with oxytetracycline (OTC). Within 12 hours, fish were transferred to aquaria in Corvallis, Oregon, where they were held for up to 48 days. The OTC produced a fluorescent band which delineated growth prior to capture from subsequent growth under laboratory conditions. Only portions of the otolith formed under natural conditions (inside the OTC band) were analyzed.

An otolith from a randomly selected fish was mounted on a slide with a toluene-based medium. It was ground using 600-grit paper along the saggital plane to a level near the central primordium. The mounting medium was then melted, the otolith was removed, washed, and remounted on its opposite side with heat-setting epoxy. The second side was then ground to the central primordium and polished with a series of diamond and alumina grits, ending with 0.05 μm alumina. The specimen was cleaned ultrasonically in detergent and water between grit changes and given final rinses in water and methanol. Prior to microprobe analysis, the specimen was carbon coated.

Beam power density and precision

Wavelength-dispersive electron microprobe analysis was performed with a Cameca SX-50 microprobe with a 40° beam angle. Three levels of beam-power density were obtained by varying the beam diameter while holding accelerating voltage and beam current constant at 15 KV and 20 nA, respectively. These voltage and current settings are common to most of the previous studies (R. Radtke, Hawaii Inst. Geophys., Univ. Hawaii, Honolulu 96822, pers. commun. 1990), although Kalish (1989) used a 10 nA current. Defocused beam diameters of 5, 7, and 10 μm resulted in beam-power densities of 1.019, 0.520, and 0.255 nA/μm. The most common beam diameter used in previous studies was 5 μm (R. Radtke, pers. commun. 1990), although Kalish (1989) rastered a 12.5 μm × 12.5 μm square.

Sr and Ca concentrations were calculated as normalized mole fractions (equivalent to the atomic ratios of Kalish 1989). Mole fractions are more informative than weight percentages for examination of Sr/Ca ratios, since the substitution of Sr for Ca in otolith aragonite theoretically occurs on a per-atom basis (e.g., Radtke 1989). Normalization also reduces effects of beam damage on concentrations.

Precision of elemental measurements was determined as the coefficient of variation (CV) (Williams 1987),

$$CV = \sigma_{\text{k-ratio}}/\text{k-ratio}$$

where the k-ratio is the ratio of x-ray counts from the otolith to those of the standard (i.e., the calibrated fraction of that element in the otolith) and $\sigma_{\text{k-ratio}}$ is the

standard deviation of that measurement. For a single microprobe analysis, this is calculated as

$$CV = \left[\left[\left[\frac{\left[\sum_{i=1}^{n} N_i^2 - \frac{\left(\sum_{i=1}^{n} N_i \right)^2}{n} \right]^{0.5}}{\left(\frac{\sum_{i=1}^{n} N_i}{n} \right)} \right]^2 \right]_{\text{Standard}} + \left[\frac{N_p + \left(\frac{t_p}{t_b} \right) * N_i}{(N_p - N_b)} \right]^2_{\text{Otolith}} \right]^{0.5}$$

where n = number of samples taken on the standard,
N_i = x-ray count (corrected for background count) from ith sample on the standard,
N_p = x-ray count for peak wavelength of element in sample,
N_b = x-ray counts from background wavelengths of element in sample,
t_p = peak wavelength counting time, and
t_b = background wavelength counting time.

Approximate 95% confidence limits for each element measured in each sample were considered ±2*CV, since the Poisson distribution underlying these calculations approximates a normal distribution when sample size (the number of x-rays detected by the spectrometer during an analysis) is high (Williams 1987). X-ray counts in this experiment were on the order of 10^2–10^3 for Sr and 10^4–10^5 for Ca. Confidence limits for the Sr/Ca ratio were also calculated as ±2*CV, but in this case the standard deviation of the k-ratio was calculated as

$$\sigma_{Sr/Ca} = \left[\left(\frac{\sigma_{Sr}}{\text{k-ratio}_{Sr}} \right)^2 + \left(\frac{\sigma_{Ca}}{\text{k-ratio}_{Ca}} \right)^2 \right]^{0.5}.$$

Sr and Ca were analysed using the TAP (Sr L-α) and PET (Ca K-α) crystals. Background counts were taken at ±(0.005*sin θ) (where θ is the angle of the spectrometer crystal when it is detecting peak counts) for the same length of time as the peak count. Due to interference with a second-order Ca K-α peak, only one background count was made for Sr. Strontianite (NMNH R10065) and calcite (USNM 136321) were used as standards.

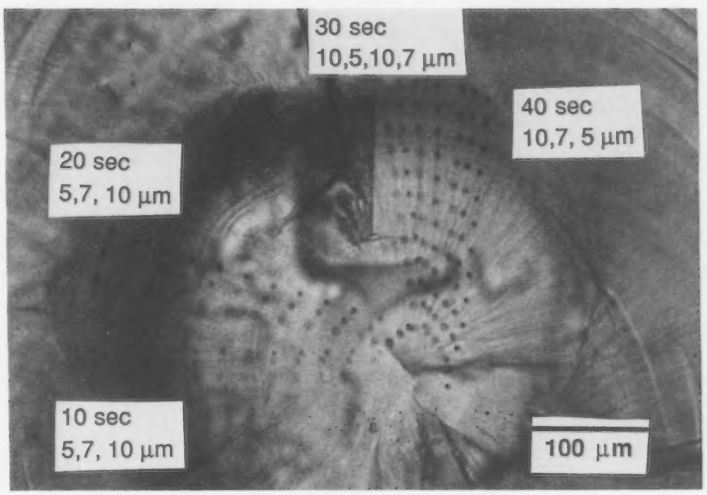

Figure 1
Photomicrograph of otolith from 65.7 mm SL juvenile Dover sole *Microstomus pacificus*, showing location of 12 microprobe transects used for analysis. Each circular area represents one analysis. Note hyaline area near central primordium at inner end of transects and more opaque area towards outer end. The 13th transect was an accidental repetition of the 10 µm, 30-sec transect. Bar indicates 100 µm.

Counting time and precision

Counting time refers to the length of time a spectrometer is collecting counts of characteristic x-rays for an element during one analysis. Counting times of 10, 20, 30, and 40 sec were compared for each beam-power density. The most commonly used counting time for both elements in previous studies was 20 sec (R. Radtke, pers. commun. 1990), although Kalish (1989) analyzed Sr at 100 sec and Ca at 20 sec. Precision was determined as with beam-power density.

Transects of twelve analyses each were made for the 12 combinations of beam power density (4) and counting time (3) (combined N=[12*3*4]=144). These transects passed from an area near the central primordium to an area just inside the discontinuity created by accessory primordia (Fig. 1). This discontinuity

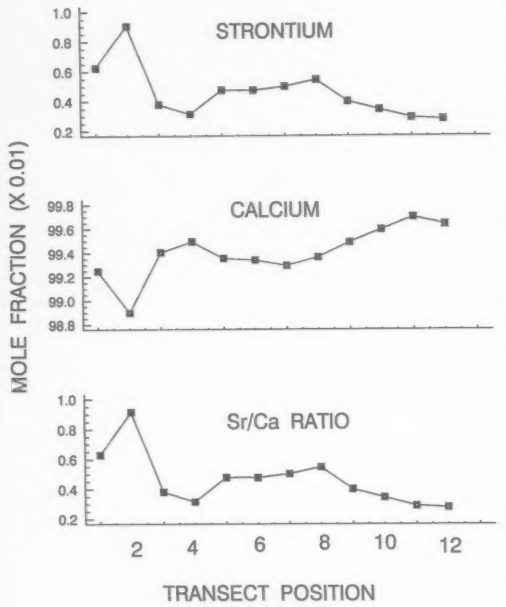

Figure 2

Example of changes in Sr and Ca concentration and the Sr/Ca ratio along one of 12 transects made on a Dover sole otolith. A 7 μm beam and 20-sec counting time were used. Position 1 is the point closest to the central primordium, and position 12 is closest to the otolith edge.

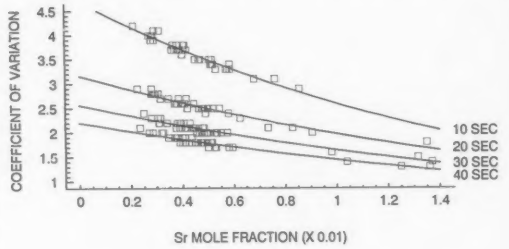

Figure 3

Relation of coefficient of variation (measurement error) to elemental concentration for transects from one Dover sole otolith. Each regression represents three transects with 12 points each (N 36). Regression equations are presented in Table 2.

Table 2

Relationship between Sr concentration and coefficient of variation (CV) for different counting times, based on microprobe transects along the saggital plane of a Dover sole *Microstomus pacificus* otolith. Each equation was derived from three transects of twelve points each (N 36). Equations are in the form: CV = exp(A + (B * Sr mole fraction)). Standard errors in parentheses.

Seconds	A	B	R^2
10	1.546	−59.261	0.940
	(0.012)	(2.558)	
20	1.150	−47.156	0.938
	(0.011)	(2.076)	
30	0.941	−44.454	0.947
	(0.010)	(1.806)	
40	0.789	−42.135	0.938
	(0.010)	(1.863)	

was >100 μm inside the OTC mark. Starting and ending points for all transects were referenced to specific growth areas identified by dark continuous bands, and the remaining points were evenly spaced between these two points. Locations at the start of the transects were in a translucent area of the otolith assumed to have little organic material (Dannevig 1955), while the end points were in a more opaque area, which probably contained more organic material.

Exposure time and accuracy

Counting time and exposure time were distinguished in this experiment. Counting time is the minimum time the specimen is exposed to the electron beam, while exposure time also includes the time necessary to collect background counts and counts of other elements.

Six sequential analyses were made at each of six locations (combined N 36) to determine changes in elemental concentration. The locations were the start and endpoints of each 20-sec transect used for the precision analysis. Sequential analyses at each location were made in increments of 20-sec counting times, which corresponded to exposure times of 65, 130, 195, 260, 325, and 390 sec. These exposure times were approximately twice as long as those which would result from an analysis of Sr and Ca alone, because S was also analyzed (results not reported).

Statistical analyses

The effect of elemental concentration on Sr precision (CV's) was examined with linear and nonlinear regressions. To determine if beam-power density affected Sr precision, multiple regressions containing normalized concentration and "dummy variables" corresponding to beam size were analyzed with partial-F tests (Neter et al. 1989:364–370). Each of the four counting times was analyzed separately.

Widths of 95% confidence intervals associated with Sr/Ca ratios were determined with linear and nonlinear regressions for each counting time. The ratios and widths of confidence intervals were then converted to temperatures using the four previously published Sr/Ca vs. temperature regressions in Table 1.

The effect of exposure time on Sr/Ca constancy was analyzed with a multiple regression containing exposure time and each location (coded as 0's and 1's) as independent variables. Locations were included to remove possible effects of initial Sr/Ca concentrations, which varied between sites. After determining that interactions and nonlinear terms did not improve a model with parallel straight lines, the common slope was compared with a slope of 0 using a t-test.

Whenever the null hypothesis could not be rejected at $\alpha = 0.05$, statistical power $(1-\beta)$ of the test was calculated as in (Neter et al. 1989:74–75). The power of a test was considered acceptable if $(1-\beta) > 0.80$ (Peterman 1990).

Results

The twelve transects made under different beam conditions on the otolith of a 65.7 mm SL juvenile Dover sole exhibited consistent patterns of strontium and calcium concentrations. Sr concentrations were highest at the two innermost positions and lowest at the two outermost positions in all transects. Sr/Ca ratios mirrored the pattern of Sr. Ca concentrations were approximately 100–500 times higher than Sr concentrations. An example of one of the 12 transects (7 μm beam at 20-sec counting time) is presented in Figure 2.

Relative error of Sr measurements decreased as counting time and elemental concentrations increased, and this was best described by an exponential regression model (Fig. 3, Table 2). The coefficient of variation was 1.4–4.2% for Sr concentrations of 0.2–1.2%. When the effect of elemental concentration was removed, Sr CV's increased with decreasing beam-power density (Table 3); however, this effect was small compared with those of elemental concentration and counting time. Differences in Sr CV's attributable to beam-power density was 0.012–0.076%.

The coefficient of variation associated with Ca measurements was 0.5% for 10- and 20-sec counts and 0.4% for 30- and 40-sec counts, regardless of Ca concentration and beam-power density.

Regressions of the widths of 95% confidence intervals for Sr/Ca determinations against measured Sr/Ca ratios are presented in Figure 4 and Table 4. These regressions include only the effects of elemental concentration and counting time; the effect of beam-power density is omitted. Although relative error decreases

Table 3

Relationship between Sr coefficient of variation (CV) and beam power density, holding Sr concentration as a nonlinear covariate, based upon microprobe transects along the saggital plane of a Dover sole otolith. Each regression represents three transects with 12 points each (N 36). Equations are in the form: $CV = A_1 + A_2Z_1 + A_3Z_2 + B_1*(\text{Sr mole fraction}) + B_2*(\text{Sr mole fraction})^2$ where A is the intercept for the 10 μm beam (0.255 nA/μm density), $A + A_2Z_1$ is the intercept for the 7 μm beam (0.520 nA/μm density), and $A + A_3Z_2$ is the intercept for the 5 μm beam (1.019 nA/μm density); Z_1 and Z_2 are dummy variables for the 7 and 5 μm beams; and B_1 and B_2 are fitted slope parameters. Partial-F tests indicate the significance of beam power density effects in the model. Standard errors in parentheses.

	Counts			
Parameter	10-sec	20-sec	30-sec	40-sec
A_1	4.990	3.394	2.767	2.420
	(0.101)	(0.043)	(0.051)	(0.041)
A_2	−0.013	−0.019	−0.027	−0.039
	(0.027)	(0.018)	(0.017)	(0.014)
A_3	−0.076	−0.055	−0.052	−0.053
	(0.027)	(0.018)	(0.017)	(0.014)
B_1	−389.80	−219.41	−169.07	−151.79
	(40.88)	(13.49)	(15.73)	(12.81)
B_2	17940.3	7746.5	5386.3	5229.6
	(3996.70)	(921.47)	(959.47)	(796.05)
R^2 (adj.)	0.954	0.969	0.959	0.962
$F^*_{(0.05, 2, 31)}$	4.479	4.833	4.531	8.443
P	0.020	0.015	0.019	0.001

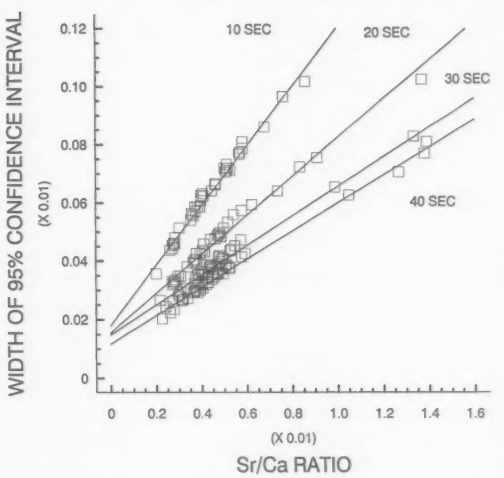

Figure 4

Relationship between Sr/Ca ratios and 95% confidence intervals of measurements at different counting times, based upon microprobe transects along the saggital plane of one Dover sole otolith. Each regression represents three transects of 12 points each (N 36). Regression equations are presented in Table 4.

Table 4

Relationship between Sr/Ca ratios and 95% confidence interval of measurements at different counting times, based upon microprobe transects along the saggital plane of a Dover sole otolith. Each equation was derived from three transects of 12 points each (N 36). Form of the relationship is: 95% CI = A + (B*Sr/Ca ratio). Standard errors in parentheses.

Seconds	A	B	R^2
10	1.791E-4	0.1024	0.9861
	(9.829E-6)	(0.0021)	
20	1.551E-4	0.0669	0.9823
	(7.990E-6)	(0.0015)	
30	1.477E-4	0.0508	0.9817
	(6.579E-6)	(0.0012)	
40	1.166E-4	0.0482	0.9888
	(4.843E-6)	(0.0009)	

with increasing Sr/Ca, the actual width of the confidence interval increases. Conversion of Sr/Ca ratios and 95% confidence limits to temperatures, using the 20-sec regression and previously published temperature vs. Sr/Ca ratios, is presented in Figure 5. Confidence limits associated with calculated temperatures were 0.6–4.7°C, depending upon species, study, and temperature level.

The model which best fit the six multiple exposures is presented in Figure 6. The common slope of $-1.3*10^{-7}$ was not different from a slope of 0 ($t_{0.05,29} = 0.176$, $P = 0.86$). This experiment could have detected a change as small as $1.86*10^{-6}$ Sr/Ca per sec increased exposure (or $1.21*10^{-4}$ for each 65-sec treatment) at $\alpha = 0.05$ and $(1-\beta) = 0.90$, had such an effect existed.

Discussion

Our results confirm that measurement error associated with Sr/Ca determinations is nontrivial. At the standard counting time of 20 sec, measurement error associated with Sr/Ca determinations (expressed as 95% confidence intervals) was equal to or greater than the Sr/Ca increment representative of a 1°C temperature change in three of the four previously-published studies. Even in Townsend et al. (1989), at temperatures <4°C, measurement error was >1°C. The highest measurement error in the studies was representative of a 4.7°C temperature change. Inferred temperature differences between otolith regions or between fish should be considered in light of these values. Statistical error in the Sr/Ca vs. temperature regressions will add to the measurement error associated with temperature calculations.

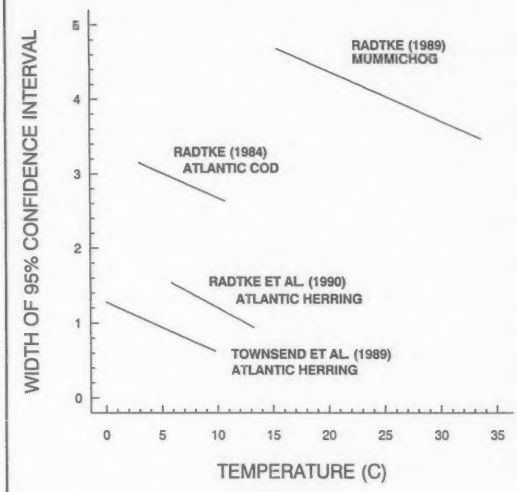

Figure 5

Relationship between back-calculated temperature estimates and 95% confidence intervals (for measurement error only) surrounding those estimates. Temperature vs. Sr/Ca conversions are from Table 1. Confidence intervals are converted from Sr/Ca confidence intervals for 20-sec counts in Table 4 and Figure 4.

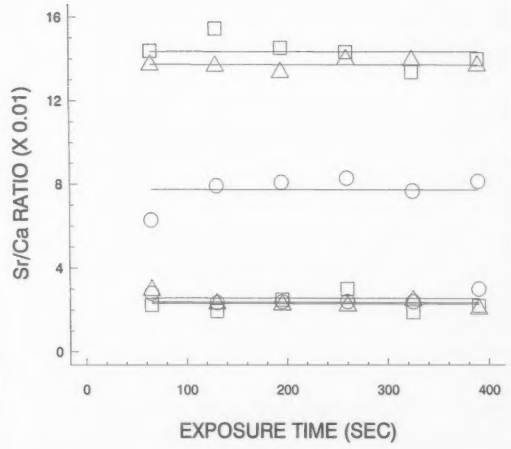

Figure 6

Relationship between Sr/Ca level and exposure time, based upon microprobe samples at six sites on one Dover sole otolith. Six sequential analyses were made at each site (N 36). The six exposure times corresponded to counting times of 20, 40, 60, 80, 100, and 120 sec. The equation describing the relationship is: Sr/Ca level = $0.0023 + (0.0054*Z_1) + (0.00026*Z_2) + (0.0114*Z_3) + (6.6\times10^{-5}*Z_4) + (0.012*Z_5) - (1.30\times10^{-7}*$ exposure time), where Z_1–Z_5 are dummy variables for locations. Adjusted $R^2 = 0.991$, $P < 0.0001$.

At least 40-sec counts would be necessary to detect a 1°C change in temperature experienced by herring (Townsend et al. 1989, Radtke et al. 1990) at all temperature levels examined in those studies. Detection of a 1°C temperature change in cod (Radtke 1984) and *Fundulus* (Radtke 1989) would require much longer counting times, beyond the range examined in this experiment.

This experiment documents the improvement in precision which is possible when otoliths are analyzed at longer counting times and higher beam power densities. Neither treatment appeared to affect the level of Sr/Ca accuracy under the range of conditions examined. Obvious burns on the otolith (Fig. 1) indicate that beam damage did occur in all of our experimental treatments, and we suspect that it also occurred in other studies using similar analytical conditions. However, whatever effect this may have had on the accuracy of the molecular weight percent concentrations for Ca and Sr, the ratio of the two elements remained constant, indicating no observable fractionation.

One implication of these results is that Sr/Ca precision can be increased, with no apparent loss of accuracy, when analyses are conducted for 40-sec rather than 20-sec counting times, and at 5 μm rather than 10 μm beam sizes, at an accelerating voltage of 20 nA. The 5 μm beam allows greater temporal resolution, which is helpful when matching the sample location to structures such as daily growth increments. These may be as small as 0.1–0.2 μm, depending upon species, growth rate, and age (Campagna and Neilson 1985).

Because the level of precision may affect conclusions of studies relating otolith Sr/Ca levels to environmental temperature, it is important to know the analytical conditions under which each study is conducted. Minimal information required includes beam current and voltage, beam size, counting time for each element, standards used, and precision of measurements. This information has not been reported in sufficient detail in some of the previous studies, making interpretation difficult. The methods described in this experiment are proposed as a means of defining measurement precision in future studies of Sr/Ca ratios in fish otoliths.

Acknowledgments

We are grateful to Douglas Markle for his advice and support. Comments by John Kalish on an earlier draft greatly improved the final version. This work was funded in part by the Oregon Sea Grant Program, Project No. NA85AA-D-SG095; Pacific Outer Continental Shelf Region of the Minerals Management Service, Department of Interior Contract No. 14-12-0001-30429; and the Oregon State University Research Office. We also thank Capt. Terry Thompson of the FV *Olympic* for donation of a portion of the ship time.

Citations

Campagna, S.E., and J. Neilson
1985 Microstructure of fish otoliths. Can. J. Fish. Aquat. Sci. 42:1014–1032.

Dannevig, E.H.
1955 Chemical composition of the zones in cod otoliths. J. Cons. Cons. Int. Explor. Mer 21:156–159.

Degens, E.T., W. Deuser, and R. Haedrich
1969 Molecular structure and composition of fish otoliths. Mar. Biol. (Berl.) 2:105–113.

Kalish, J.M.
1989 Otolith microchemistry: Validation of the effects of physiology, age, and environment on otolith composition. J. Exp. Mar. Biol. Ecol. 132:151–178.

Neter, J., W. Wasserman, and M. Kutner
1989 Applied linear regression models. Irwin, Boston, 667 p.

Peterman, R.M.
1990 Statistical power analysis can improve fisheries research and management. Can. J. Fish. Aquat. Sci. 47:2–15.

Potts, P.J.
1987 A handbook of silicate rock analysis. Chapman & Hall, NY, 622 p.

Radtke, R.L.
1984 Cod fish otoliths: Information storage structures. *In* The propagation of cod *Gadus morhua* L. Flodevigen Rapp. 1:273–298.
1987 Age and growth information available from the otoliths of the Hawaiian snapper, *Pristipomoides filamentosus*. Coral Reefs 6:19–25.
1989 Strontium-calcium concentration ratios in fish otoliths as environmental indicators. Comp. Biochem. Physiol. 92A: 189–193.

Radtke, R.L., and B. Morales-Nin
1989 Mediterranean juvenile bluefin tuna: Life history patterns. J. Fish Biol. 35:485–496.

Radtke, R.L., and T. Targett
1984 Rythmic structural and chemical patterns in otoliths of the Antarctic fish *Notothenia larsoni*: Their application to age determination. Polar Biol. 3:203–210.

Radtke, R.L., D. Townsend, S. Folsom, and M. Morrison
1990 Strontium:calcium concentration ratios in otoliths of herring larvae as indicators of environmental histories. Environ. Biol. Fish. 27:51–61.

Smith, M.P.
1986 Silver coating inhibits electron microprobe beam damage of carbonates. J. Sedimentary Petrol. 56:107–108.

Townsend, D.W., R. Radtke, M. Morrison, and S. Folsom
1989 Recruitment implications of larval herring overwintering distributions in the Gulf of Maine, inferred using a new otolith technique. Mar. Ecol. Prog. Ser. 55:1–13.

Williams, K.L.
1987 An introduction to X-ray spectrometry: X-ray fluorescence and electron microprobe analysis. Allen & Unwin, London, 370 p.

Superintendent of Documents **Subscriptions** Order Form

Order Processing Code:
* 5178

☐ **YES,** enter my subscription as follows:

Charge your order. It's Easy! MasterCard VISA

To fax your orders (202) 512–2233

____ subscriptions to **FISHERY BULLETIN (FB)** for $24.00 per year ($30.00 foreign).

The total cost of my order is $_____. Price includes regular domestic postage and handling and is subject to change.

_____
(Company or Personal Name) (Please type or print)

_____
(Additional address/attention line)

_____
(Street address)

_____
(City, State, ZIP Code)

_____
(Daytime phone including area code)

_____
(Purchase Order No.)

May we make your name/address available to other mailers? YES ☐ NO ☐

Please Choose Method of Payment:

☐ Check Payable to the Superintendent of Documents

☐ GPO Deposit Account ☐☐☐☐☐☐☐–☐

☐ VISA or MasterCard Account

☐☐☐☐☐☐☐☐☐☐☐☐☐☐☐☐

☐☐☐☐ (Credit card expiration date)

Thank you for your order!

_____
(Authorizing Signature) 11/91

Mail To: New Orders, Superintendent of Documents
P.O. Box 371954, Pittsburgh, PA 15250–7954

The National Marine Fisheries Service (NMFS) does not approve, recommend or endorse any proprietary product or proprietary material mentioned in this publication. No reference shall be made to NMFS, or to this publication furnished by NMFS, in any advertising or sales promotion which would indicate or imply that NMFS approves, recommends or endorses any proprietary product or proprietary material mentioned herein, or which has as its purpose an intent to cause directly or indirectly the advertised product to be used or purchased because of this NMFS publication.

Fishery Bulletin

Guidelines for Contributors

Form of manuscript

The document should be in the following sequence: Title Page, Abstract (not required for Note), Text, Acknowledgments, Citations, Text footnotes, Appendices, Tables, Figure legends, and Figures.

Title page should include authors' full names and mailing addresses and the senior author's telephone and FAX numbers.

Abstract Not to exceed one double-spaced typed page. Should include a sentence or two explaining to the general reader why the research was undertaken and why the results should be viewed as important. Abstract should convey the main point of the paper and outline the results or conclusions. No footnotes or references.

Text A brief introduction should portray the broad significance of the paper. The entire text should be intelligible to readers from different disciplines. All technical terms should be defined, as well as all abbreviations, acronyms, and symbols in text, equations, or formulae. Abbreviate units of measure only when used with numerals or in tables and figures to conserve space. Measurements should be expressed in metric units, with other equivalent units given in parentheses. Follow the *U.S. Government Printing Office Style Manual*, 1984 ed., and the *CBE Style Manual*, 5th ed. Fishery and invertebrate nomenclature should follow the *American Fisheries Society Special Publication 12* (for fishes), *16* (for mollusks), and *17* (for decapod crustaceans).

Text footnotes should be numbered in Arabic numerals and typed on a separate sheet from the text. Footnotes are not used for reference material or personal communications, but rather to explain or define terms in the text and for contribution numbers on the title page.

Informal sources Personal communications, unpublished data, and untitled manuscripts in preparation are noted parenthetically in the text (full name, affiliation, brief address including zip code, and month and year when appropriate).

Acknowledgments Gather all acknowledgments into a brief statement at the end of the text. Give credit only for exceptional contributions and not to those whose contributions are part of their normal duties.

Citations All titled sources should be listed in the Citations section, including unpublished and processed material. In text, cite as Smith and Jones (1977) or (Smith and Jones 1977); if more than one citation, list chronologically (Smith 1936, Jones 1975, Doe In press). All sources cited in the text should be listed alphabetically by the senior authors' surnames under the heading CITATIONS. Abbreviations of periodicals and serials should conform to *Serial Sources for the BIOSIS Data Base™*. Indicate whether sources are in a language other than English. For informal literature, include address of author or publisher. Authors are responsible for the accuracy of all citations.

Tables should supplement, not duplicate, the text. Each table should be numbered and cited consecutively, with headings short but amply descriptive so that the reader need not refer to the text. For values less than one, zeros should precede all decimal points. Indicate units of measure in column headings; do not deviate from the unit of measure within a column. Table footnotes should be noted consecutively in Roman letters across the page from left to right and then down. Since all tables are typeset, they need not be submitted camera-ready.

Figures Photographs and line drawings should be of professional quality—clear and concise—and reducible to 42 picas for full-page width or to 20 picas for a single-column width, and to a maximum 55 picas high. All graphic elements in illustrations must be proportioned to insure legibility when reduced to fit the page format. Line weight and lettering should be sharp and even. Lettering should be upper and lower case, and vertical lettering should be avoided whenever possible (except for vertical, y, axis). Zeros should precede all decimal points for values less than one. Reproductions of line artwork are accepted in the form of high-quality photographic prints from negatives or photomechanical transfer (PMT). Halftones should be sharply focused with good contrast. Micron rules should be inserted on electron micrographs, even when magnification is included in the figure legend. There should be clear distinction between identifying letters (press-on or overlay) and background of photograph. Label each figure in pencil on the back. Send only xerox copies of figures to the Scientific Editor; originals or photographic prints will be requested later when the manuscript is accepted for publication.

Copyright Government publications are in the public domain, i.e., they are not protected by copyright.

Submission of manuscript

Disks Authors are encouraged to retain manuscripts on word-processing storage media (diskettes, floppy disks) and submit a double-spaced hardcopy run from the storage media. Submit disks as MS-DOS "print" or "non-document" files (often called "ASCII files"). If a disk cannot be converted to an ASCII file, the author should indicate on the disk the source computer and software language along with the file name. Either 5¼-inch or 3½-inch disks from IBM-compatible or Apple/MacIntosh systems (non-graphics only) can be submitted, double-sided/double-density or high-density, limiting each file to 300 kilobytes. All 8-inch word-processing disks (e.g., Wang or NBI) must be converted onto 5¼- or 3½-inch MS-DOS print disks.

Send original hardcopy and two duplicated copies to:

Dr. Linda L. Jones, Scientific Editor
National Marine Mammal Laboratory
F/AKC3
National Marine Fisheries Service,
NOAA
7600 Sand Point Way NE
Seattle, WA 98115-0070
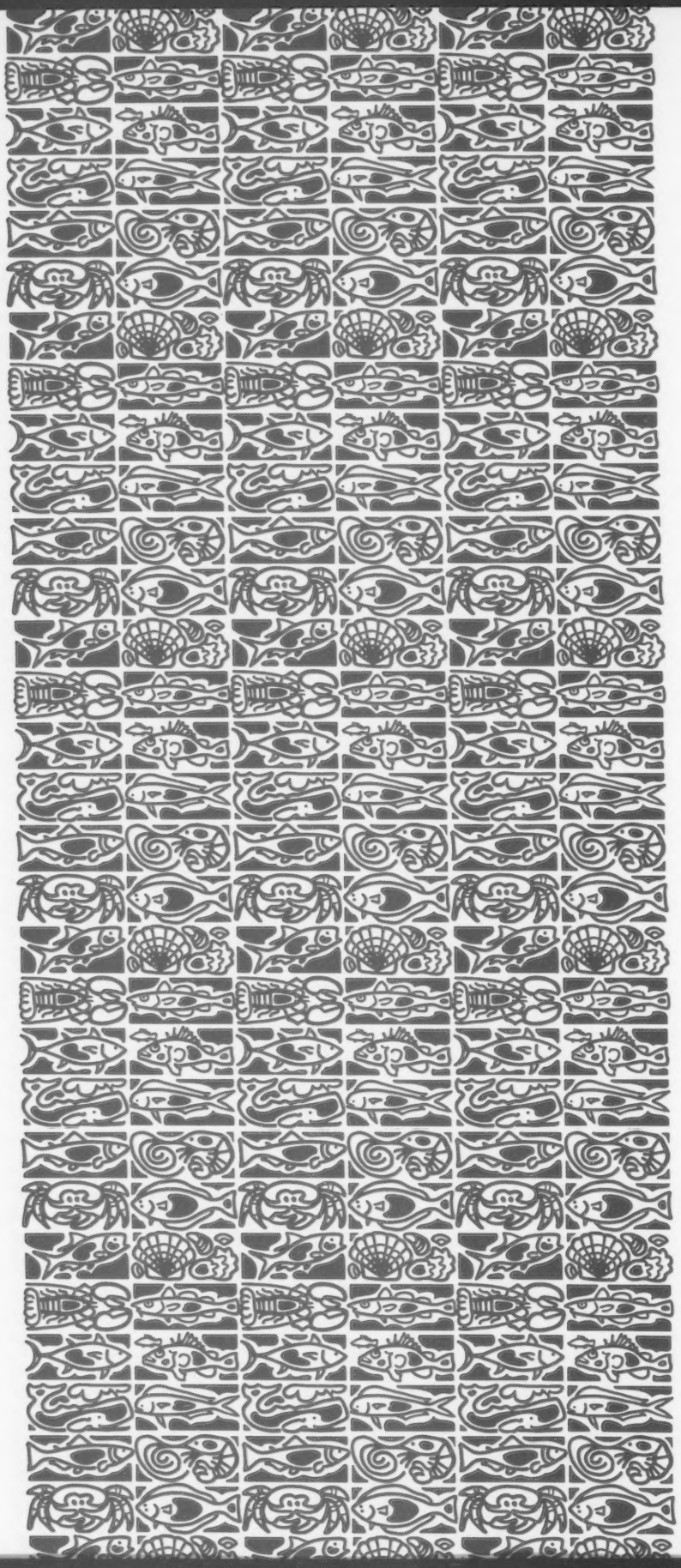
Copies of published articles and notes
The senior author and his/her organization each receive 50 separates free-of-charge. Additional copies may be purchased in lots of 100.